Year : 2021

Innate lymphoid cells in sepsis and trained immunity

Théroude Charlotte

UNIL | Université de Lausanne

Centre hospitalier universitaire vaudois

Département de Médecine
Service des Maladies Infectieuses

Innate lymphoid cells in sepsis and trained immunity

Thèse de doctorat ès sciences de la vie (PhD)

présentée à la

Faculté de biologie et de médecine
de l'Université de Lausanne

par

Charlotte THEROUDE

Master de l'Université Lyon 1, France

Jury

Prof. Matthieu Perreau, Président
Prof. Thierry Roger, Directeur de thèse
Prof. Thierry Calandra, Co-directeur de thèse
Prof. Camilla Jandus, Experte
Dr. Jeroen Geurts, Expert

Lausanne 2021

UNIL | Université de Lausanne

Centre hospitalier universitaire vaudois

Département de Médecine
Service des Maladies Infectieuses

Innate lymphoid cells in sepsis and trained immunity

Thèse de doctorat ès sciences de la vie (PhD)

présentée à la

Faculté de biologie et de médecine
de l'Université de Lausanne

par

Charlotte THEROUDE

Master de l'Université Lyon 1, France

Jury

Prof. Matthieu Perreau, Président
Prof. Thierry Roger, Directeur de thèse
Prof. Thierry Calandra, Co-directeur de thèse
Prof. Camilla Jandus, Experte
Dr. Jeroen Geurts, Expert

Lausanne 2021

UNIL | Université de Lausanne
Faculté de biologie
et de médecine

Ecole Doctorale
Doctorat ès sciences de la vie

Imprimatur

Vu le rapport présenté par le jury d'examen, composé de

Président·e	Monsieur	Prof.	Matthieu	**Perreau**
Directeur·trice de thèse	Monsieur	Prof.	Thierry	**Roger**
Co-directeur·trice	Monsieur	Prof.	Thierry	**Calandra**
Expert·e·s	Madame	Prof.	Camilla	**Jandus**
	Monsieur	Prof.	Jeroen	**Geurts**

le Conseil de Faculté autorise l'impression de la thèse de

Madame Charlotte Delphine Anne-Marie Theroude

Master, Université Claude Bernard / Lyon I, France

intitulée

Innate lymphoid cells in sepsis and trained immunity

Date de l'examen : 28 mai 2021

Date d'émission de l'imprimatur : Lausanne, le 18 juin 2021

pour le Doyen
de la Faculté de biologie et de médecine

Prof. Niko GELDNER
Directeur de l'Ecole Doctorale

Acknowledgments

I would like to thank the members of my PhD committee, Prof. Thierry Calandra, Prof. Matthieu Perreau, Prof. Camilla Jandus and Dr. Jeroen Geurts, for accepting and taking the time to examine my thesis. I would also like to additionally thank my first year and half-thesis committee president, Prof. Matthieu Perreau for the helpful discussions.

I owe my deepest gratitude to my supervisor, Prof. Thierry Roger, for his support all along my PhD. Thierry's door has always been open to discuss about experiments, to give advice, but also to take my opinion into consideration. Finally, Thierry has always helped me to prepare for various oral presentations, directly related to my PhD but also when I tried my hand on scientific mediation during events such as the "Science is wonderful" event and the international Famelab competition. Thanks to his humor and his good mood, the lab was an amazing place to spend four years in.

I would like to thank the head of our service, my co-supervisor, Prof. Thierry Calandra, for his interest, his challenging questions at the lab meetings, and for always having time to converse.

I would like to thank Irene, who happened to not only be a colleague, but also a friend with whom I started this adventure. I would also like to thank Eleonora and Marta, for their great help during my thesis. I would like to express my gratitude to Didier for being always ready to help and for his cheerful mood in all circumstances. I would like to thank all my colleagues that have accompanied me during this PhD: Tytti, Erato and Denho, for these amazing moments we had together inside and outside the lab. I am thankful to all the members of the Service of Infectious Diseases and CLE for their support during these four years and for everything they taught me.

During my PhD, I had the chance to supervise master and lab technician students. I would like to thank all of them.

I would like to thank all the members of the European Sepsis Academy for all the memory our meetings and travels have given me.

I am grateful to all my friends for their mental support and for taking my mind off from my research.

Finally, I am thankful to my family and particularly my parents Bénédicte and Fabien, and my brother Antoine, who have always supported and believed in me.

Summary

Innate immune cells are the first line of defense against infections. A recent breakthrough in immunology has been the description of the acquisition of memory by innate immune cells and their progenitors, a process called “trained immunity”. Trained immunity is induced by microbial or danger signals. Trained innate immune cells show an enhanced response to a secondary hit. Many aspects of trained immunity remain open, particularly in the field of infections. Here, we developed a model of training induced by challenging mice with yeast-derived β-glucans to characterize the impact of trained immunity on infections.

Here we first investigated: 1) the breadth and 2) the persistence of protection conferred by trained immunity. Using a large panel of preclinical models, we show that training protected mice from systemic, peritoneal, gastrointestinal and pulmonary infections induced by *Staphylococcus aureus*, *Listeria monocytogenes*, *Escherichia coli*, *Citrobacter rodentium*, *Pseudomonas aeruginosa and Streptococcus pneumoniae*. Training increased bone marrow myeloid progenitors, blood inflammatory monocytes and neutrophils, peritoneal antimicrobial macrophages, and lung monocytes and neutrophils. Monocytes/macrophages and IL-1 signaling were essential for protecting trained mice from systemic listeriosis. Most of the cellular alterations persisted over time. Accordingly, mice trained 9 weeks earlier were protected from lethal listeriosis. Thus, trained immunity confers broad, long-lasting protection from bacterial infections.

Innate lymphoid cells (ILCs) are tissue-resident cells and important sources of cytokines shaping immune responses. Thus, we explored ILC subpopulations (ILC1/2/3) during pneumococcal pneumoniae. In trained mice, the number of ILCs remained stable, but the proportion of ILCs shifted toward ILC2 involved in tissue repair. Thus, training promotes antimicrobial defense mechanisms and possibly resolution/repair mechanisms following bacterial pneumonia.

ILCs were identified recently. The expression of ILCs in humans suffering from sepsis is not known. Using two cohorts of patients constituted during this thesis, we questioned whether ILCs circulate at different levels in the blood of patients with ventilator-associated pneumoniae (VAP) and Covid-19 pneumonia. ILCs blood counts were not affected upon VAP. On the contrary, ILCs numbers decreased in patients hospitalized with Covid-19, an effect associated with disease severity. Therefore, ILCs may represent biomarkers for Covid-19 but apparently not for VAP sepsis.

Overall, our studies suggest that trained immunity could be used to enhance antimicrobial host defenses, for example by designing new vaccine adjuvants, or targeted to counter-balance the deleterious effects associated with enhanced inflammatory responses. Moreover, ILCs may represent an attractive biomarker for sepsis patients suffering from Covid-19.

Résumé

Les cellules immunitaires innées constituent la première ligne de défense contre les infections. La description de l'acquisition d'une mémoire par les cellules immunitaires innées constitue une percée récente en immunologie. Ce processus est appelé « trained immunity ou immunité entraînée ». L'immunité entraînée est induite par des signaux microbiens ou de danger. Elle fournit des cellules immunitaires innées répondant de manière accrue à un contact ultérieur avec ces mêmes types de signaux. Dans ce travail, nous avons développé un modèle préclinique d'entrainement par injection de paroi de levure à des souris, puis caractérisé l'impact de l'immunité entraînée sur les infections.

Dans un premier temps, nous avons étudié le spectre et la persistance de la protection conférée par l'immunité entraînée. L'entraînement protégeait les souris d'infections systémiques, péritonéales, gastro-intestinales et pulmonaires induites par des bactéries telles Staphylocoque, Listeria, Escherichia coli, Pseudomonas et Streptocoque. L'entraînement augmentait le nombre de cellules souches myéloïdes ainsi que les monocytes et neutrophiles du sang, de la cavité péritonéale et des poumons. Les monocytes et la signalisation induite par l'IL-1 étaient essentiels pour protéger les souris entraînées contre la listériose. La plupart des altérations cellulaires persistaient dans le temps, et les souris entraînées neuf semaines plus tôt étaient protégées contre la listériose. Ainsi, l'immunité entraînée confère une protection large et durable contre les infections bactériennes.

Les cellules lymphoïdes innées (ILCs) sont des cellules résidant dans les tissus et une source importante de cytokines qui façonnent les réponses immunitaires. Nous avons exploré les sous-populations d'ILCs (ILC1/2/3) au cours de la pneumonie à pneumocoque. Chez les souris entraînées, le nombre d'ILCs restait stable mais la proportion des ILC2, qui promeuvent la réparation tissulaire, augmentait chez les souris survivantes. Ainsi, l'entraînement favorise les mécanismes de défense antimicrobienne et peut-être les mécanismes de cicatrisation lors d'une pneumonie bactérienne.

Finalement, nous avons questionné si les ILCs circulent à des niveaux différents dans le sang de patients souffrant de pneumonie associée à la ventilation mécanique (PAVM) et de Covid-19. Le nombre d'ILCs n'était pas affecté par la PAVM. Au contraire, le nombre d'ILCs diminuait drastiquement chez les patients hospitalisés pour Covid-19. Par conséquent, les ILCs peuvent représenter des biomarqueurs pour la septicémie de Covid-19 mais pas pour la PVA.

Globalement, notre étude suggère que l'immunité entraînée pourrait être utilisée pour renforcer les défenses antimicrobiennes de l'hôte, par exemple en concevant de nouveaux adjuvants vaccinaux, ou en ciblant des inhibiteurs pour contrebalancer les effets délétères associés à l'inflammation. En outre, les ILCs pourraient servir de biomarqueur pour les patients atteints de Covid-19.

Résumé destiné à un large public

Le système immunitaire est un système de défense qui nous protège notamment contre les infections. Il est divisé en deux parties: 1) le système immunitaire inné composé de globules blancs qui reconnaissent de manière non-spécifique toutes sortes de microbes, et 2) le système immunitaire adaptatif qui génère des lymphocytes mémoires qui réagissent beaucoup plus vite et de manière plus intense lors d'une réinfection avec un même pathogène. Cette capacité de mémorisation est utilisée dans le principe des vaccins qui nous protègent contre les infections.

Le dogme selon lequel la mémoire immunitaire est l'apanage des lymphocytes et du système immunitaire adaptatif a été remis en question récemment. Ainsi, il a été démontré que le système immunitaire innée préalablement exposé à un microbe (le plus souvent un fragment de levure ou le vaccin BCG) fait preuve de mémoire en ce sens qu'il peut augmenter sa réponse lors d'une réinfection par l'intermédiaire de globules blancs appelés monocytes et neutrophiles.

Dans ce projet, nous avons cherché à définir si la mémoire du système immunitaire inné: 1) permet de protéger de toute sorte d'infections, et 2) persiste dans le temps. Nous rapportons en utilisant des modèles précliniques utilisant la souris que le développement de mémoire immunitaire innée protège les souris contre un grand nombre d'infections incluant la septicémie, péritonite, gastro-entérite et pneumonie. Par ailleurs la protection est durable au cours du temps.

Les cellules lymphoïdes innées (ILCs) sont des cellules découvertes récemment. Elles résident dans les tissus et sont une source importante de molécules solubles qui façonnent les réponses immunitaires (*i.e.* des cytokines, qui s'apparentent à des *hormones* du système immunitaire). Vu ces caractéristiques, nous avons exploré l'expression des ILCs au cours de la pneumonie à pneumocoque en relation avec l'instauration de la mémoire du système immunitaire inné. Nos résultats suggèrent que les ILCs ne sont pas affectées de par leur nombre mais possiblement de par leur fonction lors de l'acquisition de la mémoire innée, favorisant les mécanismes de défense antimicrobienne et peut-être les mécanismes de cicatrisation après une pneumonie bactérienne.

Pour terminer, nous avons questionné si les ILCs présentes dans le sang sont affectées chez les patients souffrant de pneumonie à bactérie associée à la ventilation mécanique ou de pneumonie à virus, en l'occurrence de Covid-19. Le nombre des ILCs diminuait drastiquement chez les patients hospitalisés pour Covid-19 mais pas chez les patients souffrant de pneumonie bactérienne, suggérant que les ILCs pourraient être utilisées pour estimer la sévérité de la Covid-19.

Globalement, ces travaux suggèrent que la mémoire de l'immunité innée pourrait être utilisée pour renforcer les défenses antimicrobiennes de l'hôte, par exemple en concevant de nouveaux types de vaccins. En outre, les ILCs pourraient servir de marqueur pour les patients atteints de Covid-19.

List of abbreviations

Ac	Acetyl
AHR	Aryl hydrocarbon receptor
AIDS	Acquired immunodeficiency syndrome
AnxA1	Annexin A1
AREG	Amphiregulin
Arg1	Arginase 1
ATP	Adenosine triphosphate
BCL11B	B-cell lymphoma/leukemia 11B
BCG	Bacillus Calmette–Guérin
BrdU	Bromodeoxyuridine
C3aR and C5aR	C3a and C5a receptors
C. albicans	Candida albicans
CARD	Caspase activation and recruitment domains
cAMP	Cyclic adenosine monophosphate
CCR6	C-C chemokine receptor type 6
C. difficile	*Clostridium difficile*
CDS	Cytosolic DNA sensor
cDC	Conventional DC
CD127	IL-7 receptor subunit
CHILP	Common helper innate lymphoid precursor
CLR	C-type lectin receptor
CLP	Common lymphoid progenitor
CO	Carbon monoxide
C. neoformans	*Cryptococcus neoformans*
COPD	Chronic obstructive pulmonary disease
CpG-ODN	CpG oligodeoxynucleotide
C. rodentium	*Citrobacter rodentium*
CREB	cAMP response element-binding
CRTH2	PGD2 receptor
DAMP	Danger-associated molecular pattern
DC	Dendritic cell
DC-SIGN	Dendritic Cell-Specific Intercellular adhesion molecule-3-Grabbing Non-integrin
dsRNA	Double-stranded RNA
E. coli	*Escherichia coli*
EET	Eosinophil extracellular trap
EGF	Epidermal growth factor
EILP	Early ILC precursor
Eomes	Eomesodermin
GATA-3	Gata binding protein 3
GBS	Group B streptococci
GFi-1	Transcription factor Growth factor independence 1
GMP	Granulocytes monocyte progenitors
FGF	Fibroblast growth factor
Flt3	Fms-like tyrosine kinase 3

H2S	Hydrogen sulfide
H3K4me	Methylation of histone 3 at lysine 4
H3K27/18ac	Acethylation of histone 3 at lysine 27 or 18
HCMV	Human cytomegalovirus
HIF-1α	Hypoxia-inducible factor 1-α;
HIV	Human immunodeficiency viruses
H. hepaticus	*Helicobacter hepaticus*
HMGB1	High–mobility group box 1
H. polygyrus	*Heligmosomoides polygyrus*
HSC	Hematopoietic stem cell
IBD	Inflammatory bowel disease
ICAM	Intracellular adhesion molecule
ICOS	Inducible T cell co-stimulator
ICOSL	ICOS ligand
ID2	Inhibitor of DNA binding 2
iE-DAP	Gamma-D-meso-diaminopimelic acid
IEL	Intraepithelial
IFN	Interferon
ILC	Innate lymphoid cell
ILCP	ILC progenitor
ILCreg	regulatory ILC
i.d.	Intradermally
i.n.	Intranasally
lncRNA	Long non-coding RNA
iNOS	Inducible nitric oxide synthase
i.p.	Intraperitoneally
IRF	Interferon regulatory factor
IRAK	Interleukin-1 receptor-associated kinase 1
i.t.	Intratracheally
i.v.	Intravenously
KDM5	Lysine demethylase 5
KLRG1	Killer cell lectin-like receptor subfamily G member
L. monocytogenes	*Listeria monocytogenes*
LGP2	Laboratory of genetics and physiology 2
LN	Lymph node
LRRC33	Leucine-rich repeat-containing protein 33
LPS	Lipopolysaccharide
L. sigmodontis	*Litomosoides sigmodontis*
LTA	Lipotechoic acid
LT-HSC	Long-term HSC
LTi	Lymphoid tissue-inducer cell
LTiP	LTi precursor
M. bovis	*Mycobacterium bovis*
M1 macrophage	Classically activated macrophage
M2 macrophage	Alternatively activated macrophage
MAMP	Microbial-associated molecular pattern
MAC	Membrane attack complex
MAPK	Mitogen-activated protein kinases
MCMV	Murine cytomegalovirus

MDA5	Melanoma differentiation-associated protein 5
MDSC	Myeloid derived suppressor cell
MDP	Muramyl dipeptide
Me	Methyl
MHC	Major histocompatibility
MHC-I	Class I MHC
MHC-II	Class II MHC
MINCLE	Macrophage inducible Ca2+-dependent lectin receptor
MIP-1α	Macrophage inflammatory protein-1α
miRNA	MicroRNA
MMTV	Mouse mammary tumor virus
M. leprae	*Mycobacterium leprae*
MoDC	Monocyte-derived DCs
MPLA	Monophosphoryl lipid A
mTOR	Mechanistic target of rapamycin
M. tuberculosis	*Mycobacterium tuberculosis*
mTOR	Mechanistic target of rapamycin
NAIP5	Neuronal apoptosis inhibitory protein 5
N. brasiliensis	*Nippostrongylus brasiliensis*
NCR	Natural cytotoxicity receptor
NET	Neutrophil extracellular trap
NF-κB	Nuclear factor-kappa B
NFIL3	Nuclear factor interleukin-3 regulated
NK cell	Natural killer cell
NLR	NOD-like receptor
NLRC4	NLR-CARD domain-containing 4
NLRP3	NLR family primary domain containing 3
NOD	Nucleotide oligomerization domain
NMUR1	Neuromedin-U receptor 1
NRP1	Neuropilin-1
Ox-LDL	Oxidized low-density lipoprotein
OxPHOS	Oxidative phosphorylation
PB	Peripheral blood
P. berghei	*Plasmodium berghei*
PLZF	Promyelocytic leukemia zinc finger
PRR	Pattern recognition receptor
PD-1	Programmed cell death protein 1
PD-L1	PD-1 ligand
pDC	Plasmacytoid DC
PDGF	Platelet-derived growth factor
PGD2	Prostaglandin D_2
rRNA	Ribosomal RNA
RLR	RIG-I like receptor
RIG-I	Retinoic acid-inducible gene I
RNS	Reactive nitrogen species
ROS	Reactive oxygen species
RORγt	Retinoid-related orphan receptor γt
RSV	Respiratory syncytial virus

S. aureus	*Staphylococcus aureus*
Sca-1	Stem cells antigen-1
s.c.	Subcutaneously
S. mansoni	*Schistosoma mansoni*
S. pneumoniae	*Streptococcus pneumoniae*
SPM	Specialized pro-resolving mediators
Syk	Spleen tyrosine kinase
S. enterica Typhimurium	*Salmonella enterica serovar* Typhimurium
ST2	Suppression of tumorigenicity 2 = IL-1 receptor-like 1
ST-HSC	Short-term HSC
ssRNA	Single-stranded RNA
Syk	Spleen tyrosine kinase
TCA	Tricarboxylic acid
TCF-1	T cell factor 1
TGF	Transforming growth factor
T. gondii	*Toxoplasma gondii*
Th2	Type 2 T helper cell
T. muris	*Trichuris muris*
TNF	Tumor necrosis factor
TLR	Toll-like receptor
TPA	12-O-tetradecanoylphorbol 13-acetate
Treg	T regulatory cell
T_{RM}	Tissue-resident memory cell
TRAIL	Tumor necrosis ligand superfamily member 10
TRAF-6	Tumor necrosis factor receptor-associated factor 6
TOX	Thymocyte selection-associated high-mobility group box protein
TSLP	Thymic stromal lymphopoietin
VCAM	Vascular cell adhesion molecule
VEGF	Vascular endothelial growth factor
VSV	Vesicular stomatitis virus
Y. enterocolitica	*Yersinia enterocolitica*

List of figures

List of tables

TABLE OF CONTENTS

1. INTRODUCTION

1.1. Innate immunity

The immune system is a host defense system that protects against infection. It is divided into two parts: the innate immune system and the adaptive immune system [1]. These two parts have been for a long time oppositely described as follows: the innate immune system is present in, all alive organisms, with an immediate and broad specificity response and no memory, while the adaptive immune system is absent from lower organisms, has a higher and fine specificity response, with a memory. However, recent findings are beginning to reconsider this dichotomy. Indeed, innate and adaptive immunity exhibit a range of interactions that is more complex than what was initially thought. In this section, we will focus on the innate immune response.

1.1.1. Inflammatory response during lung infection

The air we inhale carry microorganisms, which can cause respiratory infections like pneumonia. To prevent this, microorganisms have to be quickly eliminated by the immune system, through a process involving an inflammatory response (***Figure 1***). At the tissue level, inflammation is characterized by redness, swelling, pain and warmth at the site of infection, characteristic of a vasodilatation which purpose is to facilitate leukocyte extravasation [2]. The first line of defense during lung infection are the epithelial cells, which are composed of four main types: the ciliated cells, the goblet cells, the club cells and the basal cells [3]. They provide a physical barrier to pathogen invasion and secrete mucus to trap and to facilitate pathogen's expulsion. When a pathogen breaches the first line of defense, pattern recognition receptors (PRRs) on resident cells, also called sensor cells, recognize microbial-associated molecular patterns (MAMPs) and danger-associated molecular patterns (DAMPs) released by injured, dying cells or foreign agents (like bacteria or viruses) (***Figure 1***) [4, 5]. The expression of different PRRs at the cell surface allows to sense the broadest possible range of signals, as detailed in ***Table 1*** [6, 7]. Among those PRRs are the families of Toll-like receptors (TLRs), C-type lectin receptors (CLRs), NOD-like receptors (NLRs), RIG-I like receptors (RLRs)/DExD/H-box helicases RNA sensors, and cytosolic DNA sensors (CDSs). When PRRs bind their ligands, it triggers intracellular signaling pathways that culminate in the activation of the NF-κB (nuclear factor-kappa B), MAPK (mitogen-activated protein kinases) and IRF (interferon regulatory factors) pathways. It also enhances the activation of the receptor-related multiprotein complex called inflammasome (among which the best known are NLRC4 (NLR-CARD domain-containing 4) and NLRP3 (NLR family primary domain containing 3) [8]. These activations result in the production of the first-order mediators (a classification proposed by Akiko Iwasaki et al. [9]) among which cytokines (e.g. IL-1β, IL-6 and tumor necrosis factor-TNF) and chemokines (e.g. CXCR1, CXCL8 and CCL2).

Among sensor cells, monocytes and macrophages serve as key sentinels of lungs. Macrophages are primarily self-sustained resident macrophages that derive from fetal liver progenitors [10]. Later on, they differentiate in the lungs, into bronchial macrophages, alveolar macrophages [11] and interstitial macrophages [12]. In parallel to the concept of T-helper (Th) cell polarization [13], two phenotypes of alveolar macrophages have been proposed: classically activated macrophage (M1 macrophage) and alternatively activated macrophage (M2 macrophage). M1 macrophages, as type 1 Th cells, respond to inflammatory microbial factors and Th1 pro-inflammatory cytokines (LPS, interferon (IFN)γ, TNF). They display inflammatory activities, engulf and kill invading microorganisms through phagocytosis, and enhance recruitment of immune cells into the lungs [2]. M2 macrophages, as Th2 cells, are induced by Th2/anti-inflammatory cytokines (IL-4, TGF (transforming growth factor)-β) to undergo phagocytosis of apoptotic cells, resolution of inflammation and repair of tissue damage [14-16].

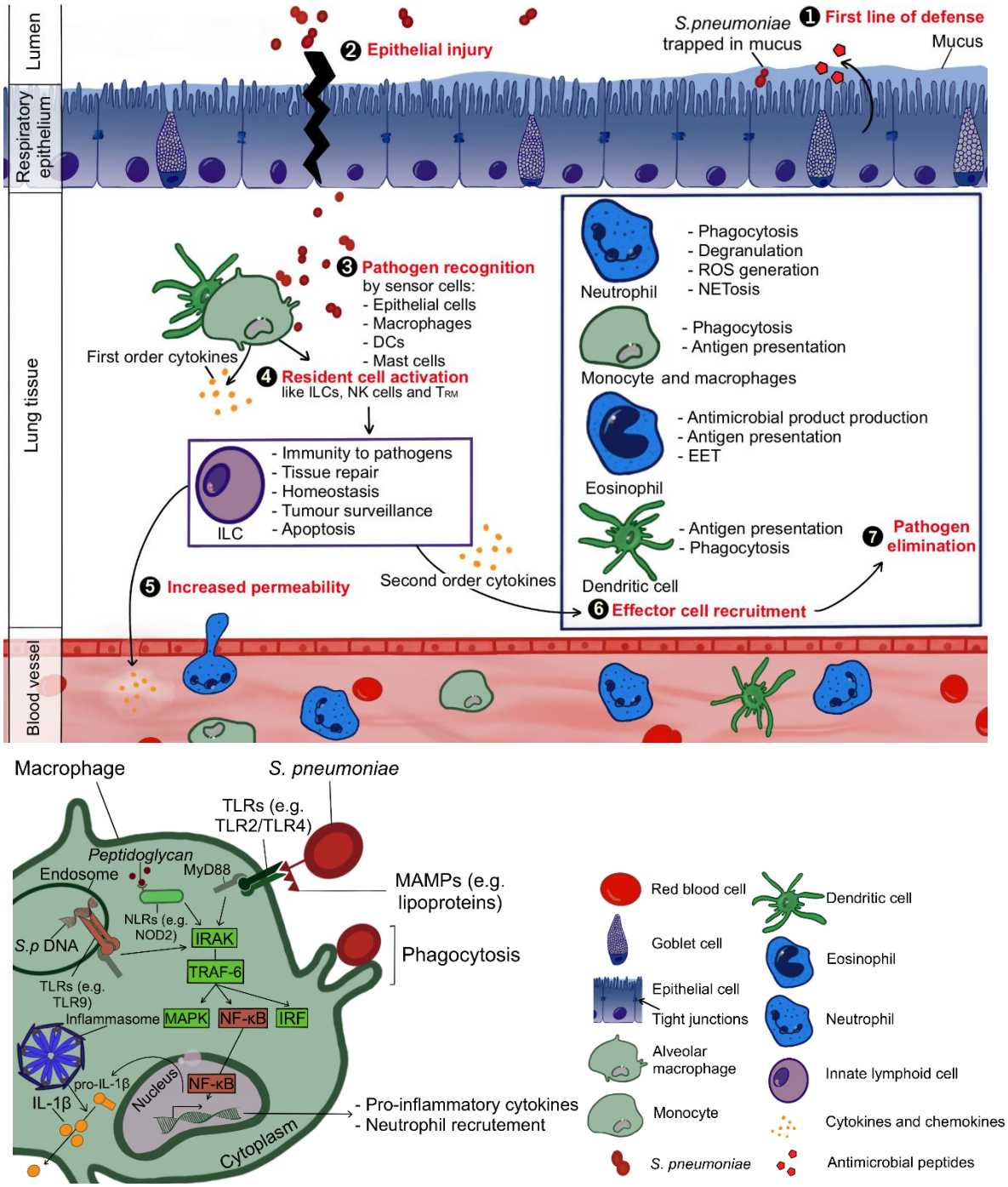

Figure 1*:* Inflammatory response in the lungs

Top) Epithelial cells form a physical barrier against microorganisms. Epithelial cells produce mucus that traps pathogens and facilitates expulsion. Epithelial cell injury is recognized by sensor cells that produce first order cytokines to activate resident cells. Resident cells produce second order cytokines that enhance permeability, and recruitment and activation of effector cells [9]. **Bottom)** PRRs like TLR2/TLR4 recognize MAMPs such as lipoprotein on the surface of *S. pneumoniae*. DNA of *S. pneumoniae* can be recognized by TLR9 and CDSs. These interactions activate the NF-κB, MAPK and IRF pathways, enhancing production of pro-inflammatory cytokines and neutrophil recruitment.

DC: dendritic cells; EET: eosinophil extracellular trap; ILCs: innate lymphoid cells; IRAK: interleukin-1 receptor-associated kinase 1; IRF: interferon regulatory factors; MAMP: microbial-associated molecular pattern; MAPK: mitogen-associated protein kinase; NLR: NOD-like receptor; NK cell: natural killer cell; NF-κB: nuclear factor-kappa B; ROS: reactive oxygen species; T_{RM}: tissue resident memory cell; TLR: toll-like receptor; TRAF-6: tumor necrosis factor receptor (TNFR)-associated factor-6.

Lung-resident dendritic cells (DCs) are recruited from the bone marrow and remain in an immature state in the lungs, until they capture an antigen and undergo a maturation process [17, 18]. There are multiple DC subsets in the lungs: conventional DCs (cDCs), plasmacytoid DCs (pDCs) and monocyte-derived DCs (moDCs) [17]. They have a central role in orchestrating both innate and adaptive immune responses, which major function is antigen presentation [19]. Indeed, the DCs primary role is to capture antigen through several pathways such as micropinocytosis, endocytosis and phagocytosis. They subsequently migrate to secondary lymphoid organs, where they present antigen to naive T cells, thereby initiating adaptive immune responses [20-22]. This migration can be modulated by complement subcomponents. The complement system is a set of plasma and cell surface proteins triggered through different routes (classical, lectin or alternative), that aid antibodies and phagocytes to clear invading pathogens (through opsonization), promote inflammation (through anaphylatoxins), and lyse pathogen (through the membrane attack complex (MAC)) [2, 23, 24].

Production of the first-order cytokines induces the activation of resident cells such as innate lymphoid cells (ILCs), natural killer (NK) cells and tissue-resident memory cells (T_{RM}) [9]. ILCs, which will be more described in the section 1.2, are tissue-resident cells that are locally renewed and expended in inflammatory conditions. They are important producers of cytokines after a rapid stimulation by surrounding sensor cells. They have an important role in maintaining tissue homeostasis within the lungs, and provide an initial response to pathogen challenge. NK cells, member of the ILC family, are rapidly recruited from the bone marrow to the lungs [25] where they recognize and bind infected host cells to induce their apoptosis through the secretion of perforin and granzyme B [19, 26, 27].

The activation of these resident cells enhances the production of second-order cytokine, leading to increased permeability and recruitment of effector cells such as monocytes, neutrophils and eosinophils [9, 28, 29]. Monocytes are recruited to the lungs in response to CCL2 and CCL7 where they can differentiate into macrophages [30]. Monocytes/macrophages initiate phagocytosis and antigen presentation. Indeed, microbial fragments remaining from phagocytosis can be presented to T lymphocytes through a complex of proteins expressed on the cell surface called major histocompatibility complex (MHC) [19]. MHC are glycoproteins that bind antigenic peptide fragments of proteins that have been synthesized within the cell (class I MHC or MHC-I) or that have been ingested by phagocytes and proteolytically process (class II MHC or MHC-II). Once in lungs, monocytes can differentiate into DCs [31]. DCs are the most adapted cells to present antigen to activated naïve T cells in the lymph nodes, making them crucial for the initiation of adaptive immune responses [20].

TNF and IL-6 produced by monocytes enhance acute phase response and recruitment of neutrophils to the lungs [32, 33]. Neutrophils contribute to pathogen eradication through phagocytosis, degranulation of toxic molecules, reactive oxygen and nitrogen species (ROS, RNS) generation and NETosis. NETosis reflects the release of neutrophil extracellular traps (NET), which are composed of chromatin scaffolds containing histones. NETs contain antimicrobial peptides and enzymes that immobilize and kill pathogens [34]. Neutrophils influence the activity and migration of other immune cells through the production of cytokines (IL-1, IL-12, IL-17, IL-23, IL-27, TGF-β) and chemokines (CCL2, CCL20, CXCL10) [19]. IL-5 is a cytokine involved in the expansion and mobilization of eosinophils into the lungs [35, 36]. This eosinophil migration is suggested to be induced by ILC2 and Th2 cells, two important producers of IL-5 [37, 38]. DCs are also acknowledged in eosinophils recruitment in lungs during allergen challenge [39]. Eosinophils possess antimicrobial properties against a broad range of pathogens. Indeed, eosinophils release cytotoxic secondary granules, cytokines (TGF-β, TGF-α), growth factors (epidermal growth factor (EGF), fibroblast growth factor (FGF), platelet-derived growth factor (PDGF), vascular endothelial growth factor (VEGF)), ROS and other mediators associated with host defense and tissue repair.

Table 1: PRRs and their ligands

PRRs	Localization	MAMPs/DAMPs	Origin of the ligand
TLR			
TLR1	Plasma membrane	Triacyl lipoprotein	Bacteria
TLR2	Plasma membrane	Lipoprotein, peptidoglycan, LTA and β-glucans	Bacteria, viruses, parasites, fungi and self
TLR3	Endolysosome	dsRNA	Viruses
TLR4	Plasma membrane	LPS, RSV and MMTV fusion protein, mannan, and glycol-inositolphosphate from *Trypanosoma* spp.	Gram-negative bacteria, viruses, self
TLR5	Plasma membrane	Flagellin	Bacteria
TLR6	Plasma membrane	Diacyl lipoprotein, LTA and β-glucans	Bacteria, viruses and fungi
TLR7	Endolysosome	ssRNA and short dsRNA	Viruses, bacteria, self
TLR8	Endolysosome	ssRNA, short dsRNA and bacterial RNA	Viruses, bacteria
TLR9	Endolysosome	CpG-ODN and hemozoin from *Plasmodium* spp.	Viruses, bacteria, protozoan parasites, fungi and self
TLR10	Endolysosome	Unknown	Unknown
TLR11	Plasma membrane	Profilin-like molecule, and flagellin	Apicomplexan parasites and bacteria
TLR12	Endolysosome	Profilin	Apicomplexan parasites
TLR13	Endolysosome	Bacterial rRNA	Gram-negative and gram-positive bacteria
RLR			
RIG-I	Cytoplasm	Short dsRNA, 5'triphosphate dsRNA	RNA and DNA viruses, bacteria
MDA5	Cytoplasm	Long dsRNA	RNA viruses, bacteria
LGP2	Cytoplasm	dsRNA	RNA viruses
NLR			
NOD1	Cytoplasm	iE-DAP	Bacteria
NOD2	Cytoplasm	MDP	Bacteria
NAIP5	Cytoplasm	Flagellin	Bacteria
NLRC4	Cytoplasm	Flagellin	Bacteria
NLRP3	Cytoplasm	ATP, crystals, pore forming toxins, K+ efflux, Ca2+ mobilization, cathepsin, ROS	Bacteria, viruses, self
CLR			
DC-SIGN	Plasma membrane	Mannose, Mannan	HIV, fungi
Dectin-1	Plasma membrane	β-glucans	Fungi, mycobacteria
Dectin-2	Plasma membrane	α-mannans, glycoproteins	Fungi, mycobacteria
MINCLE	Plasma membrane	α-mannans	Self, fungi, mycobacteria

ATP: adenosine triphosphate; CARD: caspase activation and recruitment domains; CLR: C-type lectin receptor; CpG ODN: CpG oligodeoxynucleotide; DAMP: danger-associated molecular pattern; DC-SIGN: dendritic cell-specific intercellular adhesion molecule-3-grabbing non-integrin; dsRNA: double-stranded RNA; iE-DAP: gamma-D-glutanyl-meso-diaminopimelic acid; LPS: lipopolysaccharide; LTA: lipotechoic acid; LGP2: Laboratory of Genetics and Physiology 2; MAMP: microbial-associated molecular pattern; MMTV: mouse mammary tumor virus; MDP: muramyl dipeptide; MINCLE: macrophage inducible Ca2+-dependent lectin receptor; MDA5: melanoma differentiation-associated protein 5; NLR: NOD-like receptor; NOD: nucleotide oligomerization domain; NAIP5: neuronal apoptosis inhibitory protein 5; NLRP3: NLR family primary domain containing 3; NLRC4: NLR-CARD domain-containing 4; PRR: pathogen recognition receptor; rRNA: ribosomal RNA; RSV: respiratory syncytial virus; RIG-I: retinoic acid-inducible gene I; RLR: RIG-I receptor; ROS: reactive oxygen species; TLR: Toll-like receptor; ssRNA: single-stranded RNA.

Like DCs and macrophages, eosinophils can present antigen thanks to the expression of MHC-II molecules and co-stimulatory receptors (e.g. CD80, CD86 and CD40L3). Furthermore, like neutrophils, eosinophils display antibacterial activity that involves the release of cytotoxic proteins such as major basic protein (MBP-1) and of eosinophil extracellular traps (EET) made of mitochondrial DNA-containing bactericidal trap [19, 40, 41]. Tissue injury and infection activate the coagulation cascade [28], initiate local clotting, decrease the activity of anticoagulant mechanisms and impair fibrinolytic system. These events prevent blood loss and entry of infectious microorganisms into the blood stream [2, 42, 43]. During the immune response to respiratory pathogens, primed, activated T cells migrate to the lungs where they persist as tissue resident T cells (T_{RM}) mediating optimal protective to a secondary challenge [44]. The role of adaptive immunity will not be developed further.

1.1.2. Resolution of inflammation

An uncontrolled or unresolved inflammation can lead to tissue damage, sepsis and chronic inflammation diseases like allergic asthma, psoriasis or Crohn's diseases [45-47]. Thus, the inflammatory response must be resolved to promote tissue repair and restore homeostasis. This process called resolution phase or resolution of inflammation (***Figure 2***) is initiated shortly after the beginning of the inflammatory response [48].

During initiation of inflammation, leukocytes traffic from bloodstream to the site of infection, forming the inflammatory exudate. This exudate contains key players of the resolution phase, the families of specialized pro-resolving mediators (SPMs) and include lipid mediators (lipoxins, resolvins, protectins and maresins), proteins and peptides (like annexin A1 (AnxA1), adrenocorticotropic hormone, chemerin peptides and galectin-1), gaseous mediators (hydrogen sulfilde (H_2S) and carbon monoxide (CO)), a purine (adenosine), and neuromodulators (acetylcholine and other neuropeptides) [46, 49]. These SPMs enhance the shutdown of neutrophil recruitment through a phenomenon called lipid mediator class switching. SPMs also reduce vascular permeability, promote apoptosis, activate clearance of apoptotic cells and play a role in macrophage reprogramming [48, 50-52]. All these events prevent excessive inflammation.

Once neutrophils influx ends, the remained neutrophils are trapped in the exudate and generate membrane-borne microvesicles called microparticles or ectosomes that inhibit the inflammatory response of macrophages [53]. These apoptotic neutrophils then attract macrophages to induce their clearance by efferocytosis [54]. This uptake reprograms macrophages from a pro-inflammatory (M1) to an anti-inflammatory (M2) phenotype characterized by the release of IL-1 receptor antagonist (IL-1RA), IL-10, TGF-β and VEGF [55, 56], promoting cell proliferation, tissue regeneration and wound repair [46, 50, 57]. Tissue repair and reestablishment of tissue functionality require tight interactions between macrophages, stem cells, progenitor cells and stromal cells [58]. After resolution, macrophages migrate to the draining lymph node where they present antigens from the inflamed tissue [59, 60]. Overall, inflammatory cells are eliminated from the site of inflammation through migration into the systemic circulation, lymphatic drainage or cell death (autophagy, NETosis, and caspase-mediated apoptosis) [61].

NF-κB plays a crucial role driving the inflammatory response. This signaling pathway can be inhibited through different processes. For example, the transmembrane molecule leucine-rich repeat-containing protein 33 (LRRC33) negatively regulates TLR signaling and subsequent NF-κB activation [62]. Additionally, micro RNAs (miR-126, miR-146a/b, miR-200b/c), long non-coding RNAs (lncRNA-Cox2, Morrbid, PACER, Lethe, NRON) induced during the immune response act as negative modulators of NF-κB signaling [63, 64]. More recently, myeloid-derived suppressor cells (MDSCs) [65, 66] and T regulatory cells (Tregs) [67] have emerged as important players of the resolution phase, linking innate and adaptive immune systems. MDSCs are immature myeloid cells characterized by their

immunosuppressive functions. Depletion of MDSCs increased the production of pro-inflammatory cytokines [68], showing the important role of MDSCs in the resolution of inflammation. Tregs are IL-10 producing T cells that regulate or suppress other immune cells. Tregs are essential for maintaining peripheral tolerance, suppressing sterilizing immunity, limiting antitumor immunity. Tregs promote repair and regeneration of various organ systems by controlling neutrophils and macrophages functions [69]. During infection, the barrier integrity of the airway epithelium can be damaged, leading to release of alarmins such as IL-33. ILC2 respond rapidly to IL-33 by producing TSLP (thymic stromal lymphopoietin) and IL-25, thus initiating epithelial cell repair and lung tissue homeostasis [70].

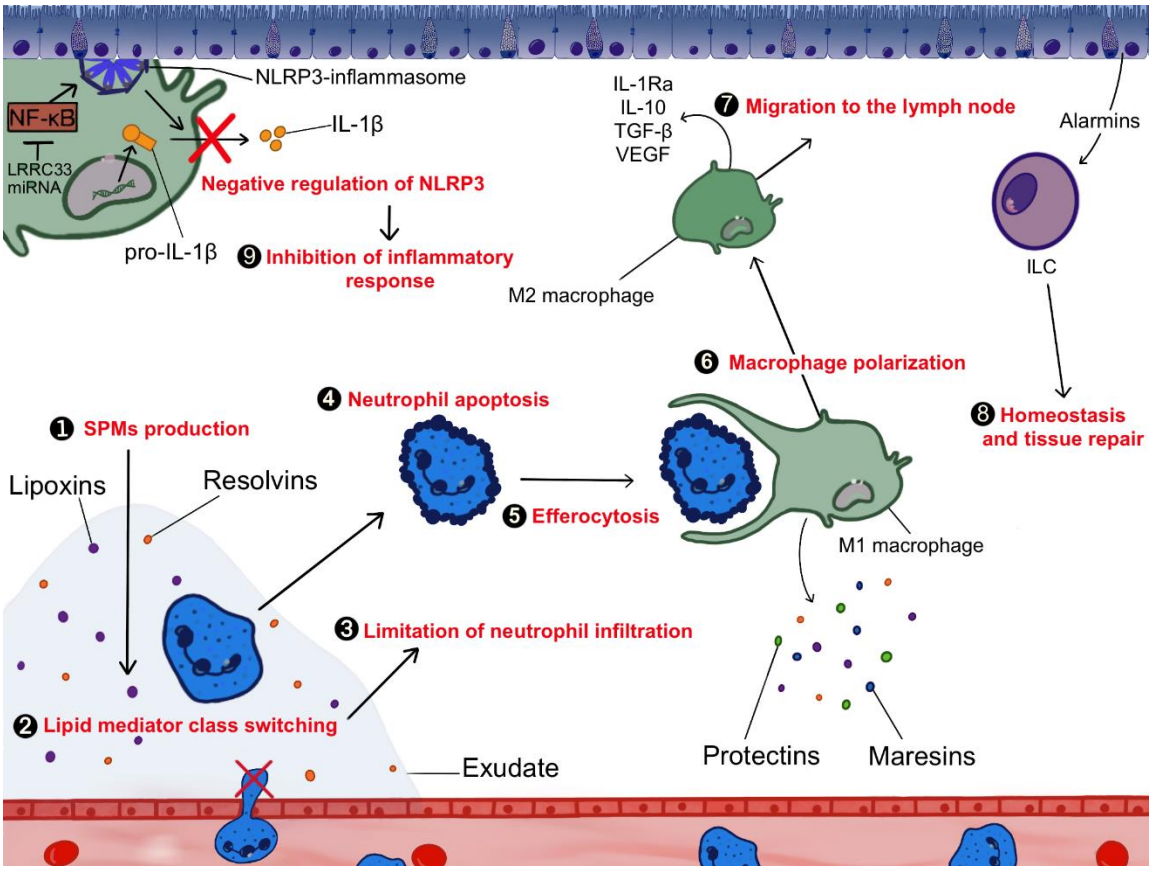

Figure 2: **Resolution of inflammation**

The inflammatory exudate is formed when leukocytes travel from the bloodstream to the site of infection. This exudate accumulates pro-resolving mediators called SPMs and lipid mediators such as lipoxins, resolvins, protectins and maresins. Lipid mediator class switching enhances the shutdown of neutrophils and other leukocytes recruitment. Apoptotic immune cells are eliminated by efferocytosis by M1 macrophages. M1 macrophages are reprogrammed into M2 macrophages, migrate to draining lymph node and present antigens from the inflamed tissue. Concomitantly, NF-κB pathway is inhibited, reducing inflammatory response. When the barrier integrity of the airway epithelium is damaged, epithelial cells activate ILC2 by producing alarmins, to enhance homeostasis and tissue repair.

ILCs: innate lymphoid cells; LRRC33: leucine-rich repeat-containing protein 33; miRNA: microRNA; M1 macrophage: Classically activated macrophage; NF-κB: nuclear factor-kappa B; NLRP3: NLR family primary domain containing 3; TGF-β: transforming growth factor beta; VEGF: vascular endothelial growth factor.

1.2. Innate lymphoid cells

ILCs have a lymphoid morphology, lack recombination activating gene and do not express cell surface markers associated with myeloid cells, DCs and conventional B and T lymphocytes, which explains why these cells were overlooked up to recently [71]. ILCs are present through the body where they play a role of environmental sensors. ILCs in both lymphoid and non-lymphoid organs are tissue-resident cells, locally renewed, expanded and activated by surrounding cells, in response to acute environmental challenges [72, 73]. Once activated, ILCs produce cytokines that shape innate and adaptive immune responses [74, 75]. Based on the cytokine they produce, the transcription factors and interleukins that regulate their development and functions, ILCs have been subcategorized into three groups: ILC1, ILC2 and ILC3, that mirror $CD4^+$ Th1, Th2 and Th17 cells, and NK cells that mirror $CD8^+$ cytotoxic T cells [27, 76-78] (***Figure 3*** and ***Figure 4***).

1.2.1. Development and regulation of ILCs

ILCs initially develop in the fetal liver and later develop in the adult bone marrow [79, 80]. They arise from common lymphoid precursors (CLPs) [81], which take their origin from hematopoietic stem cells (HSCs) (***Figure 3***). CLP are $CD127^+$ (IL-7 receptor subunit) and $Flt3^+$ (Fms-like tyrosine kinase 3). Under the expression of nuclear factor IL-3 regulated (NFIL3) [82], and thymocyte selection-associated high-mobility group box protein (TOX) [83], the CLP can differentiate into early ILC precursor (EILP) that express the transcription factor T cell factor 1 (TCF-1). This latter give rise to all ILC subsets: ILC1, ILC2, ILC3 and NK cells [84]. The differentiation of common helper innate lymphoid precursors (CHILPs) from EILP depends on inhibitor of DNA binding 2 (ID2) [85]. CHILP have a similar surface phenotype to CLP, but do not express Flt3. CHILPs, under the expression of ID2, TOX and RORγt (Retinoid-related orphan receptor γt) gives rise to the lymphoid tissue inducer precursor (LTiP), that can differentiate into lymphoid tissue inducer (LTi) under the expression of AHR (aryl hydrocarbon receptor) and RORγt [86]. LTi are also described as ILC3 $CCR6^+$ [87]. CHILP give rise to ILC progenitors (ILCPs), which are $CD127^+$ and $PD\text{-}1^+$ (programmed cell death protein 1) [88], through the expression of promyelocytic leukemia zinc finger (PLZF) and ID2 [73, 89]. However, ILCs can develop also in the absence of CD127 [90, 91]. Transcription factors such as TCF-1, ID2, PLZF, NFIL3, TOX, BCL11B (B-cell lymphoma/leukemia 11B), GFi1 (transcription factor growth factor independence 1), AHR, RORγt and GATA-3 are key elements for ILC fate commitment leading to ILC1, ILC2 and ILC3. A more recent study used CRISPR/Cas9-generated combinatorial reporter approach to study ILC development in fetal liver and adult bone marrow, confirmed the key role of GATA3 and RORγt and reported distinct origins of ILC and LTi lineages [92]. For now, it remains unclear whether ILCPs infiltrate peripheral tissues during development and differentiate locally to commit to ILC lineages. However, IL-33 signaling negatively regulates CXCR4 expression to promote ILC2 progenitors exit from the bone marrow [93]. In addition, allergic airway inflammation induced by the fungal allergen *Alternaria alternata* drives the egress of ILC2 progenitors from the bone marrow [93].

ILC1 development is strictly dependent on T-bet, on the contrary, to NK cells that rely on both T-bet and Eomes (***Figure 3***). ILC1 respond to IL-12, IL-15 and IL-18 and produce IFNγ and TNF (***Figure 4***) [76, 94]. The development of ILC2 depends on GATA-3, Gfi1 and BCL11B (***Figure 3***). They respond to IL-25, IL-33, prostaglandin D_2 (PGD2) and TSLP, constitutively express GATA-3 and produce IL-4, IL-5, IL-9, IL-13, arginase 1 (Arg1) and amphiregulin (AREG) (***Figure 4***) [76]. ILC3 are subdivided into three groups: natural cytotoxic receptor negative (NCR^-) and natural cytotoxic receptor positive (NCR^+) cells, according to the expression of natural cytotoxicity receptors (such as NKp46 and NKp44) and LTi cells. Additionally, LTi express CCR6 and/or CD4 and secrete IL-17, IL-22 and lymphotoxin [87]. Their development requires AHR (***Figure 3***). The role of LTi resides mainly in the formation of secondary lymphoid structures, and for this reason, they will not be described further [95]. The ILC3 NCR^- and

NCR^{+} respond to IL-1β, IL-6, and IL-23, constitutively express RORγt, and produce IL-17A and IL-22 (***Figure 4***) [71, 73, 96].

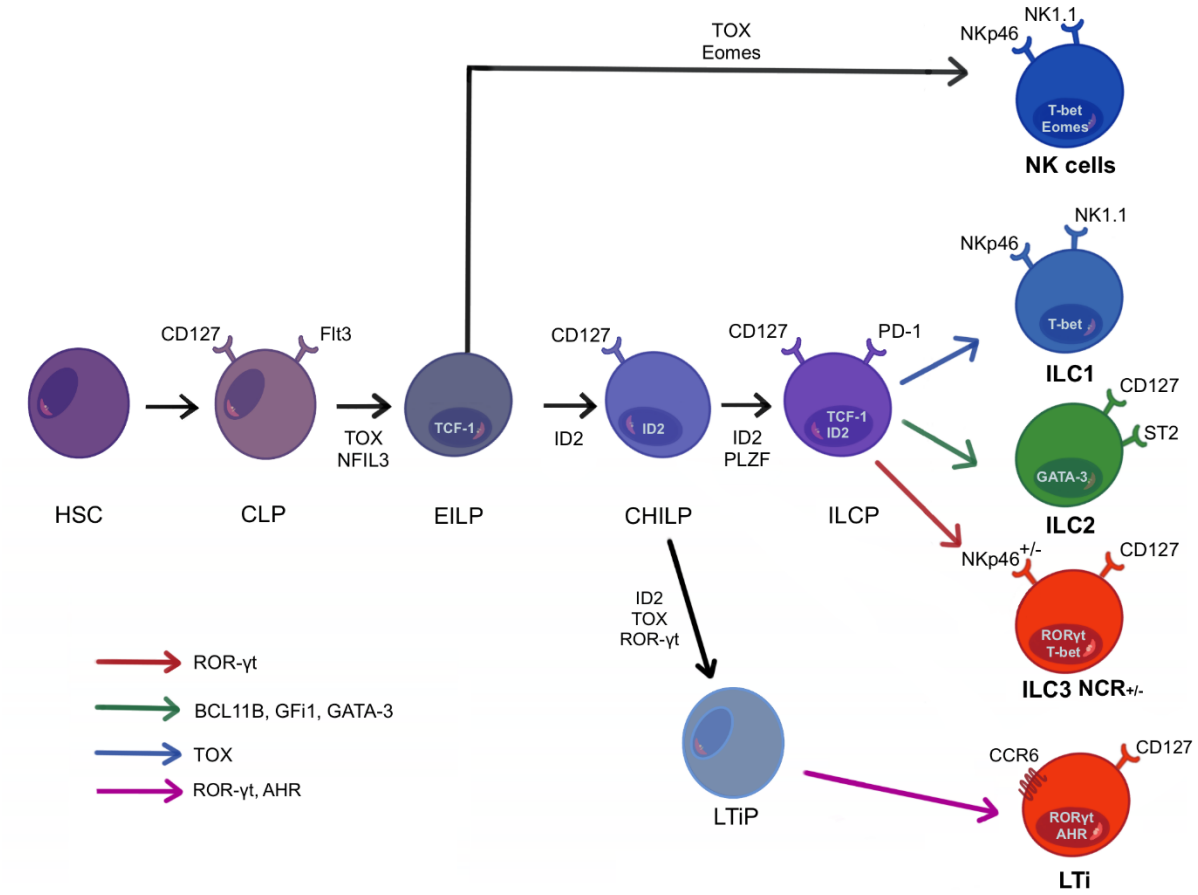

Figure 3: Development of ILCs

ILCs arise from CLP, which arise from HSC. CLP can differentiate into EILP under the expression of TOX and NFIL3. TOX and Eomes expression give rise to NK cells, while ID2 give rise to CHILP. ILC1, ILC2 and ILC3 CCR6- take their origin from ICLP that develop from CHILP, while ILC3 CCR6+ take their origin directly from CHILP. Finally, LTi take their origin from CHILP that differentiate into LTiP.

AHR: aryl hydrocarbon receptor; BCL11B: B-cell lymphoma/leukemia 11B; CD127: IL-7 receptor subunit; CLP: common lymphoid precursors; CHILP: common helper innate lymphoid precursors; EILP: early ILC precursors; Eomes: eomesodermin; FLT3: fms-like tyrosine kinase 3; GATA-3: gata binding protein 3; GFi1: transcription factor growth factor independence 1; HSC: hematopoietic stem cells; ILCP: ILC progenitors; ID2: Inhibitor of DNA binding 2; LTi: lymphoid tissue inducer; LTiP: LTi precursors; NCR: natural cytotoxicity receptor; NFIL3: nuclear factor interleukin-3 regulated; PLZF: promyelocytic leukemia zinc finger; PD-1: programmed cell death 1; RORγt: retinoid-related orphan receptor γt; ST2: suppression of tumorigenicity 2; TOX: high-mobility group box protein; TCF-1: T cell factor 1.

Figure 4: **Regulation of ILCs**
ILC1 respond to IL-12, IL-15 and IL-18 and produce IFNγ and TNF. ILC2 respond to IL-25, IL-33, TSLP and PGD2 and produce IL-4, IL-5, IL-9, IL-13, Arg1 and AREG. ILC3 respond to IL-1β and IL-23 and produce IL-17A and IL-22.

AREG: amphiregulin; Arg1: arginase 1; GATA-3: gata binding protein 3; IFNγ: interferon gamma; PGD2: prostaglandin D2; RORγt: retinoid-related orphan receptor γt; TSLP: thymic stromal lymphopoietin; TNF: tumor necrosis factor.

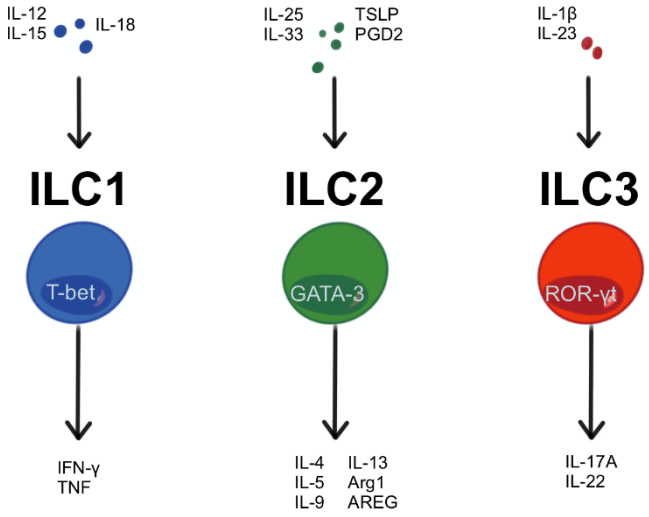

1.2.2. Localization and phenotype of ILCs

ILCPs and all ILCs are defined as lineage (i.e. CD3, CD14, CD16, CD19 and CD20) negative in mouse and human. Furthermore, ILCs are CD3ε$^-$, CD5$^-$, CD8α$^-$, CD11b$^-$, CD11c$^-$, CD19$^-$, B220$^-$, CD49b$^-$, Ter119$^-$, FcεRI$^-$, TCRα/β$^-$, TCRγ/δ$^-$ in mouse [94], and CD1a$^-$, CD3$^-$, CD14$^-$, CD19$^-$, CD34$^-$, CD94$^-$, CD123$^-$, TCRα/β$^-$, TCRγ/δ, NKG2A$^-$ and FcεRI$^-$ in human [97]. It is important to notice that accumulating evidence demonstrate that ILCs are shaped by the microenvironment, reflected by the distinct ILC profiles in different tissues. The different phenotypes will be described in this section.

Murine ILCPs are defined as α4β7$^+$, CD127$^+$, ID2$^+$, PD-1$^+$ and PLZF$^+$, as reviewed in [98] and [99]. This population can differentiate in all ILC subsets [79]. They have been described in bone marrow, liver and small intestine as described in ***Table 2***. Furthermore, ILC2 progenitors, defined as CD45$^+$, IL25R$^+$, CD127$^+$, CXCR4$^+$ cells, have also been described in lungs, and in adults and perinatal bone marrow [93, 100, 101]. In human, ILCPs are defined as CD7$^+$, CD127$^+$, CD117$^+$ cells [102]. They were described in lymph nodes, spleen, tonsils, peripheral and cord blood (***Table 3***).

Murine ILCs are defined as CD45$^+$, CD90.2$^+$ and CD127$^+$ cells [94]. In human, ILCs are defined as CD45$^+$ and CD127$^+$ cells [97]. However, recent studies have shown that CD127 expression is down regulated from the cell surface of activated ILCS [94].

ILC1 are NK1.1$^+$, NKp46$^+$, T-bet$^+$ cells and express CD49a and TRAIL in both humans and mice, but expression of these markers is often lost upon activation and can be tissue-dependent (***Table 4*** and ***Table 5***). ILC1 express C-C chemokine receptor 5, 7 and 9 (CCR5-7), CD62L (L-selectin), CXCR4 and α4β7 that regulate their migration [98, 103]. Murine ILC1 are found in various tissues and organs. In the blood, they represent the most prevalent subset of ILCs, probably representing an immature precursor that will later on differentiate in mature subset in tissues [104]. In both mouse and human, ILC1 are found in the decidua and uterus, where they dominate before puberty and increase during pregnancy, especially during second pregnancies [105-107].

Table 2: Murine ILCP localization and phenotype in organs and tissues

Organs & tissues	CD25	CD117	Flt3	GATA-3	RORγt	Sca-1	ST2	T-bet	Ref.
Bone marrow	-	+	-	n.d.	n.d.	+/-	n.d.	n.d.	[79, 93, 100, 108]
Liver[a]	-	+	-	+	-	+/-	-	-	[79, 80, 100, 108]
Small intestine[a]	-	n.d.	-	n.d.	+	n.d.	n.d.	n.d.	[100, 108]

Flt3: fms-like tyrosine kinase 3; GATA-3: gata binding protein 3; RORγt: retinoid-related orphan γt; Sca-1: Stem cells antigen-1; ST2: suppression of tumorigenicity 2 = IL-1 receptor-like 1; [a]: also detected in fetus.

Table 3: Human ILCP localization and phenotype in organs and tissues

Organs & tissues	CD34	CD45RA	CCR6	GATA-3	IFNγ	IL-1R1	NKp44	NRP-1	PLZF	RORγt	T-bet	Ref.
Cord blood	n.d.	+	-	lo	n.d.	n.d.	-	-	n.d.	-	+	[102]
LN	+	+	n.d.	n.d.	n.d.	+/-	n.d.	n.d.	n.d.	+	n.d.	[109]
PB	n.d.	+	n.d.	+/-	-	+	-	n.d.	+/-	-	-	[102, 110]
Spleen	+	+	n.d.	n.d.	n.d.	+/-	n.d.	n.d.	n.d.	+	n.d.	[109]
Tonsils	+	+	n.d.	n.d.	n.d.	+/-	n.d.	n.d.	n.d.	+	n.d.	[109]

CCR6: C-C chemokine receptor type 6; GATA-3: gata binding protein 3; IFNγ: interferon gamma; LN: lymph nodes; NRP-1: neuropilin-1; PB: peripheral blood; PLZF: promyelocytic leukemia zinc finger; RORγt: retinoid-related orphan γt.

Table 4: Murine ILC1 localization and phenotype in organs and tissues

Organs & tissues	CD16	CD49b	CD61	CD69	CD103	CD127	CD200r1	CXCR6	GATA-3	Ref.
Adipose tissue	n.d.	n.d.	n.d.	n.d.	n.d.	+	n.d.	n.d.	-	[111]
Bone marrow	n.d.	n.d.	n.d.	n.d.	n.d.	+	n.d.	n.d.	-	[100, 111]
Colon	n.d.	n.d.	n.d.	n.d.	n.d.	+	n.d.	n.d.	-	[100]
Decidua, uterus[c]	n.d.	-	n.d.	+	+	+/-	n.d.	+	int	[106, 107, 112, 113]
IEL	n.d.	n.d.	+	n.d.	n.d.	+/-	n.d.	n.d.	-	[79, 114]
Kidney	n.d.	n.d.	n.d.	n.d.	n.d.	+	n.d.	n.d.	-	[115]
Lungs	n.d.	n.d.	n.d.	n.d.	n.d.	+	n.d.	n.d.	-	[100, 116-118]
Liver[a]	+	-	n.d.	+	-	+/-	+	+	-	[79, 100, 107, 108, 111, 119, 120]
LN	n.d.	n.d.	n.d.	n.d.	n.d.	+	n.d.	n.d.	-	[100, 116]
Peyer's patches	n.d.	n.d.	n.d.	n.d.	n.d.	+	n.d.	n.d.	-	[100]
PB*	n.d.	n.d.	n.d.	n.d.	n.d.	-	n.d.	n.d.	-	[104]
Small intestine[a]	n.d.	-	+	+	-	+	+	+/-	-	[72, 100, 108, 111, 114, 116, 121-123]
Salivary gland	+	+	n.d.	+	+/-	+	+	+	-	[72]
Spleen*[b]	n.d.	-	n.d.	+/-	-	+	+	+	-	[100, 108, 116, 124, 125]
Thymus	n.d.	n.d.	n.d.	n.d.	n.d.	+	n.d.	n.d.	-	[100]

GATA-3: gata binding protein 3; IEL: intraepithelial; LN: lymph nodes; n.d.: not determined; PB: peripheral blood; RORγt: retinoid-related orphan γt; TRAIL: tumor necrosis ligand superfamily member 10; *: main ILCs subset; [a]: detected in fetus, [b]: detected in neonates; [c]: detected during pregnancy.

Table 5: Human ILC1 localization and phenotype in organs and tissues

Organs & tissues	CD49a	CD56	CD69	CD103	CD117	CD161	CCR6	Eomes	Nkp44	IFNγ	Ref.
Adipose tissue*	-	+/-	+/-	-	-	n.d.	n.d.	+/-	+/-	n.d.	[111, 116]
Cord blood	n.d.	n.d.	n.d.	n.d.	-	-	n.d.	n.d.	n.d.	n.d.	[126, 127]
Decidua, uterus[c]	-	+/-	+/-	+/-	-	n.d.	n.d.	+/-	+/-	+	[105, 113, 128, 129]
Colon*	n.d.	n.d.	n.d.	n.d.	-	n.d.	n.d.	n.d.	+/-	n.d.	[116]
Heart	n.d.	-	n.d.	n.d.	n.d.	n.d.	n.d.	n.d.	-	n.d.	[130]
Kidney	n.d.	n.d.	n.d.	n.d.	-	+	n.d.	n.d.	-	n.d.	[115]
Liver[a]	+	+	+	n.d.	+/-	n.d.	n.d.	-	+/-	n.d.	[131]
Lungs*	-	+/-	+/-	-	n.d.	n.d.	n.d.	+/-	+/-	n.d.	[116, 132]
LN*	n.d.	n.d.	n.d.	+	-	n.d.	n.d.	n.d.	+/-	n.d.	[116, 133]
PB[c]	-	+/-	+/-	-	-	n.d.	n.d.	+/-	+/-	n.d.	[110, 118, 127, 134]
Small intestine[a]	-	+/-	+/-	+/-	-	+	-	+/-	+/-	n.d.	[114, 116, 131, 133, 135, 136]
Spleen*	-	+/-	+/-	-	-	n.d.	n.d.	+/-	+/-	n.d.	[116, 134]
Skin	n.d.			n.d.	-	n.d.	n.d.	n.d.	n.d.	n.d.	[137]
Tonsils	n.d.	+/-	+/-	+/-	-	+	n.d.	+/-	+/-	n.d.	[97, 102, 114, 131, 133, 135, 138]

LN: lymph nodes; n.d.: not determined; PB: peripheral blood; *: main ILCs subset; [a]: detected in fetus, [b]: detected in neonates; [c]: detected during pregnancy.

In mouse, ILC2 are $ST2^+$ and $GATA\text{-}3^+$ cells (***Table 6***) [94]. ILC2 can be separated into tissue-resident natural ILC2 (nILC2) and transient circulating inflammatory ILC2 (iILC2) [139, 140]. nILC2 are IL-33 responsive, $KLRG1^{int}$, $Arg1^{hi}$, and $CD90^{hi}$. iILC2 are IL-25 responsive, $KLRG1^{hi}$, $Arg1^{lo}$, $CD90^{lo}$ cells and have been found in murine lungs after infections with *Nippostrongylus brasiliensis* or IL-25 administration [139, 140]. nILC2 are tissue-resident cells that are self-renewed and proliferate locally, while iILC2 are migratory cells that travel from the intestine to the lungs [72, 93, 101]. In addition, pulmonary ILC2 are a heterogeneous population, where mouse strain and *in vivo* treatment influence surface marker, i.e. phenotype. Thereby, ILC2 should be defined as a lineage negative cells expressing CD45 and the transcription factor GATA-3 [141]. Lungs, kidneys, small and large intestine, and adipose tissues of mice are composed of, almost exclusively, ILC2 subset [115, 116]. ILC2 are a relatively rare population, comprising 2-3 x 10^4 cells in the lungs of naïve mouse, representing 0.4-1% of total leukocytes [142]. Contrary to human, ILC2 could not be found in mouse decidual tissues. Few ILC2 could be detected in uterus [112, 143].

In human, ILC2 are $CD127^+$, $CD161^+$, $ST2^+$ and $CRTH2^+$ cells (***Table 7***) [144, 145]. The presence of ILC2 in decidual tissues is debated and may depend on the gestation phase. Indeed, during gestation, decidual ILC2 increase gradually (reaching up to ~80% of ILCs), and become the major ILC subset during the third trimester [129]. Finally, ILC2 predominate in ischemic cardiomyopathy and myocarditis of human heart, representing ~65% of ILCs [130].

In both human and mouse ILC3 are defined as $CD117^+$ and $ROR\gamma t^+$ cells (***Table 8*** and ***Table 9***). In mice, ILC3 $NCR^{+/-}$ are nearly exclusively located the intestine [146, 147]. Like ILC2, decidual ILC3 are higher in virgin mice and during pregnancy [112, 148]. However, human lung ILCs are composed of approximately 50-60% ILC3, together with ILC1 [73, 116]. Additionally, during asthma ILC3-like cells are observed in the bronchoalveolar lavage fluid [149]. ILC3 also increase in the skin during inflammatory diseases such as psoriasis [150, 151].

Recently, a new subpopulation of ILCs, called regulatory ILC (ILCreg) have been described in both mouse and human intestine [152, 153]. ILCreg produce IL-10. They derive from CHILP, express ID3 and SOX4, but they lack other transcription factors that are essential for the development of ILCs (such as Nfil3, ROR, GATA-3 and AHR). Mice intestines contain around 4.5 x 10^4 ILCregs [152].

Table 6: Murine ILC2 localization and phenotype in organs and tissues

Organs & tissues	CD25	CD69	CD117	CCR4	CCR8	CRTH2	ICOS	IL-17Rβ	KLRG1	NMUR1	Sca1	Ref.
Adipose tissue*	+	+	n.d.	+	+	n.d.	+	+	+	n.d.	n.d.	[101, 116, 154-157]
Bone marrow[b]	+	-	n.d.	-	-	n.d.	+	+	+/-	n.d.	n.d.	[79, 93, 101, 140, 158]
Kidney*	n.d.	n.d.	n.d.	n.d.	n.d.	n.d.	n.d.	n.d.	n.d.	n.d.	n.d.	[115]
Lungs*[a,b]	+	+	+/-	+	+	n.d.	+	+/-	+/-	+	+/-	[72, 79, 93, 101, 115, 116, 118, 140, 142, 143, 157, 159-167]
Liver	n.d.	+	+	n.d.	n.d.	n.d.	n.d.	+	+	n.d.	+	[140, 160]
LN	+	+	+	n.d.	n.d.	n.d.	n.d.	+	+	n.d.	-	[93, 116, 140, 158, 160, 168, 169]
Peritoneum	n.d.	n.d.	+	n.d.	n.d.	n.d.	n.d.	n.d.	n.d.	n.d.	+	[160, 169, 170]
Salivary glands	n.d.	n.d.	n.d.	n.d.	n.d.	n.d.	n.d.	n.d.	n.d.	n.d.	n.d.	[72]
Skin[b]	+	+	n.d.	+	+	n.d.	+	lo	+	n.d.	n.d.	[93, 101, 157, 168]
Small intestine*[a,b]	+	+	-	hi	+/-	n.d.	n.d.	hi	+/hi	+	+	[72, 79, 101, 108, 115, 116, 121-123, 133, 136, 147, 157, 162, 168, 170-177]
Spleen	n.d.	+	+	n.d.	n.d.	n.d.	+	+	+	n.d.	-	[116, 140, 158, 160, 169, 170]
Uterus*	+		+	n.d.	n.d.	n.d.	+	+	n.d.	n.d.	+	[112, 143]

CRTH2: PGD2 receptor; ICOS: inducible T cell co-stimulator; KLRG1: killer cell lectin-like receptor subfamily G member; LN: lymph nodes; n.d.: not determined; NMUR1: neuromedin-U receptor 1; Sca-1: stem cells antigen-1; *: main ILCs subset; [a]: detected in fetus, [b]: detected in neonates.

Table 7: Human ILC2 localization and phenotype in organs and tissues

Organs & tissues	CD25	CD49a	CD117	CD161	CCR4	CCR6	CRTH2	ICOS	IL-1R1	IL-17Rβ	KLRG1	NKp30	Ref.
Adenoid	+	+/-	+/-	+	+/-	+	+	+/-	n.d.	n.d.	+/-	-	[178]
Adipose tissue	+/-	n.d.	+/-	n.d.	+/-	+/-	+	+/-	n.d.	n.d.	+/-	-	[116, 154]
Colon	+	n.d.	+	+	n.d.	n.d.	+	n.d.	n.d.	n.d.	+	+	[116, 178]
Cord blood	+	-	+/-	+	+/-	+/-	+	+/-	n.d.	n.d.	+/-	+/-	[126, 127, 178]
Decidua, uterus*[c]	n.d.	n.d.	n.d.	n.d.	n.d.	n.d.	+	n.d.	n.d.	n.d.	n.d.	n.d.	[112, 129]
Heart*	n.d.	n.d.	n.d.	n.d.	n.d.	n.d.	+	n.d.	n.d.	n.d.	n.d.	n.d.	[130]
Kidney	n.d.	n.d.	n.d.	+	n.d.	n.d.	+	n.d.	n.d.	n.d.	n.d.	n.d.	[115]
Liver[a]	n.d.	n.d.	+/-	+	n.d.	n.d.	+	n.d.	n.d.	n.d.	n.d.	n.d.	[131]
Lungs[a,b]	+/-	+/-	+/-	+	+/-	+/-	+/-	+/-	+	+	+/-	-	[116, 132, 142, 144, 178, 179]
LN	n.d.	n.d.	n.d.	n.d.	n.d.	n.d.	+	n.d.	n.d.	n.d.	n.d.	n.d.	[116]
PB*[d]	+	-	+/-	+	+	+/-	+	-	+	+	+/-	+/-	[102, 110, 118, 127, 134, 144, 180, 181]
Small intestine[a]	+/-	n.d.	+/-	+	+	+/-	+	n.d.	n.d.	n.d.	+	n.d.	[116, 131, 133, 136, 144, 180]
Skin	+/-	+/-	+/-	+	+/-	+/-	+	+/-	n.d.	n.d.	+/-	-	[137, 178, 182, 183]
Spleen	+/-	+/-	+/-	+	+/-	+/-	+	+/-	n.d.	n.d.	+/-	-	[116, 134]
Tonsils	+/-	n.d.	+/-	+	n.d.	n.d.	+	n.d.	n.d.	n.d.	+	+	[97, 102, 131, 135]

ICOS: inducible T cell co-stimulator; KLRG1: killer cell lectin-like receptor subfamily G member; LN: lymph nodes; n.d.: not determined; PB: peripheral blood; *: main ILCs subset; [a]: detected in fetus, [b]: detected in neonates, [c]: detected during pregnancy.

Table 8: **Murine ILC3 localization and phenotype in organs and tissues**

Organs & tissues	CD4	CD25	CCR4	CCR6	CCR7	CCR9	CXCR5	CXCR6	MHC-II	NK1.1	NKp44	NKp46	Ref.
Adipose tissue	n.d.	n.d.	n.d.	n.d.	n.d.	n.d.	n.d.	n.d.	n.d.	n.d.	n.d.	n.d.	[116]
Bone marrow	n.d.	n.d.	n.d.	n.d.	n.d.	n.d.	n.d.	n.d.	n.d.	+	+	n.d.	[100]
Decidua or uterus[c]	n.d.	n.d.	n.d.	+/-	n.d.	n.d.	n.d.	n.d.	n.d.	+	n.d.	+/-	[105, 112, 129]
Colon	n.d.	n.d.	n.d.	n.d.	n.d.	n.d.	n.d.	n.d.	n.d.	n.d.	n.d.	n.d.	[100, 184-187]
Kidney	n.d.	n.d.	n.d.	n.d.	n.d.	n.d.	n.d.	n.d.	n.d.	n.d.	n.d.	n.d.	[115]
Liver[a]	n.d.	n.d.	n.d.	n.d.	n.d.	n.d.	n.d.	n.d.	n.d.	+	n.d.	+	[100, 131, 171, 188]
Lungs	-	n.d.	n.d.	n.d.	n.d.	n.d.	n.d.	n.d.	n.d.	+	n.d.	+	[100, 116, 118, 188, 189]
LN*	n.d.	n.d.	n.d.	n.d.	n.d.	n.d.	n.d.	n.d.	n.d.	+	n.d.	+	[100, 116, 185, 188]
Peyer's patches	n.d.	n.d.	n.d.	n.d.	n.d.	n.d.	n.d.	n.d.	n.d.	+	n.d.	+	[100]
Salivary glands	-	n.d.	n.d.	n.d.	n.d.	n.d.	n.d.	n.d.	n.d.	+	n.d.	+	[72]
Skin	n.d.	n.d.	n.d.	n.d.	n.d.	n.d.	n.d.	n.d.	n.d.	n.d.	n.d.	n.d.	[151]
Small intestine*[a]	+/-	-	+	+	hi	hi	-	+/-	+	+/-	+/-	+/-	[72, 79, 87, 100, 114, 116, 121-123, 133, 144, 147, 171, 184, 187, 188, 190-198]
Spleen	n.d.	n.d.	n.d.	n.d.	+	-	+	n.d.	+	+	+/-	+/-	[100, 116, 188, 199]
Thymus	n.d.	n.d.	n.d.	n.d.	n.d.	n.d.	n.d.	n.d.	n.d.	+	n.d.	+	[100]

MHC-II: class II major histocompatibility; LN: lymph nodes; *: main ILCs subset; [a]: detected in fetus, [b]: detected in neonates, [c]: detected during pregnancy.

Table 9: Human ILC3 localization and phenotype in organs and tissues

Organs & tissues	CD39	CD56	CD69	CD161	CCR7	CXCR5	HLA-DR	ICOS	NKp30	NKp44	Nkp46	NRP1	Ref.
Adenoid	n.d.	n.d.	n.d.	+	n.d.	n.d.	n.d.	n.d.	+/-	+/-	+/-	n.d.	[178]
Adipose tissue	n.d.	n.d.	n.d.	n.d.	n.d.	n.d.	n.d.	n.d.	n.d.	+/-	n.d.	n.d.	[116]
Colon	n.d.	n.d.	n.d.	+	n.d.	n.d.	n.d.	n.d.	+/-	n.d.	+/-	n.d.	[116, 178]
Cord blood	n.d.	n.d.	n.d.	+	n.d.	n.d.	n.d.	n.d.	+/-	n.d.	+/-	n.d.	[126, 127, 178]
Decidua or uterus*	n.d.	+/-	n.d.	n.d.	n.d.	n.d.	n.d.	n.d.	n.d.	+/-	n.d.	n.d.	[105, 112, 113, 128, 129, 200]
Heart	n.d.	n.d.	n.d.	n.d.	n.d.	n.d.	n.d.	n.d.	n.d.	n.d.	n.d.	n.d.	[130]
Liver*[a]	n.d.	+/-	n.d.	+/-	n.d.	n.d.	n.d.	n.d.	n.d.	+/-	n.d.	n.d.	[131, 201]
Lungs*[a]	+/-	n.d.	+/-	n.d.	n.d.	n.d.	+/-	+/-	n.d.	+/-	n.d.	+/-	[116, 132, 178, 201]
LN[a]	n.d.	+/-	+/-	n.d.	+/-	+/-	-	n.d.	+/-	+/-	+/-	+/-	[116, 202, 203]
PB*[c]	-	n.d.	+/-	+/-	-	-	n.d.	n.d.	n.d.	-	n.d.	-	[102, 118, 127, 134, 201, 202]
Skin	+/-	n.d.	+/-	+/-	-	n.d.	+/-	+/-	n.d.	+/-	n.d.	-	[137, 150, 178, 183]
Small intestine*[a]	+/-	n.d.	+/-	+/-	-	n.d.	+/-	+/-	n.d.	+	n.d.	-	[114, 133, 135, 136, 144, 201, 203]
Spleen	+/-	+/-	+/-	n.d.	+/-	+/-	-	-	+/-	+/-	+/-	n.d.	[116, 134, 202, 203]
Tonsils	+/-	+/-	+/-	+	+/-	n.d.	+/-	+/-	+/-	+/-	+/-	+/-	[102, 114, 135, 138, 178, 202, 203]

ICOS: inducible T cell co-stimulator; NRP1: neuropilin-1; *: main ILCs subset; [a]: detected in fetus.

1.2.3. Plasticity of ILCs

There are evidences that ILCs subsets are not stable, and modulate their phenotype upon local environmental cues (***Figure 5***). This phenomenon is called plasticity [204]. Human ILC1 can convert into ILC3-like cells producing IL-17 *in vitro* when co-cultured with pulmonary squamous cell carcinoma [205]. Conversion of NK cells into ILC1 also occurs in tumors upon stimulation with TGF-β and IL-12 [206, 207] and during *Toxoplasma gondii* infection [125]. The plasticity of ILC2 towards ILC1-like cells was described upon *in vitro* stimulation and in lungs of mice infected with influenza virus and of patients with chronic obstructive pulmonary diseases (COPD) [208-210]. Interestingly, this conversion can be reversed by IL-4 [209]. iILC2 can differentiate into nILC2 and *vice versa*, upon stimulation with a combination of IL-33 with IL-1β, IL-23, TGFβ and Notch signal [211]. In addition, mouse iILC2 produce IL-17 *in vitro*, after IL-1β, IL-6, IL-23 and TGFβ stimulation. ILC2 also have the capability to convert into ILC3-like cells producing IL-13 and IL-17, when co-cultured with *Candida albicans*, in the context of psoriasis or in the nasal polyps of patients with cystic fibrosis [140, 151, 212, 213].

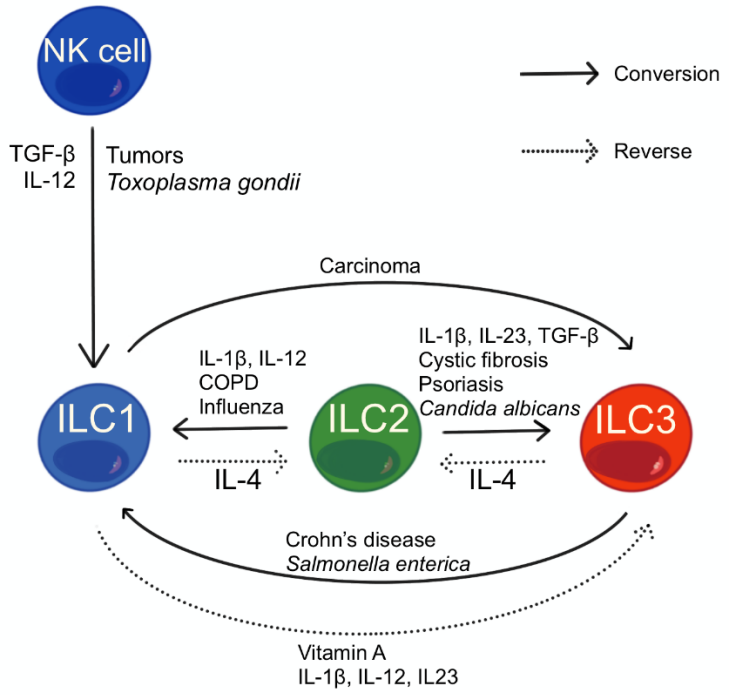

Figure 5: Plasticity of ILCs
NK cells can convert into ILC1 upon stimulation with TGF-β, IL-12, *Toxoplasma gondii* or in tumors. ILC1 can convert into ILC3 during carcinoma. ILC2 can convert into ILC1 when stimulated with IL-1β, IL-12, influenza or during chronic obstructive pulmonary disease (COPD). They can also convert into ILC3 upon stimulation with IL-1β, IL-23, TGF-β, Candida albicans or during Cystic fibrosis and psoriasis. These two conversions can reverse upon exposure to IL-4. ILC3 can convert into ILC1 during *Salmonella enterica* infection or during Crohn's disease. This conversation is reversible with exposure to vitamin A, IL-1β, IL-12 or IL-23.

In mice, ILC3 that downregulate RORγt and upregulate T-bet acquire the capacity to produce IFNγ in response to *Salmonella enterica* or IL-12 and IL-23 in the intestine, showing a conversion into ILC1-like cells [87, 133, 214]. Patients with Crohn's disease showed increased numbers of ILC1 at the expense of ILC3, suggesting that chronic inflammation might enhance conversion from an ILC3 to an ILC1 phenotype [133, 215]. In another study, the conversion from ILC3 to ILC1 phenotype in response to IL-12 was reversible following exposure to the vitamin A metabolite retinoic acid [133]. Bal et al., hypothesized that, upon acute inflammation, ILC3 rapidly convert into ILC1 and that, after resolution of the inflammation, these ILC1 reconvert into ILC3 [204].

The transcriptional networks controlling the plasticity of ILCs start to be revealed, showing an important role of transcription factors such as Ikaros, Aiolos, MAF, SMAD4, BCL-11B and BCL-6 [204, 207, 216]. However, it remains to understand how environmental cues control these transcriptional networks. It is suggested that this plasticity occurs for rapid immune responses to various infections or inflammatory environment [98].

1.2.4. Functions and interactions with other immune cells

ILCs act as a bridge between innate and adaptive immunity, behaving as immune regulators connected to their anatomical localization and cytokine profile. ILCs have a pathogenic role in cancer, metabolic and skin diseases [217]. On the contrary, they have a beneficial role in physiological processes like tissue repair, organ development and in the control of infections (***Table 10***) [74, 96]. We will describe the latter more precisely in this chapter.

Table 10: ILCs and infections

ILCs	Pathogen	Reference
ILC1	*Clostridium difficile*	[193]
	Cytomegalovirus	[119, 120, 124, 218]
	Influenza	[117, 124]
	Listeria monocytogenes	[185, 195]
	Salmonella enterica Typhimurium	[87, 219]
	Sendai virus	[124]
	Toxoplasma gondii	[125, 220]
ILC2	*COVID-19*	[110, 181]
	Heligmosomoides polygyrus	[174-177]
	Influenza	[142, 165, 166]
	Litomosoides sigmodontis	[163]
	Nippostrongylus brasiliensis	[158, 161, 162, 168, 169, 173, 221-223]
	Plasmodium berghei	[224]
	Rhinovirus	[225]
	Schistosoma mansoni	[164, 174]
	Staphylococcus aureus	[167]
	Trichuris muris	[122, 157]
	Trichinella spiralis	[226]
ILC3	*Candida albicans*	[190, 192]
	Citrobacter rodentium	[186, 187, 191, 196]
	Clostridium difficile	[123, 193]
	Helicobacter hepaticus	[147, 197, 198]
	Listeria monocytogenes	[185, 188, 195]
	Mycobacterium tuberculosis	[118, 132]
	Rotavirus	[184]
	Salmonella enterica Typhimurium	[87]
	Streptococcus pneumoniae	[189]
	Yersina enterocolitica	[194]

ILC1. ILC1 (***Figure 6***) are key cells involved in the clearance of *Toxoplasma gondii* [220]. The transfer of ILC1 into alymphoid mice sustained IFNγ production, the recruitment of monocytes, and the elimination of *T. gondii*. Using $Rag1^{-/-}$ mice lacking T and B cells and $Rag2^{-/-}$ $Il2rg^{-/-}$ mice lacking T and B cells and ILCs, Abt et al. showed that ILC1 are the major cells producing IFNγ and required to clear *Clostridium difficile* [193]. Upon *L. monocytogenes* infection by oral gavage, ILC1 are the main producer of IFNγ [195], participating to bacterial clearance. Following murine cytomegalovirus (MCMV) intraperitoneal (i.p.) infection, Sendai virus, *S. enterica* Typhimurium, *L. monocytogenes* or influenza intranasal (i.n.) infection, ILC1 rapidly produce IFNγ in response to IL-12 produced locally by DCs [87, 117, 119, 120, 124, 185, 195, 219]. Also, during sepsis, ILC1 counts are higher in peripheral blood of septic patients than healthy subjects [227].

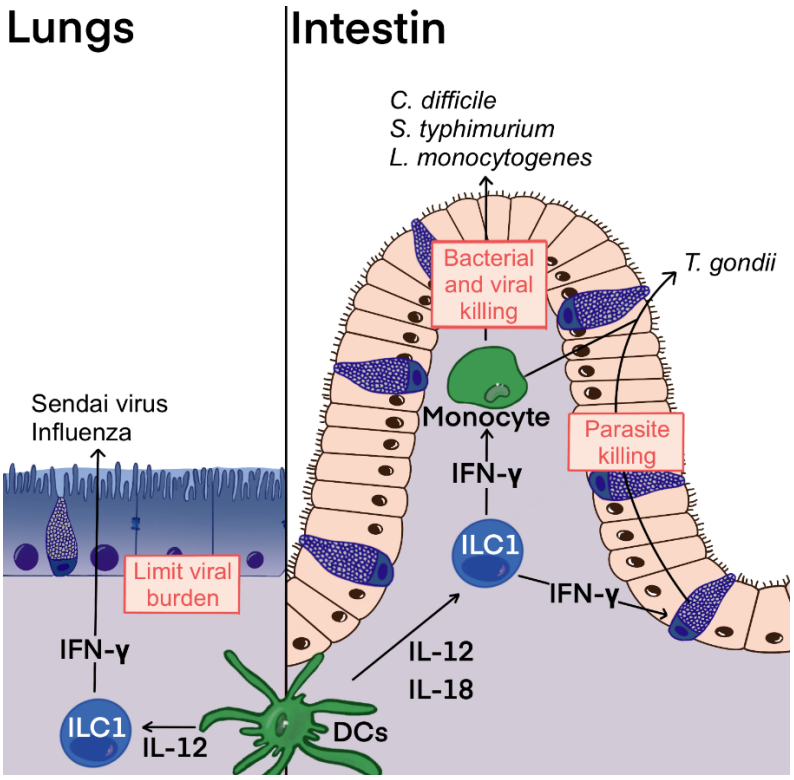

Figure 6: ILC1 and infection

In the lungs, ILC1 are activated by IL-12 produced by resident DCs. They produce IFNγ, which was associated with clearance of Sendai and influenza virus. In the intestine, IFNγ production by ILC1 was associated with increased production of mucus by goblet cells and activation of monocytes, killing *Toxoplasma gondii*. Activation of monocytes by ILC1 was also associated to bacterial or viral killing of *L. monocytogenes*, *S. enterica* Typhimurium and *C. difficile*.

ILC2. ILC2 (***Figure 7***) have been mostly studied during intestinal and lungs helminth infections [228-230] by *Nippostrongylus brasiliensis* [158, 161, 162, 168, 169, 173, 221-223], *Trichuris muris* [122, 157], *Heligmosomoides polygyrus* [174, 175], *Litomosoides sigmodontis* [163], and *Schistosoma mansoni* [164]. The adoptive transfer of ILC2 into infected mice deficient in IL-13 or IL-25 and IL-33 signaling demonstrated that ILC2 are sufficient to control infection by *N. brasiliensis* [158, 168, 221]. Following infection, epithelial cells and Tuft cells release stress mediators (like IL-25, IL-33 and TSLP) maintaining ILC2 homeostasis and activation [175-177]. IL-13 and amphiregulin (AREG) derived from ILC2 increase goblet cell hyperplasia, mucus production and activate smooth muscle cells to limit worm development and enhance worm expulsion. After subcutaneous injection of *N. brasiliensis* larvae, accumulation of eosinophils and alternatively activated (M2) macrophages in lungs results from IL-5 production by ILC2. The production of AREG, Arg1 and polarization of macrophage toward an M2 phenotype highlight the contribution of ILC2 into tissue repair [142, 166, 231, 232]. During *Trichuris muris* infection, mice treated with a lipase inhibitor or Rag1$^{-/-}$ mice have a significant reduction of ILC2 accumulation and ILC2-derived cytokines (IL-5 and IL-13). This is associated with an increased worm burden [157]. During *H. polygyrus* and *S. mansoni infection*, ILC2-derived cytokines correlate with worm clearance [174]. The administration of IL-33 prevents cerebral malaria of mice infected with *Plasmodium berghei*, which is associated with an expansion of splenic ILC2, the activation of M2 macrophages and the recruitment of Tregs [224]. ILC2 express MHC-II and therefore are able to directly interact with T cells, as demonstrated during helminth infections [169]. ILC2 express co-stimulatory molecules such as ICOS ligand (ICOSL) [161, 233, 234] and programmed cell death ligand 1 (PD-L1) [235-237] that is reported to provide a second signal for T cell activation. In a mouse model of influenza infection [142, 165, 166], ILC2 orchestrate immune response and regulate lung inflammation. ILC2 are activated by tissue-resident alveolar macrophages to produce IL-5 and IL-13 implicated in the accumulation of eosinophils during the recovery phase of infection [142, 166]. Potentially, ILC2 activate DCs and M2 macrophages as shown elsewhere [238, 239]. ILC2 also protect mice from lethal infection caused by *Staphylococcus aureus* [167], through the secretion of type 2 cytokines, promoting eosinophilia and preventing a lethal neutrophilic response. TSLP and IL-33 produced by alveolar cells induce ILC2 to produce IL-9 to coordinate epithelial cell maintenance. Autocrine IL-9 promotes IL-5 and

IL-13 production and lung homeostasis [240]. ILC2 response is induced by cytokines or growth factors produced by a variety of cells, such as IL-4 produced by basophils [241], PGD2 by mast cells [242], TGF-β and/or IL-33 by epithelial cells, endothelial cells, macrophages, NKT cells, and mast cells [165, 166, 243, 244]. IL-33 produced by DCs [245] and mast cells [246] also play a role in the activation of ILC2. *In vitro*, lung ILC2 enhance $CD4^+$ T cell proliferation and the production of Th2 cytokines [158]. IL-2 produced by T cells and B cells is associated with IL-9 production by ILC2 in papain-induced lung inflammation [247]. ILC2 expand locally in the lungs in response to *L. sigmodontis* [163]. More recently, ILC2 were described in peripheral blood of COVID-19 patients, where they oppositely showed an overall increase or decreased of ILC2 in severely ill COVID-19 patients [110, 181].

ILC3. ILC3 contribute to oral, intestinal and lung defenses. ILC3 are the predominant source of IL-22 and IL-17 during oropharyngeal candidiasis [192], *Citrobacter rodentium* colonic infection [191, 196] and *Streptococcus pneumoniae* lung infection [189] (***Figure 8***). During *C. rodentium* infection, secretion of IL-22 by ILC3 triggers epithelial cells to produce antimicrobial peptides and regulate T cell responses through the expression of MHC-II [190], protecting against intestinal infection. Later, it was shown that NCR^+ ILC3 are to some extent redundant for the control of the infection in the presence of T cells, but essential for cecal homeostasis [191]. The production of IL-22 by ILC3 is promoted by the expression of β2-integrin on intestinal macrophages [187]. ILCs can act in concert as shown for ILC1 and ILC3 during *C. difficile* infection via oral gavage [193]. ILC3-derived IFNγ is required for early protection during *Y. enterocolitica* infection [194]. During rotavirus infection, IL-1α induces IL-22 and IFNγ production by ILC3, thus curtailing replication of rotavirus [184]. In a model of *S. enterica* Typhimurium enteric infection, Klose et al. demonstrated that intestine ILC1-like ILC3 are the main producers of IFNγ, which is required to increase the production of mucus by goblet cells [87]. Oral infection with *L. monocytogenes* induces an IL-22 response by ILC3 in the intestine. However, it does not contribute to control bacteria dissemination [185, 188, 195]. ILC3 not only protect against invasive bacterial infection, they also play a role in the confinement of intestinal commensal bacteria [248]. Previous studies identified a role for ILC3 in regulating adaptive immunity, and specifically $CD4^+$ T cells in the large intestine through granulocyte-macrophage colony-stimulating factor (GM-CSF) and MHC-II. Production of IL-2 by ILC3 is significantly reduced in the small intestine of patients with Crohn's disease, and this correlates with lower frequencies of Treg cells [249]. It is speculated that ILC3 may present microbiota-derived antigens to CD4 T cells [146]. In opposition to these beneficial roles of ILC3, ILC3 contribute to *Helicobacter hepaticus*-mediated colitis through the production of IL-22 and IL-17, and the upregulated expression of costimulatory molecules such as OX40L [147, 199, 250]. This indicates that ILCs can have a pathogenic role. During *S. pneumoniae* lungs infection, ILC3 produce IL-17 and IL-22 in response to DCs-derived IL-23 and IL-1β, which promotes the recruitment of neutrophils. More recently, ILC3 were shown to accumulate in lungs of patients infected with *Mycobacterium tuberculosis*. ILC3 upregulate CXCR5, involved in the accumulation of alveolar macrophages, mediating early immune protection against tuberculosis [118]. In addition, in some inflammatory conditions, IL-22 and GM-CSF derived ILC3 may induce epithelial cells to generate neutrophil chemoattractants, leading to the accumulation of neutrophils and tissue destruction [251, 252]. ILC3 count are underrepresented in patients with septic shock, compared to ILC1 [227].

Lastly, ILCreg were described in both mouse and human intestines [152], where they contributed to the resolution of intestinal inflammation through the suppression of ILC1 and ILC3 activation via secretion of IL-10.

Taken together, ILCs are pivotal regulators of both innate and adaptive immune cells, being able to either promote or dampen the immune response depending on the environmental context. They have been shown to express PRRs on their surface [253, 254]. It remains unclear whether ILCs can regulate adaptive immune response through presentation of peptide-MHC. However, in lymph nodes, ILC3 antigen presentation is critical to regulate T and B cell responses and maintain tissue homeostasis and mutualism with the commensal microbiota [198].

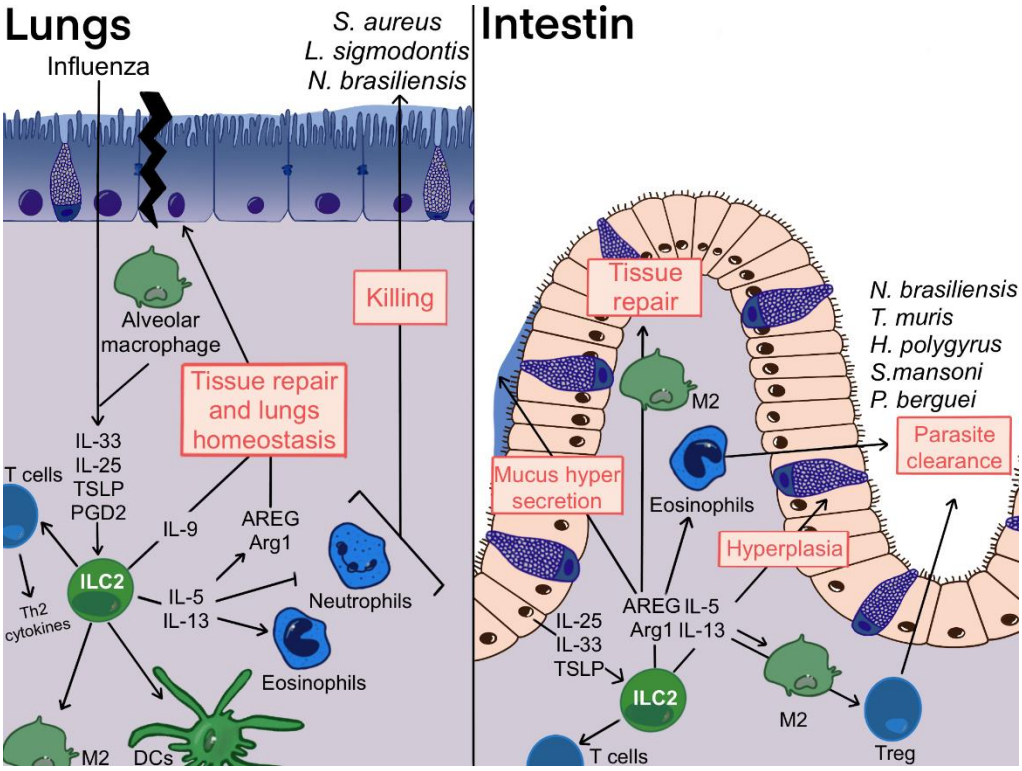

Figure 7: ILC2 and infections

In the lungs, ILC2 are activated by surrounding resident myeloid cells such as alveolar macrophages. This activation leads to a cascade of events such as the activation of T cells, macrophages, DCs, eosinophils and neutrophils leading to the killing of pathogens, tissue repair and lungs homeostasis. In the intestine, ILC2 leads activate T cells, Tregs, eosinophils and M2 macrophages promoting parasite clearance and tissue repair. Furthermore, the production of AREG, Arg1, IL-5 and IL-13 leads to the production of mucus hyper secretion and goblet cells hyperplasia, supporting parasite clearance.

AREG: amphiregulin; Arg1: arginase 1; PGD2: prostaglandin D_2; M2: alternatively activated macrophages; Th2: type 2 T helper cells; TSLP: thymic stromal lymphopoietin; Treg: T regulatory cells

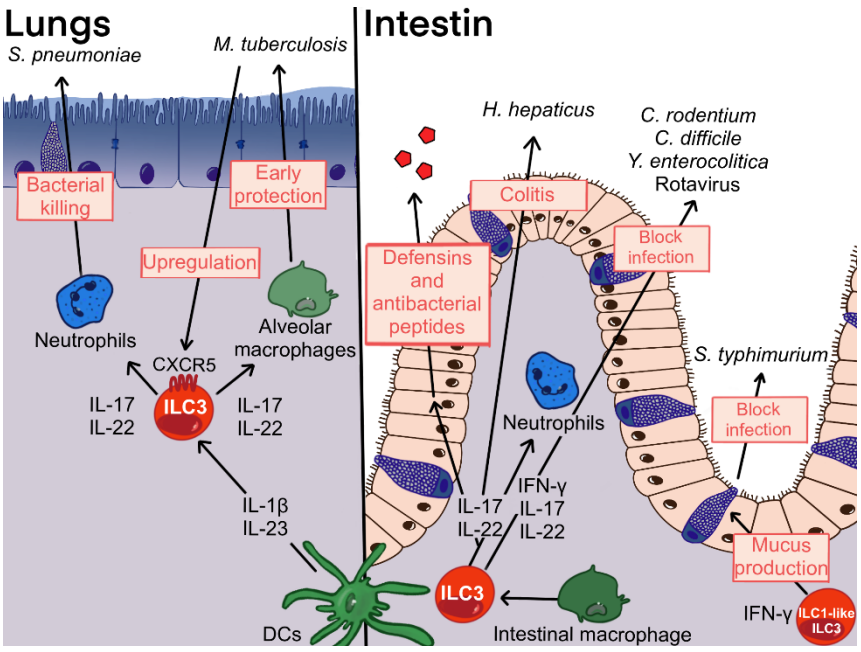

Figure 8: ILC3 and infections

In lungs, ILC3 are implicated in protection against *S. pneumoniae* and *M. tuberculosis* infection, through the recruitment of neutrophils and alveolar macrophages. In intestine, ILC3 are implicated in the protection against infection by stimulating the production of antibacterial peptides (defensins) and mucus, and promoting neutrophils recruitment. However, they also contribute to *Helicobacter hepaticus*-mediated colitis.

1.3. Innate immune memory and trained immunity

Since the demonstration by Jenner in 1796 that an infection with a mild cowpox virus protected from deadly smallpox virus, what we now call vaccination, it has become clear that the immune system can keep a memory of the pathogens it has encountered. This characteristic was attributed to the adaptive immune system through the generation of memory T and B cells [255, 256]. However, this dogma has been challenged (***Figure 9***). Pioneer studies in the 60's described that plants, that do not have an adaptive immune system, develop after a first hit a resistance to a secondary infection against a broad spectrum of microorganisms in a manner similar to immunization in mammals (reviewed in [257]), a process called systemic acquired resistance. In 2003, studies showed that invertebrates are capable of specific memory even though invertebrates do not have an adaptive immune system [258]. In the 80's, mice injected intravenously (i.v.) with a low dose of *Candida albicans* were shown to be protected against a lethal dose of *Staphylococcus aureus* injected i.v [259]. Later on, studies in mice showed that β-glucans, a cell wall component of *C. albicans*, protected T and B cells deficient mice against an infection with *C. albicans* ([260] and reviewed in [261]). Epidemiological studies in humans showed that Bacillus Calmette-Guérin (BCG) vaccine, an attenuated strain of *Mycobacterium bovis* protects not only against tuberculosis, but also against other infectious diseases, in a T- and B-lymphocytes independent manner [262], suggesting nonspecific protective effects of the vaccine ([263-265] and reviewed in [266]).

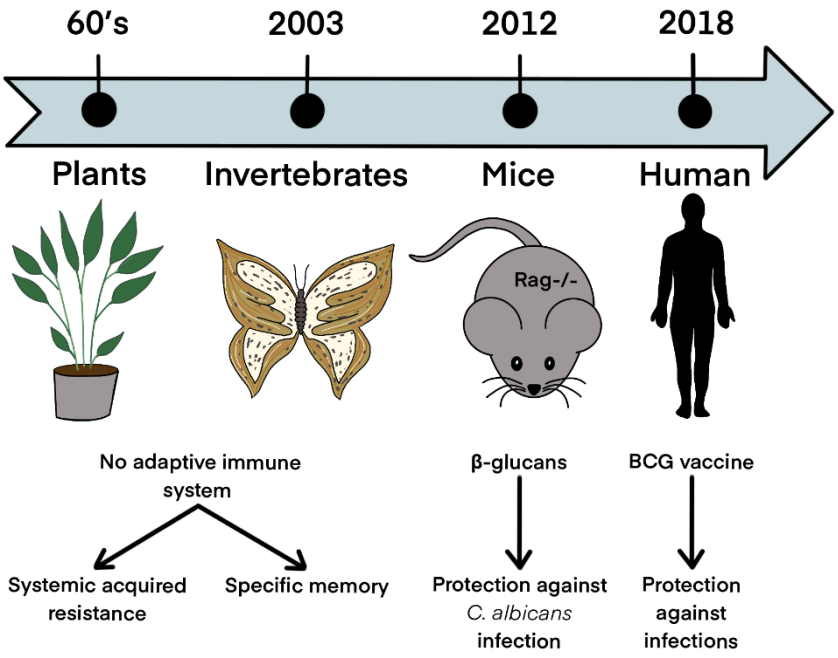

Figure 9: Reconsidering immune memory

First studies that helped reconsider the immune memory were study done in plants and invertebrates. They both develop a specific memory even though those organisms do not have an adaptive immune system. Later on, $Rag^{-/-}$ mice treated with β-glucans showed protection against *C. albicans* infection. Finally, recent studies demonstrate that BCG vaccination enhances protection against various infections. BCG: Bacillus Calmette-Guérin.

These observations were put together by Mihai Netea and colleagues (Radboud University Medical Center, Nijmegen, The Netherlands) who proposed in 2011 the concept of trained immunity that defines a "heightened response to a secondary infection that can be exerted both toward the same microorganism and a different one" [267]. Thus, trained immunity, also called innate immune memory, reflects the capacity of the innate immune system to be reprogramed after a primary stimulation, in order to mount a stronger response upon a secondary stimulation (***Figure 10***). The first stimulation induces metabolic and epigenetic changes, which stimulate and imprint hematopoiesis [268, 269]. The metabolic and epigenetic changes result in the production of trained innate immune cells with an

increased capacity to respond to a secondary trigger, infectious or not infectious (for example by transformed cells). Thus, trained immunity may add inflammation in pathological situations.

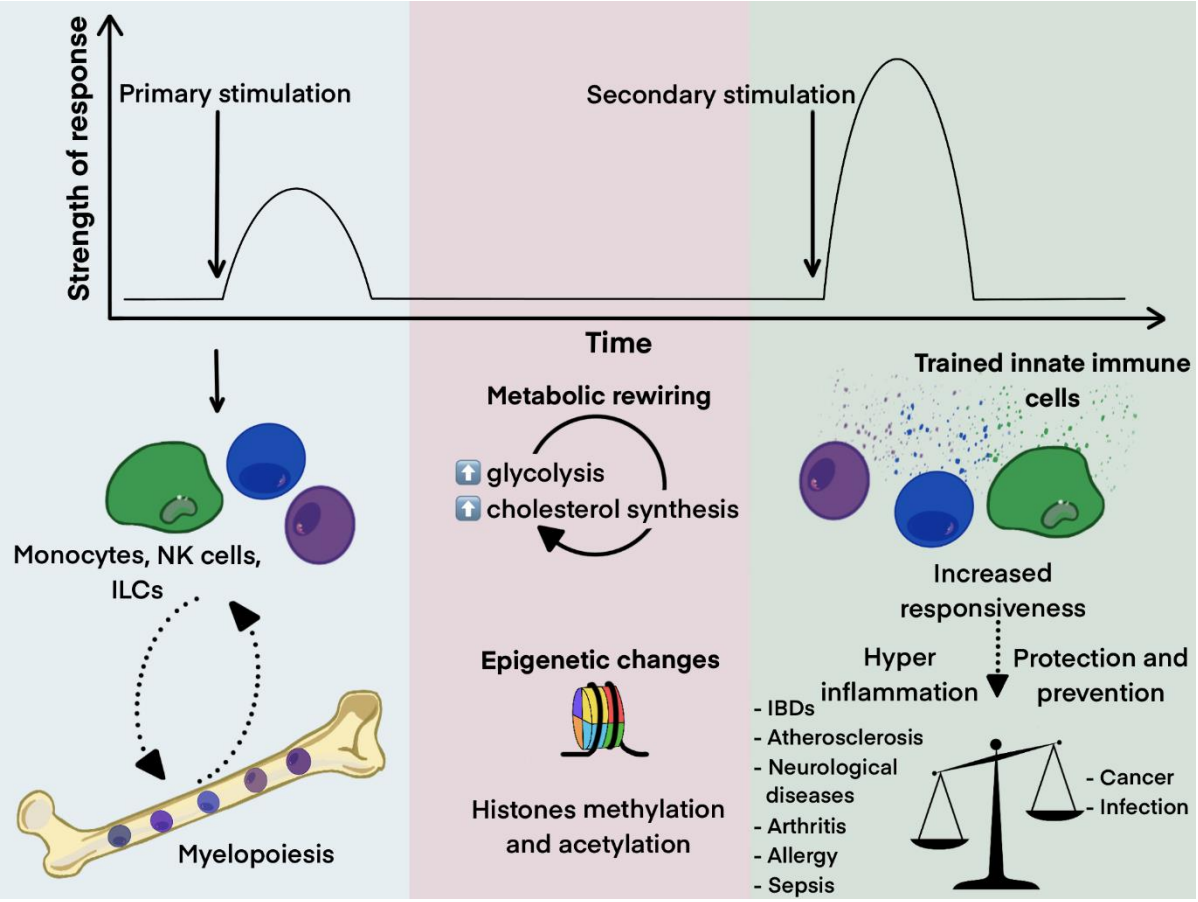

Figure 10: Innate immune memory (Adapted from [270])
A primary stimulation by BCG or β-glucans activate innate immune cells (monocytes, NK cells, ILCs) and induce metabolic and epigenetic changes which promote myelopoiesis and the generation of trained innate immune cells with an increased responsiveness to heterologous secondary stimulation. While contributing to long-term nonspecific protection against infections or prevention of certain forms of cancers, trained immunity may also promotes inflammation and increase susceptibility to inflammatory diseases. IBD: Inflammatory bowel disease; ILCs: innate lymphoid cells; NK cells: natural killer cells.

1.3.1. Inducers of training

Various agents induce trained immunity, but they do not all reprogram the same cells in the same way. The nature, dose and duration of exposure to MAMPs/DAMPs influence the reprograming of innate immune cells. Actually, a stimulus can induce either training or tolerance depending on its concentration [271]. As an example, LPS, a well-recognized inducer of tolerance, can confer trained immunity [272]. BCG and β-glucans are the two most used priming agents in studies on trained immunity, but heterologous protection occurs with many microbial components, inactivated whole organisms, live whole organisms and non-microbial components as detailed in ***Table 11***.

Table 11: Inducers of trained immunity

Primary stimulation		Secondary stimulation		Ref.
Microbial product				
Adenovirus	i.n.	*Streptococcus pneumoniae*	i.t.	[273]
β-glucans	i.p.	*Candida albicans*	i.v.	[274]
β-glucans	i.p.	*Escherichia coli*	i.p.	[275]
β-glucans	i.p.	*Citrobacter rodentium*	i.t.	[275]
β-glucans	i.p.	*Staphylococcus aureus*	i.v.	[274-277]
β-glucans	i.p.	*Listeria monocytogenes*	i.v.	[275]
β-glucans	i.p.	*Pseudomonas aeruginosa*	i.n.	[275]
β-glucans	i.p.	*Leishmania braziliensis*	s.c.	[278]
Chitin from *S. cerevisiae*	i.p.	*Candida albicans*	i.v.	[279]
CpG-ODN	i.p.	*Listeria monocytogenes*	i.p.	[280]
CpG-ODN	i.p.	*Escherichia coli*	neocortex	[281]
Lipid A mimetics	i.n.	*Yersinia pestis*	i.n.	[282]
LPS (2 injections)	i.p.	GBS	i.v.	[283]
LPS	i.p.	*Staphylococcus aureus*	i.p.	[272]
LPS	i.p.	*Pseudomonas aeruginosa*	i.p.	[284]
LPS	i.p.	LPS	i.p.	[285]
MPLA	i.v.	*Staphylococcus aureus*	i.t.	[286]
Pseudomonas aeruginosa flagellin	*in vitro*	*Aspergillus fumigatus*	*in vitro*	[287]
S. enterica Typhimurium flagellin	i.p.	*S. enterica* Typhimurium, rotavirus	i.t.	[288, 289]
Inactivated whole organisms				
BCG vaccine	i.v.	*Candida albicans*	i.v.	[262]
BCG vaccine	i.p.	*Plasmodium yoelii*	i.p.	[290]
BCG vaccine	i.d.	Yellow fever virus	i.d.	[291]
BCG vaccine	i.d.	*Mycobacterium tuberculosis*	*ex vivo*	[292]
BCG vaccine	i.d.	*Staphylococcus aureus*	*ex vivo*	[292]
BCG vaccine	i.d.	*Candida albicans*	*ex vivo*	[292]
BCG vaccine	*in vitro*	Pam_3CSK_4, LPS, TNF	*in vitro*	[293]
Candida albicans	i.p.	GBS	i.v.	[294]
Propionibacterium acnes	i.v.	*Salmonella typhimurium*	i.v.	[295]
Live whole organisms				
Candida albicans	i.n.	*Pseudomonas aeruginosa*	i.n.	[296]
Candida albicans	i.v.	*Staphylococcus aureus*	i.v.	[259]
Herpesvirus	i.n.	*Listeria monocytogenes*	i.p.	[297]
Influenza virus	i.n.	Influenza virus	i.n.	[298]
Lactobacillus plantarum	i.n.	Pneumovirus	i.n.	[299]
S. enterica Typhimurium	i.p.	LPS	i.p.	[285]
Strongyloides venezuelensis	s.c.	*Nippostrongylus brasiliensis*	s.c.	[300]
Staphylococcus aureus	s.c.	*Staphylococcus aureus*	s.c.	[301]
Vaccinia virus	*in vitro*	Vaccinia virus	*in vitro*	[302]
Trichinella spiralis	*in vivo*	*Trichinella spiralis*	*in vivo*	[226]
Synthetic & non-microbial products				
Combination Pam_3CSK_4, muramyl dipeptide, and flagellin	*in vitro*	*S. enterica* Typhimurium	*in vitro*	[303]
Ox-LDL	*in vitro*	Pam_3CSK_4, LPS, TNF	*in vitro*	[293]
Muramyl dipeptide	s.c.	*Toxoplasma gondii*	i.p.	[304]

Imiquimod (TLR7 and NLRP3 agonist)	Topical	Vitamin D analogue calcipotriol, topical TPA (induces hyperplasia), epidermal abrasion wounding, *Candida albicans*	-	[305]

CpG-ODN: CpG oligodeoxynucleotide; GBS: Group B streptococci; i.d.: intradermally; i.n.: intranasally; i.p.: intraperitoneally; i.v.: intravenously; i.t.: intratracheally; MPLA: monophosphoryl lipid A; NLRP3: NLR family primary domain containing 3; Ox-LDL: oxidized low-density lipoprotein; s.c.: subcutaneously; TPA: 12-O-tetradecanoylphorbol 13-acetate.

Many studies described innate immune memory characteristics of monocytes and macrophages following *in vitro* re-simulation with PAMPs or DAMPs. However, considering that mature myeloid cells are usually short-lived, quickly raised the question how innate immune memory could be maintained over time. The conundrum was resolved when β-glucans and BCG were reported to reprogram bone marrow (BM) hematopoietic stem cells (HSCs) to intensify hematopoiesis and generate circulating trained myeloid cells [268, 269, 306, 307].

1.3.2. Mechanisms of trained immunity

The molecular mechanisms underlying the acquisition of a trained immune phenotype include metabolic and epigenetic modifications associated with the functional reprogramming of cells [270, 308] (***Figure 11***). Functional reprogramming of cells is induced by activation of PRRs, and leads to the activation of intracellular signaling cascades (like PI3K (phosphoinositol 3-kinase)/AKT/mTOR (mammalian target of rapamycin) and MAP kinase pathways) and *in fine* metabolic and epigenetic changes [274, 309-311]. Metabolic changes usually include a shift from oxidative phosphorylation (OXPHOS) to aerobic glycolysis, a phenomenon known as the Warburg effect. The shift is regulated by the mTOR/HIF-1α (hypoxia-inducible factor-1α), mevalonate and glutamate pathways [312-314]. It activates the cholesterol synthesis pathway and glutaminolysis that refills the TCA cycle, and it blocks the itaconate pathway. Metabolites such as fumarate, mevalonate and succinate accumulate, assist epigenetic modifiers and enhance trained immunity. For example, fumarate inhibits the histone lysine demethylase KDM5, while succinate activates HIF-1α that controls glycolysis and the transcription of the *Il1b* gene. Accordingly, IL-1β has been involved in the establishment of trained immunity induced by BCG, β-glucans and Western diet [269, 291, 307, 315]. The metabolic adaptation generates rapidly energy to support secretory and bactericidal functions of innate immune cells. Indeed, increase of glucose consumption concomitant to activation of glycolysis is observed during trained immunity [268]. In monocytes/macrophages, high concentrations of β-glucans sensing through dectin-1 activates an AKT/mTOR/HIF-1α pathway driving the Warburg effect. However, low concentrations of β-glucans, BCG or oxidized LDL (Ox-LDL) can activate both OXPHOS and glycolysis [274, 310, 316]. Furthermore, the anti-inflammatory metabolite itaconate regulates the balance between tolerance and trained immunity [317].

Metabolites affect the activity of epigenetic modifiers. For example, acetyl-CoA is a group donor to histone acetyltransferase, S-adenosylmethionine (SAM) is a methyl group donor to DNA and histone methyltransferases, α-ketoglutarate (α-KG) a cofactor of DNA and histone demethylases and NAD^+ a cofactor of histone deacetylase. Genome-wide comparison of the epigenetic landscapes of trained and non-trained PBMCs, monocytes, macrophages and HSCs revealed numerous differentially regulated sites. The establishment of trained immunity is associated with an increase in marks of open chromatin including mono and tri-methylation of histone 3 and lysine 4 (H3K4me1 and H3K4me3), and acetylation of H3K27 or H3K18 (H3K27ac or H3K18ac) at enhancers and promoters of genes associated with metabolic, immune and host defense pathways [260, 261, 291, 311, 318, 319]. Assay for transposase-accessible chromatin using sequencing (ATAC-seq) confirmed increased chromatin accessibility at sites encompassing genes associated with inflammation, immune response and myeloid differentiation in trained conditions [268, 269, 284, 306]**.** Consequently, these genes are more robustly transcribed. As mentioned above, IL-1β contributes to trained immunity induced by BCG, β-glucans and Western diet.

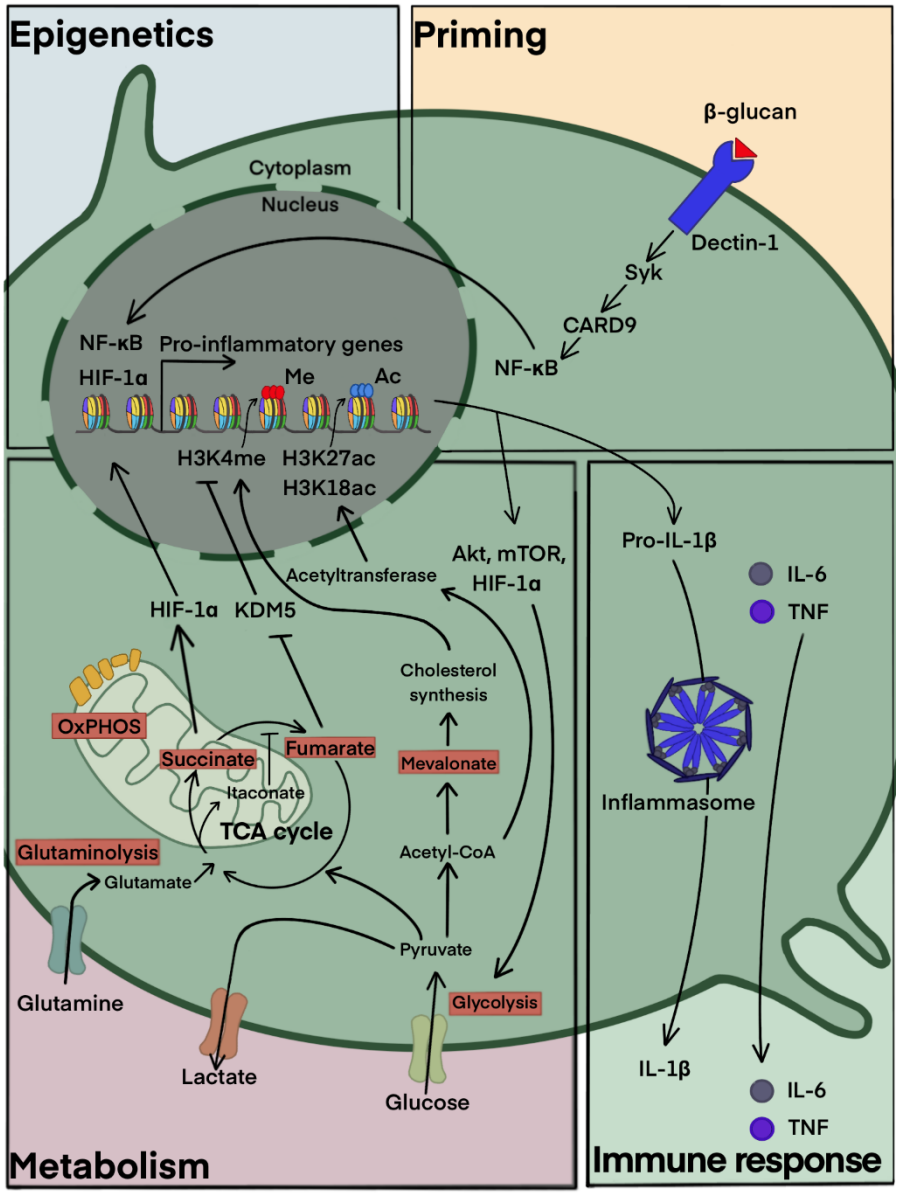

Figure 11: Mechanisms involved in trained immunity

Priming: A priming agent such as β-glucans activates a signaling pathway leading to the activation of NF-κB. Akt, mTOR and HIF-1α pathways. ***Metabolism:*** Trained cells exhibit an overall upregulation of glycolysis, TCA, OxPHOS and glutaminolysis metabolism. Glycolysis provides pyruvate that is metabolized into acetyl-CoA or lactate and be used in the TCA cycle. Acetyl-CoA can also derived from fatty acids through β-oxidation. The conversation of glutamate into α-ketoglutarate by glutaminolysis can also replenish the TCA cycle in carbon. Succinate can inhibit the degradation of HIF-1α, promoting transcription of proinflammatory genes. It can also inhibit the enzymatic activity of KDM5. Acetyl-CoA can provide acetyl for histone acetyl transferases. The oxidation of succinate to fumarate enhance production of ATP by the OxPHOS pathway [322, 323]. ***Epigenetics:*** Metabolites working as cofactors of epigenetic enzymes or donors of epigenetic modifications promote epigenetic changes, facilitating the transcription of proinflammatory genes such as *IL1b*, *IL6* and *TNF*. ***Immune response:*** This production leads to increase immune responses.

Ac: acetyl; CARD9: caspase recruitment domain family member 9; KDM5: lysine demethylase 5; HIF-1α: hypoxia-inducible factor 1-α; H3K4me: methylation of histone 3 at lysine 4; H3K27/18ac: acetylation of histone 3 at lysine 27 or 18; Me: methyl; mTOR: mechanistic target of rapamycin; NF-κB: nuclear factor-kappa B; OxPHOS: oxidative phosphorylation; Syk: Spleen tyrosine kinase; TCA: tricarboxylic acid.

Among others, IL-1β signaling promotes glycolytic activity and the proliferation of HSPCs [269, 291, 307, 315]. Hence, IL-1β is considered as a central regulator of trained immunity.

Overall, induction of trained immunity by β-glucans and BCG acts at the level of BM progenitors with a shift towards myelopoiesis through induction of persistent transcriptional and epigenetic changes in HSCs. Interestingly, β-glucans also trigger nuclear factor of activated T cells (NFAT) to increase the transcription of gene-priming lncRNAs. lncRNAs are key modulators of gene activity, linking nuclear organization to gene regulation [320]. This epigenetic memory is not only present in mature cells, but is also transmitted to HSCs and progenitors of innate immune cells, leading to the generation of trained monocytes and macrophages [268, 269, 321]. Overall, these modifications promote heightened immune responses as reported in numerous articles and described in the next section.

1.3.3. Innate immune cells and memory

NK cells were the first non-T, non-B cells reported to have memory features lasting up to 4 weeks [324]. The acquisition of memory features by NK cells follows phases that parallel those of T cells and B cells (expansion, contraction and memory). Additionally, NK cells and $CD8^+$ T cells share epigenetic and transcriptional programs underlying immunological memory properties [325]. Memory NK cells differentially express inhibitory and activating NK receptors. Memory NK cells are induced in various conditions listed in ***Table 12***.

Table 12: NK cells in trained immunity

Condition	Host	Effect	Ref.
BCG vaccination	Human	• Increased production of IL-1β and IL-6 by NK cells upon secondary *ex vivo* challenges in BCG vaccinated volunteers	[292]
Cytokines	Mouse	• Increased production of IFNγ	[326]
Haptens	Mouse	• NK cell accumulation	[324]
		• NK cell memory property depend on CXCR6 expression	[327]
Hantavirus	Human	• Rapid expansion of NK cells • NK cells detected up to 60 days after infection • Expression of NKG2C by NK cells	[328]
HCMV	Human	• Rapid degranulation and release of cytokines • Increased production of cytokines	[329-331]
HIV	Mice	• NK cell memory property depend on CXCR6 expression	[327]
Influenza	Mice	• NK cell memory property depend on CXCR6 expression	[327]
	Mice	• Liver memory NK cells protected mice against secondary influenza infection	[298]
MCMV	Mouse	Memory NK cells: • Detected up to 70 days post-infection • With an increased production of cytokines by NK cells • Undergo a rapid degranulation	[332, 333]
		• Antigen specificity for MCMV-encoded glycoprotein	[334, 335]
		• Clonal proliferation of NK cells	[336, 337]
		• Persistence of NK cells during contraction and memory phases	[338]
Pregnancies	Mouse	• NK cells highly express the memory cell marker CXCR6	[107]
Vaccinia virus	Mouse	• NK memory cells protect against secondary vaccinia virus infection	[302]
VSV	Mouse	• NK cell memory property depend on CXCR6 expression	[327]

BCG: Bacillus Calmette–Guérin; HCMV: human cytomegalovirus; HIV: human immunodeficiency virus; MCMV: murine cytomegalovirus; VSV: vesicular stomatitis virus.

Multiple studies reported that exposure of monocytes or macrophages to diverse products enhance their response towards an unrelated pathogen, as described in ***Table 13*** and discussed in previous sections. Alveolar macrophages were described with a long-term memory property in murine lungs. Indeed, during adenoviral infection, alveolar macrophages up-regulate MHC-II molecules, glycolysis and expression of genes implicated in immune defenses [273]. These memory alveolar macrophages exposed to adenoviral infection confer long-lasting protection against *S. pneumoniae* and *E. coli* infections through increased production of chemokines and neutrophils recruitment to the lungs. Resident macrophages of the brain (microglia) can be primed during inflammatory processes and have an amplified response during a second insult [339-341]. Exposure of pregnant mice or neonatal mice to an inflammatory stimulus (LPS, poly (I:C), and live bacteria) causes alterations in microglial response to a second stimulus given in adulthood [342-345]. In addition, after axonal injury, the microglia exhibits an excessive production of IL-1 and phagocytic response in the optic nerve in response to LPS challenge [346]. A single i.p. injection of LPS suppressed the release of IL-1β in the brain in response to a second LPS challenge. In this article, the authors showed that the first LPS challenge leads to epigenetic silencing of *Il1b* promoter in microglia [285].

Few reports suggested that ILCs and DCs display some kind of memory properties. For ILCs, this has been proposed for ILC1 and ILC2 in response to MCMV, allergens, *N. brasiliensis* and *T. spiralis* (***Table 14***). Murine DCs exposed to *Cryptococcus neoformans* show an increased production of IFNγ and TNF upon *ex vivo* challenge with *C. neoformans*, 70 days after a first infection [347]. This shows possible memory property of DCs. Neutrophils from BCG vaccinated healthy volunteers show long-term epigenetic and immunophenotypic changes associated with increased activation, and increase activity against *M. tuberculosis*, *C. albicans* and LPS [348]. The acquisition of a trained phenotype is widely described for circulating leukocytes with short half-lives, while monocytes with trained features are found up to 1 year after BCG vaccination [292, 319]. This is explained by the fact that the induction of trained immunity affects stem cells, among which hematopoietic stem and progenitor cells (HSPCs) in the bone marrow (***Table 15***). Priming with β-glucans, BCG vaccination and Western diet promote hematopoiesis, with a bias towards myelopoiesis [268, 269, 306, 307]. Most importantly, memory property is not restricted to immune cells, and has been described in non-immune cells such as endothelial cells, skin epithelial cells and vascular smooth muscle cells (***Table 16***). While this may have huge consequences for host responses, unfortunately little has been reported in the literature. The concept of “extended trained immunity” has been proposed to include all cell types with the potential of memorizing microbial encounters [349].

Table 13: Monocytes/macrophages and trained immunity

Condition	Host	Effect	Ref.
Adenovirus	Mouse	Alveolar macrophages: • Up-regulation of MHC-II molecules • Long lasting protection against *S. pneumoniae* and *E. coli* • Increased production of chemokines • Increased neutrophils recruitment to the site of infection	[273]
C. albicans	Mouse	• Enhanced cytokines production by monocytes • β-glucans enhance stable changes of trimethylation at H4K4	[260]
E. coli	Mouse	• Increase of monocytes • Increased cytokine production	[275]
	Rat	• Rats treated postnatally with *E.coli* show microglial memory cell marker at 16 months of age	[342]
Influenza virus	Mice	• Increased production of IL-6 by alveolar macrophages • Increased protection against a secondary infection by *S. pneumoniae* infection 1 month after influenza challenge	[350]
L. monocytogenes	Mouse	• Increase of monocytes • Increased cytokines production	[275]
LPS	Human	• Epigenetic changes with increased H3K4m1 and H3K27ac marks.	[311]
	Mouse	• Dramatic increase expression of IL-1β, PTX3, iNOS in the brain • Neutrophil infiltration in the brain • Expression of IL-1β by microglial cells	[344]
		• IL-1β and IL-6 transcripts in microglial cells	[346]
		• Increased brain IL-1β, TNF and IL-12 levels	[345]
		• LPS injection in the brain suppress IL-1β release in response to a secondary LPS challenge	[285]
N. brasiliensis	Mouse	• Macrophages isolated 45 days after infection show accelerated parasite clearance when transfer to naïve recipients mice • Primed macrophages increase mortality of parasite *in vitro* • Macrophages primed by neutrophils	[351]
Poly (I:C)	Mouse	• Altered microglial transcriptome and phagocytic function	[343]
S. pneumoniae	Mouse	• Long-lasting remodeling of alveolar macrophages with enhanced protection against another pneumococcal serotype up to 6 months • Trained alveolar macrophages have an altered metabolism	[352]
	Human	• Alveolar macrophages from *S. pneumoniae*-colonized individuals show increased opsonophagocytosis to pneumococcus up to 3 months after experimental pneumococcal colonization	[353]

		• Increased response against *S. pyogenes*, *S. aureus* and *E. coli*	
***S. enterica* Typhimurium**	Mouse	• Increased brain IL-1β, TNF and IL-12 levels • Microglia display an activated phenotype	[345]

Table 14: ILCs and trained immunity

Cell	Condition	Host	Effect	Ref.
ILC1	MCMV	Mouse	• Transcriptional and epigenetic modification • Increased production of inflammatory cytokines and antigen specificity • Migration properties	[120]
	Allergen-immuno therapy	Human	• Stable increase of ILC1 at the expense of ILC2, for up to 3 years of allergen-immuno therapy • High expression of CD25	[354]
ILC2	Allergens	Mouse	• High production of IL-5 and IL-13	[355]
	BrdU	Mouse	• High production of IL-13	[356]
	N. brasiliensis	Mouse	• Increased production of IL-5 and IL-13, which enhances eosinophils accumulation in lungs	[300]
	T. spiralis	Mouse	• ILC2s primed mucus production	[226]

BrdU: bromodeoxyuridine; MCMV: murine cytomegalovirus.

Table 15: Stem cells and trained immunity

Condition	Host	Effect	Ref.
Allergy	Human	• Basal cell hyperplasia • Phenotypic shifts in secretory cell antimicrobial expression of respiratory epithelial stem cells • Intrinsic memory of IL-4/IL-13 exposure	[357]
Arthritis	Both	• Persistence of inflammation controlled by epigenetic changes in fibroblasts	[358]
BCG vaccination	Mouse	• Increased myelopoiesis, dependently on IFNγ	[268]
	Human	• Persistent myeloid transcriptomic bias on HSCs, regulated by HNF1a and HNF1b • Resulted in persistent training of monocytes	[306]
β-glucans	Mouse	• Increased myelopoiesis, dependently on IL-1β	[269]
Cecal ligation and puncture	Mouse	• Increased myelopoiesis • Increased production of IL-6 • Transcriptional reprogramming	[359]
LPS	Rat	• Epigenetic modifications • Increased expression of IL-6 and IL-8	[360]
L. monocytogenes	Mouse	• Increase of HSCs	[275]
P. aeruginosa	Mouse	• LPS-exposed HSCs show long-term protection *against P. aeruginosa* infection • LPS-exposed HSCs have an increased inflammatory response • LPS induce persisting epigenetic changes in HSCs	[284]
PRR stimulation	Human	• Intestinal stromal cells produced prolonged pro-inflammatory cytokines • Epigenetic modifications and immuno-metabolic mechanisms	[303]
S. aureus	Mouse	• Increased phagocytic killing capacity by bone marrow-derived macrophages *in vitro*	[361]
M. leprae	Mouse	• Epigenetic modifications of progenitor Shwann cells	[362]

PRR: pathogen recognition receptor.

Table 16: Non-immune cells and trained immunity

Cell	Condition	Host	Effect	Ref.
Endothelial cells	LPS	Human	• Increased expression of TLR-4	[363]
			• Increased production of CCL2	[364]
			• Increased production of IL-8	[365]
			• Increased production of IL-1α and IL-1β	[366]
	LPS or IFNγ	Human	• Increased expression of TLR2	[367]
	Ox-LDL	Human	• Pro-inflammatory memory profile • Metabolic and epigenetic reprogramming • Increased expression of TLR2	[368]
Skin epithelial cells	Skin inflammation	Mouse	• Long lived epithelial cells • Increased wound-healing • Memory capacity dependent on IL-1β	[305]
Vascular smooth muscle cells	Ox-LDL or BCG treatment	Human	• Increased production of IL-6, IL-8, CCL2 • Metabolic and epigenetic modifications	[293]

BCG: Bacillus Calmette-Guérin; OxLDL: oxidized low-density lipoprotein; TLR: Toll-like receptor.

1.3.4. Clinical implications of trained immunity

Understanding the mechanisms of trained immunity opens a broad range of therapeutic possibilities. First, trained immunity confers protection from infections. However, it should be noted that most mouse studies tested one single microorganism using one single training agent, making it difficult to drive broad conclusions about protection. This is why, as we will see in section 3.1 [275], we initiated a program to characterize more broadly the interplay between trained immunity and sepsis. Second, in the field of vaccination, trained immunity could provide improve vaccine efficacy or increase the immune response in poor vaccine responders. Trained immunity can be induced by adjuvants (such as TLR agonists and cytokines) [369]. A recent study showed that injection of BCG vaccination to health volunteers increase the protection against viremia induced by yellow fever vaccination [291]. As an example of therapeutic strategy, trained immunity-based treatments could be administered to increased efficiency of the current COVID-19 vaccines. Third, improving immune responses by trained immunity may be beneficial to fight against oncologic diseases. Indeed, BCG is a modulator of immune system during cancer [370]. The FDA approved intravesical BCG instillation as an adjuvant immunotherapy for the treatment of bladder cancer in 1990, making BCG the first FDA-approved immunotherapy treatment [371, 372]. Still today, BCG remains the gold-standard for patients with high-risk non-muscle-invasive bladder cancer, and it has been proposed that BCG immunotherapy relies on trained immunity [373]. Immune paralysis is observed in tumor microenvironment where MDSCs develop [374]. MDSCs undergo temporary epigenetic modification to carry out their functions [375]. This could be used in the design of new trained immunity-based immunotherapy [376]. However, excessive activation of the immune system may promote tumorigenesis or tumor progression through local inflammation, and because cancer cells rely on glycolytic metabolism or transcription factors such as HIF-1α. Hence, trained immunity can be either beneficial or detrimental during oncologic processes. Besides cancer, low-grade persistent inflammation may favor the development of inflammatory, age-associated disorders such as familial fever syndromes, neurological diseases, arthritis, atherosclerosis, type 2 diabetes and systemic lupus erythematosus [349]. Going along with this assumption, recent studies showed that a Western diet, rich in fats, sugars, salt and low in fiber, promotes the establishment of trained phenotype [307, 377]. Therefore, trained immunity might be fine-tuned in order to improve or to dampen the immune system according to the environmental situation.

1.4. Sepsis

While trained immunity protects from infections, conversely, infections and sepsis may induce trained immunity as suggested in a model of cecal ligation and puncture induced sepsis [359]. Sepsis may be caused by highly virulent pathogens or genetic predispositions impairing the mounting of appropriate inflammatory responses. Inappropriate inflammatory and immune responses, by default or by excess, can result in uncontrolled microbial growth, tissue injury, vascular collapse and multiorgan failure. Indeed, the latest definition of sepsis published in 2016, Sepsis-3, defines sepsis as “a life-threatening organ dysfunction caused by a dysregulated host response to infection” [378]. Septic shock is a subset of sepsis with circulatory, cellular and metabolic abnormalities profound enough to substantially increase mortality [378]. From an immuno-pathogenetic point of view, sepsis is characterized by an exacerbation of antimicrobial defense mechanisms, culminating into the so-called “cytokine storm” liable of tissue injury, organ dysfunctions and early mortality. The early inflammatory response is associated with a parallel shift towards resolution of inflammation and tissue repair. While necessary for restoring homeostasis, this change is involved in sepsis-induced immuno-paralysis or immunosuppression responsible for long-term immune disabilities and the development of secondary, nosocomial infections accounting for late mortality. Community-acquired pneumonia (CAP) and ventilator-associated pneumonia (VAP) are among the most common infections responsible of sepsis [379-381]. Some patients surviving sepsis develop chronic critical illness (CCI) characterized

by long-lasting immunosuppression. This state, characterized by persistent low-grade inflammation associated with catabolism and malnutrition, is known as persistent inflammation immunosuppression and catabolism syndrome (PICS). PICS is associated with long-term morbidity, late organ failures and late mortality [66].

1.4.1. Epidemiology

Sepsis is among the leading causes of mortality with around fifty million cases per year, resulting in over eleven million deaths and huge costs for society [382]. Sepsis is a primary cause of death from infection and of preventable deaths, representing 19.7% of all global deaths. Neonates, infants, seniors and immunosuppressed patients are at high risk of developing sepsis [383]. Both incidence and case-fatality rates of sepsis are higher in males than females [384]. The incidence and mortality of sepsis are higher in sub-Saharan Africa, Oceania and Southeast Asia. This is mainly due to a lack of improved medical care and hygiene, contaminated drinking water [385].

The most common sites of infection are the lungs (60% of adult and 40% of pediatric sepsis cases), abdomen, urinary tract, bloodstream and skin/soft tissue [382]. The etiologic infectious organism is identified in about 60-65% of patients with sepsis [386-389]. Bacteria are predominant, with 35-45% gram negative bacteria and 30-40% are gram positive bacteria, followed by fungi in 12-16% of the cases [382]. Most common microorganisms isolated from children and adults with sepsis include *Escherichia coli*, *Klebsiella spp.*, *Enterobacter*, *Pseudomonas spp.*, *Proteus fragilis*, *Bacteroides fragilis*, *Staphylococcus aureus*, *Streptococcus pneumoniae* and *pyogenes, Enterococcus* and *Candida spp.* [386-388, 390].

1.4.2. Immune response in lungs during sepsis

Lung is the most common site of infection leading to sepsis (i.e. pneumosepsis). During sepsis, the host response to infection is disturbed and can results into acute lung injury and acute respiratory distress syndrome (ARDS), causing irreversible damage to the lungs (***Figure* 12**) [391, 392]. The initial inflammatory phase of sepsis can be accompanied by fever, hypotension, tachycardia and tachypnea [393]. Many biological pathways are (over) activated, such as the complement, the coagulation, the kinin and inflammatory signaling (MAPK, IRFs, NF-κB) pathways. Consequently, elevated amounts of pro-inflammatory cytokines (TNF, IL-6, IL-12, IFNγ), chemokines and anaphylatoxins are produced [394]. C5a anaphylatoxin is a chemoattractant for neutrophils, monocytes and macrophages [395]. C5a enhances the generation of ROS, granular enzymes, pro-inflammatory cytokines and chemokines by neutrophils and the production of pro-inflammatory cytokines by macrophages, amplifying the inflammatory response [395]. Additionally, bronchoalveolar epithelial cells increase the expression of complement receptors C3aR and C5aR, which further contribute to neutrophil, basophil, monocyte and lymphocyte infiltration and participates to severe acute lung injury [396, 397].

Neutrophil infiltration into the lungs depends on the expression of adhesion molecules like intracellular adhesion molecule-1 (ICAM-1) and vascular cell adhesion molecule-1/VCAM-1, integrins, whose expression increases on endothelial cells, together with pro-inflammatory cytokines and chemokines (CXCL1, CXCL2, CXCL8, CXCL10, CCL-3, macrophage inflammatory protein-1α/MIP-1α) [398-403]. As aforementioned, the endothelial barrier function, which is maintained by cell cytoskeleton (actin) and tight junctions, is impaired. This is partly due to a disruption in the integrity of the endothelium in response to neutrophil adhesion and release of pro-inflammatory and oxidative mediators (reviewed in [404]). This enhances vascular fluid leakage, creating a massive loss of intravascular proteins and plasma fluids into the extravascular space [405]. Moreover, coagulation promoted by inflammatory cytokines and complement activation cause damage to the endothelium [406, 407]. Platelets become a source of P-selectin for neutrophils attachment, which in turn produce NETs [47]. This is accompanied with vasodilation that leads to tissue edema [407]. The major threat is that breakdown of the endothelial barrier leads to uncontrolled bleeding and organ dysfunction [408-410]. Exposure of

neutrophils to a systemic inflammatory environment increases their life span due to suppression of apoptosis [411, 412].

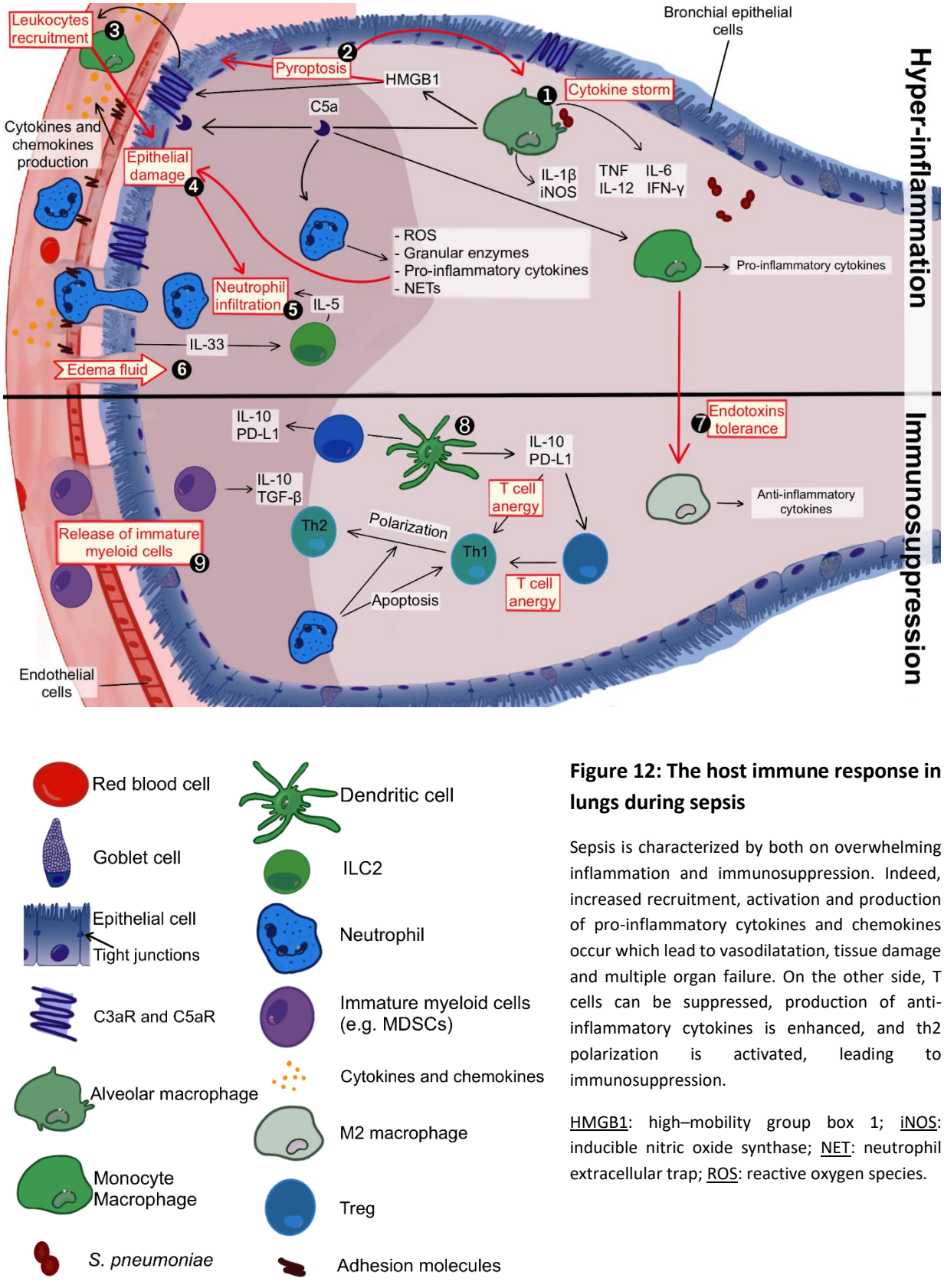

Figure 12: The host immune response in lungs during sepsis

Sepsis is characterized by both on overwhelming inflammation and immunosuppression. Indeed, increased recruitment, activation and production of pro-inflammatory cytokines and chemokines occur which lead to vasodilatation, tissue damage and multiple organ failure. On the other side, T cells can be suppressed, production of anti-inflammatory cytokines is enhanced, and th2 polarization is activated, leading to immunosuppression.

HMGB1: high–mobility group box 1; iNOS: inducible nitric oxide synthase; NET: neutrophil extracellular trap; ROS: reactive oxygen species.

Alveolar macrophages promote neutrophil infiltration into the lungs [413]. In addition, high–mobility group box 1 (HMGB1) released by alveolar macrophages upregulates ICAM-1 and VCAM-1 [414] and promotes pyroptosis of macrophages and endothelial cells [415]. HMGB1 activates the NLRP3 inflammasome and subsequent IL-1β release. IL-1β reduces cyclic adenosine monophosphate (cAMP) and cAMP response element-binding (CREB) in pulmonary endothelial cells, inducing pulmonary vascular endothelial damage and leakage [416], which is exacerbated by the production of inducible NOS (iNOS) by alveolar macrophages [417]. In the resolution phase, macrophages undergo reprogramming (M1 to M2) towards the production of anti-inflammatory mediators [418, 419].

DCs are depleted in the acute inflammatory phase of sepsis, and as a consequence produce less IL-12 for T cell help [420, 421]. Surviving DCs express reduced levels of HLA-DR and produce more IL-10, enhancing immunosuppression [422]. DCs can also be responsible for T cell anergy or proliferation of Tregs [423]. NK cells participate in hyper-inflammation state observed during sepsis [424, 425] but they can also participate in the immunosuppressive stage by producing IL-10 when stimulated by DCs [426].

Parallel to inflammation, immunosuppression occurs during sepsis [427]. It is marked by an increase expression of C-reactive protein (CRP), the most important marker for PIICS [428], neutrophilia and release of immature myeloid cells [429-431]. Immature neutrophils induce T cell suppression and Th2 polarization [432, 433], a loss of monocyte inflammatory cytokine production and antigen presentation [434] and an increase in MDSCs [435]. Both immature neutrophils and MDSCs secrete anti-inflammatory cytokines such as IL-10 and TGF-β. An increase of PD-L1 is also observed during sepsis, suppressing T cell function [436]. Additionally, the suppressor activity of Tregs is increase and subsequently causes T cell anergy [437, 438].

1.4.3. Immuno-regulatory therapies

Current therapies of sepsis are based on control of the infection, adequate antibiotic prescription and supportive measures, as reviewed elsewhere [439]. The first clinical study in sepsis dates back to 1982, and tested the activity of endotoxin (LPS) antiserum. Since then, around 100 phase II or phase III clinical trials testing more than 20 targets of microbial or host origin have been performed, unfortunately with overall negative results [440-442]. Thus, there is no sepsis-specific drug on the market. Despite intensive research, management of sepsis continues to carry controversy [443]. A major issue with sepsis management is the lack of effective tools for early diagnosis and treatment decision-making [439]. Attempts at developing effective therapies to prevent sepsis have proven to be difficult. In 2017, the World Health Assembly and the WHO adopted a resolution to improve the prevention, diagnosis and management of sepsis.

Therapeutic approaches have targeted hyper-inflammation or immunosuppression in sepsis, (***Table 17***, reviewed in [444]), up to now without real success. Two main reasons account for the failures of the clinical trials testing immunotherapy in sepsis: 1) partial knowledge of the pathophysiological mechanisms of sepsis, and 2) heterogeneity of the disease, which reflects heterogeneous and evolutive immune status of patients [427, 445-447]. Hence, theranostics approaches have to be implemented to follow-up the immune status and select the most suitable host-directed immunotherapy (stimulatory or inhibitory) to be initiated in a personalized manner [448-450]. This is the goal of ongoing national and international initiatives, among which the H2020 ImmunoSep (Personalized immuno-therapy in sepsis: a precision medicine-based approach) and HDM-FUN (Host directed medicine in invasive fungal infection) consortia for which our Service is a partner. This was also an objective of the H2020 Marie Skłodowska-Curie “European Sepsis Academy: towards new biomarkers to improve sepsis management” consortium in which I was recruited to perform my PhD.

Table 17: Past and future host-targeted therapies in sepsis

Target		Ref.
Targets to dampen immune over-activation and related organ failure		
Inhibition of innate immune response	TNF	[451-459]
	TLR signaling	[451-459]
	Inflammasome/IL-1 targeting	[460-466]
	Pyroptosis	[467-470]
	cGAS-STING signaling	[471-474]
	C3a and C5a blockage	[475-480]
Immunothrombosis	Activated protein C (APC)	[481-483]
Endothelial dysfunction	Angiopoietin 1 and 2	[484, 485]
	Adrenomedullin	[486-489]
Pleiotropic drugs	Hydrocortisone, ascorbic acid, thiamine, antibiotics	[490-501]
Target for stimulation/restoration of immune responses		
	FLT3L, GM-CSF, IFNγ, IL-7, IL-15	[502-504]
	Anti-IL-10	[505, 506]
	Anti-CD40, anti-OX40	[507-513]
	Mesenchymal stem cells	[514, 515]
	Immune checkpoint inhibitors (anti-PD1/PDL1 and -CTLA4)	[516-520]

We will comment on some of the host-directed therapies that have been tested and/or developed for sepsis (***Table 17***). Studies in the early 90's investigating the role of TNF during sepsis showed that it is highly increased and associated with sepsis pathogenesis [521, 522]. This prompted the development of anti-TNF monoclonal antibodies, which were among the first immunomodulatory therapy tested in clinical trials. While some studies have shown that neutralizing TNF increased mortality [452, 453], others have shown that it could reduce mortality [454]. A systematic meta-analysis of 17 studies with 8971 patients suggest that, in the most severely ill patients, anti-TNF therapy may improve survival [523]. Targeting the TLR pathways is promising for cancer but possibly also sepsis, either through inhibition of TLR pathways during the acute inflammatory phase or by using TLR agonists as adjuvants to reverse immunosuppression [455, 524]. However, clinical trials with the TLR4 antagonist Eritoran (Esai company) did not meet primary endpoints in a large clinical study and was abandoned as a sepsis therapy [525]. Inhibition of inflammasome pathways has also been proposed as an interesting target, with a focus on NLRP3, IL-1β and IL-18. In fact, the recombinant IL-1R antagonist (IL-1RA) anakinra is being tested to dampen inflammatory responses in sepsis patients preselected based on their immune profile. As previously discussed, pyroptosis is an inflammatory lytic programmed cell death associated with sepsis. As such, targeting pyroptosis may improve sepsis survival. cGAS-STING pathways is triggered in response to DNA in the cytoplasm [526], leading to phosphorylation and activation of IRF3 and TBK1. STING, TBK1 and IRF3 have all been found significantly increased in PBMCs of septic patients. This makes the cGAS-STING pathway a good target for sepsis therapy [527]. Blocking C5a and C3a has also improved survival in various clinical studies [475-480].

During sepsis, the coagulation system is strongly activated and there is growing evidence suggesting that thrombosis has a major impact on immune defenses. In this direction, the role of activated protein C (rhAPC) has been discussed. Recombinant human APC (rhAPC, trademark Xigris®, Eli Lilly) has been approved in 2001 as a sepsis-specific drug. Unfortunately, 10 years later it was withdrawn from the market following a large randomized, double-blind, placebo-controlled, multicenter trial showing no beneficial effect of the drug [528]. Following the coagulation system impairment, endothelial impairment is also targeted in sepsis therapy. In this interest, angiopoietin reduces leukocyte transmigration and cytokine production [529, 530] and hold promises. Additionally, adrenomedullin possess anti-inflammatory properties by regulating endothelial cells [531].

Pleiotropic drugs such as antibiotics, hydrocortisone and vitamins have been investigated for their immunomodulatory functions [490-498]. Low-dose corticosteroids may reduce mortality of sepsis, however, several studies suggest that corticosteroid could have no or even negative effects [498, 532, 533]. On the contrary, a relatively novel strategy is to restore immune responses in patients with immunosuppression. One of the possibilities for that is to use immuno-stimulatory cytokines and growth factors such as IFNγ [505, 506], GM-CSF [502-504] and IL-7 [507-513]. Additionally, mesenchymal stem cells are known to reduce organ injury and mortality in animal model of sepsis, increasing their function could also be beneficial in human sepsis [514, 515]. Finally, targeting immune checkpoint pathways using anti-PD1/PDL1 and anti-CTLA4 have more recently gained a lot of attention in order to prevent apoptotic cell death and restore the function of primarily lymphocytes. The use of checkpoint inhibitors is being investigating in sepsis treatment [516-520].

2. AIMS

When we started this work, trained immunity had just been shown to protect from candidiasis and staphylococcal infection, and myeloid progenitors, monocyte and macrophages to be the main drivers of innate immune training. Numerous questions were open, such as the breadth and the length of protection conferred by trained immunity, as well as the implication or cell types beyond monocytes/macrophages. To start addressing these questions, we defined four objectives, the first three ones being based on the usage of preclinical mouse models of infection/sepsis, and the fourth one based on human studies:

1. The **first objective** was to determine the range of infections against which training is protective, the cells and the functions involved in this protection (**Section 3.1**).

2. The **second objective** was to investigate whether training induced by β-glucans protect from pneumococcal infection and the dynamic of lung ILCs (**Section 3.2**).

3. The **third objective** was to evaluate whether trained immunity induced by β-glucans confers long-lasting protection against listeriosis (**Section 3.3**).

4. The **fourth objective** was to investigate the modulation of peripheral ILCs during airway infections in humans, in order to address whether ILCs could be used as (bio) markers of disease severity (**Section 3.4**).

3. RESULTS

This part is divided into four sections:

1. Trained immunity confers broad-spectrum long-term protection against infections
2. Trained immunity increases lung phagocytes and protects from pneumococcal pneumonia
3. Trained immunity confers long lasting protection from listeriosis
4. ILCs in human infections

3.1. Trained immunity confers broad-spectrum long-term protection against infections

Eleonora Ciarlo[1], Tytti Heinonen[1], Charlotte Théroude[1], Fatemeh Asgari[1], Jacobus Herderschee[1], Didier Le Roy[1], Mihai G. Netea[3,4], Thierry Roger[1]

[1]Infectious Diseases Service, Department of Medicine, Lausanne University Hospital and University of Lausanne, Epalinges, Switzerland

[2]Department of Biomedical Sciences, Humanitas University, Milan, Italy

[3]Radboud Center for Infectious Diseases (RCI), and Department of Internal Medicine, Radboud University Medical Center, Nijmegen, The Netherlands

[4]Department for Genomics & Immunoregulation, Life and Medical Sciences Institute (LIMES), University of Bonn, Bonn, Germany

***The Journal of Infectious Diseases**. 2020 Nov 9;222(11):1869-1881. doi: 10.1093/infdis/jiz692.*

Summary

Induction of trained immunity is associated with metabolic, epigenetic and functional reprograming of innate immune cells. Yet, the overall impact of trained immunity on host defenses and ability to survive infections remains largely unknown. To address that question, we developed a model of training induction by zymosan, a cell-wall preparation rich in b-glucans. Here we show that priming trained immunity through a unique protocol protected mice from an amazingly large panel of infections with leading etiologic agents of sepsis, including systemic infections, peritonitis, enteritis and pneumonia. Trained immunity increased bone marrow myeloid progenitors and circulating Ly6C^{high} (antimicrobial) monocytes and PMNs, and amplified blood antimicrobial responses. Monocytes/macrophages and IL-1 signaling were required to protect trained mice from listeriosis. Thus, trained immunity confers broad-spectrum protection against lethal infections, including at anatomical sites distant from the priming site. These observations support the development of trained immunity-based strategies to improve host defenses against infections.

Contribution to the work: I participated to the cell population analysis. I helped with *in vivo* experiments. I revised the paper.

The Journal of Infectious Diseases

MAJOR ARTICLE

Trained Immunity Confers Broad-Spectrum Protection Against Bacterial Infections

Eleonora Ciarlo,[1] Tytti Heinonen,[1] Charlotte Théroude,[1] Fatemeh Asgari,[2] Didier Le Roy,[1] Mihai G. Netea,[3,4] and Thierry Roger[1]

[1]Infectious Diseases Service, Department of Medicine, Lausanne University Hospital and University of Lausanne, Epalinges, Switzerland, [2]Department of Biomedical Sciences, Humanitas University, Milan, Italy, [3]Radboud Center for Infectious Diseases, and Department of Internal Medicine, Radboud University Medical Center, Nijmegen, The Netherlands, and [4]Department for Genomics & Immunoregulation, Life and Medical Sciences Institute, University of Bonn, Bonn, Germany

Background. The innate immune system recalls a challenge to adapt to a secondary challenge, a phenomenon called *trained immunity*. Training involves cellular metabolic, epigenetic and functional reprogramming, but how broadly trained immunity protects from infections is unknown. For the first time, we addressed whether trained immunity provides protection in a large panel of preclinical models of infections.

Methods. Mice were trained and subjected to systemic infections, peritonitis, enteritis, and pneumonia induced by *Staphylococcus aureus, Listeria monocytogenes, Escherichia coli, Citrobacter rodentium,* and *Pseudomonas aeruginosa*. Bacteria, cytokines, leukocytes, and hematopoietic precursors were quantified in blood, bone marrow, and organs. The role of monocytes/macrophages, granulocytes, and interleukin 1 signaling was investigated using depletion or blocking approaches.

Results. Induction of trained immunity protected mice in all preclinical models, including when training and infection were initiated in distant organs. Trained immunity increased bone marrow hematopoietic progenitors, blood Ly6C^{high} inflammatory monocytes and granulocytes, and sustained blood antimicrobial responses. Monocytes/macrophages and interleukin 1 signaling were required to protect trained mice from listeriosis. Trained mice were efficiently protected from peritonitis and listeriosis for up to 5 weeks.

Conclusions. Trained immunity confers broad-spectrum protection against lethal bacterial infections. These observations support the development of trained immunity-based strategies to improve host defenses.

Keywords. innate immunity; infection; sepsis; trained immunity; peritonitis; *Listeria*; pneumonia; monocyte/macrophage; neutrophil; stem cell.

We used preclinical models to demonstrate that trained immunity confers broad-spectrum protection against bacterial infections. Trained immunity increased myeloid progenitors and circulating inflammatory monocytes and neutrophils, and depletion or neutralization of monocytes/macrophages and interleukin 1 signaling impaired trained immunity-mediated protection.

Innate immune cells express pattern recognition receptors specific for microbial-associated and danger-associated molecular patterns that are released by stressed or injured cells. The interaction of pattern recognition receptors with microbial- or danger-associated molecular patterns activates intracellular signaling pathways that coordinate metabolic adaptation, epigenetic changes, and gene expression. The cellular and soluble mediators mobilized on infection regulate the development of the inflammatory response, the establishment of antimicrobial cellular and humoral responses, and the restoration of homeostasis once the pathogen has been contained or eradicated. Dysfunctions in these processes may have dramatic consequences for the infected host, as observed in patients with sepsis [1–5].

It has long been thought that immunological memory was restricted to antigen-specific memory and a privilege of the adaptive immune system carried by lymphocytes. However, the description of systemic acquired resistance in plants, specific memory in invertebrates, antigen-specific memory by natural killer cells, and heterologous protection conferred by BCG, smallpox, and measles vaccines suggested the existence of a form of innate immune memory [6–13]. The term *trained immunity* was proposed to reflect the fact that the innate immune system recalls or adapts to a first challenge to mount a robust response to a secondary challenge by a similar or dissimilar microbial stimulus [14, 15]. The concept of innate immune training was posed by showing that a nonlethal challenge

Received 30 August 2019; editorial decision 20 December 2019; accepted 30 December 2019; published online December 31, 2019.

Correspondence: Thierry Roger, Infectious Diseases Service, Lausanne University Hospital and University of Lausanne, CLED.04.407, Chemin des Boveresses 155, CH-1066 Epalinges, Switzerland (Thierry.Roger@chuv.ch).

The Journal of Infectious Diseases® 2020;222:1869–81

DOI: 10.1093/infdis/jiz692

by *Candida albicans* improved the innate immune response of mice [16].

The molecular mechanisms underlying trained immunity include metabolic, epigenetic, and functional reprogramming of bone marrow myeloid precursors and innate immune cells. β-glucan, a fungal cell wall compound commonly used to study trained immunity, is detected by monocytes/macrophages through the dectin 1 receptor. Dectin 1 triggering activates a PI3K (phosphoinositol 3-kinase)/AKT/mTOR (mammalian target of rapamycin)/HIF-1α (hypoxia-inducible factor-1α) pathway that induces a metabolic shift toward aerobic glycolysis, increases glutaminolysis that replenishes the tricarboxylic acid cycle, activates the cholesterol synthesis pathway, and blocks the itaconate pathway [16–21]. As a consequence, metabolites such as fumarate, succinate, and mevalonate accumulate and act as cofactors of epigenetic modifiers and as amplifiers of trained immunity [19, 22]. β-glucan, *C. albicans*, and BCG vaccine induce genome-wide epigenetic changes, including monomethylation and trimethylation of histone (H) 3 lysine (K) 4 and acetylation of H3K27 at promoters and enhancers of genes associated with metabolic, immune, and host defense pathways [16, 23, 24]. Hence, trained monocytes/macrophages produce increased levels of cytokines (tumor necrosis factor [TNF], interleukin 1β [IL-1β], and interleukin 6 [IL-6]) when challenged with microbial compounds [16, 19, 24, 25].

Whether the induction of trained immunity confers a wide-ranging advantage during infections is unknown. Therefore, we questioned to which extent trained immunity protects from heterologous infections and at anatomic sites distant from the priming training site. Our results showed that a unique training scheme potently protected mice from clinically relevant pathogens inoculated through diverse routes to induce peritonitis, systemic infections, enteritis and pneumonia. Trained immunity was particularly efficient at protecting mice from lethal listeriosis, which was dependent on monocytes/macrophages and interleukin 1 (IL-1) signaling.

MATERIALS AND METHODS

Products used in this study are described in Supplementary Table 1.

Ethics Statement

Animal experimentation was approved by the Service des Affaires Vétérinaires, Direction Générale de l'Agriculture, de la Viticulture et des Affaires Vétérinaires, état de Vaud (Epalinges, Switzerland) under authorizations 876.9 and 877.9 and performed according to Swiss and Animal Research: Reporting of In Vivo Experiments (ARRIVE) guidelines.

Mice, Cells, and Bacteria

C57BL/6J (wild-type, MyD88$^{-/-}$, and Toll-like receptor [TLR] 2$^{-/-}$), and BALB/cByJ female mice (Charles River Laboratories) were 8–10 weeks old. Mice were housed under specific pathogen-free conditions (license VD-H04). Mice were free of mouse hepatitis and norovirus. Bone marrow cells were cultured in Roswell Park Memorial Institute medium [26], supplemented with 50 IU/mL macrophage colony-stimulating factor (M-CSF) (ImmunoTools) to generate bone marrow–derived macrophages (BMDMs). BMDMs were trained as described elsewhere [18, 23]. Bone marrow cells were cultured for 24 hours with 10 µg/mL zymosan and M-CSF, washed, cultured 6 days in fresh medium containing M-CSF, detached, enumerated, and seeded (2×10^6 cells/mL) in 96-well plates.

Peritoneal cells obtained by a peritoneal lavage were plated at 10^5 cells/well in 96-well plate in 100 µL of Roswell Park Memorial Institute, washed after 4 hours, and stimulated for 24 hours. *Listeria monocytogenes* 10403S, methicillin-resistant *Staphylococcus aureus* AW7, and *Escherichia coli* O18 were grown in brain-heart infusion broth, *Citrobacter rodentium* DBS100 in LB Broth Miller, *Pseudomonas aeruginosa* PAO1 in LB Broth Lennox, and *C. albicans* 5102 in yeast extract–peptone-dextrose [27–30]. Heat inactivation was performed for 2 hours at 70°C.

Flow Cytometry

Cells were collected and stained as described in the **Supplementary Methods**, using antibodies described in Supplementary Table 1 [31, 32]. Data were acquired using an Attune NxT Flow Cytometer (Thermo Fisher Scientific) and analyzed using FlowJo_V10_CL software (FlowJo). Gating strategies are presented in Supplementary Figure 1.

Whole-Blood Bactericidal Assay and Cytokine Production

The whole-blood assay is described in the **Supplementary Methods**. Cytokines were quantified by means of enzyme-linked immunosorbent assay, a ProCarta kit (Invitrogen), and a Bio-Plex 200 system (Bio-Rad) [33].

Isolation of Bone Marrow Monocytes and Chromatin Immunoprecipitation

The isolation of bone marrow monocytes and chromatin immunoprecipitation were performed as described in the **Supplementary Methods** [34].

In Vivo Models

Age-matched female mice were randomly divided into groups. Mice were injected intraperitoneally with 1 mg of zymosan or heat-killed *C. albicans* or intravenously with 0.1 mg of zymosan before bacterial challenge. Staphylococcal sepsis was also tested in BALB/cByJ mice. Enteritis was induced in TLR2$^{-/-}$ mice deprived of food for 8 hours before bacterial challenge. The role of monocytes/macrophages was assessed using mice injected intraperitoneally with 200 µL of clodronate or phosphate-buffered saline liposomes (LIPOSOMA research) 7 and 4 days before infection. The role of polymorphonuclear neutrophils (PMNs) was assessed using mice injected intraperitoneally with 100 µg of 1A8 anti-Ly6G monoclonal antibody (mAb) or 2A3

immunoglobulin G2a isotype control mAb (Bio X Cell) 6 days, 3 days, and 1 day before infection.

Cell depletion (≥95% and ≥60% for monocytes/macrophages and PMNs, respectively) was evaluated on the day of infection by means of flow cytometry. Depletion in trained mice reduced PMNs to levels similar to those measured in isotype control mAb-treated untrained mice (mean [standard deviation], 3.7 [1.2] vs 2.7 [0.7] × 10^6 PMNs/mL; n = 8; $P > .05$). To assess the role of IL-1 signaling, mice were injected intraperitoneally with 500 µg of anakinra (Kineret; Sobi) 6, 5, 4, and 3 days before infection. Body weight, severity score, and survival were recorded at least once daily [35].

Statistical Analyses

Graphics represent data obtained from individual mice, or boxes with minimum-to-maximum whiskers. Data were analyzed for normal distribution and homogeneity of variances and compared with the appropriate parametric (2-tailed unpaired Student *t*) or nonparametric (2-tailed Mann-Whitney) statistical test. The false discovery rate was controlled, when necessary. The Kaplan-Meier method was used for building survival curves, and differences were analyzed using the log-rank sum test. Analyses were performed using PRISM version 8.0.1 software (GraphPad Software). *P* values were 2 sided.

RESULTS

Impact of Trained Immunity on *E. coli* Peritonitis

C57BL/6J mice were trained with zymosan, a cell wall preparation rich in β-glucan, given intraperitoneally 7 and 3 days before infection [18] unless specified otherwise (Figure 1A). In a first model, control and trained mice were challenged intraperitoneally with *E. coli*. Trained mice coped much better with peritonitis than control mice, showing lower severity scores, absence of *E. coli* dissemination in the blood, and improved survival rates (92% vs 23% survival; $P < .001$) (Figure 1B). Cytokine levels were increased in the blood of trained mice (Figure 1B), likely reflecting diffusion from the peritoneal cavity in which trained cells responded massively to *E. coli*.

Supporting this assumption, peritoneal cells from trained mice produced high levels of TNF and IL-6 in response to lipopolysaccharide (LPS) stimulation (Figure 1C). Moreover, the peritoneal cavity of trained mice contained more leukocytes, among which were more phagocytes (Figure 1D). PMNs were increased 8.2-fold, and there was a shift in the macrophage population. In control mice, the peritoneal cavity contained mainly homeostatic large peritoneal macrophages (LPMs) that virtually disappeared in trained mice at the expense of inflammatory and bactericidal small peritoneal macrophages (SPMs).

Impact of Trained Immunity on Systemic Staphylococcal and *Listeria* Infections

To explore whether trained immunity protected from systemic infections, C57BL/6J mice were injected intravenously with methicillin-resistant *S. aureus*. Trained mice survived better than control mice (31% vs 0% survival; $P = .006$) and had 10-fold less bacteria in blood 2 days after infection (Figure 2A). Very similar results were obtained using BALB/cByJ mice (Supplementary Figure 2*A*), and subsequent experiments were all performed using C57BL/6J mice.

Mice were challenged intravenously with a lethal dose of *L. monocytogenes*. Most strikingly, all trained mice survived infection, whereas all control mice died within 5 days (Figure 2B). Bacteria were not detected in blood collected from trained mice 2 and 3 days after infection, whereas up to 10^5 colony-forming units/mL were measured in the circulation of control mice (Figure 2B and Supplementary Figure 2B). Trained mice had 2–3-log lower counts of *L. monocytogenes* in spleen, liver, and kidney (Figure 2B), and *L. monocytogenes* was undetectable in organs collected from mice surviving infection for 1–2 months.

Confirming an efficient control of bacterial burden in trained mice, cytokines and chemokines were detected at much lower concentrations in blood collected 3 days after infection (Figure 2B). Training mice with zymosan given intravenously as a single dose 7 days before infection also efficiently reduced bacterial burden, suggesting that training can be induced through diverse routes (Figure 2C). Because training was demonstrated by challenging mice with heat-killed *C. albicans* [16], we questioned whether a similar approach would protect from listeriosis. Mice trained with heat-killed *C. albicans* were powerfully protected from lethal listeriosis ($P = .002$) and had greatly reduced bacteremia (Figure 2D). Thus, trained immunity efficiently protected mice from systemic bacterial infections.

Impact of Trained Immunity on Enteritis and Pneumonia

To extend the panel of microorganisms and routes of inoculation tested, we developed models of enteritis and pneumonia. Enteritis induced by *C. rodentium* was established in TLR2$^{-/-}$ mice, because the bacteria are cleared quickly in immunocompetent animals. All mice lost weight and had some diarrhea, but none died. Trained and control mice recovered their initial weights 7 and 18 days after infection, respectively. Trained mice showed improved weight from day 7 to day 30 ($P < .01$) (Figure 3A). Pneumonia was induced by an intranasal challenge with *P. aeruginosa*. The survival of trained mice was largely improved ($P = .02$) (Figure 3B). Overall, trained immunity protected mice in all the preclinical models tested, suggesting the enhancement of broad mechanisms of defense.

Impact of Trained Immunity on Blood Antimicrobial Activity and Myelopoiesis

Trained immunity protected mice remarkably well from systemic listeriosis (92 of 96 trained mice survived vs 0 of 74 control mice; n = 5 experiments). We reasoned that blood should provide an efficient barrier against *L. monocytogenes* burden. Ex vivo, the blood of trained mice limited the growth of *L. monocytogenes* better than that of control mice (Figure 4A),

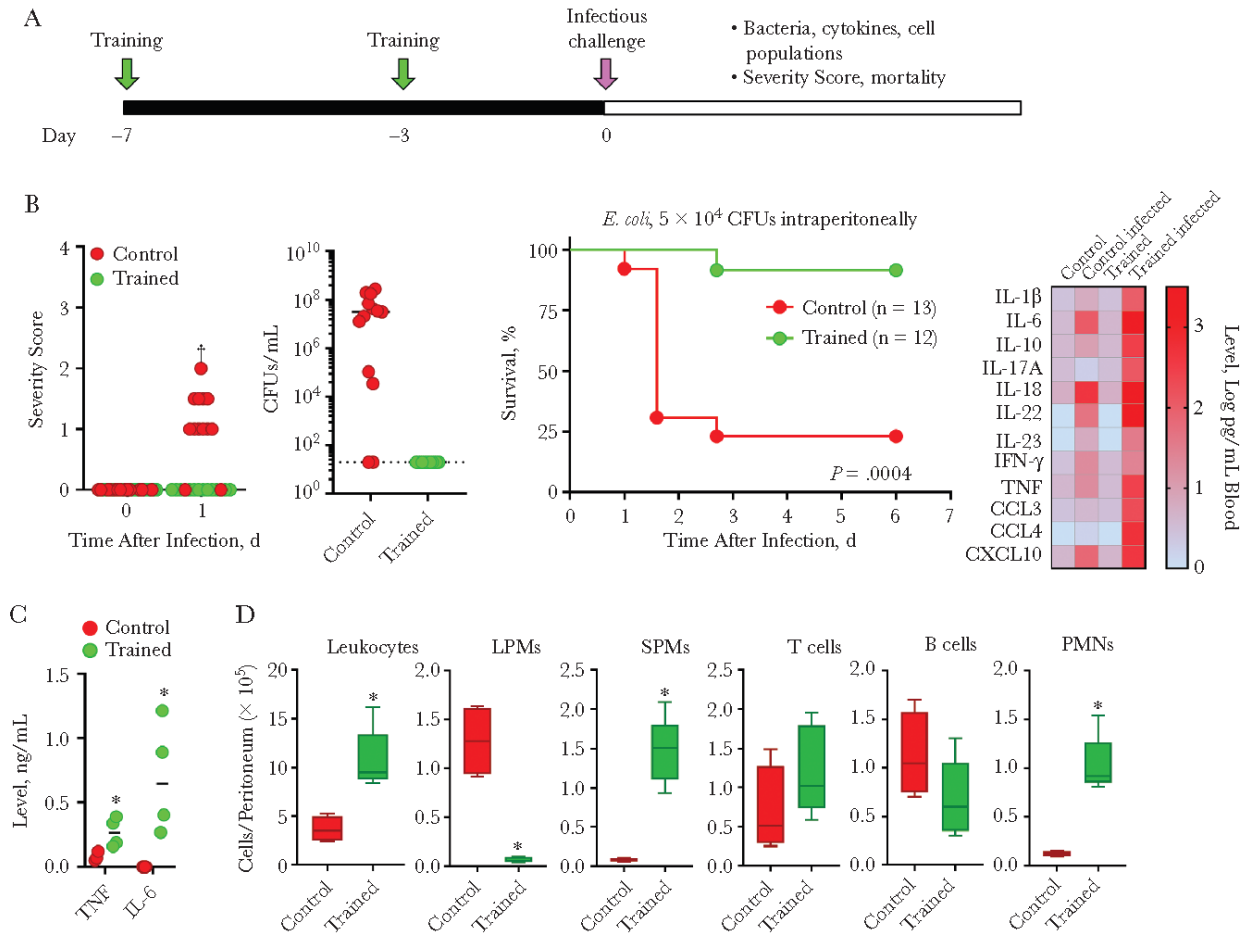

Figure 1. Trained immunity protects from *Escherichia coli* peritonitis. *A*, Experimental model to study protection from infection mediated by trained immunity. Unless specified otherwise, training was induced by 2 intraperitoneal injections of 1 mg zymosan, performed 4 days apart (at –7 and –3 days) using C57BL/6J mice. *B*, Control and trained mice were challenged intraperitoneally with 10^4 colony-forming units (CFUs) of *E. coli*. Severity score and survival were recorded. Blood was collected 18 hours after infection to quantify bacteria (Dashed line indicates lower limit of detectio) and cytokines using Luminex technology (n = 6 mice per group). *C*, Tumor necrosis factor (TNF) and interleukin 6 (IL-6) production by peritoneal cells from control and trained mice exposed ex vivo for 6 hours (TNF) or 24 hours (IL-6) to 10 ng/mL lipopolysaccharide. *D*, Leukocytes in the peritoneal cavity of control and trained mice before infection (n = 4–5 mice). *$P \leq .05$; †$P \leq .001$. Abbreviations: CCL, C-C motif chemokine ligand; CXCL, C-X-C motif chemokine ligand; IFN, interferon; IL-1β (etc), interleukin 1β (etc); LPMs, large peritoneal macrophages; PMNs, polymorphonuclear neutrophils; SPMs, small peritoneal macrophages; TNF, tumor necrosis factor.

and it was more reactive to microbial products, as shown by increased production of TNF and IL-6 in response to LPS, CpG, Pam_3CSK_4, *L. monocytogenes* and *C. albicans* (Figure 4B).

We then quantified leukocytes in control and trained mice, using blood collected before and 2 days after infection with *L. monocytogenes* (Figure 4C). Training increased leukocyte counts 1.6 fold, reflecting more $Ly6C^{high}$, $Ly6C^{int}$, and $Ly6C^{low}$ monocytes (inflammatory, intermediate, and nonclassic monocytes) and PMNs (7.6-, 3.9-, 1.9-, and 4.7-fold increase, respectively, vs control; $P < .05$). In trained mice, $Ly6C^{high}$ and $Ly6C^{int}$ monocytes expressed more CD11b/Itgam (2.5- and 1.8-fold higher mean fluorescence intensity), indicative of a primed/activated phenotype (Supplementary Figure 3). Conversely, PMNs expressed lower CD11b (2.5 lower mean fluorescence intensity), which is associated with an immature status [36]. The absolute numbers of T and B lymphocytes were not affected.

L. monocytogenes induced a massive depletion of leukocytes 2 days after infection, which was less pronounced in trained mice (2.9- vs 11.5-fold decrease in trained vs control mice) (Figure 4C). $Ly6C^{high}$ and $Ly6C^{low}$ monocytes were more preserved in trained mice. PMNs were rather stable in trained mice, but they decreased 9.9-fold in control mice. T cells and B cells decreased 4–7-fold in trained mice, but 40-fold in control mice. The relative preservation of blood leukocytes suggested an enhanced hematopoiesis in trained mice. Indeed, the bone marrow of trained mice contained more long-term hematopoietic stem cells and more multipotent progenitors (MPPs), including more myeloid-biased MPP3 and lymphoid-biased MPP4 (Figure 4D).

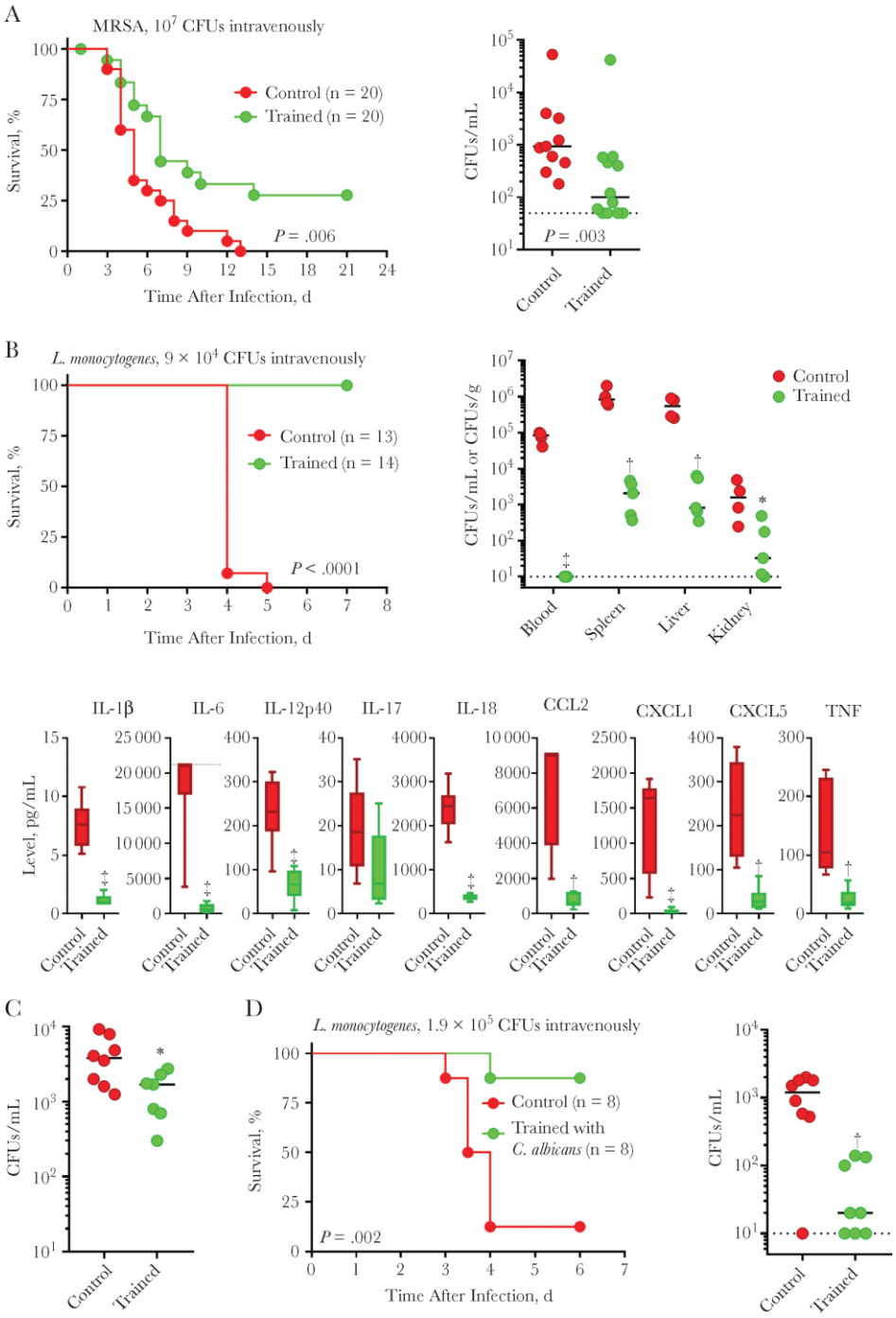

Figure 2. Trained immunity protects from systemic staphylococcal and *Listeria* infections. *A*, Control and trained mice were challenged intravenously with 10^7 colony-forming units (CFUs) of methicillin-resistant *Staphylococcus aureus* (MRSA). Survival was recorded. Blood was collected 2 days after infection to quantify bacteria. *B*, Control and trained mice were challenged intravenously with 9×10^4 CFUs of *Listeria monocytogenes*. Survival was recorded. Blood, spleen, liver, and kidney were collected 3 days after infection to quantify bacteria. Dashed line indicates lower limit of detection. Blood was collected 2 days after infection to quantify cytokines using Luminex technology (n = 6 mice per group). Dashed line indicates upper limit of detection. *C*, Control mice and mice trained with zymosan intravenously (0.1 mg at day −7) were infected intravenously with 10^5 CFUs of *L. monocytogenes*. Blood was collected 2 days after infection to quantify bacteria. *D*, Control mice and mice trained with heat-killed *Candida albicans* were infected intravenously with 1.9×10^5 CFUs of *L. monocytogenes*. Survival was recorded, and blood was collected 2 days after infection to quantify bacteria. *$P \leq .05$; †$P \leq .01$; ‡$P \leq .001$. Abbreviations: CCL, C-C motif chemokine ligand; CXCL, C-X-C motif chemokine ligand; IL-1β (etc), interleukin 1β (etc); TNF, tumor necrosis factor.

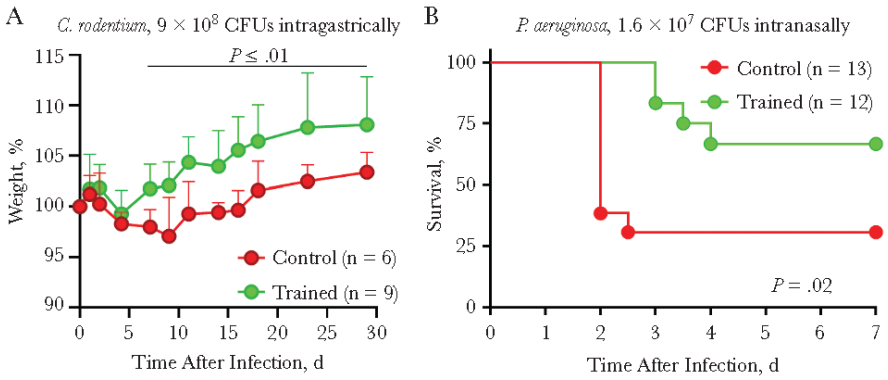

Figure 3. Trained immunity protects from enteritis and pneumonia. *A*, Weight of control and trained mice challenged intragastrically with 9×10^8 colony-forming units (CFUs) of *Citrobacter rodentium*. *B*, Survival of control and trained mice challenged intranasally with 1.6×10^7 CFUs of *Pseudomonas aeruginosa*.

Role of Monocytes/Macrophages and IL-1 Signaling

We analyzed the impact of depleting monocytes/macrophages by treating mice with clodronate liposomes during induction of training. Clodronate treatment fully abolished the protection conferred by training (Figure 5A). Because PMNs were also increased during training, we tested the impact of PMN depletion using anti-Ly6G mAb. In both trained and control mice, the depletion of PMNs modified neither survival nor bacteremia (Figure 5B). Two days after infection, PMNs were still fully depleted from the blood of anti-Ly6G mAb-treated mice, whether trained mice or control mice (Figure 5C). These observations suggested that monocytes are central effector cells for the protection against listeriosis conferred by trained immunity.

We tested the contribution of IL-1β/IL-1 signaling, because IL-1β has been proposed to play a role in trained immunity [37]. IL-1β was detected at higher concentrations in blood from trained mice (Figure 6A). Blood from trained mice showed a trend toward producing higher levels of IL-1β on exposure to *L. monocytogenes*, and BMDMs trained in vitro with zymosan produced higher levels of IL-1β in response to *L. monocytogenes* (Figure 6A).

Because MyD88 is the adaptor signaling molecule downstream interleukin 1R, we quantified leukocytes as a surrogate of IL-1 signaling-mediated training in MyD88$^{-/-}$ mice. None of the changes observed in trained wild-type mice were detected in trained MyD88$^{-/-}$ mice, which behaved similarly to untrained MyD88$^{-/-}$ mice (Supplementary Figure 4). The role of IL-1 signaling was tested in mice treated daily for 4 days with recombinant IL-1 receptor antagonist (anakinra) during the induction of trained immunity (Figure 6B-C). Severity score and weight loss ($P < .01$ and $P < .001$, respectively) were increased in anakinra-treated mice. Accordingly, 3 of 8 anakinra-treated trained mice died of listeriosis, whereas all trained mice survived infection ($P = .06$). The partial effect on mortality rate was related to a partial (1.4-fold) reduction in Ly6C^{high} monocytes ($P = .02$) (Figure 6C). These data supported the assumption that IL-1 signaling is involved in the antilisterial activity conferred by trained immunity. Interestingly, chromatin immunoprecipitation assays performed on monocytes isolated 3 weeks after the induction of training revealed increased marks associated with active chromatin (H3K4me1 and H3K4me3, Figure 6D) and trained immunity [16, 23, 24].

Length of Protection Conferred by Trained Immunity

The length of protection conferred by trained immunity against lethal bacterial infections is unknown. To start filling that gap, we analyzed mice trained up to 5 weeks earlier (Figure 7A). In the peritoneal cavity, leukocytes steadily increased from 2 to 5 weeks after training, reaching a maximum after 5 weeks (Figure 7B). The decreased number of LPMs remained drastic at all time points, whereas the number of SPMs increased 2–5 weeks after training. PMNs reached a maximum value 2 week after training and remained stable for up to 5 weeks. In line with these observations, mice trained 5 weeks earlier were protected from *E. coli* peritonitis, as shown by reduced weight loss and bacterial dissemination into the blood compared with untrained mice (Figure 7C). Blood cytokine levels increased mainly 1–2 weeks after training, and returned to baseline levels 5 weeks after challenge (Figure 7D). Moreover, blood leukocyte counts were back to normal 5 weeks after training (Figure 7D). Impressively, mice trained 1, 2, 4, or 5 weeks earlier were all protected from listeriosis, in term of both survival and bacteremia (Figure 7D).

DISCUSSION

We report the first broad analysis of the impact of trained immunity on bacterial infections. Trained immunity protected mice from a large panel of clinically relevant bacterial pathogens inoculated systemically and locally to induce peritonitis, enteritis, and pneumonia.

In all models, bacterial dissemination was controlled. In the peritonitis model, this results from a massive accumulation of PMNs and SPMs in the peritoneal cavity. At baseline, SPMs

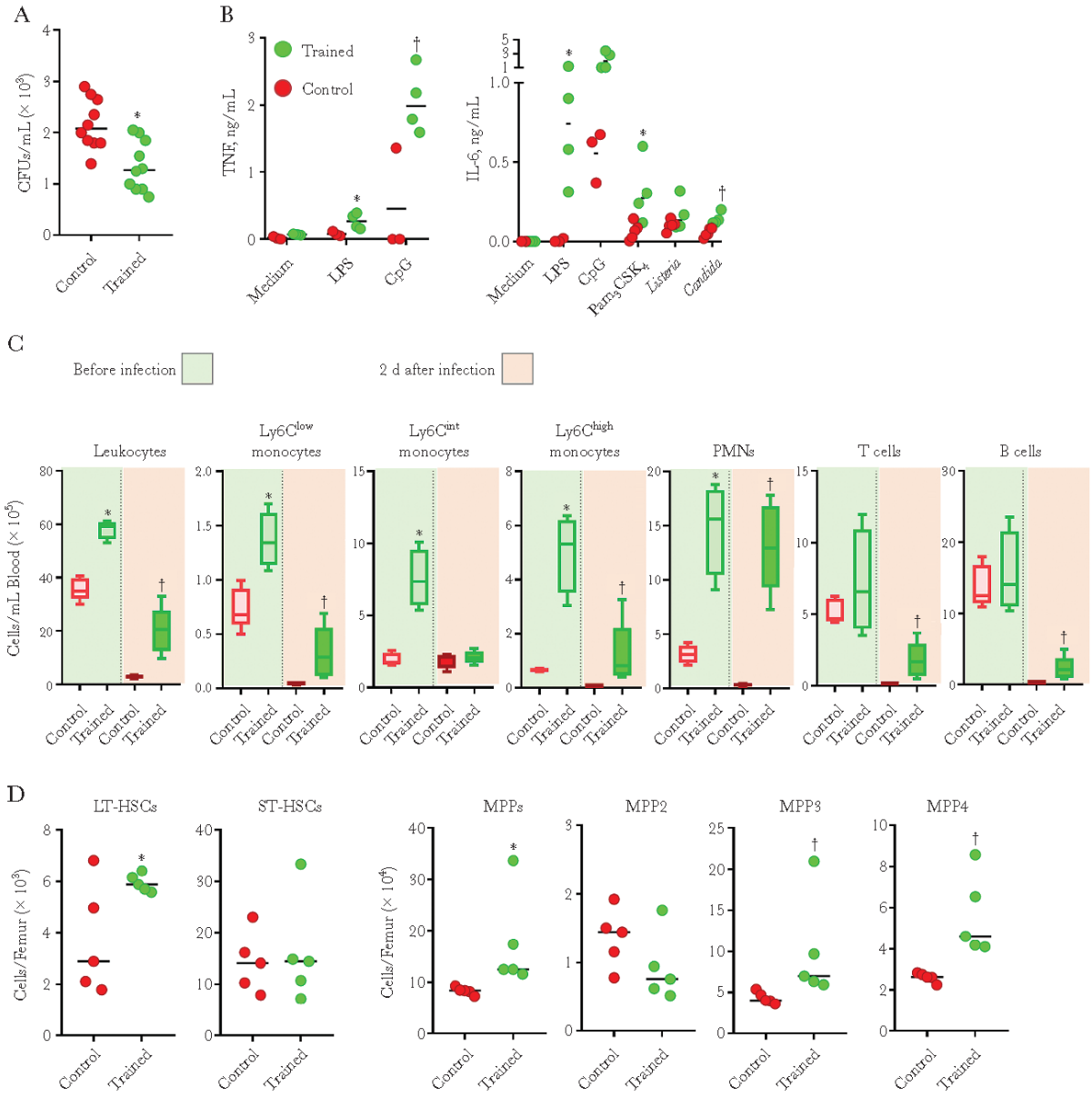

Figure 4. Trained immunity increases blood antimicrobial activity and stimulates myelopoiesis. *A*, Bacteria in whole blood from control and trained mice exposed ex vivo for 2 hours to 1.2×10^3 colony-forming units (CFUs)/mL of *Listeria monocytogenes*. *B*, Tumor necrosis factor (TNF) and interleukin 6 (IL-6) production by whole blood from control and trained mice exposed ex vivo for 6 hours (TNF) or 24 hours (IL-6) to 10 ng/mL lipopolysaccharide (LPS), 10 µmol/L CpG, 100 ng/mL Pam_3CSK_4, 10^7 heat-killed *L. monocytogenes*, and 10 mg/mL heat-killed *Candida albicans*. *C*, Leukocytes in blood collected from control and trained mice before infection (*left part*) and 2 days after an intravenous challenge with 1.1×10^5 CFUs of *L. monocytogenes* (*right part*) (n = 5 mice per group). *D*, Long-term and short-term hematopoietic stem cells (LT-HSCs and ST-HSCs), multipotent progenitors (MPPs), MPP2, MPP3, and MPP4 in the bone marrow of control and trained mice. *$P \leq .05$; †$P \leq .01$. Abbreviation: PMNs, polymorphonuclear neutrophils.

represent <10% of peritoneal macrophages, which are composed mainly of self-maintaining LPMs. Local inflammation triggers the migration of LPMs to the omentum, where these cells produce growth factors and chemokines that stimulate myelopoiesis and induce the influx of PMNs and inflammatory monocytes, which are precursors of SPMs [38]. Hence, LPMs and SPMs play key roles as initiator and effector cells of trained immunity when training and infection occur in the peritoneum.

Stimulation of myelopoiesis greatly increased blood leukocyte counts, above all those of PMNs and Ly6C^{high} inflammatory monocytes exhibiting a primed/activated phenotype. Changes in peripheral blood gave an indubitable advantage to trained mice during systemic infections, as demonstrated in models of listeriosis and staphylococcal infection. The picture was rather unexpected in the model of listeriosis, because almost all trained mice survived a challenge equivalent to 10–20

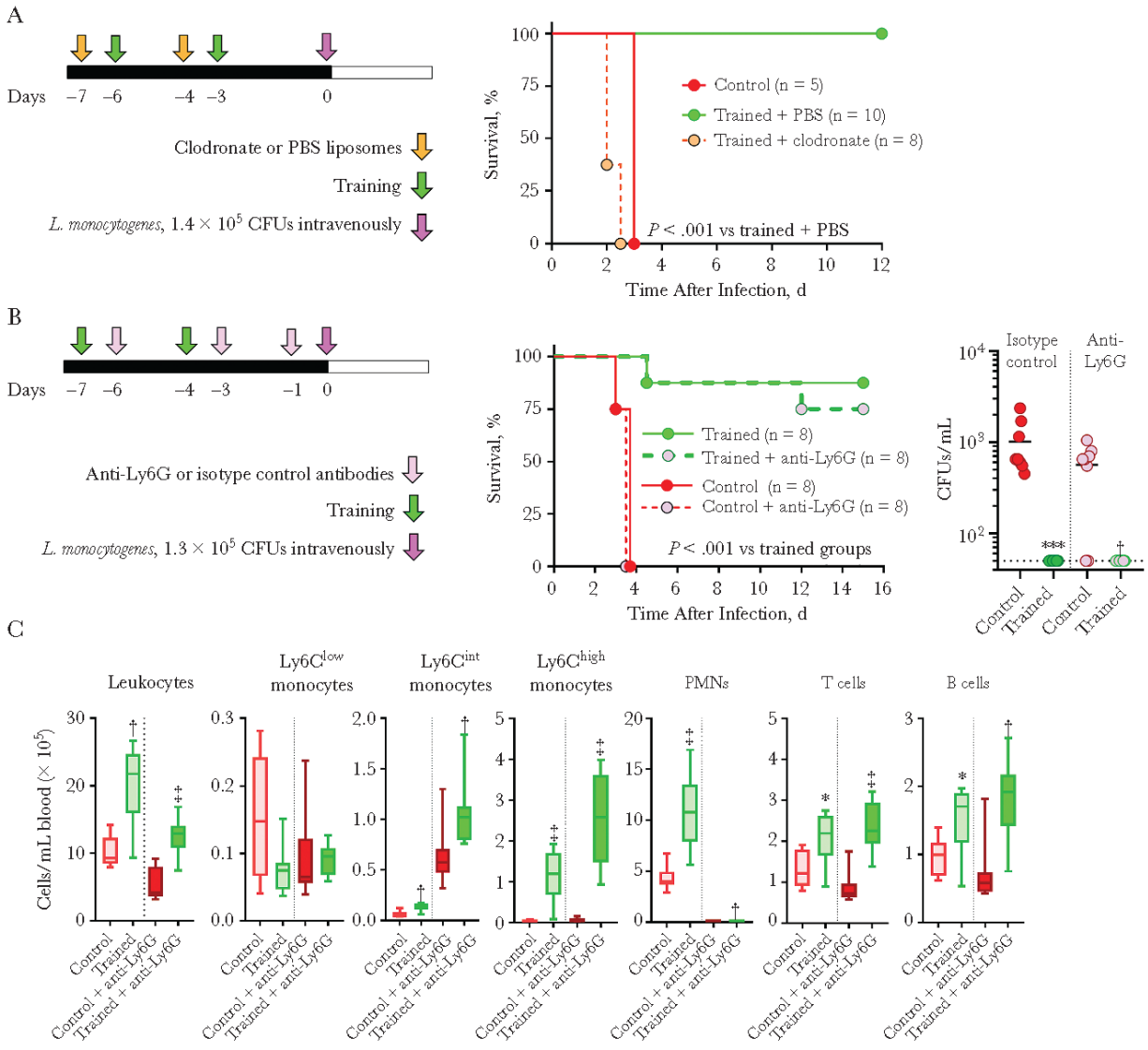

Figure 5. Monocytes/macrophages are essential to protect trained mice from listeriosis. *A*, Experimental model to study the role of monocytes/macrophages in trained immunity (*left*) and survival of mice treated with clodronate or phosphate-buffered saline (PBS) liposomes and challenged intravenously with 1.4×10^5 colony-forming units (CFUs) of *Listeria monocytogenes* (*right*). *B*, Experimental model to study the role of polymorphonuclear neutrophils (PMNs) in trained immunity (*left*). Survival of mice treated with anti-Ly6G or isotype control antibody and challenged intravenously with 1.3×10^5 CFUs of *L. monocytogenes* (*middle*) and bacteria in blood collected 18 hours after infection (right). *C*, Leukocytes in blood collected 2 days after infection with *L. monocytogenes* (n = 8 mice per group.) * $P \leq .01$; † $P \leq .01$; ‡ $P \leq .001$.

times the LD_{100}. Results of cell depletion experiments suggested that monocytes/macrophages were the main drivers of protection. This is in agreement with the fact that inflammatory monocytes were essential whereas PMNs were dispensable for clearing bacteria during the early and late phases of systemic infection by *L. monocytogenes* [39]. Circulating inflammatory monocytes migrated to foci of infection in liver and spleen to give rise to TNF- and inducible nitric oxide synthase–producing dendritic cells and monocyte-derived macrophages that replenished Kupffer cells dying through necroptosis. This helped enhance antibacterial immunity and restore tissue integrity [40, 41].

Trained immunity protected mice from enteritis and pneumonia, pointing to distant effects. Intraperitoneal injections of LPS induced epigenetic reprogramming of brain resident macrophages and modulated neuropathology in models of Alzheimer disease and stroke [42]. The broad effects of trained immunity during infections may result from the action of soluble mediators that directly or indirectly stimulate the response of intestinal, airway, and lung parenchyma cells or resident immune cells. For example, adenoviral infection improved the activity of self-renewing memory alveolar macrophages that promoted neutrophilia and protected from *Streptococcus pneumoniae* lung infection [43].

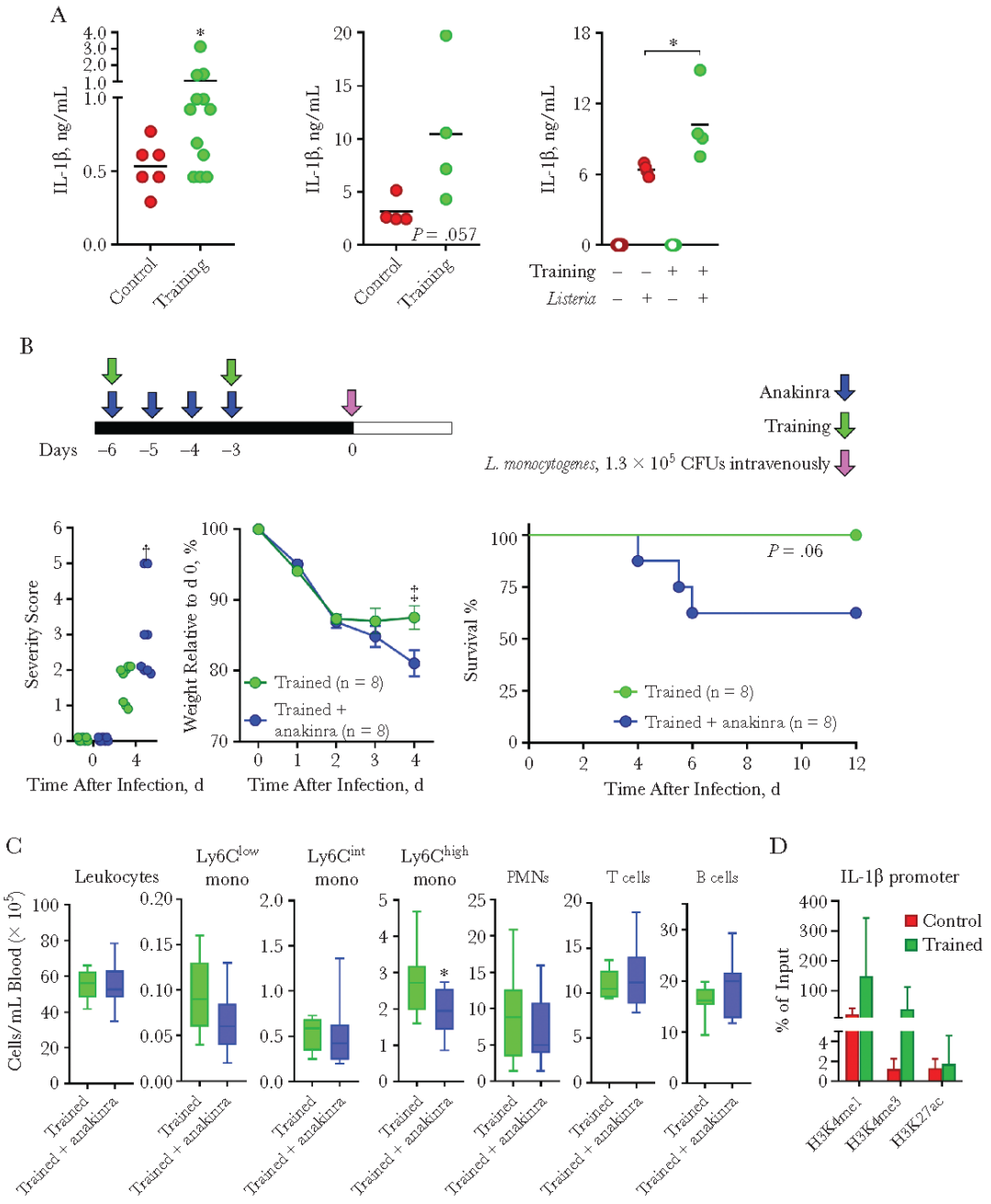

Figure 6. Interleukin 1 (IL-1) signaling participates to protect trained mice from listeriosis. *A*, Interleukin 1β (IL-1β) concentrations in blood collected from control and trained mice at day 0 (*left*), in whole blood from control and trained mice exposed ex vivo for 6 hours to 10^8 heat-killed *Listeria monocytogenes* (*middle*), and in cell culture supernatants of control and trained bone marrow–derived macrophages cultured for 24 hours with or without 1 live *L. monocytogenes* per cell (*right*). *B*, Experimental model to study the role of IL-1 signaling in trained immunity (*top*). Severity score, weight loss, and survival (*bottom*) of mice trained with or without anakinra treatment and challenged intravenously with 1.3×10^5 colony-forming units (CFUs) of *L. monocytogenes* (n = 8 mice per group). *C*, Leukocytes in blood collected just before infection from mice trained with or without anakinra (n = 9–10 mice per group). *D*, H3K4me1, H3K4me3 and H3K27ac signal at the *Il1b* promoter of bone marrow monocytes isolated from mice trained or not 3 weeks earlier were quantified by chromatin immunoprecipitation followed by real-time polymerase chain reaction and expressed as percentage of input (n = 4 mice per group). *$P \leq .05$; †$P \leq .01$; ‡$P \leq .001$. Abbreviation: PMNs, polymorphonuclear neutrophils.

Bone marrow hematopoietic stem and progenitor cells adapted to acute and chronic peripheral inflammation and infection through cell-extrinsic and cell-intrinsic mechanisms, increasing proliferation and skewing toward the myeloid lineage to provide activated innate immune cells [44–46]. Our training protocol increased the number of hematopoietic stem cells and MPPs, accounting for higher leukocyte counts before and during infection. In the same vein, the adoptive transfer

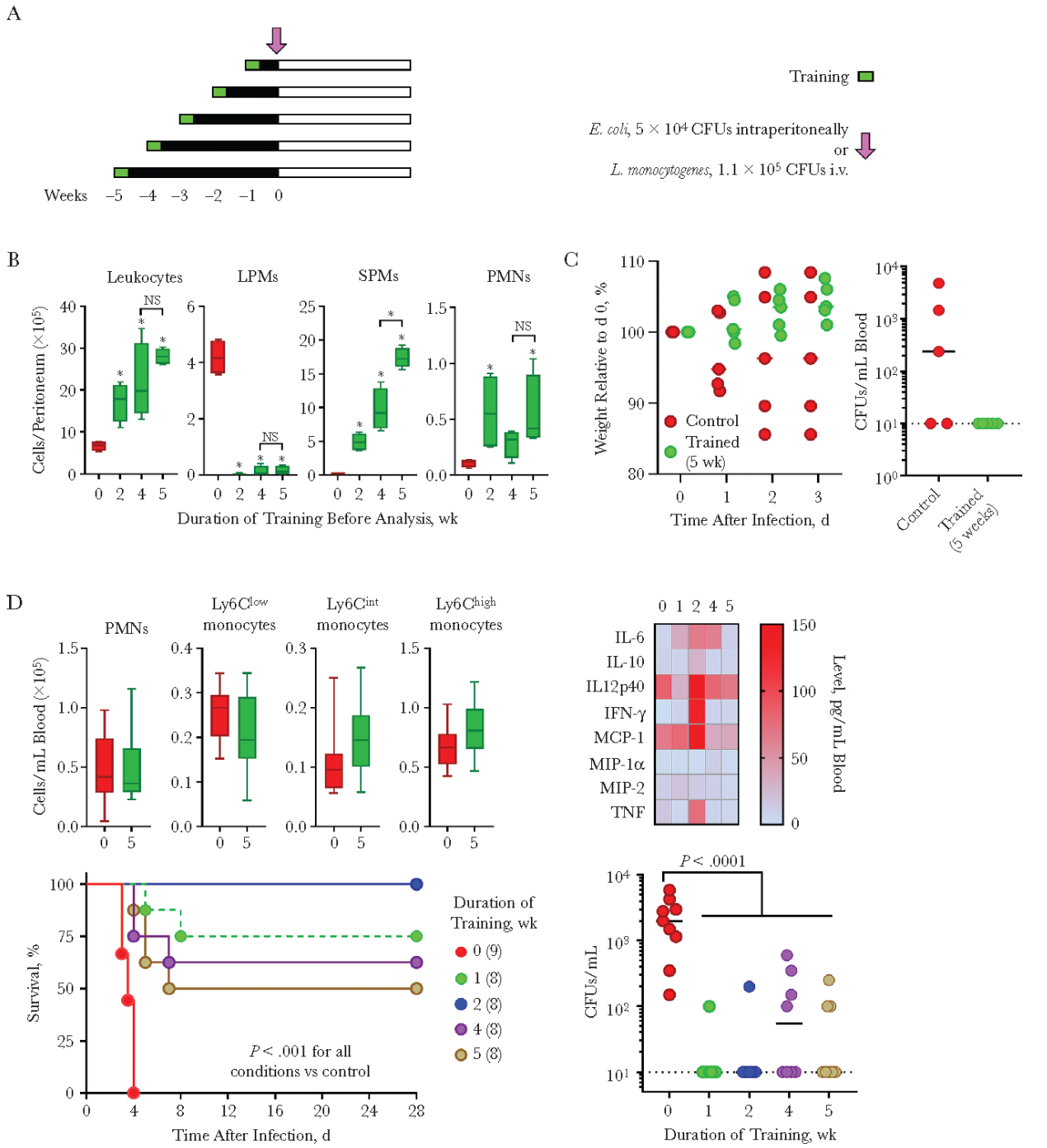

Figure 7. Trained immunity protects from peritonitis and listeriosis for at least 5 weeks. *A*, Experimental model to study the effects of training over time. *B*, Leukocytes in the peritoneal cavity of mice trained 0, 2, 4, and 5 weeks earlier (n = 5 mice per group). *C*, Weight loss and bacteria in blood collected 2 days after an intraperitoneal challenge with 5×10^4 colony-forming units (CFUs) of *Escherichia coli*. *D*, Leukocytes (n = 8–10) and cytokines (n = 6) in blood of mice trained 0, 1, 2, 4 and 5 weeks earlier (*top*). Survival and bacteria in blood collected 2 days after infection of mice challenged intravenously with 1.1×10^5 CFUs of *Listeria monocytogenes*). #$P \leq .05$. Abbreviations: IFN, interferon; IL-6 (etc), interleukin 6 (etc); LPMs, large peritoneal macrophages; MCP, monocyte chemoattractant protein; MIP, macrophage inflammatory protein; NS, not significant; PMNs, polymorphonuclear neutrophils; SPMs, small peritoneal macrophages; TNF, tumor necrosis factor.

in naive mice of long-term hematopoietic stem cells or bone marrow cells collected from mice trained with β-glucan and BCG vaccine increased the proportion of blood $Gr1^+CD11b^+$ myeloid cells and protected from pulmonary tuberculosis [25, 44]. We are performing experiments to delineate the length of protection conferred by trained immunity. This information

will be valuable for preclinical and clinical development of trained immunity-based therapeutics.

The diversity of the models of infection tested supports wide effects of trained immunity. Work will be required to establish whether trained immunity protects from additional bacterial, fungal and viral infections. Trained immunity is most typically induced with β-glucan, which promotes T-helper (Th) 1/Th17 proinflammatory responses essential to fight bacteria, viruses, and fungi. However, training might be tipped toward Th2 immune responses beneficial during parasitic infections [47].

IL-1β has gained attention as a possible hub regulating trained immunity [24, 37, 44–46]. Uninfected trained mice expressed increased blood levels of IL-1β, and treatment with anakinra compromised trained immunity, indicating that IL-1 signaling played a role. Trained peripheral blood mononuclear cells produced higher levels of IL-1β, and IL-1β itself fueled human monocytes to produce higher levels of cytokines on stimulation [17]. In vivo, BCG vaccine–induced IL-1β production was correlated with the capacity to control viremia in healthy subjects challenged with yellow fever vaccine [24]. IL-1 family members can affect trained immunity through manifold mechanisms [37]. Interestingly, training mice with β-glucan sustained IL-1β signaling that promoted glycolytic activity and proliferation of hematopoietic stem and progenitor cells [44]. This aspect is highly relevant for listeriosis, which affects blood leukocytes and constrains vigorous myelopoiesis. Inflammasomes control IL-1β secretion and are likely to be involved in trained immunity. Supporting this hypothesis, feeding *Ldr*$^{-/-}$ atherosclerotic mice a Western diet induced an oxidized low-density lipoprotein/NOD-like receptor family, pyrin domain containing 3 (NLRP3)/IL-1 axis, leading to the establishment of trained immunity [45].

Induction of trained immunity is an attractive approach to increase vaccine efficacy and resistance to pathogens. Training with β-glucan counteracted endotoxin-mediated immune tolerance associated with poor outcome in sepsis [3, 4, 21, 48]. However, immunotherapies may have doubled-edge sword effects. Low-grade inflammation sustained by trained immunity may be involved in the pathophysiology of chronic and autoinflammatory disorders [49]. Monocytes from patients with hyperimmunoglobulin D syndrome have a trained phenotype [22] and Western diet feeding induced trained immunity [45]. Interfering with the sensing of training inducers, IL-1 signaling, and inflammation, metabolic and epigenetic changes may be exploited to avoid pathogenic processes linked to trained immunity. For instance, trained immunity induced by helminth products provided an anti-inflammatory environment, attenuating the development of experimental autoimmune encephalomyelitis [50].

In summary, induction of trained immunity remodeled bone marrow and blood cellular compartments, providing efficient barriers against bacterial infections. Protection was remarkably broad when considering the pathogens and sites of infection tested. These data support the development of trained immunity-based strategies to improve the efficacy of vaccines and host defenses against infections, and they may give clues about the pathological processes underlying inflammatory and autoimmune disorders.

Notes

Author contributions. E. C., T. H., and D. L. R. performed the in vitro experiments. E. C., T. H., C. T., F. A., and D. L. R. performed the in vivo experiments. T. R. conceived the project. M. G. N. provided protocols and discussed the project. E. C. and T. R. designed the experiments and wrote the article. All authors discussed the results and revised the article.

Financial support. This work was supported by the Swiss National Science Foundation (grants 149511 and 173123 to T. R.), the Société Académique Vaudoise (scholarship to T. H.), and the European Sepsis Academy Horizon 2020 Marie Skłodowska-Curie Action: Innovative Training Network (grant 676129 to C. T. and F. A.).

Potential conflicts of interest. All authors: No reported conflicts. All authors have submitted the ICMJE Form for Disclosure of Potential Conflicts of Interest. Conflicts that the editors consider relevant to the content of the manuscript have been disclosed.

References

1. Savva A, Roger T. Targeting Toll-like receptors: promising therapeutic strategies for the management of sepsis-associated pathology and infectious diseases. Front Immunol **2013**; 4:387.
2. Singer M, Deutschman CS, Seymour CW, et al. The Third International Consensus Definitions for Sepsis and Septic Shock (Sepsis-3). JAMA **2016**; 315:801–10.
3. van der Poll T, van de Veerdonk FL, Scicluna BP, Netea MG. The immunopathology of sepsis and potential therapeutic targets. Nat Rev Immunol **2017**; 17:407–20.
4. Venet F, Monneret G. Advances in the understanding and treatment of sepsis-induced immunosuppression. Nat Rev Nephrol **2018**; 14:121–37.
5. Ciarlo E, Savva A, Roger T. Epigenetics in sepsis: targeting histone deacetylases. Int J Antimicrob Agents **2013**; 42(suppl):S8–12.
6. Kurtz J, Franz K. Innate defence: evidence for memory in invertebrate immunity. Nature **2003**; 425:37–8.
7. Sadd BM, Schmid-Hempel P. Insect immunity shows specificity in protection upon secondary pathogen exposure. Curr Biol **2006**; 16:1206–10.
8. Kachroo A, Robin GP. Systemic signaling during plant defense. Curr Opin Plant Biol **2013**; 16:527–33.
9. Goodridge HS, Ahmed SS, Curtis N, et al. Harnessing the beneficial heterologous effects of vaccination. Nat Rev Immunol **2016**; 16:392–400.
10. Farber DL, Netea MG, Radbruch A, Rajewsky K, Zinkernagel RM. Immunological memory: lessons from

the past and a look to the future. Nat Rev Immunol **2016**; 16:124–8.
11. de Bree LCJ, Koeken VACM, Joosten LAB, et al. Non-specific effects of vaccines: Current evidence and potential implications. Semin Immunol **2018**; 39:35–43.
12. Netea MG, Schlitzer A, Placek K, Joosten LAB, Schultze JL. Innate and adaptive immune memory: an evolutionary continuum in the host's response to pathogens. Cell Host Microbe **2019**; 25:13–26.
13. Cerwenka A, Lanier LL. Natural killer cell memory in infection, inflammation and cancer. Nat Rev Immunol **2016**; 16:112–23.
14. Netea MG, Quintin J, van der Meer JW. Trained immunity: a memory for innate host defense. Cell Host Microbe **2011**; 9:355–61.
15. Netea MG, Joosten LA, Latz E, et al. Trained immunity: a program of innate immune memory in health and disease. Science **2016**; 352:aaf1098.
16. Quintin J, Saeed S, Martens JHA, et al. *Candida albicans* infection affords protection against reinfection via functional reprogramming of monocytes. Cell Host Microbe **2012**; 12:223–32.
17. Ifrim DC, Joosten LA, Kullberg BJ, et al. *Candida albicans* primes TLR cytokine responses through a dectin-1/Raf-1-mediated pathway. J Immunol **2013**; 190:4129–35.
18. Cheng SC, Quintin J, Cramer RA, et al. mTOR- and HIF-1α-mediated aerobic glycolysis as metabolic basis for trained immunity. Science **2014**; 345:1250684.
19. Arts RJ, Novakovic B, Ter Horst R, et al. Glutaminolysis and fumarate accumulation integrate immunometabolic and epigenetic programs in trained immunity. Cell Metab **2016**; 24:807–19.
20. Saz-Leal P, Del Fresno C, Brandi P, et al. Targeting SHIP-1 in myeloid cells enhances trained immunity and boosts response to infection. Cell Rep **2018**; 25:1118–26.
21. Dominguez-Andres J, Novakovic B, Li Y, et al. The itaconate pathway is a central regulatory node linking innate immune tolerance and trained immunity. Cell Metab **2019**; 29:211–220 e5.
22. Bekkering S, Arts RJW, Novakovic B, et al. Metabolic induction of trained immunity through the mevalonate pathway. Cell **2018**; 172:135–146 e9.
23. Saeed S, Quintin J, Kerstens HH, et al. Epigenetic programming of monocyte-to-macrophage differentiation and trained innate immunity. Science **2014**; 345:1251086.
24. Arts RJW, Moorlag S, Novakovic B, et al. BCG vaccination protects against experimental viral infection in humans through the induction of cytokines associated with trained immunity. Cell Host Microbe **2018**; 23:89–100 e5.
25. Kaufmann E, Sanz J, Dunn JL, et al. BCG educates hematopoietic stem cells to generate protective innate immunity against tuberculosis. Cell **2018**; 172:176–190 e19.
26. Ciarlo E, Roger T. Screening the impact of sirtuin inhibitors on inflammatory and innate immune responses of macrophages and in a mouse model of endotoxic shock. Methods Mol Biol **2016**; 1436:313–34.
27. Roger T, Froidevaux C, Le Roy D, et al. Protection from lethal gram-negative bacterial sepsis by targeting Toll-like receptor 4. Proc Natl Acad Sci U S A **2009**; 106:2348–52.
28. Meller S, Di Domizio J, Voo KS, et al. T_H17 cells promote microbial killing and innate immune sensing of DNA via interleukin 26. Nat Immunol **2015**; 16:970–9.
29. Roger T, Schneider A, Weier M, et al. High expression levels of macrophage migration inhibitory factor sustain the innate immune responses of neonates. Proc Natl Acad Sci U S A **2016**; 113:E997–1005.
30. Savva A, Brouwer MC, Roger T, et al. Functional polymorphisms of macrophage migration inhibitory factor as predictors of morbidity and mortality of pneumococcal meningitis. Proc Natl Acad Sci U S A **2016**; 113:3597–602.
31. Heinonen T, Ciarlo E, Le Roy D, Roger T. Impact of the dual deletion of the mitochondrial sirtuins SIRT3 and SIRT5 on anti-microbial host defenses. Front Immunol **2019**; 10:2341.
32. Heinonen T, Ciarlo E, Rigoni E, Regina J, Le Roy D, Roger T. Dual deletion of the sirtuins SIRT2 and SIRT3 impacts on metabolism and inflammatory responses of macrophages and protects from endotoxemia. Front Immunol **2019**; 10:2713.
33. Ciarlo E, Heinonen T, Herderschee J, et al. Impact of the microbial derived short chain fatty acid propionate on host susceptibility to bacterial and fungal infections in vivo. Sci Rep **2016**; 6:37944.
34. Roger T, Ding X, Chanson AL, Renner P, Calandra T. Regulation of constitutive and microbial pathogen-induced human macrophage migration inhibitory factor (MIF) gene expression. Eur J Immunol **2007**; 37:3509–21.
35. Roger T, Delaloye J, Chanson AL, Giddey M, Le Roy D, Calandra T. Macrophage migration inhibitory factor deficiency is associated with impaired killing of gram-negative bacteria by macrophages and increased susceptibility to *Klebsiella pneumoniae* sepsis. J Infect Dis **2013**; 207:331–9.
36. Silvestre-Roig C, Hidalgo A, Soehnlein O. Neutrophil heterogeneity: implications for homeostasis and pathogenesis. Blood **2016**; 127:2173–81.
37. Moorlag SJCFM, Röring RJ, Joosten LAB, Netea MG. The role of the interleukin-1 family in trained immunity. Immunol Rev **2018**; 281:28–39.
38. Buscher K, Wang H, Zhang X, et al. Protection from septic peritonitis by rapid neutrophil recruitment through omental high endothelial venules. Nat Commun **2016**; 7:10828.
39. Shi C, Hohl TM, Leiner I, Equinda MJ, Fan X, Pamer EG. $Ly6G^+$ neutrophils are dispensable for defense against systemic *Listeria monocytogenes* infection. J Immunol **2011**; 187:5293–8.
40. Serbina NV, Salazar-Mather TP, Biron CA, Kuziel WA, Pamer EG. TNF/iNOS-producing dendritic cells

mediate innate immune defense against bacterial infection. Immunity **2003**; 19:59–70.
41. Blériot C, Dupuis T, Jouvion G, Eberl G, Disson O, Lecuit M. Liver-resident macrophage necroptosis orchestrates type 1 microbicidal inflammation and type-2-mediated tissue repair during bacterial infection. Immunity **2015**; 42:145–58.
42. Wendeln AC, Degenhardt K, Kaurani L, et al. Innate immune memory in the brain shapes neurological disease hallmarks. Nature **2018**; 556:332–8.
43. Yao Y, Jeyanathan M, Haddadi S, et al. Induction of autonomous memory alveolar macrophages requires T cell help and is critical to trained immunity. Cell **2018**; 175:1634–1650 e17.
44. Mitroulis I, Ruppova K, Wang B, et al. Modulation of myelopoiesis progenitors is an integral component of trained immunity. Cell **2018**; 172:147–161 e12.
45. Christ A, Gunther P, Lauterbach MAR, et al. Western diet triggers NLRP3-dependent innate immune reprogramming. Cell **2018**; 172:162–175 e14.
46. Chavakis T, Mitroulis I, Hajishengallis G. Hematopoietic progenitor cells as integrative hubs for adaptation to and fine-tuning of inflammation. Nat Immunol **2019**; 20:802–11.
47. Yasuda K, Adachi T, Koida A, Nakanishi K. Nematode-infected mice acquire resistance to subsequent infection with unrelated nematode by inducing highly responsive group 2 innate lymphoid cells in the lung. Front Immunol **2018**; 9:2132.
48. Cheng SC, Scicluna BP, Arts RJ, et al. Broad defects in the energy metabolism of leukocytes underlie immunoparalysis in sepsis. Nat Immunol **2016**; 17:406–13.
49. Mulder WJM, Ochando J, Joosten LAB, Fayad ZA, Netea MG. Therapeutic targeting of trained immunity. Nat Rev Drug Discov **2019**; 18:553–66.
50. Quinn SM, Cunningham K, Raverdeau M, et al. Anti-inflammatory trained immunity mediated by helminth products attenuates the induction of T cell-mediated autoimmune disease. Front Immunol **2019**; 10:1109.

Supplementary information

Flow cytometry

Blood. Twenty µl of whole blood were incubated for 30 minutes in the dark at room temperature with 50 µl of antibodies diluted in cell staining medium (CSM: PBS+0.5% BSA). Reaction mixture was diluted with 500 µl of red blood cell lysis buffer (0.65 M ammonium chloride, 10 mM sodium bicarbonate, 0.1 mM EDTA, pH 7.4). After 10 minutes, cells were washed, incubated for 5 minutes with 5% paraformaldehyde (Thermo Fisher Scientific), washed and re-suspended in 1 ml CSM. Samples were kept at 4°C until acquisition. **Peritoneal cells and bone marrow (BM) cells**. Peritoneal cells were obtained by a peritoneal lavage. BM cells obtained from femurs were incubated for 5 minutes on ice with 3 ml ice cold lysis buffer. Peritoneal and BM cells were washed and enumerated, and 5 x 105 or 106 cells were incubated for 30 minutes in the dark at 4°C with 50 µl live/dead dye (Fixable Viability Dye eFluor™ 450 or LIVE/DEAD™ Fixable Violet, Thermo Fisher Scientific), then with 50 µl 2.4G2 monoclonal antibody, and finally with 50 µl of antibodies diluted in CSM. Cells were fixed and kept as detailed for blood. Eight hundred µl of cell suspensions were acquired using an Attune NxT Flow Cytometer (Thermo Fisher scientific). Flow cytometry data were analyzed using FlowJo_V10_CL software (FlowJo LLC, Ashland OR). Gating strategies are presented in **Figure S1**. The antibody mixtures to stain blood cells contained anti-CD3, CD11b, CD45, Ly6C and Ly6G or anti-CD19 and CD45. The antibody mixtures to stain peritoneal cells contained anti-CD11c, CD19, F4/80 and MHC II or anti-CD3 and CD45. The antibody mixtures to stain BM cells contained a lineage cocktail (anti-B220, CD3, CD11b, CD19, Ly-76 and Ly6C/G), anti-CD16/32, CD34, CD117/c-kit and Ly6A/E/Sca-1.

Whole blood bactericidal assay and cytokine production

For bactericidal assay, 20 µl blood were added to 130 µl RPMI GlutaMAX™ containing 1.2 x 103 CFU/ml L. monocytogenes and incubated for 2 hours. Reaction mixtures were plated on blood agar plates. For cytokine production, 20 µl blood were diluted 1:5 in RPMI GlutaMAX™ and incubated for 6 or 24 hours with 10 ng/ml LPS, 10 µM CpG ODN, 100 ng/ml Pam3CSK4, and 107 heat killed L. monocytogenes. Supernatants were collected. Dots are mean of technical triplicates obtained with one mouse.

Isolation of BM monocytes and chromatin immunoprecipitation (ChIP)

Bone marrow (BM) cells were obtained from tibias and femurs of mice. Bone marrow monocytes were isolated with the Monocyte Isolation Kit (BM) (Miltenyi Biotec, Bergisch Gladbach, Germany) following manufacturer's protocol. Briefly, 5×10^7 cells were sequentially incubated with FcR Blocking Reagent, Biotin-Antibody Cocktail (targeting non-monocytic cells), and Anti-Biotin MicroBeads. Magnetic separation was performed trough LS columns. Purity was assessed by flow cytometry. Monocytes were identified according to FSC/SSC parameters as lineage negative (Ter119, B220, CD19, CD3, NK1.1, Ly6G, TCRgd), CD11b+ and CD115+ cells. Purity was above 80% for all samples. One million monocytes were used for each ChIP recation. Chomatin Immunoprecipitation was performed using the MAGnify™ Chromatin Immunoprecipitation System (Invitrogen by Life Technologies, Carlsbad, CA) following manufacturer's recommendations. Cells were cross-linked with 1% formaldehyde for 10 minutes and lysed with the lysis buffer. Shearing of the chromatin was achieved by sonication (8 cycles, amplitude: 30%, 30 s on, 30 s off; using a Branson Digital Sonifier 450, Branson Ultrasonics, Danbury, CT). Chromatin was diluted in Dilution Buffer containing protease Inhibitors. Amounts of material corresponding to 105 cells were used for immunoprecipitations using magnetic beads coupled to anti-H3K4me1, anti-H3K4me3, anti-H3K27Ac, anti-Rpb1 NTD or anti-rabbit negative controls. Chromatin was washed. Crosslinking was reversed and DNA purified with DNA Purification Magnetic Beads. PCRs were performed in duplicate with 1.25 µl DNA, 1.25 µl H2O, 0.62 µl of primers (10 nM) targeting the IL1b promoter (Forward: TCAGTTTTGTTGTGAAATCAGT, Reverse: CAGGGTTTGTTGTCCAACTT; from Kaushik et al., Journal of Neurochemistry 2013; PMID 23895397) and 3.12 µl KAPA SYBR Green Fast (Kapa Biosystems, Wilmington, MA) using a QuantStudio™ 12K Flex system (Life Technologies, Carlsbad, CA). Data were normalized to input controls and express as % input.

Supplementary Table 1

Reagent	Brand/origin	Identifier/reference
Antibodies and chemicals		
Anti mouse CD11b, APC eFluor 780 (clone M1/70)	eBioscience	RRID: AB_1603193; Cat #47-0112-82
Anti mouse CD11c APC (clone N418)	BioLegend	RRID: AB_313779; Cat #117310
Anti mouse CD11c PE-eFluor610 (clone N418)	eBioscience	RRID: AB_2574530; Cat #61-0114
Anti mouse CD19 PE-Cy7 (clone 1D3)	eBioscience	RRID: AB_657663; Cat #25-0193
Anti mouse CD3e PE (clone 145-2C11)	eBioscience	RRID: AB_465496; Cat #12-0031
Anti mouse CD4 BV711 (clone GK1.5)	BioLegend	RRID:AB_2564586; Cat #100447
Anti mouse CD45, FITC (clone 30-F11)	eBioscience	RRID: AB_465050; Cat #11-0451
Anti mouse CD8a AlexaFluor700 (clone 53-6.7)	eBioscience	RRID: AB_494005; Cat #56-0081
Anti mouse F4/80 AlexaFluor700 (clone BM8)	eBioscience	RRID: AB_2574503; Cat #56-4801
Anti mouse F4/80 APC (clone BM8)	eBioscience	RRID: AB_469452; Cat #17-4801
Anti mouse Ly6C PerCpCy5.5 (clone HK1.4)	eBioscience	RRID: AB_2723343; Cat #45-5932-82
Anti mouse Ly6G BV605 (clone 1A8)	BD Biosciences	Cat #563005
Anti mouse Ly6G PE (clone 1A8)	BD Biosciences	Cat #551461
Anti mouse MHC Class II (IA/IE), PE (clone M5/114.15.2)	eBioscience	RRID: AB_465928; Cat #12-5321-81
Anti-mouse B220, PE-Cy7 (clone RA3-6B2)	BioLegend	RRID: AB_313005; Cat #103222
Anti-mouse CD117 (c-Kit), APC (clone2B8)	BioLegend	RRID: AB_313221; Cat #105812
Anti-mouse CD11b, PE-Cy7 (clone M1/70)	BioLegend	RRID: AB_312799; Cat #101216
Anti-mouse CD150 (SLAM), PerCP-Cy5.5 (clone TC15-12F12.2)	BioLegend	RRID: AB_2303663; Cat #115922
Anti-mouse CD135 (Flt3), PE (clone A2F10)	eBioscience	RRID: AB_465859; Cat #12-1351
Anti-mouse CD16/CD32, Alexa Fluor 700 (clone 93)	eBioscience	RRID: AB_493994; Cat #56-0161
Anti-mouse CD3, PE-Cy7 (clone 17A2)	BioLegend	RRID: AB_1732057; Cat #100220
Anti-mouse CD3, APC (clone 17A2)	eBioscience	RRID: AB_10597589; Cat # 17-0032-82
Anti-mouse CD48, APC-Cy7 (clone HM48-1)	BioLegend	RRID: AB_2561463; Cat #103432
Anti-mouse Ly6A/E (Sca-1), Super Bright 600 (clone D7)	eBioscence	RRID: AB_2663622; Cat #63-5981
Anti-mouse Ly6C/G, PE-Cy7 (clone RB6-8C5)	BioLegend	RRID: AB_313381; Cat #108416
Anti-mouse Ly-76, PE-Cy7 (clone TER-119)	BioLegend	RRID: AB_2281408; Cat #116222
Anti-mouse Gr-1, PE-Cy7 (clone RB6-8C5)	BioLegend	RRID: AB_313381; Cat #108416
Anti-mouse CD115 BV421 (clone AFS98)	BioLegend	RRID: AB_2562667; Cat # 135513
Anti-mouse CD11b APC (clone M1/70)	eBioscience	RRID: AB_469343; Cat # 17-0112-82
Anti-mouse CD3 PE-Cy7 (clone 145-2C11)	eBioscience	RRID: AB_469572; Cat #25-0031-82
Anti-mouse TCR gamma/delta PE-Cy7 (clone GL3)	eBioscience	RRID: AB_2573464; Cat #25-5711-82
Anti-mouse Ly6G PE-Cy7 (clone 1A8)	BioLegend	RRID: AB_1877261; Cat # 127618
Anti-mouse NK1.1 PE-Cy7 (clone PK136)	BD Biosciences	Cat #552878
Anti-mouse B220 PE-Cy7 (clone RA3-6B2)	eBioscience	RRID: AB_469627; Cat # 25-0452-82
Anti-mouse CD19 PE-Cy7 (clone 6D5)	BioLegend	RRID: AB_313655; Cat # 115520
Anti-mouse Ter 119 PE-Cy7 (clone TER-119)	BioLegend	RRID: AB_2281408; Cat # 116222
Anti-mouse Ly6G (clone 1A8)	Bio X Cell	RRID: AB_1107721; Cat #BE0075
Anti-mouse trinitrophenol, IgG2a isotype control (clone 2A3)	Bio X Cell	RRID: AB_1107769; Cat #BE0089
Rabbit polyclonal anti-H3K4me1	Diagenode	Cat #C15410037
Rabbit polyclonal anti-H3K4me3	Diagenode	Cat #C15410003
Rabbit polyclonal anti-H3K27Ac	Diagenode	Cat #C15410196
Rabbit monoclonal anti-Rpb1 NTD (D8L4Y)	Cell Signaling Technology	Cat #14958
2-mercaptoethanol	Gibco	31350010
96-well Clear Polystyrene Microplates	Corning	3799
Ammonium chloride	Sigma-Aldrich Merck	A0171
Brain Heart Infusion broth	Oxoid	CM1135
BSA	Sigma-Aldrich Merck	A7906
Clodronate Liposomes & Control Liposomes (PBS)	LIPOSOMA reserarch	CP-020-020

Columbia III Agar with 5% Sheep Blood	BD Biosciences	254098
EDTA, Titriplex® III	Merck	1.08418
FBS Superior	Biochrom, Merck group	S 0615
Fixable Viability Dye eFluor™ 450	Invitrogen	65-0863
IMDM, GlutaMAX™	Gibco	31980
Kineret® (Anakinra)	Sobi	
LB Broth Base Lennox	Invitrogen	12780052
LIVE/DEAD™ Fixable Violet	Invitrogen	L34955
M Tubes	Miltenyi Biotec	130-096-335
M-CSF	ImmunoTools	12343115
Microvette® CB 300 K2E	SARSTEDT	16.444
Penicillin/streptomycin	Gibco	15140122
PFA, Pierce™ 16% Formaldehyde (w/v)	Thermo Fisher scientific	28908
RPMI Medium 1640 - GlutaMAX™-I	Gibco	61870
Sodium bicarbonate	Sigma-Aldrich Merck	S6014
Ultrapure LPS from *Salmonella minnesota*	List Biological Laboratories	#434
Versene Solution	Gibco	15040033
Yeast Extract-Peptone-Dextrose broth	BD Biosciences	242820
Zymosan A from *Saccharomyces cerevisiae*	Sigma-Aldrich Merck	Z4250
Mouse Custom ProcartaPlex 17-plex	Invitrogen	PPX-17-MX7DPRR
Mouse IL-6 DuoSet ELISA	R&D Systems	DY406
Mouse TNF-alpha DuoSet ELISA	R&D Systems	DY410
ProcartaPlex Mix&Match Mouse 15-plex (IFNγ, IL-1β, IL-2, IL-4, IL-6, IL-10, IL-12p70, IL-17A, IL-18, IL-22, IL-23, CXCL10, CCL3, CCL4, TNF)	Invitrogen	PPX-15-MXDJXJ4
ProcartaPlex Mix&Match Mouse 17-plex (ENA-78/CXCL5, G-CSF, Gro-α/KC, IFNγ, IL-1α, IL-1β, IL-3, IL-6, IL-10, IL-12p40, IL-17A, IL-18, CXCL10, CCL2, CCL3, CXCL2, TNF)	Invitrogen	PPX-17-MX7DPRR
MAGnify™ Chromatin Immunoprecipitation System	Life Technologies	#49-2024
Monocyte Isolation Kit (BM), mouse	Miltenyi Biotec	#130-100-629
Bacteria and yeasts		
Candida albicans 5102	Isolated from a septic patient hospitalized at CHUV	doi.org/10.1093/infdis/jis673
Citrobacter rodentium DBS100	ATCC	51459
Escherichia coli O18:K1:H7	Isolated from a septic patient hospitalized at CHUV	doi.org/10.1093/infdis/jis673
Listeria monocytogenes 10403S	BEI RESOURCES (Gift from Prof. Zehn, Technical University of Munich, Freising, Germany)	NR-13223
Pseudomonas aeruginosa PAO1	ATCC	HER-1018 [PAO1]
Staphylococcus aureus AW7	Isolated from a septic patient hospitalized at CHUV	doi.org/10.1093/infdis/jis673
Mice		
C57BL/6J	Charles River Laboratories	632
BALB/cByJ	Charles River Laboratories	627
C57BL/6JMyD88-/-	Prof. Shizuo Akira, Osaka University, Osaka, Japan	doi.org/10.1016/S1074-7613(00)80596-8
C57BL/6JTLR2-/-	Prof. Shizuo Akira, Osaka University, Osaka, Japan	doi.org/10.1016/S1074-7613(00)80119-3
Software		
Prism 8	GraphPad Software	
FlowJo_V10_CL 10	FlowJo LLC	
Others		
Feeding tube for rodents, 1.1 x 50 mm, for 1 ml serine	ECIMED, Boissy-Saint-Léger, France	V0104050

Figure S1

A. Blood and bone marrow

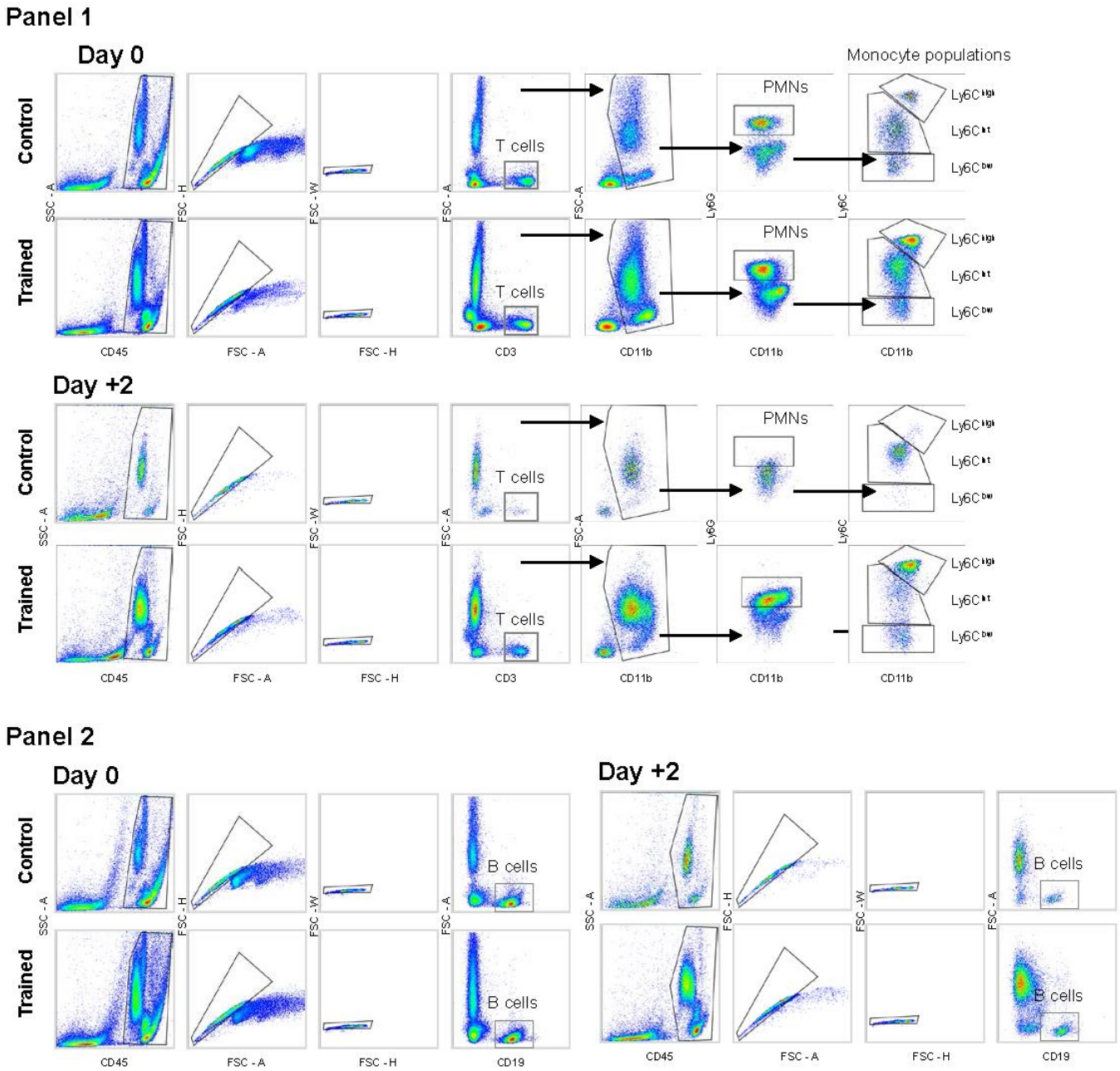

Figure S1

B. Bone marrow HSCs and MPPs

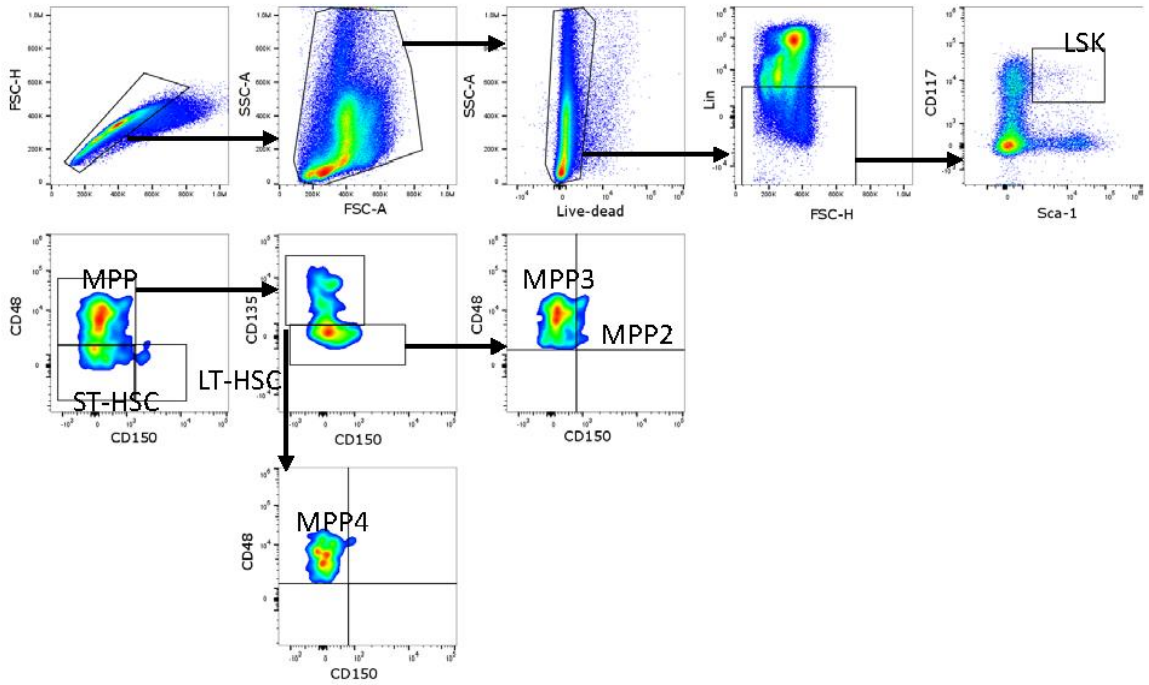

C. Peritoneal cells

Panel 1

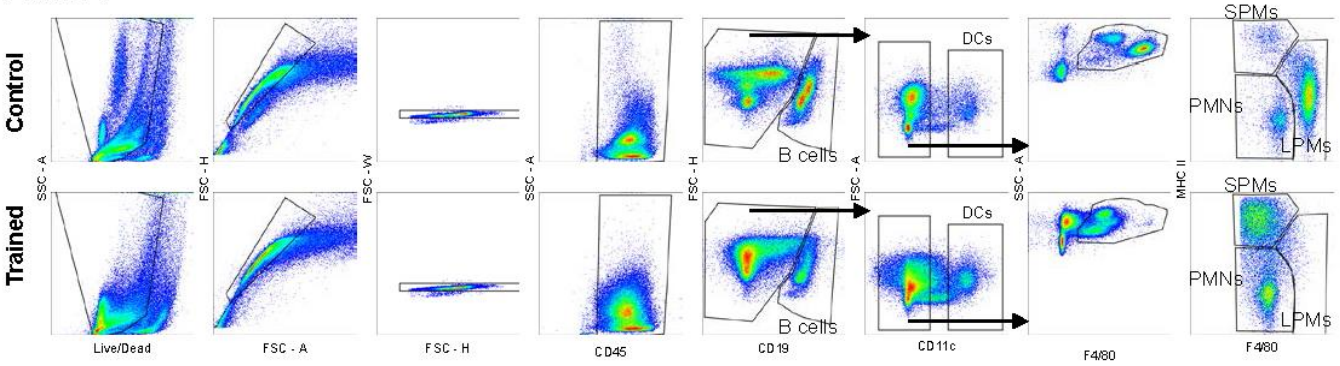

Panel 2

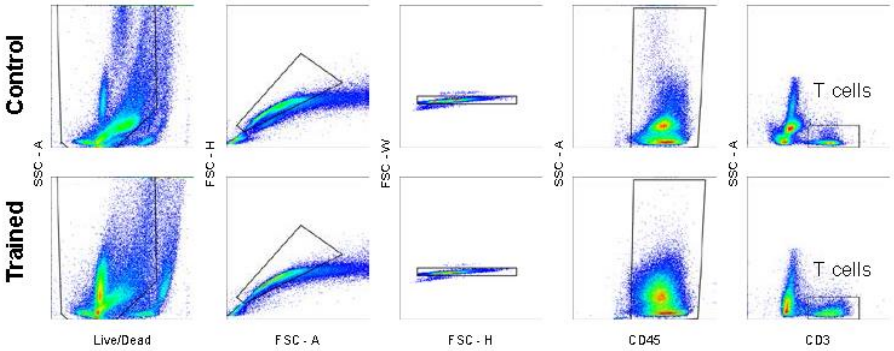

Figure S2

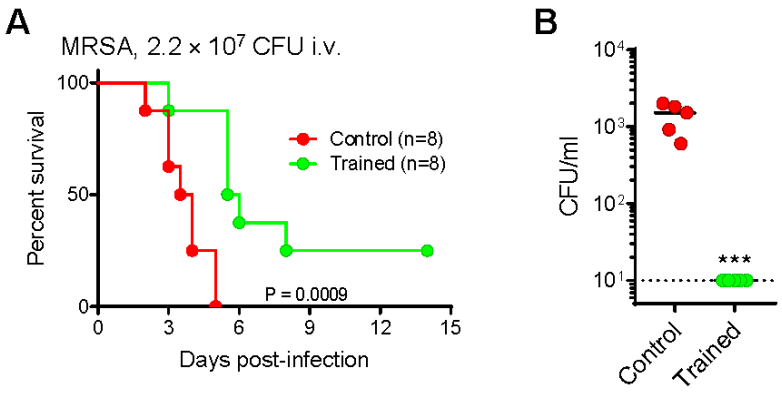

Figure S3

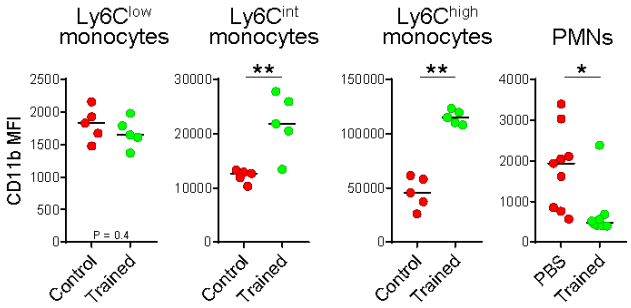

Figure S4

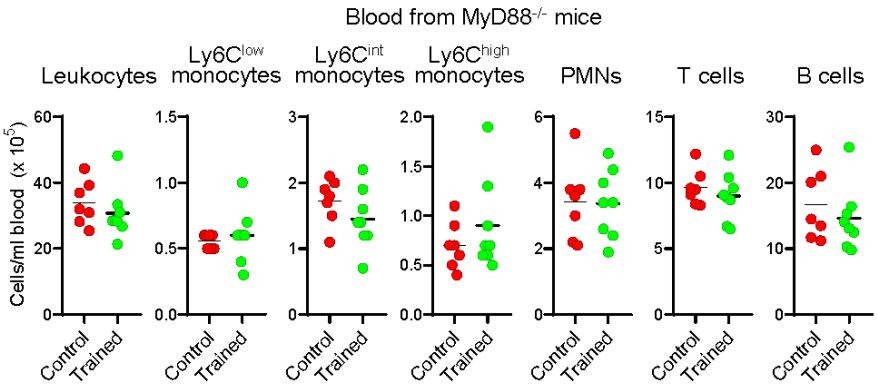

Additional data for reviewers

Additional Figure 1

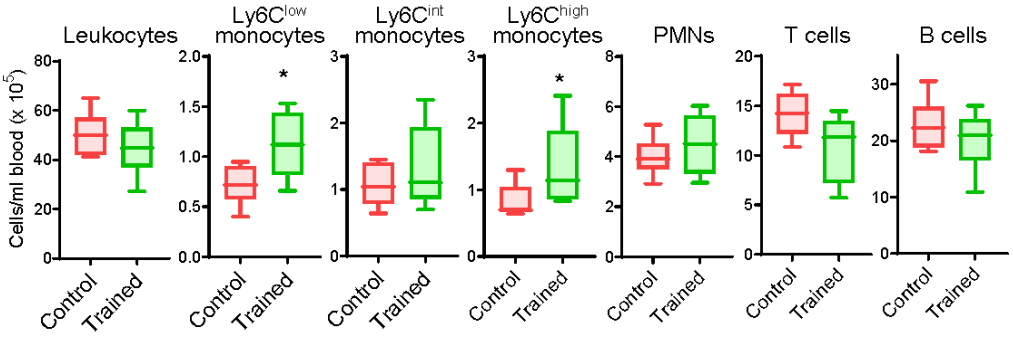

Additional Figure 1. Leukocytes in the blood of control mice and mice trained with zymosan i.v. (0.1 mg at day -7). N = 8 mice per group. *, P ≤ .05.

Additional Figure 2

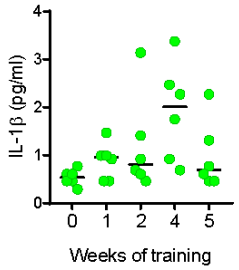

Additional Figure 1. IL-1β in the blood of mice trained 0, 1, 2, 4 and 5 weeks earlier.

Supplementary Figure Legends

Figure S1. A, Gating strategy for the analysis of blood and bone marrow by flow cytometry. The figure shows examples obtained using control and trained mice, analyzed just before infection (day 0) and 2 days post-infection (day +2) with L. monocytogenes. **B**, Gating strategy for the analysis of bone marrow long-term and short-term hematopoietic stem cells (LT-HSCs and ST-HSCs), multipotent progenitors (MPPs), MPP2, MPP3 and MPP4 by flow cytometry. **C**, Gating strategy for the analysis of peritoneal cells by flow cytometry. LPMs: large peritoneal macrophages; SPMs: small peritoneal macrophages.

Figure S2. A, Control and trained BALB/cBy mice were challenged i.v. with 2.2 x 10^7 CFU methicillin-resistant S. aureus (MRSA). Survival was recorded. **B**, Control and trained C57BL/6J mice were challenged i.v. with 9 x 10^4 CFU L. monocytogenes. Blood was collected 2 days after infection to quantify bacteria. The dashed line indicates the lower limit of detection. Each dot represents one mouse. ***, $P \leq .001$.

Figure S3. Mean fluorescence intensity (MFI) of CD11b expressed by blood Ly6Clow, Ly6Cint and Ly6Chigh monocytes and PMNs in control and trained mice. Each dot represents one mouse. *, $P \leq .05$; **, $P \leq .01$.

Figure S4. Leukocytes in blood from MyD88-/- mice challenged 7 and 3 days earlier with zymosan (trained) or PBS (control). Each dot represents one mouse.

3.2. Trained immunity increases lung phagocytes and protects from pneumococcal pneumonia

Charlotte Théroude[1], Rémi Porte[2], Barbara Bottazzi[2], Marta Reverte[1], Irene T. Schrijver[1], Eleonora Ciarlo[1], Didier Le Roy[1], Thierry Calandra[1], Cecilia Garlanda[2], Thierry Roger[1]

[1]Infectious Diseases Service, Department of Medicine, Lausanne University Hospital and University of Lausanne, Epalinges, Switzerland

[2]Department of Inflammation & Immunology, Humanitas Clinical and Research Center IRCCS, Rozzano (Milan), Italy

Submitted for publication.

Summary

Trained immunity confers broad-spectrum protection against lethal infections, including at anatomical sites distant from the priming site, such as the lungs. Yet, the overall impact of trained immunity on host lung defenses and ability to survive against lethal pneumococcal infection remains largely unknown. To address that question, we trained mice with zymosan, a cell-wall preparation rich in β-glucans, as previously described. Here, we show that priming protected mice from a lethal pneumococcal infection by *S. pneumoniae*. Trained immunity increases lungs neutrophils and monocytes Ly6C^{high} prior to or during early time point of the infection. Furthermore, phagocytosis was increased in bone marrow derived neutrophils. All of which contributed to the protection against lethal pneumococcal infections. These observations support the development of trained immunity-based therapies to improve defenses against infections.

Contribution to the work: I participated to or performed all experiments. I co-write and revised the paper.

ABSTRACT

Trained immunity is defined by the capacity of the immune system to develop an enhanced innate immune response against a secondary infection. The induction of trained immunity protects from various types of bacterial infections. Yet, whether trained immunity impact on lethal pneumococcal infection remains to be defined. To address this question, we evaluated the impact of training on innate immune defenses in the lungs of mice challenged with *Streptococcus pneumoniae*. Training was associated with an increase of lung polymorphonuclear neutrophils (PMNs) and Ly6C^{high} monocytes. While all control mice died from pneumococcal pneumonia, trained mice controlled bacterial burden in lungs and spleen, had reduced lung injury, and were protected from lethal infection. The resolution of infection in trained mice was associated with a reduction of lung PMNs. PMNs from trained mice showed increased phagocytosis and NETosis, and increased metabolic activity oriented towards mitochondrial respiration. Altogether, these data indicate that trained immunity confers protection against lethal pneumococcal infection.

Keywords: Trained immunity, innate immunity, *Streptococcus pneumoniae*, neutrophils, monocytes, innate lymphoid cells, NETs, metabolism

INTRODUCTION

Streptococcus pneumoniae is responsible of infections ranging from otitis media to severe invasive diseases such as pneumonia, meningitis and bacteremia. Pneumococcal severe infections are a major public health issue, accentuated by the problematic of antibiotic resistance and the rise of infections due to serotypes uncovered by current vaccines [1-3]. Overall, *S. pneumoniae* infections account for around 2.5 million death annually, primarily in children and elderlies [4, 5]. The World Health Organization published in 2017 a list of 12 global priority pathogens including *S. pneumoniae* to fight against.

S. pneumoniae colonizes the mucosal surfaces of the upper airways, but under certain circumstances evades host immune control allowing invasion of sterile sites like middle ear spaces, lungs, bloodstream and meninges [6]. Among innate immune cells, polymorphonuclear neutrophils (PMNs) represent an essential component of the host response to pulmonary infection, through the production of granules, serine proteases, antimicrobial peptides, neutrophil extracellular traps (NETs), reactive oxygen species (ROS), and phagocytosis (reviewed in [7]). During acute otitis media caused by *S. pneumoniae*, PMNs are the most predominant innate immune cells recruited to the focus of infection [8]. Phagocytosis, degranulation of antimicrobial mediators and production of NETs were implicated in elimination of *S. pneumoniae* [9]. Similarly, elastase, a serine protease produced by PMNs is critical to fight *S. pneumoniae* lung infection [10, 11]. However, the antimicrobial activities of PMNs are harmful to lung tissues. While early PMNs influx is essential to control pneumococcal infection, the extended presence of PMNs in lungs is responsible of pulmonary damage and poor outcome [12]. Macrophages sense *S. pneumoniae* through TLR2/TLR4 and TLR9, phagocytose and kill the bacteria before undergoing apoptosis [13-15]. Innate lymphoid cells (ILCs) are tissue-resident cells that can renew locally, and that are expanding and being activated by cues released by surrounding tissue cells responding to acute environmental challenges [16, 17]. ILC1, ILC2 and ILC3, which mirror CD4^{+} Th1, Th2 and Th17 cells [18], have been implicated in inflammatory or recovery phases following infection with influenza virus and *S. pneumoniae* and airway hyper-reactivity [19-24].

Vaccination is based on the fact that the immune system can keep a memory of the pathogens it has encountered, a characteristic attributed to the adaptive immune system through memory T and B cells [25, 26]. However, pioneer studies described in plants a process called systemic acquired resistance, reflecting the fact that plants expose to a pathogen could develop resistance to a secondary infection [27]. In 2003, studies showed that invertebrates develop specific memory, without owning adaptive immune system [28]. Mice infected with a low dose of *Candida albicans* or β-glucans, a cell wall component of *C. albicans*, were protected from a lethal dose of *Staphylococcus aureus* [29, 30]. Later on, human vaccinated with Bacillus Calmette-Guérin (BCG) vaccine showed protection not only against tuberculosis, but also against other infectious diseases, in a T- and B- cells independent manner [31-34]. The term “trained immunity” was proposed to define a “heightened response to a secondary infection that can be exerted both toward the same microorganism and a different one” [35]. The molecular mechanisms involved in trained immunity include metabolic, epigenetic and functional reprogramming of monocytes, macrophages and NK cells [36, 37]. While trained immunity may protect from infections, it may participate to the development of inflammatory pathological situations [38].

We have recently shown that trained immunity protects from bacterial infections [39], but whether it protects from pneumococcal infections remains unknown. Here we developed a model of pneumococcal pneumonia to address the protective role of trained immunity. We report that trained immunity increased lung PMNs and monocytes, increased the anti- bactericidal activity of PMNs, and protected from lethal pneumococcal pneumonia.

MATERIALS AND METHODS

Products used in this study are described in **Supplementary Table 1**.

Ethics statement

Animal experiments performed in Lausanne were approved by the Service des Affaires Vétérinaires, Direction Générale de l'Agriculture, de la Viticulture et des Affaires Vétérinaires, état de Vaud (Epalinges, Switzerland) under authorizations 3287, 876.9 and 877.9 and performed according to Swiss and ARRIVE guidelines. Animal experiments performed in Milano were conformed to protocols approved by the Humanitas Clinical and Research Center (Rozzano, Milan, Italy) in compliance with national (4D.L. N.116, G.U., suppl. 40, 18-2-1992) and international law and policies (2010/63/EU, and National Institutes of Health Guide for the Care and Use of Laboratory Animals, U.S. National Research Council, 2011).

Bacteria preparation

S. pneumoniae serotype 3 (American Type Collection 6303™) was grown on 5% sheep blood agar plates. Colonies were used to inoculate Todd Hewitt yeast broth (THYB, Sigma-Aldrich). Cultures were incubated at 37°C until an OD_{600} of 0.7-0.9. A green fluorescent protein (GFP) expressing strain of *S. pneumoniae* was constructed as described previously [40]. Clinical isolate E1586 was grown in THYB until an OD_{600} of 0.1, and incubated for 12 min at 37°C with 100 ng/ml of synthetic competence-stimulating peptide 1 (Eurogentec), and for 20 min at 30°C with PhlpA-hlpA-gfp_Camr DNA fragment (gift from Jan-Willem Veening, UNIL, Lausanne). Bacteria were diluted 10 x in THYB, incubated 1.5 hours at 37°C and platted on Tryptic Soy Agar plates (BD Biosciences) containing 5% sheep blood and 4.5 µg/mL chloramphenicol. Colony forming units (CFU) were determined by plating serial dilution of the inoculum on blood agar plates. Cultures stored for up to 3 months at -80°C in THYB containing 12% glycerol.

Mice and *in vivo* model of infection

C57BL/6J mice (Charles River Laboratories) were 8-10 weeks old. Mice were housed under specific pathogen-free conditions in the animal facility of Epalinges, Switzerland (license VD-H04) or in the animal facility of the Humanitas Clinical and research center IRCCS. Mice were kept in a temperature-controlled environment with a 12 hours light/dark cycle in air-conditioned room and with free access to food and water. Age-matched female mice were randomly divided into groups and injected intraperitoneally (i.p.) with PBS (control) or 1 mg of zymosan (trained) 7 and 3 days before usage [39]. Mice were anesthetized by an i.p. injection of 1.25 g/kg ketamine and 12.5 mg/kg xylazine. Mice were infected by an intranasal (i.n.) challenge with 5×10^4 CFU *S. pneumoniae*. Body weight, severity score, and survival were recorded at least once daily [41]. Mice were sacrificed at selected times by CO_2 to collect organs. Lungs were homogenized as described in *Flow cytometry* section. Spleen were homogenized with an UltraTurrax homogenizer (IKA-Werke, Staufen, Germany).

Cell population analyses by flow cytometry

Bronchoalveolar lavages (BALs) were performed as previously described [42]. Briefly, a catheter was inserted in the trachea, PBS was instilled and then gently retracted. Following BAL collection, lungs were collected and added to a solution containing collagenase D (2 mg/mL) and DNAse (80 U/mL), fetal calf serum (FCS), and HEPES (10 mM, pH 7.0). Samples were transferred into GentleMACS C-tube, and dissociated for 30 min using gentleMACS Octo Dissociator with heaters on program 37C_m_LDK_1. Cell suspensions were incubated for 3 min with 3 mL of red blood cell (RBC) lysis buffer (0.65 M ammonium chloride, 10 mM sodium bicarbonate, 0.1 mM EDTA, pH 7.4). Cells from BALs and lungs were washed, resuspended in cell staining medium (CSM: PBS containing 0.5% BSA), enumerated, and incubated for 30 min at 4°C in the dark with 50 µL live/dead dye, then 50 µL 2.4G2 monoclonal antibody (Ab), and finally 50 µL of Abs diluted in CSM. For intracellular staining, cells were first permeabilized by for 30 min at room temperature in 200 µL 1 x fixation/permeabilization solution (eBioscience). Antibodies in 50 µL 1 x permeabilization buffer were added to the cells, and incubation for 30 min at room temperature protected from light. The Ab mix to stain leukocytes in lungs and BAL contained anti-CD45, Siglec-F, CD11b, Ly6G and Ly6C Abs. Gating strategies for lungs and BALs are presented in **Figure 1 and Figure S2.** The Ab mix to stain ILCs contained a lineage antibody cocktail

(Lin: anti-CD8, CD3, CD5, CD11b, CD19, CD45R/B220, CD49b, TCRγδ, Ter119, CD11c, TCRβ and FcεRIα Abs), anti-CD45, CD90, CD127, ROR-γt, and GATA3 Abs. Gating strategy is presented in **Figure 3**. For ILC1 staining, the Ab mix contained Lin, anti-CD45, CD90, CD127, IFN-γ and T-bet Abs. For ILC2 staining, the Ab mix contained Lin, anti-CD45, CD90, CD127, GATA3, IL-4 and IL-5 Abs. Gating strategy of ILC1 and ILC2 are presented **Figure S3**. Ab mixes to stain lung progenitors contained a lineage antibody cocktail (anti-CD19, B220, CD3e, CD11b, Gr-1 and Ter119 Abs). Panel 1 contained anti-Sca-1, CD150, CD135, CD48 and CD117 Abs. Panel 2 contained anti-Sca-1, CD127, CD117, CD16/32 and CD34 Abs. Gating strategies are presented in **Figure S4**. Antibodies are described in **Supplementary Table 1**. Data were acquired on an Attune NxT Flow Cytometer (Thermo Fisher Scientific) or a BD LSRFortessa (BD Biosciences) and analyzed using FlowJo_V10_CL (FlowJo LLC, Ashland, OR) or BD FACSDiva software.

Cytokine measurements

Cytokines were quantified by ELISA or a multiplex Mouse Custom ProcartaPlex (Thermo Fisher Scientific) using a Bio-Plex 200 system (Bio-Rad, Hercules, CA) [43].

***In vivo* bioluminescence imaging**

Mice were injected i.p. with 200 mg/kg luminol (Carbosynth) and imaged using an In-Vivo XtremeTM II SPF animal chamber with high-efficiency particulate air filters (Bruker, Billerica, MA) as previously described [44]. Bioluminescence imaging was analyzed using Molecular Imaging software (Bruker). Regions of interest (ROI) were set on the lungs and peritoneum and the bioluminescent signals were expressed in units of photons per second (P/s).

Lungs histology

Lungs were excised, fixed in 4% paraformaldehyde and embedded in paraffin. Three tissues sections of 3 µm thickness collected at a distance of 150 µm were stained with hematoxylin and eosin (H&E). A blind histological evaluation evaluated the number of small (<0.5 mm) and large (>0.5 mm) foci in each section. The total number of foci were determined, and a total score (calculated as follows: [(foci <0.5 mm x 1) + (foci >0.5 mm) x 3] were calculated. Additionally, intravascular leukocyte rolling/adhesion, bronchiolar damage, perivascular edema and hemorrhage, and intra-alveolar hemorrhages were scored according to the histological grading system reported in **Supplementary Table 2**.

Bacteria phagocytosis and killing assays

Polymorphonuclear neutrophils (PMNs) were isolated from the bone marrow of femurs and tibias using the mouse Neutrophil Isolation Kit (Miltenyi, Bergisch Gladbach, Germany) as previously described [45]. For phagocytosis assays, PMNs at 2.5 x 10^5/mL were incubated for 1 hour at 37°C in RPMI medium containing 10^6 CFU/mL GFP-expressing *S. pneumoniae*. Extracellular fluorescence was quenched by incubation for 1 min with 0.25 mg/mL trypan blue. Cells were analyzed flow cytometry using an Attune NxT Flow Cytometer. For killing assay, PMNs at 5 x 10^8/mL were incubated for 1 hour at 37°C in RPMI medium containing 10^6 CFU/mL *S. pneumoniae*. Serial dilutions of reaction mixtures were plated on blood agar plates (BD Biosciences), and colonies enumerated 24 hours later.

NETosis and ROS production by PMNs

To measure NETosis, 2.5 x 10^5 PMNs/mL were incubated for 1 hour at 37°C in RPMI medium containing 10^6 CFU/mL *S. pneumoniae* and 5 µM Sytox green. Fluorescence (Em_{504}, Ex_{523}) was recorded using a Synergy plate reader (BioTek, Winooski, VT). NETs were observed using a EVOS M7000 Imaging System (Thermo Fisher Scientific) with Plan Apochromat 2x and 10x objectives. To measure ROS production, 2.5 x 10^5 PMNs/mL were incubated for 1 hour at 37°C in RPMI medium containing 0.1 mM M H_2O_2 (Sigma Aldrich) or 10^6 CFU/mL *S. pneumoniae*. MitoSOX (Thermofisher) was added at 5 µM during the last 10 min of incubation. Signals were detected by flow cytometry using an Attune NxT Flow Cytometer.

Metabolic activity

The metabolic activity of PMNs was measured on a 96-well format using a Seahorse XFe96 Analyzer (Agilent, Santa Clara, CA) [47, 48]. PMNs were seeded at 1.5 x 10^5 cells/well at in Seahorse XFe96 plates pre-coated with Cell-Tak (Corning). PMNs were pre-incubated in 180 µl of assay medium (Seahorse XF DMEM pH 7.4 supplemented with 2 mM L-glutamine, 1 mM pyruvate and 25 mM glucose (Gibco™)) for 1 hour at 37°C in a CO_2-free incubator. Oxygen consumption rate (OCR) was recorded using the Seahorse Cell Mito Stress Test protocol, which relies on the sequential addition of 1 µM oligomycin, 2 µM carbonyl cyanide 4-(trifluoromethoxy) phenylhydrazone (FCCP) and 0.5/0.5 µM rotenone + antimycin A (Rot/AA) (Sigma-Aldrich). Glycolytic proton efflux rates (GlycoPER) was recorded using

Seahorse Glycolytic Rate Test protocol which relies on the sequential addition of 0.5/0.5 µM Rot/AA and 50 µM 2-deoxyglucose (2-DG) (Sigma-Aldrich). Results were analysed using the Wave Desktop software (Agilent). At the end of measurements, cells were lysed with a mixture of 1 x RIPA Lysis and Extraction Buffer IV (Bio Basic, Toronto, Canada) and cOmplete Protease Inhibitor Cocktail (Merck, Darmstadt, Germany) in PBS. Protein concentrations were determined using a Pierce BCA Protein Assay Kit (Thermofisher Scientific) and used to normalize results according to protein concentration per well.

Statistical analyses

Graphics represent data obtained from individual mice, or violin plots. Data were analyzed for normal distribution and homogeneity of variances and compared with the appropriate parametric (2-tailed unpaired Student t test) or nonparametric (2-tailed Mann-Whitney test) statistical test. The Kaplan-Meier method was used for building survival curves, and differences were analyzed using the log-rank sum test. P values were 2 sided. Analyses were performed using PRISM version 8.0.1 software (GraphPad Software).

RESULTS

Trained immunity increases lung PMNs and Ly6C^{high} monocytes

The induction of trained immunity increased bone marrow hematopoiesis and blood leukocytes [39]. To study whether trained immunity affected additional compartments, we evaluated the immune cell status in the lungs of control and trained mice (**Figure 1A**). Macrophages, eosinophils, PMNs and monocytes were detected in lungs of control and trained mice (**Figure 1B**). t-SNE plots showed an overall increase of myeloid cells in trained mice when compared to control mice (**Figure 1C**). This was reflected by a 2.7 and 3.5-fold increase of PMNs and Ly6C^{high} monocytes ($P < .01$ and $P < .001$ *vs* control) (**Figure 1D**). Eosinophils were increased 1.7-fold in trained mice ($P = .05$), and expressed 1.1-fold less of the inhibitory receptor Siglec-F ($P < .05$) (**Figure S1**). Macrophages counts were slightly decreased in trained mice ($P < .05$). Myeloid cell counts were similar in BALs from control trained mice (**Figure S2**). A multiplex cytokine assay (G-CSF, IFNγ, IL-1α, IL-1β, IL-6, IL-10, IL-12p40, IL-18, TNF, CCL2, CCL3, CXCL2, CXCL5 and CXCL10) showed increased concentrations of G-CSF, IL-1β, IL-6 and CXCL2 in the lungs of trained mice (**Figure 2A**). Whole body inflammation was assessed by luminol-generated bioluminescence (**Figure 2B**). Bioluminescence signals were not detected in control mice, nor in the lungs of trained mice. As expected, a strong signal was detected in the region of the peritoneal cavity of trained mice ($P < .01$).

ILCs are tissue resident cells that play an important role in lung inflammation and innate immune responses, and lung ILC2 have been suggested to acquire memory capacity. Thus, we measured total ILCs and ILC1, ILC2 and ILC3 in lungs (**Figure 3A**). We detected 2.3-11.2 x 10^4 ILCs in lungs. ILC1, ILC2 and ILC3 represented 76-95%, 3.4-20.2% and 0.1- 2.5% of all ILCs. Total ILCs were slightly reduced in trained mice (**Figure 3B**), which mainly resulted from a 2-fold decreased in ILC2 ($P <.05$). ILC1 proportion was higher in trained than in control mice at the expense of ILC2 proportion (ILC1 and ILC2 in control vs trained: 89 ± 6.1% vs 94 ± 1.6% and 10 ± 4.8 vs 6±1.4%). The expression levels (depicted by the mean fluorescence intensity) of GATA3 in ILC2 were similar in control and trained mice while we observed a slight increase of ROR-γt in ILC3 (**Figure S3A**). The proportions of ILCs positive for IFNγ, IL-4 and IL-5 were low (0.5-5% of ILCs). Yet we detected a trend for more IFNγ$^+$ ILC1 ($P = .095$) (**Figure S3B**) and more IL-4$^+$ and IL-5$^+$ ILC2 (3.9 and 1.7-fold increase, $P <.05$ and $P < .01$ vs control, respectively) (**Figure S3C**) in the lungs of trained mice. Training increased central myelopoiesis [39], and lungs can be a reservoir for hematopoietic progenitors [46-48]. However, training did not increase hematopoietic progenitors in lungs (**Figure S4**). This observation suggested that PMNs were recruited to the lungs following the induction of trained immunity, while macrophages might expand locally.

Trained immunity protects from pneumococcal infection

The rise of phagocytes in the lungs of trained mice suggested that training might protect from lung infection. To address that possibility, we developed a model of pneumonia induced by intranasal instillation of 5x10^4 CFU *S pneumoniae* serotype 3 (**Figure 4A**). All control mice died within 5 days. In sharp contrast, 53% of trained mice survived infection ($P < 10^{-4}$) (**Figure 4B**). Accordingly, trained mice had 120- and 44-fold less bacteria in lungs and spleen 36 hours post-infection. Histological evaluation of lungs collected 24-48 hours after infection showed stronger inflammation and the presence of abscesses in control mice (**Figure 4C**). The numbers of large bronchopneumonia foci and the lung

histological scores were reduced in trained mice compared to control mice (**Figure 4D**).

Dynamics of immune cells in lungs during pneumococcal infection

We then investigated the dynamics of immune cells in the lungs of mice undergoing pneumonia, focusing first on PMNs, macrophages, monocytes and eosinophils. t-SNE plots showed an overall increase of myeloid cells in trained mice compared to control mice (**Figure 5A**). This was reflected by 1.5-, 2.9 and 2-fold more PMNs, Ly6C^{low} monocytes and eosinophils at 12 hours post-infection ($P < 0.05$, $P < .01$ and $P < .05$, respectively) (**Figure 5B**). At 36 hours post-infection, 5-fold more eosinophils were detected in the lungs of trained mice ($P < .001$), while PMNs counts were 2.6-fold lower. This evolution was mainly due to PMNs raising 5.3-fold in control mice while they remained pretty constant in trained mice. Macrophages counts did not change over time in control and trained mice. However, while macrophages from controlled mice decreased Siglec-F expression during the course of infection, macrophages from trained mice kept stable expression levels (Siglec-F MFI median in control vs trained macrophages at 12 and 36 hours: 4826 vs 4263 and 3777 vs 4439, $P < 0.05$ for both) (**Figure S5**). Going well along these data, lung cytokines levels were globally lower in trained mice than in control mice 36 hours after infection (**Figure 6A**). Moreover, bioluminescence imaging 36 hours post-infection showed lower bioluminescence signals in the area of the lungs of trained mice than control mice (**Figure 6B**). The numbers of PMNs, macrophages and monocytes were much lower in BALs than in lungs, while eosinophils were not detected (**Figure S6**). None of these populations were different between control and trained mice except for PMNs measured 36 post-infection. Indeed, similar to the situation observed in lungs, PMNs increased much more strongly in BALs from control than trained mice (control vs trained macrophages at 12 and 36 hours: 2285 vs 2465 and 18200 vs 6235 PMNs/BAL, $P = 0.4$ and $P < 0.01$) (**Figure S6**).

We then focused on ILCs since ILC1 are important players involved in anti-bacterial defenses, while ILC2 have an important role in tissue repair. Total ILCs, ILC1 and ILC3 did not differ between control and trained mice 12 hours and 36 hours post-infection. ILC2 (total number and % of ILCs) decreased in control mice, while they slightly increased in trained mice (control vs trained at 12 and 36 hours: 4010 vs 2725 and 1210 vs 2890 ILC2/lungs, $P = 0.2$ and $P = 0.03$) (**Figure 7A**). As a result of these modifications, between 12 hours and 36 hours post-infection, the ILC1/ILC2 ratio increased 1.6-fold in control mice while it decreased by around two times in trained mice. No differences of expression of GATA3 in ILC2 and ROR-γt in ILC3 were detected at any time point (**Figure 7B**). Additionally, no differences in the proportions of IFNγ producing ILC1 and IL-4 and IL-5 producing ILC2 were observed (**Figure S7A-7B**).

Trained immunity increases phagocytosis, NETosis and ROS production by PMNs

PMNs play an important role in early defense mechanisms against pneumococcal infection. The fact that PMNs were upregulated in the lungs of trained mice before infection suggested that these cells could participate in protecting from pneumococcal pneumoniae. To get clues about mechanisms through which PMNs may hold that role, we compared phagocytosis, NETosis and ROS production by control and trained PMNs.

To assess phagocytosis, PMNs were incubated for 1 hour with *S. pneumoniae* engineered to express GFP. As shown in **Figure 8A**, 38% of PMNs from trained mice phagocytosed *S. pneumoniae*, while only 20% of PMNs from control mice did ($P < 0.001$). The production of NETs was quantified using a Sytox Green assay and visualized by fluorescent microscopy (**Figure 8B**). NETs were not detected when PMNs were cultured in medium. Incubation of PMNs with *S. pneumoniae* stimulated NETosis to a greater extent by trained than by control PMNs, as attested by a 2.6-fold higher Sytox Green assay signal using trained PMNs ($P < 0.001$). Accordingly, more numerous NETs were observed by imaging trained PMNs. Finally, the production of mitochondrial ROS was quantified by flow cytometry using MitoSOX dye (**Figure 8C**). H_2O_2 used as a positive control of measurement gave a strong fluorescent signal (MFI in control vs trained PMNs: 35.4 vs 41.4, $P < 0.001$). A weak signal was detected in PMNs cultured with medium, which was 2.0-fold higher using trained than control PMNs ($P = 0.01$). The addition of *S. pneumoniae* amplified 2.5-6-fold baseline signal, but the production of mitochondrial ROS production was similar using control and trained PMNs. Overall, these data suggested that trained PMNs were better armed to control *S pneumoniae* burden.

Trained immunity increases mitochondrial respiration of PMNs

Metabolic rewiring of innate immune cells accompany the development of host defense mechanisms. Thus we analyzed glycolysis and mitochondrial respiration in control and trained PMNs using the SeaHorse technology (**Figure 9A**). No differences of basal and compensatory glycolysis were observed between control and trained PMNs (**Figure 9A**). In contrast, trained PMNs showed 2.5-fold higher oxygen consumption rate (OCR), which reflects mitochondrial respiration, when compared to control PMNs (*P*

< 0.0001) (**Figure 9B**). Trained neutrophils also showed 1.7-fold increased space respiratory capacity, reflecting the capability of the cells to respond to an energetic demand ($P < 0.05$). Lastly, trained PMNs had 2.4-fold higher mitochondrial-derived ATP production than control neutrophils ($P < 0.0001$). Thus, trained neutrophils showed an overall shift towards mitochondrial respiration, which was also documented by measuring the mitoOCR/glycoPER ratio ($P < 0.05$).

DISCUSSION

We report that the induction of trained immunity increased lung phagocytes, antimicrobial activity of PMNs and protected from pneumococcal infection. Taken together with our previous observations [39], these results indicate that trained immunity confers broad-spectrum protection against lethal bacterial infections.

Bacterial dissemination was controlled in trained mice, resulting from the accumulation of PMNs and Ly6C^{high} monocytes in lungs. We have previously shown that monocytes were required to protect trained mice from listeriosis. Confirming the important role of monocytes in pneumococcal infection protection induced by trained immunity. Nevertheless, another recent study demonstrated that alveolar macrophages were the only cells showing adaptive characteristics after resolution of mild bacterial pneumoniae. These modifications were lasting up to 6 months after infection [49]. Our results suggested that an early influx of PMNs was essential to control the infection, while an excessive and extended influx of PMNs was harmful to host lung tissue [12].

Pneumococcal capsule protected against phagocytosis by PMNs [40] and pneumolysin, a toxin secreted by *S. pneumoniae* was associated with killing of PMNs [50]. Phagocytosis by trained PMNs was increased compared to untrained PMNs, showing that pneumococcal capsule was not efficient enough to protect against trained neutrophils. Whether trained immunity was implicated in pneumolysin secretion by *S. pneumoniae* or susceptibility towards their killing effect on PMNs remains to be determined. *S. pneumoniae* regularly encounters toxic oxygen radical on the airway surfaces from the host metabolism and immune system. As such, *S. pneumoniae* developed defenses to cope with oxygen radicals [51]. This could explain the fact that we did not observed differences of ROS production between trained and untrained PMNs, when cells were stimulated with *S. pneumoniae*.

NETs have been involved in the elimination of *S. pneumoniae* mediated otitis media [9]. We observed an increased capacity to produce NETs by trained PMNs, which may participate to limit bacterial dissemination. Interestingly, lungs of trained mice contained more CXCL1 and CXCL2, two neutrophils chemoattractants expressed by macrophages [52], of IL- 1β and IL-6 that are pro-inflammatory cytokines implicated in PMNs survival and recruitment [53, 54]. These data could explain why we observe an accumulation of neutrophils in lungs of trained mice. After training, eosinophils had lower expression of Siglec-F in lungs of trained mice, a mouse function paralog of the human Siglec-8 that induces apoptosis in eosinophils [55], justifying the accumulation of eosinophils in lungs of trained mice before and after *S. pneumoniae* infection. IL-6 is also responsible for iron sequestration by macrophages, limiting iron availability to bacteria. This could contribute to the decreased of bacterial burden and dissemination observed in lungs of trained mice [56].

The significant differences observed 36 hours post-infection, particularly with regard to ILC2 cell counts were probably subsequent to the reduced bacterial burden and dissemination observed. ILC2 increase in lungs of trained mice at late time point after the infection might be a consequence of reduced lung injury. Indeed, ILC2 are known to promote tissue repair during influenza virus infection [19, 21], parasite infections [57, 58], and allergy [59] by production of amphiregulin (AREG) and arginase (ARG1). Additionally, ILC2-producing IL-4, IL-5 and IL-13 cells have been implicated in the recruitment and maintenance of eosinophils during the recovery phase of influenza infection [19, 21]. ILC2 producing IL-4 and IL-5 cells increased drastically during the infection, which could explain the significant increase of eosinophils, as well as the reduced lungs injury observed in trained mice.

Eosinophils are traditionally perceived as detrimental cells, causing lung tissue damage via the release of cytotoxic granules [60]. However, some reports suggested that eosinophils can have homeostatic functions. As such, production of IL-4 or IL-10 by activated eosinophils was necessary for hepatocyte [61] and muscle regeneration [62] and resolution of lung-allergic responses [63]. Additionally, eosinophils directly contributed to coagulation, an important process during epithelial injury and remodeling, since they produce key factors of coagulation (tissue factor thrombin) and fibrinolysis (plasminogen) [64]. These observations provide evidence that eosinophils contribute to tissue repair, a concept elaborated in the Local Immunity And Remodeling/repair (LIAR) hypothesis [65].

Mucociliary clearance is one of the primary innate defense mechanisms of the lungs. Mucous trap inhaled pathogens, while the cilia beat in metachronal waves to expel pathogens. Abnormal cilia result in a deficient mucociliary clearance and chronic lung diseases and observed in patients with primary cilia dyskinesia, cystic fibrosis, or asthma [66, 67]. Recently, two groups reported that ILC2 mediated mucous production during helminth [68] and rhinovirus [69] infections. Interestingly, a first gastrointestinal helminths infection induced an innate mucin response driven by ILC2, priming peripheral barrier sites, including the lungs, for protection against a secondary helminth infection. This could also be related to the accumulation of ILC2 in the lungs of trained mice. Similarly, lungs exposed to *C. albicans* led to the recruitment and activation of ILCs. This recruitment was associated by the secretion of IL-22 and protection from a secondary infection with *Pseudomonas aeruginosa* [70].

Trained PMNs acquired energy mainly through oxidative metabolism under steady state, confirming the metabolic rewiring observed elsewhere [36]. Considering the major problematic of antibiotic resistance and the emergence of infection by serotypes of *S. pneumoniae* uncovered by current vaccines, trained immunity could be used to increase vaccine efficacy or increase the resistance to pathogens. Currently, BCG-mediated trained immunity strategies have been proposed to improve host defenses against severe acute respiratory syndrome coronavirus 2 (SARS-CoV2) infection [71-83]. This follows reports showing that BCG vaccination of health volunteers reduced viremia induced by yellow fever vaccination [84].

In summary, induction of trained immunity increased lungs phagocytes, providing efficient barrier against *Streptococcus pneumoniae* infection. These data support the idea of trained-immunity-based therapy against lethal pneumococcal infection.

AUTHORSHIP

TR conceived the project. CT, RP, MR, DLR designed, performed and analyzed experiments. BB, ITS, TC and CG provided reagents, analyzed and interpreted results. CT and TR wrote the paper. All the authors revised the paper..

ACKNOWLEDGMENTS

TR is supported by the Swiss National Science Foundation (SNSF, grant number 320030_149511 and 310030_173123), by the European Sepsis Academy Horizon 2020 Marie Skłodowska-Curie Action: Innovative Training Network (MSCA-ESA-ITN, grant number 676129, to support CT and ITS), by Fondation Carigest/Promex Stiftung für die Forschung (Geneva, Switzerland) and Fondation Biochimie (Epalinges, Switzerland). CT and ITS received a scholarship from the Société Académique Vaudoise (Lausanne, Switzerland).

CONFLICT OF INTEREST DISCLOSURE

The authors declare no competing financial interests.

FIGURES

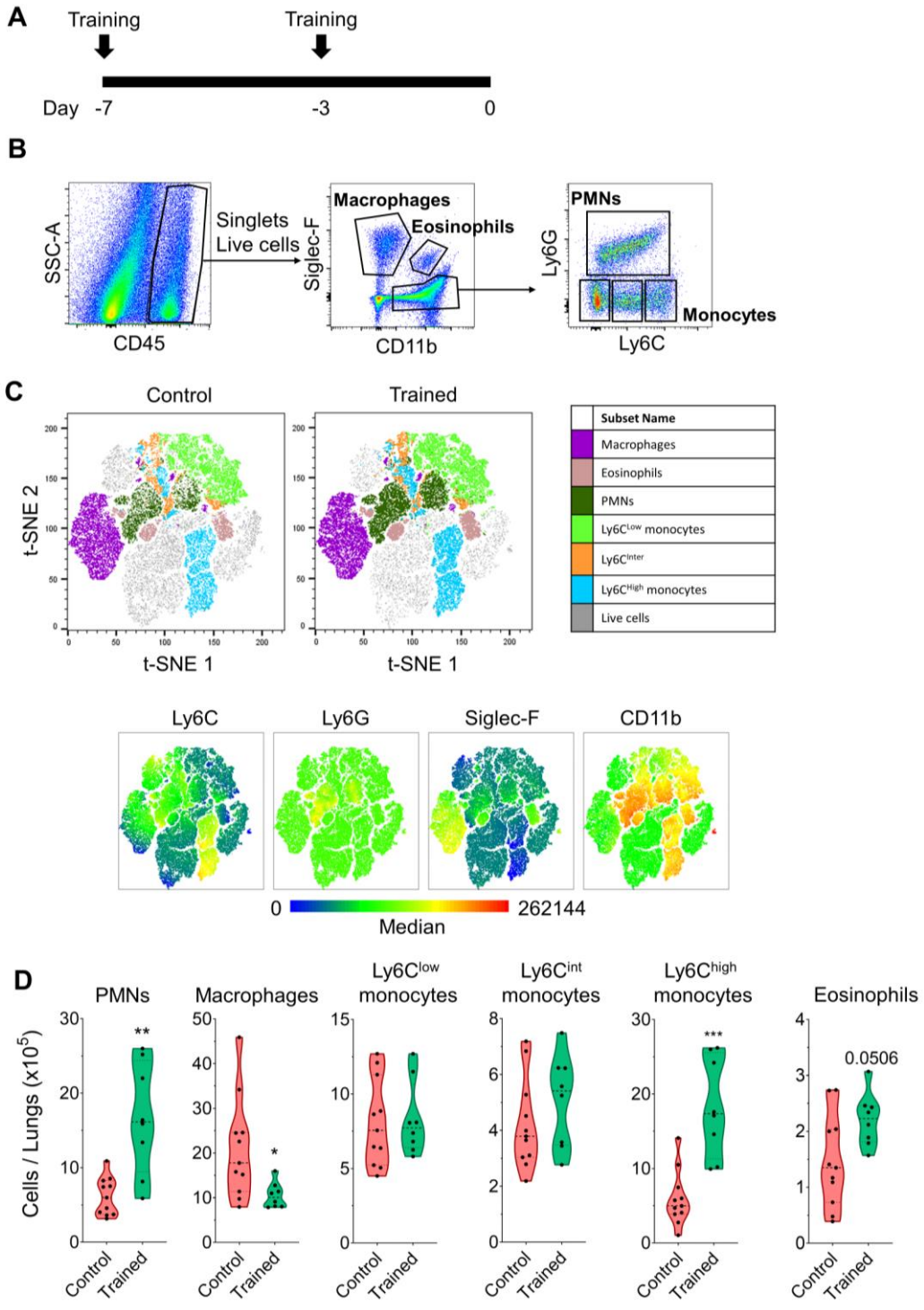

Figure 1. Trained immunity increases myeloid cells in the lungs. ***A.*** Experimental model to study effect of trained immunity. ***B***. Gating strategy used for flow cytometry analysis of leukocytes in the lungs. ***C***. t-SNE plots of leukocyte subpopulations in the lungs of control and trained mice. ***D***. Number of PMNs, macrophages, Ly6C^{low}, Ly6C^{int} and Ly6C^{high} monocytes and eosinophils in the lungs of control and trained mice. Each dot represents one mouse (n=8-11 mice). * $P < 0.05$, ** $P < 0.01$, *** $P < 0.001$.

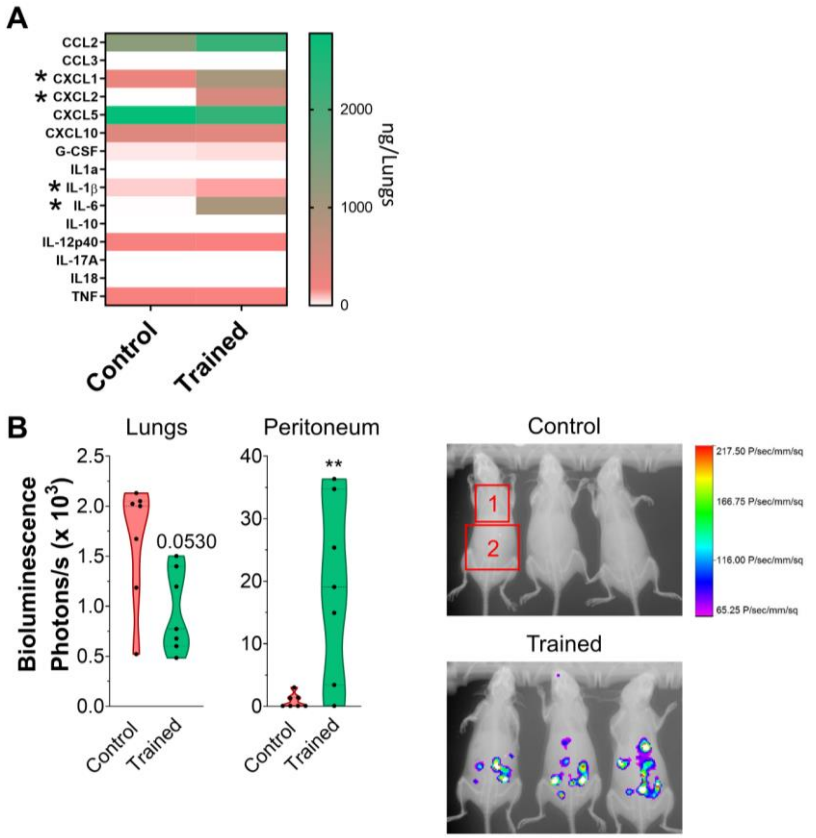

Figure 2. Trained immunity increases inflammation in lungs. ***A***. Lungs were collected from control and trained mice to quantify cytokines by Luminex technology (n=4 mice). ***B***. Bioluminescence was quantified in control and trained mice using *In vivo* Xtreme II technology. CCL, C-C motif chemokine ligand; CXCL, C-X-C motif chemokine ligand; IFN, interferon; IL-, interleukin. * $P < 0.05$, ** $P < 0.01$, *** $P < 0.001$.

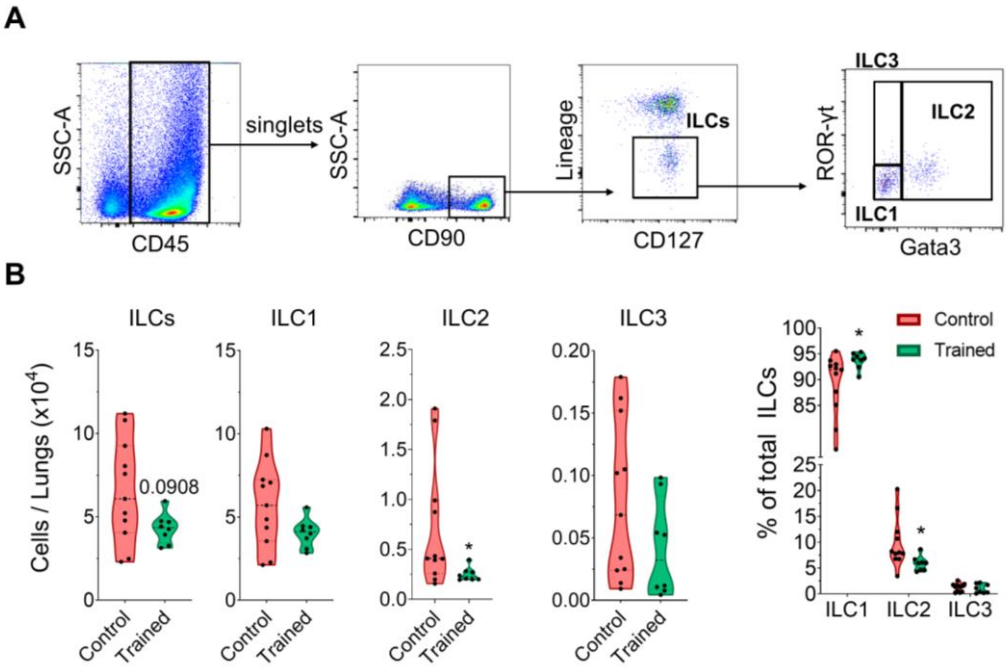

Figure 3. ILCs in lungs of trained mice. ***A.*** Gating strategy used for flow cytometry analysis of ILCs in lungs. ***B***. Numbers and proportions of ILCs, ILC1, ILC2, ILC3 in the lungs of control and trained mice (n=8-11 mice). * $P < 0.05$.

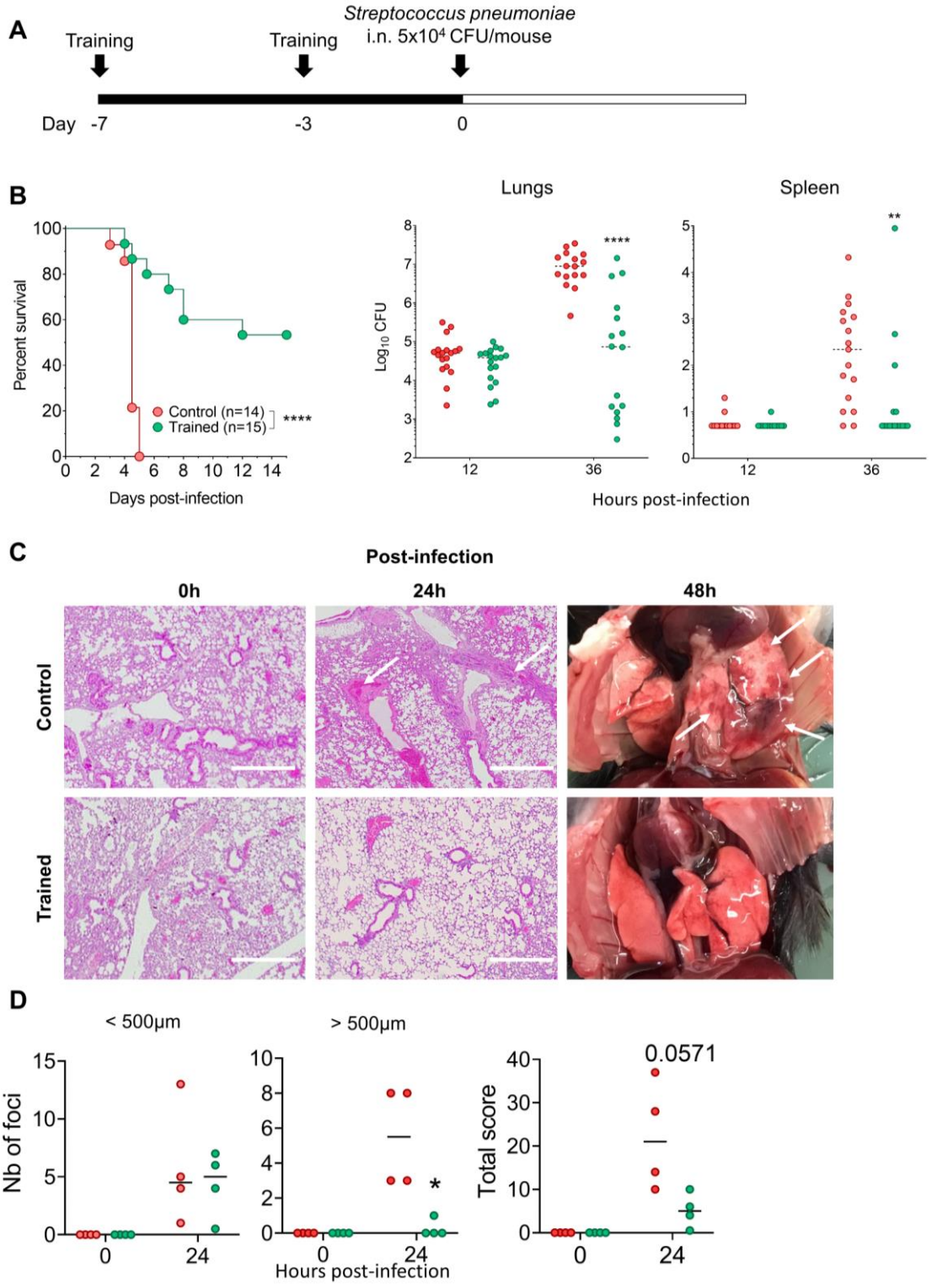

Figure 4. Trained immunity protects from pneumococcal infection. ***A.*** Experimental model. Mice were infected i.n. with 5 x 10^4 CFU *S. pneumoniae*. ***B***. Mouse survival was recorded up to 14 days after infection. Lungs and spleen were collected 12 and 36 hours after infection to quantify bacteria. ***C***. Hematoxylin and eosin (H&E) staining of lungs sections of control and trained mice at 10x magnification, and image of lungs. ***D***. The number of foci was determined, and total score calculated (n=4 mice). Each dot represents one mouse. * $P < 0.05$.

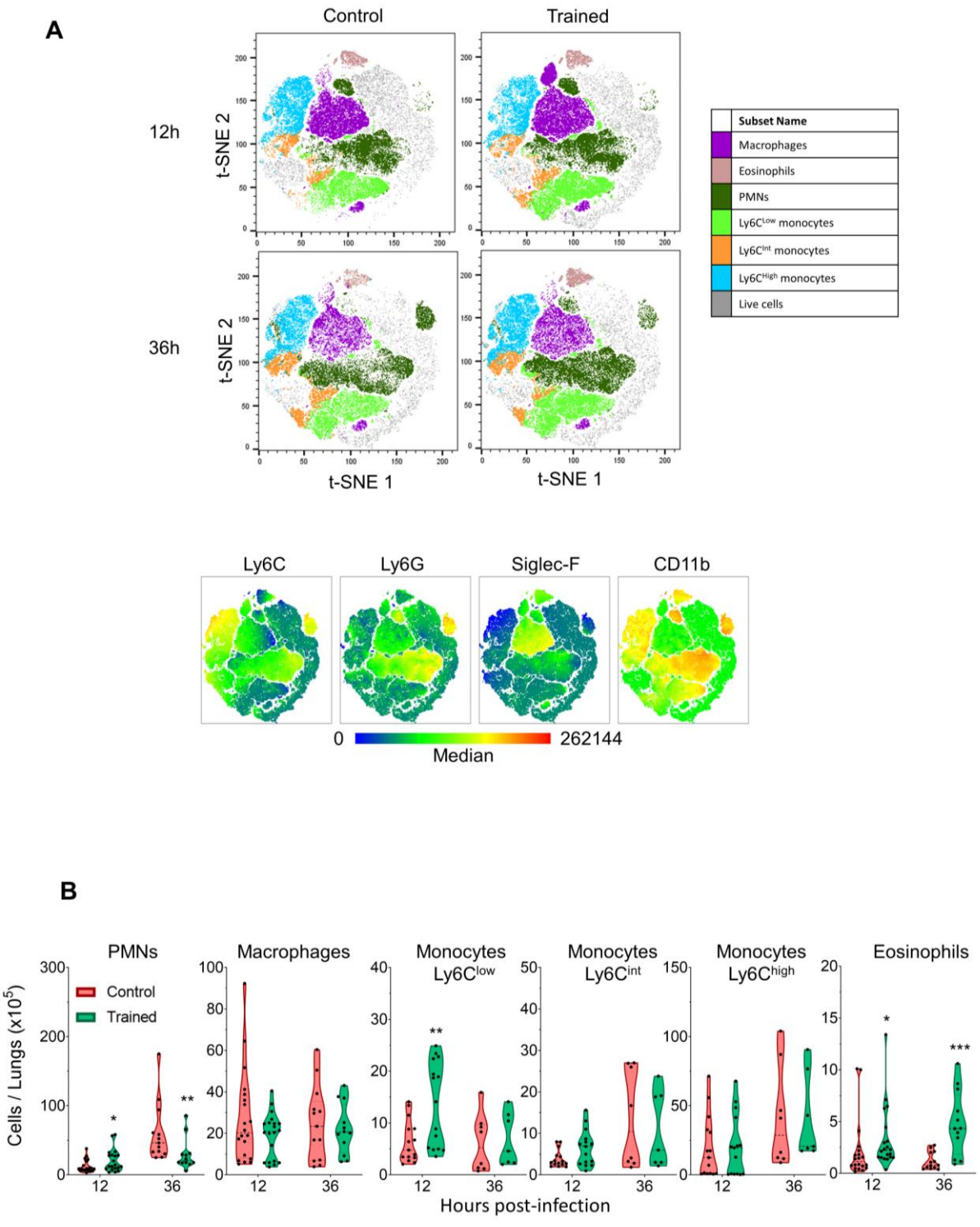

Figure 5. PMNs increase in lungs of control but not trained mice with pneumococcal infection. ***A.*** t-SNE plot of lung leukocytes from control and trained mouse 12 and 36 hours post-infection. ***B***. Number of PMNs, macrophages, Ly6C^{low}, Ly6C^{int} and Ly6C^{high} monocytes and eosinophils in the lungs of control and trained mice (n=12-20 mice). * $P < 0.05$, ** $P < 0.01$, *** $P < 0.001$.

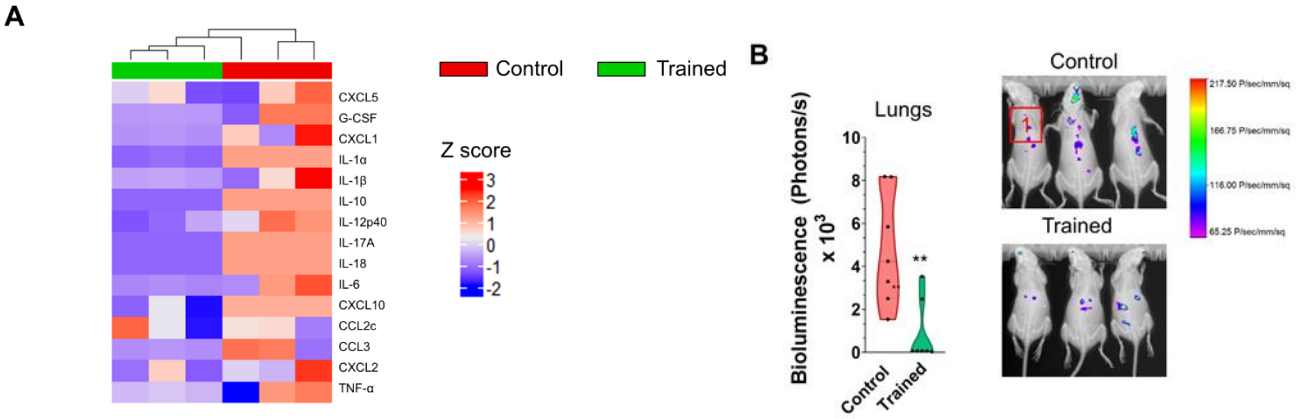

Figure 6. Reduced inflammation in the lungs of trained mice following pneumococcal infection. ***A***. Lungs were collected 36 hours after infection. Cytokines were quantified by Luminex (n=3 mice). ***B***. Bioluminescence was quantified in control and trained mice 36 hours after infection using *In vivo* Xtreme II technology. Each dot represents one mouse. * $P < 0.05$.

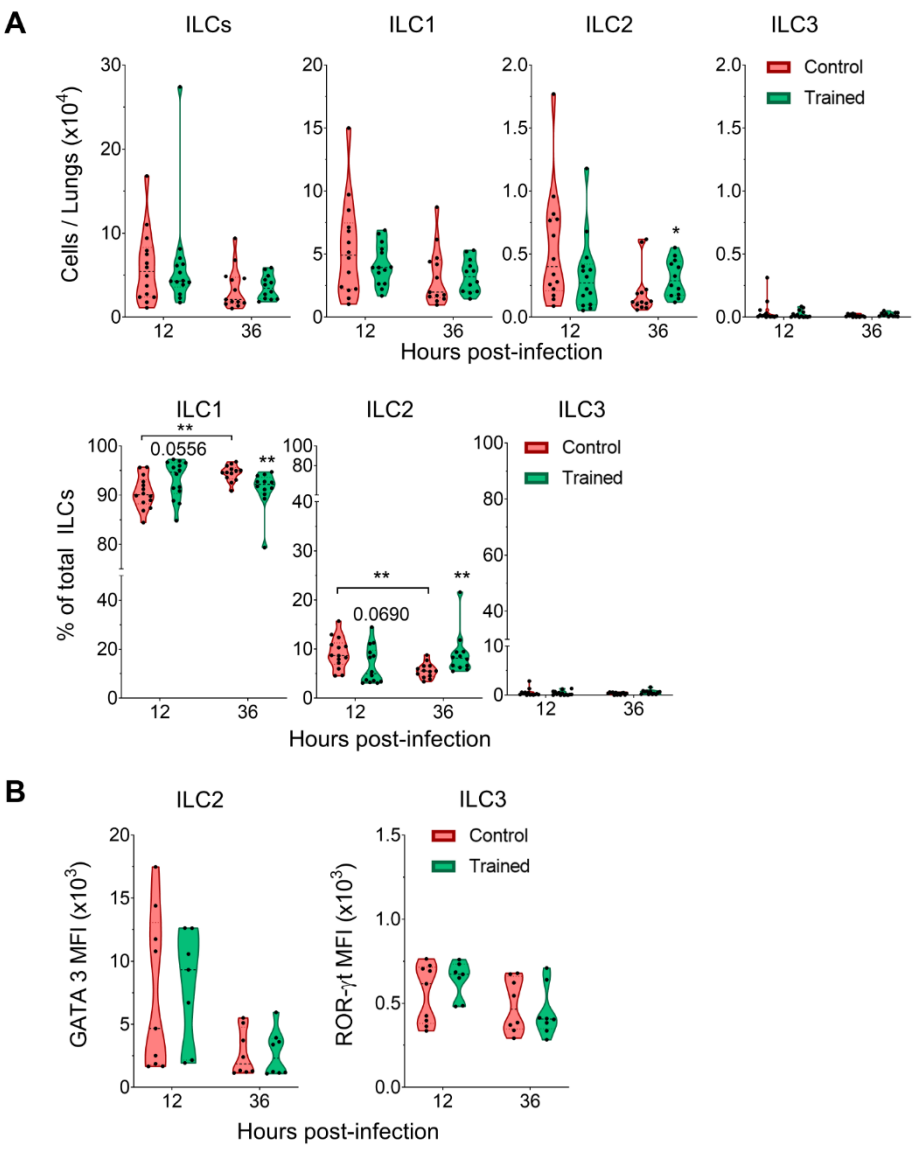

Figure 7. Modulation of lung ILCs during pneumococcal infection. ***A.*** ILCs in the lungs of control and trained mice 12 and 36 hours post-infection (n=13-20 mice). ***B***. Mean fluorescence intensity (MFI) of GATA3 expressed by ILC2 and ROR-γt expressed by ILC3 in control and trained mice 12 and 36 hours post infection (n=7-10 mice).

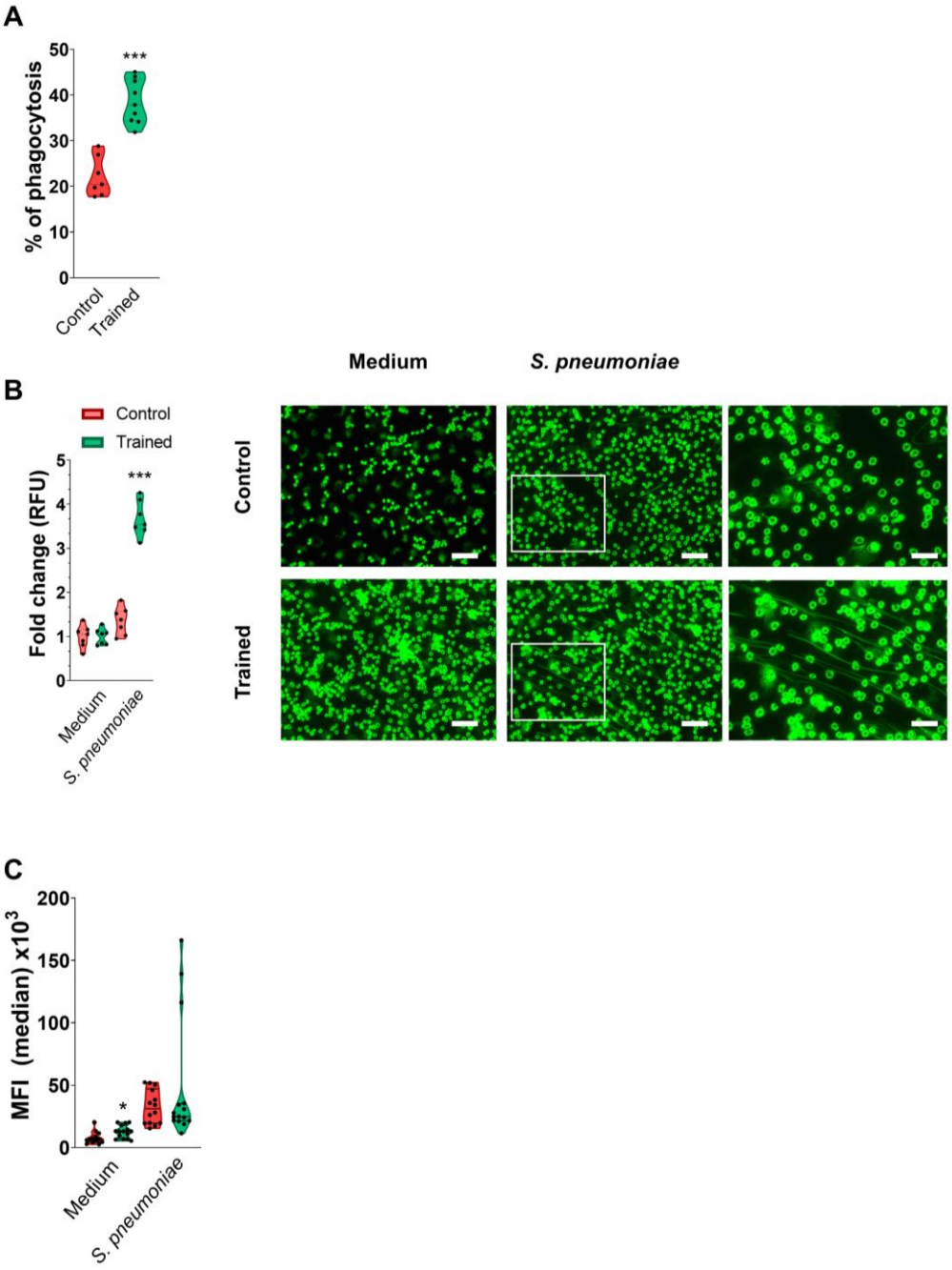

Figure 8. Trained immunity increases phagocytosis and by trained PMNs. ***A.*** PMNs were incubating for 1 hour with 10^6 CFU/mL GFP-expressing *S. pneumoniae* and analyzed by flow cytometry to quantify the percentage of PMNs phagocytosing bacteria (n=7-9 mice). ***B***. NETs production by PMNs from control and trained mice after 1 hour of culture with 10^6 CFU/mL *S. pneumoniae*. NETs were quantified using the Sytox Green assay. Results were expressed relative to values obtained using PMNs cultured in medium set at 1. NETs were visualized by fluorescent microscopy (40 and 160 x magnification). ***C***. Median fluorescence intensity (MFI) of PMNs cultured 1 hour with medium, 0.1 mM H_2O_2 or 10^6 CFU/mL *S. pneumoniae* and stained with MitoSOX determined by flow cytometry. (n=7-10 mice). * $P < 0.05$, ** $P < 0.01$, *** $P < 0.001$.

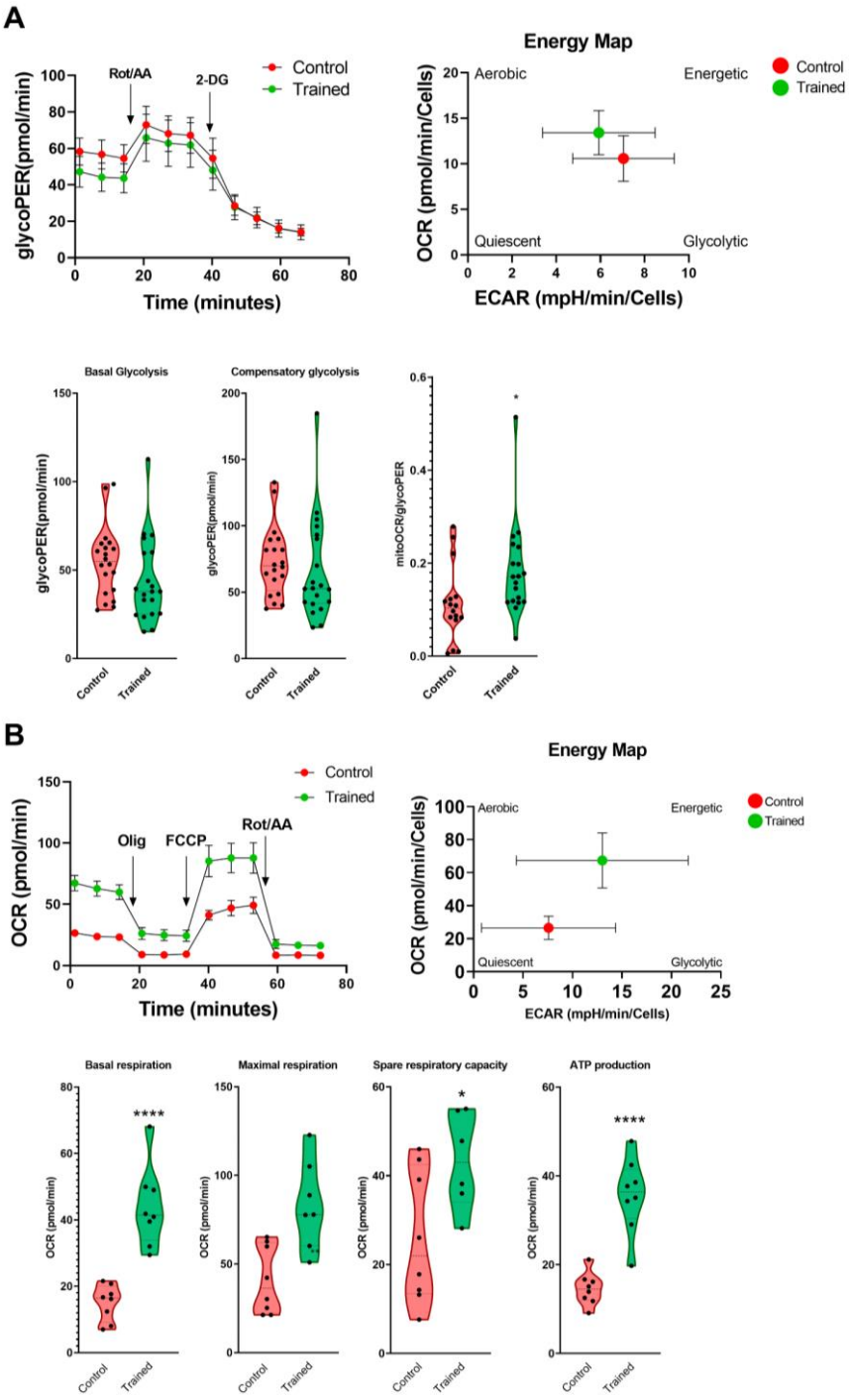

Figure 9. Trained immunity increases mitochondrial respiration by PMNs. ***A.*** Glycolysis was represented as glycolytic proton efflux rate (GlycoPER). ***B***. Mitochondrial respiration was represented as oxidative consumption rate (OCR). Measurements were performed using a Seahorse XFe96 Analyzer. 2-DG, 2-deoxy-D-glucose; ECAR, extracellular acidification rate; FCCP, carbonyl cyanide-p-trifluoromethoxyphenyl-hydrazon; Olig, oligomycin; Rot/AA, rotenone and antimycin A. Each dot represents one mouse. * $P < 0.05$, ** $P < 0.01$, *** $P < 0.001$, **** $P < 0.0001$.

SUPPLEMENTARY Figures

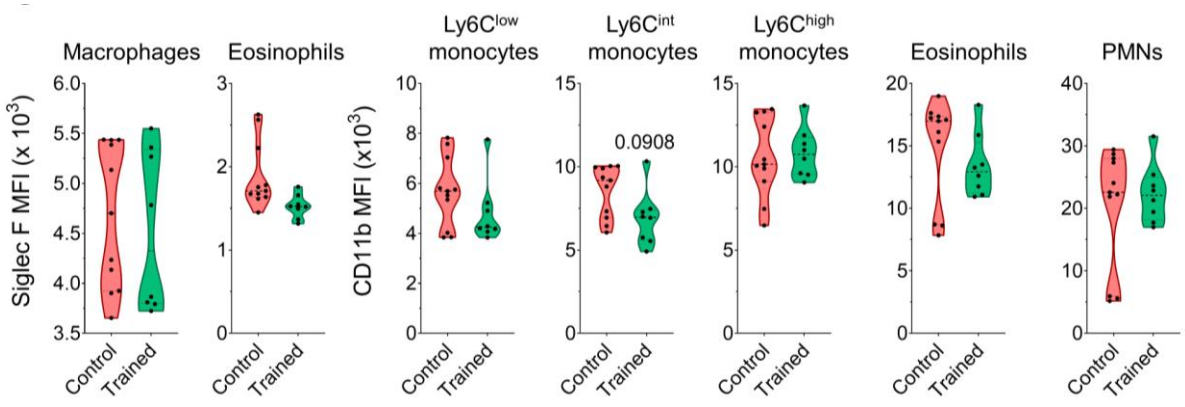

Figure supplementary 1. Mean fluorescence intensity (MFI), determined by flowcytometry, of Siglec-F expressed by lung macrophages and eosinophils and CD11b expressed by lungs monocytes, eosinophils and PMNs in control and trained mice (n= 8-11 mice). * $P < 0.05$.

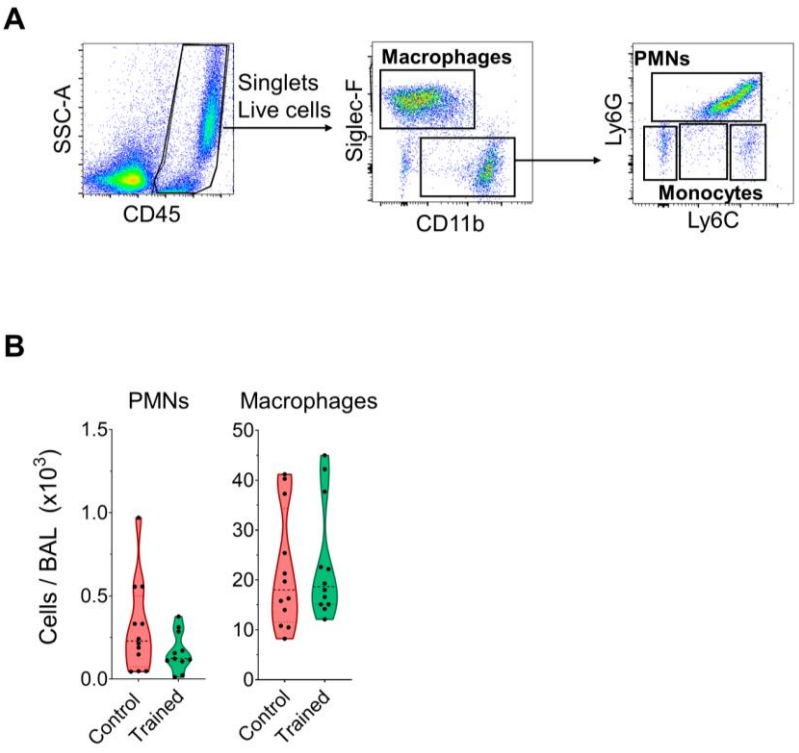

Figure supplementary 2. ***A*****.** Gating strategy for the analysis by flow cytometry of leukocytes in BALs. ***B***. PMNs and macrophages in BALs of control and trained mice (n=8-11 mice).

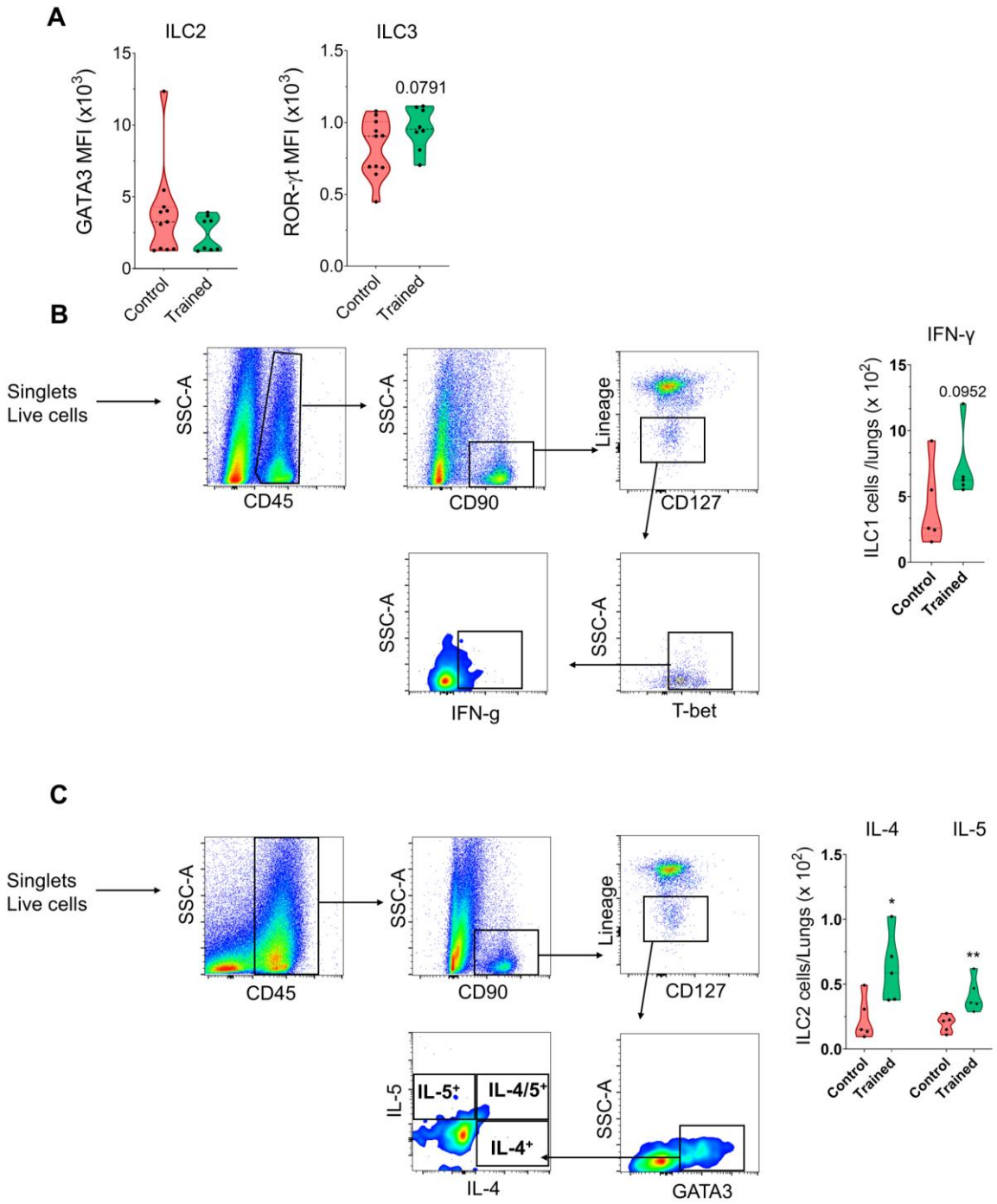

Figure supplementary 3. ***A.*** MFI of GATA3 expressed by lung ILC2 and ROR-γt expressed by lung ILC3. ***B***. Gating strategy for the analysis of ILC1 producing IFNγ by flow cytometry. ***C***. Gating strategy for the analysis of ILC2 producing IL-4 and IL-5 by flow cytometry. Each dot represents one mouse. * $P < 0.05$; ** $P < 0.01$.

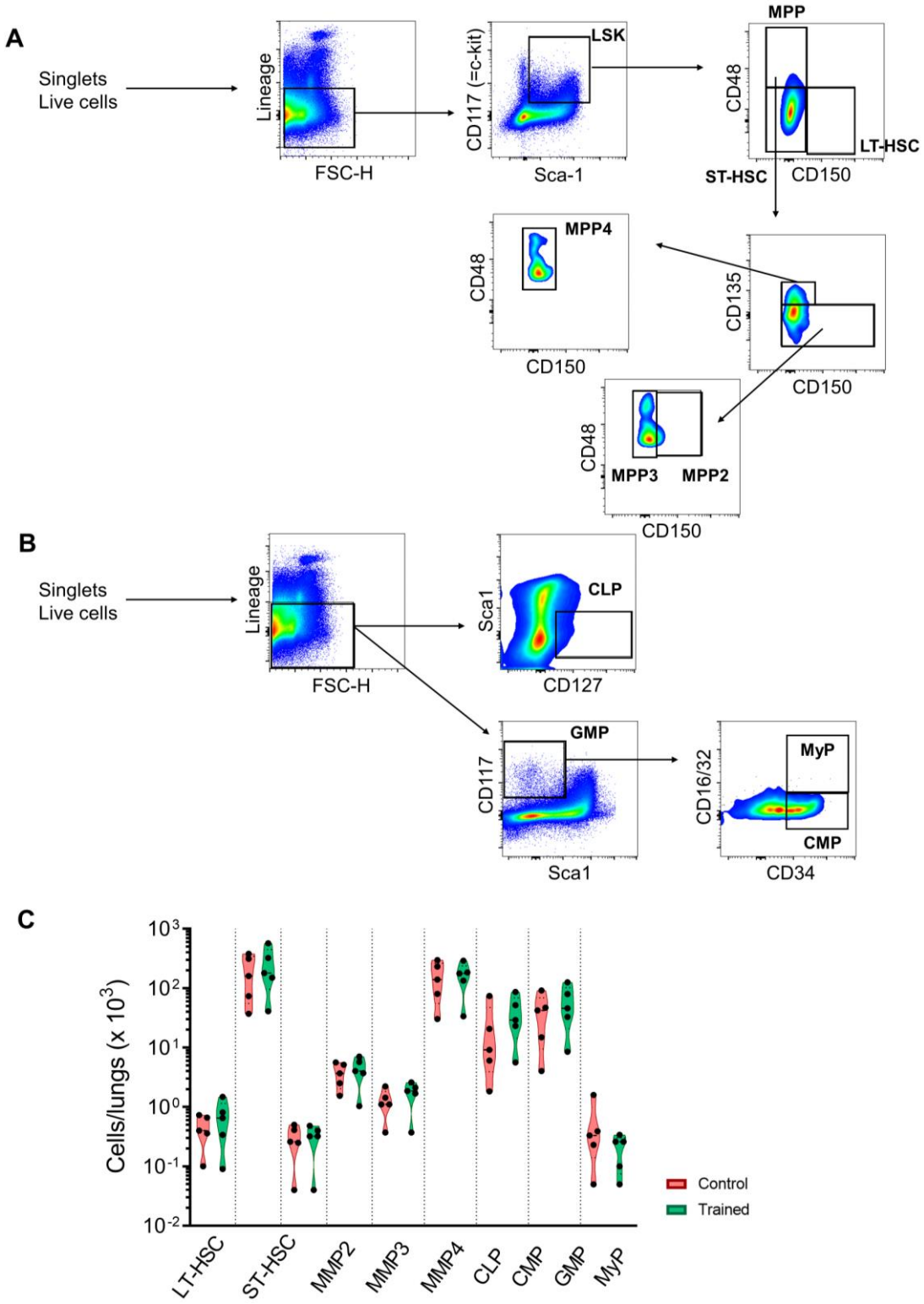

Figure supplementary 4. *A*. Gating strategy for the analysis of LT-HSC, ST-HSC, MPP4, MPP3 and MPP2 in lungs. ***B***. Gating strategy for the analysis of CLP, GMP, MyP and CMP in lungs. ***C***. Lungs progenitors in control and trained mice (n=5 mice). CLP, common lymphoid progenitors; CMP, common myeloid progenitors; GMP, granulocyte-monocyte progenitors; LT-HSC, long-term hematopoietic stem cells; LSK, lineage $Sca1^{+}Kit^{+}$; MPP, multipotent progenitors; MyP, myeloid progenitors; ST-HSC, short-term hematopoietic stem cells.

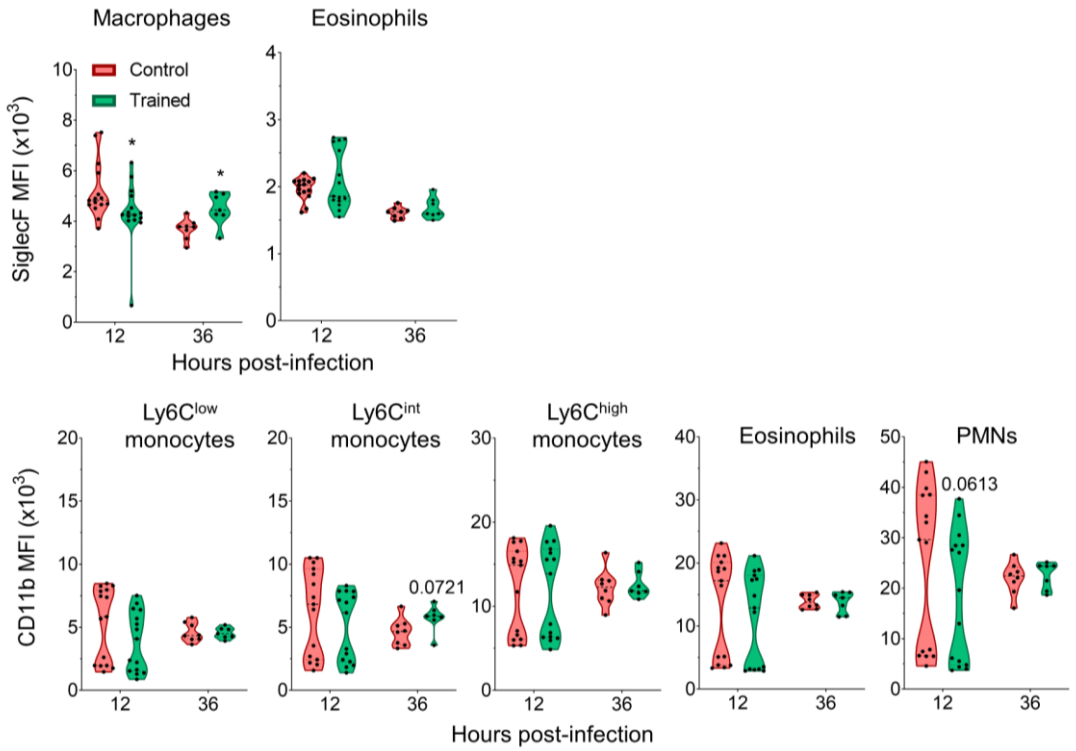

Figure supplementary 5. MFI of Siglec-F expressed by lung macrophages and eosinophils and CD11b expressed by lung monocytes, eosinophils and PMNs in control and trained mice 12 and 36 hours post-infection with *S. pneumoniae* (n= 12-20 mice). * $P < 0.05$.

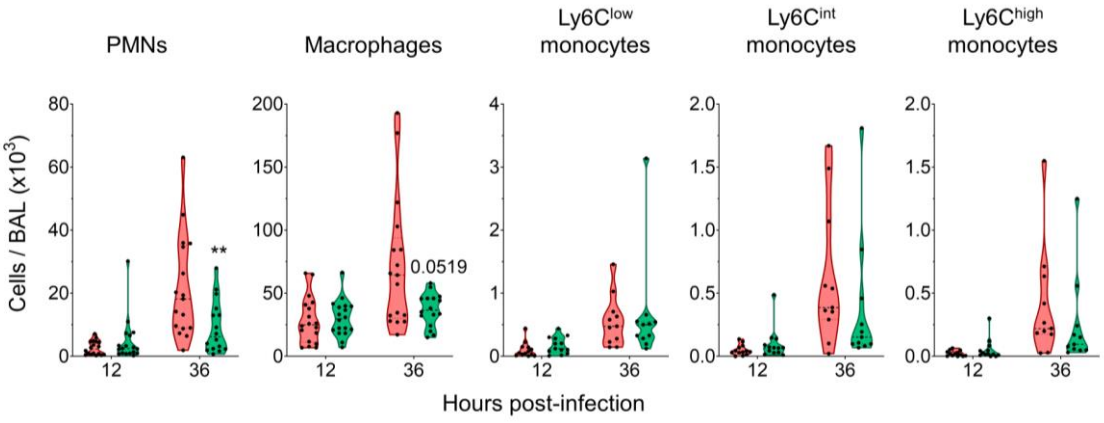

Figure supplementary 6. PMNs, macrophages and monocytes in BALs of control and trained mice 12 and 36 hours post-infection with *S. pneumoniae* (n=12-20 mice).

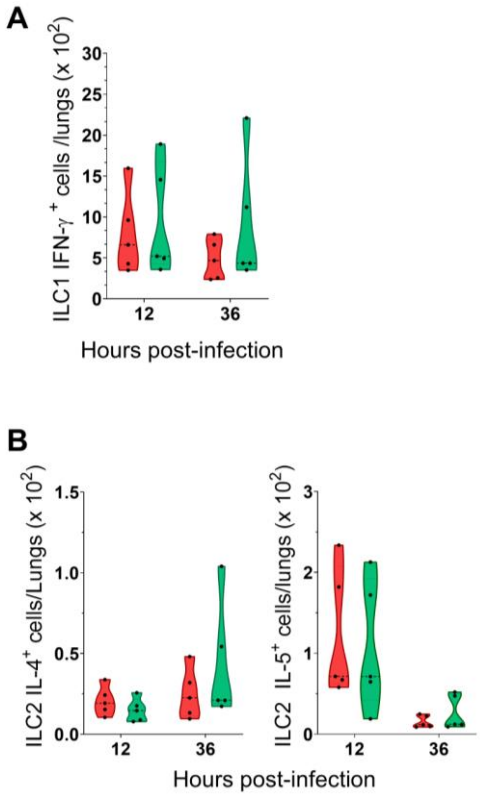

Figure supplementary 7. Lungs were collected from control and trained mice (n=5/group) 12 and 36 hours post-infection with *S. pneumoniae*. ***A*.** ILC1 producing IFNγ determined by flow cytometry. ***B***. ILC2 producing IL-4 and IL-5 determined by flow cytometry.

REFERENCES

1. Takeuchi, N., et al., *First report on multidrug-resistant non-encapsulated Streptococcus pneumoniae isolated from a patient with pneumonia.* J Infect Chemother, 2020.
2. Micek, S.T., et al., *Characteristics and outcomes among a hospitalized patient cohort with Streptococcus pneumoniae infection.* Medicine (Baltimore), 2020. **99**(18): p. e20145.
3. Daniels, C.C., P.D. Rogers, and C.M. Shelton, *A Review of Pneumococcal Vaccines: Current Polysaccharide Vaccine Recommendations and Future Protein Antigens.* J Pediatr Pharmacol Ther, 2016. **21**(1): p. 27-35.
4. Rodriguez, B.F., et al., *Streptococcus pneumoniae: the forgotten microorganism in neonatal sepsis.* Fetal Pediatr Pathol, 2015. **34**(3): p. 202-5.
5. Collaborators, G.B.D.L.R.I., *Estimates of the global, regional, and national morbidity, mortality, and aetiologies of lower respiratory infections in 195 countries, 1990-2016: a systematic analysis for the Global Burden of Disease Study 2016.* Lancet Infect Dis, 2018. **18**(11): p. 1191-1210.
6. Weiser, J.N., D.M. Ferreira, and J.C. Paton, *Streptococcus pneumoniae: transmission, colonization and invasion.* Nat Rev Microbiol, 2018. **16**(6): p. 355-367.
7. Pechous, R.D., *With Friends Like These: The Complex Role of Neutrophils in the Progression of Severe Pneumonia.* Front Cell Infect Microbiol, 2017. **7**: p. 160.
8. Wang, W., et al., *Interleukin 17A promotes pneumococcal clearance by recruiting neutrophils and inducing apoptosis through a p38 mitogen-activated protein kinase-dependent mechanism in acute otitis media.* Infect Immun, 2014. **82**(6): p. 2368-77.
9. Schachern, P.A., et al., *Neutrophil Extracellular Traps and Fibrin in Otitis Media: Analysis of Human and Chinchilla Temporal Bones.* JAMA Otolaryngol Head Neck Surg, 2017. **143**(10): p. 990-995.
10. Standish, A.J. and J.N. Weiser, *Human neutrophils kill Streptococcus pneumoniae via serine proteases.* J Immunol, 2009. **183**(4): p. 2602-9.
11. Hahn, I., et al., *Cathepsin G and neutrophil elastase play critical and nonredundant roles in lung-protective immunity against Streptococcus pneumoniae in mice.* Infect Immun, 2011. **79**(12): p. 4893-901.
12. Bou Ghanem, E.N., et al., *Extracellular Adenosine Protects against Streptococcus pneumoniae Lung Infection by Regulating Pulmonary Neutrophil Recruitment.* PLoS Pathog, 2015. **11**(8): p. e1005126.
13. Paterson, G.K. and T.J. Mitchell, *Innate immunity and the pneumococcus.* Microbiology (Reading), 2006. **152**(Pt 2): p. 285-293.
14. Tomlinson, G., et al., *TLR-mediated inflammatory responses to Streptococcus pneumoniae are highly dependent on surface expression of bacterial lipoproteins.* J Immunol, 2014. **193**(7): p. 3736-45.
15. Dockrell, D.H., et al., *Immune-mediated phagocytosis and killing of Streptococcus pneumoniae are associated with direct and bystander macrophage apoptosis.* J Infect Dis, 2001. **184**(6): p. 713-22.
16. Gasteiger, G., et al., *Tissue residency of innate lymphoid cells in lymphoid and nonlymphoid organs.* Science, 2015. **350**(6263): p. 981-5.
17. Lai, D.M., Q. Shu, and J. Fan, *The origin and role of innate lymphoid cells in the lung.* Mil Med Res, 2016. **3**: p. 25.
18. Vivier, E., et al., *Innate Lymphoid Cells: 10 Years On.* Cell, 2018. **174**(5): p. 1054-1066.
19. Monticelli, L.A., et al., *Innate lymphoid cells promote lung-tissue homeostasis after infection with influenza virus.* Nat Immunol, 2011. **12**(11): p. 1045-54.
20. Chang, Y.J., et al., *Innate lymphoid cells mediate influenza-induced airway hyper-reactivity independently of adaptive immunity.* Nat Immunol, 2011. **12**(7): p. 631-8.
21. Gorski, S.A., Y.S. Hahn, and T.J. Braciale, *Group 2 innate lymphoid cell production of IL-5 is regulated by NKT cells during influenza virus infection.* PLoS Pathog, 2013. **9**(9): p. e1003615.
22. Van Maele, L., et al., *Activation of Type 3 innate lymphoid cells and interleukin 22 secretion in the lungs during Streptococcus pneumoniae infection.* J Infect Dis, 2014. **210**(3): p. 493-503.
23. Kim, H.Y., et al., *Innate lymphoid cells responding to IL-33 mediate airway hyperreactivity independently of adaptive immunity.* J Allergy Clin Immunol, 2012. **129**(1): p. 216-27 e1-6.
24. Thio, C.L., et al., *Regulation of type 2 innate lymphoid cell-dependent airway hyperreactivity by butyrate.* J Allergy Clin Immunol, 2018. **142**(6): p. 1867-1883 e12.
25. Puissant, B. and B. Combadiere, *Keeping the memory of smallpox virus.* Cell Mol Life Sci, 2006. **63**(19-20): p. 2249-59.
26. Kurosaki, T., K. Kometani, and W. Ise, *Memory B cells.* Nat Rev Immunol, 2015. **15**(3): p. 149-59.

27. Sticher, L., B. Mauch-Mani, and J.P. Metraux, *Systemic acquired resistance.* Annu Rev Phytopathol, 1997. **35**: p. 235-70.
28. Kurtz, J. and K. Franz, *Innate defence: evidence for memory in invertebrate immunity.* Nature, 2003. **425**(6953): p. 37-8.
29. Bistoni, F., et al., *Evidence for macrophage-mediated protection against lethal Candida albicans infection.* Infect Immun, 1986. **51**(2): p. 668-74.
30. Quintin, J., et al., *Candida albicans infection affords protection against reinfection via functional reprogramming of monocytes.* Cell Host Microbe, 2012. **12**(2): p. 223-32.
31. Kleinnijenhuis, J., et al., *Bacille Calmette-Guerin induces NOD2-dependent nonspecific protection from reinfection via epigenetic reprogramming of monocytes.* Proc Natl Acad Sci U S A, 2012. **109**(43): p. 17537-42.
32. Roth, A., et al., *BCG vaccination scar associated with better childhood survival in Guinea-Bissau.* Int J Epidemiol, 2005. **34**(3): p. 540-7.
33. Aaby, P., et al., *Randomized trial of BCG vaccination at birth to low-birth-weight children: beneficial nonspecific effects in the neonatal period?* J Infect Dis, 2011. **204**(2): p. 245-52.
34. Garly, M.L., et al., *BCG scar and positive tuberculin reaction associated with reduced child mortality in West Africa. A non-specific beneficial effect of BCG?* Vaccine, 2003. **21**(21-22): p. 2782-90.
35. Netea, M.G., J. Quintin, and J.W. van der Meer, *Trained immunity: a memory for innate host defense.* Cell Host Microbe, 2011. **9**(5): p. 355-61.
36. Ferreira, A.V., J. Domiguez-Andres, and M.G. Netea, *The Role of Cell Metabolism in Innate Immune Memory.* J Innate Immun, 2020: p. 1-9.
37. van der Heijden, C., et al., *Epigenetics and Trained Immunity.* Antioxid Redox Signal, 2018. **29**(11): p. 1023-1040.
38. Netea, M.G., et al., *Defining trained immunity and its role in health and disease.* Nat Rev Immunol, 2020.
39. Ciarlo, E., et al., *Trained immunity confers broad-spectrum protection against bacterial infections.* J Infect Dis, 2019.
40. Kjos, M., et al., *Bright fluorescent Streptococcus pneumoniae for live-cell imaging of host-pathogen interactions.* J Bacteriol, 2015. **197**(5): p. 807-18.
41. Roger, T., et al., *Macrophage migration inhibitory factor deficiency is associated with impaired killing of gram-negative bacteria by macrophages and increased susceptibility to Klebsiella pneumoniae sepsis.* J Infect Dis, 2013. **207**(2): p. 331-9.
42. Van Hoecke, L., et al., *Bronchoalveolar Lavage of Murine Lungs to Analyze Inflammatory Cell Infiltration.* J Vis Exp, 2017(123).
43. Ciarlo, E., et al., *Impact of the microbial derived short chain fatty acid propionate on host susceptibility to bacterial and fungal infections in vivo.* Sci Rep, 2016. **6**: p. 37944.
44. Reverte, M. and N. Fasel, *Leishmania Parasite Quantification by Bioluminescence in Murine Models.* Bio Protoc, 2019. **9**(22): p. e3431.
45. Heinonen, T., et al., *Impact of the Dual Deletion of the Mitochondrial Sirtuins SIRT3 and SIRT5 on Anti-microbial Host Defenses.* Front Immunol, 2019. **10**: p. 2341.
46. Lefrancais, E., et al., *The lung is a site of platelet biogenesis and a reservoir for haematopoietic progenitors.* Nature, 2017. **544**(7648): p. 105-109.
47. Hillel-Karniel, C., et al., *Multi-lineage Lung Regeneration by Stem Cell Transplantation across Major Genetic Barriers.* Cell Rep, 2020. **30**(3): p. 807-819 e4.
48. Mitroulis, I., et al., *Modulation of Myelopoiesis Progenitors Is an Integral Component of Trained Immunity.* Cell, 2018. **172**(1-2): p. 147-161 e12.
49. Guillon, A., et al., *Pneumonia recovery reprograms the alveolar macrophage pool.* JCI Insight, 2020. **5**(4).
50. Kadioglu, A., et al., *Upper and lower respiratory tract infection by Streptococcus pneumoniae is affected by pneumolysin deficiency and differences in capsule type.* Infect Immun, 2002. **70**(6): p. 2886-90.
51. Yesilkaya, H., et al., *Streptococcus pneumoniae and reactive oxygen species: an unusual approach to living with radicals.* Trends Microbiol, 2013. **21**(4): p. 187-95.
52. De Filippo, K., et al., *Mast cell and macrophage chemokines CXCL1/CXCL2 control the early stage of neutrophil recruitment during tissue inflammation.* Blood, 2013. **121**(24): p. 4930-7.
53. Prince, L.R., et al., *The role of interleukin-1beta in direct and toll-like receptor 4-mediated neutrophil activation and survival.* Am J Pathol, 2004. **165**(5): p. 1819-26.
54. Fielding, C.A., et al., *IL-6 regulates neutrophil trafficking during acute inflammation via STAT3.* J Immunol, 2008. **181**(3): p. 2189-95.
55. Mao, H., et al., *Mechanisms of Siglec-F-induced eosinophil apoptosis: a role for caspases but not for SHP-1, Src kinases, NADPH oxidase or reactive oxygen.* PLoS One, 2013. **8**(6): p. e68143.

56. Ganz, T. and E. Nemeth, *Iron sequestration and anemia of inflammation.* Semin Hematol, 2009. **46**(4): p. 387-93.
57. Turner, J.E., et al., *IL-9-mediated survival of type 2 innate lymphoid cells promotes damage control in helminth-induced lung inflammation.* J Exp Med, 2013. **210**(13): p. 2951-65.
58. Allen, J.E. and T.E. Sutherland, *Host protective roles of type 2 immunity: parasite killing and tissue repair, flip sides of the same coin.* Semin Immunol, 2014. **26**(4): p. 329-40.
59. Doherty, T.A. and D.H. Broide, *Airway innate lymphoid cells in the induction and regulation of allergy.* Allergol Int, 2019. **68**(1): p. 9-16.
60. Rosenberg, H.F., K.D. Dyer, and P.S. Foster, *Eosinophils: changing perspectives in health and disease.* Nat Rev Immunol, 2013. **13**(1): p. 9-22.
61. Goh, Y.P., et al., *Eosinophils secrete IL-4 to facilitate liver regeneration.* Proc Natl Acad Sci U S A, 2013. **110**(24): p. 9914-9.
62. Heredia, J.E., et al., *Type 2 innate signals stimulate fibro/adipogenic progenitors to facilitate muscle regeneration.* Cell, 2013. **153**(2): p. 376-88.
63. Takeda, K., et al., *Eosinophils contribute to the resolution of lung-allergic responses following repeated allergen challenge.* J Allergy Clin Immunol, 2015. **135**(2): p. 451-60.
64. Coden, M.E. and S. Berdnikovs, *Eosinophils in wound healing and epithelial remodeling: Is coagulation a missing link?* J Leukoc Biol, 2020.
65. Lee, J.J., et al., *Eosinophils in health and disease: the LIAR hypothesis.* Clin Exp Allergy, 2010. **40**(4): p. 563-75.
66. Bustamante-Marin, X.M. and L.E. Ostrowski, *Cilia and Mucociliary Clearance.* Cold Spring Harb Perspect Biol, 2017. **9**(4).
67. Tilley, A.E., et al., *Cilia dysfunction in lung disease.* Annu Rev Physiol, 2015. **77**: p. 379-406.
68. Campbell, L., et al., *ILC2s mediate systemic innate protection by priming mucus production at distal mucosal sites.* J Exp Med, 2019. **216**(12): p. 2714-2723.
69. Han, M., et al., *IL-1beta prevents ILC2 expansion, type 2 cytokine secretion and mucus metaplasia in response to early-life rhinovirus infection in mice.* Allergy, 2020.
70. Mear, J.B., et al., *Candida albicans airway exposure primes the lung innate immune response against Pseudomonas aeruginosa infection through innate lymphoid cell recruitment and interleukin-22-associated mucosal response.* Infect Immun, 2014. **82**(1): p. 306-15.
71. Sharma, A.R., et al., *BCG as a game-changer to prevent the infection and severity of COVID- 19 pandemic?* Allergol Immunopathol (Madr), 2020.
72. Escobar, L.E., A. Molina-Cruz, and C. Barillas-Mury, *BCG vaccine protection from severe coronavirus disease 2019 (COVID-19).* Proc Natl Acad Sci U S A, 2020.
73. O'Neill, L.A.J. and M.G. Netea, *BCG-induced trained immunity: can it offer protection against COVID-19?* Nat Rev Immunol, 2020.
74. Curtis, N., et al., *Considering BCG vaccination to reduce the impact of COVID-19.* The Lancet, 2020.
75. Redelman-Sidi, G., *Could BCG be used to protect against COVID-19?* Nat Rev Urol, 2020.
76. Abbas, A.M., et al., *The effect of BCG vaccine in the era of COVID-19 pandemic.* Scand J Immunol, 2020: p. e12947.
77. Miyasaka, M., *Is BCG vaccination causally related to reduced COVID-19 mortality?* EMBO Mol Med, 2020.
78. Kerboua, K.E., *The perplexing question of trained immunity versus adaptive memory in COVID-19.* J Med Virol, 2020.
79. Macedo, A. and C. Febra, *Relation between BCG coverage rate and COVID-19 infection worldwide.* Med Hypotheses, 2020. **142**: p. 109816.
80. Klinger, D., et al., *Significantly Improved COVID-19 Outcomes in Countries with Higher BCG Vaccination Coverage: A Multivariable Analysis.* Vaccines (Basel), 2020. **8**(3).
81. Madan, M., et al., *TB infection and BCG vaccination: are we protected from COVID-19?* Public Health, 2020. **185**: p. 91-92.
82. Kinoshita, M. and M. Tanaka, *Impact of routine infant BCG vaccination in young generation on prevention of local COVID-19 spread in Japan.* J Infect, 2020.
83. Covian, C., et al., *Could BCG Vaccination Induce Protective Trained Immunity for SARS-CoV- 2?* Front Immunol, 2020. **11**: p. 970.
84. Arts, R.J.W., et al., *BCG Vaccination Protects against Experimental Viral Infection in Humans through the Induction of Cytokines Associated with Trained Immunity.* Cell Host Microbe, 2018. **23**(1): p. 89-100 e5.

Supplementary Table 1

Reagent	Brand/origin	Identifier/catalog reference #
Antibodies		
Anti-mouse CD3, APC (clone 17A2)	eBioscience	RRID: AB_10597589; #17-0032-82
Anti-mouse CD3, FITC (clone 17A2)	eBioscience	RRID: AB_11-0032-82; #2572431
Anti-mouse CD3, PE-Cy7 (clone 17A2)	BioLegend	RRID: AB_1732057; #100220
Anti-mouse CD5, FITC (clone 53-7.3)	eBioscience	RRID: AB_464908; #11-0051-82
Anti-mouse CD8a, FITC (clone 53-6.7)	BioLegend	RRID: AB_312745; #100706
Anti-mouse CD11b, APC-Cy7 (clone M1/70)	BD Biosciences	RRID: AB_2033993; #561039
Anti-mouse CD11b, FITC (clone M1/70.15.11.5)	Miltenyi Biotec	RRID: AB_244270; #130-081-201
Anti-mouse CD11b, PE-Cy7 (clone M1/70)	BioLegend	RRID: AB_312799; #101216
Anti-mouse CD11c, FITC (clone N418)	eBioscience	RRID: AB_464940; #11-0114-82
Anti-mouse CD16/CD32, Alexa Fluor 700 (clone 93)	eBioscience	RRID: AB_493994; #56-0161
Anti-mouse CD19, FITC (clone 1D3)	eBioscience	RRID:AB_657666; #11-0193-82
Anti-mouse CD19, FITC (clone 1D3)	eBioscience	RRID: AB_657663; #25-0193-82
Anti-mouse CD34, PE-Cy7 (clone RAM34)	eBioscience	RRID: AB_465021; #11-0341-82
Anti-mouse CD45, Brilliant violet 605 (clone 30-F11)	BD Biosciences	RRID:AB_2737976; #563053
Anti-mouse CD45, AlexaFluor700 (clone 30-F11)	eBioscience	RRID:AB_891454; #56-0451-82
Anti-mouse CD45R (B220), FITC (clone RA3-6B2)	eBioscience	RRID:AB_465054; #11-0452-82
Anti-mouse CD45R (B220), PE-Cy7 (clone RA3-6B2)	BioLegend	RRID: AB_313005; #103222
Anti-mouse CD48, APC-Cy7 (clone HM48-1)	BioLegend	RRID: AB_2561463; #103432
Anti-mouse CD49b, FITC (clone DX5)	Miltenyi Biotec	RRID:AB_2660456; #130-102-258
Anti-mouse CD90/Thy1.2, APC-Cy7 (clone 53-2.1)	eBioscience	RRID:AB_469422; #17-0902-82
Anti-mouse CD117 (c-Kit), APC (clone2B8)	BioLegend	RRID: AB_313221; #105812
Anti-mouse CD127, PE-Cyanine7 (clone A7R34)	eBioscience	RRID:AB_469649; #25-1271-82
Anti-mouse CD127, PE (clone A7R34)	eBioscience	RRID:AB_465843; #12-1271-81
Anti-mouse CD135 (Flt3), PE (clone A2F10)	eBioscience	RRID:AB_465859; #12-1351-82
Anti-mouse CD150 (SLAM), PerCP/Cyanine5.5 (clone TC15-12F12.2)	BioLegend	RRID:AB_2303663; #115922
Anti-mouse CD170 (Siglec F), eFluor 660 (clone 1RNM44N)	eBioscience	RRID:AB_2574186; #50-1702-80
Anti-mouse FcεRIα, FITC (clone MAR-1)	Miltenyi Biotec	RRID:AB_2660610; #130-102-264
Anti-mouse GATA3, Brilliant violet 711 (clone L50-823)	BD Biosciences	RRID: AB_2739242; #565449
Anti-mouse Gr-1, PE-Cy7 (clone RB6-8C5)	BioLegend	RRID: AB_313381; #108416
Anti-mouse IFN-gamma, PE (clone XMG1.2)	BD Biosciences	RRID:AB_395376; #554412
Anti-mouse IL-4, Brilliant violet 421 (clone 11B11)	BD Biosciences	RRID:AB_2737889; #562915
Anti-mouse IL-5, APC (clone TRFK5)	BD Biosciences	RRID:AB_398548; #554396
Anti-mouse Ly6A/E (Sca-1), Super Bright 600 (clone D7)	eBioscence	RRID: AB_2663622; #63-5981
Anti-mouse Ly6A/E (Sca-1), FITC (clone D7)	eBioscence	RRID: AB_465333; #11-5981-82

Anti-mouse Ly6C, FITC (clone AL-21 (RUO))	BD Biosciences	RRID:AB_10584332; #561085
Anti-mouse Ly6G, PE-CF594 (clone 1A8)	BD Biosciences	RRID:AB_2737730; #562700
Anti-mouse MHC Class II (IA/IE), PE (clone M5/114.15.2)	eBioscience	RRID: AB_465928; #12-5321-81
Anti-mouse ROR gamma (t), APC (clone AFKJS-9)	eBioscience	RRID: AB_1633425; 17-6988-80
Anti-mouse T-bet, APC (clone 4B10)	BioLegend	RRID: AB_10901173; #644814
Anti-mouse TCR beta, FITC (clone H57-597)	Invitrogen	RRID: AB_2539041; MA5-17651
Anti-mouse TCR gamma/delta, FITC (clone GL3)	eBioscience	RRID: AB_465238; #11-5711-82
Anti-mouse Ter119, PE-Cy7 (clone TER-119)	BioLegend	RRID: AB_2281408; #116222
Anti-mouse Ter119, FITC (clone Ter119)	Miltenyi Biotec	RRID: AB_2660080; #130-102-257
Fixable Viability Dye eFluor™ 450	Invitrogen	65-0863
LIVE/DEAD™ Fixable Violet	Invitrogen	L34955
Zombie Yellow™ Fixable Viability Kit	BioLegend	423103
Chemicals		
2-deoxyglucose	Sigma-Aldrich	D6134
5x RIPA Buffer IV with Triton-X-100 (pH 7.4)	Bio Basic	RB4478
Ammonium chloride	Sigma-Aldrich Merck	A0171
Antimycin A from *Streptomyces* sp.	Sigma-Aldrich	A8674
Carbonyl cyanide-p-trifluoromethoxyphenylhydrazone (FCCP)	Sigma-Aldrich	C2910
Celltak	Corning	354240
Collagenase D	Sigma-Aldrich Merck	11088866001
cOmplete, Mini, EDTA-free Protease Inhibitor Cocktail	Roche	11836170001
DAPI (4',6-Diamidino-2-Phenylindole, Dihydrochloride)	Invitrogen	D1306
DNAse I	Sigma-Aldrich Merck	11284932001
EDTA, Titriplex® III	Merck	1.08418
Fetal calf serum (FCS)	Bioconcept	2-01F30-I
Fixation/Permeabilization concentrate	eBioscience	00-5123-43
Fixation/Permeabilization diluent	eBioscience	00-5223-56
HEPES	Bioconcept	5-31F00-H
Hydrogen peroxide (H_2O_2) solution 30% (w/w) in H_2O	Sigma-Aldrich	H1009
Luminol sodium salt	Carbosynth	20666-12-0
Neutrophil isolation kit (mouse)	Miltenyi	130-097-658
Oligomycin	Sigma-Aldrich	A8674
ProcartaPlex Mix&Match Mouse 17-plex (ENA-78/CXCL5, G-CSF, Gro-α/KC, IFNγ, IL-1α, IL-1β, IL-3, IL-6, IL-10, IL-12p40, IL-17A, IL-18, IP-10/CXCL10, MCP-1/CCL2, MIP-1α/CCL3, MIP-2/CXCL2, TNF	Invitrogen	PPX-17-MX7DPRR
PFA, Pierce™ 16% Formaldehyde (w/v)	Thermo Fisher scientific	28908
Permeabilization buffer	eBioscience	00-8333
Phosphate buffered saline (PBS)	GROSSE APOTHEKE	100 0 324 00

Pierce BCA Protein Assay Kit	Thermofisher Scientific	23227
RPMI 1640 Medium, GlutaMAX	Gibco (ThermoFisher)	61870-010
Seahorse XFp Fluk Pak	Agilent	103025
Sodium bicarbonate solution (7.5%)	Sigma-Aldrich Merck	S8761
SYTOX Green Nucleic Acid Stain	Invitrogen	S7020
Todd Hewitt Broth	Sigma-Aldrich Merck	T1438
Triton X-100	Bio-Rad	161-0407
Rotenone	Sigma-Aldrich	R8875
XF 1.0 M Glucose solution	Agilent	103577
XF 100 mM Pyruvate solution	Agilent	103578
XF 200 mM Glutamine solution	Agilent	103579
Yeast extract	Sigma-Aldrich Merck	70161
Zymosan A from *Saccharomyces cerevisiae*	Sigma-Aldrich Merck	Z4250
Materials		
96-well Clear Polystyrene Microplates	Corning	3799
Columbia III Agar with 5% Sheep Blood	BD Biosciences	254098
GentleMACS C Tube	Miltenyi Biotec	130-096-334
Bacteria		
Streptococcus pneumoniae		ATCC 6303
Mice		
C57BL/6J	Charles River Laboratories	632
Software		
Adope Photoshop	Adope 22.3	
BD FACSDiva software.	BD	
FlowJo_V10_CL 10	FlowJo LLC	
Molecular Imaging (MI) software	BRUKER	
Prism 8	GraphPad Software	
R	RStudio Team (2020)	
SeaHorse Analytics	Agilent	

Supplementary Table 2: Grading system

Finding	Score				
	0	**1**	**2**	**3**	**4**
Leukocyte rolling/ adhesion	Absent	Minimal (rare cells, occasional blood vessels)	Mild (small number of cells, multiple blood vessels)	Moderate (moderate number of cells, multiple blood vessels)	Marked (large number of cells, multiple blood vessels)
Peribronchial/ Perivascular Interstitial leukocyte infiltration	Absent	Minimal	Mild	Moderate	Marked
Bronchiolar damage	Absent	Occasional degenerated epithelial cells (vacuolar, swollen)	Multifocal degenerated epithelial cells (vacuolar swollen)	Numerous degenerated epithelial cells + sloughing	Numerous degenerated epithelial cells + sloughing + intraluminal inflammatory cells
Intralesional bacteria	Absent	Present			
Intralesional foreign body material 0-1	Absent	Present			
Perivascular edema; perivascular hemorrhage	Absent	Minimal (or focal)	Mild (or multifocal, < 10% of blood vessels)	Moderate (or multifocal, 10-50% of blood vessels)	
Intra-alveolar hemorrhage	Absent	Minimal (or focal)	Mild (or multifocal, < 10% of lung parenchyma)	Moderate (or multifocal, 10-50% of lung parenchyma)	

3.3. Trained immunity confers prolonged protection from listeriosis

Charlotte Théroude*, Marta Reverte*, Tytti Heinonen*, Eleonora Ciarlo*, Irene Schrijver, Florian Pralong, Didier Le Roy, Thierry Roger

Infectious Diseases Service, Department of Medicine, Lausanne University Hospital and University of Lausanne, CH-1066 Epalinges, Switzerland

*, equal contribution

Submitted for publication.

Summary

Trained immunity characterizes the capacity of memory of the innate immune system. Its induction is associated with epigenetic, metabolic and functional reprograming of innate immune cells. Following our demonstration that the induction of trained immunity protects from a broad-range of infectious insults, we questioned whether these protective effects last long after induction. To address that question, mice were trained with β-glucans and challenged 1-9 weeks later with *Listeria monocytogenes*. Blood, bone marrow and spleen were collected to quantify hematopoietic progenitors, leukocytes, bacteria and antimicrobial activity. Mice trained for 9 weeks showed increased myelopoiesis. Their blood contained 2-fold more Ly6C^{high} monocytes and neutrophils, produced more G-CSF, IFNγ, IL-1α, IL-1β, IL-6, IL-10, TNF and CXCL2 in response to LPS, and controlled better the growth of *L. monocytogenes*. In line with these observations, while control mice were bacteremic and died from listeriosis, mice trained 9 weeks earlier were sterile and survived infection. Listeriosis induced the depletion of leukocytes, which was counterbalanced by trained immunity. Overall, our results support long-lasting protection afforded by trained immunity against systemic listeriosis. We are currently running experiments to better define the window of protection conferred by trained immunity.

Contribution to the work: I participated to or performed the cell population analysis. I helped with *in vivo* experiments. I revised the paper

Trained immunity confers prolonged protection from listeriosis

Charlotte Théroude*, Marta Reverte*, Tytti Heinonen*, Eleonora Ciarlo*, Irene T. Schrijver, Florian Pralong, Didier Le Roy, Thierry Roger

Infectious Diseases Service, Department of Medicine, Lausanne University Hospital and University of Lausanne, CH-1066 Epalinges, Switzerland

*Equal contribution

Short title: Trained immunity protects from listeriosis for up to 9 weeks

Corresponding author: Thierry Roger, Infectious Diseases Service, Lausanne University Hospital and University of Lausanne, CLED.04.407, Chemin des Boveresses 155, CH-1066 Epalinges, Switzerland

Tel. +41 21 314 1038;+41 79 556 8069; Thierry.Roger@chuv.ch; ORCID 0000-0002-9358-0109

Number of figures: 8

Supplementary data file: 1

Abstract

Trained immunity refers to the ability of innate immune cells exposed to a first challenge to provide an enhanced response to a secondary homologous or heterologous challenge. We reported previously that training induced one week earlier with β-glucan confers protection against a broad-spectrum of lethal bacterial infections. Yet, whether this protection persists over time is unknown. To tackle that issue, we analyzed the immune status and the response to *Listeria monocytogenes* of mice trained 9 weeks earlier. The induction of trained immunity increased bone marrow myelopoiesis and blood counts of Ly6C^{high} inflammatory monocytes and polymorphonuclear neutrophils (PMNs). *Ex vivo*, the blood from trained mice produced increased levels of cytokines in response to microbial products and limited the growth of *Listeria monocytogenes*. Upon infection with *L. monocytogenes*, peripheral blood leukocytes and especially PMNs were massively depleted in control mice but largely preserved in trained mice. PMNs from trained mice showed enhanced glycolytic activity in response to *L. monocytogenes*. Showing an efficient control of infection in trained mice, bacterial burden and dissemination in blood and liver (bacterial counting and histological analyses) as well as systemic cytokines and inflammation (multiplex bead assay and *in vivo* bioluminescence imaging) were strongly reduced in trained mice. In full agreement with these results, mice trained 9 weeks earlier were powerfully protected from lethal listeriosis. Altogether, these data suggest that trained immunity may confer prolonged protection from lethal bacterial infection.

Key words: Trained immunity, innate immunity, infection, sepsis, listeria, neutrophils, myelopoiesis, immunometabolism

Introduction

Innate immune cells express pattern-recognition receptors (PRRs) involved in the sensing of microbial-associated molecular patterns (MAMPs) and damage-associated molecular patterns (DAMPs) released by injured or stressed cells. The main families of PRRs are Toll-like receptors (TLRs), NOD-like receptors (NLRs), c-type lectins receptors (CLRs), RNA sensors (RIG-I-like receptors and DExD/H-box helicases) and cytosolic DNA sensors (CDSs) (1, 2). The interaction of PRRs with MAMPs/DAMPs triggers intracellular signaling pathways among which nuclear factor-κB (NF-κB), mitogen-activated protein kinases (MAPKs) and interferon (IFN) response factor (IRF) signaling pathways that drive gene expression and tweak effector functions of innate immune cells. Innate immune cells adapt their metabolism to meet the energy requirements necessary for defense functions, which is associated with epigenetic changes that modulate gene expression and cellular functions.

The restriction of immunological memory to the adaptive immune system has been challenged by the observations of systemic acquired resistance in plants and nonspecific effects of vaccines and *Candida albicans* infection on host defenses in vertebrates (3, 4). The concept of trained immunity was proposed to account for innate immune memory in mammals (5). Recent consensus definitions adopted for adaptive programs induced in innate immune cells restrict trained immunity to characterize "faster and greater response against a secondary challenge with homologous or even heterologous pathogens" (6). Trained immunity induced by MAMPs/DAMPs has been studied principally using the fungal cell wall component β-glucan, *Candida albicans* and the Bacillus Calmette-Guérin (BCG). The impact of training is commonly assessed one week after induction. The molecular mechanisms underlying trained immunity include metabolic, epigenetic and functional reprogramming of cells. These adaptations were initially described in monocytes and macrophages, and later extended to hematopoietic stem cells (HSCs), non-immune cells and stem cells including skin and lung epithelial stem cells (7-16). Epigenetic changes affecting DNA and chromatin in trained monocytes/macrophages promote their metabolic rewiring and expression of proinflammatory genes.

Contrary to adaptive immune memory, innate immune memory conferred by trained immunity is not antigen specific, suggestive of broad effects. This goes along with human epidemiological studies reporting strong non-specific effects on host defenses of live vaccines (BCG, polio, smallpox, measles), and proof of principle studies showing that BCG vaccination protects from controlled infection by yellow fever and malaria (17-20). Further demonstrating the broad effects of trained immunity, we reported that trained immunity conferred protection from clinically relevant pathogens inoculated through diverse routes to induce peritonitis, systemic infections, enteritis and pneumonia (21).

Many aspects of trained immunity remain to be addressed (22, 23). Among others, the length of protection conferred by trained immunity against deleterious infections is unknown. In the present study we questioned whether trained immunity induced persistent changes to protect from acute listeriosis. We show that myelopoiesis was increased 9 weeks after the induction of training, affecting peripheral blood leukocyte pool and functions. Moreover, mice trained 9 weeks prior to infection were remarkably protected from lethal listeriosis.

Materials and methods

Ethics statement. Animal experiments were approved by the Service des Affaires Vétérinaires, Direction Générale de l'Agriculture, de la Viticulture et des Affaires Vétérinaires (DGAV), état de Vaud (Epalinges, Switzerland) under authorizations n° 876.8/9 and 877.9/10 and performed according to Swiss and ARRIVE guidelines and according to Directive 2010/63/EU of European Union.

Mice. Experiments were performed with 8 to 10-week-old C57BL/6J female mice (Charles River Laboratories, Saint-Germain-sur-l'Arbresle, France). Mice were acclimated one week at least before usage. Mice were housed under specific pathogen-free and mouse hepatitis and mouse norovirus free conditions of the animal facility of the Centre des Laboratoires d'Epalinges (Switzerland, license VD-H04). Housing conditions were 21±2°C, 55±10% humidity, and 14-hours (h) light/10-h dark cycles. Food (SAFE or KILIBA NAGAF) and water (local filtered and autoclaved water or Innovive Aquavive®) were given ad libitum. Mice were injected intra-peritoneally (i.p.) twice at 4 days apart with 1 mg zymosan (Sigma-Aldrich, St-louis, MO) to induce training (**Figure 1**). Bone marrow cells were collected from femurs and tibias, while blood was collected from the submandibular vein in EDTA-tubes (Sarstedt, Nümbrech, Germany) (24, 25).

Reagents. Details about reagents, kits and antibodies used for flow cytometry analyses are reported in **Supplementary information**. Zymosan A from *Saccharomyces cerevisiae* and phytohemagglutinin-L (PHA) from *Phaseolus vulgaris* were from Sigma-Aldrich, *Salmonella minnesota* ultra-pure lipopolysaccharide (LPS) from List Biologicals Laboratories (Campbell, CA), and CpG ODN 1826 (CpG) from Microsynth (Balgach, Switzerland). *Listeria monocytogenes* 10403S (*L. monocytogenes*) was grown in brain heart infusion broth (Thermo Fisher Scientific, Waltham, MA). *Candida albicans* 5102 (*C. albicans*) was cultured in yeast extract-peptone-dextrose (BD Biosciences, Franklin Lakes, NJ) (26). Microorganisms were washed with PBS and heat-inactivated for 2 h at 56°C (*C. albicans*) or 70°C (*L. monocytogenes*).

Flow cytometry. Bone marrow cells were incubated 5 minutes (min) on ice with 3 ml ice-cold red blood cell (RBC) lysis buffer (0.65 M ammonium chloride, 10 mM sodium bicarbonate, 0.1 mM EDTA, pH 7.4). Cells were washed with cell staining medium (CSM: PBS containing 0.5% BSA (Sigma-Aldrich) and enumerated (27). Five times 10^5-10^6 cells were incubated 30 min in the dark at 4°C with 50 µl live/dead dye (Fixable Viability Dye eFluor™ 450 or LIVE/DEAD™ Fixable Violet, Thermo Fisher Scientific), then with 50 µl of 2.4G2 monoclonal antibody (cell culture supernatant of confluent cells, ATCC® HB-197™, ATCC, Manassas, VA) and finally with 50 µl of antibodies diluted in CSM to identify bone marrow progenitors or leukocytes (21). Cells were washed, incubated 5 min with 5% paraformaldehyde (PFA, Thermo Fisher Scientific), washed and re-suspended in 1 ml CSM. For whole blood staining, 20 µl of whole blood were incubated 30 min in the dark at room temperature with 50 µl of antibodies diluted in CSM. Reaction mixtures were diluted with 500 µl of RBC lysis buffer and incubated for 10 min. Cells were washed, incubated 5 min with 5% PFA, washed and re-suspended in 1 ml CSM. Throughout procedures, samples were centrifuged for 5 min at 400 x g and 4°C, and washing steps were performed with 1 ml CSM.

Eight hundred microliters of cell suspensions were acquired using an Attune NxT Flow Cytometer (Thermo Fisher Scientific) linked to an autosampler. Flow cytometry data were analyzed using FlowJo v.10 software (FlowJo LLC, Ashland, OR). Gating strategies were as described previously (21, 28). The antibody mixture to stain BM progenitor cells contained a lineage cocktail (anti-B220, CD3, CD11b, CD19, Ly-76 and Ly6C/G antibodies), and anti-CD16/32, CD34, CD117/c-kit and Ly6A/E/Sca-1 antibodies. The antibody mixture to stain BM and blood leukocytes contained anti-CD3, CD11b, CD19, CD45, Ly6C and Ly6G antibodies (**Supplementary information**).

***Ex vivo* blood stimulation assay**. Twenty microliters of blood were incubated with 80 µl of stimulus diluted in RPMI (Thermo Fisher Scientific). After 6 h or 24 h, reactions were mixed by

gentle up and down pipetting and centrifuged for 5 min at 400 x g and 4°C. Supernatants were collected to quantify cytokines.

Cytokine measurements. Cytokine concentrations were determined with DuoSet ELISA kits (R&D systems, Minneapolis, MN) using VersaMax Microplate Reader (Molecular Devices, San José, CA) and Mouse Custom ProcartaPlex (Thermo Fisher Scientific) using a Bioplex 200 system (Bio-Rad, Hercules, CA) (27).

Bacterial growth assay. Twenty microliters of blood in 96-well plates were incubated for 2 h with 6 x 10^4 CFU of *L. monocytogenes* in 130 µl RPMI without additives. Plates were shacked for 1 min at 400 rpm using a microplate shaker (Edmund Buhler, Bodelshausen, Germany) and serial dilutions of blood were plated on Columbia III Agar with 5% Sheep blood medium (BD Biosciences). Plates were incubated for 24 h at 37°C, and colonies were enumerated.

Metabolic activity. Polymorphonuclear neutrophils (PMNs) were isolated from the bone marrow of femurs and tibias using the mouse Neutrophil Isolation Kit (Miltenyi Biotec, Bergisch Gladbach, Germany). Metabolic parameters were determined using a Seahorse XFe96 Analyzer (Agilent, Santa Clara, CA) (29). PMNs were seeded at 1.5 x 10^5 cells per well in Seahorse XFe96 plates (Agilent) pre-coated with 22.4 µg/ml CellTak (Corning, Corning, NY) diluted in 0.1 M sodium bicarbonate pH 8.0 (Sigma-Aldrich). PMNs were plated in assay medium (Seahorse XF DMEM pH 7.4 supplemented with 2 mM glutamine, 1 mM pyruvate and 10 or 25 mM glucose (Agilent) for glycolytic activity or mitochondrial respiration, respectively). PMNs were incubated for 30 min with or without 10^8 heat-killed *L monocytogenes* in assay medium at 37°C without CO_2. Glycolytic activity, depicted by means of proton efflux rate (glycoPER), was assessed following Seahorse Cell Glycolytic Rate protocol (user guide kit 103344-100, Agilent), which consists of the sequential addition of 0.5/0.5 µM rotenone + antimycin A (Rot/AA) and 50 mM 2-deoxyglucose (2-DG, Sigma-Aldrich). Mitochondrial respiration, depicted by means of oxygen consumption rate (OCR), was assessed following Seahorse Mito Stress protocol (user guide kit 103015-100, Agilent), which consists of subsequent injections of 1 µM oligomycin (oligo), 2 µM carbonyl cyanide 4-(trifluoromethoxy) phenylhydrazone (FCCP) and 0.5/0.5 µM Rot/AA (Sigma-Aldrich). Results were analyzed using Wave Desktop software (Agilent). Cells were lysed with a mixture of RIPA Buffer IV (Bio Basic, Markham, Canada) and a complete protease inhibitor cocktail tablet (Roche Life Science, Basel, Switzerland) in PBS. Data were normalized to protein content quantified using the Pierce BCA Protein Assay Kit (Thermo Fisher Scientific). Data are represented as means ± SEM from 3-5 mice analyzed in quadruplicate.

RNA analyses. Total RNA was isolated, reverse transcribed and used in real-time PCR analyses performed using a QuantStudio™ 12K Flex system (Life Technologies, Carlsbad, CA) (27). Reactions, tested in triplicates, consisted of 2 µl cDNA, 2 µl H_2O, 1 µl 0.5 µM primers and 5 µl Fast SYBR® Green Master Mix (Life Technologies). Gene expression was analyzed using the threshold cycle (C_T) method $2^{-\Delta\Delta Ct}$. Data were normalized to *Actin* expression and were reported to the expression in control PMNs set at 1. Primers are listed in **Supplementary information**.

***In vivo* model of listeriosis**. Listeriosis was induced by challenging mice intravenously (i.v.) with 1.7-2.0 x 10^5 CFU *L. monocytogenes*. Blood was collected 2 days post-infection to quantify bacteria and cytokines and analyze cell populations. In some experiments, mice were sacrificed to collect bone marrow, liver and spleen. Body weight loss, severity score and survival were registered at least twice daily by 2-3 operators. The severity score was graded 0-5 based on mobility, posture, appearance and weight loss. The criteria were approved by the Service des Affaires Vétérinaires, DGAV, and are available upon request. Mice were sacrificed when they met a severity score of 4, while a dead mouse was assigned a score of 5 (28).

Quantification of inflammation *in vivo* by bioluminescence imaging. Mice were injected i.p. with 200 mg/kg luminol (Carbosynth, Staad, Switzerland). After 10 min, mice were anesthetized

using isoflurane in a veterinary induction chamber for rodents (PS-0346, Rothacher Medical GmbH, Heitenried, Germany) and transferred to an In-Vivo XtremeTM II SPF animal chamber with high-efficiency particulate air (HEPA) filters (BRUKER, Billerica, MA). Image acquisition was performed using an In-Vivo Xtreme II system (BRUKER) with luminescence and X Ray modalities. The capture values for luminescence modality were 10 min exposure time, binning 8x8 pixels, fSTOP 1.1 and field of view (FOV) and for X Ray modality parameters were 5 sec exposure time, binning 1x1 pixels, fSTOP 4 and FOV 19 cm. Images were analyzed using the Molecular Imaging software v.7.5.3 from BRUKER. Regions of interest (ROI) were set on the upper peritoneal cavity and the net bioluminescent signals were expressed in units of photons per second (P/s).

Histology. Liver was fixed overnight in 4% PFA, washed with PBS and embedded into paraffin. Transversal liver sections 5 µm thick were stained with hematoxylin and eosin (H&E) at the Mouse Pathology Facility of the University of Lausanne (Epalinges, Switzerland). Images were acquired using an EVOS M7000 Imaging System (Thermo Fisher Scientific) with Plan Apochromat 2x and 10x objectives using bright field contrast. Representative images of sections are shown. Liver sections were reconstructed to quantify the number of foci. The size and number of foci were determined using EVOS™ Analysis software v.1.4.

Statistical analyses. Data were analyzed using PRISM v.8.3.0 software (GraphPad Software, La Jolla, CA, USA) and R software v.3.6.0 (R Foundation for Statistical Computing, Vienna, Austria). Groups were compared by two-tailed unpaired t tests or by ANOVA followed by Dunnett's multiple comparisons test. Mouse survival was analyzed using the Kaplan-Meier method. *P* values < 0.05 were considered to be statistically significant. *, $P < 0.05$; **, $P \leq 0.01$; ***, $P \leq 0.001$; ****, $P \leq 0.0001$ unless *P* values are mentioned in figures.

Results

Training for 9 weeks sustains myelopoiesis

The impact of training on immune parameters is mostly assessed within a week of induction (11, 14-16, 21). To determine whether trained immunity persists for a longer period, we compared control mice with mice trained 9 weeks earlier (**Figure 1A**). We analyzed immune and progenitor cells in bone marrow and peripheral blood compartments. In the bone marrow, the number of LSK ($Lin^-Sca1^+cKit^+$) hematopoietic progenitors, long-term (LT) HSCs ($CD48^-CD150^+$ LSKs), short-term (ST) HSCs ($CD48^-CD150^-$ LSKs) (**Figure 1B**), myeloid-biased multipotent progenitors (MPPs) MPP2 ($Flt3^-CD48^+CD150^+$ LSKs) and lymphoid-biased MPP4 ($Flt3^+CD48^+CD150^-$ LSKs) were similar in control and trained mice. On the contrary, the number of myeloid-biased MPP3 ($Flt3^-CD48^+CD150^-$ LSKs) was increased 2.1-fold in trained mice ($P = 0.03$) (**Figure 1B**). In line, common myeloid progenitors (CMPs) and granulocyte-monocyte progenitors (GMPs) were increased 1.5 and 1.6-fold in the bone marrow of trained mice ($P = 0.028$ and 0.014, respectively) (**Figure 1C**). We then compared bone marrow leukocyte subpopulations (**Figure 1D**). Following increased myelopoiesis, the bone marrow from trained mice contained 1.6-fold more $CD45^+$ leukocytes ($P = 0.006$) (**Figure 1D**). This increase resulted from a rise of PMNs and to a lesser extent of $Ly6C^{high}$ inflammatory/classical monocytes and $Ly6C^{int}$ monocytes (3.1, 2.1, 2.2-fold-increase, $P < 0.005$). The counts of $Ly6C^{low}$ nonclassical/patrolling monocytes and T cells were not altered, while the counts of B cells were reduced 2-fold ($P = 0.006$).

The blood from trained mice contained 1.7 and 2.4-fold more $Ly6C^{high}$ monocytes and PMNs ($P < 10^{-4}$ and $P = 0.0003$), while the counts of $Ly6C^{low/int}$ monocytes, T cells and B cells were not affected (**Figure 2A**). IL-1β is an important regulator of hematopoiesis (30). It has been involved in the induction of trained immunity induced by BCG, β-glucan and Western diet and to

promote the proliferation of HSCs (19, 31, 32). Thus, we quantified IL-1β in the blood of mice trained for 0, 1, 2, 4, 5 and 9 weeks (**Figure 2B**). Interestingly, IL-1β concentrations were 1.6-3.6 higher in trained mice than in control mice. The highest concentrations were measured 4 weeks after training ($P = 0.009$ versus control). We also measured IL-6, IL-12p40 and TNF to consider systemic inflammation induced by trained immunity. IL-6 was slightly increased in some mice, but results were not statically significantly different from control mice. IL-12p40 and TNF were at highest (but low) levels 2 weeks after training ($P = 0.0006$ versus control) and were back to control levels in mice trained 4 weeks onwards (**Figure 2B**). Overall, these data indicated that training increased myelopoiesis and Ly6C^{high} monocytes and PMNs in peripheral blood for up to 9 weeks.

Training for 9 weeks sustains the antimicrobial response of whole blood

Leukocytes form a major barrier against systemic infection. Hence, we tested the reactivity of whole blood collected from control mice and trained mice against a range of stimuli including LPS, PHA, CpG, and heat killed *L. monocytogenes* and *C. albicans* (**Figure 3A**). The blood of mice trained 9 weeks earlier produced more IL-6 upon exposure to LPS, PHA and CpG ($P < 0.05$) than the blood of control mice. IL-6 levels were higher also in response to heat-killed *L. monocytogenes* and *C. albicans*, though differences did not reach statistical significance. To extend our analyses, we performed a multiplex immunoassay (Luminex) to quantify 15 cytokines (G-CSF, IFNγ, IL-1α, IL-1β, IL-6, IL-10, IL-12p40, IL-18, TNF, CCL2, CCL3, CXCL2, CXCL5 and CXCL10) expressed by whole blood exposed to LPS (**Figure 3B**). Globally, the blood from trained mice produced more cytokines, with results reaching statistical significance for G-CSF, IFNγ, IL-1α, IL-1β, IL-6, IL-10, TNF and CXCL2. To mimic infectious conditions, we measured the capacity of whole blood to limit the growth of live *L. monocytogenes*. Blood was incubated for 2 h with *L. monocytogenes*, and the number of bacteria was quantified (**Figure 3C**). The blood from trained mice contained more efficiently the growth of *L. monocytogenes*, as shown by 1.5-fold lower bacterial counts in the blood from trained mice than from control mice ($P = 0.016$).

Training for 9 weeks preserves leukocytes during listeriosis and increases the glycolysis of PMNs

Our observations suggested that mice trained for 9 weeks should be protected from infection. To verify this assumption, we used a preclinical model of sepsis to compare the behavior of control mice to that of mice trained 9 weeks earlier. In some experiments we included mice trained 1 week earlier, used as a reference. Mice were infected i.v. with *L. monocytogenes*. Two days post-infection, listeriosis induced a profound depletion of peripheral blood leukocytes (around 10-fold decrease, compare cell counts in **Figure 2** and **Figure 4**). Training 1 week prior to infection preserved leukocyte counts ($P < 0.01$), including those of Ly6C^{low} monocytes, Ly6C^{int} monocytes, Ly6C^{high} monocytes, PMNs, T cells and B cells ($P < 0.01$-10^{-4}). Though less efficient, training 9 weeks prior to infection preserved leukocyte counts to some extent. Results were statistically significance for Ly6C^{high} monocytes ($P < 0.01$), PMNs ($P < 0.001$) and T cells ($P < 0.05$). B cell counts were heterogeneous but higher (around 6-fold) in mice trained for 9 weeks than in control mice ($P = 0.09$), while Ly6C^{int} monocytes were decreased around 2-fold ($P < 10^{-3}$) (**Figure 4**).

The induction of trained immunity has been associated with metabolic rewiring in myeloid cells, favoring aerobic glycolysis over oxidative phosphorylation (OXPHOS) (33-37). Considering that PMNs were particularly preserved in trained mice, we compared the metabolic parameters of PMNs isolated 2 days post-infection from control mice and mice trained for 9 weeks (**Figure 5A-C**). PMNs from trained mice showed an increased glycolytic rate upon exposure to *L. monocytogenes* (1.6-3.2-fold increase *vs* control PMNs) (**Figure 5A-B**). In agreement, PMNs from

trained mice expressed 1.7-fold more of glucose receptor 1 (*Glut1*) mRNA (**Figure 5C**). No major differences were noticed when comparing the oxidative metabolism of PMNs from trained and control mice (**Figure 5C**). These results supported the assumption that training promoted glycolytic metabolism to sustain antimicrobial activity.

Training for 9 weeks protects from listeriosis

To visualize mouse response to infection with *L. monocytogenes*, we performed *in vivo* bioluminescence imaging. One and 2 days post-infection, mice were injected with luminol which reacts with superoxide generated in phagosomes and reflecting myeloperoxidase of tissue-infiltrating neutrophils. As shown in **Figure 6**, luminol-mediated bioluminescent signals were detected in the abdomen of mice, which was in agreement with the rapid colonization of liver upon systemic infection with *L. monocytogenes*. The signals were globally lower in mice trained 9 weeks earlier than in control mice (P = 0.05 and 0.06 at days 1 and 2 post-infection). It likely reflected lower bacteria spreading and subsequent antimicrobial inflammatory response in the organs of trained mice.

Two days post infection all control mice were strongly bacteremic, while mice trained 1 week and 9 weeks earlier were all but one sterile (P <10^{-4}) (**Figure 7A**). To confirm these observations, we performed histology on the liver (**Figure 7 B-D**). The number and the size of inflammatory foci were 1.8- and 1.3-fold lower in mice trained 9 weeks earlier than in control mice, respectively (P = 0.05 and P <10^{-4}). The efficient control of bacterial dissemination and burden was further attested by the fact that the blood from mice trained 9 weeks earlier contained lower levels of a broad range of cytokines (IL-1β, IL-6, IL-10, IL-12p40, IL-17A, IL-18, IFNγ, TNF, CCL2 and CXCL5) (**Figure 8A**). Control mice lost more weight than mice trained 1 week or 9 weeks earlier (P < 0.01 *vs.* control) (**Figure 8B**). Accordingly, while all control mice died of infection within 4 days, 75% of mice trained for 1 or 9 weeks survived the infection (1 and 9 weeks of training *vs.* control: P < 10^{-4} and P = 0.0003, respectively) (**Figure 8C**).

Discussion

Trained immunity protects from candidiasis and chronic and acute bacterial infections (14, 21). Extending these observations, we report that, 9 weeks after the induction of trained immunity, mice were still fully protected in a model of lethal listeriosis. This survival advantage was associated with increased myelopoiesis and blood leukocytes especially PMNs, and metabolic rewiring in PMNs.

The blood from mice trained for 9 weeks produced more cytokines upon stimulation with PAMPs and mitogen, and restricted more efficiently the growth of *L. monocytogenes* than blood from control mice. Along with this observation, monocytes/macrophages trained with β-glucan or BCG produced increased levels of cytokines when exposed to microbial compounds and displayed superior microbicidal responses (10, 14, 16, 19, 26, 38). The short lifetime of PMNs and monocytes raised the question how innate immune memory persists over time in these cells. This was answered when β-glucan and BCG were shown to reprogram bone marrow HSCs generating trained myeloid cells (10, 11, 31).

Innate immune cells besides PMNs and monocytes may acquire memory properties and participate to host defense responses. For example, memory skills have been attributed to microglia, dendritic cells, liver resident group 1 innate lymphoid cells (ILC1) and lung resident ILC2 obtained from mice exposed to LPS, *Cryptococcus neoformans*, cytomegalovirus, allergens

and IL-33 (7, 9, 34, 39-43). Of great interest, the concept of training has been extended to non-immune cells. For instance, skin and respiratory epithelial progenitor stem cells exposed to inflammatory pressure as well as fibroblasts exposed to IFNβ display memory characteristics (12, 13, 44). Stem cells promote immune cell recruitment and repair mechanisms when they sense breaches in epithelial barriers. Moreover, stem cells respond to signals from recruited immune cells. This suggests bidirectional communication between stroma, stem cells and immune cells to optimize defense responses in trained conditions.

Nine weeks of training persistently stimulated myelopoiesis as demonstrated by increased bone marrow CMPs and GMPs, supporting a central role of HSCs in the establishment of a functional trained phenotype. The rise of myeloid progenitors paralleled the rise of $Ly6C^{high}$ inflammatory monocytes and PMNs in peripheral blood, and the resistance of trained mice to listeriosis. Besides protecting from infections, PMNs are involved in pathophysiological processes. Interestingly, PMNs from mice trained with β-glucan promoted anti-tumor activity (45). Given that PMNs are abundant in the tumor microenvironment and that BCG vaccination enhanced the functions of blood PMNs in humans (46), trained immunity might be targeted for cancer treatment (47). Upon recognition of DAMPs and PAMPs, cells undergo a metabolic shift to meet energy requirements for prompt responses. As archetypal examples, inflammatory macrophages and PMNs favor aerobic glycolysis over OXPHOS, while anti-inflammatory macrophages rely on fatty acid oxidation and the TCA cycle to generate ATP (48). The induction of trained immunity rewired the metabolism of bone marrow progenitors and monocytes, which was characterized by an increase of glycolysis and cholesterol metabolism (11, 33, 34). Accordingly, PMNs from trained mice showed increased glycolytic activity when exposed to *L. monocytogenes*.

IL-1β circulated at low, but increased levels in the peripheral blood of mice up to 9 weeks after the induction of trained immunity. IL-1β promoted the proliferation of HSPCs and myelopoiesis as well as innate immune responses of monocytes (11, 30-32). Blocking IL-1 signaling through pharmacological or genetic approaches (using the IL-1 receptor antagonist anakinra or using *Il1r* or *Nlrp3* knockout mice) blunted the acquisition of a trained phenotype in mice fed with a Western diet or challenged with BCG, and reduced resistance to mycobacterial infection and listeriosis. Furthermore, functional and genetic studies in healthy volunteers suggested that IL-1β underlined the establishment of trained immunity induced by BCG and oxidized low-density lipoprotein (19, 21, 32, 49). Altogether, IL-1β may represent a hub regulating trained immunity induced by PAMPs and DAMPs. Considering that targeting IL-1 signaling has been proposed to represent an efficient way to modulate trained immunity pathways (50), it would be interesting to determine how long persist subnormal levels of IL-1β in the circulation. However, possibly minutes levels of IL-1β may act locally to stimulate myelopoiesis or have an important biological impact.

Mice trained 9 weeks earlier cleared bacteria and survived infection induced with an inoculum of *L. monocytogenes* equivalent to 20 times the LD_{100} in control mice. Furthermore, organs collected up to 2 months after the infectious challenge were sterile (blood, spleen and liver, data not shown), suggesting effective bacterial clearance in trained mice. The adoptive transfer in naive mice of bone marrow cells or long-term HSCs collected from mice 4 weeks after the induction of training increased the proportion of blood $Gr1^+CD11b^+$ myeloid cells and protected from pulmonary tuberculosis (10, 11). Alveolar macrophages showed marks of trained immunity 16 weeks following an intranasal challenge of adenovirus (7, 9). In healthy humans, BCG vaccination generated PBMCs, monocytes and neutrophils with increased enhanced effector functions 3 months after inoculation, and protected from protected from experimental infection with the yellow fever vaccine given 4 weeks after BCG (19, 46, 51, 52). Taken all together, these models support the assumption that trained immunity has persistent effects on immune responses

in humans and mice. Intriguingly, BCG vaccination promoted granulopoiesis and protected neonate mice from polymicrobial sepsis 3 days but not 13 days after vaccination. However, the protected effect of BCG vaccination vanished when infection was delayed for 10 days (53). This might indicate that, in this specific mouse model, BCG protected from polymicrobial sepsis in a narrow time window around birth. Detailed analysis of age-dependent effectiveness of trained immunity induction, especially at the extremes of age, will be critical to optimize interventions based on trained immunity.

In summary, the induction of trained immunity durably protected from systemic listeriosis by increasing myelopoiesis and the antimicrobial response of mature innate immune cells. Further studies will be required to delineate the persistence of trained immunity. This will give information necessary to consider the possible influence of trained immunity on the development of inflammatory and age-associated diseases and the development of trained-immunity based strategies to enhance or inhibit innate immune responses.

References

1. Savva A, Roger T. Targeting toll-like receptors: promising therapeutic strategies for the management of sepsis-associated pathology and infectious diseases. Front Immunol. 2013;4:387.
2. Broz P, Monack DM. Newly described pattern recognition receptors team up against intracellular pathogens. Nat Rev Immunol. 2013;13(8):551-65.
3. Cassone A. The Case for an Expanded Concept of Trained Immunity. mBio. 2018;9(3).
4. Farber DL, Netea MG, Radbruch A, Rajewsky K, Zinkernagel RM. Immunological memory: lessons from the past and a look to the future. Nat Rev Immunol. 2016;16(2):124-8.
5. Netea MG, Quintin J, van der Meer JW. Trained immunity: a memory for innate host defense. Cell Host Microbe. 2011;9(5):355-61.
6. Divangahi M, Aaby P, Khader SA, Barreiro LB, Bekkering S, Chavakis T, et al. Trained immunity, tolerance, priming and differentiation: distinct immunological processes. Nat Immunol. 2021;22(1):2-6.
7. Yao Y, Jeyanathan M, Haddadi S, Barra NG, Vaseghi-Shanjani M, Damjanovic D, et al. Induction of Autonomous Memory Alveolar Macrophages Requires T Cell Help and Is Critical to Trained Immunity. Cell. 2018;175(6):1634-50 e17.
8. de Laval B, Maurizio J, Kandalla PK, Brisou G, Simonnet L, Huber C, et al. C/EBPbeta-Dependent Epigenetic Memory Induces Trained Immunity in Hematopoietic Stem Cells. Cell Stem Cell. 2020;26(5):657-74 e8.
9. Wendeln AC, Degenhardt K, Kaurani L, Gertig M, Ulas T, Jain G, et al. Innate immune memory in the brain shapes neurological disease hallmarks. Nature. 2018;556(7701):332-8.
10. Kaufmann E, Sanz J, Dunn JL, Khan N, Mendonca LE, Pacis A, et al. BCG Educates Hematopoietic Stem Cells to Generate Protective Innate Immunity against Tuberculosis. Cell. 2018;172(1-2):176-90 e19.
11. Mitroulis I, Ruppova K, Wang B, Chen LS, Grzybek M, Grinenko T, et al. Modulation of Myelopoiesis Progenitors Is an Integral Component of Trained Immunity. Cell. 2018;172(1-2):147-61 e12.
12. Naik S, Larsen SB, Gomez NC, Alaverdyan K, Sendoel A, Yuan S, et al. Inflammatory memory sensitizes skin epithelial stem cells to tissue damage. Nature. 2017;550(7677):475-80.

32. Christ A, Gunther P, Lauterbach MAR, Duewell P, Biswas D, Pelka K, et al. Western Diet Triggers NLRP3-Dependent Innate Immune Reprogramming. Cell. 2018;172(1-2):162-75 e14.
33. Arts RJ, Novakovic B, Ter Horst R, Carvalho A, Bekkering S, Lachmandas E, et al. Glutaminolysis and Fumarate Accumulation Integrate Immunometabolic and Epigenetic Programs in Trained Immunity. Cell Metab. 2016;24(6):807-19.
34. Arts RJW, Carvalho A, La Rocca C, Palma C, Rodrigues F, Silvestre R, et al. Immunometabolic Pathways in BCG-Induced Trained Immunity. Cell Rep. 2016;17(10):2562-71.
35. Bekkering S, Arts RJW, Novakovic B, Kourtzelis I, van der Heijden C, Li Y, et al. Metabolic Induction of Trained Immunity through the Mevalonate Pathway. Cell. 2018;172(1-2):135-46 e9.
36. Dominguez-Andres J, Novakovic B, Li Y, Scicluna BP, Gresnigt MS, Arts RJW, et al. The Itaconate Pathway Is a Central Regulatory Node Linking Innate Immune Tolerance and Trained Immunity. Cell Metab. 2019;29(1):211-20 e5.
37. Fanucchi S, Dominguez-Andres J, Joosten LAB, Netea MG, Mhlanga MM. The Intersection of Epigenetics and Metabolism in Trained Immunity. Immunity. 2021;54(1):32-43.
38. Ifrim DC, Joosten LA, Kullberg BJ, Jacobs L, Jansen T, Williams DL, et al. Candida albicans primes TLR cytokine responses through a Dectin-1/Raf-1-mediated pathway. J Immunol. 2013;190(8):4129-35.
39. Cerwenka A, Lanier LL. Natural killer cell memory in infection, inflammation and cancer. Nat Rev Immunol. 2016;16(2):112-23.
40. Martinez-Gonzalez I, Matha L, Steer CA, Ghaedi M, Poon GF, Takei F. Allergen-Experienced Group 2 Innate Lymphoid Cells Acquire Memory-like Properties and Enhance Allergic Lung Inflammation. Immunity. 2016;45(1):198-208.
41. Steer CA, Matha L, Shim H, Takei F. Lung group 2 innate lymphoid cells are trained by endogenous IL-33 in the neonatal period. JCI Insight. 2020;5(14).
42. Weizman OE, Song E, Adams NM, Hildreth AD, Riggan L, Krishna C, et al. Mouse cytomegalovirus-experienced ILC1s acquire a memory response dependent on the viral glycoprotein m12. Nat Immunol. 2019;20(8):1004-11.
43. Verma M, Michalec L, Sripada A, McKay J, Sirohi K, Verma D, et al. The molecular and epigenetic mechanisms of innate lymphoid cell (ILC) memory and its relevance for asthma. J Exp Med. 2021;218(7).
44. Kamada R, Yang W, Zhang Y, Patel MC, Yang Y, Ouda R, et al. Interferon stimulation creates chromatin marks and establishes transcriptional memory. Proc Natl Acad Sci U S A. 2018;115(39):E9162-E71.
45. Kalafati L, Kourtzelis I, Schulte-Schrepping J, Li X, Hatzioannou A, Grinenko T, et al. Innate Immune Training of Granulopoiesis Promotes Anti-tumor Activity. Cell. 2020;183(3):771-85 e12.
46. Moorlag S, Rodriguez-Rosales YA, Gillard J, Fanucchi S, Theunissen K, Novakovic B, et al. BCG Vaccination Induces Long-Term Functional Reprogramming of Human Neutrophils. Cell Rep. 2020;33(7):108387.
47. Netea MG, Joosten LAB, van der Meer JWM. Hypothesis: stimulation of trained immunity as adjunctive immunotherapy in cancer. J Leukoc Biol. 2017;102(6):1323-32.
48. O'Neill LA, Pearce EJ. Immunometabolism governs dendritic cell and macrophage function. J Exp Med. 2016;213(1):15-23.
49. Moorlag S, Khan N, Novakovic B, Kaufmann E, Jansen T, van Crevel R, et al. beta-Glucan Induces Protective Trained Immunity against Mycobacterium tuberculosis Infection: A Key Role for IL-1. Cell Rep. 2020;31(7):107634.
50. Moorlag S, Roring RJ, Joosten LAB, Netea MG. The role of the interleukin-1 family in trained immunity. Immunol Rev. 2018;281(1):28-39.

51. Kleinnijenhuis J, Quintin J, Preijers F, Benn CS, Joosten LA, Jacobs C, et al. Long-lasting effects of BCG vaccination on both heterologous Th1/Th17 responses and innate trained immunity. J Innate Immun. 2014;6(2):152-8.
52. Kleinnijenhuis J, Quintin J, Preijers F, Joosten LA, Ifrim DC, Saeed S, et al. Bacille Calmette-Guerin induces NOD2-dependent nonspecific protection from reinfection via epigenetic reprogramming of monocytes. Proc Natl Acad Sci U S A. 2012;109(43):17537-42.
53. Brook B, Harbeson DJ, Shannon CP, Cai B, He D, Ben-Othman R, et al. BCG vaccination-induced emergency granulopoiesis provides rapid protection from neonatal sepsis. Sci Transl Med. 2020;12(542).

Acknowledgments

TR is supported by the Swiss National Science Foundation (SNSF, grant number 320030_149511 and 310030_173123), by Fondation Carigest/Promex Stiftung für die Forschung (Genève, Switzerland), Fondation Biochimie (Epalinges, Switzerland) and the European Sepsis Academy Horizon 2020 Marie Skłodowska-Curie Action: Innovative Training Network (MSCA-ESA-ITN, grant number 676129, support to CT and IS). TH, CT and IS received a scholarship from the Société Académique Vaudoise (Lausanne, Switzerland).

Contribution to the field

The term trained immunity was coined recently to reflect that the innate immune system recalls and adapts to an initial challenge to mount an improved response to a secondary challenge. Trained immunity is studied mainly using fungal cell wall component β-glucan and the BCG vaccine as priming agents. Trained immunity is not antigen specific, suggestive of broad effects. Indeed, we have recently shown that induction of training by β-glucan challenge one week before infection powerfully protects mice from lethal and chronic infections including peritonitis, blood-born infections, enteritis and pneumonia. Among the open questions related to trained immunity, the length of protection against deleterious infections is unknown. In our study, we show that mice trained 9 weeks prior to infection were remarkably protected from acute, lethal listeriosis. The protection was associated with increased myelopoiesis, blood leukocytes, metabolism and antimicrobial defenses in trained mice. Overall, our data suggest that trained immunity has persistent effects on antimicrobial host defenses. This information is important considering the possible influence of trained immunity on the development of inflammatory and age-associated diseases, and the development of trained-immunity based strategies to enhance or inhibit innate immune responses.

Supplementary Information

Reagents

Reagent	Source	Identifier
2-Deoxyglucose	Sigma-Aldrich	D6134
Antimycin A from *Streptomyces sp.*	Sigma-Aldrich	A8674
Brain Heart Infusion	Oxoid	CM1135
Carbonyl cyanide-p-trifluoromethoxyphenylhydrazone	Sigma-Aldrich	C2910
Celltak	Corning	354240
Columbia III Agar with 5% Sheep Blood	BD	254098
cOmplete, EDTA-free Protease Inhibitor Cocktail	Roche	11836170001
CpG: G*GGTCAACGTTGAG*G*G*G*G*G	Microsynth	
Fetal bovine serum	Biochrom AG (Merck)	S 0615
HBSS no phenol red no Ca+ no Mg+	ThermoFisher	88284
IMDM, GlutaMAX	ThermoFisher	31980-022
KAPA SYBR Green Fast ROX low	Kapa Biosystems	KK4620
LPS ultrapure from *Salmonella minnesota*	List Biologicals	434
LS columns	Miltenyi Biotec	130-042-401
Luminol sodium salt	Carbosynth	FL02733
Mouse Custom ProcartaPlex	Invitrogen	PPX-MX7DPRR
Mouse IL-10 ELISA development kit	Mabtech	3432-1H-20
Mouse IL-1b Elisa Ready-SET-Go!	eBioscience	88-7013-88
Mouse IL-6 DuoSet ELISA	R&D Systems	DY406
Mouse TNF-α DuoSet ELISA	R&D Systems	DY410
Neutrophil Isolation Kit, mouse	Miltenyi Biotec	130-097-658
Oligomycin from *Streptomyces diastatochromogenes*	Sigma-Aldrich	A4876
Pam_3CSK_4	EMC microcollections	L2000
Penicillin-streptomycin	ThermoFisher	15140-122
Phytohemagglutinin, M form (PHA)	ThermoFisher	10576015
QuantiTect reverse transcription kit	Qiagen	205313
Rotenone	Sigma-Aldrich	R8875
RPMI 1640 Medium, GlutaMAX	ThermoFisher	61870-010
XF 100 mM Pyruvate solution	Agilent	103578
XF 200 mM Glutamine solution	Agilent	103579
Seahorse XFp Fluk Pak	Agilent	103025
XF 1.0 M Glucose solution	Agilent	103577
5x RIPA Buffer IV with Triton-X-100 (pH 7.4)	Bio Basic	RB4478
Seahorse XF DMEM Medium, pH 7.4	Agilent	103575
Sodium Bicarbonate solution (7.5%)	Sigma-Aldrich	S8761

Mouse strains

Name	Source	Identifier
C57BL/6J mice	Charles River	632

Microorganisms

Species	Strain	Reference
C. albicans	5102	
L. monocytogenes	10403s	NCBI:txid393133

Antibodies and viability dyes used for flow cytometry

Target	Clone name	Coupling	Brand	Reference
B220	RA3-6B2	PE-Cy7	BioLegend	103222
B220	RA-6B2	Brilliant Violet 570	BioLegend	103237
CD117	2B8	APC	BioLegend	105812
CD11b	M1/70	APC-eFluor780	eBioscience	47-0112
CD11b	M1/70	PE-Cy7	BioLegend	101216
CD11b	M1/70	PercCP-Cy5.5	eBioscience	45-0112
CD11c	N418	APC	BioLegend	117310
CD11c	N418	PE	BioLegend	117307
CD135	A2F10	PE	eBioscience	12-1351
CD150	TC15-12F12.2	PerCP-Cy5.5	BioLegend	115922
CD19	1D3	PE-Cy7	eBioscience	25-0193
CD3e	17A2	APC	eBioscience	17-0032
CD3e	17A2	PE-Cy7	BioLegend	100220
CD4	GK1.5	APC-Cy7	BioLegend	100414
CD41	MWReg30	eFluor450	eBioscience	48-0411

CD45	30-F11	FITC	BD Biosciences	553079
CD48	HM48-1	APC-Cy7	BioLegend	103432
CD8a	53-6.7	FITC	BioLegend	100706
Fixable Aqua	-	-	ThermoFisher	L34957
Fixable Violet	-	-	ThermoFisher	L34955
Ly6C	HK1.4	PerCP-Cy5.5	eBioscience	45-5932
Ly6C/G	RB6-8C5	PE-Cy7	BioLegend	108416
Ly6G	1A8	eFluor450	eBioscience	48-9668
Ly-76	TER119	PE-Cy7	BioLegend	116222
MHCII	M5/114.15.2	PE	eBioscience	12-5321
Sca-1	D7	FITC	eBioscience	11-5981
Zombie	-	-	BioLegend	77168

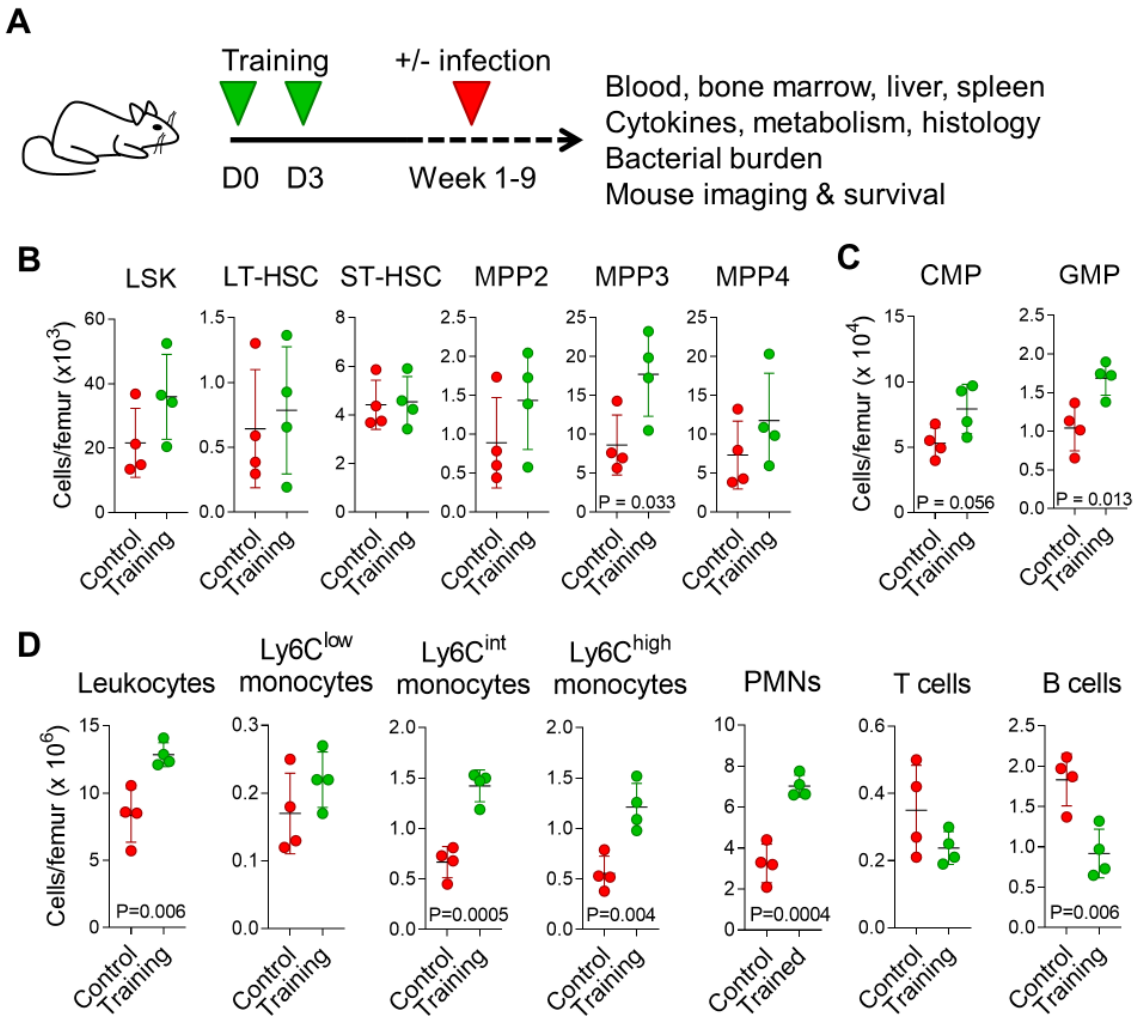

Figure 1. Training for 9 weeks promotes myelopoiesis.

(A) Experimental model to study trained immunity. **(B-D)** Bone marrow cells were collected from control mice and mice trained for 9 weeks (*n* = 4/group) and analyzed by flow cytometry for hematopoietic progenitors (LSK), long-term hematopoietic stem cells (LT-HSC), short-term HSC (ST-HSC), multipotent progenitors (MMP) 2, MPP3 and MPP4 **(B)**, common myeloid progenitors (CMP) and granulocyte-monocyte progenitors (GMP) **(C)** as well as CD45$^+$ leukocytes, Ly6C^{low}, Ly6C^{int} and Ly6C^{high} monocytes (CD11b$^+$Ly6G$^-$), PMNs (Ly6G$^+$), T cells (CD3$^+$) and B cells (B220$^+$) **(D)**. Each dot represents a mouse. Lines represent mean and SD. *P* values are given in the graphs.

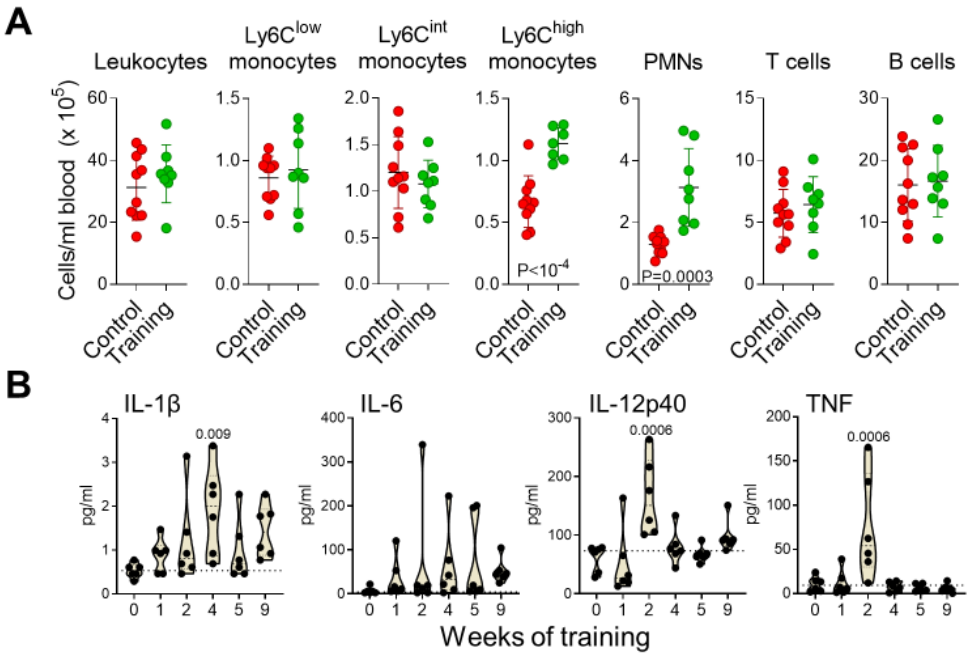

Figure 2. Training for 9 weeks increases blood inflammatory monocytes and PMNs.
(A) Blood counts of CD45$^+$ leukocytes, Ly6C^{low}, Ly6C^{lint} and Ly6C^{high} monocytes (CD11b$^+$Ly6G$^-$), PMNs (Ly6G$^+$), T cells (CD3$^+$) and B cells (B220$^+$) in control mice (*n* = 10) and mice trained for 9 weeks (*n* = 8). **(B)** Blood concentrations of IL-1β, IL-6, IL-12p40 and TNF in control mice (and mice trained for 1-9 weeks (*n* = 6/group). Each dot represents a mouse. Lines represent mean and SD. *P* values are given in the graphs.

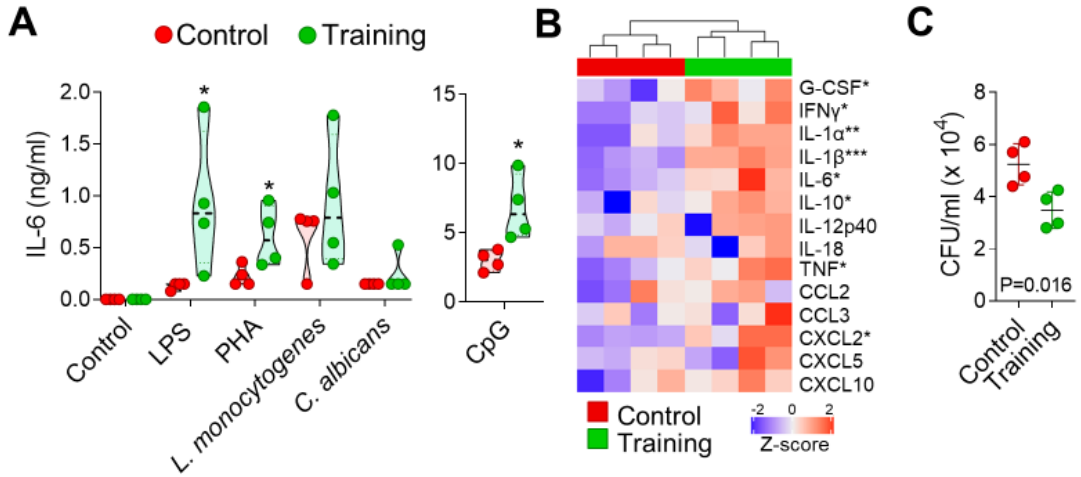

Figure 3: Training for 9 weeks promotes whole blood antimicrobial responses.
Blood was collected from control mice and mice trained for 9 weeks (*n* = 4/group). **(A-B)** Blood was incubated for 6 h with 10 ng/ml LPS, 1 µg/ml PHA, 10 µM CpG and 10^8 heat-killed *L. monocytogenes* and *C. albicans*. The concentrations of IL-6 in blood supernatants were quantified by ELISA. Each dot represents a mouse, and the horizontal lines the mean. *, *P* < 0.05 **(A)**. The concentrations of G-CSF, IFNγ, IL-1α, IL-1β, IL-6, IL-10, IL-12p40, IL-17A, IL-18, TNF, CCL2, CCL3, CXCL1, CXCL2, CXCL5 and CXCL10 in blood supernatants were quantified by multiplex immunoassay (Luminex). Heatmap and hierarchical clustering of cytokine levels was performed using Z-score normalization **(B)**. **(C)** Blood was incubated for 2 h with 6 x 10^4 CFU *L. monocytogenes*. Bacteria were enumerated by plating serial dilutions of blood on blood agar plates and incubation for 24 h. Each dot represents a mouse. The horizontal lines represent the mean and SD. *, P < 0.05; **, P < 0.01; ***, P < 0.001 vs. control.

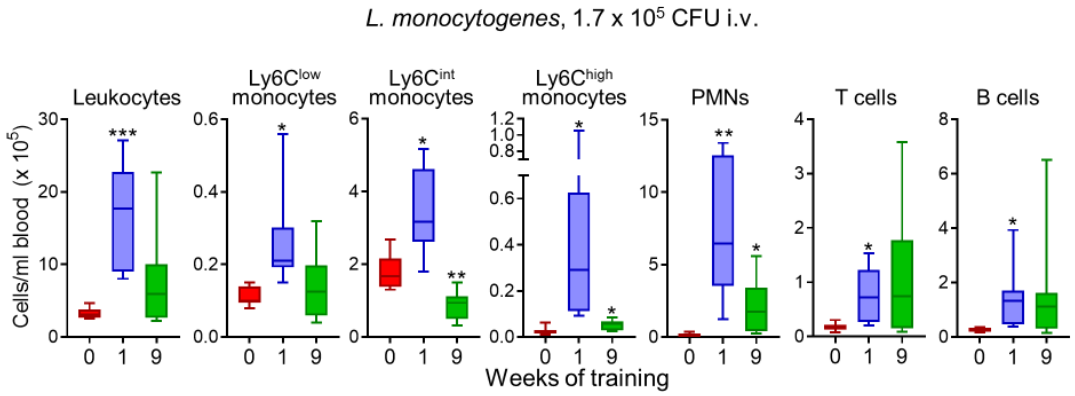

Figure 4. Training for 9 weeks limits leukocyte depletion induced by listeriosis.
Control mice and mice trained for 1 week and 9 weeks were challenged i.v. with 1.7 x 10^5 CFU *L. monocytogenes*. Blood was collected 2 days after infection to quantify $CD45^+$ leukocytes, $Ly6C^{low}$, $Ly6C^{lint}$ and $Ly6C^{high}$ monocytes ($CD11b^+Ly6G^-$), PMNs ($Ly6G^+$), T cells ($CD3^+$) and B cells ($B220^+$). Graphs represent boxplots with min-to-max whiskers. The horizontal line shows the mean. n = 8-9 mice/group. *, $P < 0.05$; **, $P < 0.01$; ***, $P < 0.001$.

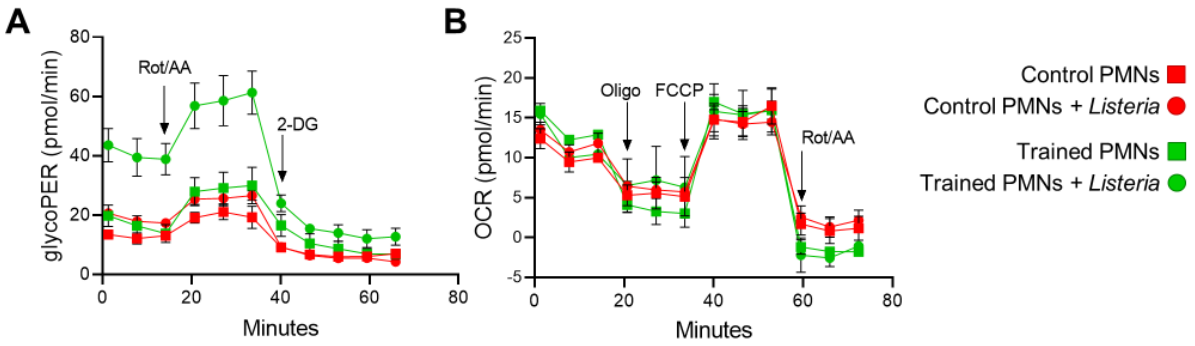

Figure 5. Training for 9 weeks increases the metabolism of PMNs.
PMNs were isolated from the bone marrow of control (n=5) and trained (n=4) mice infected with 2 x 10^5 CFU *L. monocytogenes* for 48 h. PMNs were incubated for 30 min with or without 10^8 heat-killed *L monocytogenes* and metabolic activity was analyzed using the SeahorseXFe96 analyzer. **(A)** Glycolytic activity was determined using Glycolytic Rate kit, which consisted of consecutive injections of 0.5/0.5 µM Rot/AA (rotenone/antimycin A) and 50 mM 2-DG (2-deoxyglucose). Glycolytic activity is depicted by means of proton efflux rate (glycoPER) adjusted to protein concentration per condition. **(B)** Mitochondrial respiration was analyzed using Mito Stress kit, which consisted of consecutive injections of 1 µM oligo (oligomycin), 2 µM FCCP (carbonyl cyanide 4-(trifluoromethoxy) phenylhydrazone) and 0.5/0.5 µM Rot/AA. Mitochondrial respiration is depicted by means of oxygen consumption rate (OCR) adjusted to protein concentration per condition and represented as OCR. Data are means ± SEM from 5-4 mice aged 10–12 weeks analyzed in quadruplicate.

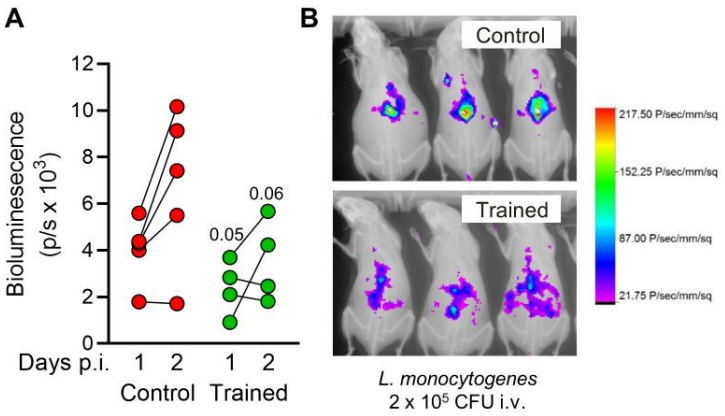

Figure 6. Training for 9 weeks reduces *Listeria*-induced inflammation measured by bioluminescence imaging.

Control mice and mice trained for 9 weeks were challenged i.v. with 1.7 x 10^5 CFU *L. monocytogenes*. One day and 2 days post infection, inflammatory levels were measured by luminol-generated bioluminescence using an Xtreme II (BRUKER) imaging system. Bioluminescence was recorded by imaging. **(A)** Quantification of bioluminescent signals. Each dot represents a mouse. Lines connect results obtained from one animal analyzed 1 and 2 days post infection (p.i.). **(B)** Representative images of control and trained mice analyzed 2 days p days p.i. displayed as an overlay of luminescent and X Ray modalities.

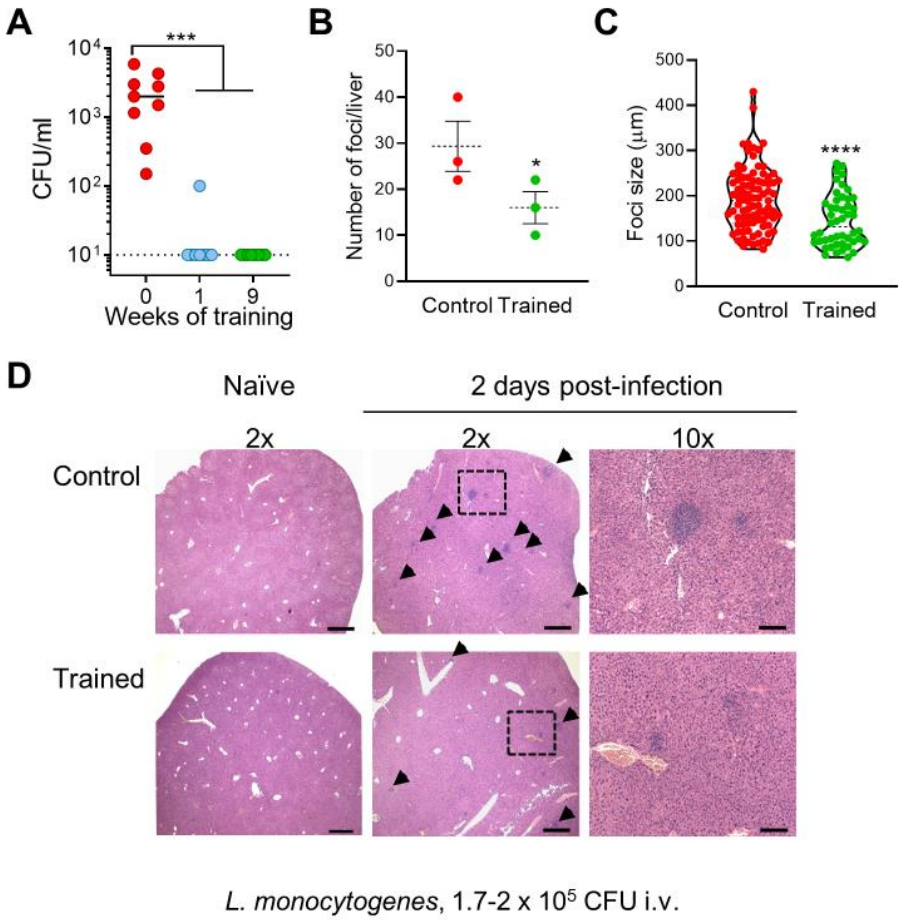

Figure 7. Training for 9 weeks prevents *Listeria* burden and dissemination.
Control mice and mice trained for 9 weeks were challenged i.v. with 1.7-2 x 10^5 CFU *L. monocytogenes*. **(A)** Blood was collected 2 days p.i. to quantify bacteria. Each dot represents a mouse. The plain and dotted horizontal lines represent median and limit of detection, respectively. **(B-D)** Liver were collected 2 days p.i. and liver sections stained with hematoxylin and eosin. Naïve mice were used as negative control. The number of foci per liver section (**B**) and the size of the foci (**C**) were determined by quantified using EVOS Analysis software. Representative images of liver sections imaged at 2x and 10x using an EVOS M7000 microscope **(C)**. Nuclei (dark purple) and cytoplasm components (pink) are represented. Scale bar represents 750 µm or 150 µm for 2x and 10x images, respectively. Arrows point to foci and the doted square to the area zoomed 10x. *, $P < 0.05$; ***, $P < 0.001$; ****, $P < 0.0001$ *vs.* control.

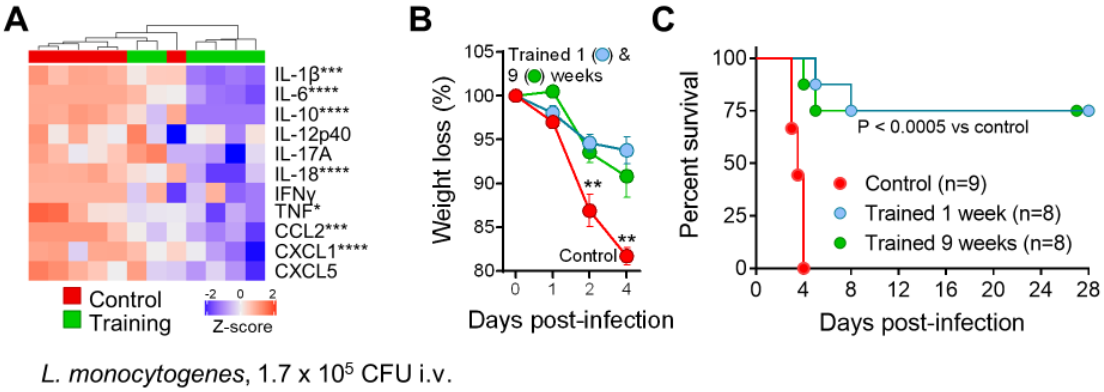

Figure 8. Training for 9 weeks increase mice survival from lethal listeriosis.
Control mice and mice trained for 1 week and 9 weeks were challenged i.v. with 1.7 x 10^5 CFU *L. monocytogenes*. **(A)** Blood was collected 2 days after infection to quantify cytokines (IL-1β, IL-6, IL-10, IL-12p40, IL-17A, IL-18, IFNγ, TNF, CCL2, CXCL1, and CXCL5). Each dot represents a mouse. The plain and dotted horizontal lines represent median and limit of detection, respectively. Heatmap and hierarchical clustering of cytokine levels was performed using Z-score normalization. **(B-C)** Weight loss and survival of mice. *, $P < 0.05$; **, $P < 0.01$; ***, $P < 0.001$; ****, $P < 0.0001$ *vs.* control.

3.4. ILCs in human infections: the PIPOVAP and IMMUNO-SARS-CoV-2 studies

We poorly understand what is responsible for the dysregulated host response in sepsis patients. Considering that ILCs sense environmental cues and regulate inflammation and host defenses, we hypothesized that ILCs might be involved in immune dysregulation occurring in sepsis, and may represent biomarkers for human sepsis. To test this hypothesis, we studied blood ILCs in septic patients from two clinical studies: PIPOVAP and IMMUNO-SARS-CoV-2.

Method. Blood samples were collected in EDTA tubes at CHUV and transferred to the laboratory within 2 hours. One hundred µl blood in round bottom tube were mixed with 50 µl of an antibody assortment (containing a lineage cocktail made of antibodies directed against CD5, CD14, CD16, CD19, CD34, CD94, CD123, CD303, FCεRI, TCRαβ and TCRγδ) (**Table 18**). Blood was stained for 20 minutes on ice in the dark. Cells were fixed and lysed by adding 1.5 ml 1-step Fix/Lyse Solution (eBioscience™ Cat # 00-5333-54) and incubation 15-60 minutes at room temperature. Samples were washed with cell staining medium (CSM: PBS containing 0.5% BSA (Sigma-Aldrich, Darmstadt, Germany) centrifuged at 500g for 5 minutes at room temperature and re-suspended in 1ml CSM for acquisition on an Attune NxT Flow cytometer (Thermo Fisher scientific). Alternatively, samples were stored in buffer for up to 48 hours at 2-8°C and protected from light before washing and acquisition. The gating strategy used to identify ILCs subpopulations is presented in ***Figure 13***.

Table 18: Antibodies used for detection of ILC in peripheral blood samples

Target	Clone	Fluorochrome	Brand	Reference
TCRab	T10B9.1A-31	FITC	BD	555547
CD3	UCHT1	AlexaFluor 700	eBioscience	56-0038-42
CD16	HI16a	FITC	ImmunoTools	21810163
CD127	HIL-7R-M21	PE-Cy7	BD	560822
CD14	18D11	FITC	ImmunoTools	21620143
CD45	2D1	APC-H7	BD	560178
CD303	AC144	FITC	Miltenyi Biotec	130-090-510
CD336	p44-8	PE	BD	558563
TCRgd	B1	FITC	BD	559878
CD34	581	FITC	Biolegend	343504
CD56	B159	PerCP-Cy5.5	BD	560842
CD123	6H6	FITC	BD	11-1239-42
CD294	BM16	AlexaFluor 647	BD	558042
CD335	9-E2	BV 421	BD	564065
FceRI	AER-37	FITC	eBioscience	11-5899-42
CD19	HIB19	FITC	ImmunoTools	21810193
CD5	UCHT2	FITC	eBioscience	11-0059-41
CD94	HP-3D9	FITC	BD	555888
CD117	104D2	BV 605	Biolegend	313218

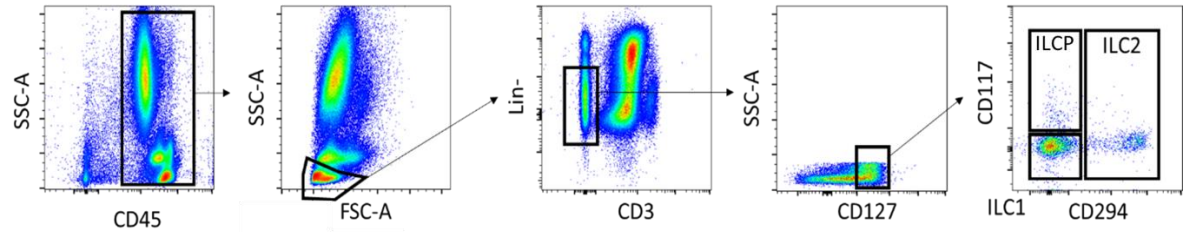

Figure 13*: Gating strategy of ILCs in blood*

PIPOVAP study. PIPOVAP stands for Profile, Interaction and PrOgnosis in Ventilator Associated Pneumoniae (***Table 19***). PIPOVAP is a prospective, two-center (CHUV and Lille University Hospital), observational research project assessing the consequences of using carbapenems in ventilator-associated-pneumoniae (VAP). Within the PIPOVA study, we embedded a study of blood cell study in peripheral blood. Here we report the analysis of circulating ILCs in patients at inclusion, one day, and five days after infection, before extubation and after exit from Intensive Care Unit (ICU) (***Figure 14***). Twenty-seven ICU patients were enrolled in the PIPOVAP study by CHUV. Unfortunately, we did not get any sample from the Lille site. Males represented 59% of the cohort, median age was 63 years and SOFA score 11.5 (***Table 19***). Among the 27 patients, 8 controls were patients that did not develop VAP and did not receive antibiotics, 10 patients developed VAP, and 9 patients developed another type of infection (urinary infections or unknown).

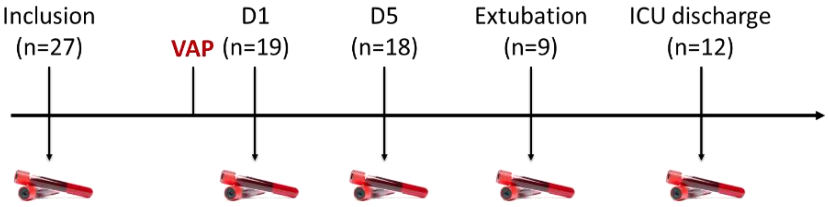

Figure 14: Overview of sample collection for the PIPOVAP study.

Table 19: Descriptive characteristics of PIPOVAP cohort study (medians (IQR) or N (%)).

General information	
Number of subjects/patients	27
Gender, Male	16 (59%)
Age (years)	63 [51-68]
Severity of illness (at admission)	
SOFA score	11.5 [10-14]

Results are presented in ***Figure 15***. In controls, ILCs represented around 0.5 x 10^6 cells/ml blood. More than 90% of ILCs were ILC1, while ILC2 and ILCP represented a small proportion of blood ILCs. Although numbers are small and caution advised, ILCs counts and repartition seemed to be similar in controls and infected patients, before and after extubation (***Figure 15***).

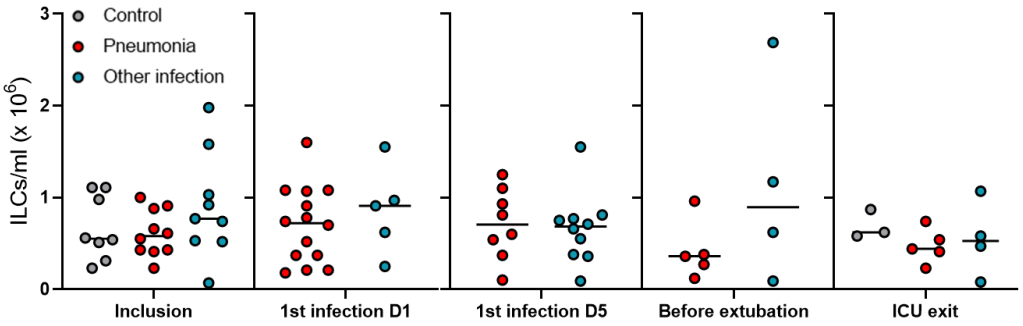

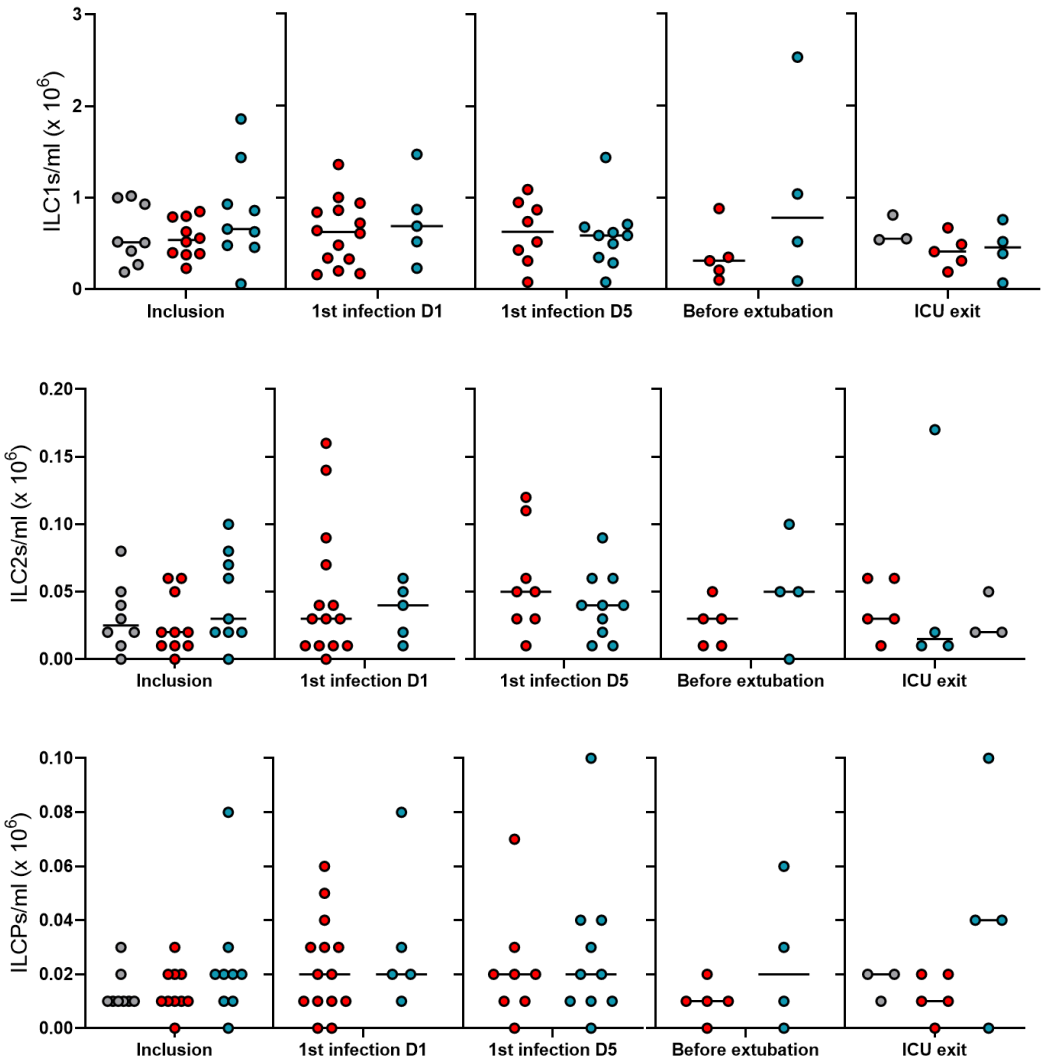

Figure 15: ILCs in peripheral blood of VAP patients (PIPOVAP study).

SARS-CoV-2 study. The SARS-CoV-2 study is an ongoing collaborative study between the Departments of Immunology and Allergy, Internal Medicine, Intensive Care and Infectious Diseases of CHUV. The study called "Defining the immune signatures associated with ICU and non-ICU hospitalized SARS-CoV-2 infected individuals at the time of admission/diagnosis and longitudinally" aims, among other objectives, to characterize immune signatures associated with ICU and non-ICU hospitalized SARS-CoV-2 infected individuals, and to define whether immune signatures are associated with the outcome of infected patients. Fifty-six patients were enrolled (***Table 20***). Males represented 70% of the cohort, the median age was 62 years. Fifty patients (89%) were intubated and 22 patients (39%) were admitted in ICU. Samples were obtained from 20 patients (36%) 3 months after admission.

Table 20: Descriptive characteristics of IMMUNO-SARS-CoV-2 study (medians (IQR) or N (%)).

General information	
Number of subjects/patients	56
Gender, Male	39 (70%)
Age (years)	62 [54-75]
Number of samples 3 months after admission	20 (36%)
Severity of illness	
Intubated	50 (89%)
ICU admission	22 (39%)

White cell counts were in the normal range, yet increased in ICU versus non-ICU patients (8.3 versus 6.7 x 10^9 cells per liter). Lymphocytes counts were similar (0.9 x 10^9 cells per L) in both groups. NK cells and ILCs counts (data not showed) and proportions were significantly lower in patients when compared to healthy volunteers (***Figure 16***). These observations were in line with results obtained in another clinical study [181]. Furthermore, severely ill patients that required intubation or an ICU admission had significantly less NK cells, ILC1s and ILC2s. Three months after admission, patients showed an increase of ILCs when compared to levels measured at admission, which reached levels measured in healthy controls. In contrast, patients had still lower proportions of NK cells compared to healthy control. This was more significant for severely ill patients. Interestingly, no differences in ILCs ratio were observed in this study, meaning ILCs subpopulations were similarly affected.

These two clinical studies suggest that ILCs are dynamic cell populations, which systemic levels respond to organ specific injury. Despite the disappointingly, identical ILCs counts in patients suffering from VAP, preliminary data observed in IMMUNO-SARS-CoV-2 study showed the potential role of ILCs in immune responses against SARS-CoV-2, and particularly to the severity of COVID-19. In this direction, peripheral blood proportions of ILCs could be used as biomarkers for disease severity. Additionally, considering that NK cells and ILC1 are mainly implicated in pro-inflammatory responses toward infection a rapid restoration to their initial proportion could improve patients' outcome.

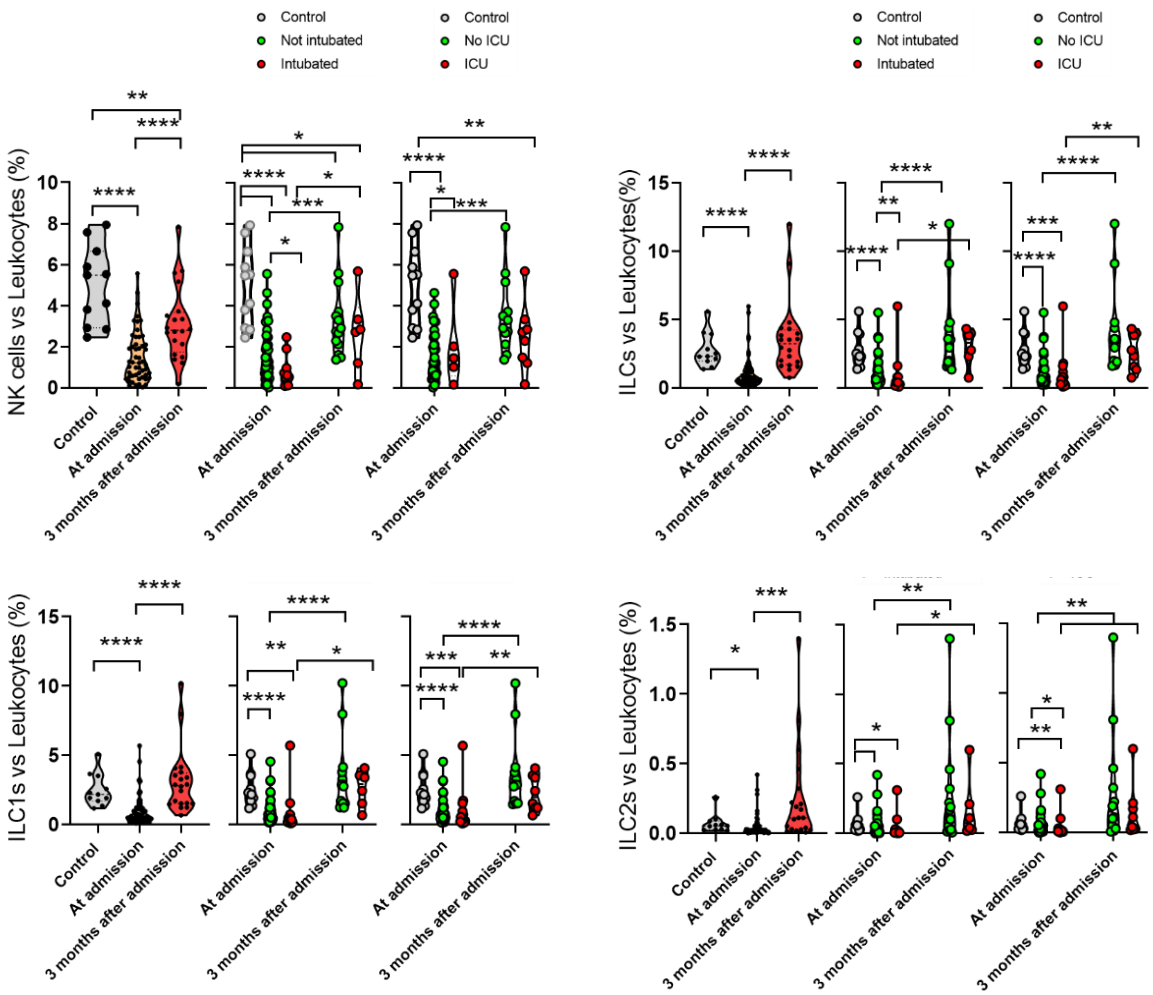

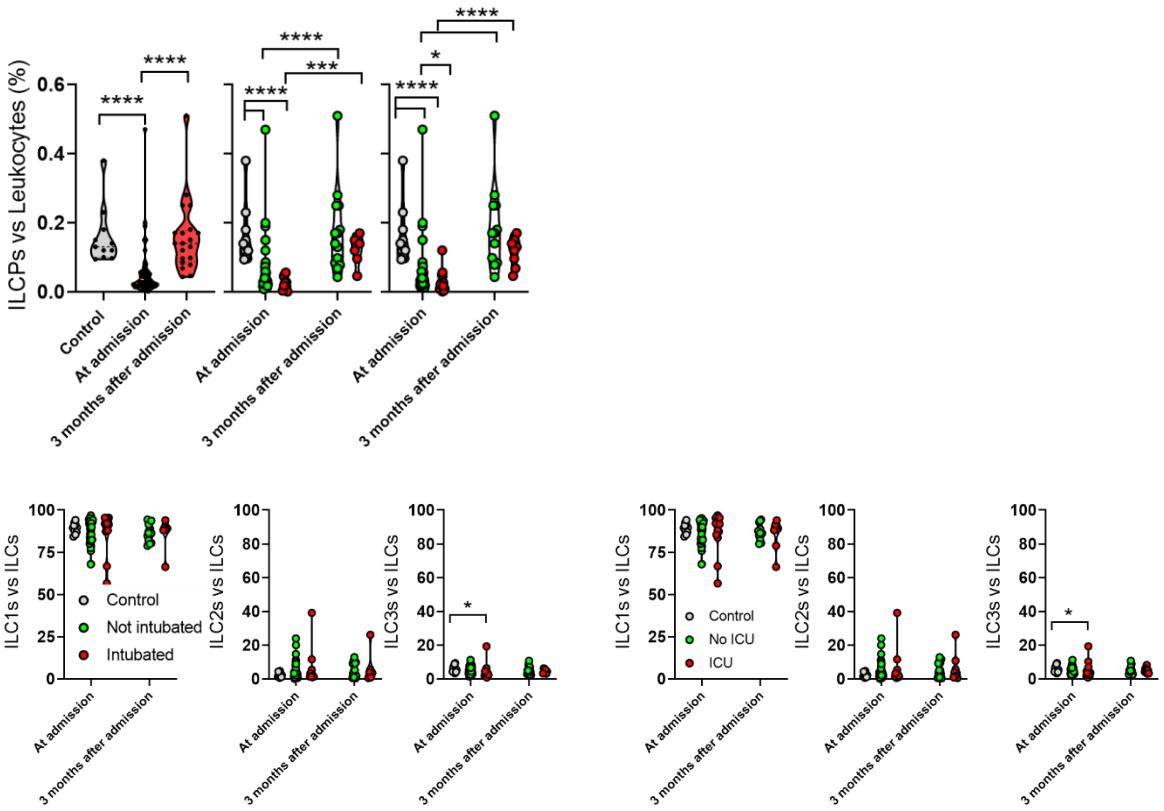

Figure 16: ILCs in blood of SARS-CoV-2 infected patients (IMMUNO-SARS-coV-2 study).

4. GENERAL DISCUSSION AND PERSPECTIVES

4.1. Trained immunity and infections

Looking backwards, innate immune memory gets its roots in the description more than 50 years ago of systemic acquired resistance in plants. Acquired memory protecting from reinfections was then reported in *Macrocyclops albidus* and insects lacking an adaptive immune system [258, 534, 535]. Pioneer mouse studies in the 70's-90's and early reports describing the non-specific protection from infectious diseases by vaccines were the basis of the belief that trained immunity would protect from any kind of infection. Yet, experimental designs analyzed one training agent and one single infectious microorganism, making difficult to draw general conclusions about the antimicrobial effectiveness of experimental trained immunity. Additionally, when we started this work, the nature of the cells underlying trained immunity was largely unknown, as well as the persistence of innate immune memory. Here we aimed addressing these questions.

4.1.1. Breadth of protection

To question about the breadth of protection conferred by trained immunity induced by β-glucans (zymosan), mice were tested using a large panel of infections. Remarkably, training protected mice from *E. coli* peritonitis, systemic blood infections by *S. aureus* and *L. monocytogenes*, *C. rodentium* enteritis and *P. aeruginosa* pneumonia. In a subsequent study, we showed that an identical training protocol protected from lethal *S. pneumoniae* pneumonia. Altogether, trained immunity confers broad-spectrum protection against heterologous microbial infections (see ***Table 21***), even when infection initiates at anatomical sites distant from the priming/training site. We extended our observations in a model of flu induced by H1N1 virus. In a pilot experiment, trained mice did not lose weight following infection, suggesting that training may protect from viral infection as well (***Figure 17***). We are currently challenging further this hypothesis in models of infection with H1N1 and mouse hepatitis virus (MHV) (using as readouts systemic and local cytokines concentrations and leukocytes counts, lung and liver histopathology and damage, mouse morbidity and mortality).

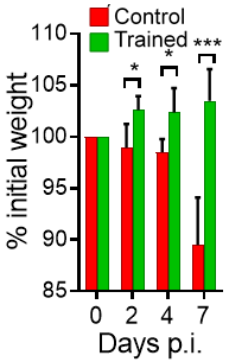

***Figure 17* : Trained immunity protects from H1N1 infection.**

*Control and trained C57BL/6 mice (n=5 mice/group) were challenged i.n. with 100 pfu H1N1. Weight was recoded and expressed relative to initial weight set at 100% (n=5 per group). *, P ≤ 0.05; ***, P ≤ 10-3.*

The clinical relevance of these observations gets credits from the results from the phase III ACTIVATE, a randomized clinical trial for enhanced trained immune responses through BCG vaccination to prevent infections of the elderly, which revealed that BCG vaccination increases the time to first infection and protects against viral respiratory infections [536]. Moreover, a few weeks ago, results from an investigator-blind randomized controlled trial in Uganda demonstrated that BCG-induced non-specific effects on heterologous infectious in neonates [537].

Trained immunity-based strategies might be used to fight severe acute respiratory syndrome coronavirus 2 (SARS-CoV2). Supporting this assumption, epidemiological studies reported non-specific effects of live vaccines and proof of principle studies showed that BCG vaccination protects healthy volunteers from controlled infection by YF and malaria [290, 291, 538-540]. Quadrivalent inactivated influenza vaccine induces trained immunity responses against SARS-CoV-2, and SARS-CoV-2 infection was less frequently detected in Dutch hospital employees vaccinated against influenza in the

2019/2020 winter season (Debisarun et al. https://doi.org/10.1101/2020.10.14.20212498). While debated, BCG vaccination was proposed to protect health care workers and to lower the incidence and/or severity of SARS-CoV2. [541-553]. Clinical trials are addressing that question in Australia, Denmark, France, Greece, South Africa and The Netherlands (https://www.clinicaltrials.gov/). This is of particular interest since HSCs, which are targeted during BCG-induced training, develop a memory phenotype and pass their memory to their progeny. This could be an advantageous target for the development of prevention or therapeutic treatments. However, while administration of BCG or β-glucans confers protections against *M. tuberculosis* infection [268, 306], a first administration of *M. tuberculosis* suppresses myelopoiesis and impairs development of protective immunity against a secondary infection with *M. tuberculosis* [554]. Whether this phenomenon is restricted to *M. tuberculosis* or occurs with other pathogens is unknown.

Experimental studies in the field of trained immunity mainly use as a training agent β-glucans that stimulate T helper (Th)1/Th17 proinflammatory responses critical to fight against bacteria, viruses and fungi. However, adaptive traits are acquired by the innate system exposed to a broad range of microbial products including β-glucans, chitin, peptidoglycan and muramyldipeptide, LPS and lipid A, CpG ODN, flagellin, as well as microorganisms (*C. albicans*, BCG, herpes virus, adenovirus, *Lactobacillus plantarum*). Not surprisingly, nematode-infected mice also acquired resistance to a subsequent infection with an unrelated nematode, suggesting that trained immunity can be skewed towards Th2 immune responses beneficial during parasitic infections [300]. This is important in the perspective of a possible role of trained immunity in the development of disorders linked to either Th1 or Th2 pathogenic responses (***Table 21***).

Table 21: Clinical implications of trained immunity (including our observations)

Effect	Condition/infectious agent	Ref.
Infectious diseases		
Protection	Candidiasis	[262, 292]
	C. rodentium	[275]
	COVID-19	[541-553]
	E. coli	[273, 275, 353]
	Influenza	[298]
	Leprosy	[555]
	L. monocytogenes	[275]
	Malaria	[290, 538, 539]
	Measles	[556]
	Meningitis	[557]
	M. tuberculosis	[265, 321, 558]
	N. brasiliensis	[351]
	P. aeruginosa	[275, 284]
	Sepsis	[376]
	S. pneumoniae	[273, 350, 352]
	S. pyogenes	[353]
	S. mansoni	[559]
	S. aureus	[275-277, 353, 361, 560, 561]
	Vaccinia virus	[302]
Impaired protection	*M. tuberculosis*	[554]
Vaccination		
Increase efficacy of vaccination	AIDS	[369]
	Yellow fever vaccination	[291]
Cancer		
Prevention	Bladder cancer	[371, 562]
	Leukemia	[563]

	Lymphoma	[370]
	Melanoma	[564]
Other inflammatory diseases		
Hyper-inflammation	Atherosclerosis	[565-568]
	Allergies	[569]
	IBD	[570]
	Neurological diseases	[341, 571]
	Transplant rejection	[572]
Reduced inflammation	Multiple sclerosis	[573, 574]

4.1.2. Cellular basis of infectious control by trained immunity

Initial reports identified PBMCs and blood derived monocytes/macrophages as trainable cells [260]. However, it became quickly evident that training should be sustained by cell renewal considering the short half-life of myeloid cells. We hypothesized that training affects bone marrow progenitors through epigenetic modifications. Indeed, we observed that training increased hematopoietic progenitors (LSKs), CMPs, GMPs and MMP3. In the meantime, millstone publications by Kaufmann et al. and Mitroulis et al. in *Cell* reported comprehensive analyses of the impact of trained immunity on bone marrow myeloid progenitors [268, 269].

During emergency myelopoiesis, HSCs migrate through the blood to induce extramedullary hematopoiesis. Interestingly, we observed that the size of the spleen increased twice up to 2 months after training. At that time point, the spleen contained more hematopoietic progenitors, including long-term and short-term HSCs, MMP2 and MMP3 (***Figure 18***). These data advocate for a role of extramedullary (splenic) hematopoiesis supporting trained immunity. Thus, it would be interesting to compare the transcriptome and epigenome of bone marrow and spleen HSCs to define whether common mechanisms are engaged in distant organs. Of note, training did not increase hematopoietic progenitors in lungs, suggesting that lung PMNs might be recruited while lung macrophages might expand locally during training (unpublished data).

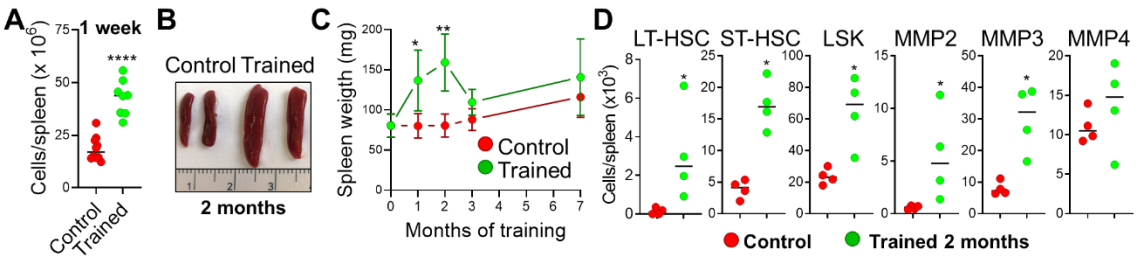

Figure 18 : **Trained immunity stimulates extramedullamry hematopoiesis.**
Mice were trained or not with zymosan as described in [275]. **A**) Splenocytes counts; **B**) spleen size; **C**) spleen weight; and **D**) spleen hematopoietic progenitors. *, $P \leq 0.05$; **, $P \leq 10^{-2}$; ****, $P \leq 10^{-4}$.

The peripheral blood as well as lungs of trained mice contained more leukocytes especially PMNs and Ly6C^{high} monocytes. Depletion and blocking experiments demonstrated that IL-1 signaling and monocytes/macrophages were required to protect trained mice from listeriosis, while PMNs were not required. These data are in agreement with the fact that IL-1β stimulates myelopoiesis and has been involved in the establishment of trained immunity [269, 291, 307, 315]. Although PMNs were dispensable during listeriosis, mature neutrophils are subjected to functional reprogramming by BCG-induced trained immunity [348], and β-glucan-induced trained immunity was associated with neutrophil reprogramming toward an anti-tumor phenotype [575].

Interestingly, the lungs of trained mice also contained more eosinophils. While these cells are traditionally perceived as detrimental, causing lung tissue damage via the release of cytotoxic granules [576], they also mediate homeostatic functions. As such, production of IL-4 or IL-10 by activated

eosinophils was necessary for hepatocyte and muscle regeneration and resolution of lung-allergic responses [577-579]. Additionally, they contribute to tissue remodeling and repair by producing key factors of coagulation (tissue factor thrombin) and fibrinolysis (plasminogen) (reviewed in [580]). These observations have been put together by Lee et al. who proposed the hypothesis “local immunity and remodeling/repair” (LIAR) [581].

The total number and subtypes proportions of lung ILCs were not modulated by training. In trained mice surviving infection, the number of ILCs also remained stable, but the proportion of ILCs shifted toward ILC2 probably subsequent to reduced bacterial burden. ILC2 accumulation in lungs of trained mice at late time point after the infection might reflect the ongoing repair mechanisms and/or be a consequence of reduced lung injury. Indeed, ILC2 promote tissue repair during influenza viral and parasitic infections [142, 166, 231, 232], and allergy [582] by production of amphiregulin (AREG) and arginase 1 (ARG1). Memory characteristics of ILCs have been reported in the literature. Memory ILC1 were identified in lymph nodes, where they acquire properties to migrate and reside in the liver via a CXCR6-CXCL16 axis [583]. Additionally, ILC1 expand in mice following MCMV infection. Those ILC1 acquire transcriptional and epigenetic modifications and demonstrate an enhanced protective response following a secondary challenge with MCMV [120]. In a recent article, ILC2s mediated systemic innate protection during *T. spiralis* infection by priming mucus production at distal mucosal sites [226]. Following allergen inhalation, ILC2 adopt a memory-like phenotype [355]. Memory ILC2 produce higher levels of IL-5 and IL-13 and initiate more efficiently Th2 responses during recall responses, in an unspecific manner. In neonatal lungs, ILC2 activation by endogenous IL-33 has significant effects on ILC2 functions in adulthood. Steer *et al*., showed that neonatal ILC2 persist in adulthood and respond more intensely to IL-33 [356], suggesting that memory ILC2 respond more efficiently to challenges later in life. Thus, while our data do not demonstrate a direct effect of training induction on lung ILCs, additional experiments are required, for example to check whether ILCs from trained mice produce more mediators that those from control mice. Additionaly, we plan to perform scRNA-seq and scATAC-seq on lungs of control and trained mice to pinpoint on cell to cell interactions and mechanisms accounting for protective effects of training in pneumococcal pneumonia [584].

4.1.3. Persistence of trained immunity

From a pathophysiological perspective, a central question is whether trained immunity has persistent effects on the immune system. Indeed, as we will discuss later, whether the immune system returns to homeostatic level or promotes the development of inflammatory diseases is unknown.

We analyzed mice trained for up to 9 weeks. In these mice, blood monocytes and PMNs as well as bone marrow CMPs and GMPs were increased. The blood from mice trained for 9 weeks produced increased levels of cytokines in response to microbial products and limited the growth of *Listeria*. Impressively, mice trained 9 weeks earlier controlled bacterial burden and survived listeriosis while all control mice died. These data suggest that increased myelopoiesis accounts for prolonged protection from infection conferred by trained immunity [275]. Others have shown that training durably affects the innate immunity system. For example, the adoptive transfer in naive mice of long-term HSCs or bone marrow cells collected from mice trained 4 weeks earlier increased the proportion of blood $Gr1^+CD11b^+$ myeloid cells and protected from pulmonary tuberculosis [268, 269]. Alveolar macrophages showed marks of trained immunity 16 weeks after an i.n. challenge of adenovirus [273]. Interestingly, adaptive immune cells such as effector $CD8^+$ lymphocytes were necessary to initiate this process, unravelling an adaptive to innate immunity signaling for the induction of trained immunity. Moreover, i.p. delivery of LPS into mice mediated epigenetic reprogramming of microglia (i.e. brain-resident macrophages) and brain immune training and tolerance that persisted for 6 months [341]. In the same vein, some weeks ago the group from Yasmine Belkaid (NIH, Bethesda, MD) showed that mice infected with *Yersinia pseudotuberculosis* were protected against intestinal *Klebsiella pneumoniae* infection up to 15 weeks after primary infection [585]. BCG vaccination induced changes in bone marrow HSPCs and blood $CD14^+$ monocytes detected 90 days after vaccination [306], and

protected healthy volunteers from experimental infection with the YF vaccine given 4 weeks after BCG vaccination [291]. In adult humans, BCG vaccination increased the response of PBMCs and circulating monocytes to unrelated pathogens 3 months post-vaccination, a phenomenon that largely vanished 1 year post-vaccination [319].

We started to test whether training initiated for up to 18 months confers a protective advantage towards bacterial infections. Unfortunately, these experiments had to be stopped earlier than planned due to restrictions imposed because of COVID-19, and all animals had to be used promptly or scarified. In that context, we decided to perform pilot experiments with mice analyzed 1 week and 1, 3 and 7 months after training induction (***Figure 19A***). In the peritoneal cavity, training induced a massive accumulation of antimicrobial small peritoneal macrophages (SMPs) that persisted for at least 1 month, and a less pronounced rise of PMNs. Cellularity returned to control levels within 3-7 months (***Figure 19B***). Peritoneal cells collected 7 months after training produced more IL-6 in response to LPS, CpG and bacteria, suggesting long-term effects on cell reactivity (***Figure 19C***). Mice trained 7 months earlier coped with *E. coli* peritonitis better than control mice, showing a trend for increased survival (***Figure 19D***). We then analyzed the blood compartment of trained mice. Training increased blood leukocytes, monocytes and PMNs early after induction. Numbers decreased at 3 months and returned to normal after 7 months (***Figure 20A***). The blood from mice trained for 3 months controlled better the growth of *Listeria*, and produced more cytokines (results reaching statistical significance for 8 cytokines) in response to LPS stimulation (***Figure 20B***). Accordingly, mice trained for 3 months survived better systemic listeriosis (***Figure 20C***). Impressively, mice trained for 7 months resisted better to listeriosis as shown by reduced weight loss, and a trend towards increased survival (***Figure 20D***).

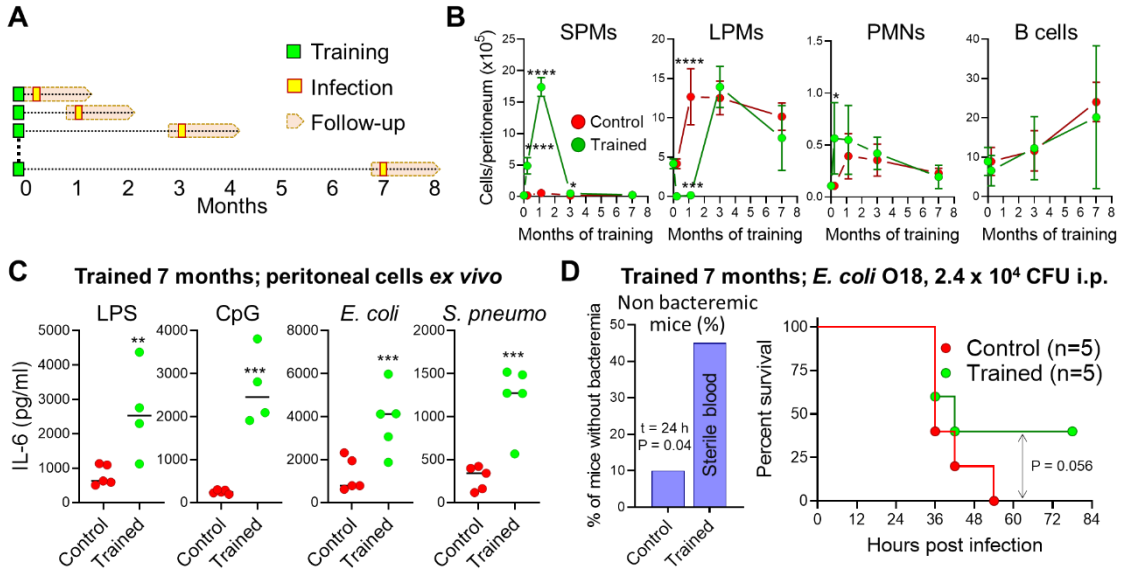

Figure 19: Trained immunity confers long-term protection from peritonitis

A) Experimental model. **B)** Leukocytes in the peritoneal cavity. SPMs/LPMs: Small/large peritoneal macrophages. **C)** IL-6 production by peritoneal cells collected 7 months after training and stimulated *ex vivo* for 6 h with LPS (100 ng/ml), CpG (0.5 µM), *E. coli* and *S. pneumoniae* (10^6 and 10^7 bacteria/ml). **D)** Bacteremia (in % of sterile mice, n=10 and 9) and survival (n=5) of mice trained for 7 months and challenged i.p. with *E. coli*. *, $P \leq 0.05$; **, $P \leq 10^{-2}$; ***, $P \leq 10^{-3}$; ****, $P \leq 10^{-4}$.

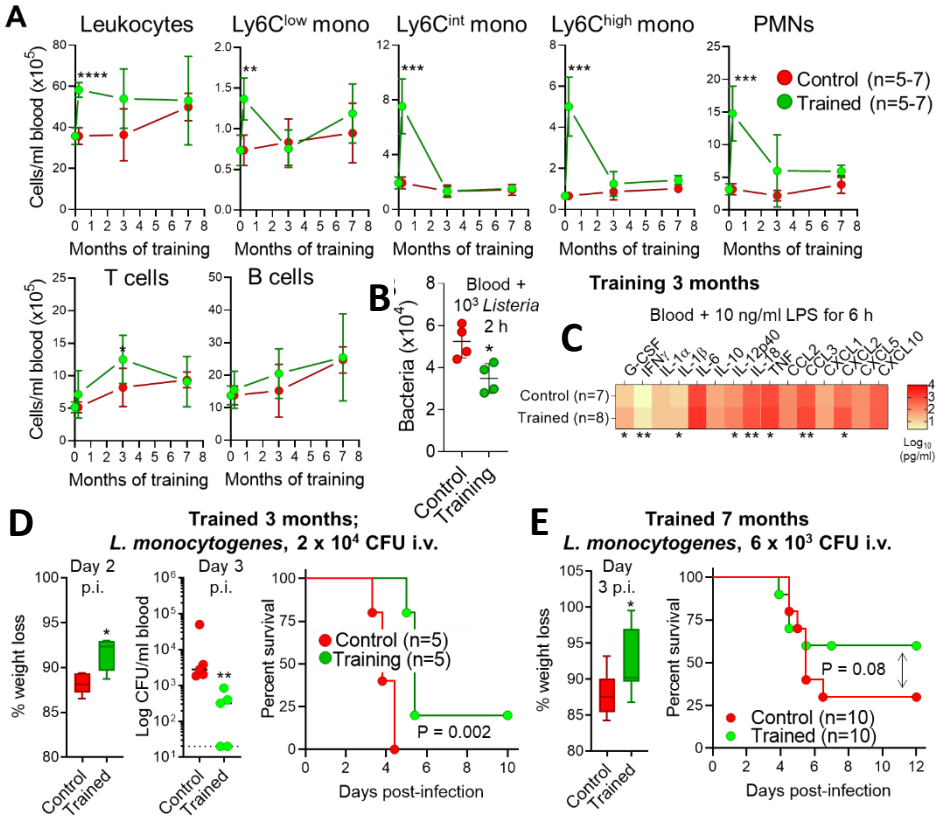

Figure 20: Trained immunity confers long-term protection from listeriosis

A) Blood leukocyte counts. Blood collected 3 months after training was incubated for 2 h with *L. monocytogenes* before enumerating bacteria (**B**) and for 6 h with 10 ng/ml LPS before measuring cytokines (n=9) (**C**). **D-E)** Weight lost, bacteremia and survival of mice trained for 3 months (**D**) and 7 months (**E**) and challenged i.v. with *L.* monocytogenes. *, $P \leq 0.05$; **, $P \leq 10^{-2}$; ***, $P \leq 10^{-3}$; ****, $P \leq 10^{-4}$.

Overall, these studies suggested that trained immunity have prolonged effects on innate immune responses. However, while BCG vaccination protected neonates from sepsis in a mouse model of neonatal polymicrobial sepsis, the effect was time limited and disappeared when infection was delayed for 10 days [586]. This could indicate that the effectiveness of trained immunity generation is age-dependent, which will require further studies for confirmation. The observations discussed in this chapter suggest that training has persistent effects that impede a prompt return at homeostasis of the innate immune system once challenged. Consequently, it interrogates about the possible deleterious impact of training on developing inflammatory and autoimmune disorders, especially age-associated diseases. Long-term follow-up of trained mice could indicate whether they are prone to develop auto-inflammatory or autoimmune diseases.

Going one-step further persistence of trained immunity, one may question whether trained immunity has intergenerational i.e. can be transmitted from parents to their progeny. Indeed, strong data indicate that phenotypes and disease risks can be transmitted through sperm and oocytes in the absence of DNA variations [587]. While the term intergenerational is self-explanatory, transgenerational inheritance characterizes mechanisms unrelated to a direct effect on the affected descendent, so that the definition excludes mechanisms possibly affecting oocytes carried by a female embryo. Transgenerational inheritance effects are responsible for the phenotypes observed in the F2 and F3 generations for male and female transmission, respectively. Evidences of intergenerational and transgenerational inheritance have been reported for invertebrates and vertebrates including rodents and humans [587]. Non-DNA sequence-based inheritance mechanisms transmitted through gametes include DNA methylation, histone post-translational modifications and miRNAs, sncRNAs, piRNAs and tsRNAs [588-595]. Additionally, nutrition, microbiome, metabolome and behavioral traits of parents

may affect phenotypes and disease susceptibility of progeny. Intergenerational inheritance of immune traits was observed in plants and insects, rarely in mammals [587, 596-598]. Amazingly, maternally transferred IgA influenced gut RORγ+ Treg numbers through multiple generations [599]. Male mice surviving lethal sepsis produced sperm with an altered methylome, and gave rise to offspring with impaired cytokine response to LPS challenge [600]. The exposure of female mice (pregnant or prior to matting) to *Aspergillus fumigatus*, LPS, probiotics, allergens and diesel exhaust particles had a strong impact on the immune response of offspring [601-608]. These observations support the hypothesis that trained immunity has an intergenerational part. To challenge this assumption, F1 mice obtained by crossing naïve or trained males with naïve females were challenged with *L. monocytogenes*. Amazingly, F1 progeny from trained males resisted infection (data not shown) indicating that protection from lethal listeriosis conferred by trained immunity is heritable. Ongoing experiments are analyzing sperm DNA methylome and bone marrow monocyte transcriptome and epigenome to unravel molecular pathways and mechanisms involved in training inheritance through males.

4.2. Trained immunity and non-infectious inflammatory diseases

A possible downside of trained immunity is the development of sterile inflammatory diseases such as familial fever syndromes, neurological diseases, arthritis, atherosclerosis, type 2 diabetes and systemic lupus erythematosus [307, 341, 376, 565, 570, 609-611]. Although this has not been firmly demonstrated, numerous arguments support this assumption besides the fact that the induction of training increases the response of innate immune cells. For example, monocytes from patients with hyperimmunoglobulin D syndrome, who are mevalonate kinase deficient and accumulate mevalonate, have a trained phenotype [313]. Western diet feeding of $Ldr^{-/-}$ atherosclerotic mice induced an oxidized low-density lipoprotein/NLRP3/IL-1 axis leading to the establishment of trained immunity [307, 377], and Western diet likely underlies so-called modern civilization diseases including obesity, diabetes, hypertension, Crohn's disease, coronary heart disease, autoimmune diseases, and cancer. Innate immune specific memory dependent on paired immunoglobulin-like receptors (PIR-A) was responsible of graft rejection mediated by monocytes and macrophages [612]. In a mouse model of Alzheimer disease, trained immunity affecting microglia exacerbated cerebral β-amyloidosis [273, 341]. Lastly, a recent study performed in Tanzania showed that urban living is associated with an inflammatory status resembling immune status observed during training [613]. Therefore, we can speculate that allergy or asthma could be the result from a training effect due to urban living.

To start challenging the possible involvement of trained immunity in sterile inflammatory diseases, we analyzed leukocyte content in the heart of control and trained mice. Interestingly, while heart/body weight ratio was similar in control and trained mice (as a control spleen weight was increased in trained mice), PMN counts increased 3-fold and there was a shift towards inflammatory monocytes in the pericardium of mice trained for 1 week (***Figure 21***). These preliminary results obtained in collaboration with Dr. Jérôme Lugrin (Services of Adult Intensive Care Medicine & Thoracic Surgery, CHUV) deserve deeper investigations. For example, we can analyze the impact of training in a model of myocardial infarction that closely mimics myocardial infarction in humans [614]. This might reveal cross-compartment communications, since myocardial infarction induced epigenetic reprograming of BM myeloid cells toward an immunosuppressive state that translate into tumor-associated monocyte myeloid derived suppressor cells (MDSCs) [615]. Going well along, our preliminary data showed an increase in monocytes MDSCs in bone marrow of trained mice (data not shown).

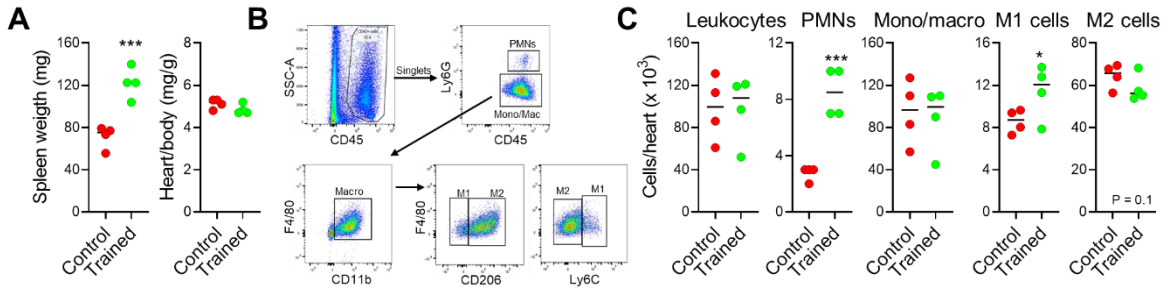

Figure 21: Training increases inflammatory cells in heart
C57BL/6 mice were trained or not with zymosan as described in [275] and sacrificed 1 week later for analysis. **A)** Spleen weight and heart/body weight ratio. **B)** Gating strategy to analyze heart immune cells. **C)** Absolute counts of leukocytes in the heart. M1 and M2 cells were defined as $CD206^{+}$ / $Ly6C^{-}$ and $CD206^{-}$ / $Ly6C^{+}$, respectively. *, $P \leq 0.05$; **, $P \leq 10^{-2}$; ***, $P \leq 10^{-3}$; ****, $P \leq 10^{-4}$.

Considering that patients with hyper immunoglobulin D syndrome are susceptible to skin rash [616], we hypothesized that training impacts on skin inflammation. We collaborated with Dr Jeremy Di Domizio (Service of Dermatology, CHUV) to test training in a model of skin inflammation and wounding induced by tape stripping [617]. We observed that trained mice had, visually, a lower inflammatory status 18 hours after the initial skin insult (***Figure 22***).

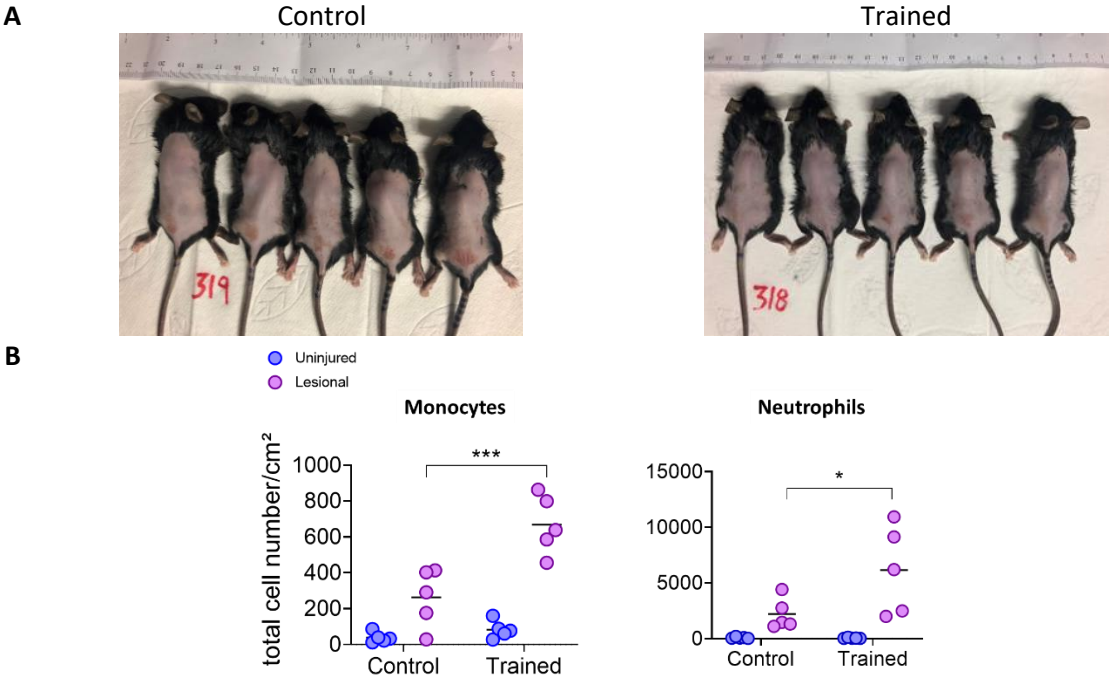

Figure 22: Trained immunity in skin inflammation
C57BL/6 mice were trained or not with zymosan as described in [275] and used 1 week later. Mice were anesthetized and shaved and depilated. Inflammation was induced by 10 tape stripping. After 18 h, mice were sacrificed, pictured, and 30 mg of injured dorsal skin was excised and digested with a mixture of 1 dispase and collagenase for 1 h at 37°C before analyzing leukocytes by flow cytometry. **A)** Photography showing inflamed skin. **B)** Absolute counts of monocytes and neutrophils per cm^2 of skin. *, $P \leq 0.05$; ***, $P \leq 10^{-3}$.

Biopsies were obtained from lesional skin and lesion-free skin to analyze leukocytes. Contrary to our expectations, the number of monocytes and neutrophils were similar in uninjured skin from control and trained mice, while lesional regions from trained mice contained more monocytes. The model of tape stripping was originally developed to study wound healing in sterile conditions. However, most

recent observations indicate that commensal bacteria colonizing skin wounds (mimicked by *S. epidermidis* recolonization in germ-free mice) activate neutrophils to produce CXCL10 involved in the recruitment and activation of plasmacytoid DCs (pDCs). In turn, activated produce type I IFNs which promote wound closure through acting on macrophages and fibroblasts that produce growth factors required for healing among which FGF2 (basic fibroblast growth factor/FGF-β) and TGF-β [618]. Of note, 1 week after injury, lesions healed better in trained than in control mice (data not shown). Therefore, we may postulate that trained immunity might favor wound healing in this model. To challenge this hypothesis, we should look at the actors involved in healing, i.e. neutrophils- CXCL10-pDCs-IFNs-macrophages-fibroblast-growth factors.

A provoking question is whether trained immunity is advantageous or disadvantageous during tumorigenesis. The answer will likely depend on the onset of training and the onset of tumorigenesis, possibly on the type and localization of the tumor. As mentioned above, myocardial infarction, which can be titled by trained immunity, accelerates breast cancer via innate immune reprogramming [615]. Trained immunity reprogrammed neutrophils enhancing their anti-tumor phenotype [575]. Overall, we need to better understand the beneficial or potentially deleterious consequences of trained immunity in order to advance towards therapeutic applications of trained immunity.

4.3. Therapeutic perspectives in trained immunity

Because of its impact on immune parameters, trained immunity may promote beneficial or harmful effects on the host (***Table 21***). As possible beneficial effects, trained immunity can be used to improve host defenses against infections or cancer development as already shown with BCG instillation in patients with bladder cancer. Deciphering training agents and training routes would be important in order to develop new adjuvants to improve vaccine efficacy. Among others, caution must be taken to the effects of training induced by vaccination. Indeed, the use of non-live vaccine was associated with overall increase mortality [619] while the use of live-attenuated vaccines was associated with significantly lower mortality [620], especially in girls [621]. Moreover, maternal priming with BCG affects outcome in BCG vaccinated newborns with a reduction in mortality of 66% [540].

A possible downside of trained immunity is the development of sterile inflammatory diseases. In these conditions, reverting the training phenotype by targeting immune, metabolic or epigenetic alterations might be an effective therapy. For example, inhibitors of the mTOR pathway, hydroxyl methylglutaryl-CoA inhibitors that prevent mevalonate synthesis or NLRP3 inflammasome inhibitors are drugs that may be used to revert or modulate trained phenotypes [274, 312, 376, 622]. Targeting specific innate immune cells using a nanoparticle delivery approach may improve the specificity of the drugs and prevent off-target effects [376]. In a mouse model of heart transplantation, donor allografts have a local training of graft-infiltrating monocytes-derived cells, which was associated with allograft rejection [572]. A nano-immunotherapeutic approach inhibiting co-stimulation between CD40 and TRAF6 inhibited CD8 T cells and promoted Tregs. This improved allograft survival [610].

Western diet promotes the establishment of trained phenotype [307, 377]. In addition to be strongly associated with obesity and related metabolic diseases, evidences show that Western diet can also promotes inflammation due to the structural and behavioral changes of the microbiome [623]. A first study showed that mice harboring a microbiota derived from a wild mouse population were protected against lethal viral infection [624]. Recently, Stacy et al. reported that colonization resistance was not only dependent on host microbiota interaction but also on previous intestinal infection [585]. The microbiota was trained to prevent colonization by heterologous infection. Pilot experiments performed in our laboratory indicated that trained immunity modified gut microbiota. Additionally, trained immunity was less efficient at protecting from infections mice pre-treated with antibiotics (data not shown). In these conditions, we can imagine using fecal or microbial community transplantation to modulate trained immunity and fight the threat of antibiotic resistance [625].

Sepsis being characterized by both an excessive inflammatory response and immunosuppression [626], patients with sepsis might not react similarly to the same treatment. Our training models showed that mice survived different models of infection. Single cell studies combining transcriptome and mass cytometry analyses in these models could give clues about the mechanisms regulating immune responses during training and explain how mice control an infection and simultaneously give hints to find better biomarkers to diagnose or treat sepsis. Training agents could, for example provide therapeutic benefit during the immunoparalysis phase of sepsis [376].

4.4. ILCs in airway diseases

We developed clinical trials to look at ILCs in patients with pulmonary infections. The goal was to determine whether we could use peripheral blood counts of ILCs (and more globally other immune cell populations among which myeloid derived suppressor cells or MDSCs) as biomarkers, for example of disease severity. Disappointingly, ILCs counts and proportions were identical in patients suffering from VAP. However, patients suffering from SARS-CoV-2 infections had fewer ILCs compared to healthy controls, and this was associated with worse outcomes.

Patients infected by SARS-CoV-2 responsible of COVID-19 disease pandemic can develop severe illness with a high fatality rate due to lung damage. As such, ILC2 involvement in immune responses to COVID-19 has also been recently investigated [181]. ILCs were reduced in severely ill patients, while showing an increase proportion of the ILC2 sub-population. An increase in IL-5 and IL-13 was observed in patients compared to healthy donors, which may be attributed to a cytokine secretion by ILC2. Additionally, NKG2D$^+$ ILC2 population increased in severely ill patients compared to mildly ill patients or control, while CD25 and KLRG1 decreased. This is in line with the known up-regulation of NKG2D receptor upon viral infections [627]. However, NKG2D+ ILC2 population was associated with a significantly reduced proportion of patients requiring mechanical ventilation. This may indicate a protective role of this cell subset during SARS-CoV-2 infection. In another recent article, ILCs were largely depleted from the circulation of COVID-19 patients when compared with healthy controls [110]. ILC2 frequency decreased in severe COVID-19 patients. Lastly, a study confirmed a significant decreased of ILCs in COVID-19 patients compared to uninfected controls [628]. In addition, higher ILC counts were associated with faster hospital discharge. The differences obtained between the different studies, as well as our own study, might be explained by the phenotype used to identify ILCs as well as the donor characteristics.

ILCs were dramatically impaired in peripheral blood of HIV-1 infected patients [629-631]. In a primary study, HIV-1 infection induced persistent activation of pDCs, production of type I IFNs, increase CD95 expression on ILC3s, and ILC3 apoptosis. This depletion could explain the impaired intestinal barrier function driven by IL-17/IL-22 loss [632], resulting from chronic HIV-1 infection [633]. Under these conditions, therapies targeting pDCs or type I IFN might restore the function of ILC3 and improve the intestinal barrier integrity of HIV-1 infected patients. In a second study, circulating ILCs were severely depleted during acute phase of HIV-1 infection, despite antiretroviral t and resolution of viremia peak [634]. However, when administrated during acute infection, antiretroviral therapy preserved ILC numbers. A study from 2020 demonstrated that children infected with HIV-1 at birth have a depletion in circulating and tonsil resident ILCs [631]. An early *in utero* or up to 2-3 years old antiretroviral therapy could preserve ILCs, while a late treatment was inefficient. Finally, another study showed that ILCs depletion in HIV-1 infected patient was associated with neutrophil infiltration of the gut lamina propria, type 1 interferon activation and NK cells skewing towards a pro-inflammatory state, explaining chronic inflammation observed in people infected with HIV-1 [635].

Blood counts of ILC1 and ILC3 decreased in patients with sepsis due to an increase apoptosis, while ILCs showed a decreased in HLA-DR expression [636]. The lower expression of MHC-II recalls that observed in peripheral blood monocytes and used as a biomarker of sepsis [637]. Newborns ingested

ILCs through breast milk, of which ILC1 were the largest population with high levels of IFNɣ, possibly shaping the oral and intestinal microbiome of newborns to adapt to the post-delivery environment. Thus, ILC1 may play a significant role in neonatal sepsis [638]. However another study showed that ILC1 counts were higher in septic patients than in healthy subjects, while ILC2 and ILC3 counts were lower [227]. Interestingly, ILC3 within total ILCs counts were overrepresented in patients with severe sepsis. ILC2 migrated to the lungs in response to S1P [639], where they could be activated by IL-33 released by surrounding cells has seen during cecal ligation and puncture sepsis [170, 640]. IL-33 was associated with acute lung injury and cecal ligation and puncture increased the production of IL-5 by pulmonary ILC2, leading to neutrophil infiltration and acute lung injury [640]. Conversely, pulmonary ILC2 produced IL-9 in response to IL-33, preventing pyroptosis of pulmonary endothelial cells and lung injury [641]. Therefore, therapies targeting ILCs can be developed in to dampen or to increase ILC's inflammatory properties according to patient status. New therapeutic tools could explore ILCs homeostasis properties to fine tune inflammation during by infections.

4.5. Perspectives

Follow-up studies have been mentioned in this discussion. To sum-up, our principal working hypothesis for the training project are that:

1. Trained immunity has long-lasting effects on central and peripheral hematopoiesis as well as on circulating and tissue myeloid cells that confer protection from severe infections,
2. Intergenerational inheritance, and possibly transgenerational inheritance, of epigenetic characters is associated with trained immunity confers protection from severe infections,
3. Induction of trained immunity is associated with changes of the gut microbiome that might be exploited to modulate antimicrobial host defenses.

Overall, targeting trained immunity may have important therapeutic implications, ranging from the design of vaccines that stimulate adaptive and innate immune memory to the development of inducers of trained immunity to counter-balance immuno-paralysis observed in cancer and sepsis, and to avoid the possible deleterious impact of trained immunity on the development of age-associated pathologies. Finally, considering the usage of peripheral ILCs counts or distribution as disease biomarkers for pulmonary infections, our results were not satisfying enough to deepen further this axis of research. A main reason could be that tissue ILCs more than peripheral blood ILCs could be interesting targets of study, with all ethical and technical associated difficulties. Thus, we will envisage focusing on bacteremic patients.

5. REFERENCES

1. Chaplin, D.D., *Overview of the immune response.* J Allergy Clin Immunol, 2010. **125**(2 Suppl 2): p. S3-23.
2. Sherwood, E.R. and T. Toliver-Kinsky, *Mechanisms of the inflammatory response.* Best Pract Res Clin Anaesthesiol, 2004. **18**(3): p. 385-405.
3. Leiva-Juarez, M.M., J.K. Kolls, and S.E. Evans, *Lung epithelial cells: therapeutically inducible effectors of antimicrobial defense.* Mucosal Immunol, 2018. **11**(1): p. 21-34.
4. Medzhitov, R., *Recognition of microorganisms and activation of the immune response.* Nature, 2007. **449**(7164): p. 819-26.
5. Schaefer, L., *Complexity of danger: the diverse nature of damage-associated molecular patterns.* J Biol Chem, 2014. **289**(51): p. 35237-45.
6. Takeuchi, O. and S. Akira, *Pattern recognition receptors and inflammation.* Cell, 2010. **140**(6): p. 805-20.
7. Broz, P. and D.M. Monack, *Newly described pattern recognition receptors team up against intracellular pathogens.* Nat Rev Immunol, 2013. **13**(8): p. 551-65.
8. Latz, E., T.S. Xiao, and A. Stutz, *Activation and regulation of the inflammasomes.* Nat Rev Immunol, 2013. **13**(6): p. 397-411.
9. Iwasaki, A., E.F. Foxman, and R.D. Molony, *Early local immune defences in the respiratory tract.* Nat Rev Immunol, 2017. **17**(1): p. 7-20.
10. Hoeffel, G., et al., *C-Myb(+) erythro-myeloid progenitor-derived fetal monocytes give rise to adult tissue-resident macrophages.* Immunity, 2015. **42**(4): p. 665-78.
11. Guilliams, M., et al., *Alveolar macrophages develop from fetal monocytes that differentiate into long-lived cells in the first week of life via GM-CSF.* J Exp Med, 2013. **210**(10): p. 1977-92.
12. Tan, S.Y. and M.A. Krasnow, *Developmental origin of lung macrophage diversity.* Development, 2016. **143**(8): p. 1318-27.
13. Burberry, A., et al., *Infection mobilizes hematopoietic stem cells through cooperative NOD-like receptor and Toll-like receptor signaling.* Cell Host Microbe, 2014. **15**(6): p. 779-91.
14. Joshi, N., J.M. Walter, and A.V. Misharin, *Alveolar Macrophages.* Cell Immunol, 2018. **330**: p. 86-90.
15. Xue, J., et al., *Transcriptome-based network analysis reveals a spectrum model of human macrophage activation.* Immunity, 2014. **40**(2): p. 274-88.
16. Italiani, P. and D. Boraschi, *From Monocytes to M1/M2 Macrophages: Phenotypical vs. Functional Differentiation.* Front Immunol, 2014. **5**: p. 514.
17. Kopf, M., C. Schneider, and S.P. Nobs, *The development and function of lung-resident macrophages and dendritic cells.* Nat Immunol, 2015. **16**(1): p. 36-44.
18. Ginhoux, F., et al., *The origin and development of nonlymphoid tissue CD103+ DCs.* J Exp Med, 2009. **206**(13): p. 3115-30.
19. Elliott, D.E., S.S. Siddique, and J.V. Weinstock, *Innate immunity in disease.* Clin Gastroenterol Hepatol, 2014. **12**(5): p. 749-55.
20. Banchereau, J., et al., *Immunobiology of dendritic cells.* Annu Rev Immunol, 2000. **18**: p. 767-811.
21. Alvarez, D., E.H. Vollmann, and U.H. von Andrian, *Mechanisms and consequences of dendritic cell migration.* Immunity, 2008. **29**(3): p. 325-42.
22. Condon, T.V., et al., *Lung dendritic cells at the innate-adaptive immune interface.* J Leukoc Biol, 2011. **90**(5): p. 883-95.
23. Hajishengallis, G., et al., *Novel mechanisms and functions of complement.* Nat Immunol, 2017. **18**(12): p. 1288-1298.
24. Zheng, D., T. Liwinski, and E. Elinav, *Inflammasome activation and regulation: toward a better understanding of complex mechanisms.* Cell Discov, 2020. **6**: p. 36.
25. Trinchieri, G., *Biology of natural killer cells.* Adv Immunol, 1989. **47**: p. 187-376.

26. Tosi, M.F., *Innate immune responses to infection.* J Allergy Clin Immunol, 2005. **116**(2): p. 241-9; quiz 250.
27. Culley, F.J., *Natural killer cells in infection and inflammation of the lung.* Immunology, 2009. **128**(2): p. 151-63.
28. Ashley, N.T., Z.M. Weil, and R.J. Nelson, *Inflammation: Mechanisms, Costs, and Natural Variation.* Annual Review of Ecology, Evolution, and Systematics, 2012. **43**(1): p. 385-406.
29. Epelman, S., K.J. Lavine, and G.J. Randolph, *Origin and functions of tissue macrophages.* Immunity, 2014. **41**(1): p. 21-35.
30. Goritzka, M., et al., *Alveolar macrophage-derived type I interferons orchestrate innate immunity to RSV through recruitment of antiviral monocytes.* J Exp Med, 2015. **212**(5): p. 699-714.
31. Lin, K.L., et al., *CCR2+ monocyte-derived dendritic cells and exudate macrophages produce influenza-induced pulmonary immune pathology and mortality.* J Immunol, 2008. **180**(4): p. 2562-72.
32. Maus, U.A., et al., *Monocytes are potent facilitators of alveolar neutrophil emigration during lung inflammation: role of the CCL2-CCR2 axis.* J Immunol, 2003. **170**(6): p. 3273-8.
33. Espinosa, V., et al., *Inflammatory monocytes orchestrate innate antifungal immunity in the lung.* PLoS Pathog, 2014. **10**(2): p. e1003940.
34. Brinkmann, V., et al., *Neutrophil extracellular traps kill bacteria.* Science, 2004. **303**(5663): p. 1532-5.
35. Rothenberg, M.E. and S.P. Hogan, *The eosinophil.* Annu Rev Immunol, 2006. **24**: p. 147-74.
36. Blanchard, C. and M.E. Rothenberg, *Biology of the eosinophil.* Adv Immunol, 2009. **101**: p. 81-121.
37. Bernink, J.H., K. Germar, and H. Spits, *The role of ILC2 in pathology of type 2 inflammatory diseases.* Curr Opin Immunol, 2014. **31**: p. 115-20.
38. Nakayama, T., et al., *Th2 Cells in Health and Disease.* Annu Rev Immunol, 2017. **35**: p. 53-84.
39. Yi, S., et al., *Eosinophil recruitment is dynamically regulated by interplay among lung dendritic cell subsets after allergen challenge.* Nat Commun, 2018. **9**(1): p. 3879.
40. Linch, S.N. and J.A. Gold, *The role of eosinophils in non-parasitic infections.* Endocr Metab Immune Disord Drug Targets, 2011. **11**(2): p. 165-72.
41. Wen, T. and M.E. Rothenberg, *The Regulatory Function of Eosinophils.* Microbiol Spectr, 2016. **4**(5).
42. Esmon, C.T., *The interactions between inflammation and coagulation.* Br J Haematol, 2005. **131**(4): p. 417-30.
43. Palta, S., R. Saroa, and A. Palta, *Overview of the coagulation system.* Indian J Anaesth, 2014. **58**(5): p. 515-23.
44. Snyder, M.E. and D.L. Farber, *Human lung tissue resident memory T cells in health and disease.* Curr Opin Immunol, 2019. **59**: p. 101-108.
45. Neurath, M.F., *Resolution of inflammation: from basic concepts to clinical application.* Semin Immunopathol, 2019. **41**(6): p. 627-631.
46. Sugimoto, M.A., et al., *Resolution of Inflammation: What Controls Its Onset?* Front Immunol, 2016. **7**: p. 160.
47. Levi, M. and T. van der Poll, *Inflammation and coagulation.* Crit Care Med, 2010. **38**(2 Suppl): p. S26-34.
48. Serhan, C.N. and J. Savill, *Resolution of inflammation: the beginning programs the end.* Nat Immunol, 2005. **6**(12): p. 1191-7.
49. Serhan, C.N., *Pro-resolving lipid mediators are leads for resolution physiology.* Nature, 2014. **510**(7503): p. 92-101.
50. Ortega-Gomez, A., M. Perretti, and O. Soehnlein, *Resolution of inflammation: an integrated view.* EMBO Mol Med, 2013. **5**(5): p. 661-74.
51. Stables, M.J., et al., *Transcriptomic analyses of murine resolution-phase macrophages.* Blood, 2011. **118**(26): p. e192-208.

52. Serhan, C.N., et al., *Novel anti-inflammatory--pro-resolving mediators and their receptors.* Curr Top Med Chem, 2011. **11**(6): p. 629-47.
53. Gasser, O. and J.A. Schifferli, *Activated polymorphonuclear neutrophils disseminate anti-inflammatory microparticles by ectocytosis.* Blood, 2004. **104**(8): p. 2543-8.
54. Fox, S., et al., *Neutrophil apoptosis: relevance to the innate immune response and inflammatory disease.* J Innate Immun, 2010. **2**(3): p. 216-27.
55. Fadok, V.A., et al., *Macrophages that have ingested apoptotic cells in vitro inhibit proinflammatory cytokine production through autocrine/paracrine mechanisms involving TGF-beta, PGE2, and PAF.* J Clin Invest, 1998. **101**(4): p. 890-8.
56. Michlewska, S., et al., *Macrophage phagocytosis of apoptotic neutrophils is critically regulated by the opposing actions of pro-inflammatory and anti-inflammatory agents: key role for TNF-alpha.* FASEB J, 2009. **23**(3): p. 844-54.
57. Chen, L., et al., *Inflammatory responses and inflammation-associated diseases in organs.* Oncotarget, 2018. **9**(6): p. 7204-7218.
58. Leibovich, S.J. and R. Ross, *The role of the macrophage in wound repair. A study with hydrocortisone and antimacrophage serum.* Am J Pathol, 1975. **78**(1): p. 71-100.
59. Bellingan, G.J., et al., *In vivo fate of the inflammatory macrophage during the resolution of inflammation: inflammatory macrophages do not die locally, but emigrate to the draining lymph nodes.* J Immunol, 1996. **157**(6): p. 2577-85.
60. Dorhoi, A., et al., *MDSCs in infectious diseases: regulation, roles, and readjustment.* Cancer Immunol Immunother, 2019. **68**(4): p. 673-685.
61. Fullerton, J.N. and D.W. Gilroy, *Resolution of inflammation: a new therapeutic frontier.* Nat Rev Drug Discov, 2016. **15**(8): p. 551-67.
62. Liu, J., et al., *Identification and characterization of a unique leucine-rich repeat protein (LRRC33) that inhibits Toll-like receptor-mediated NF-kappaB activation.* Biochem Biophys Res Commun, 2013. **434**(1): p. 28-34.
63. Taganov, K.D., et al., *NF-kappaB-dependent induction of microRNA miR-146, an inhibitor targeted to signaling proteins of innate immune responses.* Proc Natl Acad Sci U S A, 2006. **103**(33): p. 12481-6.
64. Perry, M.M., et al., *Rapid changes in microRNA-146a expression negatively regulate the IL-1beta-induced inflammatory response in human lung alveolar epithelial cells.* J Immunol, 2008. **180**(8): p. 5689-98.
65. Gabrilovich, D.I., *Myeloid-Derived Suppressor Cells.* Cancer Immunol Res, 2017. **5**(1): p. 3-8.
66. Schrijver, I.T., C. Theroude, and T. Roger, *Myeloid-Derived Suppressor Cells in Sepsis.* Front Immunol, 2019. **10**: p. 327.
67. Vignali, D.A., L.W. Collison, and C.J. Workman, *How regulatory T cells work.* Nat Rev Immunol, 2008. **8**(7): p. 523-32.
68. Arocena, A.R., et al., *Myeloid-derived suppressor cells are key players in the resolution of inflammation during a model of acute infection.* Eur J Immunol, 2014. **44**(1): p. 184-94.
69. Li, J., et al., *Regulatory T-Cells: Potential Regulator of Tissue Repair and Regeneration.* Front Immunol, 2018. **9**: p. 585.
70. Drake, L.Y. and H. Kita, *Group 2 innate lymphoid cells in the lung.* Adv Immunol, 2014. **124**: p. 1-16.
71. Walker, J.A., J.L. Barlow, and A.N. McKenzie, *Innate lymphoid cells--how did we miss them?* Nat Rev Immunol, 2013. **13**(2): p. 75-87.
72. Gasteiger, G., et al., *Tissue residency of innate lymphoid cells in lymphoid and nonlymphoid organs.* Science, 2015. **350**(6263): p. 981-5.
73. Lai, D.M., Q. Shu, and J. Fan, *The origin and role of innate lymphoid cells in the lung.* Mil Med Res, 2016. **3**: p. 25.
74. Artis, D. and H. Spits, *The biology of innate lymphoid cells.* Nature, 2015. **517**(7534): p. 293-301.

75. Eberl, G., J.P. Di Santo, and E. Vivier, *The brave new world of innate lymphoid cells.* Nat Immunol, 2015. **16**(1): p. 1-5.
76. Vivier, E., et al., *Innate Lymphoid Cells: 10 Years On.* Cell, 2018. **174**(5): p. 1054-1066.
77. Zhong, C., M. Zheng, and J. Zhu, *Lymphoid tissue inducer-A divergent member of the ILC family.* Cytokine Growth Factor Rev, 2018. **42**: p. 5-12.
78. Abel, A.M., et al., *Natural Killer Cells: Development, Maturation, and Clinical Utilization.* Front Immunol, 2018. **9**: p. 1869.
79. Constantinides, M.G., et al., *A committed precursor to innate lymphoid cells.* Nature, 2014. **508**(7496): p. 397-401.
80. Cherrier, M., S. Sawa, and G. Eberl, *Notch, Id2, and RORgammat sequentially orchestrate the fetal development of lymphoid tissue inducer cells.* J Exp Med, 2012. **209**(4): p. 729-40.
81. Michieletto, M.F. and J. Henao-Mejia, *Ontogeny and heterogeneity of innate lymphoid cells and the noncoding genome.* Immunol Rev, 2021.
82. Seillet, C., et al., *Nfil3 is required for the development of all innate lymphoid cell subsets.* J Exp Med, 2014. **211**(9): p. 1733-40.
83. Seehus, C.R., et al., *The development of innate lymphoid cells requires TOX-dependent generation of a common innate lymphoid cell progenitor.* Nat Immunol, 2015. **16**(6): p. 599-608.
84. Yang, Q., et al., *TCF-1 upregulation identifies early innate lymphoid progenitors in the bone marrow.* Nat Immunol, 2015. **16**(10): p. 1044-50.
85. Yokota, Y., et al., *Development of peripheral lymphoid organs and natural killer cells depends on the helix-loop-helix inhibitor Id2.* Nature, 1999. **397**(6721): p. 702-6.
86. Aliahmad, P., B. de la Torre, and J. Kaye, *Shared dependence on the DNA-binding factor TOX for the development of lymphoid tissue-inducer cell and NK cell lineages.* Nat Immunol, 2010. **11**(10): p. 945-52.
87. Klose, C.S., et al., *A T-bet gradient controls the fate and function of CCR6-RORgammat+ innate lymphoid cells.* Nature, 2013. **494**(7436): p. 261-5.
88. Yu, Y., et al., *Single-cell RNA-seq identifies a PD-1(hi) ILC progenitor and defines its development pathway.* Nature, 2016. **539**(7627): p. 102-106.
89. Zhou, L. and G.F. Sonnenberg, *In Situ Support of ILC Precursors.* Immunity, 2020. **52**(2): p. 207-209.
90. Spits, H. and J.P. Di Santo, *The expanding family of innate lymphoid cells: regulators and effectors of immunity and tissue remodeling.* Nature Immunology, 2010. **12**(1): p. 21-27.
91. Robinette, M.L., et al., *IL-15 sustains IL-7R-independent ILC2 and ILC3 development.* Nature Communications, 2017. **8**(1).
92. Kasal, D.N. and A. Bendelac, *Multi-transcription factor reporter mice delineate early precursors to the ILC and LTi lineages.* J Exp Med, 2021. **218**(2).
93. Stier, M.T., et al., *IL-33 promotes the egress of group 2 innate lymphoid cells from the bone marrow.* J Exp Med, 2018. **215**(1): p. 263-281.
94. Gomez-Cadena, A., et al., *Detecting and analyzing murine innate lymphoid cells.* Methods Enzymol, 2020. **631**: p. 329-342.
95. Lane, P.J., et al., *Lymphoid tissue inducer cells: pivotal cells in the evolution of CD4 immunity and tolerance?* Front Immunol, 2012. **3**: p. 24.
96. Ignacio, A., C.N.S. Breda, and N.O.S. Camara, *Innate lymphoid cells in tissue homeostasis and diseases.* World J Hepatol, 2017. **9**(23): p. 979-989.
97. Bjorklund, A.K., et al., *The heterogeneity of human CD127(+) innate lymphoid cells revealed by single-cell RNA sequencing.* Nat Immunol, 2016. **17**(4): p. 451-60.
98. Guia, S. and E. Narni-Mancinelli, *Helper-like Innate Lymphoid Cells in Humans and Mice.* Trends Immunol, 2020.
99. Klose, C.S.N. and D. Artis, *Innate lymphoid cells control signaling circuits to regulate tissue-specific immunity.* Cell Res, 2020.

100. Klose, C.S.N., et al., *Differentiation of type 1 ILCs from a common progenitor to all helper-like innate lymphoid cell lineages.* Cell, 2014. **157**(2): p. 340-356.
101. Schneider, C., et al., *Tissue-Resident Group 2 Innate Lymphoid Cells Differentiate by Layered Ontogeny and In Situ Perinatal Priming.* Immunity, 2019. **50**(6): p. 1425-1438 e5.
102. Lim, A.I., et al., *Systemic Human ILC Precursors Provide a Substrate for Tissue ILC Differentiation.* Cell, 2017. **168**(6): p. 1086-1100 e10.
103. Kim, C.H., S. Hashimoto-Hill, and M. Kim, *Migration and Tissue Tropism of Innate Lymphoid Cells.* Trends Immunol, 2016. **37**(1): p. 68-79.
104. Dutton, E.E., et al., *Peripheral lymph nodes contain migratory and resident innate lymphoid cell populations.* Sci Immunol, 2019. **4**(35).
105. Vacca, P., et al., *Heterogeneity of NK Cells and Other Innate Lymphoid Cells in Human and Murine Decidua.* Front Immunol, 2019. **10**: p. 170.
106. Filipovic, I., et al., *Molecular definition of group 1 innate lymphoid cells in the mouse uterus.* Nat Commun, 2018. **9**(1): p. 4492.
107. Li, M., et al., *Molecular signature and functional analysis of uterine ILCs in mouse pregnancy.* J Reprod Immunol, 2017. **123**: p. 48-57.
108. Bando, J.K., H.E. Liang, and R.M. Locksley, *Identification and distribution of developing innate lymphoid cells in the fetal mouse intestine.* Nat Immunol, 2015. **16**(2): p. 153-60.
109. Scoville, S.D., et al., *A Progenitor Cell Expressing Transcription Factor RORgammat Generates All Human Innate Lymphoid Cell Subsets.* Immunity, 2016. **44**(5): p. 1140-50.
110. Garcia, M., et al., *Innate lymphoid cell composition associates with COVID-19 disease severity.* Clin Transl Immunology, 2020. **9**(12): p. e1224.
111. Wang, H., et al., *Adipose group 1 innate lymphoid cells promote adipose tissue fibrosis and diabetes in obesity.* Nat Commun, 2019. **10**(1): p. 3254.
112. Doisne, J.M., et al., *Composition, Development, and Function of Uterine Innate Lymphoid Cells.* J Immunol, 2015. **195**(8): p. 3937-45.
113. Montaldo, E., et al., *Unique Eomes(+) NK Cell Subsets Are Present in Uterus and Decidua During Early Pregnancy.* Front Immunol, 2015. **6**: p. 646.
114. Fuchs, A., et al., *Intraepithelial type 1 innate lymphoid cells are a unique subset of IL-12- and IL-15-responsive IFN-gamma-producing cells.* Immunity, 2013. **38**(4): p. 769-81.
115. Riedel, J.H., et al., *IL-33-Mediated Expansion of Type 2 Innate Lymphoid Cells Protects from Progressive Glomerulosclerosis.* J Am Soc Nephrol, 2017. **28**(7): p. 2068-2080.
116. Yudanin, N.A., et al., *Spatial and Temporal Mapping of Human Innate Lymphoid Cells Reveals Elements of Tissue Specificity.* Immunity, 2019. **50**(2): p. 505-519 e4.
117. Vashist, N., et al., *Influenza-Activated ILC1s Contribute to Antiviral Immunity Partially Influenced by Differential GITR Expression.* Front Immunol, 2018. **9**: p. 505.
118. Ardain, A., et al., *Group 3 innate lymphoid cells mediate early protective immunity against tuberculosis.* Nature, 2019. **570**(7762): p. 528-532.
119. Picarda, G., et al., *Cytomegalovirus Evades TRAIL-Mediated Innate Lymphoid Cell 1 Defenses.* J Virol, 2019. **93**(16).
120. Weizman, O.E., et al., *Mouse cytomegalovirus-experienced ILC1s acquire a memory response dependent on the viral glycoprotein m12.* Nat Immunol, 2019. **20**(8): p. 1004-1011.
121. Gury-BenAri, M., et al., *The Spectrum and Regulatory Landscape of Intestinal Innate Lymphoid Cells Are Shaped by the Microbiome.* Cell, 2016. **166**(5): p. 1231-1246 e13.
122. Glover, M., et al., *Trickle infection and immunity to Trichuris muris.* PLoS Pathog, 2019. **15**(11): p. e1007926.
123. Fachi, J.L., et al., *Acetate coordinates neutrophil and ILC3 responses against C. difficile through FFAR2.* J Exp Med, 2020. **217**(3).
124. Weizman, O.E., et al., *ILC1 Confer Early Host Protection at Initial Sites of Viral Infection.* Cell, 2017. **171**(4): p. 795-808 e12.
125. Park, E., et al., *Toxoplasma gondii infection drives conversion of NK cells into ILC1-like cells.* Elife, 2019. **8**.

126. Bianca Bennstein, S., et al., *OMIP-055: Characterization of Human Innate Lymphoid Cells from Neonatal and Peripheral Blood.* Cytometry A, 2019. **95**(4): p. 427-430.
127. Vely, F., et al., *Evidence of innate lymphoid cell redundancy in humans.* Nat Immunol, 2016. **17**(11): p. 1291-1299.
128. Vacca, P., et al., *Identification of diverse innate lymphoid cells in human decidua.* Mucosal Immunol, 2015. **8**(2): p. 254-64.
129. Xu, Y., et al., *Innate lymphoid cells at the human maternal-fetal interface in spontaneous preterm labor.* Am J Reprod Immunol, 2018. **79**(6): p. e12820.
130. Bracamonte-Baran, W., et al., *Non-cytotoxic Cardiac Innate Lymphoid Cells Are a Resident and Quiescent Type 2-Commited Population.* Front Immunol, 2019. **10**: p. 634.
131. Forkel, M., et al., *Composition and functionality of the intrahepatic innate lymphoid cell-compartment in human nonfibrotic and fibrotic livers.* Eur J Immunol, 2017. **47**(8): p. 1280-1294.
132. Maertzdorf, J., et al., *Mycobacterium tuberculosis Invasion of the Human Lung: First Contact.* Front Immunol, 2018. **9**: p. 1346.
133. Bernink, J.H., et al., *Interleukin-12 and -23 Control Plasticity of CD127(+) Group 1 and Group 3 Innate Lymphoid Cells in the Intestinal Lamina Propria.* Immunity, 2015. **43**(1): p. 146-60.
134. Audia, S., et al., *Altered distribution and function of splenic innate lymphoid cells in adult chronic immune thrombocytopenia.* J Autoimmun, 2018. **93**: p. 139-144.
135. Bernink, J.H., et al., *Human type 1 innate lymphoid cells accumulate in inflamed mucosal tissues.* Nat Immunol, 2013. **14**(3): p. 221-9.
136. Li, N., et al., *Mass cytometry reveals innate lymphoid cell differentiation pathways in the human fetal intestine.* J Exp Med, 2018. **215**(5): p. 1383-1396.
137. Bruggen, M.C., et al., *In Situ Mapping of Innate Lymphoid Cells in Human Skin: Evidence for Remarkable Differences between Normal and Inflamed Skin.* J Invest Dermatol, 2016. **136**(12): p. 2396-2405.
138. Cella, M., et al., *Subsets of ILC3-ILC1-like cells generate a diversity spectrum of innate lymphoid cells in human mucosal tissues.* Nat Immunol, 2019. **20**(8): p. 980-991.
139. Miller, M.M., et al., *BATF acts as an essential regulator of IL-25-responsive migratory ILC2 cell fate and function.* Sci Immunol, 2020. **5**(43).
140. Huang, Y., et al., *IL-25-responsive, lineage-negative KLRG1(hi) cells are multipotential 'inflammatory' type 2 innate lymphoid cells.* Nat Immunol, 2015. **16**(2): p. 161-9.
141. Entwistle, L.J., et al., *Pulmonary Group 2 Innate Lymphoid Cell Phenotype Is Context Specific: Determining the Effect of Strain, Location, and Stimuli.* Frontiers in Immunology, 2020. **10**.
142. Monticelli, L.A., et al., *Innate lymphoid cells promote lung-tissue homeostasis after infection with influenza virus.* Nat Immunol, 2011. **12**(11): p. 1045-54.
143. Bartemes, K., et al., *IL-33-Responsive Group 2 Innate Lymphoid Cells Are Regulated by Female Sex Hormones in the Uterus.* J Immunol, 2018. **200**(1): p. 229-236.
144. Mjosberg, J.M., et al., *Human IL-25- and IL-33-responsive type 2 innate lymphoid cells are defined by expression of CRTH2 and CD161.* Nat Immunol, 2011. **12**(11): p. 1055-62.
145. Spits, H., et al., *Innate lymphoid cells--a proposal for uniform nomenclature.* Nat Rev Immunol, 2013. **13**(2): p. 145-9.
146. Powell, N., et al., *The transcription factor T-bet regulates intestinal inflammation mediated by interleukin-7 receptor+ innate lymphoid cells.* Immunity, 2012. **37**(4): p. 674-84.
147. Buonocore, S., et al., *Innate lymphoid cells drive interleukin-23-dependent innate intestinal pathology.* Nature, 2010. **464**(7293): p. 1371-5.
148. Boulenouar, S., et al., *Adipose Type One Innate Lymphoid Cells Regulate Macrophage Homeostasis through Targeted Cytotoxicity.* Immunity, 2017. **46**(2): p. 273-286.
149. Kim, H.Y., et al., *Interleukin-17-producing innate lymphoid cells and the NLRP3 inflammasome facilitate obesity-associated airway hyperreactivity.* Nat Med, 2014. **20**(1): p. 54-61.

150. Villanova, F., et al., *Characterization of innate lymphoid cells in human skin and blood demonstrates increase of NKp44+ ILC3 in psoriasis.* J Invest Dermatol, 2014. **134**(4): p. 984-991.
151. Bielecki, P., et al., *Skin-resident innate lymphoid cells converge on a pathogenic effector state.* Nature, 2021.
152. Wang, S., et al., *Regulatory Innate Lymphoid Cells Control Innate Intestinal Inflammation.* Cell, 2017. **171**(1): p. 201-216 e18.
153. Zeng, B., et al., *ILC3 function as a double-edged sword in inflammatory bowel diseases.* Cell Death Dis, 2019. **10**(4): p. 315.
154. Brestoff, J.R., et al., *Group 2 innate lymphoid cells promote beiging of white adipose tissue and limit obesity.* Nature, 2015. **519**(7542): p. 242-6.
155. Hams, E., et al., *Cutting edge: IL-25 elicits innate lymphoid type 2 and type II NKT cells that regulate obesity in mice.* J Immunol, 2013. **191**(11): p. 5349-53.
156. Lee, M.W., et al., *Activated type 2 innate lymphoid cells regulate beige fat biogenesis.* Cell, 2015. **160**(1-2): p. 74-87.
157. Wilhelm, C., et al., *Critical role of fatty acid metabolism in ILC2-mediated barrier protection during malnutrition and helminth infection.* J Exp Med, 2016. **213**(8): p. 1409-18.
158. Neill, D.R., et al., *Nuocytes represent a new innate effector leukocyte that mediates type-2 immunity.* Nature, 2010. **464**(7293): p. 1367-70.
159. Saluzzo, S., et al., *First-Breath-Induced Type 2 Pathways Shape the Lung Immune Environment.* Cell Rep, 2017. **18**(8): p. 1893-1905.
160. Price, A.E., et al., *Systemically dispersed innate IL-13-expressing cells in type 2 immunity.* Proc Natl Acad Sci U S A, 2010. **107**(25): p. 11489-94.
161. Molofsky, A.B., et al., *Interleukin-33 and Interferon-gamma Counter-Regulate Group 2 Innate Lymphoid Cell Activation during Immune Perturbation.* Immunity, 2015. **43**(1): p. 161-74.
162. Ricardo-Gonzalez, R.R., et al., *Tissue-specific pathways extrude activated ILC2s to disseminate type 2 immunity.* J Exp Med, 2020. **217**(4).
163. Boyd, A., et al., *Pleural cavity type 2 innate lymphoid cells precede Th2 expansion in murine Litomosoides sigmodontis infection.* Exp Parasitol, 2015. **159**: p. 118-26.
164. Hams, E., et al., *IL-25 and type 2 innate lymphoid cells induce pulmonary fibrosis.* Proc Natl Acad Sci U S A, 2014. **111**(1): p. 367-72.
165. Chang, Y.J., et al., *Innate lymphoid cells mediate influenza-induced airway hyper-reactivity independently of adaptive immunity.* Nat Immunol, 2011. **12**(7): p. 631-8.
166. Gorski, S.A., Y.S. Hahn, and T.J. Braciale, *Group 2 innate lymphoid cell production of IL-5 is regulated by NKT cells during influenza virus infection.* PLoS Pathog, 2013. **9**(9): p. e1003615.
167. Krishack, P.A., et al., *Protection against Staphylococcus aureus bacteremia-induced mortality depends on ILC2s and eosinophils.* JCI Insight, 2019. **4**(6).
168. Spencer, S.P., et al., *Adaptation of innate lymphoid cells to a micronutrient deficiency promotes type 2 barrier immunity.* Science, 2014. **343**(6169): p. 432-7.
169. Oliphant, C.J., et al., *MHCII-mediated dialog between group 2 innate lymphoid cells and CD4(+) T cells potentiates type 2 immunity and promotes parasitic helminth expulsion.* Immunity, 2014. **41**(2): p. 283-95.
170. Chun, T.T., et al., *Group 2 Innate Lymphoid Cells (ILC2s) Are Key Mediators of the Inflammatory Response in Polymicrobial Sepsis.* Am J Pathol, 2018. **188**(9): p. 2097-2108.
171. Frascoli, M., et al., *Heightened Immune Activation in Fetuses with Gastroschisis May Be Blocked by Targeting IL-5.* J Immunol, 2016. **196**(12): p. 4957-66.
172. Ricardo-Gonzalez, R.R., et al., *Tissue signals imprint ILC2 identity with anticipatory function.* Nat Immunol, 2018. **19**(10): p. 1093-1099.
173. Huang, Y., et al., *S1P-dependent interorgan trafficking of group 2 innate lymphoid cells supports host defense.* Science, 2018. **359**(6371): p. 114-119.
174. Pelly, V.S., et al., *IL-4-producing ILC2s are required for the differentiation of TH2 cells following Heligmosomoides polygyrus infection.* Mucosal Immunol, 2016. **9**(6): p. 1407-1417.

175. Shimokawa, C., et al., *Mast Cells Are Crucial for Induction of Group 2 Innate Lymphoid Cells and Clearance of Helminth Infections.* Immunity, 2017. **46**(5): p. 863-874 e4.
176. von Moltke, J., et al., *Tuft-cell-derived IL-25 regulates an intestinal ILC2-epithelial response circuit.* Nature, 2016. **529**(7585): p. 221-5.
177. Howitt, M.R., et al., *Tuft cells, taste-chemosensory cells, orchestrate parasite type 2 immunity in the gut.* Science, 2016. **351**(6279): p. 1329-33.
178. Simoni, Y., et al., *Human Innate Lymphoid Cell Subsets Possess Tissue-Type Based Heterogeneity in Phenotype and Frequency.* Immunity, 2018. **48**(5): p. 1060.
179. De Grove, K.C., et al., *Characterization and Quantification of Innate Lymphoid Cell Subsets in Human Lung.* PLoS One, 2016. **11**(1): p. e0145961.
180. Kramer, B., et al., *Compartment-specific distribution of human intestinal innate lymphoid cells is altered in HIV patients under effective therapy.* PLoS Pathog, 2017. **13**(5): p. e1006373.
181. Gomez-Cadena, A., et al., *Severe COVID-19 patients exhibit an ILC2 NKG2D(+) population in their impaired ILC compartment.* Cell Mol Immunol, 2020.
182. Salimi, M., et al., *A role for IL-25 and IL-33-driven type-2 innate lymphoid cells in atopic dermatitis.* J Exp Med, 2013. **210**(13): p. 2939-50.
183. Teunissen, M.B.M., et al., *Composition of innate lymphoid cell subsets in the human skin: enrichment of NCR(+) ILC3 in lesional skin and blood of psoriasis patients.* J Invest Dermatol, 2014. **134**(9): p. 2351-2360.
184. Hernandez, P.P., et al., *Interferon-lambda and interleukin 22 act synergistically for the induction of interferon-stimulated genes and control of rotavirus infection.* Nat Immunol, 2015. **16**(7): p. 698-707.
185. Zou, M., et al., *Acute neonatal Listeria monocytogenes infection causes long-term, organ-specific changes in immune cell subset composition.* Eur J Microbiol Immunol (Bp), 2020.
186. Lin, Y.D., et al., *Vitamin D Is Required for ILC3 Derived IL-22 and Protection From Citrobacter rodentium Infection.* Front Immunol, 2019. **10**: p. 1.
187. Wang, B., et al., *Macrophage beta2-Integrins Regulate IL-22 by ILC3s and Protect from Lethal Citrobacter rodentium-Induced Colitis.* Cell Rep, 2019. **26**(6): p. 1614-1626 e5.
188. Reynders, A., et al., *Identity, regulation and in vivo function of gut NKp46+RORgammat+ and NKp46+RORgammat- lymphoid cells.* EMBO J, 2011. **30**(14): p. 2934-47.
189. Van Maele, L., et al., *Activation of Type 3 innate lymphoid cells and interleukin 22 secretion in the lungs during Streptococcus pneumoniae infection.* J Infect Dis, 2014. **210**(3): p. 493-503.
190. Guo, X., et al., *Induction of innate lymphoid cell-derived interleukin-22 by the transcription factor STAT3 mediates protection against intestinal infection.* Immunity, 2014. **40**(1): p. 25-39.
191. Rankin, L.C., et al., *Complementarity and redundancy of IL-22-producing innate lymphoid cells.* Nat Immunol, 2016. **17**(2): p. 179-86.
192. Gladiator, A., et al., *Cutting edge: IL-17-secreting innate lymphoid cells are essential for host defense against fungal infection.* J Immunol, 2013. **190**(2): p. 521-5.
193. Abt, M.C., et al., *Innate Immune Defenses Mediated by Two ILC Subsets Are Critical for Protection against Acute Clostridium difficile Infection.* Cell Host Microbe, 2015. **18**(1): p. 27-37.
194. Seo, G.Y., et al., *LIGHT-HVEM Signaling in Innate Lymphoid Cell Subsets Protects Against Enteric Bacterial Infection.* Cell Host Microbe, 2018. **24**(2): p. 249-260 e4.
195. Dulson, S.J., et al., *STAT4 Directs a Protective Innate Lymphoid Cell Response to Gastrointestinal Infection.* J Immunol, 2019. **203**(9): p. 2472-2484.
196. Chu, C., et al., *Anti-microbial Functions of Group 3 Innate Lymphoid Cells in Gut-Associated Lymphoid Tissues Are Regulated by G-Protein-Coupled Receptor 183.* Cell Rep, 2018. **23**(13): p. 3750-3758.
197. Bostick, J.W., et al., *Dichotomous regulation of group 3 innate lymphoid cells by nongastric Helicobacter species.* Proc Natl Acad Sci U S A, 2019. **116**(49): p. 24760-24769.

198. Melo-Gonzalez, F., et al., *Antigen-presenting ILC3 regulate T cell-dependent IgA responses to colonic mucosal bacteria.* J Exp Med, 2019. **216**(4): p. 728-742.
199. von Burg, N., et al., *Activated group 3 innate lymphoid cells promote T-cell-mediated immune responses.* Proc Natl Acad Sci U S A, 2014. **111**(35): p. 12835-40.
200. Croxatto, D., et al., *Group 3 innate lymphoid cells regulate neutrophil migration and function in human decidua.* Mucosal Immunol, 2016. **9**(6): p. 1372-1383.
201. Marquardt, N., et al., *Fetal CD103+ IL-17-Producing Group 3 Innate Lymphoid Cells Represent the Dominant Lymphocyte Subset in Human Amniotic Fluid.* J Immunol, 2016. **197**(8): p. 3069-3075.
202. Bar-Ephraim, Y.E., et al., *Cross-Tissue Transcriptomic Analysis of Human Secondary Lymphoid Organ-Residing ILC3s Reveals a Quiescent State in the Absence of Inflammation.* Cell Rep, 2017. **21**(3): p. 823-833.
203. Hoorweg, K., et al., *Functional Differences between Human NKp44(-) and NKp44(+) RORC(+) Innate Lymphoid Cells.* Front Immunol, 2012. **3**: p. 72.
204. Bal, S.M., K. Golebski, and H. Spits, *Plasticity of innate lymphoid cell subsets.* Nat Rev Immunol, 2020.
205. Koh, J., et al., *IL23-Producing Human Lung Cancer Cells Promote Tumor Growth via Conversion of Innate Lymphoid Cell 1 (ILC1) into ILC3.* Clin Cancer Res, 2019. **25**(13): p. 4026-4037.
206. Gao, Y., et al., *Tumor immunoevasion by the conversion of effector NK cells into type 1 innate lymphoid cells.* Nat Immunol, 2017. **18**(9): p. 1004-1015.
207. Cortez, V.S., et al., *SMAD4 impedes the conversion of NK cells into ILC1-like cells by curtailing non-canonical TGF-beta signaling.* Nat Immunol, 2017. **18**(9): p. 995-1003.
208. Ohne, Y., et al., *IL-1 is a critical regulator of group 2 innate lymphoid cell function and plasticity.* Nat Immunol, 2016. **17**(6): p. 646-55.
209. Bal, S.M., et al., *IL-1beta, IL-4 and IL-12 control the fate of group 2 innate lymphoid cells in human airway inflammation in the lungs.* Nat Immunol, 2016. **17**(6): p. 636-45.
210. Silver, J.S., et al., *Inflammatory triggers associated with exacerbations of COPD orchestrate plasticity of group 2 innate lymphoid cells in the lungs.* Nat Immunol, 2016. **17**(6): p. 626-35.
211. Zhang, K., et al., *Cutting Edge: Notch Signaling Promotes the Plasticity of Group-2 Innate Lymphoid Cells.* J Immunol, 2017. **198**(5): p. 1798-1803.
212. Cai, T., et al., *IL-17-producing ST2(+) group 2 innate lymphoid cells play a pathogenic role in lung inflammation.* J Allergy Clin Immunol, 2019. **143**(1): p. 229-244 e9.
213. Bernink, J.H., et al., *c-Kit-positive ILC2s exhibit an ILC3-like signature that may contribute to IL-17-mediated pathologies.* Nat Immunol, 2019. **20**(8): p. 992-1003.
214. Vonarbourg, C., et al., *Regulated expression of nuclear receptor RORgammat confers distinct functional fates to NK cell receptor-expressing RORgammat(+) innate lymphocytes.* Immunity, 2010. **33**(5): p. 736-51.
215. Li, J., et al., *Enrichment of IL-17A(+) IFN-gamma(+) and IL-22(+) IFN-gamma(+) T cell subsets is associated with reduction of NKp44(+) ILC3s in the terminal ileum of Crohn's disease patients.* Clin Exp Immunol, 2017. **190**(1): p. 143-153.
216. Califano, D., et al., *Transcription Factor Bcl11b Controls Identity and Function of Mature Type 2 Innate Lymphoid Cells.* Immunity, 2015. **43**(2): p. 354-68.
217. Ebbo, M., et al., *Innate lymphoid cells: major players in inflammatory diseases.* Nat Rev Immunol, 2017.
218. Kvestak, D., et al., *NK/ILC1 cells mediate neuroinflammation and brain pathology following congenital CMV infection.* J Exp Med, 2021. **218**(5).
219. Castleman, M.J., et al., *Enteric bacteria induce IFNgamma and Granzyme B from human colonic Group 1 Innate Lymphoid Cells.* Gut Microbes, 2019: p. 1-17.
220. Klose, C.S. and D. Artis, *Innate lymphoid cells as regulators of immunity, inflammation and tissue homeostasis.* Nat Immunol, 2016. **17**(7): p. 765-74.

221. McKenzie, G.J., et al., *A distinct role for interleukin-13 in Th2-cell-mediated immune responses.* Current Biology, 1998. **8**(6): p. 339-342.
222. Chu, C., et al., *The ChAT-acetylcholine pathway promotes group 2 innate lymphoid cell responses and anti-helminth immunity.* Sci Immunol, 2021. **6**(57).
223. Roberts, L.B., et al., *Acetylcholine production by group 2 innate lymphoid cells promotes mucosal immunity to helminths.* Sci Immunol, 2021. **6**(57).
224. Besnard, A.G., et al., *IL-33-mediated protection against experimental cerebral malaria is linked to induction of type 2 innate lymphoid cells, M2 macrophages and regulatory T cells.* PLoS Pathog, 2015. **11**(2): p. e1004607.
225. Han, M., et al., *IL-1beta prevents ILC2 expansion, type 2 cytokine secretion and mucus metaplasia in response to early-life rhinovirus infection in mice.* Allergy, 2020.
226. Campbell, L., et al., *ILC2s mediate systemic innate protection by priming mucus production at distal mucosal sites.* J Exp Med, 2019. **216**(12): p. 2714-2723.
227. Carvelli, J., et al., *Imbalance of Circulating Innate Lymphoid Cell Subpopulations in Patients With Septic Shock.* Front Immunol, 2019. **10**: p. 2179.
228. Nausch, N. and F. Mutapi, *Group 2 ILCs: A way of enhancing immune protection against human helminths?* Parasite Immunol, 2018. **40**(2).
229. Loser, S., K.A. Smith, and R.M. Maizels, *Innate Lymphoid Cells in Helminth Infections-Obligatory or Accessory?* Front Immunol, 2019. **10**: p. 620.
230. Filbey, K., T. Bouchery, and G. Le Gros, *The role of ILC2 in hookworm infection.* Parasite Immunol, 2018. **40**(2).
231. Turner, J.E., et al., *IL-9-mediated survival of type 2 innate lymphoid cells promotes damage control in helminth-induced lung inflammation.* J Exp Med, 2013. **210**(13): p. 2951-65.
232. Allen, J.E. and T.E. Sutherland, *Host protective roles of type 2 immunity: parasite killing and tissue repair, flip sides of the same coin.* Semin Immunol, 2014. **26**(4): p. 329-40.
233. Paclik, D., et al., *ICOS regulates the pool of group 2 innate lymphoid cells under homeostatic and inflammatory conditions in mice.* Eur J Immunol, 2015. **45**(10): p. 2766-72.
234. Maazi, H., et al., *ICOS:ICOS-ligand interaction is required for type 2 innate lymphoid cell function, homeostasis, and induction of airway hyperreactivity.* Immunity, 2015. **42**(3): p. 538-51.
235. Mallett, G., A. Laurence, and S. Amarnath, *Programmed Cell Death-1 Receptor (PD-1)-Mediated Regulation of Innate Lymphoid Cells.* Int J Mol Sci, 2019. **20**(11).
236. Taylor, S., et al., *PD-1 regulates KLRG1(+) group 2 innate lymphoid cells.* J Exp Med, 2017. **214**(6): p. 1663-1678.
237. Schwartz, C., et al., *ILC2s regulate adaptive Th2 cell functions via PD-L1 checkpoint control.* J Exp Med, 2017. **214**(9): p. 2507-2521.
238. Halim, T.Y., et al., *Group 2 innate lymphoid cells license dendritic cells to potentiate memory TH2 cell responses.* Nat Immunol, 2016. **17**(1): p. 57-64.
239. Li, D., et al., *IL-33 promotes ST2-dependent lung fibrosis by the induction of alternatively activated macrophages and innate lymphoid cells in mice.* J Allergy Clin Immunol, 2014. **134**(6): p. 1422-1432 e11.
240. Mohapatra, A., et al., *Group 2 innate lymphoid cells utilize the IRF4-IL-9 module to coordinate epithelial cell maintenance of lung homeostasis.* Mucosal Immunol, 2016. **9**(1): p. 275-86.
241. Motomura, Y., et al., *Basophil-derived interleukin-4 controls the function of natural helper cells, a member of ILC2s, in lung inflammation.* Immunity, 2014. **40**(5): p. 758-71.
242. Barnig, C., et al., *Lipoxin A4 regulates natural killer cell and type 2 innate lymphoid cell activation in asthma.* Sci Transl Med, 2013. **5**(174): p. 174ra26.
243. Taube, C., et al., *IL-22 is produced by innate lymphoid cells and limits inflammation in allergic airway disease.* PLoS One, 2011. **6**(7): p. e21799.
244. Takatori, H., et al., *Regulatory Mechanisms of IL-33-ST2-Mediated Allergic Inflammation.* Front Immunol, 2018. **9**: p. 2004.

245. Besnard, A.G., et al., *IL-33-activated dendritic cells are critical for allergic airway inflammation.* Eur J Immunol, 2011. **41**(6): p. 1675-86.
246. Hsu, C.L., C.V. Neilsen, and P.J. Bryce, *IL-33 is produced by mast cells and regulates IgE-dependent inflammation.* PLoS One, 2010. **5**(8): p. e11944.
247. Wilhelm, C., et al., *An IL-9 fate reporter demonstrates the induction of an innate IL-9 response in lung inflammation.* Nat Immunol, 2011. **12**(11): p. 1071-7.
248. Sonnenberg, G.F., et al., *Innate lymphoid cells promote anatomical containment of lymphoid-resident commensal bacteria.* Science, 2012. **336**(6086): p. 1321-5.
249. Zhou, L., et al., *Innate lymphoid cells support regulatory T cells in the intestine through interleukin-2.* Nature, 2019. **568**(7752): p. 405-409.
250. Castellanos, J.G., et al., *Microbiota-Induced TNF-like Ligand 1A Drives Group 3 Innate Lymphoid Cell-Mediated Barrier Protection and Intestinal T Cell Activation during Colitis.* Immunity, 2018. **49**(6): p. 1077-1089 e5.
251. Penny, H.A., S.H. Hodge, and M.R. Hepworth, *Orchestration of intestinal homeostasis and tolerance by group 3 innate lymphoid cells.* Semin Immunopathol, 2018. **40**(4): p. 357-370.
252. Magri, G., et al., *Innate lymphoid cells integrate stromal and immunological signals to enhance antibody production by splenic marginal zone B cells.* Nat Immunol, 2014. **15**(4): p. 354-364.
253. Robinette, M.L. and M. Colonna, *Innate lymphoid cells and the MHC.* HLA, 2016. **87**(1): p. 5-11.
254. Salimi, M., et al., *Activated innate lymphoid cell populations accumulate in human tumour tissues.* BMC Cancer, 2018. **18**(1): p. 341.
255. Puissant, B. and B. Combadiere, *Keeping the memory of smallpox virus.* Cell Mol Life Sci, 2006. **63**(19-20): p. 2249-59.
256. Kurosaki, T., K. Kometani, and W. Ise, *Memory B cells.* Nat Rev Immunol, 2015. **15**(3): p. 149-59.
257. Sticher, L., B. Mauch-Mani, and J.P. Metraux, *Systemic acquired resistance.* Annu Rev Phytopathol, 1997. **35**: p. 235-70.
258. Kurtz, J. and K. Franz, *Innate defence: evidence for memory in invertebrate immunity.* Nature, 2003. **425**(6953): p. 37-8.
259. Bistoni, F., et al., *Evidence for macrophage-mediated protection against lethal Candida albicans infection.* Infect Immun, 1986. **51**(2): p. 668-74.
260. Quintin, J., et al., *Candida albicans infection affords protection against reinfection via functional reprogramming of monocytes.* Cell Host Microbe, 2012. **12**(2): p. 223-32.
261. Netea, M.G., et al., *Trained immunity: A program of innate immune memory in health and disease.* Science, 2016. **352**(6284): p. aaf1098.
262. Kleinnijenhuis, J., et al., *Bacille Calmette-Guerin induces NOD2-dependent nonspecific protection from reinfection via epigenetic reprogramming of monocytes.* Proc Natl Acad Sci U S A, 2012. **109**(43): p. 17537-42.
263. Roth, A., et al., *BCG vaccination scar associated with better childhood survival in Guinea-Bissau.* Int J Epidemiol, 2005. **34**(3): p. 540-7.
264. Aaby, P., et al., *Randomized trial of BCG vaccination at birth to low-birth-weight children: beneficial nonspecific effects in the neonatal period?* J Infect Dis, 2011. **204**(2): p. 245-52.
265. Garly, M.L., et al., *BCG scar and positive tuberculin reaction associated with reduced child mortality in West Africa. A non-specific beneficial effect of BCG?* Vaccine, 2003. **21**(21-22): p. 2782-90.
266. Blok, B.A., et al., *Trained innate immunity as underlying mechanism for the long-term, nonspecific effects of vaccines.* J Leukoc Biol, 2015. **98**(3): p. 347-56.
267. Netea, M.G., J. Quintin, and J.W. van der Meer, *Trained immunity: a memory for innate host defense.* Cell Host Microbe, 2011. **9**(5): p. 355-61.
268. Kaufmann, E., et al., *BCG Educates Hematopoietic Stem Cells to Generate Protective Innate Immunity against Tuberculosis.* Cell, 2018. **172**(1-2): p. 176-190 e19.

269. Mitroulis, I., et al., *Modulation of Myelopoiesis Progenitors Is an Integral Component of Trained Immunity.* Cell, 2018. **172**(1-2): p. 147-161 e12.
270. Ferreira, A.V., J. Domiguez-Andres, and M.G. Netea, *The Role of Cell Metabolism in Innate Immune Memory.* J Innate Immun, 2020: p. 1-9.
271. Ifrim, D.C., et al., *Trained immunity or tolerance: opposing functional programs induced in human monocytes after engagement of various pattern recognition receptors.* Clin Vaccine Immunol, 2014. **21**(4): p. 534-45.
272. Yoshida, K., et al., *The transcription factor ATF7 mediates lipopolysaccharide-induced epigenetic changes in macrophages involved in innate immunological memory.* Nat Immunol, 2015. **16**(10): p. 1034-43.
273. Yao, Y., et al., *Induction of Autonomous Memory Alveolar Macrophages Requires T Cell Help and Is Critical to Trained Immunity.* Cell, 2018. **175**(6): p. 1634-1650 e17.
274. Cheng, S.C., et al., *mTOR- and HIF-1alpha-mediated aerobic glycolysis as metabolic basis for trained immunity.* Science, 2014. **345**(6204): p. 1250684.
275. Ciarlo, E., et al., *Trained immunity confers broad-spectrum protection against bacterial infections.* J Infect Dis, 2019.
276. Di Luzio, N.R. and D.L. Williams, *Protective effect of glucan against systemic Staphylococcus aureus septicemia in normal and leukemic mice.* Infect Immun, 1978. **20**(3): p. 804-10.
277. Marakalala, M.J., et al., *Dectin-1 plays a redundant role in the immunomodulatory activities of beta-glucan-rich ligands in vivo.* Microbes Infect, 2013. **15**(6-7): p. 511-5.
278. Dos Santos, J.C., et al., *beta-Glucan-Induced Trained Immunity Protects against Leishmania braziliensis Infection: a Crucial Role for IL-32.* Cell Rep, 2019. **28**(10): p. 2659-2672 e6.
279. Rizzetto, L., et al., *Fungal Chitin Induces Trained Immunity in Human Monocytes during Cross-talk of the Host with Saccharomyces cerevisiae.* J Biol Chem, 2016. **291**(15): p. 7961-72.
280. Klinman, D.M., J. Conover, and C. Coban, *Repeated administration of synthetic oligodeoxynucleotides expressing CpG motifs provides long-term protection against bacterial infection.* Infect Immun, 1999. **67**(11): p. 5658-63.
281. Ribes, S., et al., *Intraperitoneal prophylaxis with CpG oligodeoxynucleotides protects neutropenic mice against intracerebral Escherichia coli K1 infection.* J Neuroinflammation, 2014. **11**: p. 14.
282. Airhart, C.L., et al., *Induction of innate immunity by lipid A mimetics increases survival from pneumonic plague.* Microbiology, 2008. **154**(Pt 7): p. 2131-2138.
283. Bessede, A., et al., *Aryl hydrocarbon receptor control of a disease tolerance defence pathway.* Nature, 2014. **511**(7508): p. 184-90.
284. de Laval, B., et al., *C/EBPbeta-Dependent Epigenetic Memory Induces Trained Immunity in Hematopoietic Stem Cells.* Cell Stem Cell, 2020. **26**(5): p. 657-674 e8.
285. Schaafsma, W., et al., *Long-lasting pro-inflammatory suppression of microglia by LPS-preconditioning is mediated by RelB-dependent epigenetic silencing.* Brain Behav Immun, 2015. **48**: p. 205-21.
286. Roquilly, A., et al., *Toll-like receptor-4 agonist in post-haemorrhage pneumonia: role of dendritic and natural killer cells.* Eur Respir J, 2013. **42**(5): p. 1365-78.
287. Bigot, J., et al., *Respiratory Epithelial Cells Can Remember Infection: A Proof-of-Concept Study.* J Infect Dis, 2020. **221**(6): p. 1000-1005.
288. Vijay-Kumar, M., et al., *Flagellin treatment protects against chemicals, bacteria, viruses, and radiation.* J Immunol, 2008. **180**(12): p. 8280-5.
289. Zhang, B., et al., *Viral infection. Prevention and cure of rotavirus infection via TLR5/NLRC4-mediated production of IL-22 and IL-18.* Science, 2014. **346**(6211): p. 861-5.
290. Matsumoto, S., et al., *Mycobacterium bovis bacillus calmette-guerin induces protective immunity against infection by Plasmodium yoelii at blood-stage depending on shifting immunity toward Th1 type and inducing protective IgG2a after the parasite infection.* Vaccine, 2000. **19**(7-8): p. 779-87.

291. Arts, R.J.W., et al., *BCG Vaccination Protects against Experimental Viral Infection in Humans through the Induction of Cytokines Associated with Trained Immunity.* Cell Host Microbe, 2018. **23**(1): p. 89-100 e5.
292. Kleinnijenhuis, J., et al., *BCG-induced trained immunity in NK cells: Role for non-specific protection to infection.* Clin Immunol, 2014. **155**(2): p. 213-9.
293. Schnack, L., et al., *Mechanisms of Trained Innate Immunity in oxLDL Primed Human Coronary Smooth Muscle Cells.* Front Immunol, 2019. **10**: p. 13.
294. Scaringi, L., et al., *Antibody-independent protection in mice against type Ia group B streptococcus lethal infection.* FEMS Immunol Med Microbiol, 1994. **9**(2): p. 151-62.
295. Gumenscheimer, M., et al., *Beneficial or deleterious effects of a preexisting hypersensitivity to bacterial components on the course and outcome of infection.* Infect Immun, 2002. **70**(10): p. 5596-603.
296. Mear, J.B., et al., *Candida albicans airway exposure primes the lung innate immune response against Pseudomonas aeruginosa infection through innate lymphoid cell recruitment and interleukin-22-associated mucosal response.* Infect Immun, 2014. **82**(1): p. 306-15.
297. Barton, E.S., et al., *Herpesvirus latency confers symbiotic protection from bacterial infection.* Nature, 2007. **447**(7142): p. 326-9.
298. Li, T., et al., *Respiratory Influenza Virus Infection Induces Memory-like Liver NK Cells in Mice.* J Immunol, 2017. **198**(3): p. 1242-1252.
299. Gabryszewski, S.J., et al., *Lactobacillus-mediated priming of the respiratory mucosa protects against lethal pneumovirus infection.* J Immunol, 2011. **186**(2): p. 1151-61.
300. Yasuda, K., et al., *Nematode-Infected Mice Acquire Resistance to Subsequent Infection With Unrelated Nematode by Inducing Highly Responsive Group 2 Innate Lymphoid Cells in the Lung.* Front Immunol, 2018. **9**: p. 2132.
301. Chan, L.C., et al., *Innate Immune Memory Contributes to Host Defense against Recurrent Skin and Skin Structure Infections Caused by Methicillin-Resistant Staphylococcus aureus.* Infect Immun, 2017. **85**(2).
302. Gillard, G.O., et al., *Thy1+ NK [corrected] cells from vaccinia virus-primed mice confer protection against vaccinia virus challenge in the absence of adaptive lymphocytes.* PLoS Pathog, 2011. **7**(8): p. e1002141.
303. Owens, B.M., et al., *CD90(+) Stromal Cells are Non-Professional Innate Immune Effectors of the Human Colonic Mucosa.* Front Immunol, 2013. **4**: p. 307.
304. Krahenbuhl, J.L., et al., *Effects of muramyl dipeptide treatment on resistance to infection with Toxoplasma gondii in mice.* Infect Immun, 1981. **31**(2): p. 716-22.
305. Naik, S., et al., *Inflammatory memory sensitizes skin epithelial stem cells to tissue damage.* Nature, 2017. **550**(7677): p. 475-480.
306. Cirovic, B., et al., *BCG Vaccination in Humans Elicits Trained Immunity via the Hematopoietic Progenitor Compartment.* Cell Host Microbe, 2020.
307. Christ, A., et al., *Western Diet Triggers NLRP3-Dependent Innate Immune Reprogramming.* Cell, 2018. **172**(1-2): p. 162-175 e14.
308. van der Heijden, C., et al., *Epigenetics and Trained Immunity.* Antioxid Redox Signal, 2018. **29**(11): p. 1023-1040.
309. Batbayar, S., D.H. Lee, and H.W. Kim, *Immunomodulation of Fungal beta-Glucan in Host Defense Signaling by Dectin-1.* Biomol Ther (Seoul), 2012. **20**(5): p. 433-45.
310. Arts, R.J.W., et al., *Immunometabolic Pathways in BCG-Induced Trained Immunity.* Cell Rep, 2016. **17**(10): p. 2562-2571.
311. Saeed, S., et al., *Epigenetic programming of monocyte-to-macrophage differentiation and trained innate immunity.* Science, 2014. **345**(6204): p. 1251086.
312. Arts, R.J., L.A. Joosten, and M.G. Netea, *Immunometabolic circuits in trained immunity.* Semin Immunol, 2016. **28**(5): p. 425-430.
313. Bekkering, S., et al., *Metabolic Induction of Trained Immunity through the Mevalonate Pathway.* Cell, 2018. **172**(1-2): p. 135-146 e9.

314. Arts, R.J., et al., *Glutaminolysis and Fumarate Accumulation Integrate Immunometabolic and Epigenetic Programs in Trained Immunity.* Cell Metab, 2016. **24**(6): p. 807-819.
315. Chavakis, T., I. Mitroulis, and G. Hajishengallis, *Hematopoietic progenitor cells as integrative hubs for adaptation to and fine-tuning of inflammation.* Nat Immunol, 2019. **20**(7): p. 802-811.
316. Keating, S.T., et al., *Rewiring of glucose metabolism defines trained immunity induced by oxidized low-density lipoprotein.* J Mol Med (Berl), 2020. **98**(6): p. 819-831.
317. Dominguez-Andres, J., et al., *The Itaconate Pathway Is a Central Regulatory Node Linking Innate Immune Tolerance and Trained Immunity.* Cell Metab, 2019. **29**(1): p. 211-220 e5.
318. Kamada, R., et al., *Interferon stimulation creates chromatin marks and establishes transcriptional memory.* Proc Natl Acad Sci U S A, 2018. **115**(39): p. E9162-E9171.
319. Kleinnijenhuis, J., et al., *Long-lasting effects of BCG vaccination on both heterologous Th1/Th17 responses and innate trained immunity.* J Innate Immun, 2014. **6**(2): p. 152-8.
320. Fanucchi, S., et al., *Immune genes are primed for robust transcription by proximal long noncoding RNAs located in nuclear compartments.* Nat Genet, 2019. **51**(1): p. 138-150.
321. Moorlag, S., et al., *beta-Glucan Induces Protective Trained Immunity against Mycobacterium tuberculosis Infection: A Key Role for IL-1.* Cell Rep, 2020. **31**(7): p. 107634.
322. Martinez-Reyes, I. and N.S. Chandel, *Mitochondrial TCA cycle metabolites control physiology and disease.* Nat Commun, 2020. **11**(1): p. 102.
323. Ryan, D.G. and L.A.J. O'Neill, *Krebs Cycle Reborn in Macrophage Immunometabolism.* Annu Rev Immunol, 2020. **38**: p. 289-313.
324. O'Leary, J.G., et al., *T cell- and B cell-independent adaptive immunity mediated by natural killer cells.* Nat Immunol, 2006. **7**(5): p. 507-16.
325. Schlums, H., et al., *Cytomegalovirus infection drives adaptive epigenetic diversification of NK cells with altered signaling and effector function.* Immunity, 2015. **42**(3): p. 443-56.
326. Cooper, M.A., et al., *Cytokine-induced memory-like natural killer cells.* Proc Natl Acad Sci U S A, 2009. **106**(6): p. 1915-9.
327. Paust, S., et al., *Critical role for the chemokine receptor CXCR6 in NK cell-mediated antigen-specific memory of haptens and viruses.* Nat Immunol, 2010. **11**(12): p. 1127-35.
328. Bjorkstrom, N.K., et al., *Rapid expansion and long-term persistence of elevated NK cell numbers in humans infected with hantavirus.* J Exp Med, 2011. **208**(1): p. 13-21.
329. Rolle, A., et al., *IL-12-producing monocytes and HLA-E control HCMV-driven NKG2C+ NK cell expansion.* J Clin Invest, 2014. **124**(12): p. 5305-16.
330. Hammer, Q., et al., *Peptide-specific recognition of human cytomegalovirus strains controls adaptive natural killer cells.* Nat Immunol, 2018. **19**(5): p. 453-463.
331. Newhook, N., N. Fudge, and M. Grant, *NK cells generate memory-type responses to human cytomegalovirus-infected fibroblasts.* Eur J Immunol, 2017. **47**(6): p. 1032-1039.
332. Sun, J.C., J.N. Beilke, and L.L. Lanier, *Adaptive immune features of natural killer cells.* Nature, 2009. **457**(7229): p. 557-61.
333. Min-Oo, G. and L.L. Lanier, *Cytomegalovirus generates long-lived antigen-specific NK cells with diminished bystander activation to heterologous infection.* J Exp Med, 2014. **211**(13): p. 2669-80.
334. Arase, H., et al., *Direct recognition of cytomegalovirus by activating and inhibitory NK cell receptors.* Science, 2002. **296**(5571): p. 1323-6.
335. Brown, M.G., et al., *Vital involvement of a natural killer cell activation receptor in resistance to viral infection.* Science, 2001. **292**(5518): p. 934-7.
336. Adams, N.M., et al., *Cytomegalovirus Infection Drives Avidity Selection of Natural Killer Cells.* Immunity, 2019. **50**(6): p. 1381-1390 e5.
337. Grassmann, S., et al., *Distinct Surface Expression of Activating Receptor Ly49H Drives Differential Expansion of NK Cell Clones upon Murine Cytomegalovirus Infection.* Immunity, 2019. **50**(6): p. 1391-1400 e4.

338. Sun, J.C. and L.L. Lanier, *NK cell development, homeostasis and function: parallels with CD8(+) T cells.* Nat Rev Immunol, 2011. **11**(10): p. 645-57.
339. Neher, J.J. and C. Cunningham, *Priming Microglia for Innate Immune Memory in the Brain.* Trends Immunol, 2019. **40**(4): p. 358-374.
340. Haley, M.J., et al., *Microglial Priming as Trained Immunity in the Brain.* Neuroscience, 2019. **405**: p. 47-54.
341. Wendeln, A.C., et al., *Innate immune memory in the brain shapes neurological disease hallmarks.* Nature, 2018. **556**(7701): p. 332-338.
342. Bilbo, S.D., *Early-life infection is a vulnerability factor for aging-related glial alterations and cognitive decline.* Neurobiol Learn Mem, 2010. **94**(1): p. 57-64.
343. Mattei, D., et al., *Maternal immune activation results in complex microglial transcriptome signature in the adult offspring that is reversed by minocycline treatment.* Transl Psychiatry, 2017. **7**(5): p. e1120.
344. Cunningham, C., et al., *Central and systemic endotoxin challenges exacerbate the local inflammatory response and increase neuronal death during chronic neurodegeneration.* J Neurosci, 2005. **25**(40): p. 9275-84.
345. Puntener, U., et al., *Long-term impact of systemic bacterial infection on the cerebral vasculature and microglia.* J Neuroinflammation, 2012. **9**: p. 146.
346. Palin, K., et al., *Systemic inflammation switches the inflammatory cytokine profile in CNS Wallerian degeneration.* Neurobiol Dis, 2008. **30**(1): p. 19-29.
347. Hole, C.R., et al., *Induction of memory-like dendritic cell responses in vivo.* Nat Commun, 2019. **10**(1): p. 2955.
348. Moorlag, S., et al., *BCG Vaccination Induces Long-Term Functional Reprogramming of Human Neutrophils.* Cell Rep, 2020. **33**(7): p. 108387.
349. Cassone, A., *The Case for an Expanded Concept of Trained Immunity.* mBio, 2018. **9**(3).
350. Aegerter, H., et al., *Influenza-induced monocyte-derived alveolar macrophages confer prolonged antibacterial protection.* Nat Immunol, 2020. **21**(2): p. 145-157.
351. Chen, F., et al., *Neutrophils prime a long-lived effector macrophage phenotype that mediates accelerated helminth expulsion.* Nat Immunol, 2014. **15**(10): p. 938-46.
352. Guillon, A., et al., *Pneumonia recovery reprograms the alveolar macrophage pool.* JCI Insight, 2020. **5**(4).
353. Mitsi, E., et al., *Nasal Pneumococcal Density Is Associated with Microaspiration and Heightened Human Alveolar Macrophage Responsiveness to Bacterial Pathogens.* Am J Respir Crit Care Med, 2020. **201**(3): p. 335-347.
354. Eljaszewicz, A., et al., *Trained immunity and tolerance in innate lymphoid cells, monocytes, and dendritic cells during allergen-specific immunotherapy.* J Allergy Clin Immunol, 2020.
355. Martinez-Gonzalez, I., et al., *Allergen-Experienced Group 2 Innate Lymphoid Cells Acquire Memory-like Properties and Enhance Allergic Lung Inflammation.* Immunity, 2016. **45**(1): p. 198-208.
356. Steer, C.A., et al., *Lung group 2 innate lymphoid cells are trained by endogenous IL-33 in the neonatal period.* JCI Insight, 2020.
357. Ordovas-Montanes, J., et al., *Allergic inflammatory memory in human respiratory epithelial progenitor cells.* Nature, 2018. **560**(7720): p. 649-654.
358. Frank-Bertoncelj, M., et al., *Epigenetically-driven anatomical diversity of synovial fibroblasts guides joint-specific fibroblast functions.* Nat Commun, 2017. **8**: p. 14852.
359. Bomans, K., et al., *Sepsis Induces a Long-Lasting State of Trained Immunity in Bone Marrow Monocytes.* Front Immunol, 2018. **9**: p. 2685.
360. Liu, G.Y., et al., *Short-term memory of danger signals or environmental stimuli in mesenchymal stem cells: implications for therapeutic potential.* Cell Mol Immunol, 2016. **13**(3): p. 369-78.

361. Chan, L.C., et al., *Protective immunity in recurrent Staphylococcus aureus infection reflects localized immune signatures and macrophage-conferred memory.* Proc Natl Acad Sci U S A, 2018. **115**(47): p. E11111-E11119.
362. Masaki, T., et al., *Reprogramming adult Schwann cells to stem cell-like cells by leprosy bacilli promotes dissemination of infection.* Cell, 2013. **152**(1-2): p. 51-67.
363. Faure, E., et al., *Bacterial lipopolysaccharide activates NF-kappaB through toll-like receptor 4 (TLR-4) in cultured human dermal endothelial cells. Differential expression of TLR-4 and TLR-2 in endothelial cells.* J Biol Chem, 2000. **275**(15): p. 11058-63.
364. Anand, A.R., R. Bradley, and R.K. Ganju, *LPS-induced MCP-1 expression in human microvascular endothelial cells is mediated by the tyrosine kinase, Pyk2 via the p38 MAPK/NF-kappaB-dependent pathway.* Mol Immunol, 2009. **46**(5): p. 962-8.
365. Anand, A.R., et al., *The tyrosine kinase Pyk2 mediates lipopolysaccharide-induced IL-8 expression in human endothelial cells.* J Immunol, 2008. **180**(8): p. 5636-44.
366. Marceau, F., et al., *Effects of experimental conditions on the production of interleukin-1 alpha and -1 beta by human endothelial cells cultured in vitro.* Int J Immunopharmacol, 1992. **14**(4): p. 525-34.
367. Faure, E., et al., *Bacterial lipopolysaccharide and IFN-gamma induce Toll-like receptor 2 and Toll-like receptor 4 expression in human endothelial cells: role of NF-kappa B activation.* J Immunol, 2001. **166**(3): p. 2018-24.
368. Sohrabi, Y., et al., *OxLDL-mediated immunologic memory in endothelial cells.* J Mol Cell Cardiol, 2020.
369. Sui, Y. and J.A. Berzofsky, *Myeloid Cell-Mediated Trained Innate Immunity in Mucosal AIDS Vaccine Development.* Front Immunol, 2020. **11**: p. 315.
370. Sokal, J.E., C.W. Aungst, and M. Snyderman, *Delay in progression of malignant lymphoma after BCG vaccination.* N Engl J Med, 1974. **291**(23): p. 1226-30.
371. Fuge, O., et al., *Immunotherapy for bladder cancer.* Res Rep Urol, 2015. **7**: p. 65-79.
372. Guallar-Garrido, S. and E. Julian, *Bacillus Calmette-Guerin (BCG) Therapy for Bladder Cancer: An Update.* Immunotargets Ther, 2020. **9**: p. 1-11.
373. van Puffelen, J.H., et al., *Trained immunity as a molecular mechanism for BCG immunotherapy in bladder cancer.* Nat Rev Urol, 2020.
374. Hou, A., et al., *Targeting Myeloid-Derived Suppressor Cell, a Promising Strategy to Overcome Resistance to Immune Checkpoint Inhibitors.* Front Immunol, 2020. **11**: p. 783.
375. Zhang, C., et al., *Epigenetics in myeloid derived suppressor cells: a sheathed sword towards cancer.* Oncotarget, 2016. **7**(35): p. 57452-57463.
376. Mulder, W.J.M., et al., *Therapeutic targeting of trained immunity.* Nat Rev Drug Discov, 2019. **18**(7): p. 553-566.
377. Christ, A., M. Lauterbach, and E. Latz, *Western Diet and the Immune System: An Inflammatory Connection.* Immunity, 2019. **51**(5): p. 794-811.
378. Singer, M., et al., *The Third International Consensus Definitions for Sepsis and Septic Shock (Sepsis-3).* JAMA, 2016. **315**(8): p. 801-10.
379. Ceccato, A. and A. Torres, *Sepsis and community-acquired pneumonia.* Annals of Research Hospitals, 2018. **2**: p. 7-7.
380. Feldman, C. and R. Anderson, *The Role of Streptococcus pneumoniae in Community-Acquired Pneumonia.* Semin Respir Crit Care Med, 2016. **37**(6): p. 806-818.
381. Christaki, E., *Host immune response in sepsis due to ventilator-associated pneumonia: how is it different?* Crit Care, 2009. **13**(6): p. 1009.
382. Rudd, K.E., et al., *Global, regional, and national sepsis incidence and mortality, 1990–2017: analysis for the Global Burden of Disease Study.* The Lancet, 2020. **395**(10219): p. 200-211.
383. Kempker, J.A. and G.S. Martin, *The Changing Epidemiology and Definitions of Sepsis.* Clin Chest Med, 2016. **37**(2): p. 165-79.
384. Angus, D.C., et al., *Epidemiology of severe sepsis in the United States: analysis of incidence, outcome, and associated costs of care.* Crit Care Med, 2001. **29**(7): p. 1303-10.

385. Vincent, J.L., *Highlighting the huge global burden of sepsis.* Anaesth Crit Care Pain Med, 2020.
386. Vincent, J.L., et al., *Sepsis in European intensive care units: results of the SOAP study.* Crit Care Med, 2006. **34**(2): p. 344-53.
387. Weiss, S.L., et al., *Global epidemiology of pediatric severe sepsis: the sepsis prevalence, outcomes, and therapies study.* Am J Respir Crit Care Med, 2015. **191**(10): p. 1147-57.
388. Blanco, J., et al., *Incidence, organ dysfunction and mortality in severe sepsis: a Spanish multicentre study.* Crit Care, 2008. **12**(6): p. R158.
389. Brun-Buisson, C., et al., *EPISEPSIS: a reappraisal of the epidemiology and outcome of severe sepsis in French intensive care units.* Intensive Care Med, 2004. **30**(4): p. 580-8.
390. Opal, S.M., et al., *Systemic host responses in severe sepsis analyzed by causative microorganism and treatment effects of drotrecogin alfa (activated).* Clin Infect Dis, 2003. **37**(1): p. 50-8.
391. Kumar, V. and S. Chhibber, *Acute lung inflammation in Klebsiella pneumoniae B5055-induced pneumonia and sepsis in BALB/c mice: a comparative study.* Inflammation, 2011. **34**(5): p. 452-62.
392. Kumar, V., *Pulmonary Innate Immune Response Determines the Outcome of Inflammation During Pneumonia and Sepsis-Associated Acute Lung Injury.* Frontiers in Immunology, 2020. **11**.
393. Hotchkiss, R.S., et al., *Sepsis and septic shock.* Nat Rev Dis Primers, 2016. **2**: p. 16045.
394. Guo, R.F. and P.A. Ward, *Role of C5a in inflammatory responses.* Annu Rev Immunol, 2005. **23**: p. 821-52.
395. Riedemann, N.C., et al., *Regulatory role of C5a on macrophage migration inhibitory factor release from neutrophils.* J Immunol, 2004. **173**(2): p. 1355-9.
396. Drouin, S.M., et al., *Expression of the complement anaphylatoxin C3a and C5a receptors on bronchial epithelial and smooth muscle cells in models of sepsis and asthma.* J Immunol, 2001. **166**(3): p. 2025-32.
397. Bosmann, M. and P.A. Ward, *Role of C3, C5 and anaphylatoxin receptors in acute lung injury and in sepsis.* Adv Exp Med Biol, 2012. **946**: p. 147-59.
398. Tsokos, M., *Immunohistochemical detection of sepsis-induced lung injury in human autopsy material.* Leg Med (Tokyo), 2003. **5**(2): p. 73-86.
399. Ness, T.L., et al., *Immunomodulatory role of CXCR2 during experimental septic peritonitis.* J Immunol, 2003. **171**(7): p. 3775-84.
400. Standiford, T.J., et al., *Macrophage inflammatory protein-1 alpha mediates lung leukocyte recruitment, lung capillary leak, and early mortality in murine endotoxemia.* J Immunol, 1995. **155**(3): p. 1515-24.
401. Sawa, Y., et al., *LPS-induced IL-6, IL-8, VCAM-1, and ICAM-1 expression in human lymphatic endothelium.* J Histochem Cytochem, 2008. **56**(2): p. 97-109.
402. Zhang, P., M. Xie, and J.A. Spitzer, *Hepatic neutrophil sequestration in early sepsis: enhanced expression of adhesion molecules and phagocytic activity.* Shock, 1994. **2**(2): p. 133-40.
403. Kobayashi, Y., *The role of chemokines in neutrophil biology.* Front Biosci, 2008. **13**: p. 2400-7.
404. Angus, D.C. and T. van der Poll, *Severe sepsis and septic shock.* N Engl J Med, 2013. **369**(9): p. 840-51.
405. Walter, J.M., J. Wilson, and L.B. Ware, *Biomarkers in acute respiratory distress syndrome: from pathobiology to improving patient care.* Expert Rev Respir Med, 2014. **8**(5): p. 573-86.
406. Levi, M. and T. van der Poll, *Coagulation and sepsis.* Thromb Res, 2017. **149**: p. 38-44.
407. Aird, W.C., *The role of the endothelium in severe sepsis and multiple organ dysfunction syndrome.* Blood, 2003. **101**(10): p. 3765-77.
408. Levi, M., *Pathogenesis and treatment of disseminated intravascular coagulation in the septic patient.* J Crit Care, 2001. **16**(4): p. 167-77.
409. Deutschman, C.S. and K.J. Tracey, *Sepsis: current dogma and new perspectives.* Immunity, 2014. **40**(4): p. 463-75.

410. Ward, P.A., *The harmful role of c5a on innate immunity in sepsis.* J Innate Immun, 2010. **2**(5): p. 439-45.
411. Wagner, C., et al., *Differentiation of polymorphonuclear neutrophils in patients with systemic infections and chronic inflammatory diseases: evidence of prolonged life span and de novo synthesis of fibronectin.* J Mol Med (Berl), 2000. **78**(6): p. 337-45.
412. Taneja, R., et al., *Delayed neutrophil apoptosis in sepsis is associated with maintenance of mitochondrial transmembrane potential and reduced caspase-9 activity.* Crit Care Med, 2004. **32**(7): p. 1460-9.
413. Wang, Z., et al., *Alveolar macrophages from septic mice promote polymorphonuclear leukocyte transendothelial migration via an endothelial cell Src kinase/NADPH oxidase pathway.* J Immunol, 2008. **181**(12): p. 8735-44.
414. Wang, H., H. Yang, and K.J. Tracey, *Extracellular role of HMGB1 in inflammation and sepsis.* J Intern Med, 2004. **255**(3): p. 320-31.
415. Deng, M., et al., *The Endotoxin Delivery Protein HMGB1 Mediates Caspase-11-Dependent Lethality in Sepsis.* Immunity, 2018. **49**(4): p. 740-753 e7.
416. Xiong, S., et al., *IL-1beta suppression of VE-cadherin transcription underlies sepsis-induced inflammatory lung injury.* J Clin Invest, 2020. **130**(7): p. 3684-3698.
417. Farley, K.S., et al., *Effects of macrophage inducible nitric oxide synthase in murine septic lung injury.* Am J Physiol Lung Cell Mol Physiol, 2006. **290**(6): p. L1164-72.
418. Cavaillon, J.M. and M. Adib-Conquy, *Bench-to-bedside review: endotoxin tolerance as a model of leukocyte reprogramming in sepsis.* Crit Care, 2006. **10**(5): p. 233.
419. Ellaban, E., G. Bolgos, and D. Remick, *Selective macrophage suppression during sepsis.* Cell Immunol, 2004. **231**(1-2): p. 103-11.
420. Wen, H., et al., *Severe sepsis exacerbates cell-mediated immunity in the lung due to an altered dendritic cell cytokine profile.* Am J Pathol, 2006. **168**(6): p. 1940-50.
421. Dreschler, K., et al., *Altered phenotype of blood dendritic cells in patients with acute pneumonia.* Respiration, 2012. **83**(3): p. 209-17.
422. Poehlmann, H., et al., *Phenotype changes and impaired function of dendritic cell subsets in patients with sepsis: a prospective observational analysis.* Crit Care, 2009. **13**(4): p. R119.
423. Faivre, V., et al., *Human monocytes differentiate into dendritic cells subsets that induce anergic and regulatory T cells in sepsis.* PLoS One, 2012. **7**(10): p. e47209.
424. Hotchkiss, R.S., et al., *Sepsis-induced apoptosis causes progressive profound depletion of B and CD4+ T lymphocytes in humans.* J Immunol, 2001. **166**(11): p. 6952-63.
425. Zeerleder, S., et al., *Activated cytotoxic T cells and NK cells in severe sepsis and septic shock and their role in multiple organ dysfunction.* Clin Immunol, 2005. **116**(2): p. 158-65.
426. Perona-Wright, G., et al., *Systemic but not local infections elicit immunosuppressive IL-10 production by natural killer cells.* Cell Host Microbe, 2009. **6**(6): p. 503-12.
427. van der Poll, T., et al., *The immunopathology of sepsis and potential therapeutic targets.* Nat Rev Immunol, 2017. **17**(7): p. 407-420.
428. Nakamura, K., et al., *C-reactive protein clustering to clarify persistent inflammation, immunosuppression and catabolism syndrome.* Intensive Care Med, 2020. **46**(3): p. 437-443.
429. Gentile, L.F., et al., *Persistent inflammation and immunosuppression: a common syndrome and new horizon for surgical intensive care.* J Trauma Acute Care Surg, 2012. **72**(6): p. 1491-501.
430. Hu, D., et al., *Persistent inflammation-immunosuppression catabolism syndrome, a common manifestation of patients with enterocutaneous fistula in intensive care unit.* J Trauma Acute Care Surg, 2014. **76**(3): p. 725-9.
431. Vanzant, E.L., et al., *Persistent inflammation, immunosuppression, and catabolism syndrome after severe blunt trauma.* J Trauma Acute Care Surg, 2014. **76**(1): p. 21-9; discussion 29-30.
432. Delano, M.J., et al., *MyD88-dependent expansion of an immature GR-1(+)CD11b(+) population induces T cell suppression and Th2 polarization in sepsis.* J Exp Med, 2007. **204**(6): p. 1463-74.

433. Taneja, R., et al., *Immature circulating neutrophils in sepsis have impaired phagocytosis and calcium signaling.* Shock, 2008. **30**(6): p. 618-22.
434. Munoz, C., et al., *Dysregulation of in vitro cytokine production by monocytes during sepsis.* J Clin Invest, 1991. **88**(5): p. 1747-54.
435. Cuenca, A.G., et al., *A paradoxical role for myeloid-derived suppressor cells in sepsis and trauma.* Mol Med, 2011. **17**(3-4): p. 281-92.
436. Boomer, J.S., et al., *Immunosuppression in patients who die of sepsis and multiple organ failure.* JAMA, 2011. **306**(23): p. 2594-605.
437. Hotchkiss, R.S., et al., *Apoptotic cell death in patients with sepsis, shock, and multiple organ dysfunction.* Crit Care Med, 1999. **27**(7): p. 1230-51.
438. Drewry, A.M., et al., *Persistent lymphopenia after diagnosis of sepsis predicts mortality.* Shock, 2014. **42**(5): p. 383-91.
439. Rello, J., et al., *Sepsis: A Review of Advances in Management.* Adv Ther, 2017.
440. Annane, D., *Adjunctive treatment in septic shock: What's next?* Presse Med, 2016. **45**(4 Pt 2): p. e105-9.
441. Davies, R., K. O'Dea, and A. Gordon, *Immune therapy in sepsis: Are we ready to try again?* J Intensive Care Soc, 2018. **19**(4): p. 326-344.
442. Kumar, V., *Immunometabolism: Another Road to Sepsis and Its Therapeutic Targeting.* Inflammation, 2018.
443. Gotts, J.E. and M.A. Matthay, *Sepsis: pathophysiology and clinical management.* BMJ, 2016. **353**: p. i1585.
444. Steinhagen, F., et al., *Immunotherapy in sepsis - brake or accelerate?* Pharmacol Ther, 2020. **208**: p. 107476.
445. Cohen, J., et al., *Sepsis: a roadmap for future research.* Lancet Infect Dis, 2015. **15**(5): p. 581-614.
446. Venet, F. and G. Monneret, *Advances in the understanding and treatment of sepsis-induced immunosuppression.* Nat Rev Nephrol, 2018. **14**(2): p. 121-137.
447. Cecconi, M., et al., *Sepsis and septic shock.* Lancet, 2018. **392**(10141): p. 75-87.
448. Peters van Ton, A.M., et al., *Precision Immunotherapy for Sepsis.* Front Immunol, 2018. **9**: p. 1926.
449. Rubio, I., et al., *Current gaps in sepsis immunology: new opportunities for translational research.* Lancet Infect Dis, 2019. **19**(12): p. e422-e436.
450. Stanski, N.L. and H.R. Wong, *Prognostic and predictive enrichment in sepsis.* Nat Rev Nephrol, 2020. **16**(1): p. 20-31.
451. Tracey, K.J., et al., *Anti-cachectin/TNF monoclonal antibodies prevent septic shock during lethal bacteraemia.* Nature, 1987. **330**(6149): p. 662-4.
452. Fisher, C.J., Jr., et al., *Treatment of septic shock with the tumor necrosis factor receptor:Fc fusion protein. The Soluble TNF Receptor Sepsis Study Group.* N Engl J Med, 1996. **334**(26): p. 1697-702.
453. Abraham, E., et al., *p55 Tumor necrosis factor receptor fusion protein in the treatment of patients with severe sepsis and septic shock. A randomized controlled multicenter trial. Ro 45-2081 Study Group.* JAMA, 1997. **277**(19): p. 1531-8.
454. Panacek, E.A., et al., *Efficacy and safety of the monoclonal anti-tumor necrosis factor antibody F(ab')2 fragment afelimomab in patients with severe sepsis and elevated interleukin-6 levels.* Crit Care Med, 2004. **32**(11): p. 2173-82.
455. Savva, A. and T. Roger, *Targeting toll-like receptors: promising therapeutic strategies for the management of sepsis-associated pathology and infectious diseases.* Front Immunol, 2013. **4**: p. 387.
456. Daubeuf, B., et al., *TLR4/MD-2 monoclonal antibody therapy affords protection in experimental models of septic shock.* J Immunol, 2007. **179**(9): p. 6107-14.
457. Meng, G., et al., *Antagonistic antibody prevents toll-like receptor 2-driven lethal shock-like syndromes.* J Clin Invest, 2004. **113**(10): p. 1473-81.

458. Plitas, G., et al., *Toll-like receptor 9 inhibition reduces mortality in polymicrobial sepsis.* J Exp Med, 2008. **205**(6): p. 1277-83.
459. Spiller, S., et al., *TLR4-induced IFN-gamma production increases TLR2 sensitivity and drives Gram-negative sepsis in mice.* J Exp Med, 2008. **205**(8): p. 1747-54.
460. Fu, Q., et al., *NLRP3/Caspase-1 Pathway-Induced Pyroptosis Mediated Cognitive Deficits in a Mouse Model of Sepsis-Associated Encephalopathy.* Inflammation, 2019. **42**(1): p. 306-318.
461. Liu, Y., et al., *Scutellarin Suppresses NLRP3 Inflammasome Activation in Macrophages and Protects Mice against Bacterial Sepsis.* Front Pharmacol, 2017. **8**: p. 975.
462. Sui, D.M., et al., *Resveratrol Protects against Sepsis-Associated Encephalopathy and Inhibits the NLRP3/IL-1beta Axis in Microglia.* Mediators Inflamm, 2016. **2016**: p. 1045657.
463. Sarkar, A., et al., *Caspase-1 regulates Escherichia coli sepsis and splenic B cell apoptosis independently of interleukin-1beta and interleukin-18.* Am J Respir Crit Care Med, 2006. **174**(9): p. 1003-10.
464. Vanden Berghe, T., et al., *Simultaneous targeting of IL-1 and IL-18 is required for protection against inflammatory and septic shock.* Am J Respir Crit Care Med, 2014. **189**(3): p. 282-91.
465. Fisher, C.J., Jr., et al., *Initial evaluation of human recombinant interleukin-1 receptor antagonist in the treatment of sepsis syndrome: a randomized, open-label, placebo-controlled multicenter trial.* Crit Care Med, 1994. **22**(1): p. 12-21.
466. Opal, S.M., et al., *Confirmatory interleukin-1 receptor antagonist trial in severe sepsis: a phase III, randomized, double-blind, placebo-controlled, multicenter trial. The Interleukin-1 Receptor Antagonist Sepsis Investigator Group.* Crit Care Med, 1997. **25**(7): p. 1115-24.
467. Cheng, K.T., et al., *Caspase-11-mediated endothelial pyroptosis underlies endotoxemia-induced lung injury.* J Clin Invest, 2017. **127**(11): p. 4124-4135.
468. Chu, L.H., et al., *The oxidized phospholipid oxPAPC protects from septic shock by targeting the non-canonical inflammasome in macrophages.* Nat Commun, 2018. **9**(1): p. 996.
469. Rathkey, J.K., et al., *Chemical disruption of the pyroptotic pore-forming protein gasdermin D inhibits inflammatory cell death and sepsis.* Sci Immunol, 2018. **3**(26).
470. Stevens, N.E., et al., *Therapeutic targeting of HMGB1 during experimental sepsis modulates the inflammatory cytokine profile to one associated with improved clinical outcomes.* Sci Rep, 2017. **7**(1): p. 5850.
471. Zeng, L., et al., *ALK is a therapeutic target for lethal sepsis.* Sci Transl Med, 2017. **9**(412).
472. Shirota, H., et al., *Suppressive oligodeoxynucleotides protect mice from lethal endotoxic shock.* J Immunol, 2005. **174**(8): p. 4579-83.
473. Steinhagen, F., et al., *Suppressive oligodeoxynucleotides containing TTAGGG motifs inhibit cGAS activation in human monocytes.* Eur J Immunol, 2018. **48**(4): p. 605-611.
474. Ge, W., et al., *LDK378 improves micro- and macro-circulation via alleviating STING-mediated inflammatory injury in a Sepsis rat model induced by Cecal ligation and puncture.* J Inflamm (Lond), 2019. **16**: p. 3.
475. Karasu, E., et al., *Targeting Complement Pathways in Polytrauma- and Sepsis-Induced Multiple-Organ Dysfunction.* Front Immunol, 2019. **10**: p. 543.
476. Ward, P.A., R.F. Guo, and N.C. Riedemann, *Manipulation of the complement system for benefit in sepsis.* Crit Care Res Pract, 2012. **2012**: p. 427607.
477. Keshari, R.S., et al., *Inhibition of complement C5 protects against organ failure and reduces mortality in a baboon model of Escherichia coli sepsis.* Proc Natl Acad Sci U S A, 2017. **114**(31): p. E6390-E6399.
478. Silasi-Mansat, R., et al., *Complement inhibition decreases the procoagulant response and confers organ protection in a baboon model of Escherichia coli sepsis.* Blood, 2010. **116**(6): p. 1002-10.
479. Shao, Z., et al., *Carboxypeptidase B2 deficiency reveals opposite effects of complement C3a and C5a in a murine polymicrobial sepsis model.* J Thromb Haemost, 2015. **13**(6): p. 1090-102.

480. Ren, J., et al., *Complement depletion deteriorates clinical outcomes of severe abdominal sepsis: a conspirator of infection and coagulopathy in crime?* PLoS One, 2012. **7**(10): p. e47095.
481. Vincent, J.L., et al., *Effect of a Recombinant Human Soluble Thrombomodulin on Mortality in Patients With Sepsis-Associated Coagulopathy: The SCARLET Randomized Clinical Trial.* JAMA, 2019. **321**(20): p. 1993-2002.
482. Abraham, E., et al., *Efficacy and safety of tifacogin (recombinant tissue factor pathway inhibitor) in severe sepsis: a randomized controlled trial.* JAMA, 2003. **290**(2): p. 238-47.
483. Warren, B.L., et al., *Caring for the critically ill patient. High-dose antithrombin III in severe sepsis: a randomized controlled trial.* JAMA, 2001. **286**(15): p. 1869-78.
484. Kumpers, P., et al., *The synthetic tie2 agonist peptide vasculotide protects against vascular leakage and reduces mortality in murine abdominal sepsis.* Crit Care, 2011. **15**(5): p. R261.
485. Stiehl, T., et al., *Lung-targeted RNA interference against angiopoietin-2 ameliorates multiple organ dysfunction and death in sepsis.* Crit Care Med, 2014. **42**(10): p. e654-62.
486. Miksa, M., et al., *Vasoactive hormone adrenomedullin and its binding protein: anti-inflammatory effects by up-regulating peroxisome proliferator-activated receptor-gamma.* J Immunol, 2007. **179**(9): p. 6263-72.
487. Yang, J., et al., *Human adrenomedullin and its binding protein ameliorate sepsis-induced organ injury and mortality in jaundiced rats.* Peptides, 2010. **31**(5): p. 872-7.
488. Zhou, M., S.R. Maitra, and P. Wang, *Adrenomedullin and adrenomedullin binding protein-1 protect endothelium-dependent vascular relaxation in sepsis.* Mol Med, 2007. **13**(9-10): p. 488-94.
489. Marino, R., et al., *Plasma adrenomedullin is associated with short-term mortality and vasopressor requirement in patients admitted with sepsis.* Crit Care, 2014. **18**(1): p. R34.
490. Marik, P.E., et al., *Hydrocortisone, Vitamin C, and Thiamine for the Treatment of Severe Sepsis and Septic Shock: A Retrospective Before-After Study.* Chest, 2017. **151**(6): p. 1229-1238.
491. Kim, W.Y., et al., *Combined vitamin C, hydrocortisone, and thiamine therapy for patients with severe pneumonia who were admitted to the intensive care unit: Propensity score-based analysis of a before-after cohort study.* J Crit Care, 2018. **47**: p. 211-218.
492. Kim, S.R., et al., *Ascorbic acid reduces HMGB1 secretion in lipopolysaccharide-activated RAW 264.7 cells and improves survival rate in septic mice by activation of Nrf2/HO-1 signals.* Biochem Pharmacol, 2015. **95**(4): p. 279-89.
493. Seymour, C.W., et al., *Severe sepsis in pre-hospital emergency care: analysis of incidence, care, and outcome.* Am J Respir Crit Care Med, 2012. **186**(12): p. 1264-71.
494. Fowler, A.A., 3rd, et al., *Effect of Vitamin C Infusion on Organ Failure and Biomarkers of Inflammation and Vascular Injury in Patients With Sepsis and Severe Acute Respiratory Failure: The CITRIS-ALI Randomized Clinical Trial.* JAMA, 2019. **322**(13): p. 1261-1270.
495. Barber, A.E., et al., *Glucocorticoid therapy alters hormonal and cytokine responses to endotoxin in man.* J Immunol, 1993. **150**(5): p. 1999-2006.
496. Keh, D., et al., *Immunologic and hemodynamic effects of "low-dose" hydrocortisone in septic shock: a double-blind, randomized, placebo-controlled, crossover study.* Am J Respir Crit Care Med, 2003. **167**(4): p. 512-20.
497. Oppert, M., et al., *Low-dose hydrocortisone improves shock reversal and reduces cytokine levels in early hyperdynamic septic shock.* Crit Care Med, 2005. **33**(11): p. 2457-64.
498. Pourmand, A., et al., *The controversial role of corticosteroids in septic shock.* Am J Emerg Med, 2019. **37**(7): p. 1353-1361.
499. Giamarellos-Bourboulis, E.J., et al., *Effect of clarithromycin in patients with suspected Gram-negative sepsis: results of a randomized controlled trial.* J Antimicrob Chemother, 2014. **69**(4): p. 1111-8.

500. Spyridaki, A., et al., *Effect of clarithromycin in inflammatory markers of patients with ventilator-associated pneumonia and sepsis caused by Gram-negative bacteria: results from a randomized clinical study.* Antimicrob Agents Chemother, 2012. **56**(7): p. 3819-25.
501. Tsaganos, T., et al., *Clarithromycin Leads to Long-Term Survival and Cost Benefit in Ventilator-Associated Pneumonia and Sepsis.* Antimicrob Agents Chemother, 2016. **60**(6): p. 3640-6.
502. Nierhaus, A., et al., *Reversal of immunoparalysis by recombinant human granulocyte-macrophage colony-stimulating factor in patients with severe sepsis.* Intensive Care Med, 2003. **29**(4): p. 646-51.
503. Meisel, C., et al., *Granulocyte-macrophage colony-stimulating factor to reverse sepsis-associated immunosuppression: a double-blind, randomized, placebo-controlled multicenter trial.* Am J Respir Crit Care Med, 2009. **180**(7): p. 640-8.
504. Bo, L., et al., *Granulocyte-colony stimulating factor (G-CSF) and granulocyte-macrophage colony stimulating factor (GM-CSF) for sepsis: a meta-analysis.* Crit Care, 2011. **15**(1): p. R58.
505. Docke, W.D., et al., *Monocyte deactivation in septic patients: restoration by IFN-gamma treatment.* Nat Med, 1997. **3**(6): p. 678-81.
506. Delsing, C.E., et al., *Interferon-gamma as adjunctive immunotherapy for invasive fungal infections: a case series.* BMC Infect Dis, 2014. **14**: p. 166.
507. Shindo, Y., et al., *Interleukin 7 immunotherapy improves host immunity and survival in a two-hit model of Pseudomonas aeruginosa pneumonia.* J Leukoc Biol, 2017. **101**(2): p. 543-554.
508. Unsinger, J., et al., *IL-7 promotes T cell viability, trafficking, and functionality and improves survival in sepsis.* J Immunol, 2010. **184**(7): p. 3768-79.
509. Venet, F., et al., *IL-7 restores lymphocyte functions in septic patients.* J Immunol, 2012. **189**(10): p. 5073-81.
510. Francois, B., et al., *Interleukin-7 restores lymphocytes in septic shock: the IRIS-7 randomized clinical trial.* JCI Insight, 2018. **3**(5).
511. Guo, Y., et al., *IL-15 Enables Septic Shock by Maintaining NK Cell Integrity and Function.* J Immunol, 2017. **198**(3): p. 1320-1333.
512. Inoue, S., et al., *IL-15 prevents apoptosis, reverses innate and adaptive immune dysfunction, and improves survival in sepsis.* J Immunol, 2010. **184**(3): p. 1401-9.
513. Guo, Y., et al., *Immunobiology of the IL-15/IL-15Ralpha complex as an antitumor and antiviral agent.* Cytokine Growth Factor Rev, 2017. **38**: p. 10-21.
514. Keane, C., M. Jerkic, and J.G. Laffey, *Stem Cell-based Therapies for Sepsis.* Anesthesiology, 2017. **127**(6): p. 1017-1034.
515. Schlosser, K., et al., *Effects of Mesenchymal Stem Cell Treatment on Systemic Cytokine Levels in a Phase 1 Dose Escalation Safety Trial of Septic Shock Patients.* Crit Care Med, 2019. **47**(7): p. 918-925.
516. Patil, N.K., et al., *Targeting Immune Cell Checkpoints during Sepsis.* Int J Mol Sci, 2017. **18**(11).
517. Brahmamdam, P., et al., *Delayed administration of anti-PD-1 antibody reverses immune dysfunction and improves survival during sepsis.* J Leukoc Biol, 2010. **88**(2): p. 233-40.
518. Zhang, Y., et al., *PD-L1 blockade improves survival in experimental sepsis by inhibiting lymphocyte apoptosis and reversing monocyte dysfunction.* Crit Care, 2010. **14**(6): p. R220.
519. Grimaldi, D., et al., *Nivolumab plus interferon-gamma in the treatment of intractable mucormycosis.* Lancet Infect Dis, 2017. **17**(1): p. 18.
520. Hotchkiss, R.S., et al., *Immune Checkpoint Inhibition in Sepsis: A Phase 1b Randomized, Placebo-Controlled, Single Ascending Dose Study of Antiprogrammed Cell Death-Ligand 1 Antibody (BMS-936559).* Crit Care Med, 2019. **47**(5): p. 632-642.
521. Beutler, B. and G.E. Grau, *Tumor necrosis factor in the pathogenesis of infectious diseases.* Crit Care Med, 1993. **21**(10 Suppl): p. S423-35.
522. de Groote, M.A., et al., *Plasma tumor necrosis factor levels in patients with presumed sepsis. Results in those treated with antilipid A antibody vs placebo.* JAMA, 1989. **262**(2): p. 249-51.
523. Lv, S., et al., *Anti-TNF-alpha therapy for patients with sepsis: a systematic meta-analysis.* Int J Clin Pract, 2014. **68**(4): p. 520-8.

524. Smith, M., et al., *Trial Watch: Toll-like receptor agonists in cancer immunotherapy.* Oncoimmunology, 2018. **7**(12): p. e1526250.
525. Opal, S.M., et al., *Effect of eritoran, an antagonist of MD2-TLR4, on mortality in patients with severe sepsis: the ACCESS randomized trial.* JAMA, 2013. **309**(11): p. 1154-62.
526. Ablasser, A. and Z.J. Chen, *cGAS in action: Expanding roles in immunity and inflammation.* Science, 2019. **363**(6431).
527. Bode, C., et al., *Suppressive oligodeoxynucleotides promote the development of Th17 cells.* PLoS One, 2013. **8**(7): p. e67991.
528. Ranieri, V.M., et al., *Drotrecogin alfa (activated) in adults with septic shock.* N Engl J Med, 2012. **366**(22): p. 2055-64.
529. Gamble, J.R., et al., *Angiopoietin-1 is an antipermeability and anti-inflammatory agent in vitro and targets cell junctions.* Circ Res, 2000. **87**(7): p. 603-7.
530. Pizurki, L., et al., *Angiopoietin-1 inhibits endothelial permeability, neutrophil adherence and IL-8 production.* Br J Pharmacol, 2003. **139**(2): p. 329-36.
531. Geven, C., M. Kox, and P. Pickkers, *Adrenomedullin and Adrenomedullin-Targeted Therapy As Treatment Strategies Relevant for Sepsis.* Front Immunol, 2018. **9**: p. 292.
532. Sprung, C.L., et al., *Hydrocortisone therapy for patients with septic shock.* N Engl J Med, 2008. **358**(2): p. 111-24.
533. Annane, D., et al., *Hydrocortisone plus Fludrocortisone for Adults with Septic Shock.* N Engl J Med, 2018. **378**(9): p. 809-818.
534. Kachroo, A. and G.P. Robin, *Systemic signaling during plant defense.* Curr Opin Plant Biol, 2013. **16**(4): p. 527-33.
535. Sadd, B.M. and P. Schmid-Hempel, *Insect immunity shows specificity in protection upon secondary pathogen exposure.* Curr Biol, 2006. **16**(12): p. 1206-10.
536. Giamarellos-Bourboulis, E.J., et al., *Activate: Randomized Clinical Trial of BCG Vaccination against Infection in the Elderly.* Cell, 2020. **183**(2): p. 315-323 e9.
537. Prentice, S., et al., *BCG-induced non-specific effects on heterologous infectious disease in Ugandan neonates: an investigator-blind randomised controlled trial.* Lancet Infect Dis, 2021.
538. Walk, J., et al., *Outcomes of controlled human malaria infection after BCG vaccination.* Nat Commun, 2019. **10**(1): p. 874.
539. Berendsen, M.L., et al., *BCG vaccination is associated with reduced malaria prevalence in children under the age of 5 years in sub-Saharan Africa.* BMJ Glob Health, 2019. **4**(6): p. e001862.
540. Berendsen, M.L.T., et al., *Maternal Priming: Bacillus Calmette-Guerin (BCG) Vaccine Scarring in Mothers Enhances the Survival of Their Child With a BCG Vaccine Scar.* J Pediatric Infect Dis Soc, 2020. **9**(2): p. 166-172.
541. Sharma, A.R., et al., *BCG as a game-changer to prevent the infection and severity of COVID-19 pandemic?* Allergol Immunopathol (Madr), 2020.
542. Escobar, L.E., A. Molina-Cruz, and C. Barillas-Mury, *BCG vaccine protection from severe coronavirus disease 2019 (COVID-19).* Proc Natl Acad Sci U S A, 2020.
543. O'Neill, L.A.J. and M.G. Netea, *BCG-induced trained immunity: can it offer protection against COVID-19?* Nat Rev Immunol, 2020.
544. Curtis, N., et al., *Considering BCG vaccination to reduce the impact of COVID-19.* The Lancet, 2020.
545. Redelman-Sidi, G., *Could BCG be used to protect against COVID-19?* Nat Rev Urol, 2020.
546. Abbas, A.M., et al., *The effect of BCG vaccine in the era of COVID-19 pandemic.* Scand J Immunol, 2020: p. e12947.
547. Miyasaka, M., *Is BCG vaccination causally related to reduced COVID-19 mortality?* EMBO Mol Med, 2020.
548. Kerboua, K.E., *The perplexing question of trained immunity versus adaptive memory in COVID-19.* J Med Virol, 2020.

549. Macedo, A. and C. Febra, *Relation between BCG coverage rate and COVID-19 infection worldwide.* Med Hypotheses, 2020. **142**: p. 109816.
550. Klinger, D., et al., *Significantly Improved COVID-19 Outcomes in Countries with Higher BCG Vaccination Coverage: A Multivariable Analysis.* Vaccines (Basel), 2020. **8**(3).
551. Madan, M., et al., *TB infection and BCG vaccination: are we protected from COVID-19?* Public Health, 2020. **185**: p. 91-92.
552. Kinoshita, M. and M. Tanaka, *Impact of routine infant BCG vaccination in young generation on prevention of local COVID-19 spread in Japan.* J Infect, 2020.
553. Covian, C., et al., *Could BCG Vaccination Induce Protective Trained Immunity for SARS-CoV-2?* Front Immunol, 2020. **11**: p. 970.
554. Khan, N., et al., *M. tuberculosis Reprograms Hematopoietic Stem Cells to Limit Myelopoiesis and Impair Trained Immunity.* Cell, 2020. **183**(3): p. 752-770 e22.
555. Cunha, S.S., et al., *Neonatal BCG protection against leprosy: a study in Manaus, Brazilian Amazon.* Lepr Rev, 2004. **75**(4): p. 357-66.
556. Higgins, J.P., et al., *Association of BCG, DTP, and measles containing vaccines with childhood mortality: systematic review.* BMJ, 2016. **355**: p. i5170.
557. Walker, V., G. Selby, and I. Wacogne, *Does neonatal BCG vaccination protect against tuberculous meningitis?* Arch Dis Child, 2006. **91**(9): p. 789-91.
558. Rodrigues, L.C., P. Mangtani, and I. Abubakar, *How does the level of BCG vaccine protection against tuberculosis fall over time?* BMJ, 2011. **343**: p. d5974.
559. Tribouley, J., J. Tribouley-Duret, and M. Appriou, *[Effect of Bacillus Callmette Guerin (BCG) on the receptivity of nude mice to Schistosoma mansoni].* C R Seances Soc Biol Fil, 1978. **172**(5): p. 902-4.
560. Torre, C., et al., *Staphylococcus aureus Promotes Smed-PGRP-2/Smed-setd8-1 Methyltransferase Signalling in Planarian Neoblasts to Sensitize Anti-bacterial Gene Responses During Re-infection.* EBioMedicine, 2017. **20**: p. 150-160.
561. Wong Fok Lung, T., et al., *Staphylococcus aureus small colony variants impair host immunity by activating host cell glycolysis and inducing necroptosis.* Nat Microbiol, 2020. **5**(1): p. 141-153.
562. Redelman-Sidi, G., M.S. Glickman, and B.H. Bochner, *The mechanism of action of BCG therapy for bladder cancer--a current perspective.* Nat Rev Urol, 2014. **11**(3): p. 153-62.
563. Powles, R.L., et al., *Maintenance of remission in acute myelogenous leukaemia by a mixture of B.C.G. and irradiated leukaemia cells.* Lancet, 1977. **2**(8048): p. 1107-10.
564. Stewart, J.H.t. and E.A. Levine, *Role of bacillus Calmette-Guerin in the treatment of advanced melanoma.* Expert Rev Anticancer Ther, 2011. **11**(11): p. 1671-6.
565. Bekkering, S., et al., *Trained innate immunity and atherosclerosis.* Curr Opin Lipidol, 2013. **24**(6): p. 487-92.
566. Leentjens, J., et al., *Trained Innate Immunity as a Novel Mechanism Linking Infection and the Development of Atherosclerosis.* Circ Res, 2018. **122**(5): p. 664-669.
567. Bekkering, S., et al., *Innate immune cell activation and epigenetic remodeling in symptomatic and asymptomatic atherosclerosis in humans in vivo.* Atherosclerosis, 2016. **254**: p. 228-236.
568. Shirai, T., et al., *The glycolytic enzyme PKM2 bridges metabolic and inflammatory dysfunction in coronary artery disease.* J Exp Med, 2016. **213**(3): p. 337-54.
569. Mulder, W.J.M., et al., *Therapeutic targeting of trained immunity.* Nat Rev Drug Discov, 2019.
570. Dabritz, J. and T.R. Menheniott, *Linking immunity, epigenetics, and cancer in inflammatory bowel disease.* Inflamm Bowel Dis, 2014. **20**(9): p. 1638-54.
571. Noz, M.P., et al., *Trained Immunity Characteristics Are Associated With Progressive Cerebral Small Vessel Disease.* Stroke, 2018. **49**(12): p. 2910-2917.
572. Braza, M.S., et al., *Inhibiting Inflammation with Myeloid Cell-Specific Nanobiologics Promotes Organ Transplant Acceptance.* Immunity, 2018. **49**(5): p. 819-828 e6.
573. Ristori, G., et al., *Use of Bacille Calmette-Guerin (BCG) in multiple sclerosis.* Neurology, 1999. **53**(7): p. 1588-9.

574. Ristori, G., et al., *Effects of Bacille Calmette-Guerin after the first demyelinating event in the CNS.* Neurology, 2014. **82**(1): p. 41-8.
575. Kalafati, L., et al., *Innate Immune Training of Granulopoiesis Promotes Anti-tumor Activity.* Cell, 2020. **183**(3): p. 771-785 e12.
576. Rosenberg, H.F., K.D. Dyer, and P.S. Foster, *Eosinophils: changing perspectives in health and disease.* Nat Rev Immunol, 2013. **13**(1): p. 9-22.
577. Goh, Y.P., et al., *Eosinophils secrete IL-4 to facilitate liver regeneration.* Proc Natl Acad Sci U S A, 2013. **110**(24): p. 9914-9.
578. Heredia, J.E., et al., *Type 2 innate signals stimulate fibro/adipogenic progenitors to facilitate muscle regeneration.* Cell, 2013. **153**(2): p. 376-88.
579. Takeda, K., et al., *Eosinophils contribute to the resolution of lung-allergic responses following repeated allergen challenge.* J Allergy Clin Immunol, 2015. **135**(2): p. 451-60.
580. Coden, M.E. and S. Berdnikovs, *Eosinophils in wound healing and epithelial remodeling: Is coagulation a missing link?* J Leukoc Biol, 2020.
581. Lee, J.J., et al., *Eosinophils in health and disease: the LIAR hypothesis.* Clin Exp Allergy, 2010. **40**(4): p. 563-75.
582. Doherty, T.A. and D.H. Broide, *Airway innate lymphoid cells in the induction and regulation of allergy.* Allergol Int, 2019. **68**(1): p. 9-16.
583. Wang, X., et al., *Memory formation and long-term maintenance of IL-7Ralpha(+) ILC1s via a lymph node-liver axis.* Nat Commun, 2018. **9**(1): p. 4854.
584. Bossel Ben-Moshe, N., et al., *Predicting bacterial infection outcomes using single cell RNA-sequencing analysis of human immune cells.* Nat Commun, 2019. **10**(1): p. 3266.
585. Stacy, A., et al., *Infection trains the host for microbiota-enhanced resistance to pathogens.* Cell, 2021. **184**(3): p. 615-627 e17.
586. Brook, B., et al., *BCG vaccination-induced emergency granulopoiesis provides rapid protection from neonatal sepsis.* Sci Transl Med, 2020. **12**(542).
587. Perez, M.F. and B. Lehner, *Intergenerational and transgenerational epigenetic inheritance in animals.* Nat Cell Biol, 2019. **21**(2): p. 143-151.
588. Peters, J., *The role of genomic imprinting in biology and disease: an expanding view.* Nat Rev Genet, 2014. **15**(8): p. 517-30.
589. Hammoud, S.S., et al., *Distinctive chromatin in human sperm packages genes for embryo development.* Nature, 2009. **460**(7254): p. 473-8.
590. Jacquemont, S., et al., *Mirror extreme BMI phenotypes associated with gene dosage at the chromosome 16p11.2 locus.* Nature, 2011. **478**(7367): p. 97-102.
591. Gaydos, L.J., W. Wang, and S. Strome, *Gene repression. H3K27me and PRC2 transmit a memory of repression across generations and during development.* Science, 2014. **345**(6203): p. 1515-8.
592. Alhazzazi, T.Y., et al., *A Novel Sirtuin-3 Inhibitor, LC-0296, Inhibits Cell Survival and Proliferation, and Promotes Apoptosis of Head and Neck Cancer Cells.* Anticancer Res, 2016. **36**(1): p. 49-60.
593. Grishok, A., H. Tabara, and C.C. Mello, *Genetic requirements for inheritance of RNAi in C. elegans.* Science, 2000. **287**(5462): p. 2494-7.
594. Luteijn, M.J. and R.F. Ketting, *PIWI-interacting RNAs: from generation to transgenerational epigenetics.* Nat Rev Genet, 2013. **14**(8): p. 523-34.
595. Bagijn, M.P., et al., *Function, targets, and evolution of Caenorhabditis elegans piRNAs.* Science, 2012. **337**(6094): p. 574-578.
596. Heard, E. and R.A. Martienssen, *Transgenerational epigenetic inheritance: myths and mechanisms.* Cell, 2014. **157**(1): p. 95-109.
597. Eggert, H., J. Kurtz, and M.F. Diddens-de Buhr, *Different effects of paternal trans-generational immune priming on survival and immunity in step and genetic offspring.* Proc Biol Sci, 2014. **281**(1797).

598. Hernandez Lopez, J., et al., *Trans-generational immune priming in honeybees.* Proc Biol Sci, 2014. **281**(1785): p. 20140454.
599. Ramanan, D., et al., *An Immunologic Mode of Multigenerational Transmission Governs a Gut Treg Setpoint.* Cell, 2020. **181**(6): p. 1276-1290 e13.
600. Bomans, K., et al., *Paternal sepsis induces alterations of the sperm methylome and dampens offspring immune responses-an animal study.* Clin Epigenetics, 2018. **10**: p. 89.
601. Niedzwiecki, M., et al., *Prenatal exposure to allergen, DNA methylation, and allergy in grandoffspring mice.* Allergy, 2012. **67**(7): p. 904-10.
602. Maslowski, K.M., et al., *Regulation of inflammatory responses by gut microbiota and chemoattractant receptor GPR43.* Nature, 2009. **461**(7268): p. 1282-6.
603. Hah, Y.S., et al., *Myeloid deletion of SIRT1 aggravates serum transfer arthritis in mice via nuclear factor-kappaB activation.* PLoS One, 2014. **9**(2): p. e87733.
604. Fedulov, A.V. and L. Kobzik, *Allergy risk is mediated by dendritic cells with congenital epigenetic changes.* Am J Respir Cell Mol Biol, 2011. **44**(3): p. 285-92.
605. Gregory, D.J., et al., *Transgenerational transmission of asthma risk after exposure to environmental particles during pregnancy.* Am J Physiol Lung Cell Mol Physiol, 2017. **313**(2): p. L395-L405.
606. Blumer, N., et al., *Prenatal lipopolysaccharide-exposure prevents allergic sensitization and airway inflammation, but not airway responsiveness in a murine model of experimental asthma.* Clin Exp Allergy, 2005. **35**(3): p. 397-402.
607. Blumer, N., et al., *Perinatal maternal application of Lactobacillus rhamnosus GG suppresses allergic airway inflammation in mouse offspring.* Clin Exp Allergy, 2007. **37**(3): p. 348-57.
608. Brand, S., et al., *Epigenetic regulation in murine offspring as a novel mechanism for transmaternal asthma protection induced by microbes.* J Allergy Clin Immunol, 2011. **128**(3): p. 618-25 e1-7.
609. Netea, M.G., et al., *Defining trained immunity and its role in health and disease.* Nat Rev Immunol, 2020. **20**(6): p. 375-388.
610. Ochando, J., et al., *Trained immunity in organ transplantation.* Am J Transplant, 2020. **20**(1): p. 10-18.
611. van Tuijl, J., et al., *Immunometabolism orchestrates training of innate immunity in atherosclerosis.* Cardiovasc Res, 2019. **115**(9): p. 1416-1424.
612. Dai, H., et al., *PIRs mediate innate myeloid cell memory to nonself MHC molecules.* Science, 2020. **368**(6495): p. 1122-1127.
613. Temba, G.S., et al., *Urban living in healthy Tanzanians is associated with an inflammatory status driven by dietary and metabolic changes.* Nat Immunol, 2021. **22**(3): p. 287-300.
614. Lugrin, J., et al., *Murine Myocardial Infarction Model using Permanent Ligation of Left Anterior Descending Coronary Artery.* J Vis Exp, 2019(150).
615. Koelwyn, G.J., et al., *Myocardial infarction accelerates breast cancer via innate immune reprogramming.* Nat Med, 2020. **26**(9): p. 1452-1458.
616. van der Meer, J.W., et al., *Hyperimmunoglobulinaemia D and periodic fever: a new syndrome.* Lancet, 1984. **1**(8386): p. 1087-90.
617. Gregorio, J., et al., *Plasmacytoid dendritic cells sense skin injury and promote wound healing through type I interferons.* J Exp Med, 2010. **207**(13): p. 2921-30.
618. Di Domizio, J., et al., *The commensal skin microbiota triggers type I IFN-dependent innate repair responses in injured skin.* Nat Immunol, 2020. **21**(9): p. 1034-1045.
619. Aaby, P., et al., *Measles vaccination and reduction in child mortality: a community study from Guinea-Bissau.* J Infect, 1984. **8**(1): p. 13-21.
620. Kristensen, I., P. Aaby, and H. Jensen, *Routine vaccinations and child survival: follow up study in Guinea-Bissau, West Africa.* BMJ, 2000. **321**(7274): p. 1435-8.
621. Roth, A., et al., *Tuberculin reaction, BCG scar, and lower female mortality.* Epidemiology, 2006. **17**(5): p. 562-8.

622. Nicorescu, I., et al., *Potential epigenetic therapeutics for atherosclerosis treatment.* Atherosclerosis, 2019. **281**: p. 189-197.
623. Zinocker, M.K. and I.A. Lindseth, *The Western Diet-Microbiome-Host Interaction and Its Role in Metabolic Disease.* Nutrients, 2018. **10**(3).
624. Rosshart, S.P., et al., *Wild Mouse Gut Microbiota Promotes Host Fitness and Improves Disease Resistance.* Cell, 2017. **171**(5): p. 1015-1028 e13.
625. Pamer, E.G., *Fecal microbiota transplantation: effectiveness, complexities, and lingering concerns.* Mucosal Immunol, 2014. **7**(2): p. 210-4.
626. Hotchkiss, R.S., G. Monneret, and D. Payen, *Sepsis-induced immunosuppression: from cellular dysfunctions to immunotherapy.* Nat Rev Immunol, 2013. **13**(12): p. 862-74.
627. Lanier, L.L., *NKG2D Receptor and Its Ligands in Host Defense.* Cancer Immunol Res, 2015. **3**(6): p. 575-82.
628. Silverstein, N.J., et al., *Innate lymphoid cells and disease tolerance in SARS-CoV-2 infection.* medRxiv, 2021.
629. Guo, X. and Y.X. Fu, *The tragic fate of group 3 innate lymphoid cells during HIV-1 infection.* J Clin Invest, 2015. **125**(10): p. 3992.
630. Mudd, J.C. and J.M. Brenchley, *ILC You Later: Early and Irreparable Loss of Innate Lymphocytes in HIV Infection.* Immunity, 2016. **44**(2): p. 216-8.
631. Singh, A., et al., *Innate Lymphoid Cell Activation and Sustained Depletion in Blood and Tissue of Children Infected with HIV from Birth Despite Antiretroviral Therapy.* Cell Rep, 2020. **32**(11): p. 108153.
632. Xu, H., et al., *IL-17-producing innate lymphoid cells are restricted to mucosal tissues and are depleted in SIV-infected macaques.* Mucosal Immunol, 2012. **5**(6): p. 658-69.
633. Zhang, Z., et al., *Plasmacytoid dendritic cells promote HIV-1-induced group 3 innate lymphoid cell depletion.* J Clin Invest, 2015. **125**(9): p. 3692-703.
634. Kloverpris, H.N., et al., *Innate Lymphoid Cells Are Depleted Irreversibly during Acute HIV-1 Infection in the Absence of Viral Suppression.* Immunity, 2016. **44**(2): p. 391-405.
635. Wang, Y., et al., *HIV-1-induced cytokines deplete homeostatic innate lymphoid cells and expand TCF7-dependent memory NK cells.* Nat Immunol, 2020. **21**(3): p. 274-286.
636. Cruz-Zarate, D., et al., *Innate Lymphoid Cells Have Decreased HLA-DR Expression but Retain Their Responsiveness to TLR Ligands during Sepsis.* J Immunol, 2018. **201**(11): p. 3401-3410.
637. Cazalis, M.A., et al., *Decreased HLA-DR antigen-associated invariant chain (CD74) mRNA expression predicts mortality after septic shock.* Crit Care, 2013. **17**(6): p. R287.
638. Baban, B., et al., *Presence and Profile of Innate Lymphoid Cells in Human Breast Milk.* JAMA Pediatr, 2018. **172**(6): p. 594-596.
639. Germain, R.N. and Y. Huang, *ILC2s - resident lymphocytes pre-adapted to a specific tissue or migratory effectors that adapt to where they move?* Curr Opin Immunol, 2019. **56**: p. 76-81.
640. Xu, H., et al., *Interleukin-33 contributes to ILC2 activation and early inflammation-associated lung injury during abdominal sepsis.* Immunol Cell Biol, 2018. **96**(9): p. 935-947.
641. Lai, D., et al., *Group 2 innate lymphoid cells protect lung endothelial cells from pyroptosis in sepsis.* Cell Death Dis, 2018. **9**(3): p. 369.

6. APPENDIX

This part is divided into five sections:

6.1 Sirtuin 2 Deficiency Increases Bacterial Phagocytosis by Macrophages and Protects from Chronic Staphylococcal Infection

6.2 Sirtuin 5 Deficiency Does Not Compromise Innate Immune Responses to Bacterial Infections

6.3 Regulation of inflammation and protection against invasive pneumococcal infection by the long pentraxin PTX3

6.4 Myeloid-Derived Suppressor Cells in Sepsis

6.5 Macrophage migration inhibitory factor promotes the migration of dendritic cells through CD74 and the activation of the Src/PI3K/myosin II pathway

6.6 The big sepsis game

6.1. Sirtuin 2 Deficiency Increases Bacterial Phagocytosis by Macrophages and Protects from Chronic Staphylococcal Infection

Eleonora Ciarlo [1], Tytti Heinonen [1], Charlotte Théroude [1], Jacobus Herderschee [1], Matteo Mombelli [1], Jérôme Lugrin [1], Marc Pfefferlé [1], Beatrice Tyrrell [1], Sarah Lensch [1], Hans Acha-Orbea [2], Didier Le Roy [1], Johan Auwerx [3], Thierry Roger [1]

[1]Infectious Diseases Service, Department of Medicine, Lausanne University Hospital and University of Lausanne, Epalinges, Switzerland

[2] Department of Biochemistry, University of Lausanne, Epalinges, Switzerland.

[3] Laboratory for Integrative and Systems Physiology, Ecole Polytechnique Fédérale de Lausanne, Lausanne, Switzerland.

Front Immunol. 2017 Aug 28;8:1037. doi: 10.3389/fimmu.2017.01037. eCollection 2017.

Contribution to the work: I participated to *in vivo* experiments.

frontiers in Immunology

ORIGINAL RESEARCH
published: 28 August 2017
doi: 10.3389/fimmu.2017.01037

Sirtuin 2 Deficiency Increases Bacterial Phagocytosis by Macrophages and Protects from Chronic Staphylococcal Infection

*Eleonora Ciarlo[1], Tytti Heinonen[1], Charlotte Théroude[1], Jacobus Herderschee[1], Matteo Mombelli[1], Jérôme Lugrin[1], Marc Pfefferlé[1], Beatrice Tyrrell[1], Sarah Lensch[1], Hans Acha-Orbea[2], Didier Le Roy[1], Johan Auwerx[3] and Thierry Roger[1]**

[1] Infectious Diseases Service, Department of Medicine, Lausanne University Hospital, Epalinges, Switzerland, [2] Department of Biochemistry, University of Lausanne, Epalinges, Switzerland, [3] Laboratory for Integrative and Systems Physiology, Ecole Polytechnique Fédérale de Lausanne, Lausanne, Switzerland

OPEN ACCESS

Edited by:
Abhay Satoskar, The Ohio State University Columbus, United States

Reviewed by:
Ricardo Silvestre, Instituto de Pesquisa em Ciências da Vida e da Saúde (ICVS), Portugal
Paras K. Anand, Imperial College London, United Kingdom

***Correspondence:**
Thierry Roger
thierry.roger@chuv.ch

Specialty section:
This article was submitted to Microbial Immunology, a section of the journal Frontiers in Immunology

Received: 08 April 2017
Accepted: 11 August 2017
Published: 28 August 2017

Citation:
Ciarlo E, Heinonen T, Théroude C, Herderschee J, Mombelli M, Lugrin J, Pfefferlé M, Tyrrell B, Lensch S, Acha-Orbea H, Le Roy D, Auwerx J and Roger T (2017) Sirtuin 2 Deficiency Increases Bacterial Phagocytosis by Macrophages and Protects from Chronic Staphylococcal Infection. Front. Immunol. 8:1037. doi: 10.3389/fimmu.2017.01037

Sirtuin 2 (SIRT2) is one of the seven members of the family of NAD^+-dependent histone deacetylases. Sirtuins target histones and non-histone proteins according to their sub-cellular localization, influencing various biological processes. SIRT2 resides mainly in the cytoplasm and regulates cytoskeleton dynamics, cell cycle, and metabolic pathways. As such, SIRT2 has been implicated in the pathogenesis of neurodegenerative, metabolic, oncologic, and chronic inflammatory disorders. This motivated the development of SIRT2-directed therapies for clinical purposes. However, the impact of SIRT2 on anti-microbial host defense is largely unknown. Here, we address this question using SIRT2 knockout mice. We show that SIRT2 is the most highly expressed sirtuin in myeloid cells, especially macrophages. SIRT2 deficiency does not affect immune cell development and marginally impacts on intracellular signaling and cytokine production by splenocytes and macrophages. However, SIRT2 deficiency enhances bacterial phagocytosis by macrophages. In line with these observations, in preclinical models, SIRT2 deficiency increases survival of mice with chronic staphylococcal infection, while having no effect on the course of toxic shock syndrome toxin-1, LPS or TNF-induced shock, fulminant *Escherichia coli* peritonitis, sub-lethal *Klebsiella pneumoniae* pneumonia, and chronic candidiasis. Altogether, these data support the safety profile of SIRT2 inhibitors under clinical development in terms of susceptibility to infections.

Keywords: sirtuin, innate immunity, cytokine, macrophage, phagocytosis, sepsis, histone deacetylase, metabolism

INTRODUCTION

Innate immune cells are at the vanguard of host defense against microbial infections. Monocytes/macrophages and dendritic cells (DCs) sense microbial or danger-associated molecular patterns (MAMPs and DAMPs released by injured or stressed cells) through pattern recognition receptors (PRRs) such as toll-like receptors (TLRs), NOD-like receptors, C-type lectins, scavenger receptors, RIG-I-like receptors, and intra-cytosolic DNA sensors (1, 2). The interaction of MAMPs or DAMPs with PRRs triggers the mitogen-activated protein kinases (MAPKs), nuclear factor-κB (NF-κB), and interferon (IFN) response factor signaling pathways that coordinate immune gene expression. The

cellular and soluble mediators mobilized upon infection tightly regulate the development of the inflammatory response, the establishment of antimicrobial cellular and humoral responses, and the restoration of homeostasis once pathogens have been contained or eradicated.

The superfamily of histone deacetylases (HDACs) comprises eleven Zn-dependent HDACs (HDAC1-11) and seven NAD^+-dependent sirtuins (SIRT1-7). HDACs are epigenetic erasers catalyzing histone deacetylation, chromatin compaction, and transcriptional repression. In addition, HDACs target thousands of non-histone proteins affecting many biological processes (3). The subfamily of sirtuins attracted much interest when sirtuins were proposed to promote longevity and represent attractive therapeutic targets for age-related pathologies, such as type 2 diabetes, as well as neurodegenerative, cardiovascular, and oncologic diseases (4–6). Our knowledge about the impact of sirtuins on innate immune responses is limited. Most studies have focused on SIRT1 and SIRT6, resulting in an overall complex picture attributing both proinflammatory and anti-inflammatory properties to sirtuins (7).

Sirtuin 2 (SIRT2) was originally reported to colocalize with the microtubule network and to deacetylate α-tubulin (8). Indeed, SIRT2 is mainly cytoplasmic, although it can translocate during the G2/M transition phase of cell cycle into the nucleus where it deacetylates histone H4 lysine 16 (9). Of note, SIRT2 possesses a proficient demyristoylation activity, the physiological relevance of which remains to be established (10). By targeting numerous proteins besides histones, SIRT2 regulates cytoskeleton dynamics, cell cycle, and metabolic pathways including inhibition of adipogenesis and promotion of lipolysis and gluconeogenesis. Additionally, SIRT2 can act as a tumor suppressor gene, and is involved in myelogenesis and other brain functions. Accordingly, SIRT2 has been implicated in tumorigenesis and neurodegeneration, and likely plays a role in metabolic disorders, such as obesity and type 2 diabetes (11–13).

With respect to inflammatory processes, SIRT2 was first shown to deacetylate NF-κB p65, resulting in the expression of a subset of p65-dependent genes in mouse embryonic fibroblasts (14). SIRT2 deficiency sustained brain inflammation in a model of traumatic brain injury and increased the severity of collagen-induced arthritis and colitis (15–17). However, SIRT2 deficiency was also reported to decrease NF-κB p65-mediated inflammatory response, renal tubular inflammation, and ischemia reperfusion-induced hepatocellular inflammation (18–20). Finally, in an experimental stroke model, SIRT2 deficiency preserved neurological functions without affecting inflammatory parameters (21). Overall, the function of SIRT2 in sterile and chronic inflammatory disorders appears to be context dependent.

Because sirtuins are pleiotropic and in consideration of the development of sirtuin-targeting drugs for clinical conditions, we sought to delineate the role of SIRT2 in the innate immune response. To this end, we used SIRT2 knockout mice to investigate the response of immune cells to immunological and microbial stimuli using *in vitro* experiments and *in vivo* preclinical models. Preclinical models included models of shock as well as Gram-negative and Gram-positive bacterial infections and fungal infection. Overall, SIRT2 deficiency does not modulate cytokine production by innate immune cells, but enhances bacterial phagocytosis by macrophages. SIRT2 deficiency protects from chronic staphylococcal infection, while having no impact on toxic shock, endotoxemia, fulminant peritonitis, non-lethal pneumonia, and chronic candidiasis. These data largely support the safety, in terms of susceptibility to infections, of SIRT2 inhibitors developed for clinical applications.

MATERIALS AND METHODS

Mice, Cells, and Reagents

8- to 12-week-old female BALB/cByJ mice, C57BL/6J mice (Charles River Laboratories, Saint-Germain-sur-l'Arbresle, France), and SIRT2 knockout mice backcrossed 12 times on a C57BL/6J background (15) were used. Mice were housed under specific pathogen-free conditions and free of mouse norovirus. Splenocytes were cultured in RPMI 1640 medium containing 2 mM glutamine, 50 µM 2-ME, 100 IU/ml penicillin, 100 µg/ml streptomycin (Invitrogen, San Diego, CA) and 10% heat-inactivated fetal calf serum (FCS; Sigma-Aldrich, St. Louis, MO) (22). Bone marrow (BM) cells were cultured in IMDM (Invitrogen) containing 50 µM 2-ME, penicillin, streptomycin, and 10% FCS. Medium was supplemented with 20 ng/ml M-CSF, 20 ng/ml GM-CSF plus 20 ng/ml IL-4 (ProSpec, East Brunswick, NJ) or 200 ng/ml FMS-like tyrosine kinase 3 ligand (Flt3L, Shenandoah biotechnology, Warwick, PA) to generate BM-derived macrophages (BMDMs), BM-derived dendritic cells (BMDCs), or Flt3L-DCs, respectively. BMDCs were collected after 6 days. BMDMs and Flt3L-DCs were collected after 7 days of culture. Cells (1, 5, and 20 × 10^5) were seeded in 96-well, 24-well or 6-well plates in complete medium without growth factors and antibiotics unless specified.

Salmonella minnesota ultra pure lipopolysaccharide (LPS) was from List Biologicals Laboratories (Campbell, CA), Pam_3CSK_4 from EMC microcollections (Tübingen, Germany), CpG ODN 1826 (CpG) from InvivoGen (San Diego, CA, USA), toxic shock syndrome toxin-1 (TSST-1) and staphylococcal enterotoxin B (SEB) from Toxin Technology (Sarasota, FL, USA), concanavalin A and phytohemagglutinin (PHA) from Sigma-Aldrich, and anti-CD3ε and anti-CD28 antibodies (clones 145-2C11 and 37.51) from eBioscience (San Diego, CA, USA). Clinical strains of *Escherichia coli* (*E. coli*) O18, *E. coli* J5, *E. coli* O111, *Salmonella enterica* serovar Typhimurium C5 (*Salmonella* Typhimurium), *Klebsiella pneumoniae* caroli (*K. pneumoniae*), *Neisseria meningitis*, *Streptococcus pneumoniae*, *Staphylococcus aureus* AW7 (*S. aureus*), and Group B *Streptococcus* (GBS) were grown in brain heart infusion broth (BD Biosciences, Erembodegem, Belgium) (23–27). *Candida albicans* 5102 (*C. albicans*) (22) was cultured in yeast extract–peptone–dextrose (BD Biosciences). Microorganisms were washed in PBS and adjusted at 10^{10} CFU/ml. For *in vitro* stimulation, bacteria were heat-inactivated for 2 h at 56°C. Nocodazole and 2-deoxyglucose were from Sigma-Aldrich, cytochalasin D from Millipore (Billerica, MA, USA).

RNA Analyses

Total RNA was isolated, reverse transcribed (RNeasy and QuantiTect reverse transcription kits, Qiagen, Hilden, Germany),

and used in real-time PCRs conducted with a QuantStudio™ 12K Flex system (Life Technologies, Carlsbad, CA, USA). Reactions consisted of 1.25 µl cDNA, 1.25 µl H_2O, 0.62 µl 10 nM primers [Table S1 in Supplementary Material and Ref. (28, 29)], and 3.12 µl Fast SYBR® Green Master Mix (Life Technologies) and were tested in triplicate. Gene specific expression was normalized to hypoxanthine guanine phosphoribosyl transferase expression. Sirt2 expression levels in organs were extracted from the BioGPS resource (http://biogps.org).

Western Blot Analyses

Nuclear and total protein extracts were submitted to PAGE and transferred onto nitrocellulose membranes (30, 31). Membranes were incubated with antibodies directed against SIRT2, acetylated α-tubulin, total α-tubulin, total and phosphorylated ERK1/2, p38, JNK, and NF-κB p65 and TATA-box binding protein (used as a control of nuclear extracts) (see antibody description in Table S2 in Supplementary Material), then with a secondary horseradish peroxidase-conjugated antibody (Sigma-Aldrich) (32). Blots were imaged with the enhanced chemiluminescence Western blotting system (GE Healthcare, Little Chalfont, Royaume-Uni). Images were recorded using a Fusion Fx system (Viber Lourmat, Collégien, France).

Flow Cytometry

Single cell suspensions from thymus and spleen, or BMDMs were enumerated and incubated with 2.4G2 monoclonal antibody (mAb). Immune cell subpopulations were tracked by staining performed using mAbs described in Table S2 in Supplementary Material. Splenic $CD4^+$ $CD25^+$ $Foxp3^+$ cells were detected using The Mouse Regulatory T Cell Staining Kit (eBioscience). Data were acquired using a LSR II flow cytometer (BD Biosciences) and analyzed using FlowJo Version 10.2 software (FlowJo LLC, Ashland, OR, USA) (33).

Proliferation Assay

The proliferation of 1.5×10^5 splenocytes cultured for 48 h in 96-well plates was quantified by measuring ^{3}H-thymidine incorporation over 18 h (34).

Cytokine Measurements

Cytokine concentrations were quantified using DuoSet ELISA kits (R&D Systems, Abingdon, UK) or Luminex assays (Affimetrix eBioscience, Vienna, Austria) (35).

In Vivo Models

8- to 12-week-old female $SIRT2^{+/+}$ and $SIRT2^{-/-}$ mice (6–13 mice per group) matched for age were used. To analyze the response to TSST-1, mice were challenged intraperitoneally (i.p.) with TSST-1 (0.5 mg/kg). Models of endotoxic shock were performed by challenging mice i.p. with LPS (10 and 25 mg/kg). To induce TNF shock, mice were sensitized with D-galactosamine (30 mg/kg i.p., Sigma-Aldrich) just before being challenged with TNF (25 mg/kg i.p., Preprotech, Rocky Hill, NJ, USA). Bacterial sepsis was induced by challenging mice i.p. with 10^5 CFU *E. coli* O18, intravenously (i.v.) with 10^7 CFU *S. aureus* or 10^5 CFU *C. albicans* or intranasally (i.n.) with 30 CFU *K. pneumoniae*. Blood and spleen were collected 0, 1, 6, 8, 24, or 48 h post-challenge to quantify cytokines and bacteria (28). Body weight loss, severity score, and survival were registered at least once daily. The severity score was graded from 1 to 5 (36). Animals were euthanized when they met a severity score of 4. Two to three operators performed animal follow-up.

Phagocytosis Assays

Fluoresbrite® Yellow Green Microspheres (Polysciences Inc, Warrington, PA, USA) or FITC-labeled bacteria were added to cells at a ratio of 10 beads or bacteria/cell. After 1 h, cells were washed, incubated for 1 min with trypan blue (0.25 mg/ml) and analyzed by flow cytometry. When specified, beads were opsonized with serum for 30 min at 37°C. To assess phagocytosis of live bacteria, BMDMs (in quadruplicates or sextuplates) were incubated for 1 h with *E. coli* O18, *S. aureus*, and GBS (10 bacteria/cell). Non-adherent and extracellular bacteria were removed by washing and killed by a 30-min exposure to 100 µg/ml gentamicin (Essex Chemie, Luzern, Switzerland; for *E. coli* and GBS) or 10 µg/ml ciprofloxacin (Fresenius Kabi, Oberdorf, Switzerland; for *S. aureus*). Serial dilutions of cell lysates were plated on agar plates. Colonies were enumerated to calculate the number of phagocytosed bacteria.

Glycolytic Activity

The glycolytic activity of BMDMs was analyzed using a 96-well format Seahorse XFe® system and the Seahorse XF Glycolysis Stress Test Kit (Agilent Technologies, Santa Clara, CA, USA). Briefly, 4×10^4 BMDMs were plated in 96-well plates in IMDM medium. The next day, cells were incubated with or without 5×10^7 CFU/ml heat-killed *S. aureus* and rested 1 h in Seahorse medium without glucose. The glycolytic capacity was assessed by measuring the extracellular acidification rate following the sequentially addition of 10 mM glucose, 1 µM oligomycin, and 50 mM 2-deoxy-glucose (2-DG) according to manufacturer's instructions.

Statistical Analyses

Comparisons between the different groups were performed by analysis of variance followed by two-tailed unpaired Student's *t*-test. The Kaplan–Meier method was used for building survival curves and differences were analyzed by the log-rank sum test. All analyses were performed using PRISM (GraphPad Software). *P* values were two-sided, and $P < 0.05$ was considered to indicate statistical significance.

RESULTS

SIRT2 Is Highly Expressed by Myeloid Cells

SIRT1-7 mRNA expression was quantified in BM, BMDMs, and DCs (conventional BMDCs and Flt3L-derived DCs) (**Figure 1A**). SIRT2 was the most highly expressed sirtuin in all populations. SIRT2 was also the predominantly expressed sirtuin in RAW 264.7

macrophages and in the spleen, liver, and kidneys (**Figure 1B** and data not shown). Western blot analyses confirmed SIRT2 protein expression in BMDMs (see below). Primary osteoblasts, osteoclasts, macrophages, and mast cells expressed 2.6-fold to 7.1-fold higher levels of SIRT2 mRNA than granulocytes, NK cells, T cells, B cells, DCs, and thymocytes (**Figure 1C**). Overall, SIRT2 was highly expressed by myeloid-derived cells, suggesting that it could play a role in the control of immune responses. To address this question, SIRT2-deficient mice were used [**Figures 1D,E** and Ref. (15)].

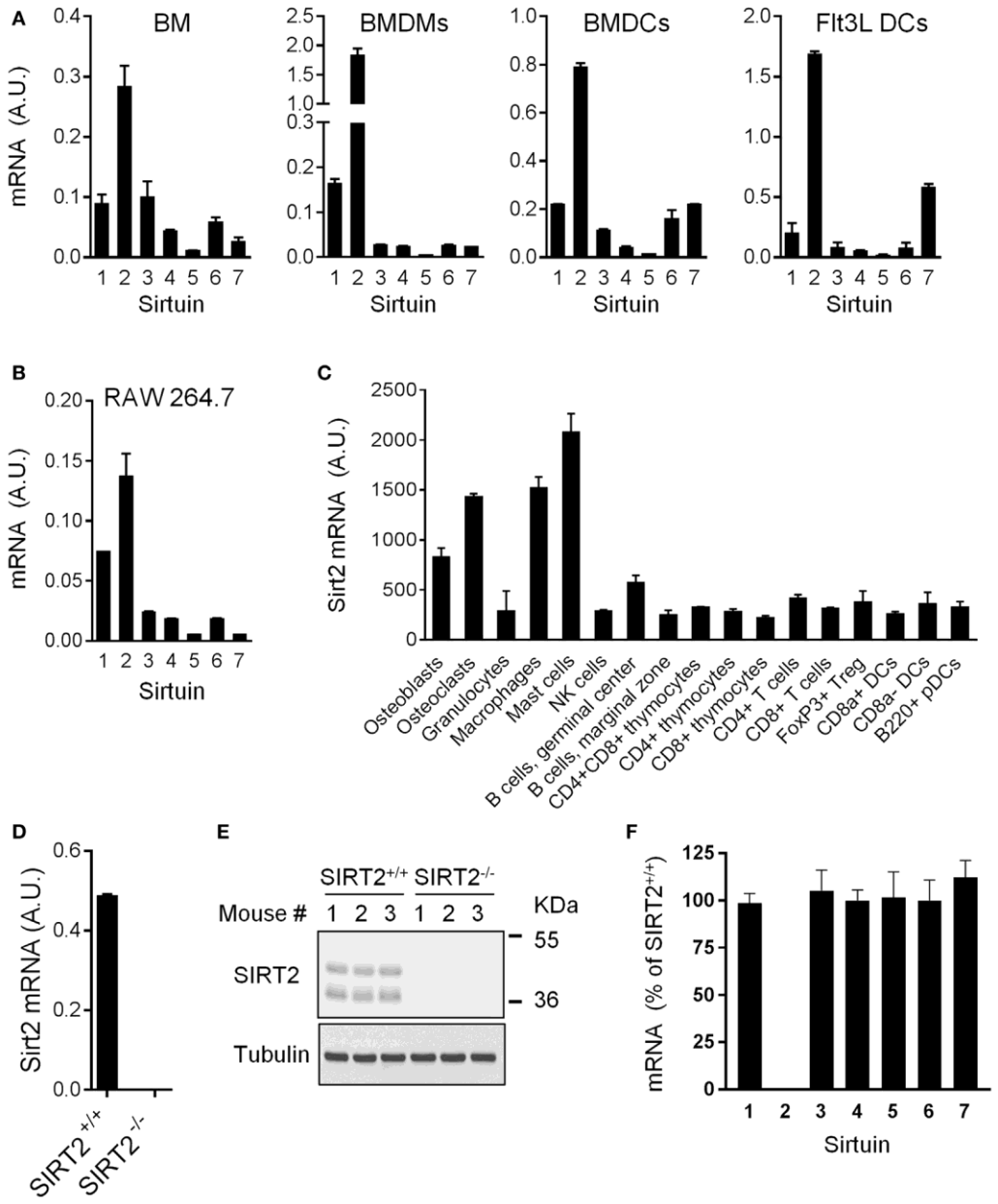

FIGURE 1 | Sirt2 is strongly expressed in myeloid cells. **(A,B)** Sirt1-7 mRNA levels in bone marrow (BM), BM-derived macrophages (BMDMs) and dendritic cells (BMDCs), and Flt3L-derived DCs **(A)** and RAW 264.7 macrophages **(B)** analyzed by RT-PCR and normalized to Hprt mRNA levels. Data are means ± SD of triplicate samples from one experiment performed with four BALB/c mice **(A)** or three preparations of RAW 264.7 macrophages **(B)**. **(C)** Sirt2 mRNA expression levels in a panel of cells (extracted from http://biogps.org). **(D,E)** Sirt2 mRNA **(D)** and Sirtuin 2 (SIRT2) protein **(E)** expression in $SIRT2^{+/+}$ and $SIRT2^{-/-}$ BMDMs assessed by RT-PCR and western blotting, respectively. Data are means ± SD from one experiment performed with three mice **(D)**. **(F)** Sirt1-7 mRNA expression levels in $SIRT2^{-/-}$ BMDMs, expressed relative to the mRNA levels in $SIRT2^{+/+}$ BMDMs set at 100%. Data are means ± SD from one experiment performed with three mice. A.U., arbitrary units. Full-length blots of panel **(E)** are presented in Figure S1 in Supplementary Material.

SIRT2 Deficiency Has No Major Impact on the Development of Immune Cells and Host Response to TSST-1

SIRT2$^{-/-}$ mice were described previously (15). These mice were born at the expected Mendelian ratio and developed without abnormalities. SIRT2 mRNA and protein were undetectable in SIRT2$^{-/-}$ BMDMs (**Figures 1D,E**). Expression levels of Sirt1 and Sirt3-7 mRNA were unaltered in SIRT2$^{-/-}$ BMDMs (**Figure 1F**), suggesting that the lack of SIRT2 was not compensated by an increase in expression of other sirtuins.

Compared to SIRT2$^{+/+}$ mice, SIRT2$^{-/-}$ mice expressed normal proportions and absolute numbers of CD4/CD8 double negative (DN1–4), double positive, and single positive (SP) thymocytes (**Table 1**). Additionally, SIRT2$^{-/-}$ mice had normal populations of splenic T cells (DN, SP, naïve, and memory), B cells (immature and mature B cells), DCs (B220$^-$ CD11c$^+$ cDCs and B220$^+$ CD11c$^+$ pDCs), and Foxp3$^+$ regulatory T cells (**Table 2**). Therefore, SIRT2 had no major impact on immune cell development.

TABLE 1 | Thymic cell subsets in SIRT2$^{+/+}$ and SIRT2$^{-/-}$ mice.

Cell subset	SIRT2$^{+/+}$	SIRT2$^{-/-}$
CD4$^+$ CD8$^+$	82.3 ± 3.1	82.9 ± 0.4
CD4$^-$ CD8$^-$	2.0 ± 0.6	1.8 ± 0.2
CD25$^+$ CD44$^+$	1.8 ± 0.6	1.6 ± 0.5
CD25$^-$ CD44$^+$	0.2 ± 0.01	0.2 ± 0.01
CD25$^+$ CD44$^-$	1.4 ± 0.6	1.3 ± 0.4
CD25$^-$ CD44$^-$	96.6 ± 1.2	96.9 ± 1.0
CD4$^+$ CD8$^-$	12.0 ± 2.3	12.1 ± 0.7
CD4$^-$ CD8$^+$	3.6 ± 0.3	3.3 ± 0.8

Data are means ± SD of four animals per group expressed as the percentage of total cells (CD4$^+$ CD8$^+$, CD4$^-$ CD8$^-$, CD4$^+$ CD8$^-$, and CD4$^-$ CD8$^+$) or percentage of CD4$^-$ CD8$^-$ parental cells (CD25$^+$ CD44$^+$, CD25$^-$ CD44$^+$, CD25$^+$ CD44$^-$ and CD25$^-$ CD44$^-$). Total cell numbers were 49.2 ± 15.4 and 55.2 ± 5.7 millions per thymus in SIRT2$^{+/+}$ and SIRT2$^{-/-}$ mice, respectively. No statistically significant differences in subset percentages or absolute numbers were detected.

TABLE 2 | Splenic cell subsets in SIRT2$^{+/+}$ and SIRT2$^{-/-}$ mice.

Cell subset	SIRT2$^{+/+}$	SIRT2$^{-/-}$
CD3$^+$ T cells (%)	27.3 ± 4.6	36.3 ± 4.8
CD4$^+$	62.3 ± 2.7	61.5 ± 4.3
CD4$^+$ CD44^{low} CD62L^{high} (naive)	46.0 ± 2.9	43.7 ± 6.8
CD4$^+$ CD44^{high} CD62L^{low} (memory)	16.3 ± 2.9	17.8 ± 6.9
CD8$^+$	31.5 ± 2.0	32.0 ± 2.9
CD8$^+$ CD44^{low} CD62L^{high} (naive)	23.1 ± 0.5	23.5 ± 0.3
CD8$^+$ CD44^{high} CD62L^{low} (memory)	8.4 ± 0.5	8.5 ± 0.3
CD4$^-$ CD8$^-$	1.3 ± 0.2	1.6 ± 0.2
B220$^+$ B cells (%)	52.2 ± 7.4	51.3 ± 3.1
B220$^+$ IgD$^+$ CD23$^+$ (mature)	45.6 ± 1.2	44.1 ± 0.9
B220$^+$, non-IgD$^+$/CD23$^+$ (immature)	6.6 ± 1.2	7.2 ± 0.9
CD11c$^+$ dendritic cells (%)	6.6 ± 0.2	6.4 ± 0.6
B220$^-$	62.8 ± 2.5	62.8 ± 4.7
B220$^+$	37.2 ± 2.5	37.2 ± 4.7
CD4$^+$ CD25$^+$ Foxp3$^+$ Tregs (%)	4.5 ± 0.4	4.7 ± 0.2

Data are means ± SD of four animals per group expressed as the percentage of CD3$^+$, B220$^+$, CD11c$^+$, and CD4$^+$ Foxp3$^+$ splenic cells or the percentage of the CD3$^+$, B220$^+$, and CD11c$^+$ parental populations expressing CD4, CD8, CD44, CD62L, IgD, and CD23. Total cell numbers were 74.2 ± 5.6 and 67.4 ± 8.7 millions per spleen in SIRT2$^{+/+}$ and SIRT2$^{-/-}$ mice, respectively. No statistically significant differences in subset percentages or absolute numbers were detected.

As a first approach to evaluate whether SIRT2 influenced immune responses, SIRT2$^{+/+}$ and SIRT2$^{-/-}$ splenocytes were exposed to microbial and immunological stimuli: LPS, CpG, concanavalin A, anti-CD3/CD28, PHA, TSST-1, and SEB. The proliferation and production of IL-2 and IFNγ (measured by ELISA) by splenocytes were not affected by SIRT2 deficiency (**Figures 2A,B**). In agreement, blood concentrations of IFNγ were similar in SIRT2$^{+/+}$ and SIRT2$^{-/-}$ mice injected with TSST-1 (**Figure 2C**), a staphylococcal superantigen responsible of toxic shock syndrome. A Luminex assay was then used to quantify TNF, IL-6, IL-10, IL-12p70, CCL3/Mip1α, CCL4/Mip1β, and CCL5/Rantes secretion by splenocytes exposed to LPS, CpG, concanavalin A, anti-CD3/CD28, PHA, TSST-1, and SEB (**Figure 2D**). No differences were observed between SIRT2$^{+/+}$ and SIRT2$^{-/-}$ splenocytes apart from a 20–28% reduction of LPS-induced IL-6, IL-10, and CCL5 and anti-CD3/CD28-induced CCL4, while the secretion of CCL5 was increased in response to anti-CD3/CD28.

SIRT2 Deficiency Increases Phagocytosis by Macrophages

Macrophages are professional phagocytic cells that play a major role in antimicrobial host defenses. Therefore, we tested whether SIRT2 deficiency had an effect on phagocytosis by BMDMs. SIRT2$^{+/+}$ and SIRT2$^{-/-}$ BMDMs were incubated with fluorescent beads and analyzed by flow cytometry (**Figures 3A–C**). A higher percentage of SIRT2$^{-/-}$ than SIRT2$^{+/+}$ BMDMs phagocytosed beads (32.4 ± 1.9 vs 24.5 ± 1.2 percent positive cells, $P = 0.002$; **Figures 3A,B**), regardless of opsonization (**Figure 3C**). SIRT2$^{-/-}$ BMDMs also exhibited higher phagocytosis using a panel of fluorescently labeled heat-inactivated bacteria (% of SIRT2$^{-/-}$ vs SIRT2$^{+/+}$ BMDMs ingesting bacteria: *E. coli* J5: 53.6 vs 43.6%, *E. coli* O111: 31.6 vs 23.0%, *Salmonella* Typhimurium: 24.1 vs 17.6%, *Neisseria meningitis*: 46.1 vs 37.2%, *S. pneumoniae*: 49.6 vs 34.7%). BMDMs were additionally exposed to live *E. coli*, *S. aureus* and GBS for 1 h before measuring the number of intracellular bacteria by plating cell lysates and enumerating colonies. Confirming the results obtained using inert beads and fluorescent bacteria, the numbers of phagocytosed *E. coli*, *S. aureus* and GBS were 1.3-fold to 1.6-fold higher using SIRT2$^{-/-}$ BMDMs (**Figure 3D**).

Macrophages express phagocytic receptors, including macrophage scavenger receptor 1 (Msr1/SR-AI/CD204), CD14, CD36, C-type lectins such as dectin-1 (encoded by Clec7a), and members of the integrin superfamily (integrin α5/Itga5/CD49e, integrin αM/Itgam/CD11b, integrin αX/Itgax/CD11c, integrin β2/Itgb2/CD18). SIRT2$^{-/-}$ and SIRT2$^{+/+}$ BMDMs expressed comparable mRNA levels of Itga5, Itga6, Itgal, Itgam, Itgax, Itgb1, Itgb2, Cd14, Cd36, Msr1, and Clec7a (**Figure 3E**). Moreover, SIRT2$^{-/-}$ and SIRT2$^{+/+}$ BMDMs expressed similar levels of membrane-bound CD11b, CD11c, CD14, and Msr1 (**Figure 3F**). Hence, SIRT2 deficiency likely improved phagocytosis by BMDMs in a phagocytic receptor independent fashion.

Stabilization of microtubules and high glycolytic activity have been associated with efficient phagocytosis by macrophages (37–40). Since SIRT2 impacts on microtubules stabilization and glucose metabolism (8, 13, 41), we questioned whether these processes influenced phagocytosis by SIRT2$^{-/-}$ BMDMs. In

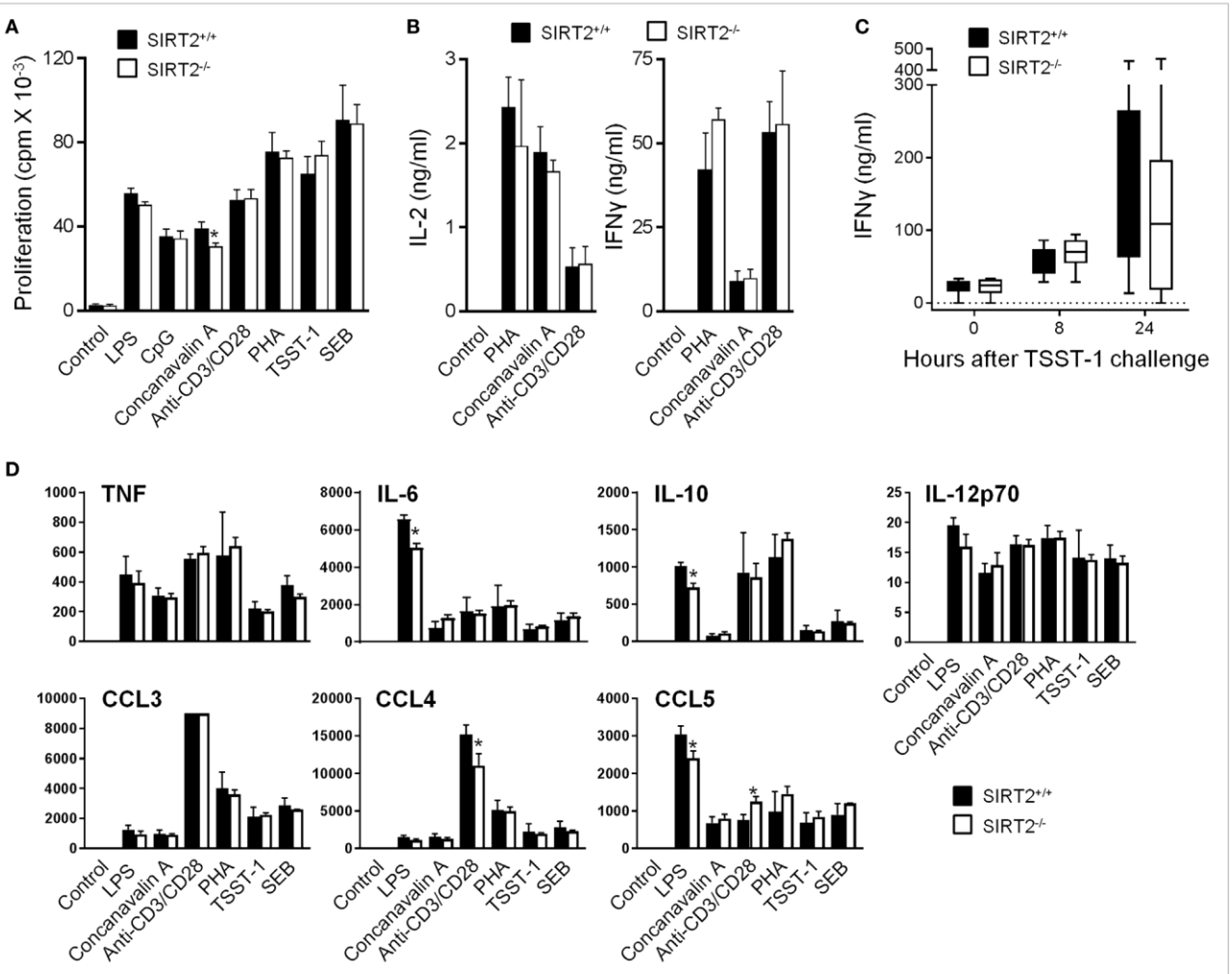

FIGURE 2 | Sirtuin 2 (SIRT2) deficiency does not affect proliferation and cytokine response of splenocytes and IFNγ production in mice challenged with toxic shock syndrome toxin-1 (TSST-1). **(A,B)** SIRT2$^{+/+}$ and SIRT2$^{-/-}$ splenocytes were incubated for 48 h with lipopolysaccharide (LPS) (5 μg/ml), CpG (2 μg/ml), concanavalin A (5 μg/ml), anti-CD3/CD28 antibodies (1 μg/ml), phytohemagglutinin (PHA) (10 μg/ml), TSST-1 (2 μg/ml), and staphylococcal enterotoxin B (SEB) (5 μg/ml). Proliferation was measured by ^{3}H-thymidine incorporation **(A)** while IL-2 and IFNγ concentrations in cell culture supernatants were quantified by ELISA **(B)**. Data are means ± SD of triplicate samples from one experiment performed with four mice and are representative of two experiments (*$P < 0.05$). **(C)** SIRT2$^{+/+}$ and SIRT2$^{-/-}$ mice ($n = 8$ per group) were injected with TSST-1 (0.5 mg/kg i.p.). Blood was collected after 0, 8, and 24 h to quantify IFNγ concentrations. Data are means ± SD. $P > 0.5$ for all time points. **(D)** SIRT2$^{+/+}$ and SIRT2$^{-/-}$ splenocytes were incubated for 48 h with LPS, CpG, concanavalin A, anti-CD3/CD28 antibodies, PHA, TSST-1, and SEB. TNF, IL-6, IL-10, IL-12p70, CCL3 (MIP-1α), CCL4 (MIP-1β), and CCL5 (RANTES) were quantified by Luminex. Data (in pg/ml) are means ± SD of one experiment performed with three mice. CCL3 values in response to anti-CD3/CD8 were over the upper limit of detection of the assay (*$P < 0.05$).

BMDMs, SIRT2 deficiency increased 1.5-fold tubulin acetylation (**Figure 3G**), a hallmark of microtubule stabilization. However, the microtubule destabilizer nocodazole did not impair the phagocytosis of *S. aureus* by BMDMs (**Figure 3H**), while the actin depolymerization agent cytochalasin D efficiently inhibited phagocytosis. Interestingly, the glycolytic activity was higher in SIRT2$^{-/-}$ than SIRT2$^{+/+}$ BMDMs exposed to *S. aureus* (**Figure 3I**). Moreover, 2-DG, which inhibits glycolysis, significantly reduced the phagocytosis of *S. aureus* by BMDMs (**Figure 3J**). Albeit preliminary, these results suggested that differences in the metabolic capacity of SIRT2$^{+/+}$ and SIRT2$^{-/-}$ BMDMs may provide a mechanism by which SIRT2 impedes phagocytosis.

SIRT2 Deficiency Does Not Affect Cytokine Response of BMDMs Exposed to Microbial Ligands and Sensitivity of Mice to Endotoxemia

Sensing of microbial ligands through TLRs initiates MAPK and NF-κB signaling involved in the control of cytokine gene expression by innate immune cells (2). To address whether SIRT2 impacted intracellular signaling, the phosphorylation of ERK1/2, p38, and JNK MAPKs in BMDMs exposed to LPS for 0, 10, 30, and 60 min was analyzed by western blotting. The rate of LPS-induced phosphorylation of ERK1/2, p38 and JNK was very similar in SIRT2$^{+/+}$

and SIRT2$^{-/-}$ BMDMs, with only a slight and late reduction of ERK1/2 phosphorylation in SIRT2$^{-/-}$ BMDMs (30% reduction at 1 hour) (**Figure 4A**). The nuclear translocation of phosphorylated NF-κB p65 was not different in SIRT2$^{+/+}$ and SIRT2$^{-/-}$ BMDMs exposed to LPS for 0, 10, 30, and 60 min ($P > 0.5$ for all time points).

SIRT2$^{+/+}$ and SIRT2$^{-/-}$ BMDMs exposed to LPS, Pam_3CSK_4, CpG (i.e., TLR4, TLR1/2 and TLR9 ligands, respectively), and *E. coli* upregulated Tnf and Il6 mRNA levels and secreted TNF and IL-6 to the same extend (**Figure 4B**). Additionally, Tlr1, Tlr2, Tlr4, and Tlr9 mRNA were modulated likewise in SIRT2$^{+/+}$

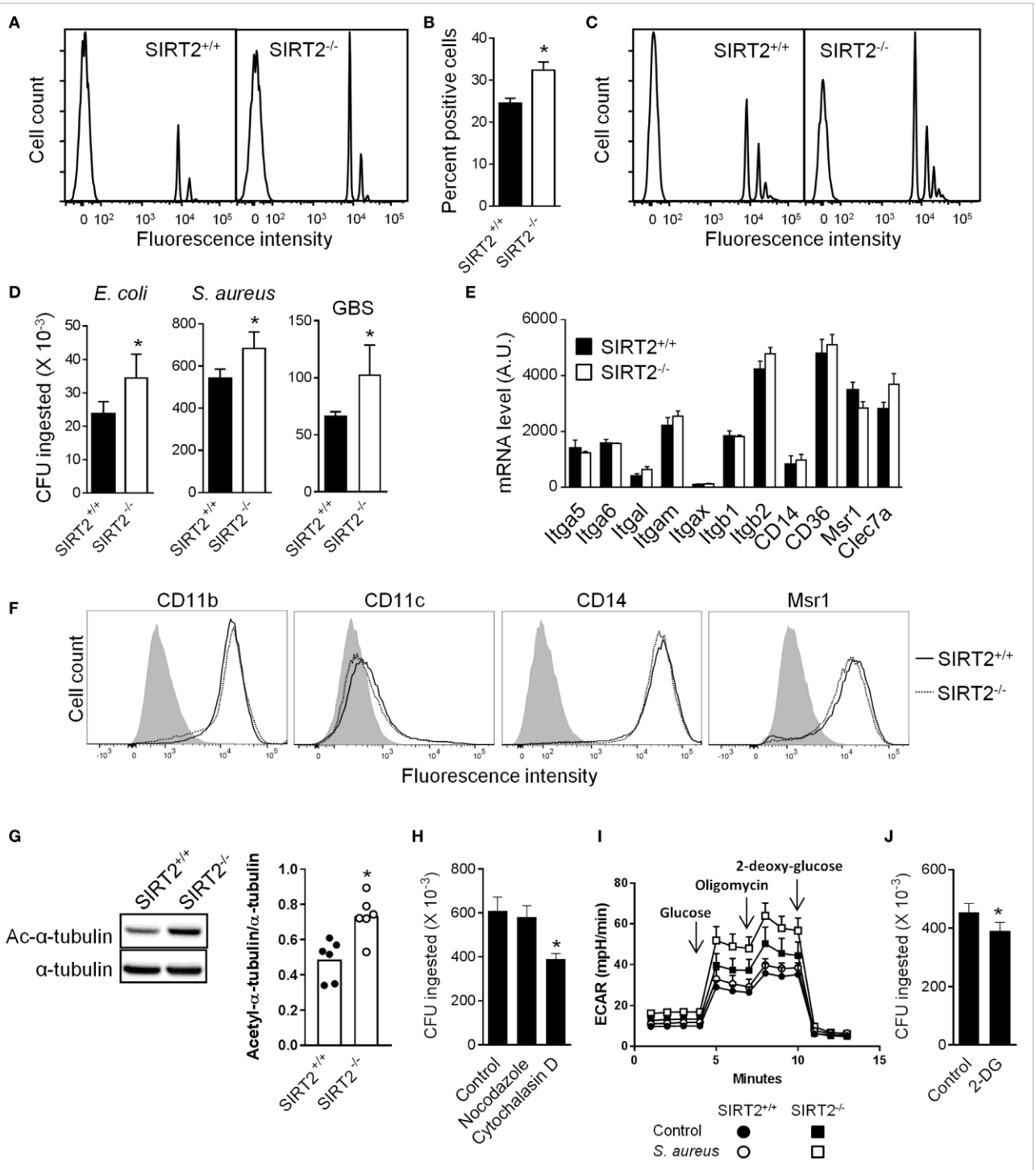

FIGURE 3 | Continued

FIGURE 3 | Continued
Sirtuin 2 (SIRT2) deficiency increases bacterial phagocytosis by macrophages. **(A–C)** SIRT2$^{+/+}$ and SIRT2$^{-/-}$ BM-derived macrophages (BMDMs) were incubated with 10 fluorescent beads [opsonized in **(C)**] per cell. After 1 h, cells were analyzed by flow cytometry. Representative histograms are depicted in **(A,C)**. The percentage of fluorescent cells was calculated **(B)**. Data are means ± SD from an experiment performed with four mice (*P = 0.002). **(D)** SIRT2$^{+/+}$ and SIRT2$^{-/-}$ BMDMs were incubated with live *Escherichia coli*, *Staphylococcus aureus*, and Group B *Streptococcus* (GBS) (10 bacteria/cell). Phagocytosis was assessed after 1 h. Data are means ± SD from one experiment performed with four (*E. coli* and GBS) or eight (*S. aureus*) mice. *P = 0.03, 0.006, and 0.03 for *E. coli*, *S. aureus*, and GBS, respectively. **(E)** Itga5, Itga6, Itgal, Itgam, Itgax, Itgb1, Itgb2, Cd14, Cd36, Msr1, and Clec7a mRNA expression levels in SIRT2$^{+/+}$ and SIRT2$^{-/-}$ BMDMs. Data are means ± SD of one experiment performed with three mice. **(F)** CD11b, CD11c, CD14, and Msr1 expression levels were analyzed by flow cytometry. The gray histogram represents staining with an isotype control antibody. **(G)** Expression levels of acetylated (Ac) and total tubulin in BMDMs were analyzed by western blotting and quantified by imaging. Data are means ± SD from six mice (right panel) (*P = 0.015). Full-length blots are presented in Figure S2 in Supplementary Material. **(H)** Phagocytosis of *S. aureus* [performed as in **(D)**] by SIRT2$^{-/-}$ BMDMs preincubated for 1 h with or without nocodazole (10 µM) and cytochalasin D (10 µM). Data are means ± SD from one experiment performed with four mice (*P = 0.008). **(I)** Glycolytic capacity of BMDMs assessed by measuring the extracellular acidification rate (ECAR) using the Seahorse XF Glycolysis Stress Test Kit as described in Section "Materials and Methods." Data are means ± SD from one experiment performed with three mice. **(J)** Phagocytosis of *S. aureus* [performed as in **(D)**] by SIRT2$^{-/-}$ BMDMs preincubated for 1 h with or without 25 mM 2-deoxy-glucose (2-DG). Data are means ± SD from one experiment performed with four mice (*P = 0.017).

and SIRT2$^{-/-}$ BMDMs (Figure S3 in Supplementary Material). SIRT2$^{+/+}$ and SIRT2$^{-/-}$ BMDMs expressed also comparable mRNA levels of Il1a, Il1b, Il10, Il12b, Il15, Il18, Il27, Ccl2/Mcp1, Ccl3/Mip1a, Ccl4/Mip1b, Ccl5/Rantes, Ccl8/Mcp2, Ccl12/Mcp5, Cxcl10/Ip10, and Cxcl11/Itac at baseline and following LPS stimulation (**Figure 4C**), and secreted comparable levels of IL-10, IL-12p70, IL-18, CXCL10, CCL2, CCL3, CCL4, and CCL5 upon exposure to LPS, Pam_3CSK_4, CpG, *E. coli*, and *S. aureus* (**Figure 4D**). Altogether, these results argued against an important role of SIRT2 in controlling proinflammatory and anti-inflammatory cytokine response by macrophages exposed to TLR ligands.

To assess the relevance of these observations *in vivo*, we developed models of endotoxemia of different severity (**Figures 5A–D**). In a mild model of endotoxemia (induced by an i.p. challenge with 10 mg/kg LPS), TNF and IL-12p40 concentrations in blood and mortality rates (83 vs 100%, $P = 0.3$) were comparable in SIRT2$^{+/+}$ and SIRT2$^{-/-}$ mice (**Figures 5A,B**). In a severe model of endotoxemia (induced by 25 mg/kg LPS), TNF, IL-6, and IL-12p40 concentrations in blood and mortality rates (88% in both groups, $P = 0.69$) were strongly increased, but remained similar in SIRT2$^{+/+}$ and SIRT2$^{-/-}$ mice (**Figures 5C,D**). Furthermore, SIRT2$^{+/+}$ and SIRT2$^{-/-}$ mice were equally sensitive to fulminant shock induced by TNF (25 mg/kg i.p. in D-galactosamine sensitized mice), the main driver of the lethal effect of endotoxemia ($P = 0.6$; **Figure 5E**). Overall, SIRT2 did not interfere with endotoxemia.

SIRT2 Deficiency Protects from Chronic Staphylococcal Infection

Considering that SIRT2 impacted phagocytosis but not cytokine expression, we hypothesized that SIRT2 deficiency should provide some benefit during chronic lethal infection but not fulminant sepsis, and should not sensitize to benign infection. Therefore, we compared the impact of SIRT2 deficiency during rapidly lethal, sub-lethal, and chronic bacterial infections induced by *E. coli*, *K. pneumonia*, and *S. aureus*, three of the most frequent causes of bacterial sepsis in humans (42).

Supporting our working hypothesis, in a model of chronic infection by *S. aureus* in which mortality occurred 3 to 16 days post i.v. challenge with the bacteria, severity score, body weight loss, and survival (SIRT2$^{+/+}$ vs SIRT2$^{-/-}$: 33.3 vs 69.2%; $P = 0.04$) were all markedly improved in SIRT2$^{-/-}$ mice (**Figure 6A**). In agreement with these findings, 48 h postinfection, only 37.5% (3/8) of SIRT2$^{-/-}$ mice were bacteremic while 71.4% (5/7) of SIRT2$^{+/+}$ mice were bacteremic (**Figure 6B**). Moreover, bacterial burden in the spleen was much lower in SIRT2$^{-/-}$ than in SIRT2$^{+/+}$ mice (1.9×10^2 vs 3.3×10^3 mean CFU/organ; $P = 0.04$). TNF was not detected in blood, while IL-6 and IL-12p40 levels were not different between SIRT2$^{-/-}$ and SIRT2$^{+/+}$ mice, although there was a trend toward lower IL-12p40 levels in SIRT2$^{-/-}$ mice (**Figure 6C**). In a model of fulminant, rapidly lethal peritonitis induced by *E. coli*, body weight loss, bacterial dissemination into the blood, and survival rate (12.5% in both groups, $P = 0.7$) were comparable in SIRT2$^{+/+}$ and SIRT2$^{-/-}$ mice (**Figure 6D**). In a non-severe model of *K. pneumoniae* pneumonia, body weight loss and survival (85.7% in both groups, $P = 0.9$) were not affected by SIRT2 deficiency (**Figure 6E**). Finally, we questioned whether SIRT2 influenced host susceptibility to a non-bacterial chronic infection. Candidiasis was induced by i.v. inoculation of 10^5 CFU/ml *C. albicans* into SIRT2$^{+/+}$ and SIRT2$^{-/-}$ mice ($n = 14$ and 16). Mice died 9–40 days postinfection, without survival differences between the SIRT2$^{+/+}$ and SIRT2$^{-/-}$ groups (71 vs 56%; $P = 0.4$), suggesting that SIRT2 deficiency did not compromise host defenses to *Candida* infection.

DISCUSSION

In the present study, we identified a unique role for SIRT2 in host–pathogen interactions. SIRT2 deficiency promoted bacterial phagocytosis by macrophages but not cytokine production. In agreement with these findings, SIRT2 deficiency protected from chronic staphylococcal infection while having no influence on the course of endotoxemia, TNF-induced shock, fulminant bacterial peritonitis, non-severe bacterial pneumonia, and chronic candidiasis. These observations are particularly relevant in light of the development of pharmacological inhibitors of SIRT2 for clinical applications (43), as they suggest that their usage would not increase susceptibility to bacterial and candidal infections.

SIRT2 was the most highly expressed sirtuin in myeloid cells. Macrophages expressed elevated levels of SIRT2, in accordance previous reports describing SIRT2 expression in microglial cells *in vivo* (16,17). Interestingly, SIRT2 deficiency had no major impact on LPS-induced MAPK activation, NF-κB nuclear translocation,

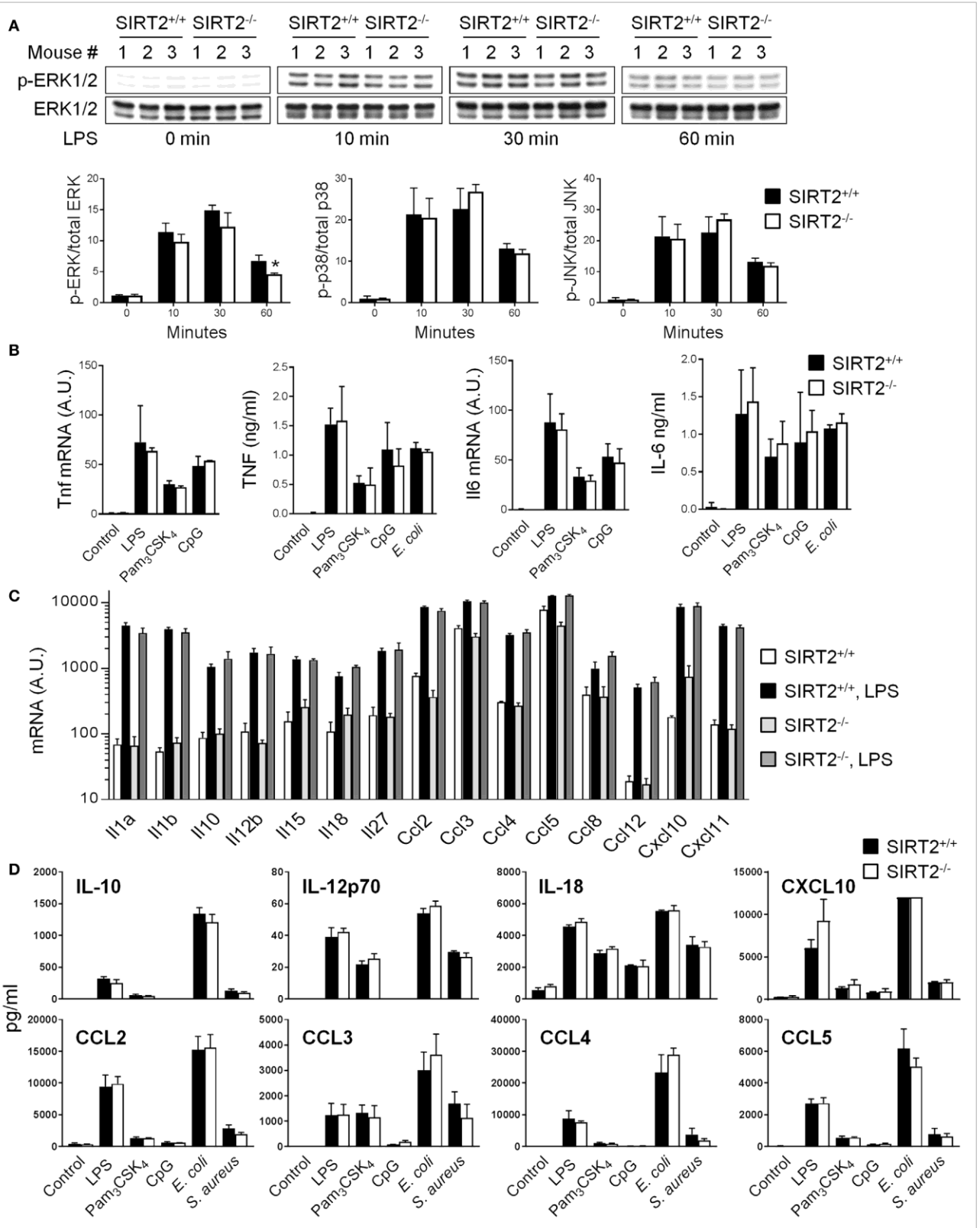

FIGURE 4 | Continued

FIGURE 4 | Contiued
Sirtuin 2 (SIRT2) deficiency does not affect the response of macrophages to microbial stimulation. SIRT2$^{+/+}$ and SIRT2$^{-/-}$ BM-derived macrophages were exposed to lipopolysaccharide (LPS) (10 ng/ml), Pam_3CSK_4 (10 ng/ml), CpG (2 μg/ml), *Escherichia coli* (10^6 CFU/ml), and *Staphylococcus aureus* (10^6 CFU/ml). **(A)** Expression levels of phosphorylated (p) and total ERK1/2 (upper panel), p38 and JNK were analyzed by western blotting and quantified by imaging. Data are means ± SD from one experiment performed with three mice (lower panel) (*$P = 0.02$). **(B)** Tnf and Il6 mRNA levels and TNF and IL-6 concentrations in cell culture supernatants 1 and 8 h after stimulation, respectively. **(C)** Il1a, Il1b, Il10, Il12b, Il15, Il18, Il27, Ccl2/Mcp1, Ccl3/Mip1a, Ccl4/Mip1b, Ccl5/Rantes, Ccl8/Mcp2, Ccl12/Mcp5, Cxcl10/Ip10, Cxcl11/Itac mRNA levels after 8 h of culture with or without LPS. **(D)** IL-10, IL-12p70, IL-18, CXCL10, CCL2, CCL3, CCL4, and CCL5 concentrations in cell culture supernatants 8 h after stimulation measured by Luminex. Data are means ± SD of triplicate samples from one experiment performed with three mice (mRNA analyses) or six mice (TNF and IL-6 secretion), or means ± SD of single measurements from one experiment performed with three mice (Luminex). CXCL10 values in response to *E. coli* were over the upper limit of detection of the assay. No statistically significant differences were detected in **(B–D)**. A.U., arbitrary units. Full-length blots of panel **(A)** are presented in Figure S4 in Supplementary Material.

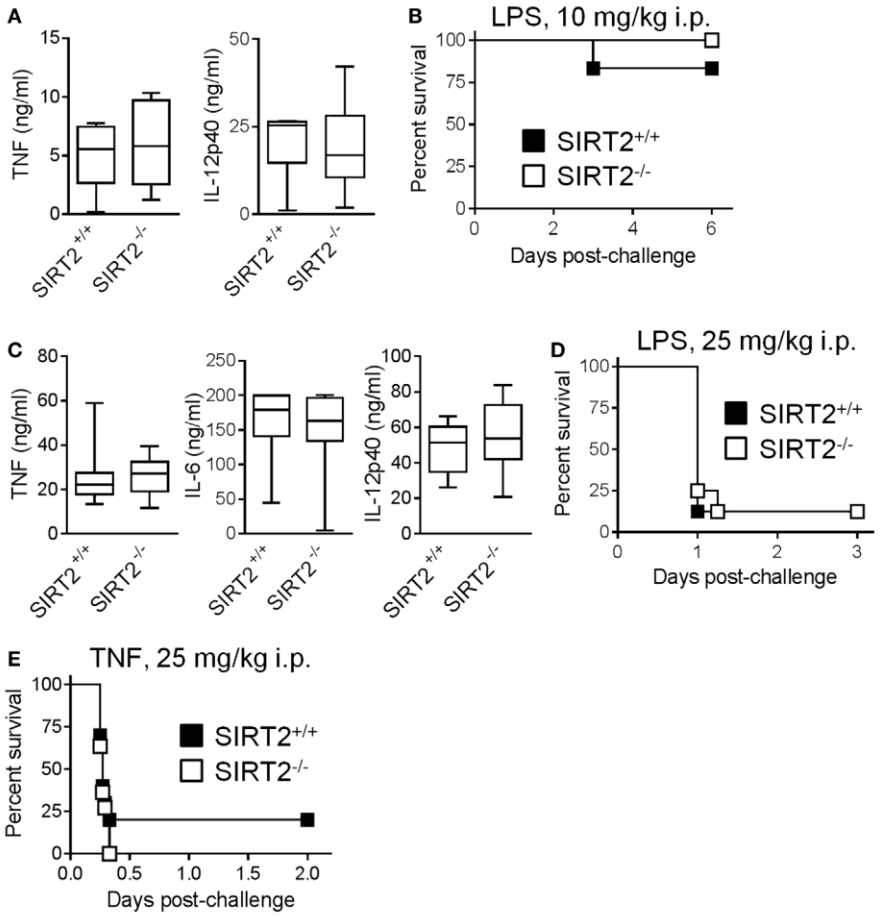

FIGURE 5 | Sirtuin 2 (SIRT2) deficiency does not affect endotoxemia and TNF-induced shock. SIRT2$^{+/+}$ and SIRT2$^{-/-}$ mice were injected i.p. with 10 mg/kg lipopolysaccharide (LPS) [**(A,B)**, $n = 6$ per group] and 25 mg/kg LPS (**C,D**, $n = 8$ per group). **(A,C)** TNF, IL-6, and IL-12p40 concentrations in blood collected 1 h (TNF) and 6 h (IL-6 and IL-12p40) after LPS challenge. $P > 0.5$ for all conditions. **(B,D)** Survival of mice. $P = 0.3$ and 0.9. **(E)** Survival of SIRT2$^{+/+}$ and SIRT2$^{-/-}$ mice ($n = 11$ per group) sensitized with 30 mg/kg D-galactosamine and challenged i.p. with 25 mg/kg TNF. $P = 0.6$.

and cytokine production in macrophages. Moreover, cytokine levels in blood were similar in SIRT2$^{+/+}$ and SIRT2$^{-/-}$ endotoxemic mice. Likewise, inflammatory parameters were comparable in SIRT2$^{+/+}$ and SIRT2$^{-/-}$ mice with experimental stroke and *Mycobacterium tuberculosis* infection (21, 44). However, contradictory findings have been reported in the literature. While SIRT2 deficiency promoted NF-κB p65 acetylation and p65-dependent gene expression, it was also reported to reduce NF-κB and p38 and JNK MAPKs activation through an increased stability of IκB and activity of MAPK phosphatase-1, respectively (14–16, 18, 20, 45). In these studies, SIRT2 deficiency sustained brain inflammation, colitis, and collagen-induced arthritis, but protected from renal and liver inflammation (15, 16, 18, 20, 45).

The discrepancy of the effects of SIRT2 on inflammatory responses mirrors conflicting results observed for other sirtuins. For example, SIRT1 protected from experimental autoimmune

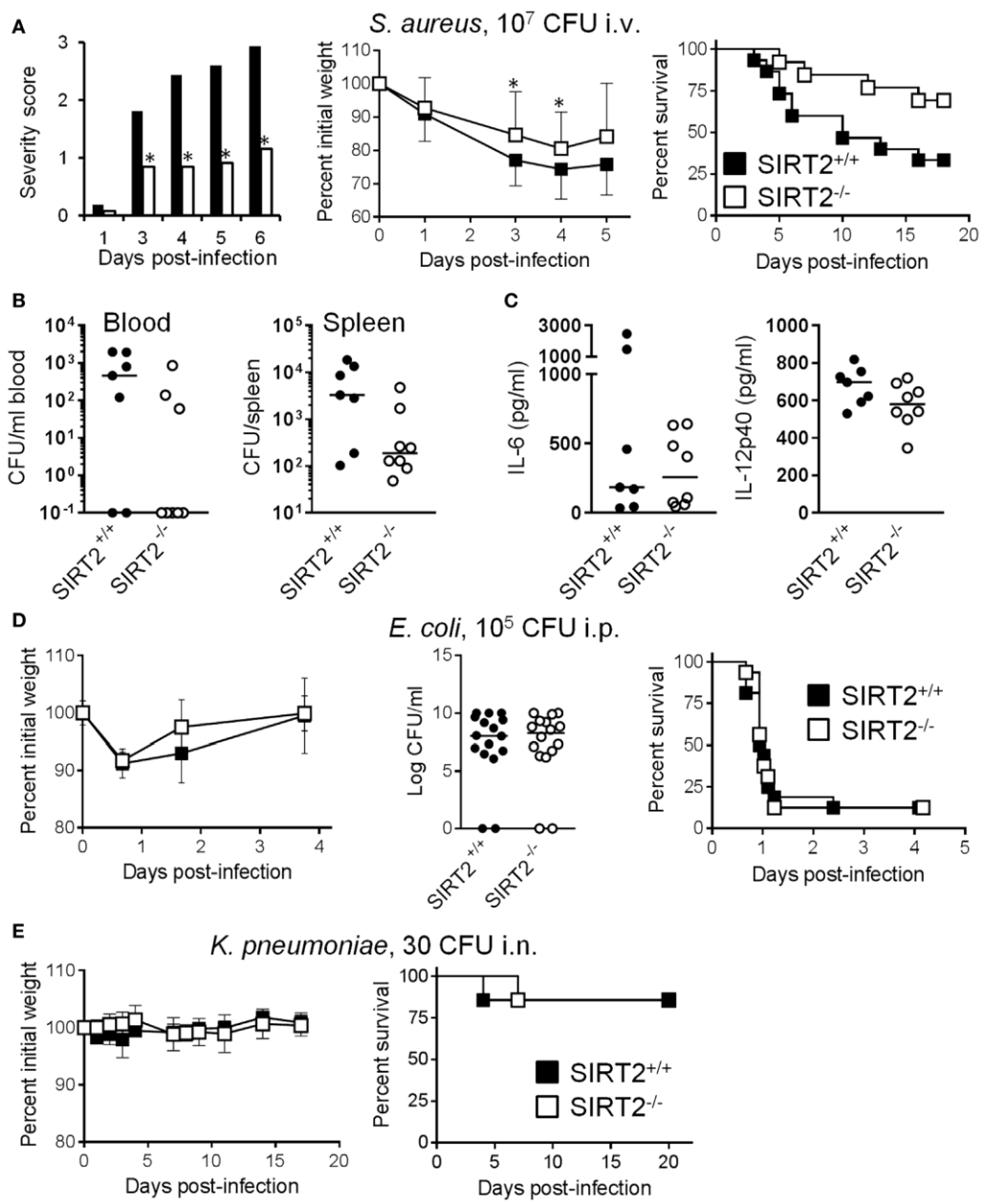

FIGURE 6 | SIRT2 deficiency protects from chronic *Staphytococcus aureus* infection. **(A)** Severity score (*$P \leq 0.01$), body weight (*$P = 0.03$ and 0.04) and survival ($P = 0.04$) of SIRT2$^{+/+}$ and SIRT2$^{-/-}$ mice challenged i.v. with 10^7 CFU *S. aureus* ($n = 13$ and 9). **(B,C)** Blood and spleen were collected from SIRT2$^{+/+}$ and SIRT2$^{-/-}$ mice ($n = 7$ and 8) 48 h after *S. aureus* challenge. Bacteria were quantified in blood and spleen **(B)** while IL-6 and IL-12p40 concentrations were quantified in blood **(C)**. Horizontal bars represent the medians. $P = 0.07$ and 0.04 in **(B)**, and $P = 0.95$ and 0.12 in **(C)**. **(D)** Body weight, bacteria in blood 18 h postinfection ($P = 0.9$), and survival ($P = 0.8$) of SIRT2$^{+/+}$ and SIRT2$^{-/-}$ mice challenged i.p. with 10^5 CFU *E. coli* ($n = 16$ per group). **(E)** Body weight and survival ($P = 0.9$) of SIRT2$^{+/+}$ and SIRT2$^{-/-}$ mice challenged i.n. with 30 CFU *K. pneumoniae* ($n = 7$ per group).

encephalomyelitis, arthritis, lung inflammation, hepatic steatosis, and insulin resistance, but promoted lupus, arthritis, allergic airway disease, and allograft rejection (46–54). SIRT6 has not only been reported to protect against liver fibrosis, atherosclerosis, osteoarthritis, and arthritis but has also been associated with increased TNF production and the development of autoimmune encephalomyelitis and cerebral ischemia (55–62). Different experimental conditions might explain these apparent conflicting results, for example qualitative and quantitative differences in caloric input or subtle variations of NAD^+ availability influencing sirtuin activity indirectly. Moreover, SIRT1, SIRT3, and SIRT6 modulate circadian function and are affected by circadian

oscillation in the abundance of NAD^+ (63, 64). Furthermore, sirtuins might primarily play a role in the development of long-lasting, chronic metabolic, and/or inflammation-related disorders while having a modest impact during acute infectious processes. For instance, SIRT3 deficiency has been reported to increase insulin resistance, diabetic cardiac dysfunction, allograft graft injury, and lung fibrosis, but had no impact on innate immune responses and susceptibility to endotoxemia or bacterial and fungal sepsis (65–73).

Two prior studies examined SIRT2 in the context of infection by intracellular bacteria. SIRT2 deletion in the myeloid compartment had no noticeable impact on host defenses against *M. tuberculosis* infection as attested by cellular infiltrates, cytokine expression, and long-term bacterial burden in lungs (44). *Listeria monocytogenes* promoted SIRT2-dependent histone H3 deacetylation and redirected host gene expression to favor infection (74). Whether other microorganisms subvert SIRT2 or other sirtuins at their own benefit is unknown.

We analyzed host responses to extracellular bacteria most frequently isolated from septic patients. Strikingly, SIRT2 deficiency enhanced the engulfment of Gram-positive and Gram-negative bacteria by macrophages, an effect apparently unrelated with a differential expression of phagocytic receptors or microtubule polymerization. This observation was surprising considering that on the one hand SIRT2 deacetylates α-tubulin and destabilizes the microtubule network (8, 41) and on the other end microtubule depolymerizating agents were reported to inhibit phagocytosis (75, 76). Yet, the effects of microtubule depolymerizating agents were tested using an immortalized macrophage-like mouse cell line and human neutrophils that may behave differently than primary BMDMs. As a positive control (77), actin depolymerization efficiently inhibited phagocytosis by BMDMs. Increased glycolysis has been associated with efficient phagocytosis by macrophages (39, 40). SIRT2 deficiency reduced HIF-1α deacetylation and destablization (78), and augmented glycolysis in human fibroblasts (79). We observed that SIRT2 deficiency increased glycolysis and that glycolysis inhibition reduced phagocytosis in BMBMs. Albeit preliminary, these results suggest that SIRT2 may influence phagocytosis through metabolic constraints.

The improved control of bacterial burden during chronic staphylococcal infection might be related to improved phagocytosis but also to enhanced autophagy in $SIRT2^{-/-}$ mice. Autophagy facilitates the clearance of cytoplasmic bacteria (80) and has been involved in host defenses and tolerance to *S. aureus* infection (81, 82). Hyperacetylation of tubulin stimulated autophagy upon nutrient deprivation, and SIRT2 deficiency increased autophagy in a colorectal cancer cell line (83, 84). Thus, by regulating tubulin acetylation and metabolic activity, SIRT2 may contribute to modulate phagocytic and autophagy defense mechanisms, though the latter has not been formally demonstrated.

From a translational perspective, it was important to define the impact of SIRT2 in preclinical models of infection. A main observation of this study is that SIRT2 deficiency protected mice from chronic staphylococcal infection, while it neither protected nor sensitized mice to TNF-induced shock, endotoxemia, rapidly lethal *E. coli* peritonitis and mild *K. pneumoniae* pneumonia. Additionally, SIRT2 deficiency did not influence the development of chronic candidiasis as it did for chronic staphylococcal infection. This may not be surprising considering differences in host–pathogen interactions during fungal and bacterial infections. Whether SIRT2 protects from other chronic bacterial infections should be tested in the future. Nonetheless, these results support the clinical development of SIRT2 inhibitors regarding their infection-related safety profile. This contrasts with inhibitors of HDAC1-11 that impaired innate immune defenses, increased susceptibility to infection in preclinical mouse models and have been associated with severe infections in patients (29, 85–89).

Overall, SIRT2 has a subtle impact on host defense responses to bacterial infections. Considering that sirtuins are intricately linked with metabolism, age-associated dysfunctions and lifespan, it will be important to analyze the impact of SIRT2 on host defenses under metabolic stress conditions and according to age. To conclude, our results are encouraging with respect to developing inhibitors of SIRT2, which are safe in terms of susceptibility to infections, for treating metabolic and neurodegenerative diseases, such as Parkinson's disease and Huntington's disease (90, 91).

ETHICS STATEMENT

Animal experimentation was approved by the Service de la Consommation et des Affaires Vétérinaires (SCAV) du Canton de Vaud (Epalinges, Switzerland) under authorizations no. 876.8 and 877.8, and performed according to Swiss and ARRIVE guidelines.

AUTHOR CONTRIBUTIONS

EC, TH, CT, JH, MM, JL, MP, BT, and SL performed *in vitro* experiments. EC, TH, CT, and DLR performed *in vivo* experiments. HA-O and JA contributed to reagents. TR conceived the project, designed the experiments, and wrote the paper. All the authors revised the paper.

FUNDING

This work was supported by grants from the Swiss National Science Foundation (SNSF) 145014, 149511, 173123 (TR), 132492 (HA-O), and 140780 (JA). TR received an interdisciplinary grant from the Faculty of Biology and Medicine of the University of Lausanne (Switzerland). CT was supported by the European Sepsis Academy Horizon 2020 Marie Skłodowska-Curie Action: Innovative Training Network (MSCA-ESA-ITN, grant number 676129). BT and SL were supported by the Summer Undergraduate Research (SUR) program of the University of Lausanne. The work in the JA laboratory was supported by the EPFL, NIH (R01AG043930), Systems X (SySX.ch 2013/153), and Velux Stiftung (1019).

SUPPLEMENTARY MATERIAL

The Supplementary Material for this article can be found online at http://journal.frontiersin.org/article/10.3389/fimmu.2017.01037/full#supplementary-material.

REFERENCES

1. Broz P, Monack DM. Newly described pattern recognition receptors team up against intracellular pathogens. *Nat Rev Immunol* (2013) 13:551–65. doi:10.1038/nri3479
2. Savva A, Roger T. Targeting toll-like receptors: promising therapeutic strategies for the management of sepsis-associated pathology and infectious diseases. *Front Immunol* (2013) 4:387. doi:10.3389/fimmu.2013.00387
3. Falkenberg KJ, Johnstone RW. Histone deacetylases and their inhibitors in cancer, neurological diseases and immune disorders. *Nat Rev Drug Discov* (2014) 13:673–91. doi:10.1038/nrd4360
4. Haigis MC, Sinclair DA. Mammalian sirtuins: biological insights and disease relevance. *Annu Rev Pathol* (2010) 5:253–95. doi:10.1146/annurev.pathol.4.110807.092250
5. Guarente L. Franklin H. Epstein Lecture: sirtuins, aging, and medicine. *N Engl J Med* (2011) 364:2235–44. doi:10.1056/NEJMra1100831
6. Verdin E. NAD(+) in aging, metabolism, and neurodegeneration. *Science* (2015) 350:1208–13. doi:10.1126/science.aac4854
7. Preyat N, Leo O. Sirtuin deacylases: a molecular link between metabolism and immunity. *J Leukoc Biol* (2013) 93:669–80. doi:10.1189/jlb.1112557
8. North BJ, Marshall BL, Borra MT, Denu JM, Verdin E. The human Sir2 ortholog, SIRT2, is an NAD+-dependent tubulin deacetylase. *Mol Cell* (2003) 11:437–44. doi:10.1016/S1097-2765(03)00038-8
9. Herskovits AZ, Guarente L. Sirtuin deacetylases in neurodegenerative diseases of aging. *Cell Res* (2013) 23:746–58. doi:10.1038/cr.2013.70
10. Teng YB, Jing H, Aramsangtienchai P, He B, Khan S, Hu J, et al. Efficient demyristoylase activity of SIRT2 revealed by kinetic and structural studies. *Sci Rep* (2015) 5:8529. doi:10.1038/srep08529
11. Donmez G, Outeiro TF. SIRT1 and SIRT2: emerging targets in neurodegeneration. *EMBO Mol Med* (2013) 5:344–52. doi:10.1002/emmm.201302451
12. Kozako T, Suzuki T, Yoshimitsu M, Arima N, Honda S, Soeda S. Anticancer agents targeted to sirtuins. *Molecules* (2014) 19:20295–313. doi:10.3390/molecules191220295
13. Gomes P, Outeiro TF, Cavadas C. Emerging role of sirtuin 2 in the regulation of mammalian metabolism. *Trends Pharmacol Sci* (2015) 36:756–68. doi:10.1016/j.tips.2015.08.001
14. Rothgiesser KM, Erener S, Waibel S, Luscher B, Hottiger MO. SIRT2 regulates NF-kappaB dependent gene expression through deacetylation of p65 Lys310. *J Cell Sci* (2010) 123:4251–8. doi:10.1242/jcs.073783
15. Lo Sasso G, Menzies KJ, Mottis A, Piersigilli A, Perino A, Yamamoto H, et al. SIRT2 deficiency modulates macrophage polarization and susceptibility to experimental colitis. *PLoS One* (2014) 9:e103573. doi:10.1371/journal.pone.0103573
16. Pais TF, Szego EM, Marques O, Miller-Fleming L, Antas P, Guerreiro P, et al. The NAD-dependent deacetylase sirtuin 2 is a suppressor of microglial activation and brain inflammation. *EMBO J* (2013) 32:2603–16. doi:10.1038/emboj.2013.200
17. Yuan F, Xu ZM, Lu LY, Nie H, Ding J, Ying WH, et al. SIRT2 inhibition exacerbates neuroinflammation and blood-brain barrier disruption in experimental traumatic brain injury by enhancing NF-kappaB p65 acetylation and activation. *J Neurochem* (2016) 136:581–93. doi:10.1111/jnc.13423
18. Jung YJ, Lee AS, Nguyen-Thanh T, Kim D, Kang KP, Lee S, et al. SIRT2 regulates LPS-induced renal tubular CXCL2 and CCL2 expression. *J Am Soc Nephrol* (2015) 26:1549–60. doi:10.1681/ASN.2014030226
19. Lee AS, Jung YJ, Kim D, Nguyen-Thanh T, Kang KP, Lee S, et al. SIRT2 ameliorates lipopolysaccharide-induced inflammation in macrophages. *Biochem Biophys Res Commun* (2014) 450:1363–9. doi:10.1016/j.bbrc.2014.06.135
20. Wang J, Koh HW, Zhou L, Bae UJ, Lee HS, Bang IH, et al. Sirtuin 2 aggravates postischemic liver injury by deacetylating mitogen-activated protein kinase phosphatase-1. *Hepatology* (2017) 65:225–36. doi:10.1002/hep.28777
21. Krey L, Luhder F, Kusch K, Czech-Zechmeister B, Konnecke B, Outeiro TF, et al. Knockout of silent information regulator 2 (SIRT2) preserves neurological function after experimental stroke in mice. *J Cereb Blood Flow Metab* (2015) 35:2080–8. doi:10.1038/jcbfm.2015.178
22. Ciarlo E, Heinonen T, Herderschee J, Fenwick C, Mombelli M, Le Roy D, et al. Impact of the microbial derived short chain fatty acid propionate on host susceptibility to bacterial and fungal infections in vivo. *Sci Rep* (2016) 6:37944. doi:10.1038/srep37944
23. Renner P, Roger T, Bochud PY, Sprong T, Sweep FC, Bochud M, et al. A functional microsatellite of the macrophage migration inhibitory factor gene associated with meningococcal disease. *FASEB J* (2012) 26:907–16. doi:10.1096/fj.11-195065
24. Roger T, Froidevaux C, Le Roy D, Reymond MK, Chanson AL, Mauri D, et al. Protection from lethal Gram-negative bacterial sepsis by targeting toll-like receptor 4. *Proc Natl Acad Sci U S A* (2009) 106:2348–52. doi:10.1073/pnas.0808146106
25. Roger T, Schneider A, Weier M, Sweep FC, Le Roy D, Bernhagen J, et al. High expression levels of macrophage migration inhibitory factor sustain the innate immune responses of neonates. *Proc Natl Acad Sci U S A* (2016) 113:E997–1005. doi:10.1073/pnas.1514018113
26. Savva A, Brouwer MC, Roger T, Valls Seron M, Le Roy D, Ferwerda B, et al. Functional polymorphisms of macrophage migration inhibitory factor as predictors of morbidity and mortality of pneumococcal meningitis. *Proc Natl Acad Sci U S A* (2016) 113:3597–602. doi:10.1073/pnas.1520727113
27. Meller S, Di Domizio J, Voo KS, Friedrich HC, Chamilos G, Ganguly D, et al. T(H)17 cells promote microbial killing and innate immune sensing of DNA via interleukin 26. *Nat Immunol* (2015) 16:970–9. doi:10.1038/ni.3211
28. Ciarlo E, Roger T. Screening the impact of sirtuin inhibitors on inflammatory and innate immune responses of macrophages and in a mouse model of endotoxic shock. *Methods Mol Biol* (2016) 1436:313–34. doi:10.1007/978-1-4939-3667-0_21
29. Roger T, Lugrin J, Le Roy D, Goy G, Mombelli M, Koessler T, et al. Histone deacetylase inhibitors impair innate immune responses to toll-like receptor agonists and to infection. *Blood* (2011) 117:1205–17. doi:10.1182/blood-2010-05-284711
30. Roger T, Ding X, Chanson AL, Renner P, Calandra T. Regulation of constitutive and microbial pathogen-induced human macrophage migration inhibitory factor (MIF) gene expression. *Eur J Immunol* (2007) 37:3509–21. doi:10.1002/eji.200737357
31. Roger T, Out TA, Jansen HM, Lutter R. Superinduction of interleukin-6 mRNA in lung epithelial H292 cells depends on transiently increased C/EBP activity and durable increased mRNA stability. *Biochim Biophys Acta* (1998) 1398:275–84. doi:10.1016/S0167-4781(98)00075-X
32. Giannoni E, Guignard L, Knaup Reymond M, Perreau M, Roth-Kleiner M, Calandra T, et al. Estradiol and progesterone strongly inhibit the innate immune response of mononuclear cells in newborns. *Infect Immun* (2011) 79:2690–8. doi:10.1128/IAI.00076-11
33. Perreau M, Vigano S, Bellanger F, Pellaton C, Buss G, Comte D, et al. Exhaustion of bacteria-specific CD4 T cells and microbial translocation in common variable immunodeficiency disorders. *J Exp Med* (2014) 211:2033–45. doi:10.1084/jem.20140039
34. Lugrin J, Ciarlo E, Santos A, Grandmaison G, dos Santos I, Le Roy D, et al. The sirtuin inhibitor cambinol impairs MAPK signaling, inhibits inflammatory and innate immune responses and protects from septic shock. *Biochim Biophys Acta* (2013) 1833:1498–510. doi:10.1016/j.bbamcr.2013.03.004
35. Vacher G, Ciarlo E, Savova-Bianchi D, Le Roy D, Hantier G, Niculita-Hirzel H, et al. Innate immune sensing of *Fusarium culmorum* by mouse dendritic cells. *J Toxicol Environ Health A* (2015) 78:871–85. doi:10.1080/15287394.2015.1051201
36. Roger T, Delaloye J, Chanson AL, Giddey M, Le Roy D, Calandra T. Macrophage migration inhibitory factor deficiency is associated with impaired killing of Gram-negative bacteria by macrophages and increased susceptibility to *Klebsiella pneumoniae* sepsis. *J Infect Dis* (2013) 207:331–9. doi:10.1093/infdis/jis673
37. Niedergang F, Di Bartolo V, Alcover A. Comparative anatomy of phagocytic and immunological synapses. *Front Immunol* (2016) 7:18. doi:10.3389/fimmu.2016.00018
38. Westermann S, Weber K. Post-translational modifications regulate microtubule function. *Nat Rev Mol Cell Biol* (2003) 4:938–47. doi:10.1038/nrm1260
39. Fensterheim BA, Guo Y, Sherwood ER, Bohannon JK. The cytokine response to lipopolysaccharide does not predict the host response to infection. *J Immunol* (2017) 198:3264–73. doi:10.4049/jimmunol.1602106
40. Pavlou S, Wang L, Xu H, Chen M. Higher phagocytic activity of thioglycollate-elicited peritoneal macrophages is related to metabolic status of the cells. *J Inflamm (Lond)* (2017) 14:4. doi:10.1186/s12950-017-0151-x

41. Yuan Q, Zhan L, Zhou QY, Zhang LL, Chen XM, Hu XM, et al. SIRT2 regulates microtubule stabilization in diabetic cardiomyopathy. *Eur J Pharmacol* (2015) 764:554–61. doi:10.1016/j.ejphar.2015.07.045
42. Annane D, Bellissant E, Cavaillon JM. Septic shock. *Lancet* (2005) 365:63–78. doi:10.1016/S0140-6736(04)17667-8
43. Villalba JM, Alcain FJ. Sirtuin activators and inhibitors. *Biofactors* (2012) 38:349–59. doi:10.1002/biof.1032
44. Cardoso F, Castro F, Moreira-Teixeira L, Sousa J, Torrado E, Silvestre R, et al. Myeloid sirtuin 2 expression does not impact long-term *Mycobacterium tuberculosis* control. *PLoS One* (2015) 10:e0131904. doi:10.1371/journal.pone.0131904
45. Lin J, Sun B, Jiang C, Hong H, Zheng Y. Sirt2 suppresses inflammatory responses in collagen-induced arthritis. *Biochem Biophys Res Commun* (2013) 441:897–903. doi:10.1016/j.bbrc.2013.10.153
46. Hah YS, Cheon YH, Lim HS, Cho HY, Park BH, Ka SO, et al. Myeloid deletion of SIRT1 aggravates serum transfer arthritis in mice via nuclear factor-kappaB activation. *PLoS One* (2014) 9:e87733. doi:10.1371/journal.pone.0087733
47. Kim SR, Lee KS, Park SJ, Min KH, Choe YH, Moon H, et al. Involvement of sirtuin 1 in airway inflammation and hyperresponsiveness of allergic airway disease. *J Allergy Clin Immunol* (2010) 125:449–60.e14. doi:10.1016/j.jaci.2009.08.009
48. Schug TT, Xu Q, Gao H, Peres-da-Silva A, Draper DW, Fessler MB, et al. Myeloid deletion of SIRT1 induces inflammatory signaling in response to environmental stress. *Mol Cell Biol* (2010) 30:4712–21. doi:10.1128/MCB.00657-10
49. Zhang J, Lee SM, Shannon S, Gao B, Chen W, Chen A, et al. The type III histone deacetylase Sirt1 is essential for maintenance of T cell tolerance in mice. *J Clin Invest* (2009) 119:3048–58. doi:10.1172/JCI38902
50. Pfluger PT, Herranz D, Velasco-Miguel S, Serrano M, Tschop MH. Sirt1 protects against high-fat diet-induced metabolic damage. *Proc Natl Acad Sci U S A* (2008) 105:9793–8. doi:10.1073/pnas.0802917105
51. Legutko A, Marichal T, Fievez L, Bedoret D, Mayer A, de Vries H, et al. Sirtuin 1 promotes Th2 responses and airway allergy by repressing peroxisome proliferator-activated receptor-gamma activity in dendritic cells. *J Immunol* (2011) 187:4517–29. doi:10.4049/jimmunol.1101493
52. Niederer F, Ospelt C, Brentano F, Hottiger MO, Gay RE, Gay S, et al. SIRT1 overexpression in the rheumatoid arthritis synovium contributes to proinflammatory cytokine production and apoptosis resistance. *Ann Rheum Dis* (2011) 70:1866–73. doi:10.1136/ard.2010.148957
53. Hu N, Long H, Zhao M, Yin H, Lu Q. Aberrant expression pattern of histone acetylation modifiers and mitigation of lupus by SIRT1-siRNA in MRL/lpr mice. *Scand J Rheumatol* (2009) 38:464–71. doi:10.3109/03009740902895750
54. Beier UH, Wang L, Bhatti TR, Liu Y, Han R, Ge G, et al. Sirtuin-1 targeting promotes Foxp3+ T-regulatory cell function and prolongs allograft survival. *Mol Cell Biol* (2011) 31:1022–9. doi:10.1128/MCB.01206-10
55. Lee HS, Ka SO, Lee SM, Lee SI, Park JW, Park BH. Overexpression of sirtuin 6 suppresses inflammatory responses and bone destruction in mice with collagen-induced arthritis. *Arthritis Rheum* (2013) 65:1776–85. doi:10.1002/art.37963
56. Xiao C, Wang RH, Lahusen TJ, Park O, Bertola A, Maruyama T, et al. Progression of chronic liver inflammation and fibrosis driven by activation of c-JUN signaling in Sirt6 mutant mice. *J Biol Chem* (2012) 287:41903–13. doi:10.1074/jbc.M112.415182
57. Ailixiding M, Aibibula Z, Iwata M, Piao J, Hara Y, Koga D, et al. Pivotal role of Sirt6 in the crosstalk among ageing, metabolic syndrome and osteoarthritis. *Biochem Biophys Res Commun* (2015) 466:319–26. doi:10.1016/j.bbrc.2015.09.019
58. Balestrieri ML, Rizzo MR, Barbieri M, Paolisso P, D'Onofrio N, Giovane A, et al. Sirtuin 6 expression and inflammatory activity in diabetic atherosclerotic plaques: effects of incretin treatment. *Diabetes* (2015) 64:1395–406. doi:10.2337/db14-1149
59. Bruzzone S, Fruscione F, Morando S, Ferrando T, Poggi A, Garuti A, et al. Catastrophic NAD+ depletion in activated T lymphocytes through Nampt inhibition reduces demyelination and disability in EAE. *PLoS One* (2009) 4:e7897. doi:10.1371/journal.pone.0007897
60. Jiang H, Khan S, Wang Y, Charron G, He B, Sebastian C, et al. SIRT6 regulates TNF-alpha secretion through hydrolysis of long-chain fatty acyl lysine. *Nature* (2013) 496:110–3. doi:10.1038/nature12038
61. Lee OH, Kim J, Kim JM, Lee H, Kim EH, Bae SK, et al. Decreased expression of sirtuin 6 is associated with release of high mobility group box-1 after cerebral ischemia. *Biochem Biophys Res Commun* (2013) 438:388–94. doi:10.1016/j.bbrc.2013.07.085
62. Van Gool F, Galli M, Gueydan C, Kruys V, Prevot PP, Bedalov A, et al. Intracellular NAD levels regulate tumor necrosis factor protein synthesis in a sirtuin-dependent manner. *Nat Med* (2009) 15:206–10. doi:10.1038/nm.1906
63. Peek CB, Affinati AH, Ramsey KM, Kuo HY, Yu W, Sena LA, et al. Circadian clock NAD+ cycle drives mitochondrial oxidative metabolism in mice. *Science* (2013) 342:1243417. doi:10.1126/science.1243417
64. Masri S, Sassone-Corsi P. Sirtuins and the circadian clock: bridging chromatin and metabolism. *Sci Signal* (2014) 7:re6. doi:10.1126/scisignal.2005685
65. Akamata K, Wei J, Bhattacharyya M, Cheresh P, Bonner MY, Arbiser JL, et al. SIRT3 is attenuated in systemic sclerosis skin and lungs, and its pharmacologic activation mitigates organ fibrosis. *Oncotarget* (2016) 7:69321–36. doi:10.18632/oncotarget.12504
66. Beier UH, Angelin A, Akimova T, Wang L, Liu Y, Xiao H, et al. Essential role of mitochondrial energy metabolism in Foxp3(+) T-regulatory cell function and allograft survival. *FASEB J* (2015) 29:2315–26. doi:10.1096/fj.14-268409
67. Bindu S, Pillai VB, Kanwal A, Samant S, Mutlu GM, Verdin E, et al. SIRT3 blocks myofibroblast differentiation and pulmonary fibrosis by preventing mitochondrial DNA damage. *Am J Physiol Lung Cell Mol Physiol* (2017) 312:L68–78. doi:10.1152/ajplung.00188.2016
68. Gao J, Zheng Z, Gu Q, Chen X, Liu X, Xu X. Deacetylation of MnSOD by PARP-regulated SIRT3 protects retinal capillary endothelial cells from hyperglycemia-induced damage. *Biochem Biophys Res Commun* (2016) 472:425–31. doi:10.1016/j.bbrc.2015.12.037
69. Lantier L, Williams AS, Williams IM, Yang KK, Bracy DP, Goelzer M, et al. SIRT3 is crucial for maintaining skeletal muscle insulin action and protects against severe insulin resistance in high-fat-fed mice. *Diabetes* (2015) 64:3081–92. doi:10.2337/db14-1810
70. Morigi M, Perico L, Rota C, Longaretti L, Conti S, Rottoli D, et al. Sirtuin 3-dependent mitochondrial dynamic improvements protect against acute kidney injury. *J Clin Invest* (2015) 125:715–26. doi:10.1172/JCI77632
71. Sosulski ML, Gongora R, Feghali-Bostwick C, Lasky JA, Sanchez CG. Sirtuin 3 deregulation promotes pulmonary fibrosis. *J Gerontol A Biol Sci Med Sci* (2017) 72:595–602. doi:10.1093/gerona/glw151
72. Yu W, Gao B, Li N, Wang J, Qiu C, Zhang G, et al. Sirt3 deficiency exacerbates diabetic cardiac dysfunction: role of Foxo3A-Parkin-mediated mitophagy. *Biochim Biophys Acta* (2017) 1863:1973–83. doi:10.1016/j.bbadis.2016.10.021
73. Ciarlo E, Heinonen T, Lugrin J, Acha-Orbea H, Le Roy D, Auwerx J, et al. Sirtuin 3 deficiency does not alter host defenses against bacterial and fungal infections. *Sci Rep* (2017) 7:3853. doi:10.1038/s41598-017-04263-x
74. Eskandarian HA, Impens F, Nahori MA, Soubigou G, Coppee JY, Cossart P, et al. A role for SIRT2-dependent histone H3K18 deacetylation in bacterial infection. *Science* (2013) 341:1238858. doi:10.1126/science.1238858
75. Horwitz SB, Chia GH, Harracksingh C, Orlow S, Pifko-Hirst S, Schneck J, et al. Trifluoperazine inhibits phagocytosis in a macrophagelike cultured cell line. *J Cell Biol* (1981) 91:798–802. doi:10.1083/jcb.91.3.798
76. Roberts RL, Nath J, Friedman MM, Gallin JI. Effects of taxol on human neutrophils. *J Immunol* (1982) 129:2134–41.
77. Hartwig JH, Stossel TP. Interactions of actin, myosin, and an actin-binding protein of rabbit pulmonary macrophages. III. Effects of cytochalasin B. *J Cell Biol* (1976) 71:295–303. doi:10.1083/jcb.71.1.295
78. Seo KS, Park JH, Heo JY, Jing K, Han J, Min KN, et al. SIRT2 regulates tumour hypoxia response by promoting HIF-1alpha hydroxylation. *Oncogene* (2015) 34:1354–62. doi:10.1038/onc.2014.76
79. Cha Y, Han MJ, Cha HJ, Zoldan J, Burkart A, Jung JH, et al. Metabolic control of primed human pluripotent stem cell fate and function by the miR-200c-SIRT2 axis. *Nat Cell Biol* (2017) 19:445–56. doi:10.1038/ncb3517
80. Huang J, Brumell JH. Bacteria-autophagy interplay: a battle for survival. *Nat Rev Microbiol* (2014) 12:101–14. doi:10.1038/nrmicro3160
81. Maurer K, Reyes-Robles T, Alonzo F III, Durbin J, Torres VJ, Cadwell K. Autophagy mediates tolerance to *Staphylococcus aureus* alpha-toxin. *Cell Host Microbe* (2015) 17:429–40. doi:10.1016/j.chom.2015.03.001
82. Wu HM, Wang J, Zhang B, Fang L, Xu K, Liu RY. CpG-ODN promotes phagocytosis and autophagy through JNK/P38 signal pathway in *Staphylococcus aureus*-stimulated macrophage. *Life Sci* (2016) 161:51–9. doi:10.1016/j.lfs.2016.07.016

83. Geeraert C, Ratier A, Pfisterer SG, Perdiz D, Cantaloube I, Rouault A, et al. Starvation-induced hyperacetylation of tubulin is required for the stimulation of autophagy by nutrient deprivation. *J Biol Chem* (2010) 285:24184–94. doi:10.1074/jbc.M109.091553
84. Inoue T, Nakayama Y, Li Y, Matsumori H, Takahashi H, Kojima H, et al. SIRT2 knockdown increases basal autophagy and prevents postslippage death by abnormally prolonging the mitotic arrest that is induced by microtubule inhibitors. *FEBS J* (2014) 281:2623–37. doi:10.1111/febs.12810
85. Li Y, Liu B, Zhao H, Sailhamer EA, Fukudome EY, Zhang X, et al. Protective effect of suberoylanilide hydroxamic acid against LPS-induced septic shock in rodents. *Shock* (2009) 32:517–23. doi:10.1097/SHK.0b013e3181a44c79
86. Mombelli M, Lugrin J, Rubino I, Chanson AL, Giddey M, Calandra T, et al. Histone deacetylase inhibitors impair antibacterial defenses of macrophages. *J Infect Dis* (2011) 204:1367–74. doi:10.1093/infdis/jir553
87. Zhang LT, Yao YM, Lu JQ, Yan XJ, Yu Y, Sheng ZY. Sodium butyrate prevents lethality of severe sepsis in rats. *Shock* (2007) 27:672–7. doi:10.1097/SHK.0b013e31802e3f4c
88. Gojo I, Jiemjit A, Trepel JB, Sparreboom A, Figg WD, Rollins S, et al. Phase 1 and pharmacologic study of MS-275, a histone deacetylase inhibitor, in adults with refractory and relapsed acute leukemias. *Blood* (2007) 109:2781–90. doi:10.1182/blood-2006-05-021873
89. Ciarlo E, Savva A, Roger T. Epigenetics in sepsis: targeting histone deacetylases. *Int J Antimicrob Agents* (2013) 42(Suppl):S8–12. doi:10.1016/j.ijantimicag.2013.04.004
90. Outeiro TF, Kontopoulos E, Altmann SM, Kufareva I, Strathearn KE, Amore AM, et al. Sirtuin 2 inhibitors rescue alpha-synuclein-mediated toxicity in models of Parkinson's disease. *Science* (2007) 317:516–9. doi:10.1126/science.1143780
91. Luthi-Carter R, Taylor DM, Pallos J, Lambert E, Amore A, Parker A, et al. SIRT2 inhibition achieves neuroprotection by decreasing sterol biosynthesis. *Proc Natl Acad Sci U S A* (2010) 107:7927–32. doi:10.1073/pnas.1002924107

Conflict of Interest Statement: The authors declare that the research was conducted in the absence of any commercial or financial relationships that could be construed as a potential conflict of interest.

Supplementary Table S1. Oligonucleotides used to quantify Sirt1-7 mRNA levels by RT-PCR

Target	Forward (5'-3')	Reverse (5'-3')
Sirt1	**agggaacctttgcctcatct**	**gaggtgttggtggcaactct**
Sirt2	**gaggtggcatggattttgac**	**agatggtagtgctggggttg**
Sirt3	**acagctacatgcacggtctg**	**gggaggtcccaagaatgagt**
Sirt4	**cgagcaaaagctcccaatag**	**gatcttgagcagcggaactc**
Sirt5	**ggccgagtttaacatggaga**	**ccgttagtgccctgctttag**
Sirt6	**acctgcaacccacaaaacat**	**ggctcagccttgagtgctac**
Sirt7	**cacatgagcatcacccgttt**	**agcccatcacagttctgagaca**

Supplementary Table S2. Antibodies used for flow cytometry analyses

Purpose	Target	Clone name	Coupling/reference
Flow cytometry	B220	RA3-6B2	eFluor® 450
	CD3	145-2C11	PE, eFluor® 450
	CD4	RM4-5	PE, FITC
	CD8	53-6.7	APC-eFluor® 780, APC-Cy7
	CD11b	M1/710	PE, APC
	CD11c	HL3	PE, APC
	CD14	Sa2-8	PE-Cy7
	CD23	B3B4	PE
	CD25	PC61.5	APC
	CD36	72-1	PE
	CD44	IM7	APC, eFluor® 450
	CD62L	MEL-14	FITC
	CD93	AA4.1	APC
	CD204	2F8	FITC
	IgD	AMS 9.1	FITC
	MHC-II	114.15.2	FITC
Western blot	α-tubulin	B-5-1-2	T5168
	Acetylated α-tubulin	6-11B-1	sc-23950
	ERK1/2	polyclonal	9102
	JNK	polyclonal	9252
	NF-κBp65	D14E12	8242
	Phospho-NF-κBp65	93H1	3033
	p38	polyclonal	9212
	Phospho-ERK1/2	polyclonal	9101
	Phospho-JNK	polyclonal	9251
	Phospho-p38	polyclonal	9211
	SIRT2	polyclonal	ab67299
	TBP	polyclonal	8515

PE: phycoerythrin; FITC: fluorescein isothiocyanate; APC: allophycocyanin. Antibodies for flow cytometry were from eBioscience, except the anti-CD204 and anti-IgD, which were from Bio-Rad and BD Biosciences (Pharmingen), respectively. Antibodies for Western blot were from Cell Signaling Technology, except the anti-α tubulin, anti-acetylated α tubulin and anti-SIRT2, which were from Sigma-Aldrich, Santa Cruz Biotechnology (Dallas, TX) and Abcam, (Cambridge, UK), respectively.

Supplementary Figure S1

Full-length blots

Panels used in Figure 1E

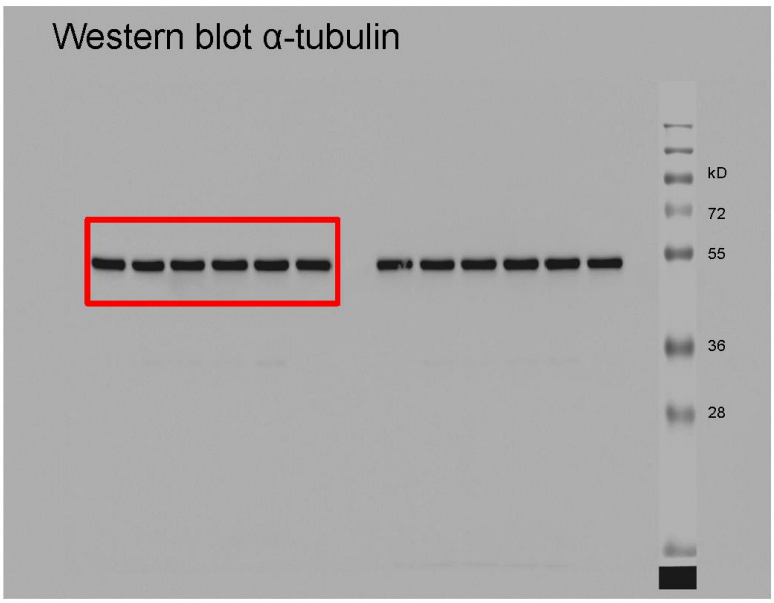

Supplementary Figure S2

Full-length blots

Panels used in Figure 3G

Western blot acetylated α-tubulin

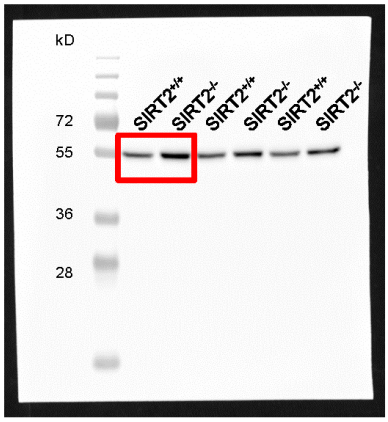

Western blot α-tubulin

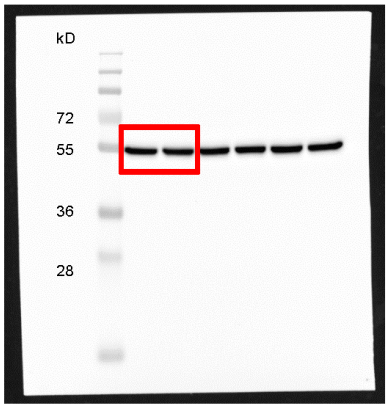

Supplementary Figure S3

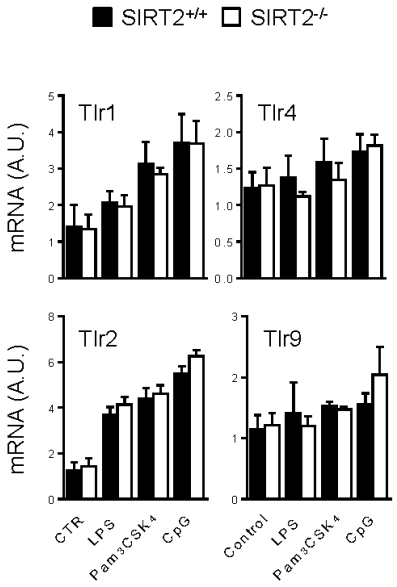

SIRT2 deficiency does not affect the expression of TLRs by macrophages to microbial stimulation. SIRT2$^{+/+}$ and SIRT2$^{-/-}$ BMDMs were exposed for 1 hour to LPS (10 ng/ml), Pam_3CSK_4 (10 ng/ml) and CpG (2 µg/ml). Tlr1, Tlr2, Tlr4 and Tlr9 mRNA levels were quantified by real-time PCR. Data are means ± SD of triplicate samples from one experiment performed with 3 mice.

Supplementary Figure S4

Full-length blots

Panels used in Figure 4A

Western blots
phospho-ERK1/2

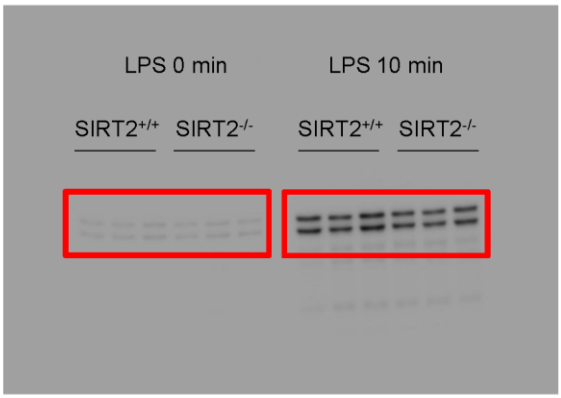

Western blots
total ERK1/2

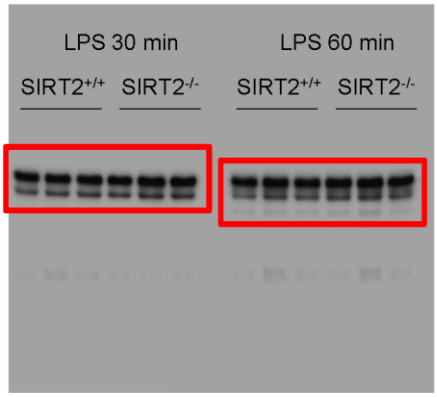

6.2. Sirtuin 5 Deficiency Does Not Compromise Innate Immune Responses to Bacterial Infections

Tytti Heinonen [1], Eleonora Ciarlo [1], Charlotte Théroude [1], Aimilia Pelekanou [1], Jacobus Herderschee [1], Didier Le Roy [1], Thierry Roger [1]

[1] Infectious Diseases Service, Department of Medicine, Lausanne University Hospital, Epalinges, Switzerland.

Front Immunol 2018 Nov 20;9:2675. doi: 10.3389/fimmu.2018.02675. eCollection 2018.

Contribution to the work: I participated to *in vivo* experiments.

frontiers in Immunology

ORIGINAL RESEARCH
published: 20 November 2018
doi: 10.3389/fimmu.2018.02675

Sirtuin 5 Deficiency Does Not Compromise Innate Immune Responses to Bacterial Infections

*Tytti Heinonen†, Eleonora Ciarlo†, Charlotte Théroude, Aimilia Pelekanou, Jacobus Herderschee, Didier Le Roy and Thierry Roger**

Infectious Diseases Service, Department of Medicine, Lausanne University Hospital, Epalinges, Switzerland

OPEN ACCESS

Edited by:
Amy Rasley,
United States Department of Energy (DOE), United States

Reviewed by:
Birgit Strobl,
Veterinärmedizinische Universität Wien, Austria
Evangelos Giamarellos-Bourboulis,
National and Kapodistrian University of Athens, Greece
Marc Le Bert,
UMR7355 Immunologie et Neurogénétique Expérimentales et Moléculaires (INEM), France

***Correspondence:**
Thierry Roger
thierry.roger@chuv.ch
orcid.org/0000-0002-9358-0109

†*These authors have contributed equally to this work*

Specialty section:
This article was submitted to Microbial Immunology, a section of the journal Frontiers in Immunology

Received: *24 April 2018*
Accepted: *30 October 2018*
Published: *20 November 2018*

Citation:
Heinonen T, Ciarlo E, Théroude C, Pelekanou A, Herderschee J, Le Roy D and Roger T (2018) Sirtuin 5 Deficiency Does Not Compromise Innate Immune Responses to Bacterial Infections. Front. Immunol. 9:2675. doi: 10.3389/fimmu.2018.02675

Sirtuin 5 (SIRT5) is a member of the family of NAD^+-dependent lysine/histone deacetylases. SIRT5 resides mainly in the mitochondria where it catalyzes deacetylation, demalonylation, desuccinylation, and deglutarylation of lysine to regulate metabolic and oxidative stress response pathways. Pharmacologic inhibitors of SIRT5 are under development for oncologic conditions, but nothing is known about the impact of SIRT5 on antimicrobial innate immune defenses. Using SIRT5 knockout mice, we show that SIRT5 deficiency does not affect immune cell development, cytokine production and proliferation by macrophages and splenocytes exposed to microbial and immunological stimuli. Moreover, preclinical models suggest that SIRT5 deficiency does not worsen endotoxemia, *Klebsiella pneumoniae* and *Streptococcus pneumoniae* pneumonia, *Escherichia coli* peritonitis, listeriosis, and staphylococcal infection. Altogether, these data support the safety profile in terms of susceptibility to infections of SIRT5 inhibitors under development.

Keywords: sirtuin, innate immunity, cytokine, macrophage, endotoxemia, sepsis, histone deacetylase, metabolism

INTRODUCTION

Innate immune cells such as monocytes/macrophages, neutrophils and dendritic cells (DCs) express pattern recognition receptors (PRRs) that mediate the sensing of microbial associated molecular patterns (such as endotoxin, lipoproteins, peptidoglycans, glucans, mannans, and nucleic acids) and danger-associated molecular patterns released by injured or infected cells. PRRs encompass Toll-like receptors (TLRs), C-type lectin receptors, NOD-like receptors, RIG-I-like receptors, and cytosolic DNA sensors (1, 2). Upon ligand sensing, PRRs initiate intracellular signaling cascades remodeling host transcriptome to promote cytokine/chemokine production and the development of antimicrobial effector mechanisms. Innate immune responses have to be tightly regulated to avoid imbalanced life-threatening immune responses.

Sirtuins belong to the highly conserved family of NAD^+-dependent lysine/histone deacetylases (HDACs). The seven mammalian sirtuins (SIRT1-7) are characterized by their domain organization, enzymatic activity and subcellular nuclear, nucleolar, cytoplasmic or mitochondrial localization. Sirtuins catalyze enzymatic reactions beyond deacetylation, and can function as ADP-ribosyltranferase, demyristolase, decrotonylase, desuccinylase, deglutarylase, demalonylase, deformylase, and demyristolase (3–7). Proteome analyses identified thousands of targets of sirtuins, and sirtuins have been involved in the regulation of many biological functions and pathological processes. Sirtuins are promising therapeutic targets for metabolic, cardiovascular, neurodegenerative, and oncologic diseases (3–7).

SIRT5 is one of the least characterized sirtuins. SIRT5 belongs, together with SIRT3 and SIRT4, to the so-called mitochondrial sirtuins. SIRT5 also localizes into the cytoplasm (8). SIRT5 was initially shown to deacetylate carbamoyl phosphate synthase (CPS1) to promote urea cycle (9). SIRT5 is a weak deacetylase and recent data suggest that SIRT5 primarily performs lysine demalonylation, desuccinylation, and deglutarylation (10, 11). SIRT5 desuccinylates and deglutarylates CSP1 to increase ammonia detoxification and desuccinylates 3-hydroxy-3-methylglutaryl-CoA synthase 2 to increase ketogenesis (10–12). SIRT5 desuccinylates succinate dehydrogenase and pyruvate dehydrogenase to repress cellular respiration and activates superoxide dismutase 1 and isocitrate dehydrogenase 2 through desuccinylation and glucose-6-phosphate dehydrogenase through deglutarylation. In this way, SIRT5 regulates NADPH homeostasis, scavenges reactive oxygen species (ROS), and increases resistance to oxidative stress (8, 13, 14). A malonylome analysis in liver identified gluconeogenesis and glycolysis as the most enriched pathways regulated by SIRT5 (15), while succinylome analyses of heart and liver identified fatty acid oxidation (FAO), amino acid metabolism and TCA cycle (8, 12, 16). Overall, SIRT5 is emerging as a key regulator of metabolism. SIRT5 protects from cardiac dysfunctions and dextran sulfate sodium-induced colitis and promotes or restricts cancer growth depending of the context (16–18). Thus, SIRT5 is a potential therapeutic target for several pathological conditions. Efforts are currently devoted to the generation of SIRT5 inhibitors such as thiosuccinyl peptides, cyclic pentapeptide harboring a central N(ε)-carboxyethyl-thiocarbamoyl-lysine residue and 3-arylthiosuccinylated and 3-benzylthiosuccinylated peptide derivatives (19–21) for specific cancer types (18, 22).

The impact of SIRT5 on antimicrobial host defenses is unknown; which is an important missing piece considering the clinical development of SIRT5 inhibitors. Using SIRT5 knockout mice, we show that SIRT5 deficiency has no major impact on immune cell development and on the response of macrophages and splenocytes to microbial stimulation. Going well along with these observations, preclinical models revealed that SIRT5 knockout mice are not particularly sensitive to endotoxemia, *Klebsiella pneumoniae* and *Streptococcus pneumoniae* pneumonia, *Escherichia coli* peritonitis, listeriosis and staphylococcal infection. Up to now, these data support the assumption that SIRT5 inhibitors should not increase patients' susceptibility to infections.

MATERIALS AND METHODS

Ethics Statement

Animal experimentation was approved by the *Service de la Consommation et des Affaires Vétérinaires* of *Canton de Vaud* (Epalinges, Switzerland) under authorizations n°VD 3287, 876.8, 876.9, 877.8, and 877.9 and performed according to Swiss and ARRIVE guidelines.

Mice, Cells and Reagents

Experiments were performed using 8 to 12-week-old C57BL/6J mice (Charles River Laboratories, Saint-Germain-sur-l'Arbresle, France) and SIRT5 knockout mice (kindly provided by Prof Johan Auwerx, Ecole Polytechnique Fédérale de Lausanne, Lausanne, Switzerland) backcrossed 7 times on a C57BL/6J background (23). Mice were housed (12 h light/dark cycle, 22°C, 70% humidity) under specific pathogen-free conditions in the animal facility of the Centre des Laboratoires d'Epalinges (CLE, Epalinges, Switzerland, license number VD-H04). Colonies were free of mouse norovirus and mouse hepatitis virus infections. Mice were fed with γ-irradiated food (Global Rodent XP 18, Provimi Kliba AG, Kaiseraugst, Switzerland) and water *ad libitum*. Mice were transferred in a BSL2 unit to perform *in vivo* models of infection.

Bone marrow-derived macrophages (BMDMs) and splenocytes were obtained and cultured as described (24, 25). For experiments, cells were seeded in complete medium without growth factors and antibiotics (1 or 20 $\times$ 10^5 cells in 96 or 6-well plates). Stimuli were *Salmonella minnesota* ultra pure LPS (InvivoGen, San Diego, CA), Pam_3CSK_4 (EMC microcollections, Tübingen, Germany), CpG ODN 1826 (CpG, InvivoGen), toxic shock syndrome toxin-1 (TSST-1, Toxin Technology, Sarasota, FL), concanavalin A (Sigma-Aldrich, St. Louis, MI), anti-CD3ε, and anti-CD28 antibodies (clones 145-2C11 and 37.51, eBioscience, San Diego, CA) and phorbol-12-myristate-13-acetate (PMA) plus ionomycin (Sigma-Aldrich) or bacteria. Clinical strains of *E. coli* O18, *S. aureus* AW7, *K. pneumoniae*, *S. pneumoniae*, and *L. monocytogenes* 10403s were grown in brain heart infusion broth (BD Biosciences, Erembodegem, Belgium), washed in 0.9% NaCl and adjusted at 10^9-10^{10} CFU/ml (26–29). Bacteria were heat-inactivated for 2 h at 56°C for *in vitro* use.

Flow Cytometry Analyses

Single cell suspensions from thymus and spleen were enumerated and incubated with 2.4G2 monoclonal antibody (mAb) (30). Cells were stained using mAbs listed in **Table S1**. Data were acquired using a LSR II flow cytometer (BD Biosciences) and analyzed using FlowJo Version 10.2 software (FlowJo LLC, Ashland OR) (31).

Western Blot Analyses

Protein extracts were submitted to PAGE and transferred onto nitrocellulose membranes (32–34). Membranes were incubated with antibodies directed against SIRT5 (8782, 1:1,000, Cell Signaling Technology, Danvers, MA) or β-actin (4967S, 1:1,000, Cell Signaling Technology) and then with a secondary HRP-conjugated antibody (31460, 1:10,000, Thermo Fisher, Waltham, MA) (35). Blots were imaged with the ECL Western blotting system (GE Healthcare, Little Chalfont, UK). Images were recorded using a Fusion Fx system (Viber Lourmat, Collégien, France) (36).

Metabolic Activity Measurements

The oxygen consumption rate (OCR, in pmole O_2/minute) and the extracellular acidification rate (ECAR, in mpH/minute) were analyzed using a 96-well format Seahorse XFe® system, the Seahorse XF Cell Mito Stress Test Kit and the Seahorse XF Glycolysis Stress Test Kit (Agilent Technologies, Santa Clara, CA). Four $\times$ 10^4 BMDMs were plated in 96-well

plates in complete IMDM medium. The next day, cells were rested one hour in Seahorse medium with or without glucose. Mitochondrial respiration was assessed by measuring OCR following the addition of 1 μM oligomycin (OM), 1 μM FCCP and 2 μM antimycinA/1 μM rotenone (AA/Rot). Glycolytic function was assessed by measuring ECAR following the addition of 10 mM glucose, 1 μM oligomycin and 50 mM 2-deoxy-glucose (2-DG).

RNA Analyses

Total RNA was isolated, reverse transcribed (RNeasy and QuantiTect reverse transcription kits, Qiagen, Hilden, Germany) and used in real-time PCR using Fast SYBR® Green Master Mix and a QuantStudio™ 12K Flex system (Life Technologies, Carlsbad, CA) as reported (24, 37). Samples were tested in triplicate. Gene specific expression was normalized to actin expression. Primers are listed in **Table S2**. Sirt5 mRNA expression levels in organs were extracted from the BioGPS resource (http://biogps.org).

Proliferation and Cytokine Measurements

The proliferation of splenocytes cultured for 48 h in 96-well plates was quantified by measuring ^{3}H-thymidine incorporation over 18 h (38). Cytokine concentrations were quantified using DuoSet ELISA kits (R&D Systems, Abingdon, UK) (39). The viability, assessed using the MTT assay (40), of resting and stimulated SIRT5$^{+/+}$ and SIRT5$^{-/-}$ BMDMs was not different.

In vivo Models

Mice were challenged intraperitoneally (i.p.) with 20 mg/kg LPS or 4×10^2 or 3×10^4 CFU *E. coli* O18, intranasally (i.n.) with 30 CFU *K. pneumoniae* or 1×10^6 CFU *S. pneumoniae* and intravenously (i.v.) with 1.2×10^3 or 9×10^4 CFU *L. monocytogenes* or 3×10^4 or 2×10^7 CFU *S. aureus*. Blood was collected to quantify cytokines and bacteria (24). At least once daily, body weight, severity score (graded from one to five) and survival were registered (41). Animals were euthanized when they met a severity score of four. Two operators performed animal follow-up.

Statistical Analyses

Comparisons between different groups were performed by analysis of variance followed by two-tailed unpaired Student's *t*-test. *In vivo* bacteria and cytokine data were analyzed using the Mann-Whitney test. Survival curves were built using the Kaplan-Meier method and differences were analyzed by the log-rank sum test. All analyses were performed using PRISM (GraphPad Software). *P* values were two-sided, and $P < 0.05$ was considered to indicate statistical significance.

RESULTS

SIRT5 Deficiency Has No Major Impact on the Development of Immune Cells

SIRT5 mRNA was ubiquitously expressed in organs, including immune organs (bone marrow, lymph nodes, spleen, and thymus). Highest levels were observed in brown adipose tissue, heart and liver (**Figure 1A**). Germline *Sirt5* knockout mice [described in (23)] were used to address whether SIRT5-deficiency affected immune cell development by analyzing thymus and spleen cell contents. The absolute numbers of cells in the thymus and the spleen of SIRT5$^{+/+}$ and SIRT5$^{-/-}$ mice were similar (**Figure 1B**). When compared to SIRT5$^{+/+}$ mice, SIRT5$^{-/-}$ mice expressed normal proportions and absolute numbers of CD4/CD8 double negative (DN), double positive (DP), and single positive (SP) thymocytes (**Figure 1C**), such as of DN1-DN4 subpopulations (CD25^{+}CD44^{+}, CD25^{-}CD44^{+}, CD25^{+}CD44^{-}, and CD25^{-}CD44^{-}). SIRT5$^{-/-}$ mice expressed normal proportions and absolute numbers of splenic CD3^{+} T cells (SP, DN as well as CD4^{+} and CD8^{+} CD44^{low}CD62L^{high} naïve and CD44^{high}CD62L^{low} memory T cells), B cells (non-IgD^{+}/CD23^{+} immature B cells and IgD^{+}CD23^{+} mature B cells) and DCs (B220^{-}CD11c^{+} conventional DCs and B220^{+}CD11c^{+} plasmacytoid DCs) (**Figure 1D**). Overall, SIRT5 deficiency had no impact on the development of the main T-cell, B-cell and DC populations.

SIRT5 Deficiency Does Not Affect the Response of Macrophages and Splenocytes to Immune Stimulation

Macrophages are highly proficient at sensing microbial products through TLRs and play a central role in anti-microbial host defenses by orchestrating innate and adaptive immune responses through the production of cytokines. Bone marrow derived macrophages (BMDMs) expressed SIRT5 protein, albeit less than liver. SIRT5 was undetectable in SIRT5$^{-/-}$ BMDMs (**Figure 2A**). SIRT5$^{-/-}$ BMDMs showed a slight increased oxygen consumption rate (OCR, readout of mitochondrial activity, **Figure 2B**) and decreased acidification rate (ECAR, readout of glycolytic activity, **Figure 2C**).

BMDMs were exposed to LPS, Pam_3CSK_4, CpG [i.e., TLR4, TLR1/TLR2, and TLR9 agonists (1, 2)] and heat killed bacteria before measuring cytokine response. SIRT5$^{+/+}$ and SIRT5$^{-/-}$ BMDMs up-regulated likewise Tnf and Il6 mRNAs (**Figures 2D,E**). Moreover, SIRT5$^{+/+}$ and SIRT5$^{-/-}$ BMDMs secreted similar levels of TNF and IL-6 in response to LPS, Pam_3CSK_4, CpG, *E. coli* and *S. aureus* (**Figures 2F,G**). In accordance with these results, SIRT5$^{+/+}$ and SIRT5$^{-/-}$ BMDMs expressed similar levels of Tlr1, Tlr2, Tlr4, and Tlr9 mRNA at baseline and upon exposure to LPS, Pam_3CSK_4, and CpG (**Figure 3**, upper panels). Finally, SIRT5$^{+/+}$ and SIRT5$^{-/-}$ BMDMs cultured with medium, LPS, Pam_3CSK_4, and CpG expressed comparable gene expression levels of CXCL1 (KC/GROα) and CXCL10 (IP10) chemokines, CD36 scavenger receptor and CD40 costimulatory molecule (**Figure 3**, lower panels).

To address further whether SIRT5 deficiency affected the response of immune cells, the proliferation of SIRT5$^{+/+}$ and SIRT5$^{-/-}$ splenocytes exposed to LPS, CpG, Pam_3CSK_4, TSST-1, and anti-CD3/CD28 was assessed by ^{3}H-thymidine incorporation, (**Figure 4A**), while the production of IL-2 by SIRT5$^{+/+}$ and SIRT5$^{-/-}$ splenocytes exposed to TSST-1, anti-CD3/CD28 and PMA plus ionomycin was measured by ELISA

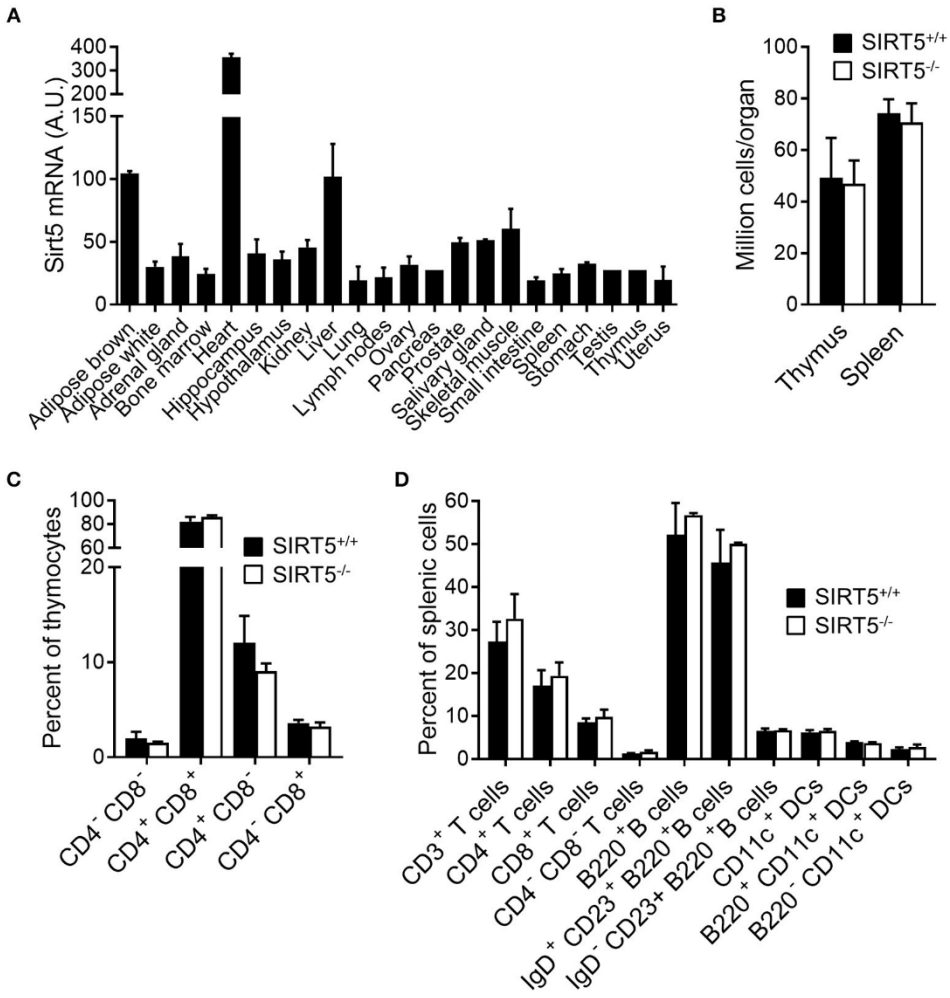

FIGURE 1 | SIRT5 deficiency does not affect immune cell development in thymus and spleen. **(A)** Sirt5 mRNA expression levels in a panel of mouse organs (extracted from the BioGPS resource). **(B)** Total cell numbers per thymus and spleen of SIRT5$^{+/+}$ and SIRT5$^{-/-}$ mice. **(C,D)** Percentages of T cell subpopulations in the thymus **(C)** and of T cells, B cells and DCs subpopulations in the spleen **(D)** of SIRT5$^{+/+}$ and SIRT5$^{-/-}$ mice. Data are means ± SD from one experiment performed with three mice and are representative of two experiments. $P > 0.5$ for all conditions **(B–D)**.

(**Figure 4B**). Neither proliferation nor IL-2 production was modified by SIRT5 deficiency. Altogether, the results argued against an important role of SIRT5 in controlling cytokine production by macrophages exposed to TLR ligands and the response of splenocytes to microbial and immune stimuli.

SIRT5 Deficiency Does not Affect Endotoxemia and Does Not Worsen Bacterial Infections

SIRT5$^{+/+}$ and SIRT5$^{-/-}$ mice were subjected to endotoxemia induced by an i.p. challenge with 20 mg/kg LPS. Consistent with the results observed *in vitro*, TNF, and IL-6 concentrations in blood collected 1 h (TNF) and 6 h (IL-6) after LPS challenge were similar in SIRT5$^{+/+}$ and SIRT5$^{-/-}$ mice ($P = 0.2$ and 0.4; **Figure 5A**). Accordingly, the mortality rates of SIRT5$^{+/+}$ and SIRT5$^{-/-}$ mice were not significantly different (75% vs. 90%; $P = 0.4$; **Figure 5B**). To mimic clinical situations, we then explored the impact of SIRT5-deficiency on host defenses in models of infections induced by challenging mice with *K. pneumoniae* and *S. pneumoniae* i.n., *E. coli* i.p. and *L. monocytogenes* and *S. aureus* i.v.

In a non-severe model of *K. pneumoniae*-induced pneumonia, body weight loss was similar in the SIRT5$^{+/+}$ and SIRT5$^{-/-}$ groups (**Figure 6A**, left panel). Moreover, mouse survival was not impaired by SIRT5 deficiency (SIRT5$^{+/+}$ vs. SIRT5$^{-/-}$: 77% vs. 100% survival; $P = 0.1$, **Figure 6A**, right panel). SIRT5 deficiency did not worsen the outcome of mice in a quickly lethal model of *S. pneumoniae*-induced pneumonia (**Figure 6B**). Two days post-infection, the proportions of bacteremic mice (6/10 vs. 5/10) and blood *S. pneumoniae* loads (SIRT5$^{+/+}$ vs. SIRT5$^{-/-}$: $4.1 \pm 2.2 \times 10^3$ CFU/ml vs. $4.8 \pm 3.6 \times 10^3$ CFU/ml; mean ± SEM; $P = 0.9$)

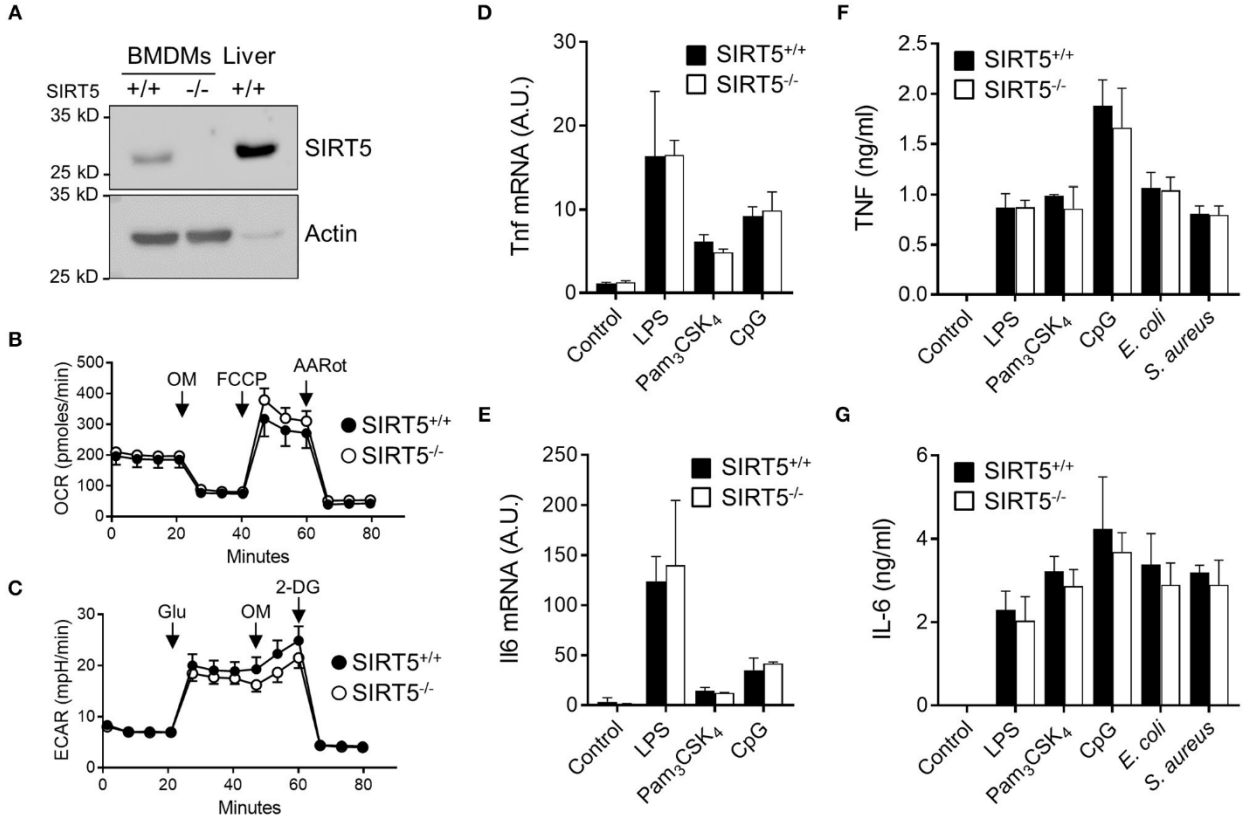

FIGURE 2 | SIRT5 deficiency does not affect TNF and IL-6 production by macrophages exposed to microbial stimuli. **(A)** SIRT5 protein expression in $SIRT5^{+/+}$ and $SIRT5^{-/-}$ BMDMs and $SIRT5^{+/+}$ liver assessed by Western blotting. Full-length blots are presented in **Figure S1**. **(B,C)** Oxygen consumption rate (OCR, **B**) and extracellular acidification rate (ECAR, **C**) of $SIRT5^{+/+}$ and $SIRT5^{-/-}$ BMDMs. Data are means ± SD from one experiment performed with two mice. **(D–G)** $SIRT5^{+/+}$ and $SIRT5^{-/-}$ BMDMs were exposed to LPS (10 ng/ml), Pam_3CSK_4 (10 ng/ml), CpG (2 μg/ml), *E. coli*, and *S. aureus* (10^6 CFU/ml). Gene expression levels were quantified by RT-PCR, normalized to actin levels, and expressed relative to $SIRT5^{+/+}$ control set at one [**(D)**: 1 h, **(E)**: 4 h]. The concentrations of TNF (4 h) and IL-6 (18 h) in cell culture supernatants were quantified by ELISA **(F,G)**. Data are means ± SD of triplicate samples from one experiment performed with three mice and are representative of two-three experiments **(A, D–G)**. $P > 0.05$ for all conditions.

were equivalent in the two groups. Accordingly, mortality rate was not significantly different (100 vs. 89% mortality; $P = 0.08$).

In a model of acute peritonitis induced by *E. coli*, bacterial dissemination into the blood ($SIRT5^{+/+}$ vs. $SIRT5^{-/-}$: 2.3 ± 1.3 × 10^8 CFU/ml vs. 3.8 ± 2.0 × 10^3 CFU/ml; mean ± SEM; $P = 0.4$) and mortality rate (73 vs. 91%, $P = 0.6$) were comparable using $SIRT5^{+/+}$ and $SIRT5^{-/-}$ mice (**Figure 6C**, plain lines). Upon challenge with a low inoculum of *E. coli*, all $SIRT5^{+/+}$ and $SIRT5^{-/-}$ mice survived (**Figure 6C**, dashed lines). During acute listeriosis, $SIRT5^{+/+}$ and $SIRT5^{-/-}$ mice displayed similar bacteremia ($SIRT5^{+/+}$ vs. $SIRT5^{-/-}$: 4.1 ± 2.2 × 10^3 CFU/ml vs. 4.8 ± 3.6 × 10^3 CFU/ml; mean ± SEM, $P = 0.8$) and survival rate ($P = 0.9$) (**Figure 7A**, plain lines). In a model of sublethal listeriosis, the mortality rate of $SIRT5^{+/+}$ and $SIRT5^{-/-}$ mice was not statistically different ($SIRT5^{+/+}$ vs. $SIRT5^{-/-}$: 100% vs. 75% survival; $P = 0.14$, **Figure 7A**, dashed lines). In a model of severe, systemic staphylococcal infection (**Figure 7B**, plain lines), there was no difference in severity score, body weight loss and survival (0 vs. 0%; $P = 0.7$) between $SIRT5^{+/+}$ and $SIRT5^{-/-}$ mice. Analogous to what observed upon challenge with low inocula of *K. pneumoniae*, *E. coli* and *L. monocytogenes* (**Figures 6A,C, 7B**), $SIRT5^{+/+}$ and $SIRT5^{-/-}$ mice were similarly resistant to sublethal staphylococcal infection (**Figure 7B**, dashed lines) suggesting that SIRT5-deficient mice are not particularly susceptible to bacterial infections.

DISCUSSION

This is the first report of the impact of SIRT5 on antimicrobial host defenses. *In vitro* studies using macrophages and splenocytes and preclinical models of endotoxemia and Gram-positive and Gram-negative bacteria infections suggest that SIRT5 deficiency has no major impact on antibacterial defenses. These observations are particularly relevant in light of the development of pharmacological inhibitors of SIRT5 for clinical applications (42).

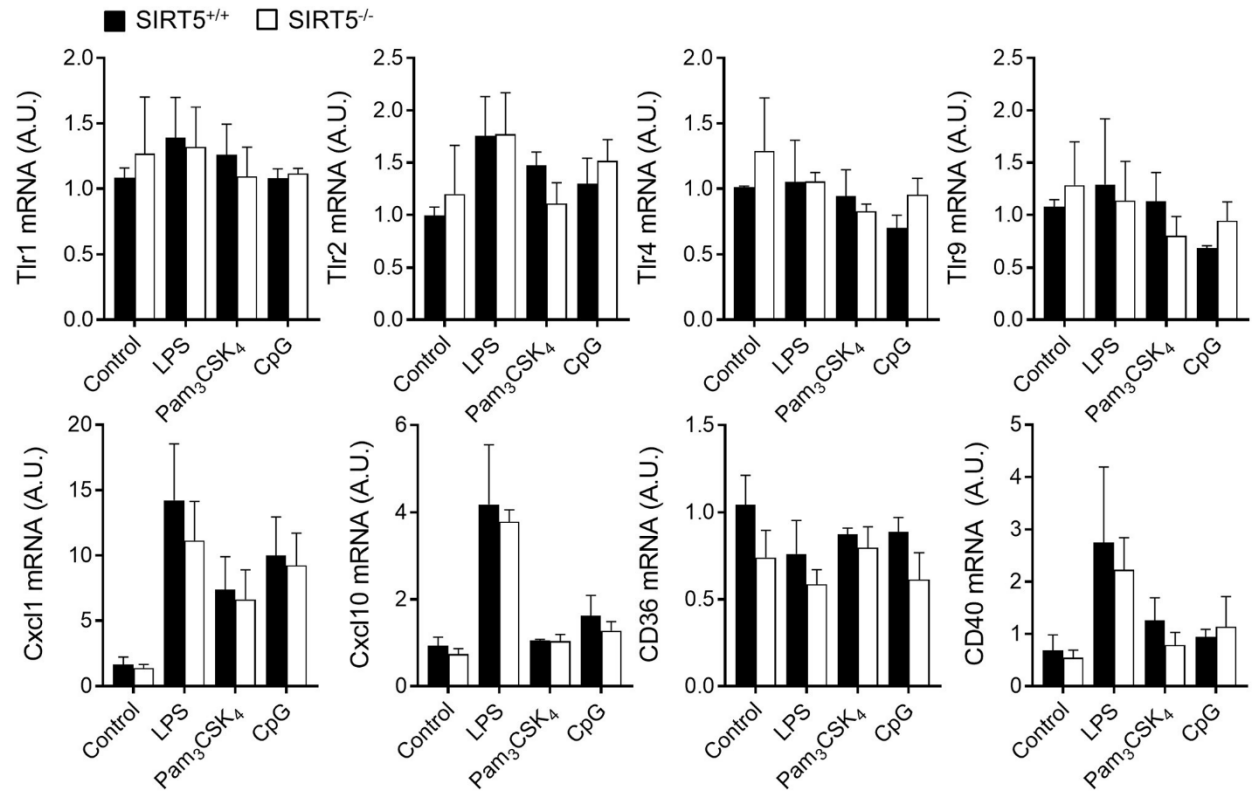

FIGURE 3 | SIRT5 deficiency does not affect macrophage response to microbial stimulation. SIRT5$^{+/+}$ and SIRT5$^{-/-}$ BMDMs were exposed for 1 h to LPS (10 ng/ml), Pam_3CSK_4 (10 ng/ml) and CpG (2 μg/ml). Gene expression levels were quantified by RT-PCR, normalized to actin levels, and expressed relative to SIRT5$^{+/+}$ control set at one. Data are means ± SD of triplicate samples from one experiment performed with three mice. $P > 0.05$ for all conditions.

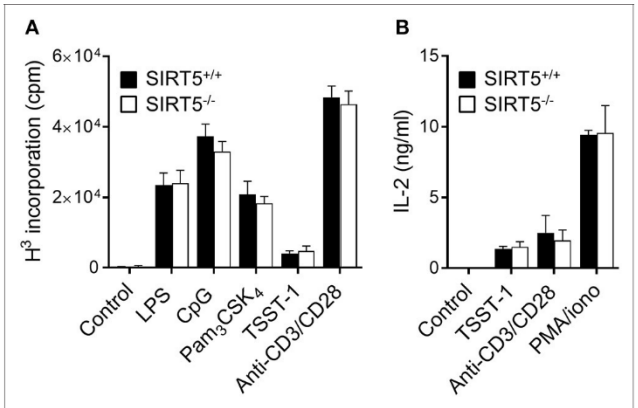

FIGURE 4 | SIRT5 deficiency does not affect proliferation of and IL-2 production by splenocytes. SIRT5$^{+/+}$ and SIRT5$^{-/-}$ splenocytes were incubated for 48 h with LPS (5 μg/ml), CpG (2 μg/ml), Pam_3CSK_4 (5 μg/ml), TSST-1 (2 μg/ml), anti-CD3/CD28 antibodies (1 μg/ml) and PMA + ionomycin (PMA/iono, 10 ng/ml/100 ng/ml). **(A)** Proliferation was measured by ^{3}H-thymidine incorporation. **(B)** IL-2 concentrations in cell culture supernatants were quantified by ELISA. Data are means ± SD of one experiment performed with three mice and are representative of two experiments. $P > 0.05$ for all conditions.

SIRT5 deficiency neither affects the development of the major T cells, B cells and DCs subsets in thymus and spleen nor the proliferation and the production of IL-2 by splenocytes. Similar observations were obtained using SIRT2$^{-/-}$and SIRT3$^{-/-}$ mice (43, 44). In SIRT1-deficient mice, CD4$^+$, CD8$^+$, and CD4$^+$CD8$^+$ thymic subpopulations were normal but highly sensitive to DNA-damaging ionizing radiation (45). Circulating T cell, B cell and monocyte counts were normal in 5 months old SIRT7$^{-/-}$ mice that developed inflammatory cardiomyopathy (46). SIRT6-deficent mice developed, after 2 weeks of life, a progeroid syndrome associated with decreased lymphocyte counts in thymus and spleen. However, lymphocyte flaw was not cell-intrinsic but linked to systemic defects (47). Overall sirtuins do not seem to affect the development of adaptive immune cells. Yet, SIRT1 was reported to influence T-helper (Th) 2, Th9, Th17 and T-regulatory (Treg) responses and SIRT3 to sustain the suppressive function of Tregs (48–52). Thus, it would be interesting to define whether SIRT5 shapes T cell responses.

SIRT5 influences diverse metabolic pathways in cardiac and hepatic cells, including urea cycle, amino acid metabolism, the TCA cycle, FAO, glycolysis and oxidative stress response (7–16). SIRT5$^{-/-}$ BMDMs showed a modest increased mitochondrial activity and decreased glycolytic

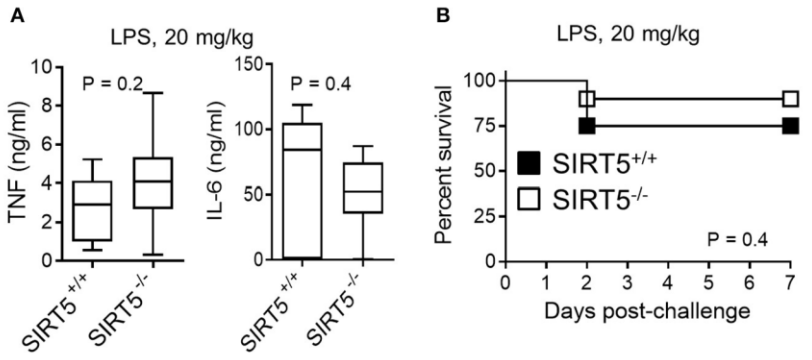

FIGURE 5 | SIRT5 deficiency does not affect endotoxemia. SIRT5$^{+/+}$ and SIRT5$^{-/-}$ female mice were injected i.p. with 20 mg/kg LPS ($n = 8$ and 10 mice per group). **(A)** TNF and IL-6 concentrations in blood collected 1 h (TNF) and 6 h (IL-6) after LPS challenge. $P = 0.2$ and 0.4. **(B)** Survival of mice. $P = 0.4$.

activity, suggesting that SIRT5 may be less influential in macrophages than in heart and liver (8, 15). Correlatively, SIRT5 mRNA and protein were expressed at much lower levels in immune organs [our data and (9)] and in primary macrophages than in liver and heart (5 and 10-fold less SIRT5 mRNA in BMDMs than in liver and heart, respectively).

SIRT5 deficiency had no major impact on LPS-induced cytokine production by macrophages and circulating TNF and IL-6 levels were similar in SIRT5$^{+/+}$ and SIRT5$^{-/-}$ endotoxemic mice. SIRT5-deficient mice under high fat diet, a condition inducing inflammation and oxidative stress, showed normal metabolic parameters and signs of inflammation attested by *Tnf*, *Cd68* (a monocyte/macrophage marker) and *Cd36* (a scavenger receptor) gene expression in the liver (23). Two recent studies analyzed the impact of SIRT5 deficiency on mouse macrophage response to LPS, leading to opposite conclusions. SIRT5$^{-/-}$ peritoneal macrophages produced reduced levels of TNF, IL-6, and MCP-1 (monocyte chemoattractant protein-1/CCL2). SIRT5 competed with SIRT2 to interact with NF-κB p65. Since SIRT2 deacetylates p65 to inhibit its transduction activity, SIRT5 indirectly promoted p65 acetylation and activity (53). In sharp contrast, LPS-stimulated SIRT5$^{-/-}$ BMDMs expressed increased levels of Tnf, Il1b, and Il6 mRNA but not Il10 mRNA. SIRT5 desuccinylated PKM2 (pyruvate kinase M2), promoting tetramer-to-dimer transition and inhibiting pyruvate kinase activity of PKM2. In that study, SIRT5 deficiency protected from DSS-induced colitis. The inconsistency of the impact of SIRT5 on inflammatory responses echoes those reported for SIRT1, SIRT2, SIRT3, and SIRT6 *in vitro* and *in vivo* [discussed in (43, 44)]. Differences in experimental conditions (BMDMs vs. peritoneal macrophages, germline vs. cell-type specific gene knockout, use of si/shRNA and pharmacological modulators of sirtuins) and subtle variations in qualitative and quantitative caloric input and NAD$^+$ availability may explain these differences. Additionally, the length of stimulation and the doses of stimulus [10 ng/ml of ultra-pure LPS here vs. 100 ng/ml of crude LPS in (17) and (53)] may have affected the results. It should also be stressed that SIRT5 deficiency was obtained by disruption of exon 4 in the case of the mice used in this study (23), while exons 2–5 were deleted in the SIRT5 knockout mice available from the Jackson Laboratory used in other studies (17, 53). Nonetheless, even in these studies, the background of the animals may have differed substantially considering that commercial knockout mice are of 85% 129 and 15% C57BL/6 backgrounds and that mice were backcrossed 10 times on a BL/6J background in one study (17) while SIRT5$^{+/+}$ and SIRT5$^{-/-}$ littermates were derived from the SIRT5$^{+/-}$ heterozygote mice in the other study (53). Of note, all broad screening proteomic analyses identified metabolic pathways as the most targeted pathways by SIRT5, while pathways commonly associated with immune/inflammatory responses (such as NF-kB, interferon-response, cytokine, cell migration and inflammation pathways) were not evidenced (8, 11, 12, 15, 16).

Endotoxemia reflects pathological situations such as fulminant meningococcemia characterized by high blood loads of endotoxin, but does not reproduce the complex host-pathogen interactions generally taking place during bacterial infections. Therefore, we sought to define the impact of SIRT5 in preclinical models of infections mimicking common clinical situations. SIRT5 deficiency did not sensitize mice to severe *S. pneumoniae* pneumonia, rapidly lethal *E. coli* peritonitis, listeriosis and staphylococcal infection. In the most stringent models, SIRT5 deficiency did not protect from lethal infection, as foreseen if SIRT5 would amplify cytokine response. SIRT5 deficiency also did not render mice particularly susceptible to bacterial infections as suggested by the results obtained using models of sub-lethal/mild infection with *K. pneumoniae*, *E. coli*, *L. monocytogenes*, and *S. aureus*. Considering the diversity of the agents (Gram-positive and Gram-negative and intracellular and extracellular bacteria) and of the routes of infection tested (i.n., i.p. and i.v.), these results so far support the assumption that SIRT5 has no dramatic influence on host defenses against bacterial infections and the clinical development of SIRT5 inhibitors for

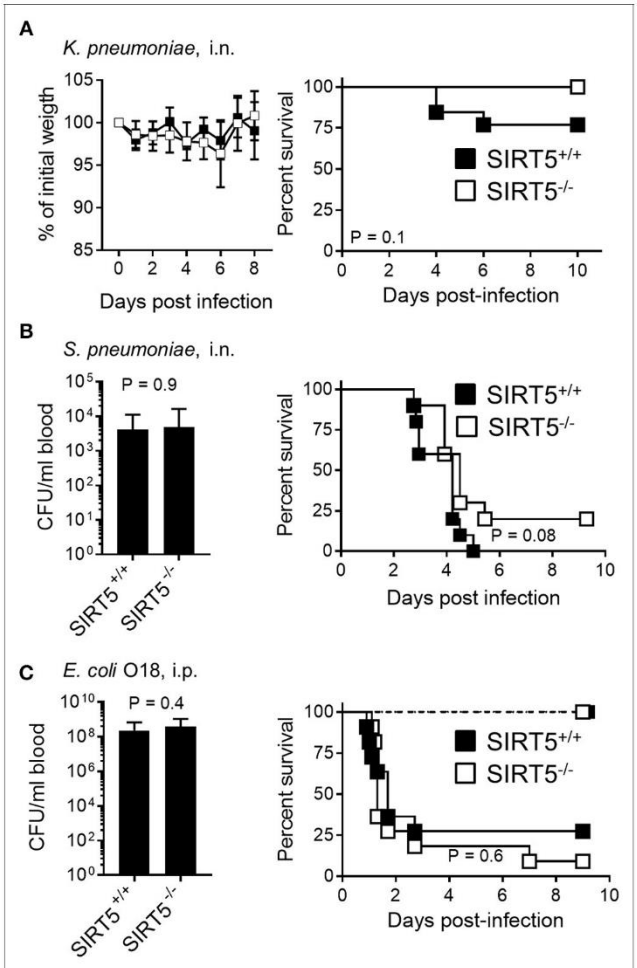

FIGURE 6 | SIRT5 deficiency does not worsen *Klebsiella pneumoniae* and *Streptococcus pneumoniae* pneumonia and *E. coli* peritonitis. SIRT5$^{+/+}$ and SIRT5$^{-/-}$ mice were injected i.n. with 30 CFU *K. pneumoniae* (**A**, $n = 11$ females + 2 males and 7 females + 3 males) or 1.6×10^6 CFU *S. pneumoniae* (**B**, $n = 10$ males per genotype) and i.p. with 4×10^2 CFU *E. coli* [**(C)**, $n = 7$ males per genotype, dashed lines] or 3×10^4 CFU *E. coli* [**C**, $n = 11$ females per genotype, plain lines]. Body weight is expressed in percentage of initial weight (**A**, left panel). Blood was collected 18 h post-infection to quantify bacteria [**(B,C)**, left panels; **(C)**: following infection with 3×10^4 CFU *E. coli*. $P = 0.9$ and 0.4]. [**(A–C)**, right panels] Survival: $P > 0.05$ for all models.

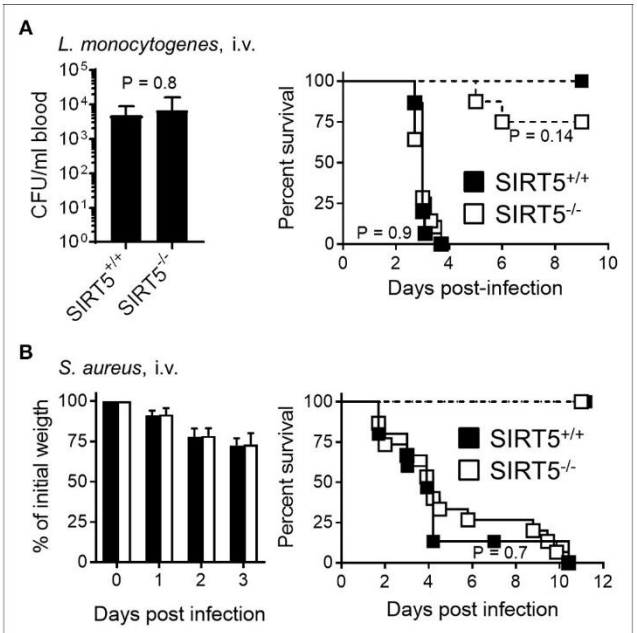

FIGURE 7 | SIRT5 deficiency does not worsen listeriosis and staphylococcal infection. SIRT5$^{+/+}$ and SIRT5$^{-/-}$ mice were injected i.v. with 1.2×10^3 CFU *L. monocytogenes* [**(A)**, $n = 5$ females + 3 males per genotype, dashed lines], 9×10^4 CFU *L. monocytogenes* [**A**, $n = 15$ and 14 females, plain lines], 3×10^4 CFU *S. aureus* (**B**, $n = 6$ females per genotype, dashed lines) or 2×10^7 CFU *S. aureus* (**B**, $n = 9$ females + 6 males per genotype, plain lines, 2 experiments). Blood was collected 48 h post-infection with 9×10^4 CFU *L. monocytogenes* to quantify bacteria (**A**, left panel, $P = 0.8$). Body weight following infection with 2–10 $\times 10^7$ CFU *S. aureus* is expressed in percentage of initial weight (**B**, left panel). Survival: $P = 0.14$ when comparing SIRT5$^{+/+}$ and SIRT5$^{-/-}$ mice challenged with 1.2×10^3 CFU *L. monocytogenes* and $P > 0.5$ for all other models.

oncologic purposes (18, 22). This contrasts with inhibitors of HDAC1-11 which impaired innate immune defenses against infections in mouse models and have been associated with episodes of severe infection when infused into cancer patients (37, 54–58). Further work will be required to test the efficacy of potential SIRT5 inhibitors (19–21) in models of cancer (18, 22) and of infections and sepsis, then to define whether these inhibitors may predispose to infections in the setting of comorbidities, e.g., in elderly patients and patients with chronic inflammatory disorders like for example colitis and diabetes mellitus.

Overall, SIRT5 does not worsen host defenses to bacterial infections under the conditions tested here. Since sirtuins are linked to metabolism, age-associated dysfunctions and lifespan, it would be of interest to investigate the role of SIRT5 under metabolic stress conditions and in older mice. To conclude, our results support the development of SIRT5 inhibitors for clinical purposes, as they suggest that these drugs would not increase patients' susceptibility to infections.

AUTHOR CONTRIBUTIONS

TH, EC, CT, AP, and DLR performed *in vitro* experiments. JH participated to flow cytometry analyses. TH, EC, CT, and DLR performed *in vivo* experiments. TR conceived the project, designed the experiments and wrote the paper. All the authors revised the paper.

FUNDING

This work was supported by grants from the Swiss National Science Foundation (SNSF) 145014, 149511, and 173123 to TR.

EC was supported by the Santos Suarez Foundation, CT by the European Sepsis Academy Horizon 2020 Marie Skłodowska-Curie Action: Innovative Training Network (MSCA-ESA-ITN, grant number 676129) and AP (present address: 4th Department of Internal Medicine, Attikon University Hospital, University of Athens Medical School, 12462 Athens, Greece) by the Porphyrogenis Foundation.

ACKNOWLEDGMENTS

We thank Filipe Pé-Curto for technical help.

SUPPLEMENTARY MATERIAL

The Supplementary Material for this article can be found online at: https://www.frontiersin.org/articles/10.3389/fimmu.2018.02675/full#supplementary-material

Figure S1 | Full-length Western blots of SIRT5 and actin expression in protein extracts obtained from SIRT5$^{+/+}$ and SIRT5$^{-/-}$ BMDMs and SIRT5$^{+/+}$ liver.

Table S1 | Antibodies used for flow cytometry analyses.

Table S2 | Oligonucleotides used in RT-PCR analyses.

REFERENCES

1. Broz P, Monack DM. Newly described pattern recognition receptors team up against intracellular pathogens. *Nat Rev Immunol.* (2013) 13:551–65. doi: 10.1038/nri3479
2. Savva A, Roger T. Targeting toll-like receptors: promising therapeutic strategies for the management of sepsis-associated pathology and infectious diseases. *Front Immunol.* (2013) 4:387. doi: 10.3389/fimmu.2013.00387
3. Choudhary C, Weinert BT, Nishida Y, Verdin E, Mann M. The growing landscape of lysine acetylation links metabolism and cell signalling. *Nat Rev Mol Cell Biol.* (2014) 15:536–50. doi: 10.1038/nrm3841
4. Guarente L. Franklin H. Epstein lecture: sirtuins, aging, and medicine *N Engl J Med.* (2011) 364:2235–44. doi: 10.1056/NEJMra1100831
5. Haigis MC, Sinclair DA. Mammalian sirtuins: biological insights and disease relevance. *Annu Rev Pathol.* (2010) 5:253–95. doi: 10.1146/annurev.pathol.4.110807.092250
6. Houtkooper RH, Pirinen E, Auwerx J. Sirtuins as regulators of metabolism and healthspan. *Nat Rev Mol Cell Biol.* (2012) 13:225–38. doi: 10.1038/nrm3293
7. van de Ven RAH, Santos D, Haigis MC. Mitochondrial sirtuins and molecular mechanisms of aging. *Trends Mol Med.* (2017) 23:320–31. doi: 10.1016/j.molmed.2017.02.005
8. Park J, Chen Y, Tishkoff DX, Peng C, Tan M, Dai L, et al. SIRT5-mediated lysine desuccinylation impacts diverse metabolic pathways. *Mol Cell* (2013) 50:919–30. doi: 10.1016/j.molcel.2013.06.001
9. Nakagawa T, Lomb DJ, Haigis MC, Guarente L. SIRT5 Deacetylates carbamoyl phosphate synthetase 1 and regulates the urea cycle. *Cell* (2009) 137:560–70. doi: 10.1016/j.cell.2009.02.026
10. Du J, Zhou Y, Su X, Yu JJ, Khan S, Jiang H, et al. Sirt5 is a NAD-dependent protein lysine demalonylase and desuccinylase. *Science* (2011) 334:806–9. doi: 10.1126/science.1207861
11. Tan M, Peng C, Anderson KA, Chhoy P, Xie Z, Dai L, et al. Lysine glutarylation is a protein posttranslational modification regulated by SIRT5. *Cell Metab.* (2014) 19:605–17. doi: 10.1016/j.cmet.2014.03.014
12. Rardin MJ, He W, Nishida Y, Newman JC, Carrico C, Danielson SR, et al. SIRT5 regulates the mitochondrial lysine succinylome and metabolic networks. *Cell Metab.* (2013) 18:920–33. doi: 10.1016/j.cmet.2013.11.013
13. Lin ZF, Xu HB, Wang JY, Lin Q, Ruan Z, Liu FB, et al. SIRT5 desuccinylates and activates SOD1 to eliminate ROS. *Biochem Biophys Res Commun.* (2013) 441:191–5. doi: 10.1016/j.bbrc.2013.10.033
14. Zhou L, Wang F, Sun R, Chen X, Zhang M, Xu Q, et al. SIRT5 promotes IDH2 desuccinylation and G6PD deglutarylation to enhance cellular antioxidant defense. *EMBO Rep.* (2016) 17:811–22. doi: 10.15252/embr.201541643
15. Nishida Y, Rardin MJ, Carrico C, He W, Sahu AK, Gut P, et al. SIRT5 regulates both cytosolic and mitochondrial protein malonylation with glycolysis as a major target. *Mol Cell* (2015) 59:321–32. doi: 10.1016/j.molcel.2015.05.022
16. Sadhukhan S, Liu X, Ryu D, Nelson OD, Stupinski JA, Li Z, et al. Metabolomics-assisted proteomics identifies succinylation and SIRT5 as important regulators of cardiac function. *Proc Natl Acad Sci USA.* (2016) 113:4320–5. doi: 10.1073/pnas.1519858113
17. Wang F, Wang K, Xu W, Zhao S, Ye D, Wang Y, et al. SIRT5 desuccinylates and activates pyruvate kinase M2 to block macrophage IL-1beta production and to prevent DSS-induced colitis in mice. *Cell Rep.* (2017) 19:2331–44. doi: 10.1016/j.celrep.2017.05.065
18. Bringman-Rodenbarger LR, Guo AH, Lyssiotis CA, Lombard DB. Emerging roles for SIRT5 in metabolism and cancer. *Antioxid Redox Signal.* (2017) 28:677–90. doi: 10.1089/ars.2017.7264
19. He B, Du J, Lin H. Thiosuccinyl peptides as Sirt5-specific inhibitors. *J Am Chem Soc.* (2012) 134:1922–5. doi: 10.1021/ja2090417
20. Liu J, Huang Y, Zheng W. A selective cyclic peptidic human SIRT5 inhibitor. *Molecules* (2016) 21:E1217. doi: 10.3390/molecules21091217
21. Kalbas D, Liebscher S, Nowak T, Meleshin M, Pannek M, Popp C, et al. Potent and selective inhibitors of human sirtuin 5. *J Med Chem.* (2018) 61:2460–71. doi: 10.1021/acs.jmedchem.7b01648
22. Rajabi N, Auth M, Troelsen KR, Pannek M, Bhatt DP, Fontenas M, et al. Mechanism-based inhibitors of the human sirtuin 5 deacylase: structure-activity relationship, biostructural, and kinetic insight. *Angew Chem Int Ed Engl.* (2017) 56:14836–41. doi: 10.1002/anie.201709050
23. Yu J, Sadhukhan S, Noriega LG, Moullan N, He B, Weiss RS, et al. Metabolic characterization of a Sirt5 deficient mouse model. *Sci Rep.* (2013) 3:2806. doi: 10.1038/srep02806
24. Ciarlo E, Roger T. Screening the impact of sirtuin inhibitors on inflammatory and innate immune responses of macrophages and in a mouse model of endotoxic shock. *Methods Mol Biol.* (2016) 1436:313–34. doi: 10.1007/978-1-4939-3667-0_21
25. Ciarlo E, Heinonen T, Herderschee J, Fenwick C, Mombelli M, Le Roy D, et al. Impact of the microbial derived short chain fatty acid propionate on host susceptibility to bacterial and fungal infections *in vivo*. *Sci Rep.* (2016) 6:37944. doi: 10.1038/srep37944
26. Renner P, Roger T, Bochud PY, Sprong T, Sweep FC, Bochud M, et al. A functional microsatellite of the macrophage migration inhibitory factor gene associated with meningococcal disease. *FASEB J.* (2012) 26:907–16. doi: 10.1096/fj.11-195065
27. Roger T, Froidevaux C, Le Roy D, Reymond MK, Chanson AL, Mauri D, et al. Protection from lethal gram-negative bacterial sepsis by targeting Toll-like receptor 4. *Proc Natl Acad Sci USA.* (2009) 106:2348–52. doi: 10.1073/pnas.0808146106
28. Roger T, Schneider A, Weier M, Sweep FC, Le Roy D, Bernhagen J, et al. High expression levels of macrophage migration inhibitory factor sustain the innate immune responses of neonates. *Proc Natl Acad Sci USA.* (2016) 113:E997–1005.doi: 10.1073/pnas.1514018113
29. Savva A, Brouwer MC, Roger T, Valls Seron M, Le Roy D, Ferwerda B, et al. Functional polymorphisms of macrophage migration inhibitory factor as predictors of morbidity and mortality of pneumococcal meningitis. *Proc Natl Acad Sci USA.* (2016) 113:3597–602. doi: 10.1073/pnas.1520727113
30. Roger T, Miconnet I, Schiesser AL, Kai H, Miyake K, Calandra T. Critical role for Ets, AP-1 and GATA-like transcription factors in regulating mouse Toll-like receptor 4 (Tlr4) gene expression. *Biochem J.* (2005) 387:355–65. doi: 10.1042/BJ20041243
31. Perreau M, Vigano S, Bellanger F, Pellaton C, Buss G, Comte D, et al. Exhaustion of bacteria-specific CD4 T cells and microbial translocation in common variable immunodeficiency disorders. *J Exp Med.* (2014) 211:2033–45. doi: 10.1084/jem.20140039

32. Roger T, Ding X, Chanson AL, Renner P, Calandra T. Regulation of constitutive and microbial pathogen-induced human macrophage migration inhibitory factor (MIF) gene expression. *Eur J Immunol.* (2007) 37:3509–21. doi: 10.1002/eji.200737357
33. Lugrin J, Ding XC, Le Roy D, Chanson AL, Sweep FC, Calandra T, et al. Histone deacetylase inhibitors repress macrophage migration inhibitory factor (MIF) expression by targeting MIF gene transcription through a local chromatin deacetylation. *Biochim Biophys Acta* (2009) 1793:1749–58. doi: 10.1016/j.bbamcr.2009.09.007
34. Tawadros T, Alonso F, Jichlinski P, Clarke N, Calandra T, Haefliger JA, et al. Release of macrophage migration inhibitory factor by neuroendocrine-differentiated LNCaP cells sustains the proliferation and survival of prostate cancer cells. *Endocr Relat Cancer* (2013) 20:137–49. doi: 10.1530/ERC-12-0286
35. Giannoni E, Guignard L, Knaup Reymond M, Perreau M, Roth-Kleiner M, Calandra T, et al. Estradiol and progesterone strongly inhibit the innate immune response of mononuclear cells in newborns. *Infect Immun.* (2011) 79:2690–8. doi: 10.1128/IAI.00076-11
36. Schneider A, Weier M, Herderschee J, Perreau M, Calandra T, Roger T, et al. IRF5 is a key regulator of macrophage response to lipopolysaccharide in newborns. *Front Immunol.* (2018) 9:1597. doi: 10.3389/fimmu.2018.01597
37. Roger T, Lugrin J, Le Roy D, Goy G, Mombelli M, Koessler T, et al. Histone deacetylase inhibitors impair innate immune responses to Toll-like receptor agonists and to infection. *Blood* (2011) 117:1205–17. doi: 10.1182/blood-2010-05-284711
38. Lugrin J, Ciarlo E, Santos A, Grandmaison G, dos Santos I, Le Roy D, et al. The sirtuin inhibitor cambinol impairs MAPK signaling, inhibits inflammatory and innate immune responses and protects from septic shock. *Biochim Biophys Acta* (2013) 1833:1498–510. doi: 10.1016/j.bbamcr.2013.03.004
39. Vacher G, Ciarlo E, Savova-Bianchi D, Le Roy D, Hantier G, Niculita-Hirzel H, et al. Innate immune sensing of fusarium culmorum by mouse dendritic cells. *J Toxicol Environ Health A* (2015) 78:871–85. doi: 10.1080/15287394.2015.1051201
40. Ferreira Lopes S, Vacher G, Ciarlo E, Savova-Bianchi D, Roger T, Niculita-Hirzel H. Primary and immortalized human respiratory cells display different patterns of cytotoxicity and cytokine release upon exposure to deoxynivalenol, nivalenol and fusarenon-X. *Toxins (Basel)* (2017) 9:337. doi: 10.3390/toxins9110337
41. Roger T, Delaloye J, Chanson AL, Giddey M, Le Roy D, Calandra T. Macrophage migration inhibitory factor deficiency is associated with impaired killing of gram-negative bacteria by macrophages and increased susceptibility to *Klebsiella pneumoniae* sepsis. *J Infect Dis.* (2013) 207:331–9. doi: 10.1093/infdis/jis673
42. Villalba JM. Alcain FJ. Sirtuin activators and inhibitors. *Biofactors* (2012) 38:349–59. doi: 10.1002/biof.1032
43. Ciarlo E, Heinonen T, Lugrin J, Acha-Orbea H, Le Roy D, Auwerx J, et al. Sirtuin 3 deficiency does not alter host defenses against bacterial and fungal infections. *Sci Rep.* (2017) 7:3853. doi: 10.1038/s41598-017-04263-x
44. Ciarlo E, Heinonen T, Theroude C, Herderschee J, Mombelli M, Lugrin J, et al. Sirtuin 2 deficiency increases bacterial phagocytosis by macrophages and protects from chronic Staphylococcal infection. *Front Immunol.* (2017) 8:1037. doi: 10.3389/fimmu.2017.01037
45. Cheng HL, Mostoslavsky R, Saito S, Manis JP, Gu Y, Patel P, et al. Developmental defects and p53 hyperacetylation in Sir2 homolog (SIRT1)-deficient mice. *Proc Natl Acad Sci USA.* (2003) 100:10794–9. doi: 10.1073/pnas.1934713100
46. Vakhrusheva O, Smolka C, Gajawada P, Kostin S, Boettger T, Kubin T, et al. Sirt7 increases stress resistance of cardiomyocytes and prevents apoptosis and inflammatory cardiomyopathy in mice. *Circ Res.* (2008) 102:703–10. doi: 10.1161/CIRCRESAHA.107.164558
47. Mostoslavsky R, Chua KF, Lombard DB, Pang WW, Fischer MR, Gellon L, et al. Genomic instability and aging-like phenotype in the absence of mammalian SIRT6. *Cell* (2006) 124:315–29. doi: 10.1016/j.cell.2005.11.044
48. Lim HW, Kang SG, Ryu JK, Schilling B, Fei M, Lee IS, et al. SIRT1 deacetylates RORgammat and enhances Th17 cell generation. *J Exp Med.* (2015) 212:607–17. doi: 10.1084/jem.20132378
49. Legutko A, Marichal T, Fievez L, Bedoret D, Mayer A, de Vries H, et al. Sirtuin 1 promotes Th2 responses and airway allergy by repressing peroxisome proliferator-activated receptor-gamma activity in dendritic cells. *J Immunol.* (2011) 187:4517–29. doi: 10.4049/jimmunol.1101493
50. Wang Y, Bi Y, Chen X, Li C, Li Y, Zhang Z, et al. Histone deacetylase SIRT1 negatively regulates the differentiation of interleukin-9-producing CD4(+) T cells. *Immunity* (2016) 44:1337–49. doi: 10.1016/j.immuni.2016.05.009
51. van Loosdregt J, Vercoulen Y, Guichelaar T, Gent YY, Beekman JM, van Beekum O, et al. Regulation of Treg functionality by acetylation-mediated Foxp3 protein stabilization. *Blood* (2010) 115:965–74. doi: 10.1182/blood-2009-02-207118
52. Beier UH, Angelin A, Akimova T, Wang L, Liu Y, Xiao H, et al. Essential role of mitochondrial energy metabolism in Foxp3(+) T-regulatory cell function and allograft survival. *FASEB J.* (2015) 29:2315–26. doi: 10.1096/fj.14-268409
53. Qin K, Han C, Zhang H, Li T, Li N, Cao X. NAD(+) dependent deacetylase Sirtuin 5 rescues the innate inflammatory response of endotoxin tolerant macrophages by promoting acetylation of p65. *J Autoimmun.* (2017) 81:120–9. doi: 10.1016/j.jaut.2017.04.006
54. Li Y, Liu B, Zhao H, Sailhamer EA, Fukudome EY, Zhang X, et al. Protective effect of suberoylanilide hydroxamic acid against LPS-induced septic shock in rodents. *Shock* (2009) 32:517–23. doi: 10.1097/SHK.0b013e3181a44c79
55. Mombelli M, Lugrin J, Rubino I, Chanson AL, Giddey M, Calandra T, et al. Histone deacetylase inhibitors impair antibacterial defenses of macrophages. *J Infect Dis.* (2011) 204:1367–74. doi: 10.1093/infdis/jir553
56. Zhang LT, Yao YM, Lu JQ, Yan XJ, Yu Y, Sheng ZY. Sodium butyrate prevents lethality of severe sepsis in rats. *Shock* (2007) 27:672–7. doi: 10.1097/SHK.0b013e31802e3f4c
57. Gojo I, Jiemjit A, Trepel JB, Sparreboom A, Figg WD, Rollins S, et al. Phase 1 and pharmacologic study of MS-275, a histone deacetylase inhibitor, in adults with refractory and relapsed acute leukemias. *Blood* (2007) 109:2781–90. doi: 10.1182/blood-2006-05-021873
58. Ciarlo E, Savva A, Roger T. Epigenetics in sepsis: targeting histone deacetylases. *Int J Antimicrob Agents* (2013) 42 (Suppl.):S8–12. doi: 10.1016/j.ijantimicag.2013.04.004

Conflict of Interest Statement: The authors declare that the research was conducted in the absence of any commercial or financial relationships that could be construed as a potential conflict of interest.

Supplementary Table S1. Antibodies used for flow cytometry analyses

Target	Clone	Coupling	Company
B220	RA3-6B2	eFluor® 450	eBioscience
CD3	145-2C11	PE, eFluor® 450	eBioscience
CD4	RM4-5	PE, FITC	eBioscience
CD8	53-6.7	APC-eFluor® 780, APC-Cy7	eBioscience
CD11b	M1/710	PE, APC	eBioscience
CD11c	HL3	PE, APC	eBioscience
CD14	Sa2-8	PE-Cy7	eBioscience
CD23	B3B4	PE	eBioscience
CD25	PC61.5	APC	eBioscience
CD44	IM7	APC, eFluor® 450	eBioscience
CD62L	MEL-14	FITC	eBioscience
CD93	AA4.1	APC	eBioscience
IgD	AMS 9.1	FITC	BD Biosciences
MHC-II	114.15.2	FITC	eBioscience

PE: phycoerythrin; FITC: fluorescein isothiocyanate; APC: allophycocyanin.

Supplementary Table S2. Oligonucleotides used in RT-PCR analyses.

Target	Forward primer (5'->3')	Reverse primer (5'->3')
Actin	CGCAAAGACCTGTATGCCAAT	GGGCTGTGATCTCCTTCTGC
Cd36	**TCCCTCACTGGAGGAAACTG**	TGT GAT ATC TGG CCT TGC TG
Cd40	ATGGCCAGTGCTGTGATTTG	GTGGCATTGGGTCTTCTCAAG
Cxcl1	CTTGAAGGTGTTGCCCTCAG	TCTCCGTTACTTGGGGACAC
Cxcl10	GGATGGCTGTCCTAGCTCTGTAC	TGGGCATGGCACATGGT
Il6	CCGGAGAGGAGACTTCACAG	CAGAATTGCCATTGCACAAC
Tlr1	CAGGCGAGCAGAGGCAAT	ATTCCTGAGGTCCCTGCTATTCT
Tlr2	CTTTTCGTTCATCTCTGGAGCAT	GATTTGACGCTTTGTCTGAGGTT
Tlr4	TCAGCAAAGTCCCTGATGACAT	ATGCCATGCCTTGTCTTCAAT
Tlr9	AGGGAGCCTCGGGAGAATC	CCCAGGGCCAGAGTCTCA
Tnf	CCAGGCGGTGCCTATGTCT	GGCCATTTGGGAACTTCTCAT

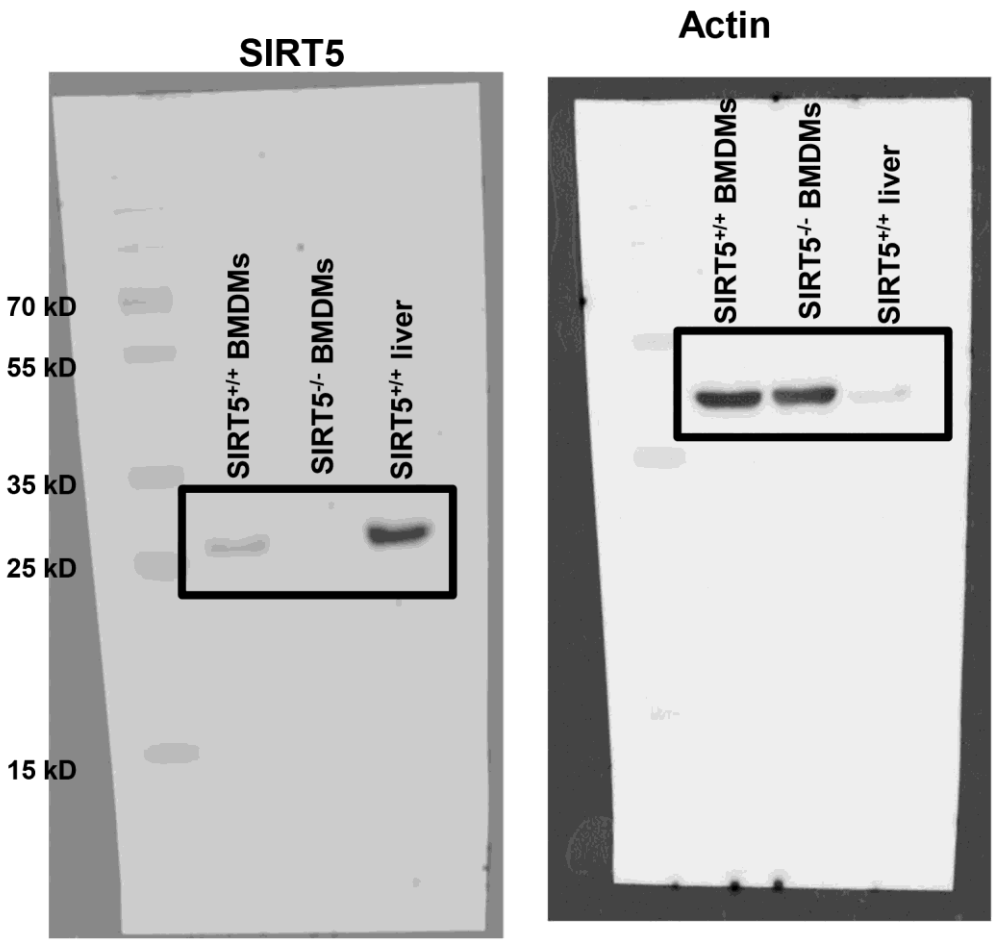

Used in Figure 1B

6.3. Regulation of inflammation and protection against invasive pneumococcal infection by the long pentraxin PTX3

Rémi Porte[1], Ana Rita Gomes[1], Charlotte Theroude[2], Raffaella Parente[1], Fatemeh Asgari[1], Marina Sironi[1], Fabio Pasqualini[1], Rosanna Asselta[1,6], Camilla Recordati[3], Andrea Doni[1], Tom Van der Poll[4], José Carlos Rodriguez-Gallego[5], Barbara Bottazzi[1], and Alberto Mantovani[1,6,7]

[1] Humanitas Clinical and Research Center IRCCS, Rozzano, Milan, Italy

[2] Infectious Diseases Service, Department of Medicine, Lausanne University Hospital and University of Lausanne, Epalinges, Switzerland.

[3] Mouse and Animal Pathology Laboratory, Fondazione Filarete, Milan, Italy

[4] Academic Medical Centre, University of Amsterdam, Netherlands

[5] Department of Immunology, Hospital Universitario de Gran Canaria Dr. Negrín, Las Palmas de Gran Canaria, Spain.

[6] Humanitas University, Department of Biomedical Sciences, Milan, Italy

[7]William Harvey Research Institute, Queen Mary University of London, Charterhouse Square, London EC1M 6BQ, UK

Submitted: PLOS Pathogens

Contribution to the work: I participated to *in vivo* experiments.

ABSTRACT

Streptococcus pneumoniae is a major pathogen in children, elderly subjects and immunodeficient patients. PTX3 is a fluid phase pattern recognition molecule (PRM) involved in resistance against selected microbial agents and in the regulation of inflammation. The present study was designed to assess the role of PTX3 in invasive pneumococcal infection. PTX3 was strongly induced during invasive pneumococcal infection in mice, and non-hematopoietic cells, endothelial cells in particular, were a major source of this PRM. The IL-1β/Myd88 pathways played a major role in induction. Ptx3-/- mice were more susceptible to invasive pneumococcal infection. Although high concentrations of PTX3 had opsonic activity in vitro, no evidence of PTX3-enhanced phagocytosis was obtained in vivo. In contrast, Ptx3-deficient mice showed enhanced recruitment of neutrophils and inflammation. Using Selp-/- mice, deficient in P-selectin, we found that protection against pneumococcus was dependent upon PTX3-mediated regulation of neutrophil inflammation. In humans, PTX3 genetic polymorphisms were associated with invasive pneumococcal infections. Thus, the fluid phase PRM plays an important role in tuning inflammation and resistance against invasive pneumococcal infection.

INTRODUCTION

Streptococcus pneumoniae (or pneumococcus) is a major leading cause of bacterial pneumonia, meningitis and sepsis in children, elders and immunodeficient patients. This pathogen is estimated to be responsible for most of the lower respiratory infections, causing around 2.5 million deaths annually worldwide [1]. Despite the widespread use of pneumococcal conjugate vaccines and antibiotic treatments, the combination of high carriage rate, its ability to become pathogenic to the host, and genetic adaptability, pneumococcus remains a significant cause of community- and hospital-acquired infections [2]. Since 2017, *S. pneumoniae* is classified as one of the 12 priority pathogens by World Health Organization.

S. pneumoniae is a Gram-positive extracellular opportunistic pathogen which colonizes the respiratory mucosa of the upper respiratory tract. Depending on the virulence factors expressed by the pathogen and host factors, the disease can evolve to pneumococcal invasive infection, where pneumococcus invade the lower respiratory tract and translocate through the blood stream into the systemic compartment [2]. The introduction over the years of pneumococcal vaccines able to protect against a variable and increasing number of different serotypes, was able to reduce the impact of the infection in susceptible populations [1,3]. However, protection was only partial for some serotypes. In particular, infection by serotype 3, associated with complicated disease course and increased risk of death [4], has not been demonstrated to be reduced by the 13-valent pneumococcal conjugate vaccine [3].

As a first line of defense against respiratory pathogens, innate immune Pattern Recognition Molecules (PRMs) recognize microbial components and modulate immune response to control infections. Among conserved PRMs, pentraxin 3 (PTX3), is a member of the pentraxin family characterized by multifunctional properties, including regulation of innate immunity during infections [5]. PTX3 is expressed by various hematopoietic and non-hematopoietic cells in response to microbial moieties and inflammatory cytokines (i.e IL-1β and TNF), and has been associated with the control of various infections by promoting different anti-microbial processes. Indeed, PTX3 participates to the elimination of microorganisms by promoting phagocytosis, activating the complement cascade and as a component of Neutrophil Extracellular Traps (NET) [6–10]. Furthermore PTX3 is described to modulate tissue remodeling [11] and inflammation via neutrophil recruitment processes (i.e complement activation and P-selectin-dependent transmigration) [12,13], both involved in the evolution of respiratory tract infections [14].

In humans, PTX3 plasma level increases in the context of inflammation and particular infectious diseases, including pneumococcal associated pathologies (i.e community-acquired pneumonia,

ventilator associated pneumonia, pneumococcal exacerbated chronic obstructive pulmonary disease), correlating with the severity of the disease and predicting the risk of mortality [8,15–21]. Single nucleotide polymorphisms (SNPs) in the PTX3 gene have been associated with patient susceptibility to respiratory infections [22–28].

The involvement of PTX3 in the control of selected respiratory pathogens and in the modulation of infection prompted us to determine the role of PTX3 in the control of pneumococcal infections. In a murine model of invasive pneumococcal infection, we observed that PTX3 genetic deficiency is associated with higher susceptibility to infection and higher respiratory tract inflammation. We also observed that PTX3, mainly produced by stromal non-hematopoietic cells during pneumococcal infection, modulates neutrophil recruitment by dampening P-selectin dependent neutrophil migration. Hence, PTX3 plays a non-redundant role in the control of S. *pneumoniae* infection, modulating neutrophil associated respiratory tissue damage and pneumococcal systemic dissemination.

MATERIALS AND METHODS

Mice

All mice used in this study were on a C57BL/6J genetic background [29]. PTX3-deficient mice were generated as described in [29]. Ptx3-/- and P-selectin (Selp-/-) double deficient mice were generated as described in [11]. Wild-type mice were obtained from Charles River Laboratories(Calco, Italy) or were cohoused littermates of the gene-deficient mice used in the study. Ptx3-/-, Csfr3r-/-, Ptx3loxP+/+Cdh5cre+/+, Ptx3loxP+/+Cdh5cre-/-, Selp-/-, Ptx3-/-Selp-/- and WT mice were bred and housed in individually ventilated cages in the SPF animal facility of Humanitas Clinical and Research Center or purchased from Charles River (Milan) and acclimated in the local animal facility for at least one weeks prior to infection. All animals were handled in a vertical laminar flow cabinet. Procedures involving animals handling and care were conformed to protocols approved by the Humanitas Clinical and Research Center (Rozzano, Milan, Italy) in compliance with national (4D.L. N.116, G.U., suppl. 40, 18-2-1992) and international law and policies (European Economic Community Council Directive 2010/63/EU, OJ L 276/33, 22.09.2010; National Institutes of Health Guide for the Care and Use of Laboratory Animals, U.S. National Research Council, 2011). All efforts were made to minimize the number of animals used and their suffering. The study was approved by the Italian Ministry of Health (742/2016-PR). Experiments were performed using sex- and age-matched mice.

Bone marrow transplantation

C57BL/6J wild-type or Ptx3-deficient mice were lethally irradiated with a total dose of 900 cGy. Then, 2h later, mice were injected in the retro-orbital plexus with 4x106 nucleated bone marrow cells obtained by flushing of the cavity of a freshly dissected femur from wild-type or Ptx3-deficient donors. Recipient mice received gentamycin (0.8 mg/ml in drinking water) starting 10 days before irradiation and maintained for 2 weeks. At 8 weeks after bone marrow transplantation, animals were infected.

Bacterial preparation

Each S. *pneumoniae* strain (supplementary Table 1) was cultured and stored has previously described [30]. Briefly, Todd-Hewitt yeast broth (THYB) (Sigma-Aldrich) was inoculated with fresh colonies grown in blood agar plates and incubated at 37°C until an optical density at 600 nm (OD600) of 0.7 to 0.9 units was reached. Cultures were stored at -80°C in THYB with 12% glycerol for up to 3 months. GFP-expressing serotype 1 was constructed as described previously [31]. Clinical isolate E1586 was grown at 37°C in THYE until an OD600 of 0.1, then 100 ng/ml of synthetic competence-stimulating peptide 1 (CSP-1; Eurogentec) was added for 12min at 37°C to activate transformation machinery. PhlpA-hlpA-gfp_Camr DNA fragment provided by Jan-Willem Veening's group [31] was added to the activated cells and incubated 20min at 30°C. Growth medium was diluted 10 times with fresh THYB medium and incubated 1.5h at 37°C. Transformants were selected by plating 5% sheep blood Tryptic Soy Agar plates

(TSA; BD Biosciences) containing 4.5 µg/ml of chloramphenicol, then cultured and stored as described above.

Recombinant PTX3

Recombinant human PTX3 was purified from culture supernatant of stably transfected Chinese hamster ovary (CHO) cells by immunoaffinity as previously described [32]. Purity of the recombinant protein was assessed by SDS-PAGE followed by silver staining. Biotinylated PTX3 (bPTX3) was obtained following standard protocols. Recombinant PTX3 contained <0.125 endotoxin units/ml as checked by the Limulus amebocyte lysate assay (BioWhittaker, Inc.). For in vivo experiments recombinant PTX3 was diluted in PBS.

Mouse model of infection

S. pneumoniae serotype 3 and serotype 1 were used to induce pneumococcal invasive infection as described previously [30,33]. For induction of pneumonia, each mouse was anesthetized by intraperitoneal injection of 100 mg/kg of ketamine plus 10 mg/kg of xylazine in 200µl of PBS. Then 5x104 or 106 colony-forming units (CFU) in 30 µL were inoculated intranasally to induce lethal infection by serotype 3 and serotype 1 respectively. Mouse survival was recorded every 12h. To rescue Ptx3 deficient mice, they were treated intraperitoneally with 10 µg/200 µl of recombinant PTX3 prior and 24h after infection. Prophylaxis or treatment have been done by intranasal instillation of 1 µg/30 µl recombinant PTX3 prior and 12h after infection respectively. Neutrophil recruitment modulation has been performed by treating intraperitoneally with 200 µg/200 µl of anti-Ly6G depleting antibody (InVivoPlus 1A8; BioXcell) or control isotype (InVivoPlus rat IgG2a; BioXcell). Blocking of P-selectin was realized by treating intraperitoneally with 50 µg/100 µl of anti-CD62P depleting antibody (rat RB40.34 NA/LE; BD Biosciences) or control isotype (rat IgG1 λ; BD Biosciences).

At indicated time, mice were sacrificed with CO2, bronchoalveolar lavage fluid (BAL), serum, lungs, and spleen were harvested and homogenated in PBS for CFU counting or in isotonic buffer (Tris HCl 50 nM, EDTA 2 mM, PMSF 1 mM [Roche Diagnostics GmbH], Triton™ X-100 1% [Merck Life Science], cOmplete™ EDTA-free protease inhibitor cocktail [Roche Diagnostics GmbH]) for protein measurement on the supernatant. Bacterial loads per organ were counted by serial dilution plated on 5% sheep blood TSA plates after 12h 37°C 5% CO2. For histological analysis, the entire lung was collected in organ cassette and fixed overnight in 4% paraformaldehyde (immunostaining) or in 4% formalin (hematoxylin eosin staining).

Lung histology and immunostaining

Immunostaining was realized on 8 µm sections from 4% paraformaldehyde (PFA)-fixed, dehydrate in sucrose solution and mounted in OCT embedding compound and stored at -80°C. PTX3 staining was performed as described previously [6]. Briefly, sections were stained with 5 µg/ml of rabbit polyclonal antibody anti-human PTX3 as a primary antibody and with MACH 1™ universal polymer (Biocare Medical) as a secondary antibody. Staining was revealed with 3,3'Diaminobenzidine (DAB; Biocare Medical) and counterstained with hematoxylin and eosin. Slides were scanned and analyzed with Image-pro (Media Cybernetics) to evaluate the percentage of stained area normalized by analyzing the same area for all animals corresponding to about 25% of the section.

Lung histological analysis was performed on fixed lungs included in paraffin and 3 µm sections were stained with hematoxylin and eosin. A blind analysis was done on 3 sections per animal distant at least of 150 µm and inflammatory foci were measured determining the area of foci and scores. Scores were determined separating small foci (<0.5 mm) and large foci (>0.5 mm) and then calculating as "Histological score = small foci + large foci x 3".

Binding assay

The binding of PTX3 on *S. pneumoniae* was assessed as described previously [34]. Briefly, 106 CFU *S. pneumoniae* were washed in PBS+/+ and suspend with 10 µg/ml, 50 µg/ml or 500 µg/ml of biotinylated recombinant PTX3 for 40min at room temperature. Bacteria were washed with PBS+/+ and stained

with streptavidin-Alexa Fluor 647 (4 µg/ml, Invitrogen) for 30min at 4°C. Washed bacteria were then fixed with 4% formalin for 15min at 4°C. Bacteria were then read by flow cytometry using FACSCanto™ II (BD Bioscience). Unstained *S. pneumoniae* were used as negative control.

Cell culture and stimulation

Human and murine endothelial cell lines were cultivated to have a confluent monolayer in 12-well culture plates (about 105 cells/well). Human Umbilical Vein Endothelial Cells (HUVEC) were grown in 1% gelatin coated wells in M199 medium (Sigma-Aldrich) containing 20% fetal bovine serum (FBS), 100 µg/ml of Endothelial Cell Growth Supplement (ECGS, Sigma-Aldrich), 100 µg/ml of heparin (Veracer; Medic Italia) and 1% penicillin and streptomycin (Pen/Strep). Murine lung capillary endothelial cell line (1G11) was grown in 1% gelatin coated wells in DMEM with 20% FBS, 100 µg/ml of ECGS, 100 µg/ml of heparin and 1% Pen/Strep.

Human neutrophils were purified from freshly collected peripheral blood in Lithium Heparin Vacutainer (BD Bioscience) and separated by a two-steps gradient separation as previously described by Kremaserova and Nauseef [35]. Briefly leukocytes and erythrocytes were separated by a 3% Dextran from Leuconostoc spp. (Sigma-Aldrich) sedimentation for 40min, then leukocytes in the supernatant were separated with Lympholyte-H Cell Separation Media (Cerdalane) and cells from the lower liquid interphase were rinsed with RPMI.

Cells were stimulated after a wash with the same culture media without Pen/Strep and then incubated with the corresponding medium containing 106 CFU *S. pneumoniae*, 20 ng/ml recombinant IL-1β (Preprotech) or 100 ng/ml lipopolysaccharide from Escherichia coli O55:B5 (LPS, Sigma-Aldrich) for 6h at 37°C. Cells were then lysate with 300 µl of PureZOL RNA isolation reagent (Bio-Rad). Human neutrophils were stimulated with 107 CFU/ml of *S. pneumoniae* serotype 3 or 10 ng/ml of phorbol myristate acetate (PMA) during 6h at 37°C, PTX3 released in the supernatant was measured by ELISA, as described below.

Neutrophil transmigration assay

Neutrophil migration assay across an endothelium monolayer was performed as previously described by Bou Ghanem and collaborators [36]. Briefly, basolateral sides of HUVEC monolayer grown 4 days on a 3 µm polyester membrane Transwell (Corning) was infected with *S. pneumoniae* (106 CFU/ml in RPMI) added the lower chamber, whereas 100 µl PBS+/+ containing 20 ng/ml recombinant IL-1β supplemented with 100 µg/ml PTX3 and/or 100 µg/ml mouse anti-human CD62P (clone AK-4, BD Bioscience) was added to the apical side (upper chamber). After 2.5h at 37˚C, 5x105 human neutrophils (in 100 µl RPMI) were added to the basolateral side. After 2.5h at 37˚C, neutrophils in the lower chamber were counted in triplicate. Neutrophil transmigration without infection was performed in parallel as negative control.

Gene expression quantification by real-time RT-PCR

Organs homogenated in PureZOL RNA isolation reagent (Bio-Rad) and cell lysate RNAs were extracted with the Direct-zol RNA Miniprep (Zymo Research) and reverse transcribed with the high-capacity cDNA archive kit (Applied Biosystems) following the manufacturer's instructions. cDNA was amplified using the Fast SYBR Green Master Mix on a QuantStudio 7 Flex Real Time PCR Systems (Applied Biosystems). The sequences of primer pairs (Sigma-Aldrich) specific for murine Gapdh (Forward, 5'-GCAAAGTGGAGATTGTTGCCAT-3', Reverse, 5'-CCTTGACTGTGCCGTTGAATTT-3') and Ptx3 (Forward, 5'-CGAAATAGACAATGGACTCCATCC-3', Reverse, 5'-CAGGCGCACGGCGT-3') were used to evaluated their expression. Relative mRNA levels (2-ΔΔCT) were determined by comparing first the PCR cycle thresholds (CT) for Ptx3 and Gapdh (ΔCT), and second, the ΔCT values for the infected/treated and uninfected/untreated (mock/control) groups (ΔΔCT). All amplifications were performed in triplicates.

ELISA

Lung homogenates and serum levels of murine C3a, C5a, CXCL1, CXCL2, IL-1β, MPO and PTX3 were determined by enzyme-linked immunosorbent assay (DuoSet ELISA Development; R&D Systems and

Cloud-Clone corp) following the manufacturer's instructions. Human PTX3 was determined with an in-house ELISA as previously described by Jaillon and collaborators [6]. Briefly, anti-PTX3 monoclonal antibody (1 µg/ml, clone MNB4) in carbonate buffer (carbonate buffer 15 mM pH 9.6) was coated overnight at 4°C in 96 well ELISA plates (Nunc). Wells were then blocked with 5% dry milk for 2h at room temperature. Cell culture supernatants, were incubated for 2h at room temperature. Biotin-labeled polyclonal rabbit anti-PTX3 antibody (100 µl/ml, clone 6B11) was used for the detection and incubated 1h at 37°C. Plates were incubated with peroxidase-labeled streptavidin (SB01-61; Biospa) for 1h at 37°C. Bound antibodies were revealed using the TMB substrate (Sigma Aldrich) and 450 nm absorbance values were read with an automatic ELISA reader (VersaMax; Molecular Devices).

Flow cytometry

BAL fluid samples were obtained after intratracheal injection of 1 ml of PBS supplemented with 5% FBS. Lung cells were isolated after digestion in PBS, supplemented with 20% FBS, 2 mM HEPES (Lonza), 100 µg/ml collagenase from Clostridium histolyticum type IV (Sigma-Aldrich) and 20 µg/ml of DNAse (Roche Diagnostics GmbH) in C-tubes processed with gentleMACS Octo Dissociator with heaters according to the manufacturer's instructions (Miltenyi Biotec). Lysate were pellet (500 g 8min) and red blood cells were lysate with 500 µl of ACK lysing buffer (Lonza) for 5min. Reaction were stopped with PBS, the cell suspensions were filtered through a 70 µm filter, count using Türk solution (Sigma-Aldrich) and 106 cells were pelleted by centrifugation (500 g, 8 min). Live/dead fixable aqua (Invitrogen) staining were realized following manufacturer's instruction and stopped in FACS buffer (PBS, 2% FBS, 2 mM EDTA, 0.05% NaN3). Fc-receptors were blocked with anti-mouse CD16/CD32 (20 µg/ml, clone 93; Invitrogen) for 20min. Cells were stained with an antibody panel able to distinguish macrophages (CD45+, CD11b-, SiglecF+), neutrophils (CD45+, CD11b+, SiglecF-, Ly6C+, Ly6G+), monocytes (CD45+, CD11b+, SiglecF-, Ly6Clow/moderate/high, Ly6G-) and eosinophils (CD45+, CD11b+, SiglecF+): anti-CD45-Brilliant Violet 605 (2 µg/ml, clone 30-F11; BD Bioscience), anti-CD11b APC-Cy7 (1 µg/ml, clone M1/70; BD Bioscience), anti-SiglecF-eFluor 660 (1.2 µg/ml, clone 1RNM44N; Invitrogen), anti-Ly6C-FITC (3 µg/ml, clone AL-21; BD Bioscience), anti-Ly6G-PE-CF594 (0.4 µg/ml, clone 1A8; BD Bioscience). Flow cytometric analysis was performed on BD LSR Fortessa and analyzed with the BD FACSDiva software.

Genotyping

DNA was obtained from 57 patients with invasive pulmonary disease (IPD) and 521 age- and sex-matched healthy controls from the cohort described by Garcia-Laorden and collaborators [37]. The genotyping was performed as previously described by Barbati and collaborators [38]. Briefly, genomic DNAs extracted from frozen EDTA-whole blood were genotyped by real time-PCR, using TaqMan. In particular, 5 µl samples containing TaqMan Genotyping Master Mix, and specific TaqMan SNP genotyping probes (rs1840680, rs2305619 and rs3816527) were mixed with 20 ng of genomic DNA and genotyped using a Quantstudio 6 Flex System according to the manufacturer's instruction (Applied Biosystems).

Statistical analysis

Results were expressed as median or mean ± SEM as indicated. Statistical differences were analyzed using the Mann-Whitney test; survival analysis was performed with the logrank test with Mantel-Cox method. All the analyses were performed with GraphPad Prism 8.0; P values <0.05 were considered significant.

As for SNP association analyses, these were performed using the PLINK v1.07 program [39]. All polymorphisms had a call rate of 100%, and were tested for Hardy-Weinberg equilibrium (HWE) in controls before inclusion in the analyses (P-HWE >0.05). In detail, deviations from HWE were tested using the exact test [40] implemented in the PLINK software. For each SNP, a standard case-control analysis using allelic chi-square test was used to provide asymptotic P values, odds ratio (OR), and 95% confidence interval (CI), always referring to the minor allele. Haplotype analysis and phasing was performed considering either all three SNPs together or by using the sliding-window option offered by

PLINK. All P values are presented as not corrected; however, in the relevant tables, Bonferroni-corrected thresholds for significance are indicated in the footnote.

RESULTS

PTX3 expression during Pneumococcal invasive infection

In order to define the relevance of PTX3 in pneumococcal respiratory disease, we first investigated whether PTX3 is induced during infection. Thus, we used a murine model of pneumococcal invasive infection induced by *S. pneumoniae* serotype 3. Mice were challenged intranasally with 5x104 CFU and sacrificed at different time points. As already described, S. *pneumoniae* serotype 3 causes bacterial colonization of the respiratory tract, then disseminates through the blood circulation and infects other organs like the spleen, resulting in death within 3 to 4 days (Fig S1A-B) [33]. As early as 6h post-infection, we detected a local expression of PTX3 in the alveolar and bronchiolar compartment near the pulmonary veins (Fig 1A-B). At 12h post-infection, we were able to detect the PTX3 specific staining in the area where we can appreciate inflammatory cells infiltration. This association was confirmed 24h post-infection, when a strong PTX3 staining was present near the recruitment site of inflammatory cells forming inflammatory foci (Fig 1A). The kinetic of PTX3 production was confirmed by the quantification of PTX3+ area (Fig 1B) and by analysis of mRNA in the lung (Fig S1C). Interestingly, local and systemic production of PTX3 was highly induced by the infection during the invasive phase (Fig 1C). During this invasive infection we observed that PTX3 was upregulated mainly in the lung, aorta and heart, while other organs like brain, kidneys and liver did not show higher PTX3 expression compared to the uninfected mice (Fig S1D).

Induction of PTX3 by IL-1β during *S. pneumoniae* infection

PTX3 has been described to be induced by primary inflammatory cytokines, i.e. IL-1β and TNF [5,8]. In this pneumococcal invasive infection model we observed a rapid induction of IL-1 β (Fig 2A), and a strong correlation between the levels of IL-1β expressed in the respiratory tract with the levels of lung PTX3 (Fig 2B). Moreover, Il1r-/- mice infected by *S. pneumonia*e showed lower PTX3 levels, locally and systemically (i.e in the lung and the serum respectively) (Fig 2C-D). *S. pneumoniae* infected Myd88-/- mice were not able to produce PTX3 in the lung and presented the same impairment of PTX3 production as Il1r-/- mice (Fig 2C-D). These data suggest that IL-1β is a major driver of PTX3 during pneumococcal infection.

Non-hematopoietic cells are a major source of PTX3 during pneumococcal infection

It has been previously reported that neutrophils contain preformed PTX3, representing an important source of the protein, rapidly released in response to proinflammatory cytokines or microbial recognition [9]. In agreement, we observed that human neutrophils release PTX3 upon stimulation with *S. pneumoniae* (Fig S2A). To investigate the involvement of neutrophils in the production of PTX3 in our model, we used mice lacking granulocyte colony-stimulating factor receptor (Csf3r-/-). These mice are characterized by a chronic neutropenia, granulocyte and macrophage progenitor cell deficiency and impaired neutrophil mobilization [29,41]. Following pneumococcal infection, Csf3r-/- mice presented lower levels of myeloperoxidase (MPO), an important marker of neutrophil recruitment, in lung homogenates at 36h post-infection (Fig S2B). By contrast, even though these mice presented a lower amount of neutrophils recruited in response to the infection, they expressed the same pulmonary levels of PTX3 as the WT mice (Fig S2B). These results suggest that neutrophils are not the main source of PTX3 in our murine model of pneumococcal invasive infection.

Since PTX3 can be produced by hematopoietic and non-hematopoietic cells, bone marrow chimeras were used to evaluate the cellular compartment responsible for PTX3 production. During pneumococcal infection, we did not observe any difference in the levels of PTX3 found in the respiratory tract and in the serum of WT mice receiving bone marrow from Ptx3-/- or WT animals,

while no PTX3 was measured in Ptx3-/- mice receiving WT or Ptx3-/- bone marrow (Fig 3A-B). These results suggest that PTX3 is mainly produced by the non-hematopoietic compartment after pneumococcal infection. Endothelial cells were described as an important source of PTX3 [5], thus we evaluated their contribution on PTX3 production during pneumococcal infection. To this aim we crossed conditional Ptx3 deficient mice (Ptx3LoxP+/+) with Cdh5-Cre mice to generate animals with the deletion of PTX3 in endothelial cells. When Ptx3LoxP+/+/Cdh5Cre+/+ mice were infected with *S. pneumoniae*, they presented approximately 50% reduction of PTX3 levels compared to PTX3-competent mice (Fig 3C-D). In-vitro experiments confirmed the ability of both murine and human endothelial cells to produce PTX3 after stimulation with *S. pneumoniae* (Fig S2C). Thus non-hematopoietic cells, mainly endothelial cells, are a major source of PTX3.

Non-redundant role of PTX3 in resistance to pneumococcal infection.

Next we evaluated the role of PTX3 in resistance against pneumococcus. When Ptx3-/- mice were infected with *S. pneumoniae* (5x104 CFU), a significant increase of the bacterial load in the lung was observed starting from 24h of infection onwards, compared to WT mice (Fig 4A). Interestingly there is no difference at earlier time points (6-18h), suggesting that PTX3 exerts a role in the control of pneumococcal infection mainly during the invasive phase. Defective local control of bacterial growth was followed by an increase of bacterial load in the systemic compartment starting at 36h post-infection (Fig 4B), which was also associated with an acceleration of the infection kinetic. Indeed, using a high dose (5x104 CFU) of pneumococcus Ptx3-/- mice had a shorted survival time compared to control (Fig 4C). Furthermore, using a lower bacterial dose (5x103 CFU) inducing around 30% mortality in WT animals, Ptx3-/- mice showed a significant higher mortality (83.3%; $P<0.001$) (Fig 4C). This phenotype is not restricted to serotype 3 pneumococcus. In fact, when mice were infected with *S. pneumoniae* serotype 1, we observed a strong PTX3 production during the invasive phase of the infection (Fig S3A) and a correlation with IL-1β levels (Fig S3B). Ptx3-/- mice infected by serotype 1 presented a higher sensitivity to the infection compared to WT animals, with a higher number of bacteria at the local site of infection and also in the systemic compartment 24h post-infection (Fig S3C-D). Overall, these data confirmed that the phenotype observed in our model of *S. pneumoniae* invasive infection is not dependent of a specific pneumococcal serotype.

The involvement of Ptx3 deficiency was confirmed by reconstituting Ptx3-/- mice with two systemic administrations of recombinant PTX3, before and 24h after the infection. As reported in Fig 4D, PTX3 administration in Ptx3-/- mice reduced lung colonization at the same level observed in WT mice. We then evaluated the antibacterial activity of PTX3 on *S. pneumoniae* serotype 3. WT animals were treated locally with 1µg of recombinant protein before infection, as a prophylaxis model, or 12h post-infection, as an on-demand model. Interestingly, in both models we observed a significant reduction, 44% and 57% respectively ($P<0.01$), of the pulmonary bacterial load compared with the CFU found in mice treated with vehicle alone (Fig 4E).

Lack of effective opsonic activity of PTX3

In an effort to explore the mechanism responsible for PTX3-mediated resistance, we first explored the effect of the recombinant protein on the in-vitro growth of *S. pneumoniae*. The incubation of *S. pneumoniae* with 25-250 µg/ml of recombinant PTX3 did not have any effect on the growth rate of the bacteria (Fig S4).

PTX3 has the capability to act as an opsonin binding selected pathogens and increasing their removal by phagocytosis [6,7,42]. To assess whether the control of the pneumococcal infection by PTX3 was due to the opsonic activity, we first analyzed PTX3 binding to S. *pneumoniae*. By using a flow cytometry assay, we analyzed PTX3 binding to *S. pneumoniae* serotype 3 mimicking the bacteria/PTX3 ratio found in the infected lung (106 CFU/100 ng PTX3). Under these conditions, we did not observe any interaction of PTX3 with bacteria and, even with an amount of PTX3 5- to 10-fold higher than the one produced in the entire lung, less than 1% of the bacteria were bound (Fig 5A). At 500 µg/ml of PTX3 (5000-fold higher than in the lung homogenates) we observed binding to only 36.4% of bacteria (Fig 5A).

We then performed a series of experiments of phagocytosis in vitro and in vivo using GFP-expressing S. pneumoniae serotype 1 (*S. pneumoniae*-GFP). In a first set of experiments, human neutrophils were incubated with PTX3-opsonized *S. pneumoniae*-GFP. We confirmed that PTX3 exerts opsonic effects, increasing the phagocytosis of pneumococcus by neutrophils, but only at very high concentrations, i.e. higher than 100 µg/ml (Fig 5B). We then moved to an in vivo setting. Since the instillation of as low as 1µg of PTX3 was sufficient to induce an antibacterial effect when administrated locally just before the infection (Fig 4E), we incubated 5x104 CFU of *S. pneumoniae* serotype 3 (i.e. the inoculum normally used for a lethal infection in our model) with 33.3 µg/ml of recombinant PTX3. Mice infected with PTX3-opsonized *S. pneumoniae* showed the same local bacterial burden at 6h to 36h after infection as mice infected with pneumococcus incubated with PBS (Fig 5C). Finally, we evaluated the phagocyting ability of neutrophils recruited in-vivo during the infection comparing WT and Ptx3 deficient mice. Interestingly, we did not observe any difference in the percentage of neutrophils phagocyting *S. pneumoniae*-GFP neither in the BAL nor in the lung (Fig 5D). These results suggest that the role of PTX3 in resistance to invasive pneumococcus infection is not accounted for by its opsonic activity of this pathogen.

Regulation of inflammation by PTX3

In pneumococcal invasive disease induced by *S. pneumoniae* serotype 3, infection was characterized by a perivascular infiltration of inflammatory cells, mainly neutrophils, around pulmonary veins and bronchioles, forming important foci (Fig S5A). The main inflammatory cell recruitment was observed during the invasive phase of the infection (starting from 24h after infection), when the pulmonary MPO was dramatically increased, (Fig S5B). We analyzed more accurately neutrophil recruitment in the lung and in the BAL of infected mice and we observed two phases of neutrophil recruitment. An initial recruitment, characterized by an increased (i.e. 3-fold compared to uninfected lung) number of neutrophils both in the BAL and in the lung parenchyma, was observed during the first 6h of infection. In the next 12h to 24h of infection we observed an important recruitment of neutrophils in the lung (i.e. 4-fold compared to uninfected lung) that translocated into the alveolar space (up to 50-fold compared to uninfected BAL) (Fig S5C-D). These two steps of recruitment have been described to have two opposite roles during the infection [36]. Indeed, the first phase is important for the early control of the infection, reducing the number of colonizing bacteria. In contrast the second phase has been associated with the development of the inflammatory environment, leading to tissue damage that could promote growth and invasion of the bacteria [36]. Given the mild expression of PTX3 during the first hours (Fig 1A), we investigated the second phase of neutrophil recruitment, comparing Ptx3 deficient and WT mice 18h after infection. At this time point Ptx3 deficiency was not associated to a higher respiratory bacterial load (Fig 4A). Interestingly, the inflammatory profile was significantly increased in Ptx3-/- mice, as shown by an increased development of foci in the lung induced by a higher inflammatory cell recruitment (Fig 6A-C). Moreover, looking at the time course of the development of pneumococcal-induced respiratory inflammation, we observed that Ptx3-/- mice had a quicker and more severe formation of inflammatory foci compared to the WT (Fig 6B-C). Flow cytometry analysis revealed that the higher inflammation in Ptx3 deficient mice was due to a significant increase of neutrophil recruitment in the BAL and the lung (Fig 6D). Moreover, we did not observe any change in the recruitment of other myeloid immune cells, i.e. macrophages, eosinophils and monocytes (Data not shown). This phenotype was also observed with the serotype 1 model of invasive pneumococcal infection (Fig S5E).

Finally, we observed that the intranasal treatment with recombinant PTX3 was also associated with a decrease in the neutrophil number in BAL and lungs, demonstrating that PTX3 has a direct role in neutrophil migration in the respiratory tract (Fig 6E).

Regulation of neutrophil recruitment by PTX3 during pneumococcal invasive infection.

It has been shown that neutrophil depletion during the invasive phase resulted in protection against infection [36]. Accordingly, neutrophil depletion by anti-Ly6G was used to assess the role of

these cells in PTX3-mediated protection against pneumococcal infection. In WT mice infected intranasally with *S. pneumoniae*, treatment with anti-Ly6G significantly reduced neutrophils infiltration in the lungs (Fig S6A). In addition, treatment with anti-Ly6G completely abolished the increased accumulation of neutrophils observed in Ptx3-/- mice (Fig S6A-B). The reduction of neutrophil recruitment in both WT and Ptx3-/- mice treated with anti-Ly6G resulted in a significant reduction of the local and systemic bacterial load, compared to mice treated with the isotype control (Fig 7A-B). In addition, Ptx3-/- mice treated with neutrophil depleting antibody were not more infected than the WT treated mice (Fig 7A-B). These results suggest that taming pneumococcus-promoting neutrophil recruitment underlies the role of PTX3 in resistance against this bacterial pathogen.

To dissect the mechanism by which PTX3 orchestrates the modulation of inflammation during pneumococcal infection, we first evaluated the level of neutrophil chemoattractants. At 18h post-infection, even though there was a higher amount of neutrophils in the airways of Ptx3-/- mice, we did not detect any differences in the levels of CXCL1 and CXCL2 between Ptx3 deficient and WT mice (Fig S6C). Since PTX3 is a well-known regulator of complement activation [43], we investigated the levels of the two anaphylatoxins C3a and C5a in the lung homogenates of infected mice. No difference in the levels of C3a and C5a, potent chemoattractants, was observed (Fig S6C). The levels of C3d, a C3 degradation product deposited on the surface of cells and a marker of complement activation in lung homogenates was similar in Ptx3 deficient and WT mice (Fig S6D).

PTX3 has been described to directly regulate inflammation by binding P-selectin and reducing neutrophil recruitment, damping the rolling on the endothelium [12,13]. We therefore investigated whether the interaction with P-selectin could be relevant in the regulation of neutrophil recruitment into the lung. We investigated the ability of PTX3 to damp the neutrophil transmigration through endothelial cell layer in vitro, using *S. pneumoniae* as the attractive signal. We observed that PTX3 could block 40% of the neutrophil migration induced by *S. pneumoniae* (Fig 7C). Moreover, the treatment of endothelial cells with anti-CD62P (P-selectin) antibody induced the same blocking effect. However, we did not observe any additional blocking effect of PTX3 in association with anti-CD62P, suggesting that PTX3 exerts its blocking effect through P-selectin. To confirm that PTX3 protects infected mice by blocking P-selectin, we used P-selectin deficient mice (Selp-/-). We observed that Selp-/- mice were partially protected from pneumococcal infection, showing a bacterial load lower than WT mice ($P<0.01$). In Selp-/- mice PTX3 treatment did not reduce the bacterial load (Fig 7D). Moreover, we treated WT and Ptx3 deficient mice with anti-P-selectin antibody (anti-CD62P), to block P-selectin-dependent neutrophil transmigration during the invasive phase of infection. Anti-CD62P treatment completely abolished the higher neutrophils recruitment in Ptx3 deficient mice (Fig S6E-F). This result suggests that the higher neutrophil infiltration observed during pneumococcal pneumonia in the absence of PTX3 is dependent on P-selectin. Importantly, the reduction of neutrophil recruitment in Ptx3 deficient mice treated with anti-CD62P is associated with a significant reduction of the local and systemic bacterial load reaching the same level observed in WT mice treated with anti-CD62P (Fig 7E-F).

Finally, to assess the role of the P-selectin pathway in PTX3-mediated resistance against invasive pneumococcus infection, we took advantage of Ptx3-/-Selp-/- double deficient mice. As shown in Fig 7G-H, genetic deficiency in P-selectin and PTX3 completely rescued the increased infection phenotype observed in Ptx3-/- mice. Thus, the defective control of invasive pneumococcal infection observed in Ptx3-/- mice is due to unleashing P-selectin-dependent recruitment of pneumococcus-promoting neutrophils.

PTX3 polymorphisms

To explore the significance of these results to human disease, we analyzed the association of human PTX3 gene polymorphisms with pneumococcal invasive disease (IPD) in a cohort of 57 patients and 521 matched healthy controls. We focused in particular on two intronic SNPs (rs2305619 and rs1840680) and a third polymorphism (rs3816527) in the coding region of the protein determining an

amino-acid substitution in position 48 (+734A/C). These SNPs are associated with increased susceptibility to infection to selected microorganisms [22,25–27]. In addition, the +734A allele was associated in various studies to decreased PTX3 levels [22,38,44].

We did not observe any difference in the frequency of the +734A allele in this cohort of patients versus controls (67.54% and 61.58%, respectively, P=0.213, Table 1). However, when we compared the frequencies of haplotypes determined by these three SNPs (rs2305619, rs3816527, rs1840680) in IPD patients and control subjects, we found that the frequency of the AAA haplotype is doubled in patients with IPD (9.67% and 4.26% respectively, P=0.0102, Table 2). The association is even more significant when considering only two SNPs (+281A and +734A), including the one associated with lower levels of the protein (11.4% and 4.94% respectively, P=0.0044, Table 2). These observations suggest that also in humans PTX3 could play a role in the control of *S. pneumoniae* infection.

DISCUSSION

S. pneumoniae is the most common cause of a range of infections, including community-acquired pneumonia, a pathological condition that affects mainly adults aged 65 years or older and infants under one year of age. It is well known that inflammation plays a crucial role during lung infections and dictates the resolution of pneumonia, but at the same time, exaggerated inflammation can be detrimental. Therefore, a strict control of the inflammatory response is essential.

The present study was aimed at assessing the role of PTX3 in invasive pneumococcal infection. PTX3 is a member of the pentraxin family highly conserved in evolution and locally produced by different cell types in response to pro-inflammatory stimuli and microbial components. The protein has multifunctional properties, including in particular a regulatory role on inflammation [5]. In a well-characterized murine model of invasive pneumococcal infection, PTX3 expression was rapidly upregulated in the alveolar and bronchiolar compartments of the lungs. The systemic dissemination of pneumococcus was associated with an increase of PTX3 serum levels. As expected, PTX3 levels were at least in part induced by IL-1β, massively produced in response to the pneumococcus.

Both myeloid and endothelial cells can produce PTX3 in response to inflammatory cytokines. Polymorphonuclear leukocytes were able to release PTX3 after stimulation with *S. pneumoniae,* however levels of the protein were similar in wild type and in neutropenic Csfr3-/- animals infected with *S. pneumoniae*. Bone marrow chimeras and conditional mice definitely demonstrated that stromal cells, and in particular endothelial cells, were a major source of PTX3 in our model of pneumococcal infection. Production of PTX3 by non-hematopoietic cells has been previously reported in other experimental settings. In a murine model of arterial thrombosis induced by FeCl3, PTX3 was only expressed by vascular cells [45]. Similarly, in a murine model of skin wound-healing, non-hematopoietic cells were the major producers of PTX3 whereas neutrophils showed a minor contribution [11].

Ptx3 genetic deficiency was associated with a higher susceptibility to *S. pneumoniae*. A defective control of bacterial load, associated with a higher mortality rate, was observed during the invasive phase of the infection, and PTX3 administration rescued the phenotype. In humans, PTX3 gene polymorphisms were already described to have an impact on the susceptibility to selected infections, in particular Mycobacterium tuberculosis, Pseudomonas aeruginosa and urinary tract infections [6,26,27]. In addition, PTX3 genetic variants are associated with the risk to develop invasive aspergillosis or Cytomegalovirus reactivation in patients undergoing allogeneic stem cell transplant [22,46]. Thus, genetic deficiency in mice and genetic polymorphisms in humans suggest that PTX3 plays an important role in the control of invasive pneumococcal infection. In the present study, in a cohort of 57 patients with IPD and 521 healthy controls haplotypes determined by PTX3 gene polymorphisms were associated with *S. pneumoniae* infection.

Various mechanisms are potentially involved in the protective role of PTX3 against infectious agents. In most cases PTX3-mediated protection has been related to the pro-phagocytic activity of the protein [6,7,42,47]. PTX3 binds selected fungal, bacterial and viral pathogens, including Aspergillus fumigatus, Pseudomonas aeruginosa, Shigella flexneri, uropathogenic Escherichia coli, Influenza virus and murine cytomegalovirus [8], acting as an opsonin and amplifying the phagocytosis of recognized microorganisms [6,7,42]. These microorganisms are naturally susceptible to phagocytosis [48–50] whereas virulent *S. pneumoniae* developed various mechanisms preventing phagocytosis [2,51]. In this study, we observed that PTX3 could bind *S. pneumoniae*, promoting its phagocytosis in vitro by human neutrophils, only at very high concentrations. Ptx3 deficiency did not affect the local phagocytosis by recruiting neutrophils and pre-opsonisation of the inoculum did not modify the kinetic of infection. Thus PTX3-mediated contribution to resistance to *S. pneumoniae* is independent of enhanced phagocytosis.

The short pentraxin CRP, distantly related to PTX3, acts as an opsonin for various microorganisms, including pneumococcus [52,53]. However, this effect is dependent on the serotype, specifically on the expression of phosphatidylcholine in the capsule. PTX3 does not interact with phosphatidylcholine [32]. In addition, serotypes 1 and 3 gave similar results in terms of kinetic of PTX3 production after infection and bacterial load in Ptx3-/- mice. These results suggest that the short pentraxin CRP and the long pentraxin PTX3 have distinct spectra of microbial recognition and role in antimicrobial resistance.

PTX3 exerts regulatory roles on complement activation by interacting with components of all the three pathways, i.e. the classical, alternative and lectin pathways. In all cases, PTX3 leads to a reduced activation of the complement cascades, thereby reducing the tissue damage associated with an activation out of control [43]. The higher susceptibility to pneumococcus infection observed in Ptx3-deficient mice was not related to failed regulation of complement activity. In fact, similar levels of complement fragments, in particular of the two anaphylatoxins C3a and C5a, were found in lung homogenates of wild type and Ptx3-/- infected mice.

In invasive pneumococcal infection neutrophils represent a double edged sword. Several lines of evidence, including depletion using anti-Ly6G antibody, suggest that in early phases of infection neutrophils are an essential component of resistance to *S. pneumoniae* as expected [36]. In contrast, during the invasive phase neutrophil depletion was protective, limiting tissue damage and associated bacterial invasion. In the present study, Ptx3 genetic deficiency was associated with uncontrolled inflammation and bacterial invasion sustained by enhanced neutrophil accumulation. These results are consistent with a yin/yang role of neutrophils in invasive pneumococcus infection.

Neutrophil infiltration at sites of bacterial invasion and inflammation is driven by chemoattractants and adhesion molecules [54]. Neutrophil attracting chemokines and complement C5a and C3a were no different in Ptx3-/- and WT mice. PTX3 has been shown to serve as a negative regulator of neutrophil recruitment by interacting with P-selectin [12,13]. In-vitro studies and in-vivo experiments which took advantage of P-selectin-deficient Selp-/- mice and Ptx3-/-Selp-/- double deficient mice were designed to assess the relevance of this pathway. The results obtained indicated that the defective control of invasive pneumococcal infection observed in Ptx3-/- mice is due to unleashing of P-selectin-dependent recruitment of neutrophils which promote bacterial invasion. Thus, by taming uncontrolled P-selectin dependent recruitment of neutrophils the fluid phase pattern recognition molecule PTX3 plays an essential role in tuning inflammation and resistance against invasive pneumococcus infection.

Figures

Fig 1. Pneumococcal invasive infection induces PTX3 expression.

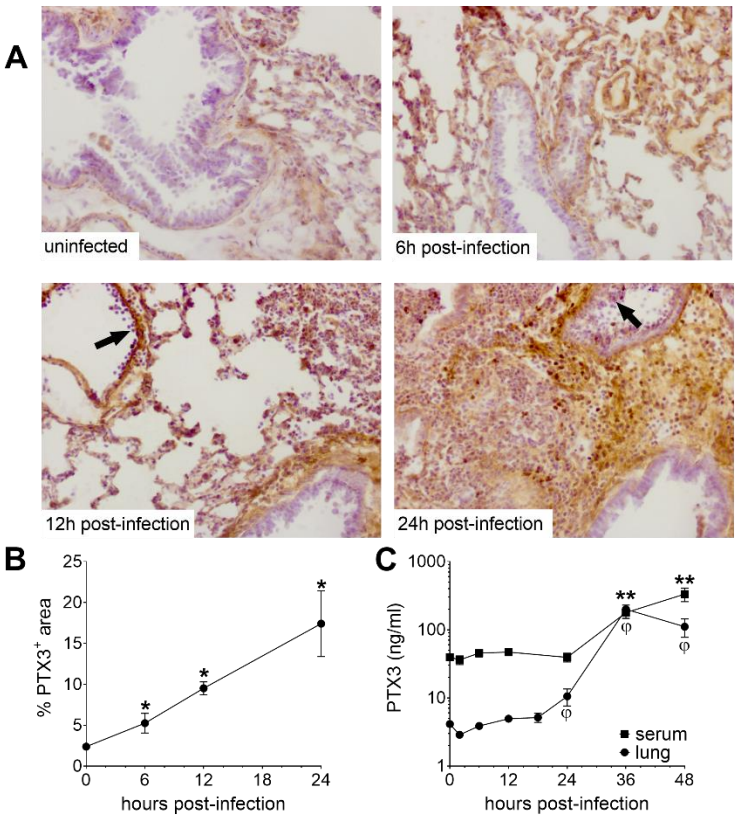

WT mice were infected intranasally with $5x10^4$ CFU of *S. pneumoniae* serotype 3 and sacrificed at the indicated time points for tissue collection. (A-B) Immunohistochemical analysis of PTX3 expression in lung sections (magnification x10) from uninfected mice and mice sacrificed 6h, 12h and 24h post-infection (n=3-6). (A) One representative images of at least three biological replicates for each condition is reported. Inflammatory cell infiltrates are indicated by arrows. (B) Sections were scanned and analyzed to determine the percentage of $PTX3^+$ area at the indicated time points. (C) PTX3 protein levels determined by ELISA in serum and lung homogenates collected at the indicated time points (n=4-10). Results are reported as mean ± SEM. Statistical significance was determined using the Mann-Whitney test comparing results to uninfected mice (ϕ or **P*<0.05 and ***P*<0.01).

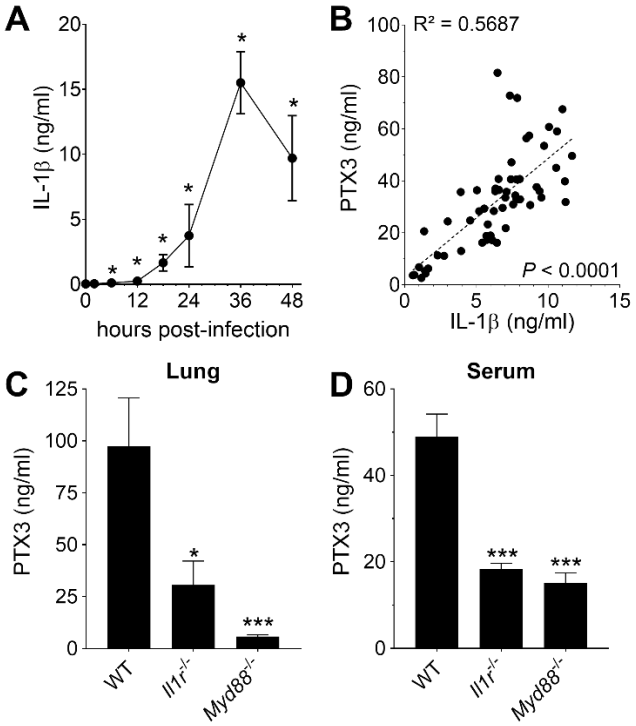

Fig 2. Role of IL-1β in induction of PTX3 during *S. pneumoniae* infection.

WT mice were infected intranasally with $5x10^4$ CFU of *S. pneumoniae* serotype 3 and sacrificed at the indicated time points for tissue collection. (A) IL-1β protein levels in lung homogenates collected at the indicated time points determined by ELISA (n=3-4). (B) Correlation between PTX3 and IL-1β protein levels in lung homogenates of all infected mice sacrificed from 2h to 48h post-infection (n=60). PTX3 protein levels determined by ELISA in lung homogenates (C) and serum (D) collected 36h post-infection in WT, *Il1r*$^{-/-}$ and *Myd88*$^{-/-}$ mice (n=7-8). Results are reported as mean ± SEM. Statistical significance was determined using the Mann-Whitney test comparing results to uninfected mice (A-B) or WT infected mice (C-D) (**P*<0.05 and ****P*<0.001).

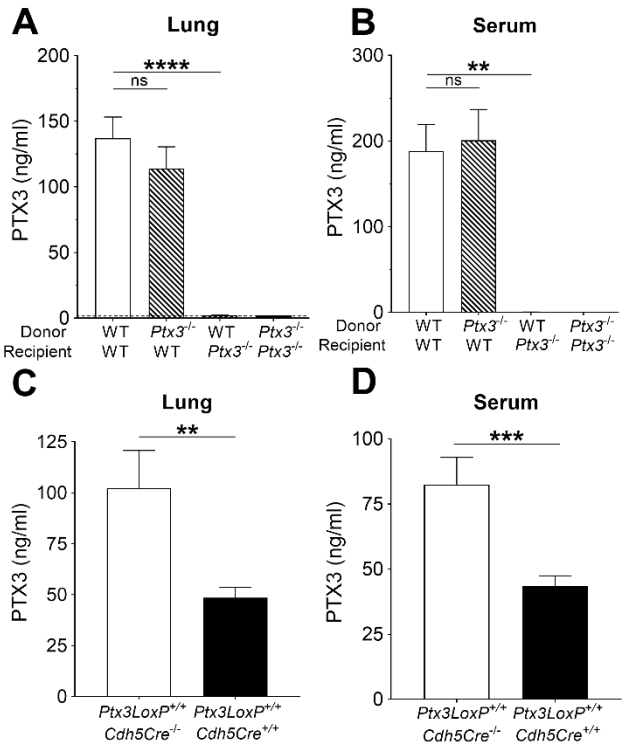

Fig 3. Non-hematopoietic cells are a major source of PTX3 during pneumococcal infections.
Mice were infected intranasally with $5x10^4$ CFU of *S. pneumoniae* serotype 3 and sacrificed at indicated time point for tissue collection. (A-B) PTX3 protein levels determined by ELISA in lung homogenates (A) and serum (B) collected 36h post-infection from chimeric mice (n=23-26). (C-D) PTX3 protein levels determined by ELISA in lung homogenates (C) and serum (D) collected 36h post-infection of *Ptx3LoxP*$^{+/+}$*Cdh5*-cre$^{-/-}$, *Ptx3LoxP*$^{+/+}$*Cdh5*-cre$^{+/+}$. Results are reported as mean ± SEM; (A-B) PTX3 detection limit is 2 ng/ml represented by a dotted line. Statistical significance was determined using the Mann-Whitney test (*P<0.05, **P<0.01, ***P<0.001 and **** P<0.0001).

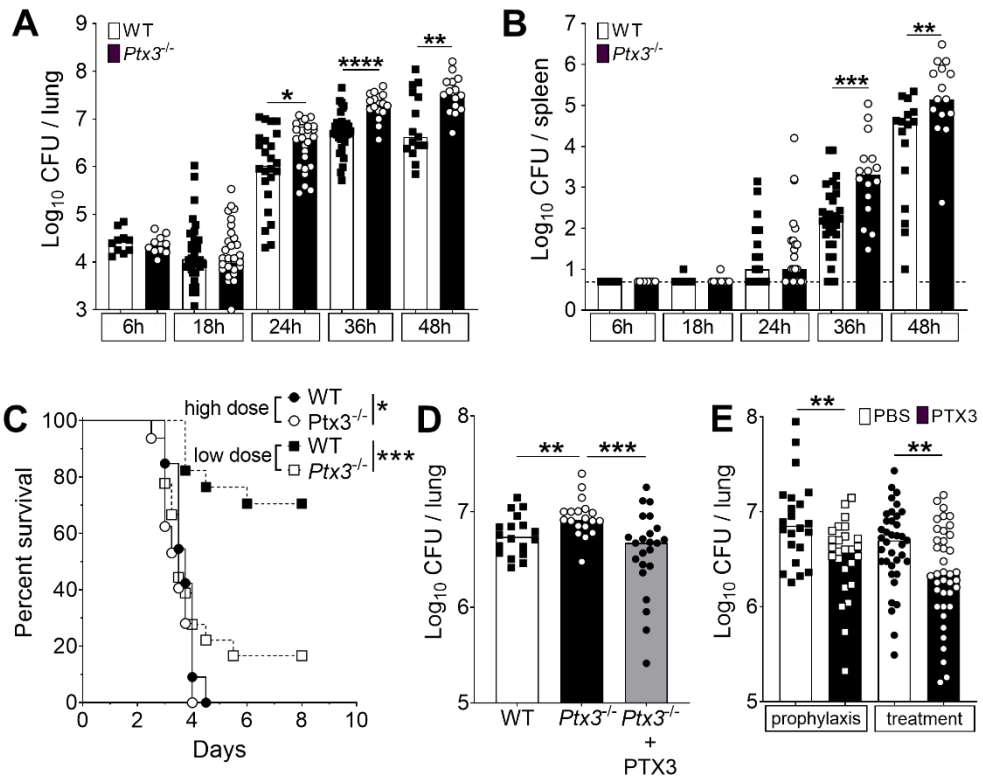

Fig 4. Defective resistance of PTX3-deficient mice to invasive pneumococcal infections.
Mice were infected intranasally with different doses of *S. pneumoniae* serotype 3 and sacrificed at the indicated time points for tissue collection. (A-B) WT and *Ptx3*$^{-/-}$ mice were infected with 5x10^4 CFU and bacterial load in lung (A) and spleen (B) was analyzed at the indicated time points (n=10-36). (C) Survival of WT and *Ptx3*$^{-/-}$ mice (n=17-33) was monitored every 6h after infection with 5x10^3 CFU (low dose) or 5x10^4 CFU (high dose). (D) Bacterial load was analyzed in lungs collected 36h post-infection from WT, *Ptx3*$^{-/-}$ and *Ptx3*$^{-/-}$ mice treated intraperitoneally with recombinant PTX3 (10µg/100µl) before the infection and 24h post-infection (n=18-23). (E) Bacterial load in lungs collected 36h post-infection from WT mice treated intranasally before the infection (prophylaxis, n=22-26) or 12h post-infection (treatment, n=37-40) with 1µg/30µl of recombinant PTX3 or PBS. Results are reported as median. CFU detection limits in the spleen is 5 CFU represented by a dotted line. Statistical significance was determined using the Mann-Whitney test for bacterial load and Log-rank (Mantel-Cox) test for survival (**P*<0.05, ***P*<0.01, ****P*<0.001 and **** *P*<0.0001).

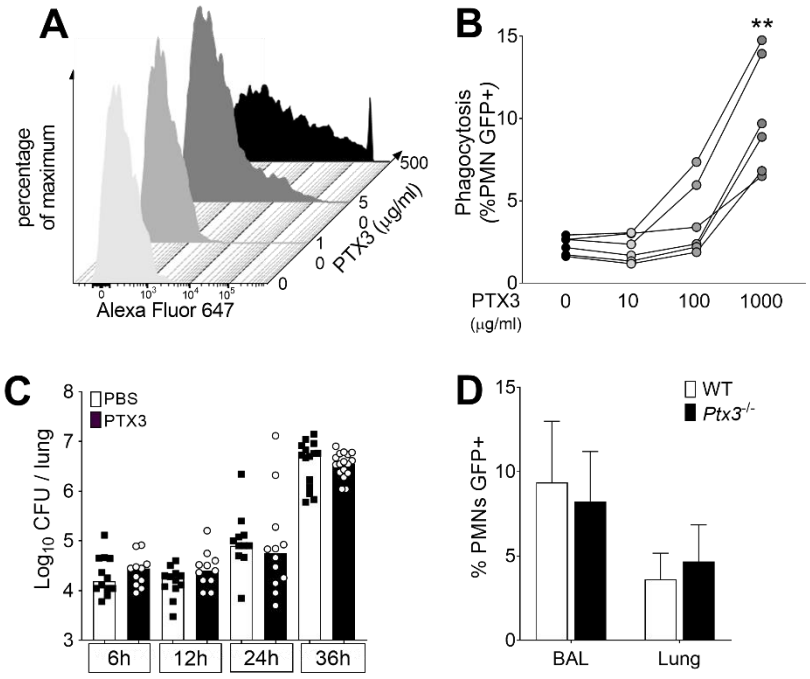

Fig 5. Role of enhanced phagocytosis in PTX3-mediated resistance to *S. pneumoniae*

(A) Binding of recombinant PTX3-biot at the indicated concentration with 10^6 CFU of *S. pneumoniae* serotype 3. PTX3 binding to *S. pneumoniae* was analyzed by flow cytometry after incubation with Streptavidin-Alexa Fluor 647. (B) *S. pneumoniae* serotype 1 expressing GFP (10^6 CFU) was pre-opsonized with indicated concentration of recombinant PTX3 and incubated 30 min with 10^5 purified human neutrophils from 6 independent donors. GFP positive neutrophils were analyzed by flow cytometry. (C) Bacterial load in lung collected at indicated time points from WT mice infected intranasally with *S. pneumoniae* serotype 3 pre-opsonized with 33µg/ml of recombinant PTX3 or non-opsonized. (n=11-17). (D) Neutrophil phagocytosis of *S. pneumoniae* serotype 1 expressing GFP was analyze by flow cytometry. BAL and lungs from WT and *Ptx3*$^{-/-}$ mice were collected 24h after infection with a lethal inoculum of PTX3 (n=9-14). Results are expressed as mean of 5 technical replicate for each time point and donor (B), median (C) and mean ± SD (D). Statistical significance was determined using a one-way ANOVA with Sidak's multiple comparison test (B) and the Mann-Whitney test (C-D) (**P<0.01).

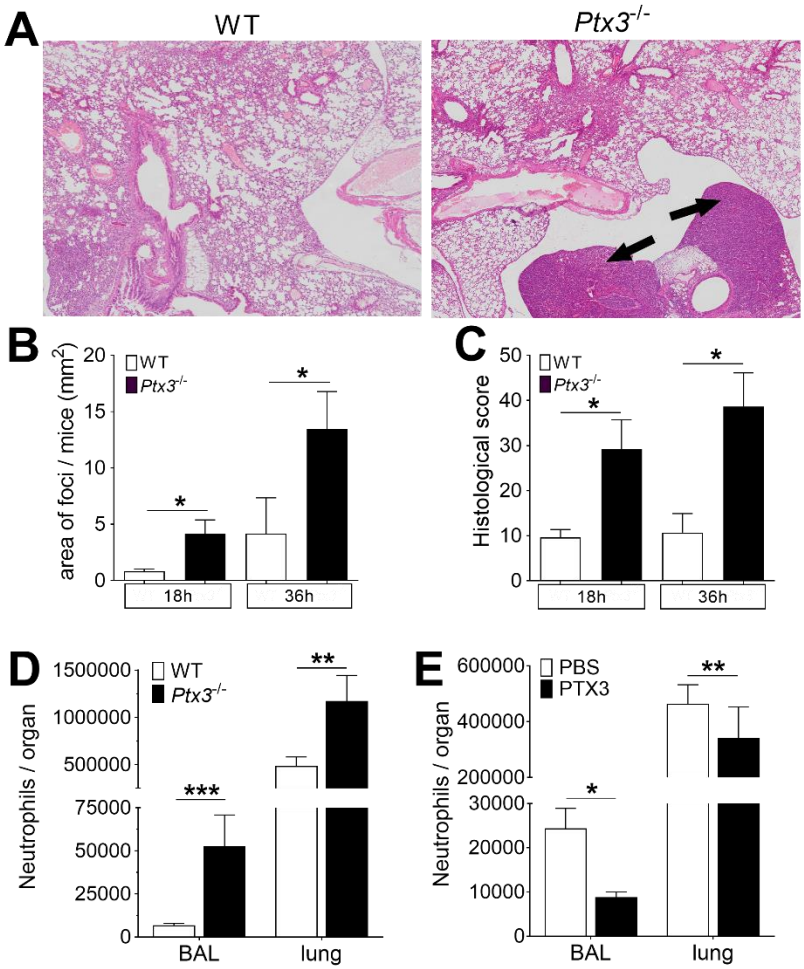

Fig 6. PTX3 regulates inflammation during pneumococcus infection.
Mice were infected intranasally with 5x10^4 CFU of *S. pneumoniae* serotype 3 and sacrificed at the indicated time points for tissue collection. (A) Hematoxylin and Eosin (H&E) staining of formalin-fixed histological sections from the lungs of WT and *Ptx3*$^{-/-}$ mice at 10x magnification. One representative image from at least ten biological replicates of WT and *Ptx3*$^{-/-}$ mice. Inflammatory cell foci are indicated by arrows. (B) Area of inflammatory cells foci measured in lungs collected 18h and 36h post-infection from WT and *Ptx3*$^{-/-}$ mice. Areas were measured on three H&E stained lung sections per mice at different depth separated by at least 100µm each (n=6-10). (C) Inflammatory histological score measured in lungs collected 18h and 36h post-infection from WT and *Ptx3*$^{-/-}$ mice. Scores (detailed in the Material and Methods section) were determined on three H&E stained lung sections per mice at different depth separated by at least 100µm each (n=6-10). (D) Neutrophil number determined by flow cytometry in BAL and lungs collected 18h post-infection from WT and *Ptx3*$^{-/-}$ mice (n=11-18). (E) Neutrophil number determined by flow cytometry in the BAL and lung collected 18h post-infection from WT mice treated intranasally 12h post-infection with recombinant PTX3 or PBS (n=11-18). Results represent the mean ± SEM. Statistical significance was determined using the Mann-Whitney test comparing results to uninfected mice (**P*<0.05, ***P*<0.01 and ****P*<0.001).

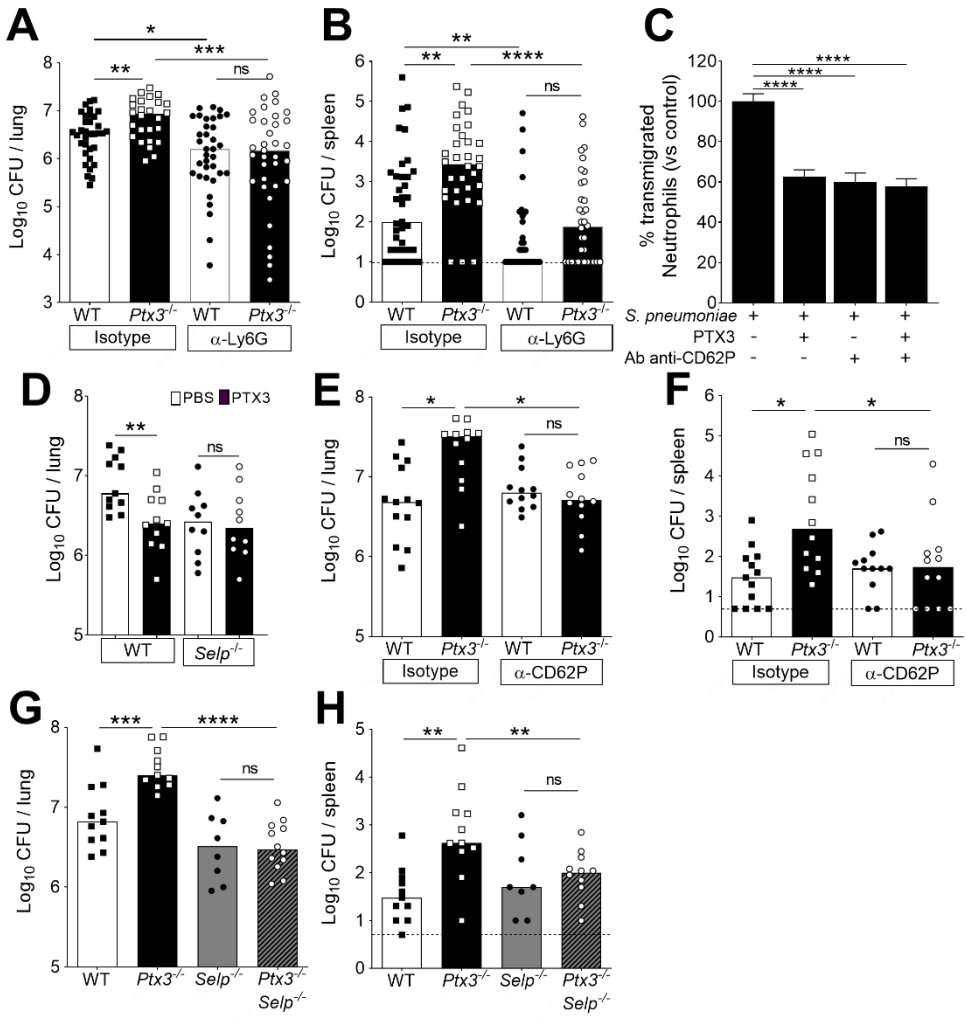

Fig 7. PTX3-mediated regulation of neutrophil recruitment.

Mice were infected intranasally with 5x10^4 CFU of *S. pneumoniae* serotype 3 and sacrificed at the indicated time points for tissue collection. (A-B) Bacterial load in lung (A) and spleen (B) collected 36h post-infection from WT and *Ptx3*$^{-/-}$ mice treated intraperitoneally 12h post-infection with 200µg/100µl of anti-Ly6G or isotype control antibodies (n=26-37). (C) Transmigration of human purified neutrophil towards *S. pneumoniae* (n=11). Results are reported as percentage of transmigrated neutrophils considering as 100% the number of transmigrated neutrophils in the control condition (i.e *S. pneumoniae* in the lower chamber and no treatment in the upper chamber). (D) Bacterial load in lungs collected 36h post-infection from WT and *Selp*$^{-/-}$ mice treated intranasally 12h post-infection with 1µg/30µl of recombinant PTX3 or PBS (n=10-11). (E-F) Bacterial load in lungs (E) and spleens (F) collected 36h post-infection from WT and *Ptx3*$^{-/-}$ mice treated intravenously 12h post-infection with 50µg/100µl of anti-CD62P or isotype control antibodies (n=12-13). (G-H) Bacterial load in lungs (G) and spleens (H) collected 36h post-infection from WT, *Ptx3*$^{-/-}$, *Selp*$^{-/-}$ and *Ptx3*$^{-/-}$*Selp*$^{-/-}$ mice (n=8-12). Results are reported as median (A-B, D-H) and mean ± SEM. CFU detection limits in the spleen is 5 CFU represented by a dotted line. Statistical significance was determined using the Mann-Whitney test (**P*<0.05, ***P*<0.01, ****P*<0.001 and **** *P*<0.0001).

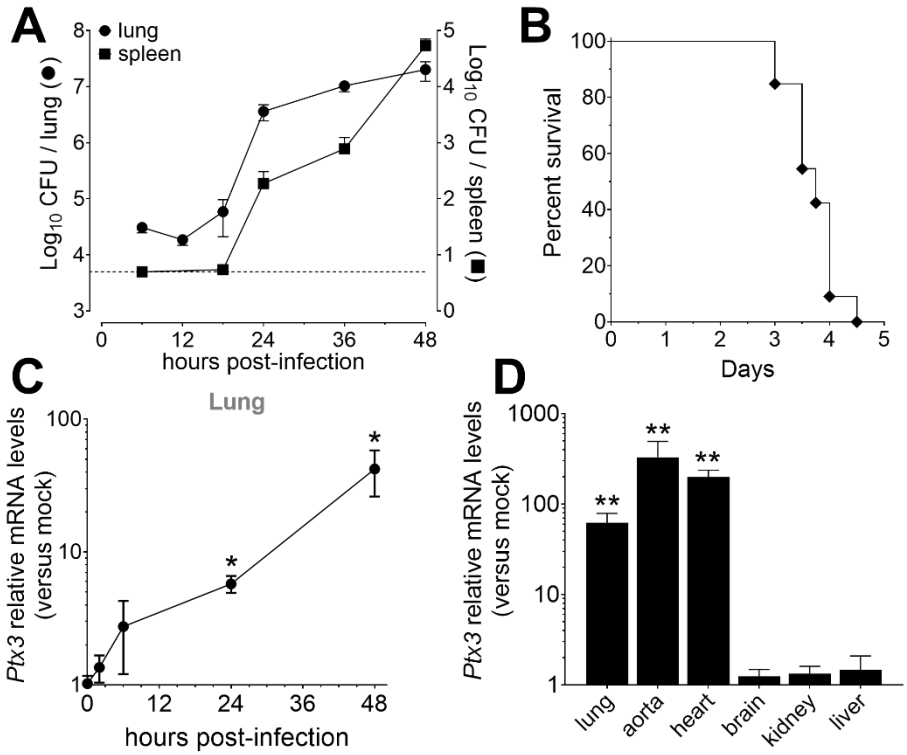

Fig S1. Pneumococcal invasive infection induces PTX3 expression.

Mice were infected intranasally with $5x10^4$ CFU of *S. pneumoniae* serotype 3 and sacrificed at the indicated time points for tissue collection. (A) Bacterial load in lung (●) and spleen (■) collected at indicated time points after infection of WT mice (n=10-21). (B) Survival of WT mice infected with a lethal inoculum of *S. pneumoniae* serotype 3. Mice were monitored every 6h (n=33) (C) Relative *Ptx3* mRNA expression determined by Real-Time quantitative PCR in lung homogenates collected at the indicated time points and normalized on uninfected mice (n=3). (D) Relative *Ptx3* mRNA expression determined by Real-Time quantitative PCR in the indicated organ homogenates collected 48h post-infection and compared to uninfected mice (n=4-5). Results are reported as the mean ± SEM. CFU detection limits in the spleen is 5 CFU represented by a dotted line. Statistical significance was determined using the Mann-Whitney test comparing results to uninfected mice (**P*<0.05 and ***P*<0.01).

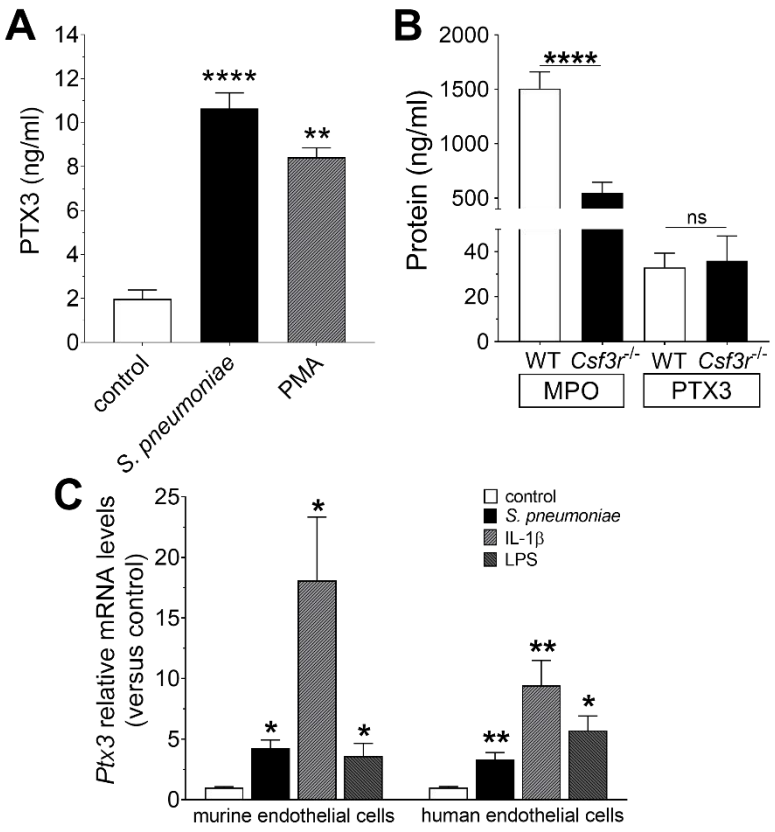

Fig S2. Cellular sources of PTX3 after stimulation with *S. pneumoniae*.
(A) PTX3 protein levels, measured by ELISA, released by 10^6 human purified neutrophils/100µl stimulated for 6h at 37°C with 10^7 CFU/ml of *S. pneumoniae* serotype 3 or 10 ng/ml of phorbol myristate acetate (PMA). (B) MPO and PTX3 protein levels determined by ELISA in lung homogenates collected 36h post intranasal infection of WT and *Csfr3*$^{-/-}$ mice with $5x10^4$ CFU of *S. pneumoniae* serotype 3 (n=18). (C) Relative *Ptx3* mRNA expression determined by Real-Time quantitative PCR in human and murine endothelial cells after 6h stimulation with 10^6 CFU *S. pneumoniae*, 20 ng/ml IL-1β or 100 ng/ml LPS (n=3-6). Results are reported as mean ± SEM. Statistical significance was determined using the Mann-Whitney test compared to control group (A, C) or to infected WT mice (B) (**P*<0.05, ***P*<0.01 and **** *P*<0.0001).

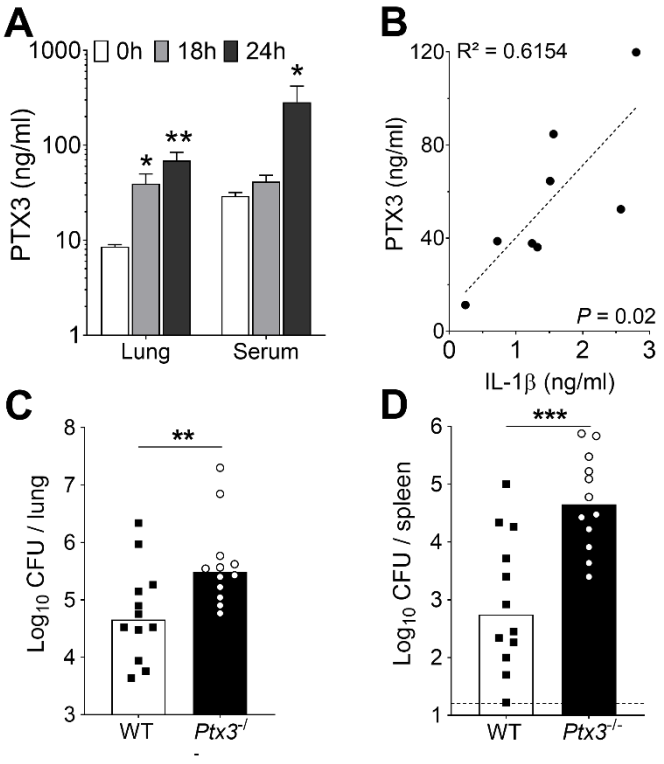

Fig S3. Infection with *S. pneumoniae* serotype 1 and bacterial growth rate in presence of PTX3.
Mice were infected intranasally with 10^6 CFU of *S. pneumoniae* serotype 1 and sacrificed at the indicated time points for tissue collection. (A) PTX3 protein levels determined by ELISA in lung homogenates and serum collected at the indicated time points (n=4-5). (B) Correlation between PTX3 and IL-1β protein levels in lung homogenates of all infected mice sacrificed from 18 to 24 hours post-infection (n=8). (C-D) Bacterial load in lung (C) and spleen (D) collected at the indicated time points after infection of WT and *Ptx3*$^{-/-}$ mice with *S. pneumoniae* serotype 1 (n=12). Results are reported as the mean ± SEM (A). Solid bars represent the median. CFU detection limits in the spleen is 5 CFU represented by a dotted line. Statistical significance was determined using the Mann-Whitney test for bacterial load compared to uninfected mice (A) and to WT infected mice (C-D) (**P*<0.05, ***P*<0.01 and ****P*<0.001).

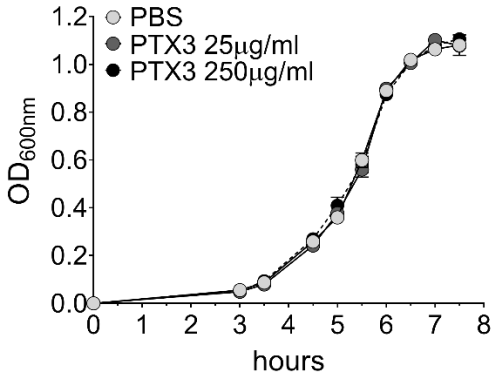

Fig S4. Lack of effect of PTX3 on *S. pneumoniae* growth rate.
Growth rate of *S. pneumoniae* serotype 3 non-opsonized or pre-opsonized with recombinant PTX3 (25-250 µg/ml for 40 min) was measured in the culture condition reported in the Material & Methods section. Absorbance (600 nm) was measured at the indicated time points (n=3) and is reported as mean ± SEM.

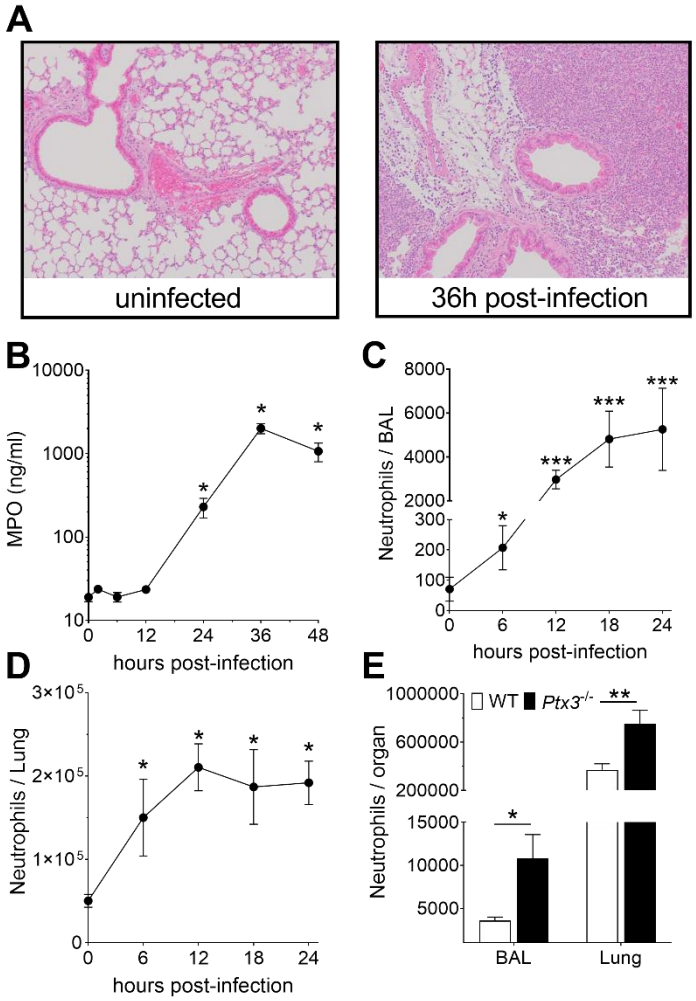

Fig S5. Neutrophil recruitment during pneumococcus invasive infection.
Mice were infected intranasally with $5x10^4$ CFU of *S. pneumoniae* serotype 3 (A-D) or with 10^6 CFU of serotype 1 (E) and sacrificed at the indicated time points for tissue collection. (A) Hematoxylin and Eosin (H&E) staining of formalin-fixed lung sections from WT mice uninfected and 36h after infection at 10x magnification. (B) MPO levels determined by ELISA in lung homogenates collected at the indicated time points (n=4). (C-D) Neutrophil number determined by flow cytometry in the BAL (C) and lung (D) collected at the indicated time points from WT mice (n=4-8). (E) Neutrophil number determined by flow cytometry in the BAL and lung collected 18h post-infection from WT and *Ptx3*$^{-/-}$ mice (n=10-13). Results are reported as mean ± SEM. Statistical significance was determined using the Mann-Whitney test comparing results to uninfected mice (**P*<0.05, ***P*<0.01 and ****P*<0.001).

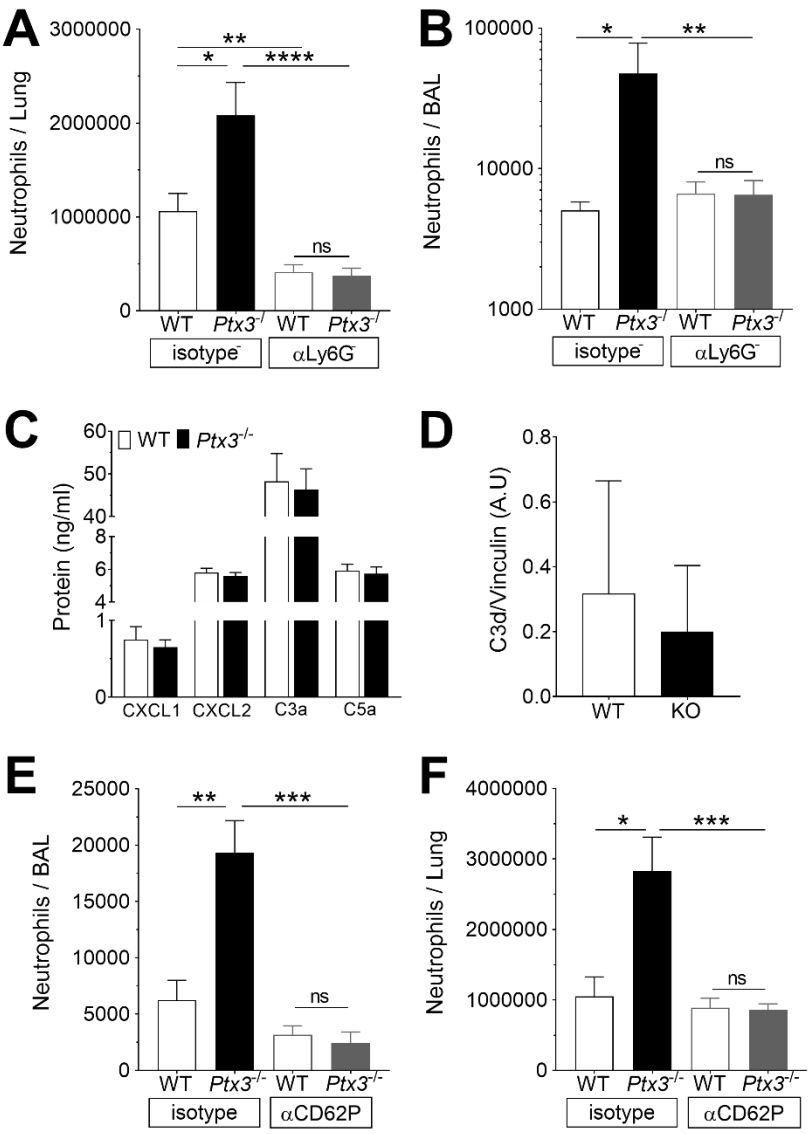

Fig S6. PTX3 modulates neutrophil recruitment.

Mice were infected intranasally with 5x10^4 CFU of *S. pneumoniae* serotype 3 and sacrificed at the indicated time points for tissue collection. (A-B) Neutrophil number determined by flow cytometry in the lung (A) and BAL (B) collected 18h post-infection from WT and *Ptx3*$^{-/-}$ mice treated intraperitoneally 12h post-infection with 200µg/100µl of anti-Ly6G or isotype control antibodies (n=9-12). (C) Chemokines (CXCL1/CXCL2) and anaphylatoxins (C3a/C5a) levels measured by ELISA in lung homogenates collected 18h post-infection from WT and *Ptx3*$^{-/-}$ mice (n=20). (D) C3d level in lung homogenates collected 36h post-infection from WT and *Ptx3*$^{-/-}$ (KO) mice, detected by western blot and normalized with vinculin expression (n=8). (E-F) Neutrophil number determined by flow cytometry in the BAL (E) and lung (F) collected 18h post-infection from WT and *Ptx3*$^{-/-}$ mice treated intraperitoneally 12h post-infection with 50µg/100µl of anti-CD62P or isotype control antibodies (n=8). Results are reported as mean ± SEM. Statistical significance was determined using the Mann-Whitney test (**P*<0.05 and ***P*<0.01).

Tables

Table 1. Frequency distribution of PTX3 gene single nucleotide polymorphisms (SNPs) in IPD patients and controls.

SNP	Alleles	Peptide shift	Associated allele	Frequency (%) IPD patients (n=57)	Frequency (%) Controls (n=521)	χ^2	OR (95%)	*P*-value*
rs2305619	+281 A/G		A G	43.86 56.14	43.44 56.56	0.007	1.02 (0.69-1.50)	0.931
rs3816527	+734 C/A	Ala→Asp	C A	32.46 67.54	38.42 61.58	1.552	0.77 (0.51-1.16)	0.213
rs1840680	+1149 A/G		A G	42.11 57.89	42.49 57.51	0.006	0.98 (0.67-1.46)	0.938

* Bonferroni-corrected threshold for significance: 0.017.

Table 2. Haplotype analysis for *PTX3* gene in IPD patients and controls.

rs2305619	rs3816527	rs1840680	Frequency (%) IPD patients (n=57)	Frequency (%) Controls (n=521)	χ^2	P-value *
G	A	G	56.15	56.51	0.005	0.9409
G	A		56.14	56.59	0.008	0.9269
	A	G	57.89	57.41	0.010	0.9202
A	C	A	32.44	38.28	1.488	0.2226
A	C		32.46	38.47	1.577	0.2091
	C	A	32.46	38.33	1.51	0.2191
A	A	A	9.67	4.26	6.604	**0.0102**
A	A		11.4	4.94	8.129	**0.0044**
	A	A	9.65	4.26	6.533	**0.0106**
A	A	G	1.73	0.95	0.610	0.4348

* Bonferroni-corrected threshold for significance: 0.017.

Significant *P* values, surviving the Bonferroni correction for multiple testing, are indicated in bold.

References

1. Troeger C, Blacker B, Khalil IA, Rao PC, Cao J, Zimsen SRM, et al. Estimates of the global, regional, and national morbidity, mortality, and aetiologies of lower respiratory infections in 195 countries, 1990–2016: a systematic analysis for the Global Burden of Disease Study 2016. The Lancet Infectious Diseases. 2018;18: 1191–1210. doi:10.1016/S1473-3099(18)30310-4
2. Weiser JN, Ferreira DM, Paton JC. Streptococcus pneumoniae: transmission, colonization and invasion. Nat Rev Microbiol. 2018;16: 355–367. doi:10.1038/s41579-018-0001-8
3. Tin Tin Htar M, Morato Martínez J, Theilacker C, Schmitt H-J, Swerdlow D. Serotype evolution in Western Europe: perspectives on invasive pneumococcal diseases (IPD). Expert Review of Vaccines. 2019;18: 1145–1155. doi:10.1080/14760584.2019.1688149
4. Weinberger DM, Harboe ZB, Sanders EAM, Ndiritu M, Klugman KP, Rückinger S, et al. Association of Serotype with Risk of Death Due to Pneumococcal Pneumonia: A Meta-Analysis. Clin Infect Dis. 2010;51: 692–699. doi:10.1086/655828
5. Garlanda C, Bottazzi B, Magrini E, Inforzato A, Mantovani A. PTX3, a Humoral Pattern Recognition Molecule, in Innate Immunity, Tissue Repair, and Cancer. Physiological Reviews. 2018;98: 623–639. doi:10.1152/physrev.00016.2017
6. Jaillon S, Moalli F, Ragnarsdottir B, Bonavita E, Puthia M, Riva F, et al. The Humoral Pattern Recognition Molecule PTX3 Is a Key Component of Innate Immunity against Urinary Tract Infection. Immunity. 2014;40: 621–632. doi:10.1016/j.immuni.2014.02.015
7. Moalli F, Doni A, Deban L, Zelante T, Zagarella S, Bottazzi B, et al. Role of complement and Fc{gamma} receptors in the protective activity of the long pentraxin PTX3 against Aspergillus fumigatus. Blood. 2010;116: 11. doi:10.1182/blood-2009-12-258376
8. Porte R, Davoudian S, Asgari F, Parente R, Mantovani A, Garlanda C, et al. The Long Pentraxin PTX3 as a Humoral Innate Immunity Functional Player and Biomarker of Infections and Sepsis. Front Immunol. 2019;10: 794. doi:10.3389/fimmu.2019.00794
9. Jaillon S, Peri G, Delneste Y, Frémaux I, Doni A, Moalli F, et al. The humoral pattern recognition receptor PTX3 is stored in neutrophil granules and localizes in extracellular traps. Journal of Experimental Medicine. 2007;204: 793–804. doi:10.1084/jem.20061301
10. Daigo K, Yamaguchi N, Kawamura T, Matsubara K, Jiang S, Ohashi R, et al. The Proteomic Profile of Circulating Pentraxin 3 (PTX3) Complex in Sepsis Demonstrates the Interaction with Azurocidin 1 and Other Components of Neutrophil Extracellular Traps. Molecular & Cellular Proteomics. 2012;11: M111.015073. doi:10.1074/mcp.M111.015073
11. Doni A, Musso T, Morone D, Bastone A, Zambelli V, Sironi M, et al. An acidic microenvironment sets the humoral pattern recognition molecule PTX3 in a tissue repair mode. 212: 21.
12. Lech M, Römmele C, Gröbmayr R, Eka Susanti H, Kulkarni OP, Wang S, et al. Endogenous and exogenous pentraxin-3 limits postischemic acute and chronic kidney injury. Kidney International. 2013;83: 647–661. doi:10.1038/ki.2012.463
13. Deban L, Russo RC, Sironi M, Moalli F, Scanziani M, Zambelli V, et al. Regulation of leukocyte recruitment by the long pentraxin PTX3. Nat Immunol. 2010;11: 328–334. doi:10.1038/ni.1854
14. Quinton LJ, Mizgerd JP. Dynamics of Lung Defense in Pneumonia: Resistance, Resilience, and Remodeling. Annu Rev Physiol. 2015;77: 407–430. doi:10.1146/annurev-physiol-021014-071937
15. Shi G-Q, Yang L, Shan L-Y, Yin L-Z, Jiang W, Tian H-T, et al. Investigation of the clinical significance of detecting PTX3 for community-acquired pneumonia. European Review for Medical and Pharmacological Sciences. 2020;24: 8477–8482. doi:10.26355/eurrev_202008_22645
16. Siljan WW, Holter JC, Michelsen AE, Nymo SH, Lauritzen T, Oppen K, et al. Inflammatory biomarkers are associated with aetiology and predict outcomes in community-acquired pneumonia: results of a 5-year follow-up cohort study. ERJ Open Res. 2019;5: 00014–02019. doi:10.1183/23120541.00014-2019
17. Kao S-J, Yang H-W, Tsao S-M, Cheng C-W, Bien M-Y, Yu M-C, et al. Plasma long pentraxin 3 (PTX3) concentration is a novel marker of disease activity in patients with community-acquired pneumonia. Clinical Chemistry and Laboratory Medicine. 2013;51. doi:10.1515/cclm-2012-0459
18. Mauri T, Coppadoro A, Bombino M, Bellani G, Zambelli V, Fornari C, et al. Alveolar pentraxin 3 as an early marker of microbiologically confirmed pneumonia: a threshold-finding prospective observational study. Crit Care. 2014;18: 562. doi:10.1186/s13054-014-0562-5
19. Bilgin H, Haliloglu M, Yaman A, Ay P, Bilgili B, Arslantas MK, et al. Sequential Measurements of Pentraxin 3 Serum Levels in Patients with Ventilator-Associated Pneumonia: A Nested Case-Control Study. Canadian Journal of Infectious Diseases and Medical Microbiology. 2018;2018: 1–8. doi:10.1155/2018/4074169
20. Thulborn SJ, Dilpazir M, Haldar K, Mistry V, Brightling CE, Barer MR, et al. Investigating the role of pentraxin 3 as a biomarker for bacterial infection in subjects with COPD. COPD. 2017;Volume 12: 1199–1205. doi:10.2147/COPD.S123528
21. Saleh MAA, van de Garde EMW, van Hasselt JGC. Host-response biomarkers for the diagnosis of bacterial respiratory tract infections. Clinical Chemistry and Laboratory Medicine (CCLM). 2019;57: 442–451. doi:10.1515/cclm-2018-0682
22. Cunha C, Aversa F, Lacerda JF, Busca A, Kurzai O, Grube M, et al. Genetic PTX3 Deficiency and Aspergillosis in Stem-Cell Transplantation. N Engl J Med. 2014;370: 421–432. doi:10.1056/NEJMoa1211161
23. Cunha C, Monteiro AA, Oliveira-Coelho A, Kühne J, Rodrigues F, Sasaki SD, et al. PTX3-Based Genetic Testing for Risk of Aspergillosis After Lung Transplant: Table 1. Clin Infect Dis. 2015;61: 1893–1894. doi:10.1093/cid/civ679

24. Brunel A-S, Wójtowicz A, Lamoth F, Spertini O, Neofytos D, Calandra T, et al. Pentraxin-3 polymorphisms and invasive mold infections in acute leukemia patients receiving intensive chemotherapy. Haematologica. 2018;103: e527–e530. doi:10.3324/haematol.2018.195453
25. He Q, Li H, Rui Y, Liu L, He B, Shi Y, et al. Pentraxin 3 Gene Polymorphisms and Pulmonary Aspergillosis in Chronic Obstructive Pulmonary Disease Patients. Clinical Infectious Diseases. 2018;66: 261–267. doi:10.1093/cid/cix749
26. Olesen R, Wejse C, Velez DR, Bisseye C, Sodemann M, Aaby P, et al. DC-SIGN (CD209), pentraxin 3 and vitamin D receptor gene variants associate with pulmonary tuberculosis risk in West Africans. Genes Immun. 2007;8: 456–467. doi:10.1038/sj.gene.6364410
27. Chiarini M, Sabelli C, Melotti P, Garlanda C, Savoldi G, Mazza C, et al. PTX3 genetic variations affect the risk of Pseudomonas aeruginosa airway colonization in cystic fibrosis patients. Genes Immun. 2010;11: 665–670. doi:10.1038/gene.2010.41
28. Wójtowicz A, Lecompte TD, Bibert S, Manuel O, Rüeger S, Berger C, et al. *PTX3* Polymorphisms and Invasive Mold Infections After Solid Organ Transplant: Figure 1. Clin Infect Dis. 2015;61: 619–622. doi:10.1093/cid/civ386
29. Ponzetta A, Carriero R, Carnevale S, Barbagallo M, Molgora M, Perucchini C, et al. Neutrophils Driving Unconventional T Cells Mediate Resistance against Murine Sarcomas and Selected Human Tumors. Cell. 2019;178: 346-360.e24. doi:10.1016/j.cell.2019.05.047
30. Porte R, Fougeron D, Muñoz-Wolf N, Tabareau J, Georgel A-F, Wallet F, et al. A Toll-Like Receptor 5 Agonist Improves the Efficacy of Antibiotics in Treatment of Primary and Influenza Virus-Associated Pneumococcal Mouse Infections. Antimicrob Agents Chemother. 2015;59: 6064–6072. doi:10.1128/AAC.01210-15
31. Kjos M, Aprianto R, Fernandes VE, Andrew PW, van Strijp JAG, Nijland R, et al. Bright Fluorescent Streptococcus pneumoniae for Live-Cell Imaging of Host-Pathogen Interactions. Schneewind O, editor. J Bacteriol. 2015;197: 807–818. doi:10.1128/JB.02221-14
32. Bottazzi B, Vouret-Craviari V, Bastone A, De Gioia L, Matteucci C, Peri G, et al. Multimer Formation and Ligand Recognition by the Long Pentraxin PTX3. Journal of Biological Chemistry. 1997;272: 32817–32823. doi:10.1074/jbc.272.52.32817
33. de Porto AP, Liu Z, de Beer R, Florquin S, de Boer OJ, Hendriks RW, et al. Btk inhibitor ibrutinib reduces inflammatory myeloid cell responses in the lung during murine pneumococcal pneumonia. Mol Med. 2019;25: 3. doi:10.1186/s10020-018-0069-7
34. Bottazzi B, Santini L, Savino S, Giuliani MM, Dueñas Díez AI, Mancuso G, et al. Recognition of Neisseria meningitidis by the Long Pentraxin PTX3 and Its Role as an Endogenous Adjuvant. Dieli F, editor. PLoS ONE. 2015;10: e0120807. doi:10.1371/journal.pone.0120807
35. Quinn MT, DeLeo FR, editors. Neutrophil: Methods and Protocols. New York, NY: Springer US; 2020. doi:10.1007/978-1-0716-0154-9
36. Bou Ghanem EN, Clark S, Roggensack SE, McIver SR, Alcaide P, Haydon PG, et al. Extracellular Adenosine Protects against Streptococcus pneumoniae Lung Infection by Regulating Pulmonary Neutrophil Recruitment. Mitchell TJ, editor. PLoS Pathog. 2015;11: e1005126. doi:10.1371/journal.ppat.1005126
37. Garcia-Laorden MI, Rodriguez de Castro F, Sole-Violan J, Payeras A, Briones ML, Borderias L, et al. The role of mannose-binding lectin in pneumococcal infection. European Respiratory Journal. 2013;41: 131–139. doi:10.1183/09031936.00174111
38. Barbati E, Specchia C, Villella M, Rossi ML, Barlera S, Bottazzi B, et al. Influence of Pentraxin 3 (PTX3) Genetic Variants on Myocardial Infarction Risk and PTX3 Plasma Levels. Stoll M, editor. PLoS ONE. 2012;7: e53030. doi:10.1371/journal.pone.0053030
39. Purcell S, Neale B, Todd-Brown K, Thomas L, Ferreira MAR, Bender D, et al. PLINK: A Tool Set for Whole-Genome Association and Population-Based Linkage Analyses. The American Journal of Human Genetics. 2007;81: 559–575. doi:10.1086/519795
40. Wigginton JE, Cutler DJ, Abecasis GR. A Note on Exact Tests of Hardy-Weinberg Equilibrium. The American Journal of Human Genetics. 2005;76: 887–893. doi:10.1086/429864
41. Liu F, Wu HY, Wesselschmidt R, Kornaga T, Link DC. Impaired Production and Increased Apoptosis of Neutrophils in Granulocyte Colony-Stimulating Factor Receptor–Deficient Mice. Immunity. 1996;5: 491–501. doi:10.1016/S1074-7613(00)80504-X
42. Garlanda C, Hirsch E, Bozza S, Salustri A, De Acetis M, Nota R, et al. Non-redundant role of the long pentraxin PTX3 in anti-fungal innate immune response. Nature. 2002;420: 182–186. doi:10.1038/nature01195
43. Haapasalo K, Meri S. Regulation of the Complement System by Pentraxins. Front Immunol. 2019;10: 1750. doi:10.3389/fimmu.2019.01750
44. Bonacina F, Moregola A, Porte R, Baragetti A, Bonavita E, Salatin A, et al. Pentraxin 3 deficiency protects from the metabolic inflammation associated to diet-induced obesity. Cardiovascular Research. 2019;115: 1861–1872. doi:10.1093/cvr/cvz068
45. Bonacina F, Barbieri SS, Cutuli L, Amadio P, Doni A, Sironi M, et al. Vascular pentraxin 3 controls arterial thrombosis by targeting collagen and fibrinogen induced platelets aggregation. Biochimica et Biophysica Acta (BBA) - Molecular Basis of Disease. 2016;1862: 1182–1190. doi:10.1016/j.bbadis.2016.03.007
46. Campos CF, Leite L, Pereira P, Vaz CP, Branca R, Campilho F, et al. PTX3 Polymorphisms Influence Cytomegalovirus Reactivation After Stem-Cell Transplantation. Front Immunol. 2019;10: 88. doi:10.3389/fimmu.2019.00088

47. Moalli F, Paroni M, Véliz Rodriguez T, Riva F, Polentarutti N, Bottazzi B, et al. The Therapeutic Potential of the Humoral Pattern Recognition Molecule PTX3 in Chronic Lung Infection Caused by *Pseudomonas aeruginosa*. JI. 2011;186: 5425–5434. doi:10.4049/jimmunol.1002035
48. Hasenberg M, Behnsen J, Krappmann S, Brakhage A, Gunzer M. Phagocyte responses towards Aspergillus fumigatus. International Journal of Medical Microbiology. 2011;301: 436–444. doi:10.1016/j.ijmm.2011.04.012
49. Schwab S, Jobin K, Kurts C. Urinary tract infection: recent insight into the evolutionary arms race between uropathogenic Escherichia coli and our immune system. Nephrology Dialysis Transplantation. 2017;32: 1977–1983. doi:10.1093/ndt/gfx022
50. Lovewell RR, Patankar YR, Berwin B. Mechanisms of phagocytosis and host clearance of *Pseudomonas aeruginosa*. American Journal of Physiology-Lung Cellular and Molecular Physiology. 2014;306: L591–L603. doi:10.1152/ajplung.00335.2013
51. Andre GO, Converso TR, Politano WR, Ferraz LFC, Ribeiro ML, Leite LCC, et al. Role of Streptococcus pneumoniae Proteins in Evasion of Complement-Mediated Immunity. Front Microbiol. 2017;8. doi:10.3389/fmicb.2017.00224
52. Szalai AJ. The antimicrobial activity of C-reactive protein. Microbes and Infection. 2002;4: 201–205. doi:10.1016/S1286-4579(01)01528-3
53. Bottazzi B, Doni A, Garlanda C, Mantovani A. An Integrated View of Humoral Innate Immunity: Pentraxins as a Paradigm. Annu Rev Immunol. 2010;28: 157–183. doi:10.1146/annurev-immunol-030409-101305
54. Maas SL, Soehnlein O, Viola JR. Organ-Specific Mechanisms of Transendothelial Neutrophil Migration in the Lung, Liver, Kidney, and Aorta. Front Immunol. 2018;9: 2739. doi:10.3389/fimmu.2018.02739

6.4. Myeloid-Derived Suppressor Cells in Sepsis

Irene T Schrijver [1], Charlotte Théroude [1], Thierry Roger [1]

[1] Infectious Diseases Service, Department of Medicine, Lausanne University Hospital, Epalinges, Switzerland.

Front Immunol. 2019 Feb 27;10:327. doi: 10.3389/fimmu.2019.00327. eCollection 2019.

Contribution to the work: I revised the manuscript.

frontiers in Immunology

MINI REVIEW
published: 27 February 2019
doi: 10.3389/fimmu.2019.00327

Myeloid-Derived Suppressor Cells in Sepsis

*Irene T. Schrijver, Charlotte Théroude and Thierry Roger**

Infectious Diseases Service, Department of Medicine, Lausanne University Hospital, Epalinges, Switzerland

Myeloid-derived suppressor cells (MDSCs) are immature myeloid cells characterized by their immunosuppressive functions. MDSCs expand during chronic and acute inflammatory conditions, the best described being cancer. Recent studies uncovered an important role of MDSCs in the pathogenesis of infectious diseases along with sepsis. Here we discuss the mechanisms underlying the expansion and immunosuppressive functions of MDSCs, and the results of preclinical and clinical studies linking MDSCs to sepsis pathogenesis. Strikingly, all clinical studies to date suggest that high proportions of blood MDSCs are associated with clinical worsening, the incidence of nosocomial infections and/or mortality. Hence, MDSCs are attractive biomarkers and therapeutic targets for sepsis, especially because these cells are barely detectable in healthy subjects. Blocking MDSC-mediated immunosuppression and trafficking or depleting MDSCs might all improve sepsis outcome. While some key aspects of MDSCs biology need in depth investigations, exploring these avenues may participate to pave the way toward the implementation of personalized medicine and precision immunotherapy for patients suffering from sepsis.

Keywords: sepsis, infectious disease, innate immunity, myeloid-derived suppressor cells, biomarker, immunosuppression, inflammation, personalized medicine

OPEN ACCESS

Edited by:
Celio Geraldo Freire-de-Lima, Universidade Federal do Rio de Janeiro, Brazil

Reviewed by:
Philip Alexander Efron, University of Florida, United States
Hugo Caire Castro-Faria-Neto, Fundação Oswaldo Cruz (Fiocruz), Brazil

***Correspondence:**
Thierry Roger
thierry.roger@chuv.ch
orcid.org/0000-0002-9358-0109

Specialty section:
This article was submitted to Microbial Immunology, a section of the journal Frontiers in Immunology

Received: *09 January 2019*
Accepted: *08 February 2019*
Published: *27 February 2019*

Citation:
Schrijver IT, Théroude C and Roger T (2019) Myeloid-Derived Suppressor Cells in Sepsis. Front. Immunol. 10:327. doi: 10.3389/fimmu.2019.00327

INTRODUCTION

Sepsis is one of the leading causes of preventable death. Sepsis is defined as a "life-threatening organ dysfunction caused by a dysregulated host response to infection" (1). The mortality rate of sepsis accounts for five-to-six million deaths of ~30 million cases per year worldwide. Sepsis incidence is rising due to the aging of the population, the burden of chronic diseases, the increasing number of immunocompromised patients, and the resistance of microorganisms to antimicrobials (2). In 2017, the World Health Assembly and the World Health Organization made sepsis a global health priority by adopting a resolution to improve the prevention, diagnosis, and management of sepsis.

Innate immune cells, such as monocytes/macrophages, dendritic cells (DCs), and neutrophils, sense microbial and danger-associated molecular patterns (MAMPs produced by microorganisms, and DAMPs released by injured or stressed cells) through pattern recognition receptors (PRRs). PRRs are grouped into five main families: toll-like receptors (TLRs), NOD-like receptors, C-type lectins, scavenger receptors, RIG-I-like receptors, and intra-cytosolic DNA sensors (3). The interaction between PRRs and MAMPs or DAMPs triggers intracellular signaling pathways that coordinate gene expression, the development of the inflammatory response, the establishment of antimicrobial cellular and humoral responses, and the restoration of homeostasis once pathogens have been contained or eradicated. Sepsis is characterized by an early exacerbation of antimicrobial defense mechanisms, the so-called hyper-inflammatory "cytokine storm," mediating

tissue injury, organ dysfunctions and early mortality, and a concomitant shift toward inflammation resolution and tissue repair. Sepsis-induced immunoparalysis (or immunosuppression) favors the development of secondary infections and long-term immune disabilities accounting for late mortality (4–8).

During the last decades, early goal-directed therapy decreased early mortality from sepsis, which contributed to shift the sepsis ICU population toward a population suffering from chronic critical illness (CCI). Indeed, a subset of ICU patients surviving sepsis develop CCI characterized by long-lasting immunosuppression associated with a persistent, low-grade, inflammation maintained by the continuing release of DAMPs. The underlying inflammation is associated with catabolism and malnutrition. The term persistent inflammation-immunosuppression and catabolism syndrome (PICS) has been proposed to characterize this degraded state. PICS is associated with long-term morbidity, late multiple organ failures and late mortality (9–11).

Clinical trials testing adjunctive therapy to dampen inflammation-related dysfunctions in sepsis have not been conclusive (12). Several reasons may account for these failures, among them the large heterogeneity of the sepsis syndrome. Nowadays, the prevalent view is that restoration of immune capacities using immuno-stimulants might be more efficient than anti-inflammatory therapies. In any case, personalized medicine should be used to define at an individual level whether inflammatory cytokines, immunoparalysis, or metabolism has to be targeted (4, 7, 13–17). In that perspective, significant efforts are devoted to the identification of genetic, molecular, and cellular biomarkers to stratify patients for clinical studies and treatment based on clinical condition and disease stage.

We poorly understand what is responsible for a dysregulated host response and the delay returning to homeostasis in sepsis patients (4–8, 18). Growing interest focuses on a subpopulation of leukocytes called myeloid-derived suppressor cells (MDSCs). MDSCs are involved in the regulation of the immune response in many pathological situations, the best-studied being cancer. A number of comprehensive reviews discusses MDSCs in the context of cancer, autoimmunity and infectious diseases [see for example (19–26)]. Interestingly, recent data suggest that MDSCs are involved in immune dysfunctions observed in sepsis. In this review, we summarize and discuss our current knowledge about the role played by MDSCs during sepsis and the potential of using MDSCs as biomarkers and therapeutic targets of sepsis.

MYELOID-DERIVED SUPPRESSOR CELLS (MDSCs)

MDSCs are immature myeloid cells that expand during chronic and acute inflammatory conditions. The premises of MDSC discovery date back more than a century when tumor progression was associated with extra-medullary haematopoiesis and neutrophilia. In the mid-1960s, Lappat and Cawein reported that subcutaneously transplanted A-280 tumor cells generate factors involved in a leucocytosis response that sustains tumor growth (27). Subsequently, leucocytosis was involved in the expansion of cells of myeloid origin with immunosuppressive activity (24). These cells express reduced levels of conventional markers for mature myeloid and lymphoid cells and were named natural suppressor cells, null cells, immature myeloid cells, or myeloid suppressor cells. In 2007, "myeloid-derived suppressor cells" was adopted as a unifying term to minimize the confusion prevailing in the literature (28).

MDSCs are defined primarily by their immunosuppressive functions. Within sepsis, one may predict that MDSCs play a dual role depending on disease progression. On the one hand, MDSCs may be beneficial by limiting hyper-inflammation during the early stages of sepsis, hence protecting from early organ dysfunction. On the other hand, MDSCs may be detrimental by amplifying long-term immunosuppression and contributing to CCI and/or PICS (8, 10). As discussed later, these two facets have been highlighted in experimental models, while clinical studies all pointed to a deleterious role of MDSCs.

Minimal phenotypic characteristics of MDSCs have been proposed, but a definite, consensual phenotyping scheme is lacking (29, 30). Two main subpopulations of MDSCs are usually considered: polymorphonuclear MDSCs (PMN-MDSCs, previously called granulocytic-MDSCs) and monocytic MDSCs (M-MDSCs), so-called because of their morphological and phenotypical homologies with PMNs and monocytes (26, 29–32). In mice, MSDCs are defined as $Gr1^+$ $CD11b^+$ cells (Gr1: granulocyte receptor-1 antigen, consisting of Ly-6G and Ly-6C antigens). PMN-MDSCs are $CD11b^+$ $Ly6G^+$ $Ly6C^{low}$ cells and M-MDSCs $CD11b^+$ $Ly6G^-$ $Ly6C^{high}$ cells. In humans, PMN-MDSCs are $CD11b^+$ $CD14^-$ $CD33^+$ ($CD15^+$ or $CD66^+$) cells and M-MDSCs $CD11b^+$ $CD14^+$ $HLA\text{-}DR^{low/-}$ $CD15^-$ cells. PMN-MDSCs overlap phenotypically with mature neutrophils but contrary to PMNs, MDSCs sediment within the PBMC fraction in ficoll gradients after density separation of whole blood. Whether low density gradient (LDGs) PMNs and PMN-MDSCs are the same entity is unclear, albeit the terms is used interchangeably in the literature. The identification of PMN-MDSCs by density gradient is further limited by the rise of not only low-density neutrophils, but also high-density $CD62L^{dim}$ neutrophils that suppress T cells in the blood of healthy humans infused with endotoxin (33). Additional markers are proposed to differentiate MDSCs from monocytes or granulocytes, for example high expression of lectin-type oxidized LDL receptor-1 (LOX-1) by PMN-MDSCs when compared to granulocytes in whole blood (33, 34).

Complicating the picture, other MDSC subsets have been described, among others early-stage MDSCs (e-MDSCs) and eosinophilic MDSCs (eo-MDSCs) (29, 35). In addition, tumor-associated macrophages (TAMs), which unlike their name suggests are present in inflammatory conditions bedsides cancer, can be considered as one of the members making up the MDSC spectrum (36, 37). Finally, MDSCs are highly plastic. They can differentiate into osteoclasts and non-suppressive mature myeloid cells, and M-MDSCs can differentiate into TAMs and PMN-MDSCs (38–41). Overall, to this day, identifying MDSCs based on cell surface phenotyping usually ends up with a mixed population, eventually containing other myeloid cell types, that

does not take into account the hallmark immunosuppressive function of MDSCs.

Adding to the above caveats, improper cell separation through density gradient and freezing whole blood or PBMC samples before flow cytometry analyses affects the detection of MDSCs, especially PMN-MDSCs. Hence, an objective of future studies is to optimize and harmonize sample handling and flow cytometry strategies (labeling, gating, and analyses) to quantify MDSCs in whole blood. This will facilitate the comparison of results from different studies to determine whether MDSCs are reliable disease biomarkers (32, 42). Strategies to identify cell surface markers discriminating MDSCs from other leukocytes using unbiased high discriminating techniques like RNA sequencing and mass cytometry analyses are starting to be used and have not yet improved the immuno-phenotyping of MDSCs (43). To summarize, the analysis of MDSCs and comparing results from different studies is complicated mainly because of: (1) the functional definition of MDSCs, (2) the lack of a defined phenotype(s) of MDSCs, and (3) the plasticity of MDSCs.

MDSCs EXPANSION AND ACTIVATION

Hematopoietic stem cells differentiate into common myeloid progenitors giving rise to immature myeloid cells. An inflammatory environment, as observed in sepsis, stimulates the egress of immature myeloid cells from the bone marrow into the blood stream and the gain immunosuppressive functions (26, 44) (**Figure 1**). The identification of mediators and molecular mechanisms underlying the expansion and the immunosuppressive functions of MDSCs may pinpoint to original therapeutic targets for various diseases. Most of our knowledge comes from disease conditions other than sepsis. In sepsis, most relevant studies analyse the impact of gene specific knockout or the infusion of MDSCs in mice exposed to polymicrobial sepsis induced by cecal ligation and puncture (CLP).

In mice subjected to CLP, MDSCs accumulate in secondary lymphoid organs, in which they represent as much as 10–20% of all leukocytes (45). In the spleen, MDSCs expand within 3–5 days, culminate after 10–14 days and stay high for at least 12 weeks. The rise of MDSCs appears to be a complex and progressive process that involves expansion and activation of immature myeloid cells through many factors. These factors are not specific to sepsis and can be redundant. The expansion of immature myeloid cells is primarily mediated by the action of growth factors (GF) and colony stimulating factors (CSF) [such as vascular endothelial-GF (VEGF), granulocyte-macrophage-CSF, macrophage-CSF (M-CSF) and stem cell factor (SCF)], DAMPs (S100 calcium-binding protein A8/A9, S100A8/9), and possibly chemokines (CXCL1, CXCL2). Activation of pathogenic MDSCs is induced by MAMPs (LPS, staphylococcal enterotoxins), DAMPs (HMGB1), cytokines (IFNγ, IL-1β, IL-4, IL-6, IL-7, IL-10, IL-13, TNF, CXCL3), and acute phase proteins (α2-macroglobulin, serum amyloid A) (26, 42, 46–56). These same factors may induce the maturation of MDSCs, with possible different outcomes. For example, M-MDSCs exposed to R848 (a TLR7/8 agonist), TNF and IFNγ differentiate into inflammatory macrophages that produce TNF and IL-12, while M-MDSCs exposed to Pam_3CSK_4 (a TLR1/2 agonist) differentiate into immunosuppressive macrophages producing IL-10 (47, 57).

Myeloid differentiation primary response 88 (MyD88), glycoprotein 130 (gp130) and nuclear factor I A (NFIA, a transcription factor) control the expansion and the immunosuppressive functions of MDSCs (**Figure 1**). MyD88 is an adaptor molecule that initiates quick nuclear factor-κB (NF-κB) signaling through the IL-1 receptor and all TLRs except TLR3. gp130 is a signal transducer co-receptor for IL-6 family cytokines that cooperates with signal transducer and activator of transcription (STAT3) and C/EBPβ to upregulate MDSCs (45, 54). MDSCs do not expand in $MyD88^{-/-}$ germline mice and in hepatocyte-specific $gp130^{-/-}$ and myeloid-specific $Nfia^{-/-}$ mice subjected to CLP (25, 45, 49, 58, 59). Additionally, $Gr1^{+}$ $CD11b^{+}$ MDSCs lacking NFI-A lose their immunosuppressive functions and stop differentiating into mature myeloid cells. The expansion of MDSCs is normal in myeloid-specific $Cebpb^{-/-}$ septic mice, but $Cebpb^{-/-}$ MDSCs produce reduced levels of IL-10 (52, 60). During CLP, triggering of a NF-κB/C/EBPβ/STAT3 axis upregulates the expression of S100A9 (also known as calgranulin B). S100A9 translocates into the nucleus to upregulate the transcription of microRNAs miR-21 and miR-181b that fine tune the expansion and the functions of MDSCs. Mice lacking S100A9 have less splenic and bone marrow MDSCs especially during late sepsis and are protected from death (61, 62). *In vivo* blockade of miR-21 and miR-181 decreases bone marrow MDSCs and improves sepsis survival (63). Recent work suggest that Nfe2l2 (nuclear factor, erythroid derived 2, Like 2; also known as NRF2) contributes to increase the metabolic activity and the expansion of $Gr1^{+}$ $CD11b^{+}$ MDSCs during endotoxemia (64).

The molecules mentioned above are not specific to MDSCs, and their genetic ablation can influence other arms of the defenses systems. To bypass this limitation, MDSCs isolated from sepsis mice are infused into wild-type recipient mice subjected to microbial insults. The adoptive transfer of Gr-1^{+} $CD11b^{+}$ MDSCs or PMN-MDSCs harvested from septic donor-mice into recipient mice protects the later from acute endotoxemia, rapidly lethal CLP and *Pseudomonas* airway infection (54, 60, 65–68). Two studies compare the benefits provided by the infusion of Gr-1^{+} $CD11b^{+}$ MDSCs taken either quickly or late after the onset of infection (i.e., 3 vs. 10–12 days post-infection). Interestingly, the transfer of early MDSCs increases while the transfer of late MDSCs decreases or does not change mortality (65, 69). Supported by additional *in vivo* and *in vitro* data (65, 69), this can be explained by the fact that, during the course of sepsis, MDSCs evolve to a more immature and anti-inflammatory state. More work will be required to appraise how much the maturation stage of MDSCs, the timing of expansion and/or infusion of MDSCs and the severity of the infectious models tip the balance toward a beneficial or a detrimental impact of MDSCs on sepsis outcome.

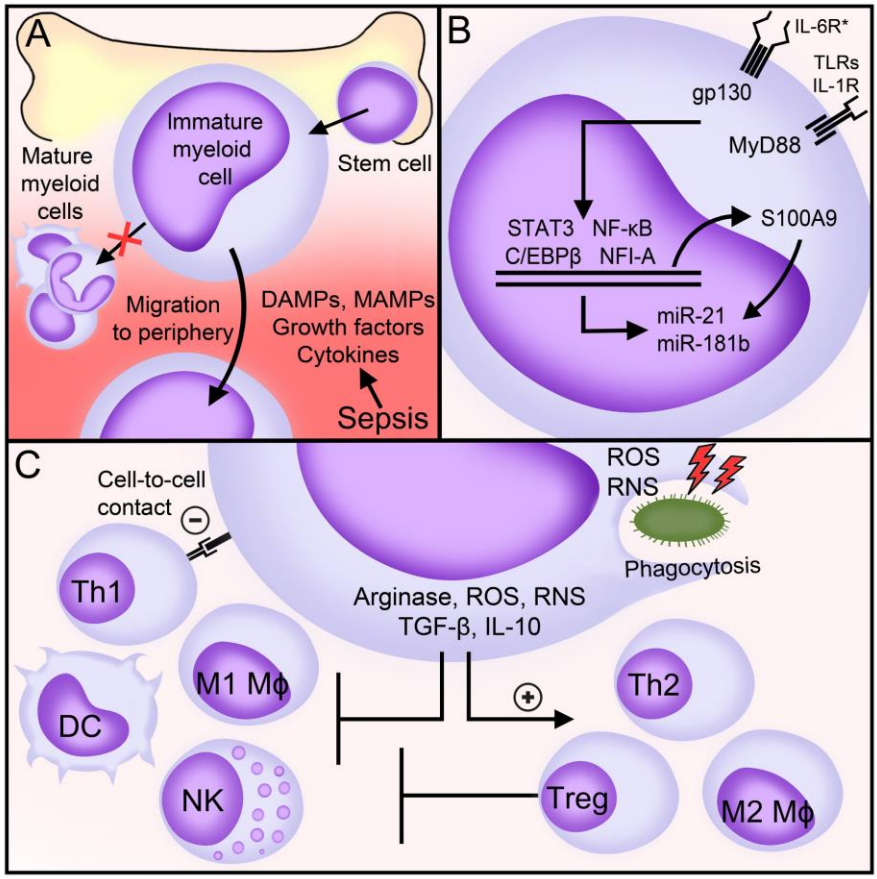

FIGURE 1 | MDSCs in sepsis. **(A)** Factors generated during sepsis induce the expansion and egress of MDSCs from the bone marrow into the peripheral blood. **(B)** Main signaling pathways involved in the expansion and the immunosuppressive functions of MDSCs during sepsis. **(C)** Biological functions of MDSCs during sepsis. See body text for detailed explanations. DAMPs, danger-associated molecular patterns; MAMPs, microbial-associated molecular patterns; IL-6R*, interleukin (IL)-6 receptor family of cytokines (commonly referred to as gp130 cytokines); gp130, glycoprotein 130; TLRs, toll-like receptors; IL-1R, interleukin-1 receptor; MyD88, Myeloid differentiation primary response 88; NF-κB, nuclear factor-κB; NFI-A, nuclear factor I A; STAT, signal transducer and activator of transcription; miR, microRNA; Mφ, macrophage; DC, dendritic cell; Th, T helper; NK, natural killer; Treg, T regulatory; IFNγ, interferon γ; ROS, reactive oxygen species; RNS, reactive nitrogen species; TGF-β, transforming growth factor-β; IL-10, interleukin-10.

As we will see in the last paragraph, the picture is clearer in clinical settings where high proportions of MDSCs indicate a poor prognosis.

The main epigenetic mechanisms, i.e., DNA methylation, histones methylation and acetylation, miRNAs and long non-coding RNAs (LncRNAs), have been implicated in the development of MDSCs with different outcomes (70). For example, inhibition of the DNA methyltransferases (DNMTs) 3a and 3b promotes the suppressive functions of MDSCs while inhibition of the histone methyltransferase SETD1B limits their suppressive function (71, 72). Pan-inhibitors of histone deacetylases (HDACs) 1–11 elicit robust expansion of M-MDSCs (73), in agreement with the observation that HDAC11 itself acts as a negative regulator of expansion and function of MDSCs (74). Interestingly, HDAC2 drives the phenotypic differentiation of M-MDSCs into PMN-MDSCs in tumor bearing mice (75), suggesting that individual HDACs have discrete, specific impact on MDSCs. Remarkably, combination therapies of inhibitors of either DNMTs or HDACs and checkpoint inhibitors (anti-PD-1 or anti-CTLA-4 antibodies) allow the eradication of checkpoint inhibitor resistant metastatic cancers by suppression of MDSCs (76). Finally, miRNAs both positively and negatively regulate the accumulation and functions of MDSCs (for instance miR-9, 17-5p, 21, 34a, 155, 181b, 210, 494, 690 vs. miR-9, 146a, 147a, 185-5p, 223, 185, 424) (70, 77). These observations, obtained in cancer models, are particularly interesting because cancer and sepsis share certain epigenetic features. Therefore, it is no surprise that oncolytic epigenetic drugs have a strong impact on innate immune responses and sepsis development (78–81). Numerous epigenetic drugs are tested in oncologic clinical trials while some are already approved for clinical applications. Altogether, these observations open a fascinating area to test epigenetic drugs targeting the expansion and/or function of MDSCs during sepsis.

IMMUNOSUPPRESSIVE FUNCTIONS OF MDSCs

MDSCs suppress the activity of immune cells through various mechanisms involving the degradation of L-arginine, the production of reactive oxygen and reactive nitrogen species (ROS, RNS), the secretion of anti-inflammatory/immunosuppressive cytokines like IL-10 and transforming growth factor (TGF)-β and the activation of T regulatory cells (Tregs) (**Figure 1**).

L-arginine becomes a semi-essential amino acid during sepsis because of increased usage and reduced production. L-arginine shortage is sustained by the production by MDSCs of arginase that metabolizes L-arginine into L-ornithine and urea (82). L-arginine depletion affects the function of T cells through a decreased expression of the CD3 zeta-chain, which is essential for T-cell receptor (TCR) signaling (50, 83). A lack of arginase also limits the activity of natural killer (NK) cells (84). ROS, RNS, IL-10, and TGF-β skew the polarization of monocytes/macrophages and T cells toward anti-inflammatory/pro-resolving M2, Th2 and regulatory phenotypes (45, 65, 85) and impair TCR and IL-2 receptor signaling, NK cell activity and DC maturation and antigen presentation (86–89) (**Figure 1**). MDSCs suppress Th1 responses though direct cell-to-cell contact, but how precisely this occurs remains to be determined (45, 85). Together with CCL5/RANTES and CCL4/MIP-1β, RNS, IL-10, and TGF-β promote the recruitment and the immunosuppressive activity of Tregs, at least in cancer and in neonates (45, 85, 90, 91). The interaction between MDSCs and Tregs in sepsis is unknown.

Splenic MDSCs harvested from CLP mice early (3–5 days) and late (10 days) after sepsis onset inhibit T cell proliferation. Early MDSCs secrete less S100A9 than late MDSCs (61) and, in response to LPS and IL-6, less TNF, IL-6, IL-10, ROS, and arginase I (65). However, in response to GM-CSF, early MDSCs produce RNS and proinflammatory cytokines while late MDSCs produce arginase, IL-10 and TGF-β (69). Of note, MDSCs can also help fight infections. Indeed, MDSCs efficiently phagocytose *E. coli* and group B streptococci (92) and clear bacteria during late sepsis through a robust production of ROS (65). Thus, MDSCs have diverse biological outputs according to their surrounding milieu and sepsis progression (54, 65). More work is required to fully understand to which extend these biological variations reflect the accumulation or the differentiation of different MDSCs subpopulations during sepsis.

DIAGNOSTIC AND PROGNOSTIC VALUES OF IMMATURE GRANULOCYTES AND MDSCs IN HUMAN SEPSIS

MDSCs make up an important proportion of immature myeloid cells. Thus, we will discuss reports analyzing immature granulocytes (IG) in adult sepsis and then move forward to studies that used more elaborated immuno-phenotyping strategies to identify MDSCs. **Table 1** provides details about the design and the main observations of these studies.

Accumulation of immature myeloid cells is one of the criteria established more than 25 years ago to characterize SIRS (systemic inflammatory response syndrome) and sepsis (107). The assessment of immature cells remained laborious up to the advent of automated cell counters. In an earliest study using automated IG counting on a small number of patients, the percentage of IG was higher in infected than in uninfected patients and was proposed to be a predictor of sepsis (93). Retrospective and prospective observational studies confirmed that IG proportion discriminates between infected and uninfected patients and is associated with disease severity (94–99) (**Table 1**). Automated cell counters can determine a delta neutrophil index (DNI), which reflects the number of immature neutrophils in the blood. A meta-analysis of ten Korean and one Egyptian studies including 1,822 sepsis patients suggests that an elevated DNI (i.e., an increased proportion of immature granulocytes) is associated with mortality (100).

Few reports demonstrate the immunosuppressive functions of immature myeloid cells in relation with sepsis and/or monitor MDSCs subpopulations using advanced flow cytometry. Since cell preparation (whole blood, with and without ficoll purification) and flow cytometry strategies are not standardized, the phenotype of MDSCs, PMN-MDSCs and M-MDSCs differs between studies (**Table 1**).

Gradient density interphase neutrophils arise during sepsis and their proportion correlates with disease severity in ICU patients. Cells isolated from septic shock patients deplete arginine and impair T cell functions *in vitro*, suggesting that they represent PMN-MDSCs (50). High levels of circulating $CD10^{dim}$ $CD16^{dim}$ IG are predictive of clinical deterioration and mortality (101, 102). This population contains a subset of $CD14^{-}$ $CD24^{+}$ myeloid suppressor cells that kill activated T cells *in vitro* (101).

The frequency of PMN-MDSCs (SSC^{high} $CD16^{+}$ $CD15^{+}$ $CD33^{+}$ $CD66b^{high}$ $CD114^{+}$ $CD11b^{+/low}$ LDG) and M-MDSCs (SSC^{low} $CD14^{+}$ $CD11b^{+}$ $CD16^{-}$ $CD15^{+}$) does not differ between non-infectious critical ill patients and sepsis patients (103). However, high levels of MDSCs are linked to nosocomial infections (**Table 1**). In a first study, PMN-MDSCs ($CD14^{-}$ $CD15^{+}$ low-density granulocytes, LDG) representing more than 36% of WBC in ICU patients sampled within 3 days of study inclusion predicts the subsequent occurrence of nosocomial infections (104). Patients that develop nosocomial infections have 2.5 times more PMN-MDSCs than patients that do not. In a second study, a close follow-up of ICU surgical patients (at days 1, 4, 7, 14, 21, and 28 or until discharge of ICU) reveals that patients with continuously high proportions of $CD33^{+}$ $CD11b^{+}$ HLA-$DR^{-/low}$ MDSCs have a longer stay in the ICU, more nosocomial infections and poor functional status at discharge (105). The percentage of total MDSCs in patients with severe sepsis/septic shock raises up to 45% of WBC, and a high proportion of MDSCs at diagnosis is associated with early mortality. Comparing cell-sorted enriched $CD33^{+}$ $CD11b^{+}$ HLA-$DR^{-/low}$ MDSCs from the blood of healthy subjects and septic patients reveals that pathogenic MDSCs dose dependently suppress IFNγ, IL-4, and IL-10 production by T cells more efficiently than MDSCs from

TABLE 1 | Studies investigating immature granulocytes and MDSCs in adults with sepsis.

Subjects	Cells/phenotypes	Observations	References
142 ED patients, 29 uninfected outpatients.	IG (automate-based determination)	Higher % in infected patients, predictor of sepsis.	(93)
70 consecutive ICU patients (51 infected, 19 uninfected).	IG (automate-based determination)	Higher % in infected patients, unrelated to day-21 and in-hospital mortality.	(94)
184 sepsis patients.	IG (automate-based determination)	Increase % associated with severity, but not predictive of mortality.	(95)
136 consecutive ICU patients.	IG (morphology and staining)	Higher % in sepsis than in uninfected patients. Unrelated to mortality.	(96)
35 sepsis and 22 non-septic consecutive burn patients, 19 healthy controls.	IG (flow cytometry)	Increase % post-burn, associated with reduced neutrophil function. Remaining elevated levels (day 7–28) associated with sepsis development	(97)
781 sepsis patients, 20 control outpatients.	IG (flow cytometry)	High % at admission related to organ failure and day-7 and day-28 mortality.	(98)
47 uninfected and 17 infected cardiac surgery patients.	IG (flow cytometry)	Increase % postoperative. Highest levels associated with secondary infection complications.	(99)
Meta-analysis (11 studies) of 1'822 sepsis patients.	Delta neutrophil index (DNI, automate-based determination)	Elevated DNI associated with mortality.	(100)
24 sepsis ICU patients, 12 hospital controls.	Interphase neutrophils (flow cytometry)	Present only in sepsis patients, proportional to sepsis severity. Suppress T-cell activity *in vitro*.	(50)
177 sepsis patients.	IG (flow cytometry)	Increase % at 48 h predictive of clinical deterioration. High % of $CD10^{dim}$ and $CD16^{dim}$ IG correlates with mortality. Kill activated T cells *in vitro*.	(101)
43 septic shock patients, 23 healthy controls.	IG (flow cytometry)	Increased % of $CD10^{dim}$ and $CD16^{dim}$ IG at days 3–4 and 6–8. Patients with lower % have better survival.	(102)
14 sepsis and 8 uninfected critically ill patients, 15 healthy controls.	M-MDSCs: SSC^{low} $CD14^{+}$ $CD11b^{+}$ $CD16^{-}$ $CD15^{+}$ PMN-MDSCs: SSC^{high} $CD16^{+}$ $CD15^{+}$ $CD33^{+}$ $CD66b^{high}$ $CD114^{+}$ $CD11b^{+/low}$	M-MDSCs but not PMN-MDSCs increase at day 13-21 post-sepsis. Similar % of M-MDSCs and PMN-MDSCs in sepsis and non-septic critical ill patients.	(103)
94 sepsis, 11 severity-matched ICU patients, 67 health donors.	M-MDSCs: Lin^{-} $CD14^{+}$ $HLA\text{-}DR^{-/low}$ PMN-MDSCs: LDG $CD14^{-}$ $CD15^{+}$ (Excluding eosinophils)	High % of PMN-MDSCs in sepsis patients. M-MDSCs are higher in gram-negative than gram-positive sepsis. PMN-MDSCs > 36% WBC at entry are associated with higher risk of nosocomial infections. PMN- and M-MDSCs suppress T-cell proliferation *in vitro*.	(104)
67 surgical patients with severe sepsis/septic shock, 18 healthy controls.	MDSCs: $CD33^{+}$ $CD11b^{+}$ $HLA\text{-}DR^{-}$ M-MDSCs: $CD14^{+}$ PMN-MDSCs: $CD14^{-}$ $CD15^{+}$	High % of MDSCs at admission correlates with early mortality. Decreasing levels of MDSCs correlate with short ICU stay. Sustained levels of MDSCs (>30% of WBC) predict nosocomial infections.	(105)
56 sepsis patients and 18 healthy controls.	M-MDSCs: $CD14^{+}$ $CD64^{+}$ $HLA\text{-}DR^{-}$ PMN-MDSCs: LDG $CD33^{+}$ $CD14^{neg/low}$ $CD64^{low}$ $CD15^{+/low}$	High % of M-MDSCs in all sepsis, but particularly in gram-negative sepsis patients. Prominent PMN-MDSCs in gram-positive sepsis. PMN-MDSCs suppress T-cell proliferation *in vitro*.	(106)

ED, emergency department; ICU, intensive care unit; IG, immature granulocytes; LDG, low density granulocytes; Lin, lineage; WBC, white blood cells.

healthy subjects, while healthy and disease MDSCs suppress T cell proliferation alike (105).

The proportion of PMN-MDSCs and M-MDSCs, defined as $CD14^{neg/low}$ $CD64^{low}$ $CD15^{+/low}$ LDG and $CD14^{+}$ $CD64^{+}$ $HLA\text{-}DR^{neg}$ leukocytes, may vary according to causative agent leading to sepsis (**Table 1**). M-MDSCs increase in all sepsis patients, predominantly in gram-negative cases, while PMN-MDSCs increase prominently in gram-positive sepsis (106). A subsequent study confirmed that M-MDSCs (Lin^{-} $CD14^{pos}$ $HLA\text{-}DR^{low/neg}$) are enriched during gram-negative sepsis, but PMN-MDSCs ($CD14^{-}$ $CD15^{+}$ LDG) do not differ according to the gram of the causative bacteria (104). Larger studies are required to ascertain that the microbial origin of sepsis shapes the pattern of MDSCs (108). This is an important parameter since M-MDSCs are more potent immunosuppressive than PMN-MDSCs on a per cell basis (109).

CONCLUDING REMARKS

MDSCs play a dual role during infection and sepsis. MDSCs expanding along emergency erythropoiesis provide a first barrier against microbial invasion by producing high amounts of bactericidal molecules like ROS and RNS and counteract the hyperinflammatory response associated with early organ dysfunctions. However, MDSCs are also detrimental by supporting the establishment and/or the maintenance of a late

protracted immunosuppressive environment. In line with a deletary role of MDSCs, all clinical studies to date associate high proportions of blood MDSCs with clinical worsening, occurrence of nosocomial infections and mortality of sepsis patients. Hence, MDSCs are attractive biomarkers, especially since these cells are barely detectable in healthy subjects. One limitation of clinical studies, not limited to the sepsis field, resides in the uneven phenotypic classification of MDSCs. One important future objective is to harmonize sample handling and flow cytometry strategies. Besides being attractive biomarkers, MDSCs are attractive therapeutic targets for sepsis. Inhibiting MDSCs-mediated immunosuppression or MDSCs trafficking or depleting MDSCs themselves (by normalizing myelopoiesis or inducing the differentiation of MDSCs into mature myeloid cells) would positively influence patient outcome. Interestingly, more than 30 clinical trials are running targeting MDSCs directly or indirectly in cancer patients (22). If ever envisaged for sepsis, these therapies will need specific evaluation since targeting MDSCs aggressively may put critically ill patients at risk of agranulocytosis. The results arising from these oncological studies, added to those from current or future studies in the field of sepsis, will give invaluable information onto whether and how MDSCs might be used to implement sepsis personalized medicine and precision immunotherapy.

AUTHOR CONTRIBUTIONS

IS and TR conceived and structured the manuscript. IS drafted the manuscript and the figure. CT revised the manuscript. TR finalized and edited the manuscript.

ACKNOWLEDGMENT

TR is supported by grants from the Swiss National Science Foundation (SNSF, grant number 173123) and the European community (Horizon 2020 Marie Skłodowska-Curie Action-European Sepsis Academy-Innovative Training Network, MSCA-ESA-ITN, grant number 676129, supporting IS and CT).

REFERENCES

1. Singer M, Deutschman CS, Seymour CW, Shankar-Hari M, Annane D, Bauer M, et al. The third international consensus definitions for sepsis and septic shock (Sepsis-3). *JAMA*. (2016) 315:801–10. doi: 10.1001/jama.2016.0287
2. Gaieski DF, Edwards JM, Kallan MJ, Carr BG. Benchmarking the incidence and mortality of severe sepsis in the United States. *Crit Care Med*. (2013) 41:1167–74. doi: 10.1097/CCM.0b013e31827c09f8
3. Savva A, Roger T. Targeting toll-like receptors: promising therapeutic strategies for the management of sepsis-associated pathology and infectious diseases. *Front Immunol*. (2013) 4:387. doi: 10.3389/fimmu.2013.00387
4. Cecconi M, Evans L, Levy M, Rhodes A. Sepsis and septic shock. *Lancet*. (2018) 392:75–87. doi: 10.1016/S0140-6736(18)30696-2
5. Hotchkiss RS, Moldawer LL, Opal SM, Reinhart K, Turnbull IR, Vincent JL. Sepsis and septic shock. *Nat Rev Dis Primers*. (2016) 2:16045. doi: 10.1038/nrdp.2016.45
6. Hotchkiss RS, Monneret G, Payen D. Sepsis-induced immunosuppression: from cellular dysfunctions to immunotherapy. *Nat Rev Immunol*. (2013) 13:862–74. doi: 10.1038/nri3552
7. van der Poll T, van de Veerdonk FL, Scicluna BP, Netea MG. The immunopathology of sepsis and potential therapeutic targets. *Nat Rev Immunol*. (2017) 17:407–20. doi: 10.1038/nri.2017.36
8. Venet F, Monneret G. Advances in the understanding and treatment of sepsis-induced immunosuppression. *Nat Rev Nephrol*. (2018) 14:121–37. doi: 10.1038/nrneph.2017.165
9. Levy MM, Rhodes A, Phillips GS, Townsend SR, Schorr CA, Beale R, et al. Surviving Sepsis Campaign: association between performance metrics and outcomes in a 7.5-year study. *Crit Care Med*. (2015) 43:3–12. doi: 10.1097/CCM.0000000000000723
10. Mira JC, Gentile LF, Mathias BJ, Efron PA, Brakenridge SC, Mohr AM, et al. Sepsis pathophysiology, chronic critical illness, and persistent inflammation-immunosuppression and catabolism syndrome. *Crit Care Med*. (2017) 45:253–62. doi: 10.1097/CCM.0000000000002074
11. Nomellini V, Kaplan LJ, Sims CA, Caldwell CC. Chronic critical illness and persistent inflammation: what can we learn from the elderly, injured, septic, and malnourished? *Shock*. (2018) 49:4–14. doi: 10.1097/SHK.0000000000000939
12. Marshall JC. Why have clinical trials in sepsis failed? *Trends Mol Med*. (2014) 20:195–203. doi: 10.1016/j.molmed.2014.01.007
13. Peters van Ton AM, Kox M, Abdo WF, Pickkers P. Precision Immunotherapy for Sepsis. *Front Immunol*. (2018) 9:1926. doi: 10.3389/fimmu.2018.01926
14. Rello J, van Engelen TSR, Alp E, Calandra T, Cattoir V, Kern WV, et al. Towards precision medicine in sepsis: a position paper from the European Society of Clinical Microbiology and Infectious Diseases. *Clin Microbiol Infect*. (2018) 24:1264–72. doi: 10.1016/j.cmi.2018.03.011
15. Talisa VB, Yende S, Seymour CW, Angus DC. Arguing for adaptive clinical trials in sepsis. *Front Immunol*. (2018) 9:1502. doi: 10.3389/fimmu.2018.01502
16. van Engelen TSR, Wiersinga WJ, Scicluna BP, van der Poll T. Biomarkers in sepsis. *Crit Care Clin*. (2018) 34:139–52. doi: 10.1016/j.ccc.2017.08.010
17. Albert-Vega C, Tawfik DM, Trouillet-Assant S, Vachot L, Mallet F, Textoris J. Immune functional assays, from custom to standardized tests for precision medicine. *Front Immunol*. (2018) 9:2367. doi: 10.3389/fimmu.2018.02367
18. Otto GP, Sossdorf M, Claus RA, Rodel J, Menge K, Reinhart K, et al. The late phase of sepsis is characterized by an increased microbiological burden and death rate. *Crit Care*. (2011) 15:R183. doi: 10.1186/cc10332
19. Betsch A, Rutgeerts O, Fevery S, Sprangers B, Verhoef G, Dierickx D, et al. Myeloid-derived suppressor cells in lymphoma: the good, the bad and the ugly. *Blood Rev*. (2018) 32:490–8. doi: 10.1016/j.blre.2018.04.006
20. Dilek N, Vuillefroy de Silly R, Blancho G, Vanhove B. Myeloid-derived suppressor cells: mechanisms of action and recent advances in their role in transplant tolerance. *Front Immunol*. (2012) 3:208. doi: 10.3389/fimmu.2012.00208
21. Dorhoi A, Du Plessis N. Monocytic myeloid-derived suppressor cells in chronic infections. *Front Immunol*. (2017) 8:1895. doi: 10.3389/fimmu.2017.01895
22. Fleming V, Hu X, Weber R, Nagibin V, Groth C, Altevogt P, et al. Targeting myeloid-derived suppressor cells to bypass tumor-induced immunosuppression. *Front Immunol*. (2018) 9:398. doi: 10.3389/fimmu.2018.00398
23. Ray A, Chakraborty K, Ray P. Immunosuppressive MDSCs induced by TLR signaling during infection and role in resolution of inflammation. *Front Cell Infect Microbiol*. (2013) 3:52. doi: 10.3389/fcimb.2013.00052
24. Talmadge JE, Gabrilovich DI. History of myeloid-derived suppressor cells. *Nat Rev Cancer*. (2013) 13:739–52. doi: 10.1038/nrc3581
25. Umansky V, Blattner C, Gebhardt C, Utikal J. CCR5 in recruitment and activation of myeloid-derived suppressor cells in melanoma. *Cancer Immunol Immunother*. (2017) 66:1015–23. doi: 10.1007/s00262-017-1988-9
26. Veglia F, Perego M, Gabrilovich D. Myeloid-derived suppressor cells coming of age. *Nat Immunol*. (2018) 19:108–19. doi: 10.1038/s41590-017-0022-x
27. Lappat EJ, Cawein M. A study of the leukemoid response to transplantable a-280 tumor in mice. *Cancer Res*. (1964) 24:302–11.

28. Gabrilovich DI, Bronte V, Chen SH, Colombo MP, Ochoa A, Ostrand-Rosenberg S, et al. The terminology issue for myeloid-derived suppressor cells. *Cancer Res.* (2007) 67:425; author reply 426. doi: 10.1158/0008-5472.CAN-06-3037
29. Bronte V, Brandau S, Chen SH, Colombo MP, Frey AB, Greten TF, et al. Recommendations for myeloid-derived suppressor cell nomenclature and characterization standards. *Nat Commun.* (2016) 7:12150. doi: 10.1038/ncomms12150
30. Damuzzo V, Pinton L, Desantis G, Solito S, Marigo I, Bronte V, et al. Complexity and challenges in defining myeloid-derived suppressor cells. *Cytometry B Clin Cytom.* (2015) 88:77–91. doi: 10.1002/cytob.21206
31. Kotsakis A, Harasymczuk M, Schilling B, Georgoulias V, Argiris A, Whiteside TL. Myeloid-derived suppressor cell measurements in fresh and cryopreserved blood samples. *J Immunol Methods.* (2012) 381:14–22. doi: 10.1016/j.jim.2012.04.004
32. Mandruzzato S, Brandau S, Britten CM, Bronte V, Damuzzo V, Gouttefangeas C, et al. Toward harmonized phenotyping of human myeloid-derived suppressor cells by flow cytometry: results from an interim study. *Cancer Immunol Immunother.* (2016) 65:161–9. doi: 10.1007/s00262-015-1782-5
33. Pillay J, Kamp VM, van Hoffen E, Visser T, Tak T, Lammers JW, et al. A subset of neutrophils in human systemic inflammation inhibits T cell responses through Mac-1. *J Clin Invest.* (2012) 122:327–36. doi: 10.1172/JCI57990
34. Condamine T, Dominguez GA, Youn JI, Kossenkov AV, Mony S, Alicea-Torres K, et al. Lectin-type oxidized LDL receptor-1 distinguishes population of human polymorphonuclear myeloid-derived suppressor cells in cancer patients. *Sci Immunol.* (2016) 1:aaf8943. doi: 10.1126/sciimmunol.aaf8943
35. Goldmann O, Beineke A, Medina E. Identification of a novel subset of myeloid-derived suppressor cells during chronic staphylococcal infection that resembles immature eosinophils. *J Infect Dis.* (2017) 216:1444–51. doi: 10.1093/infdis/jix494
36. Youn JI, Nagaraj S, Collazo M, Gabrilovich DI. Subsets of myeloid-derived suppressor cells in tumor-bearing mice. *J Immunol.* (2008) 181:5791–802. doi: 10.4049/jimmunol.181.8.5791
37. Mota JM, Leite CA, Souza LE, Melo PH, Nascimento DC, de-Deus-Wagatsuma VM, et al. Post-sepsis state induces tumor-associated macrophage accumulation through CXCR4/CXCL12 and favors tumor progression in mice. *Cancer Immunol Res.* (2016) 4:312–22. doi: 10.1158/2326-6066.CIR-15-0170
38. Kumar V, Cheng P, Condamine T, Mony S, Languino LR, McCaffrey JC, et al. CD45 Phosphatase inhibits STAT3 transcription factor activity in myeloid cells and promotes tumor-associated macrophage differentiation. *Immunity.* (2016) 44:303–15. doi: 10.1016/j.immuni.2016.01.014
39. Zhang H, Huang Y, Wang S, Fu R, Guo C, Wang H, et al. Myeloid-derived suppressor cells contribute to bone erosion in collagen-induced arthritis by differentiating to osteoclasts. *J Autoimmun.* (2015) 65:82–9. doi: 10.1016/j.jaut.2015.08.010
40. Liechtenstein T, Perez-Janices N, Gato M, Caliendo F, Kochan G, Blanco-Luquin I, et al. A highly efficient tumor-infiltrating MDSC differentiation system for discovery of anti-neoplastic targets, which circumvents the need for tumor establishment in mice. *Oncotarget.* (2014) 5:7843–57. doi: 10.18632/oncotarget.2279
41. Steding CE, Wu ST, Zhang Y, Jeng MH, Elzey BD, Kao C. The role of interleukin-12 on modulating myeloid-derived suppressor cells, increasing overall survival and reducing metastasis. *Immunology.* (2011) 133:221–38. doi: 10.1111/j.1365-2567.2011.03429.x
42. Gabrilovich DI. Myeloid-derived suppressor cells. *Cancer Immunol Res.* (2017) 5:3–8. doi: 10.1158/2326-6066.CIR-16-0297
43. Roussel M, Ferrell PB Jr., Greenplate AR, Lhomme F, Le Gallou S, Diggins KE, et al. Mass cytometry deep phenotyping of human mononuclear phagocytes and myeloid-derived suppressor cells from human blood and bone marrow. *J Leukoc Biol.* (2017) 102:437–47. doi: 10.1189/jlb.5MA1116-457R
44. Ramnath RD, Bhatia M. Substance P treatment stimulates chemokine synthesis in pancreatic acinar cells via the activation of NF-kappaB. *Am J Physiol Gastrointest Liver Physiol.* (2006) 291:G1113–9. doi: 10.1152/ajpgi.00177.2006
45. Delano MJ, Scumpia PO, Weinstein JS, Coco D, Nagaraj S, Kelly-Scumpia KM, et al. MyD88-dependent expansion of an immature GR-1(+)CD11b(+). population induces T cell suppression and Th2 polarization in sepsis. *J Exp Med.* (2007) 204:1463–74. doi: 10.1084/jem.20062602
46. Bah I, Kumbhare A, Nguyen L, McCall CE, El Gazzar M. IL-10 induces an immune repressor pathway in sepsis by promoting S100A9 nuclear localization and MDSC development. *Cell Immunol.* (2018) 332:32–8. doi: 10.1016/j.cellimm.2018.07.003
47. Bayik D, Tross D, Klinman DM. Factors influencing the differentiation of human monocytic myeloid-derived suppressor cells into inflammatory macrophages. *Front Immunol.* (2018) 9:608. doi: 10.3389/fimmu.2018.00608
48. Cheng P, Corzo CA, Luetteke N, Yu B, Nagaraj S, Bui MM, et al. Inhibition of dendritic cell differentiation and accumulation of myeloid-derived suppressor cells in cancer is regulated by S100A9 protein. *J Exp Med.* (2008) 205:2235–49. doi: 10.1084/jem.20080132
49. Dai J, Kumbhare A, Williams DA, Youssef D, Yao ZQ, McCall CE, et al. Nfia deletion in myeloid cells blocks expansion of myeloid-derived suppressor cells during sepsis. *Innate Immun.* (2018) 24:54–65. doi: 10.1177/1753425917742956
50. Darcy CJ, Minigo G, Piera KA, Davis JS, McNeil YR, Chen Y, et al. Neutrophils with myeloid derived suppressor function deplete arginine and constrain T cell function in septic shock patients. *Crit Care* (2014) 18:R163. doi: 10.1186/cc14003
51. Kulkarni U, Herrmenau C, Win SJ, Bauer M, Kamradt T. IL-7 treatment augments and prolongs sepsis-induced expansion of IL-10-producing B lymphocytes and myeloid-derived suppressor cells. *PLoS ONE.* (2018) 13:e0192304. doi: 10.1371/journal.pone.0192304
52. McClure C, McPeak MB, Youssef D, Yao ZQ, McCall CE, El Gazzar M. Stat3 and C/EBPbeta synergize to induce miR-21 and miR-181b expression during sepsis. *Immunol Cell Biol.* (2017) 95:42–55. doi: 10.1038/icb.2016.63
53. Newson J, Motwani MP, Kendall AC, Nicolaou A, Muccioli GG, Alhouayek M, et al. Inflammatory resolution triggers a prolonged phase of immune suppression through COX-1/mPGES-1-derived prostaglandin E2. *Cell Rep.* (2017) 20:3162–75. doi: 10.1016/j.celrep.2017.08.098
54. Sander LE, Sackett SD, Dierssen U, Beraza N, Linke RP, Muller M, et al. Hepatic acute-phase proteins control innate immune responses during infection by promoting myeloid-derived suppressor cell function. *J Exp Med.* (2010) 207:1453–64. doi: 10.1084/jem.20091474
55. Stoll H, Ost M, Singh A, Mehling R, Neri D, Schafer I, et al. Staphylococcal enterotoxins dose-dependently modulate the generation of myeloid-derived suppressor cells. *Front Cell Infect Microbiol.* (2018) 8:321. doi: 10.3389/fcimb.2018.00321
56. Rieber N, Singh A, Oz H, Carevic M, Bouzani M, Amich J, et al. Pathogenic fungi regulate immunity by inducing neutrophilic myeloid-derived suppressor cells. *Cell Host Microbe.* (2015) 17:507–14. doi: 10.1016/j.chom.2015.02.007
57. Wang J, Shirota Y, Bayik D, Shirota H, Tross D, Gulley JL, et al. Effect of TLR agonists on the differentiation and function of human monocytic myeloid-derived suppressor cells. *J Immunol.* (2015) 194:4215–21. doi: 10.4049/jimmunol.1402004
58. McClure C, Ali E, Youssef D, Yao ZQ, McCall CE, El Gazzar M. NFI-A disrupts myeloid cell differentiation and maturation in septic mice. *J Leukoc Biol.* (2016) 99:201–11. doi: 10.1189/jlb.4A0415-171RR
59. McPeak MB, Youssef D, Williams DA, Pritchett C, Yao ZQ, McCall CE, et al. Myeloid cell-specific knockout of NFI-A improves sepsis survival. *Infect Immun.* (2017) 85:17. doi: 10.1128/IAI.00066-17
60. McPeak MB, Youssef D, Williams DA, Pritchett CL, Yao ZQ, McCall CE, et al. Frontline science: myeloid cell-specific deletion of Cebpb decreases sepsis-induced immunosuppression in mice. *J Leukoc Biol.* (2017) 102:191–200. doi: 10.1189/jlb.4HI1216-537R
61. Dai J, Kumbhare A, Youssef D, McCall CE, El Gazzar M. Intracellular S100A9 promotes myeloid-derived suppressor cells during late sepsis. *Front Immunol.* (2017) 8:1565. doi: 10.3389/fimmu.2017.01565
62. El Gazzar M. Immunobiology of S100A8 and S100A9 proteins and their role in acute inflammation and sepsis. *Int J Immunol Immunother.* (2015) 2:2378–3672.
63. McClure C, Brudecki L, Ferguson DA, Yao ZQ, Moorman JP, McCall CE, et al. MicroRNA 21 (miR-21). and miR-181b couple with NFI-A to generate

myeloid-derived suppressor cells and promote immunosuppression in late sepsis. *Infect Immun.* (2014) 82:3816–25. doi: 10.1128/IAI.01495-14

64. Ohl K, Fragoulis A, Klemm P, Baumeister J, Klock W, Verjans E, et al. Nrf2 Is a central regulator of metabolic reprogramming of myeloid-derived suppressor cells in steady state and sepsis. *Front Immunol.* (2018) 9:1552. doi: 10.3389/fimmu.2018.01552
65. Derive M, Bouazza Y, Alauzet C, Gibot S. Myeloid-derived suppressor cells control microbial sepsis. *Intensive Care Med.* (2012) 38:1040–9. doi: 10.1007/s00134-012-2574-4
66. Chang S, Kim YH, Kim YJ, Kim YW, Moon S, Lee YY, et al. Taurodeoxycholate increases the number of myeloid-derived suppressor cells that ameliorate sepsis in mice. *Front Immunol.* (2018) 9:1984. doi: 10.3389/fimmu.2018.01984
67. Namkoong H, Ishii M, Fujii H, Yagi K, Asami T, Asakura T, et al. Clarithromycin expands CD11b+Gr-1+ cells via the STAT3/Bv8 axis to ameliorate lethal endotoxic shock and post-influenza bacterial pneumonia. *PLoS Pathog.* (2018) 14:e1006955. doi: 10.1371/journal.ppat.1006955
68. Oz HH, Zhou B, Voss P, Carevic M, Schroth C, Frey N, et al. *Pseudomonas aeruginosa* airway infection recruits and modulates neutrophilic myeloid-derived suppressor cells. *Front Cell Infect Microbiol.* (2016) 6:167. doi: 10.3389/fcimb.2016.00167
69. Brudecki L, Ferguson DA, McCall CE, El Gazzar M. Myeloid-derived suppressor cells evolve during sepsis and can enhance or attenuate the systemic inflammatory response. *Infect Immun.* (2012) 80:2026–34. doi: 10.1128/IAI.00239-12
70. Zhang C, Wang S, Liu Y, Yang C. Epigenetics in myeloid derived suppressor cells: a sheathed sword towards cancer. *Oncotarget.* (2016) 7:57452–63. doi: 10.18632/oncotarget.10767
71. Sido JM, Yang X, Nagarkatti PS, Nagarkatti M. Delta9-Tetrahydrocannabinol-mediated epigenetic modifications elicit myeloid-derived suppressor cell activation via STAT3/S100A8. *J Leukoc Biol.* (2015) 97:677–88. doi: 10.1189/jlb.1A1014-479R
72. Xin J, Zhang Z, Su X, Wang L, Zhang Y, Yang R. Epigenetic component p66a modulates myeloid-derived suppressor cells by modifying STAT3. *J Immunol.* (2017) 198:2712–20. doi: 10.4049/jimmunol.1601712
73. Rosborough BR, Castellaneta A, Natarajan S, Thomson AW, Turnquist HR. Histone deacetylase inhibition facilitates GM-CSF-mediated expansion of myeloid-derived suppressor cells *in vitro* and *in vivo*. *J Leukoc Biol.* (2012) 91:701–9. doi: 10.1189/jlb.0311119
74. Sahakian E, Powers JJ, Chen J, Deng SL, Cheng F, Distler A, et al. Histone deacetylase 11: a novel epigenetic regulator of myeloid derived suppressor cell expansion and function. *Mol Immunol.* (2015) 63:579–85. doi: 10.1016/j.molimm.2014.08.002
75. Youn JI, Kumar V, Collazo M, Nefedova Y, Condamine T, Cheng P, et al. Epigenetic silencing of retinoblastoma gene regulates pathologic differentiation of myeloid cells in cancer. *Nat Immunol.* (2013) 14:211–20. doi: 10.1038/ni.2526
76. Kim K, Skora AD, Li Z, Liu Q, Tam AJ, Blosser RL, et al. Eradication of metastatic mouse cancers resistant to immune checkpoint blockade by suppression of myeloid-derived cells. *Proc Natl Acad Sci USA.* (2014) 111:11774–9. doi: 10.1073/pnas.1410626111
77. Liu M, Zhou J, Chen Z, Cheng AS. Understanding the epigenetic regulation of tumours and their microenvironments: opportunities and problems for epigenetic therapy. *J Pathol.* (2017) 241:10–24. doi: 10.1002/path.4832
78. Ciarlo E, Savva A, Roger T. Epigenetics in sepsis: targeting histone deacetylases. *Int J Antimicrob Agents.* (2013) 42(Suppl.):S8–12. doi: 10.1016/j.ijantimicag.2013.04.004
79. Roger T, Lugrin J, Le Roy D, Goy G, Mombelli M, Koessler T, et al. Histone deacetylase inhibitors impair innate immune responses to Toll-like receptor agonists and to infection. *Blood* (2011) 117:1205–17. doi: 10.1182/blood-2010-05-284711
80. Mombelli M, Lugrin J, Rubino I, Chanson AL, Giddey M, Calandra T, et al. Histone deacetylase inhibitors impair antibacterial defenses of macrophages. *J Infect Dis.* (2011) 204:1367–74. doi: 10.1093/infdis/jir553
81. Lugrin J, Ciarlo E, Santos A, Grandmaison G, dos Santos I, Le Roy D, et al. The sirtuin inhibitor cambinol impairs MAPK signaling, inhibits inflammatory and innate immune responses and protects from septic shock. *Biochim Biophys Acta.* (2013) 1833:1498–510. doi: 10.1016/j.bbamcr.2013.03.004
82. Wijnands KA, Meesters DM, van Barneveld KW, Visschers RG, Briede JJ, Vandendriessche B, et al. Citrulline supplementation improves organ perfusion and arginine availability under conditions with enhanced arginase activity. *Nutrients.* (2015) 7:5217–38. doi: 10.3390/nu7075217
83. Bronte V, Zanovello P. Regulation of immune responses by L-arginine metabolism. *Nat Rev Immunol.* (2005) 5:641–54. doi: 10.1038/nri1668
84. Goh CC, Roggerson KM, Lee HC, Golden-Mason L, Rosen HR, Hahn YS. Hepatitis C virus-induced myeloid-derived suppressor cells suppress NK Cell IFN-gamma production by altering cellular metabolism via arginase-1. *J Immunol.* (2016) 196:2283–92. doi: 10.4049/jimmunol.1501881
85. Kostlin N, Vogelmann M, Spring B, Schwarz J, Feucht J, Hartel C, et al. Granulocytic myeloid-derived suppressor cells from human cord blood modulate T-helper cell response towards an anti-inflammatory phenotype. *Immunology.* (2017) 152:89–101. doi: 10.1111/imm.12751
86. Gabrilovich DI, Ostrand-Rosenberg S, Bronte V. Coordinated regulation of myeloid cells by tumours. *Nat Rev Immunol.* (2012) 12:253–68. doi: 10.1038/nri3175
87. Zhu J, Huang X, Yang Y. Myeloid-derived suppressor cells regulate natural killer cell response to adenovirus-mediated gene transfer. *J Virol.* (2012) 86:13689–96. doi: 10.1128/JVI.01595-12
88. Greifenberg V, Ribechini E, Rossner S, Lutz MB. Myeloid-derived suppressor cell activation by combined LPS and IFN-gamma treatment impairs DC development. *Eur J Immunol.* (2009) 39:2865–76. doi: 10.1002/eji.200939486
89. Hu CE, Gan J, Zhang RD, Cheng YR, Huang GJ. Up-regulated myeloid-derived suppressor cell contributes to hepatocellular carcinoma development by impairing dendritic cell function. *Scand J Gastroenterol.* (2011) 46:156–64. doi: 10.3109/00365521.2010.516450
90. Hatziioannou A, Alissafi T, Verginis P. Myeloid-derived suppressor cells and T regulatory cells in tumors: unraveling the dark side of the force. *J Leukoc Biol.* (2017) 102:407–21. doi: 10.1189/jlb.5VMR1116-493R
91. Lindau D, Gielen P, Kroesen M, Wesseling P, Adema GJ. The immunosuppressive tumour network: myeloid-derived suppressor cells, regulatory T cells and natural killer T cells. *Immunology.* (2013) 138:105–15. doi: 10.1111/imm.12036
92. Leiber A, Schwarz J, Kostlin N, Spring B, Fehrenbach B, Katava N, et al. Neonatal myeloid derived suppressor cells show reduced apoptosis and immunosuppressive activity upon infection with Escherichia coli. *Eur J Immunol.* (2017) 47:1009–21. doi: 10.1002/eji.201646621
93. Ansari-Lari MA, Kickler TS, Borowitz MJ. Immature granulocyte measurement using the Sysmex XE-2100. Relationship to infection and sepsis. *Am J Clin Pathol.* (2003) 120:795–9. doi: 10.1309/LT30-BV9U-JJV9-CFHQ
94. Nierhaus A, Klatte S, Linssen J, Eismann NM, Wichmann D, Hedke J, et al. Revisiting the white blood cell count: immature granulocytes count as a diagnostic marker to discriminate between SIRS and sepsis–a prospective, observational study. *BMC Immunol.* (2013) 14:8. doi: 10.1186/1471-2172-14-8
95. Ha SO, Park SH, Park SH, Park JS, Huh JW, Lim CM, et al. Fraction of immature granulocytes reflects severity but not mortality in sepsis. *Scand J Clin Lab Invest.* (2015) 75:36–43. doi: 10.3109/00365513.2014.965736
96. Mare TA, Treacher DF, Shankar-Hari M, Beale R, Lewis SM, Chambers DJ, et al. The diagnostic and prognostic significance of monitoring blood levels of immature neutrophils in patients with systemic inflammation. *Crit Care.* (2015) 19:57. doi: 10.1186/s13054-015-0778-z
97. Hampson P, Dinsdale RJ, Wearn CM, Bamford AL, Bishop JRB, Hazeldine J, et al. Neutrophil dysfunction, immature granulocytes, and cell-free DNA are early biomarkers of sepsis in burn-injured patients: a prospective observational cohort study. *Ann Surg.* (2017) 265:1241–9. doi: 10.1097/SLA.0000000000001807
98. Daix T, Guerin E, Tavernier E, Mercier E, Gissot V, Herault O, et al. Multicentric standardized flow cytometry routine assessment of patients with sepsis to predict clinical worsening. *Chest.* (2018) 154:617–27. doi: 10.1016/j.chest.2018.03.058
99. Daix T, Guerin E, Tavernier E, Marsaud JP, Hacan A, Gauthier F, et al. Immature granulocytes: a risk factor of infection after cardiac surgery. *Cytometry B Clin Cytom.* (2018) 94:887–94. doi: 10.1002/cyto.b.21739

100. Ahn C, Kim W, Lim TH, Cho Y, Choi KS, Jang BH. The delta neutrophil index (DNI). as a prognostic marker for mortality in adults with sepsis: a systematic review and meta-analysis. *Sci Rep.* (2018) 8:6621. doi: 10.1038/s41598-018-24211-7
101. Guerin E, Orabona M, Raquil MA, Giraudeau B, Bellier R, Gibot S, et al. Circulating immature granulocytes with T-cell killing functions predict sepsis deterioration. *Crit Care Med.* (2014) 42:2007–18. doi: 10.1097/CCM.0000000000000344
102. Demaret J, Venet F, Friggeri A, Cazalis MA, Plassais J, Jallades L, et al. Marked alterations of neutrophil functions during sepsis-induced immunosuppression. *J Leukoc Biol.* (2015) 98:1081–90. doi: 10.1189/jlb.4A0415-168RR
103. Patera AC, Drewry AM, Chang K, Beiter ER, Osborne D, Hotchkiss RS. Frontline science: defects in immune function in patients with sepsis are associated with PD-1 or PD-L1 expression and can be restored by antibodies targeting PD-1 or PD-L1. *J Leukoc Biol.* (2016) 100:1239–54. doi: 10.1189/jlb.4HI0616-255R
104. Uhel F, Azzaoui I, Gregoire M, Pangault C, Dulong J, Tadie JM, et al. Early expansion of circulating granulocytic myeloid-derived suppressor cells predicts development of nosocomial infections in patients with sepsis. *Am J Respir Crit Care Med.* (2017) 196:315–27. doi: 10.1164/rccm.201606-1143OC
105. Mathias B, Delmas AL, Ozrazgat-Baslanti T, Vanzant EL, Szpila BE, Mohr AM, et al. Human myeloid-derived suppressor cells are associated with chronic immune suppression after severe sepsis/septic shock. *Ann Surg.* (2017) 265:827–34. doi: 10.1097/SLA.0000000000001783
106. Janols H, Bergenfelz C, Allaoui R, Larsson AM, Ryden L, Bjornsson S, et al. A high frequency of MDSCs in sepsis patients, with the granulocytic subtype dominating in gram-positive cases. *J Leukoc Biol.* (2014) 96:685–93. doi: 10.1189/jlb.5HI0214-074R
107. Bone RC, Balk RA, Cerra FB, Dellinger RP, Fein AM, Knaus WA, et al. Definitions for sepsis and organ failure and guidelines for the use of innovative therapies in sepsis. The ACCP/SCCM Consensus Conference Committee American College of Chest Physicians/Society of Critical Care Medicine. *Chest.* (1992) 101:1644–55.
108. Patel JJ, Rosenthal MD, McClave SA, Martindale RG. Tempering the clinical effects of early myeloid-derived suppressor cell expansion in severe sepsis and septic shock. *Am J Respir Crit Care Med.* (2018) 197:677–8. doi: 10.1164/rccm.201708-1701LE
109. Kumar V, Patel S, Tcyganov E, Gabrilovich DI. The nature of myeloid-derived suppressor cells in the tumor microenvironment. *Trends Immunol.* (2016) 37:208–20. doi: 10.1016/j.it.2016.01.004

Conflict of Interest Statement: The authors declare that the research was conducted in the absence of any commercial or financial relationships that could be construed as a potential conflict of interest.

6.5. Macrophage migration inhibitory factor promotes the migration of dendritic cells through CD74 and the activation of the Src/PI3K/myosin II pathway

Annette Ives[1], Didier Le Roy[1], Charlotte Théroude[1], Jürgen Bernhagen[2], Thierry Roger[1*], Thierry Calandra[1*]

[1]Infectious Diseases Service, Department of Medicine, Lausanne University Hospital and University of Lausanne, Lausanne, Switzerland

[2]Chair of Vascular Biology, Institute for Stroke and Dementia Research (ISD), Klinikum der Universität München (KUM), Ludwig-Maximilians-University (LMU), 81377 Munich, Germany, and Munich Cluster for Systems Neurology (SyNergy), 81377 Munich, Germany.

The FASEB Journal, 2021

Contribution to the work: I participated to *in vivo* experiments and performed flow cytometry analysis.

Received: 26 June 2020 | Revised: 14 January 2021 | Accepted: 21 January 2021

DOI: 10.1096/fj.202001605R

RESEARCH ARTICLE

THE FASEB JOURNAL

Macrophage migration inhibitory factor promotes the migration of dendritic cells through CD74 and the activation of the Src/PI3K/myosin II pathway

Annette Ives[1] | **Didier Le Roy**[1] | **Charlotte Théroude**[1] | **Jürgen Bernhagen**[2,3] | **Thierry Roger**[1] | **Thierry Calandra**[1]

[1]Infectious Diseases Service, Department of Medicine, Lausanne University Hospital and University of Lausanne, Lausanne, Switzerland

[2]Chair of Vascular Biology, Institute for Stroke and Dementia Research (ISD), Klinikum der Universität München (KUM), Ludwig-Maximilians-University (LMU), Munich, Germany

[3]Munich Cluster for Systems Neurology (SyNergy), Munich, Germany

Correspondence
Thierry Calandra, Infectious Diseases Service, Department of Medicine, Lausanne University Hospital and University of Lausanne, BH-10.555, Rue du Bugnon 46, CH-1011 Lausanne, Switzerland.
Email: Thierry.Calandra@chuv.ch

Funding information
Schweizerischer Nationalfonds zur Förderung der Wissenschaftlichen Forschung (SNF), Grant/Award Number: 310030_138488, CRSII3_147662S, 316030_145014 and 310030_173123; Wilhelm Sander-Stiftung (Wilhelm Sander Foundation), Grant/Award Number: 2017.009.1; Deutsche Forschungsgemeinschaft (DFG), Grant/Award Number: SFB1123/A3; EC | Horizon 2020 Framework Programme (H2020), Grant/Award Number: 676129; Société Académique Vaudoise, Lausanne, Switzerland

Abstract

Constitutively expressed by innate immune cells, the cytokine macrophage migration inhibitory factor (MIF) initiates host immune responses and drives pathogenic responses in infectious, inflammatory, and autoimmune diseases. Dendritic cells (DCs) express high levels of MIF, but the role of MIF in DC function remains poorly characterized. As migration is critical for DC immune surveillance, we investigated whether MIF promoted the migration of DCs. In classical transwell experiments, $MIF^{-/-}$ bone marrow-derived DCs (BMDCs) or $MIF^{+/+}$ BMDCs treated with ISO-1, an inhibitor of MIF, showed markedly reduced spontaneous migration and chemotaxis. $CD74^{-/-}$ BMDCs that are deficient in the ligand-binding component of the cognate MIF receptor exhibited a migration defect similar to that of $MIF^{-/-}$ BMDCs. Adoptive transfer experiments of LPS-matured $MIF^{+/+}$ and $MIF^{-/-}$ and of $CD74^{+/+}$ and $CD74^{-/-}$ BMDCs injected into the hind footpads of homologous or heterologous mice showed that the autocrine and paracrine MIF activity acting via CD74 contributed to the recruitment of DCs to the draining lymph nodes. Mechanistically, MIF activated the Src/PI3K signaling pathway and myosin II complexes, which were required for the migration of BMDCs. Altogether, these data show that the cytokine MIF exerts chemokine-like activity for DC motility and trafficking.

KEYWORDS
chemokine, cytokine, dendritic cell, innate immunity, MIF, motility

Abbreviations: BMDCs, bone marrow-derived dendritic cells; CCL, chemokine (C-C motif) ligand; CCR, C-C motif chemokine receptor; CXCL, chemokine (C-X-C motif) ligand; CXCR, C-X-C motif chemokine receptor; DCs, dendritic cells; D-DT, D-dopachrome tautomerase; Itg, integrins; LPS, lipopolysaccharide; MII, myosin II; MIF, macrophage migration inhibitory factor; MLCII, myosin II light chain.

Thierry Roger and Thierry Calandra contributed equally to this work.

1 | INTRODUCTION

Migration of leukocytes from the bloodstream into tissues is essential for the maintenance of homeostasis, body surveillance, and the mounting of host responses to danger signals sensed by sentinel innate immune cells in injured tissues.[1-3] Inflammatory mediators released by innate immune cells trigger complex leukocyte-vessel wall interactions resulting in the trans-endothelial migration, extravasation, and navigation of leukocytes into the interstitium. Microbial products, extracellular matrix, chemokines and cytokines, and lipid mediators are key drivers of adhesion-dependent and adhesion-independent leukocyte migration.[1,4-6] The binding of chemokines to cognate G-protein-coupled receptors of leukocytes activates intracellular signaling pathways including the Rho family of GTPases, Ca^{2+} signaling, phosphoinositide 3-kinase (PI3K)-Akt, and mitogen-activated protein kinases (MAPKs) that generate a bipolar mechanosensory state for cell migration.[1-7]

Macrophages and dendritic cells (DCs) are the main sentinel cells of the innate immune system that patrol peripheral tissues. They play a fundamental role in the recruitment of leukocytes following exposure to harmful environmental compounds, microbial products, or endogenous danger molecules. Tissue macrophages are an abundant source of a broad array of cytokines and chemokines that stimulate the migration of leukocytes into peripheral tissues. DCs are a heterogeneous group of hematopoietic cells bridging innate and adaptive immunity.[8,9] Beyond the production of cytokines, one key function of the classical (also called conventional) population of DCs is their ability to capture antigens in peripheral tissues and transport them via the lymphatic vessels into the draining lymph nodes where they present antigens to naïve T cells.[3] Following the endocytosis of foreign or self-antigens, DCs undergo a maturation process and up-regulate the expression of C-C chemokine receptor (CCR) 7, which results in an increased motility and haptotaxis into the lymphatic vasculature through the interaction of CCR7 with chemokine (C-C motif) ligand (CCL) 21 expressed by the lymphatic endothelium.[3,10,11] Upon arrival in the sub-capsular sinus of the draining lymph nodes, a CCL21 gradient guides classical DCs to the T-cell–rich zone where they support the activation, maturation, and development of effector functions of antigen-specific $CD4^+$ and $CD8^+$ T cells.

Cytokines are crucial effector molecules of innate immunity that play an essential role in the activation of phagocytes, the recruitment of leucocytes, and the maturation and migration of DCs.[12] Within the superfamily of cytokines, macrophage migration inhibitory factor (MIF) occupies a special place.[13,14] MIF and its close relative D-dopachrome tautomerase (D-DT, also coined MIF-2) are the only identified members of this cytokine family.[15] MIF acts as an enzyme and a hormone, a unique feature among cytokines. Other distinctive MIF traits are its constitutive expression and circulation at high concentration in the bloodstream and body fluids.[16] MIF is released promptly by a broad range of immune and endocrine cells in response to a vast array of stimuli and stress hormones including glucocorticoids.[16-18] Within the innate immune system, monocytes, macrophages, and DCs express copious amounts of MIF, which they further upregulate during acute inflammation to support robust innate immune responses.[19-21] MIF mediates these effects via a positive regulation of the expression of Toll-like receptor 4 (TLR4), the inhibition of p53, and the counter-regulation of the immune suppressive effects of glucocorticoids.[17,22-25] Hence, MIF acts as an initiator or regulator of infectious, inflammatory, and auto-immune diseases and represents a target for the management of pathological conditions.[14,26-41] Extracellular MIF signals through a multicomponent receptor complex composed of CD74 and CD44.[42-46] CD74 also works in association with C-X-C motif chemokine receptor (CXCR) 2, CXCR4, or CXCR7.[42-46] By contrast, the intracellular MIF acts through an interaction with p53, COP9 signalosome subunit 5/c-Jun-activation domain-binding protein 1 (CSN5/JAB-1), thioredoxin-interacting protein, and ribosomal protein S19.[47-50] Downstream signaling pathways activated by MIF include the extracellular signal-regulated kinase (ERK1/2), p38, and c-jun N-terminal kinase (JNK), MAPKs and PI3K/Akt.[51-55]

Unexpectedly given its name, MIF displayed chemokine-like function as a non-cognate ligand for CXCR2 and CXCR4.[44] Subsequent work indicated that MIF promotes the chemotaxis of neutrophils, B cells, eosinophils, and myeloid-derived suppressor cells through the engagement of one or several of its receptors, that is, CD74, CRXR2, CXCR4, and CXCR7, as well as indirectly through the chemokine (C-C motif) ligand (CCL) 2/MCP-1.[46,56-59] Given that MIF is expressed abundantly in DCs and that migration is a key feature of DCs, we explored whether MIF was a *bona fide* chemotactic factor for DCs using genetic and pharmacological approaches.

2 | MATERIALS AND METHODS

2.1 | Ethical considerations

Animal experiments were approved by the Service des Affaires Vétérinaires, Direction Générale de l'Agriculture, de la Viticulture et des Affaires Vétérinaires (DGAV), état de Vaud (Epalinges, Switzerland) under authorizations n.° 876.9, 877.8, and 877.9 to TR and were performed according to Swiss and ARRIVE guidelines (http://www.nc3rs.org.uk/arrive-guidelines).

2.2 | Mice and cells

Eight to twelve-week-old BALB/cAnNCrl and C57BL/6N mice were purchased from Charles River Laboratories (L'Arbresle, France). $MIF^{-/-}$ BALB/c mice[60] and $MIF^{-/-}$ C57BL/6N mice[61] were backcrossed at least eight times onto BALB/cAnNCrl and C57BL/6N genetic backgrounds. $CD74^{-/-}$ C57BL/6N mice were obtained from Prof Richard Bucala (Yale University School of Medicine, New Haven, CT). Mice were housed under specific pathogen-free conditions in the animal facility of the Centre des Laboratoires d'Epalinges (Switzerland, license number VD-H04) at 22°C, with 70% humidity in ambient air and 12-hour light/dark cycles. Colonies were free of norovirus and mouse hepatitis virus. Bone marrow cells were cultured in IMDM containing 2 μM 2-mercaptoethanol (βME), 2 mM L-glutamine, 100 U/mL penicillin, 100 μg/mL streptomycin (Invitrogen, San Diego, CA), and 10% of heat-inactivated FCS (Biochrom AG, Berlin, Germany) supplemented with 50 ng/mL of granulocyte-macrophage colony-stimulating factor and 20 ng/mL of IL-4 (ProSpec, East Brunswick, NJ). Loosely adherent bone marrow-derived dendritic cells (BMDCs) were collected after seven days.[62] BMDCs were incubated 36 hours with 10 ng/mL Ultrapure *Salmonella minnesota* LPS (List Biologicals Laboratories, Campbell, CA) to generate activated DCs.

2.3 | Cell migration assay

Cell migration was assessed using Corning Costar Transwell cell culture inserts or Corning Transwell-COL collagen-coated membrane inserts (Corning Life Sciences BV) with 5 μm pore size (Corning BV Life Sciences, Amsterdam, NL). Briefly, $MIF^{+/+}$ and $MIF^{-/-}$ BMDCs were washed with PBS and incubated for 1 hour in RPMI 1640 medium (Invitrogen) containing 0.1% BSA (Sigma-Aldrich, Buchs, Switzerland). In some experiments, BMDCs were preincubated for 1 hour with recombinant MIF (rMIF) or inhibitors of MIF [4,5-dihydro-3-(4-hydroxyphenyl)-5-isoxazoleacetic acid methyl ester, known as ISO-1, 100 μM], CXCR2 (SB225002, 100 μM), CXCR4 (AMD3100, 100 μg/mL), MEK-1/2 (U0126, 10 μM), myosin II (blebbistatin, 100 μM), PI3K (Ly29002, 10 μM; wortmannin, 1 μM), ROCK (Y27632, 5 μM), or SRC (PP2, 10 μM; Src inhibitor-1, 5 nM). Five × 10^5 cells were transferred to the transwell inserts. The lower chamber of the transwell device contained medium with or without recombinant CCL5 (500 ng/mL), CCL19 (250 ng/mL), CCL20 (100 ng/mL), CCL21 (250 ng/mL), or CXCL12 (250 ng/mL). The number of cells migrating into the lower chamber was assessed after 6 hours. MIF was prepared as described previously.[22,44] Chemokines were from Peprotech (Rocky Hill, NJ), and other reagents were from Sigma-Aldrich (Buchs, Switzerland) or Tocris (Zug, Switzerland).

2.4 | RNA analysis

Total RNA was isolated, reversed transcribed, and used in real-time quantitative PCR conducted with a QuantStudio 12K Flex system (Life Technologies, Carlsbad, CA).[63] Primer pairs are listed in Table S1. Relative gene specific expression levels were calculated with the $2^{\Delta\Delta CT}$ method using *Hprt* as a reference gene.

2.5 | Flow cytometry analysis

BMDCs were incubated with the 2.4G2 antibody (BD Biosciences, Erembodegem, Belgium) to block non-specific binding and stained with antibodies listed in Table S2. Dead cells were excluded following 7-ADD staining. Data were acquired using a LSR II flow cytometer (BD Biosciences) and analyzed using the FlowJo 10.2 software (FlowJo LLC, Ashland OR).[64]

2.6 | Adherence to fibronectin-coated glass slides

BMDCs were seeded onto fibronectin-coated (5-6 μg/cm^2) glass multi-well microscope slides at a density of 1.5 × 10^5 cells/cm^2. After 1 hour, slides were washed with PBS, stained with DIFF QUICK (Sigma-Aldrich), and mounted with coverslips. The number of adherent cells was determined in a semi-automated manner using the Image J software.

2.7 | Western blot analysis

Total cell extracts were obtained by incubating BMDCs in 10 mM HEPES pH 7.9, 10 mM KCl, 0.1 M EDTA, 0.1 mM EGTA, 1 mM DDT, 2.5 mM PMSF, 0.6% NP-40, cOmplete, Mini Protease, and PhosSTOP phosphatase inhibitor cocktails (Roche Applied Science, Basel, Switzerland) for 10 minutes on ice. Proteins were fractioned through 8-12% PAGE and transferred onto nitrocellulose membranes (Schleicher & Schuell, Keene, NH). Membranes were incubated with antibodies described in Table S2. The signals were detected using the ECL system (GE Healthcare, Little Chalfont, UK), and the images were recorded using a Fusion Fx system (Vilber Lourmat, Collégien, France). Full-size western blots and quantification data are shown in Figures S3 and S4.

2.8 | In vivo migration assay

C57BL/6N $MIF^{+/+}$ and $MIF^{-/-}$ BMDCs and $CD74^{+/+}$ and $CD74^{-/-}$ BMDCs were differentiated for 36 hours

with 10 ng/mL Ultrapure LPS, labeled with either 5-carboxyfluorescein diacetate succinimidyl ester (CFSE) (CellTrace CFSE Cell Proliferation Kit, Invitrogen) or CellVue Claret Far-red fluorescent cell linker (Sigma-Aldrich), washed, mixed at a 1:1 ratio (5×10^6 cells of each preparation), and injected into the left hind footpad of either $MIF^{+/+}$ or $MIF^{-/-}$ mice. Twenty-four hours later, popliteal lymph nodes were collected and analyzed by flow cytometry using antibodies directed against CD3, CD11c, CD19, and MHC-II (Table S2).

2.9 | Graphical representation and statistical analyses

Graphs were plotted and statistical analyses were performed using Prism 8.3.0 (GraphPad Software, Inc). Violin plots show the 25th and 75th percentile, and the median. The bars depict mean ± SD. Comparisons between different groups were performed using the analysis of variance followed by parametric (two-tailed unpaired Student's *t*-test) or non-parametric (two-tailed Mann-Whitney test) statistical tests. *P* values less than .05 were considered to indicate statistical significance (*$P < .05$; **$P < .01$; ***$P < .005$).

3 | RESULTS

3.1 | MIF promotes spontaneous and chemokine-induced migration of DCs

To determine whether MIF regulates the migration of DCs, BMDCs derived from $MIF^{+/+}$ and $MIF^{-/-}$ mice were subjected to transwell migration assays performed in the presence or in the absence of homeostatic (CCL19, CCL21), inflammatory (CCL5, CCL20), or mixed homeostatic/inflammatory (CXCL12) chemokines acting through CCR7 (CCL19 and CCL21), CCR1/3/4/5 (CCL5), CCR6 (CCL20), and CXCR4/CXCR7 (CXCL12). The number of migrating cells was assessed after 6 hours of incubation. As shown in Figure 1A, the spontaneous migration of $MIF^{-/-}$ BMDCs was 1.9-fold (C57BL/6) and 1.6-fold (BALB/c) lower than that of $MIF^{+/+}$ BMDCs, respectively ($P = .0017$ and $P = .026$). Chemokines increased the migration of $MIF^{+/+}$ BMDCs by a factor of 2 to 3. $MIF^{-/-}$ C57BL/6 BMDCs exhibited severely impaired migration upon exposure to CCL19, CCL21, CCL5, or CCL20 (1.6-, 1.6-, 2.0-, and 1.9-fold reduction; $P = .053$, .001, .02, and .04, respectively) (Figure 1B). Interestingly, migration of $MIF^{-/-}$ BMDCs was not impaired when it was induced by CXCL12 (Figure 1B). Spontaneous migration and CCL21-induced chemotaxis of $MIF^{-/-}$ C57BL/6 BMDCs matured for 3 days with LPS were also markedly lower (2.6- to 3.1-fold) than that of $MIF^{+/+}$ C57BL/6 BMDCs (Figure S1A). Unless specified otherwise, all subsequent experiments were performed with cells derived from C57BL/6 mice.

We also performed transwell migration assays with wild-type BMDCs treated with ISO-1, an inhibitor of MIF.[65] ISO-1 reduced the spontaneous and the CCL21-induced migration of $MIF^{+/+}$ BMDCs (2-fold and 1.5-fold; $P = .041$ and $P = .016$) (Figure 1C). Next, we used a recombinant mouse MIF (rMIF) for add-back experiments in MIF-deficient BMDCs. BMDCs were incubated with rMIF for 1 hour before being used in transwell migration assays. rMIF increased in a dose-dependent manner spontaneous and CCL21-induced migration of $MIF^{-/-}$ BMDCs (2.7-fold and 5.5-fold) (Figure 1D) indicative of a paracrine effect of MIF on spontaneous and chemokine-induced migration of BMDCs.

We then examined the contribution of MIF receptors to the migration of BMDCs using $CD74^{+/+}$ and $CD74^{-/-}$ BMDCs and pharmacological inhibitors of CXCR2 (SB225002) and CXCR4 (AMD3100) (Figure 1E,F). Like $MIF^{-/-}$ BMDCs, $CD74^{-/-}$ BMDCs exhibited a marked decrease of spontaneous and chemokine-induced (CCL19 or CCL21) migration (1.8-, 2.0-, and 1.9-fold; $P = .001$, .011, and .09, respectively) (Figure 1E). The CXCR4 inhibitor AMD3100 exhibited a small effect on CCL21-induced but not on spontaneous chemotaxis of $MIF^{+/+}$ BMDCs ($P = .016$). The CXCR2 inhibitor SB225002 did not affect migration (Figure 1F).

Taken together, these results show that MIF plays an important role in the spontaneous migration and in the chemotaxis of DCs and that it exerts its effects predominantly in a CD74-dependent manner.

3.2 | MIF deficiency impairs the migration of DCs into draining lymph nodes

To evaluate the effect of autocrine and paracrine MIF on the migration of DCs in vivo, we used a model of adoptive cell transfer. Fluorochrome-labelled, LPS-matured $MIF^{+/+}$ and $MIF^{-/-}$ BMDCs were injected in the footpads of $MIF^{+/+}$ and $MIF^{-/-}$ mice, and the number of cells that migrated into the popliteal draining lymph nodes was assessed after 24 hours by flow cytometry. As shown in Figure 2A, $MIF^{+/+}$ mice injected with $MIF^{+/+}$ BMDCs had the highest number of cells migrating into the draining lymph nodes. Migrating BMDCs were reduced by 36% ($P = .004$) in $MIF^{+/+}$ mice injected with $MIF^{-/-}$ BMDCs, by 36% ($P = .002$) in $MIF^{-/-}$ mice injected with $MIF^{+/+}$ BMDCs, and by 54% ($P = .0006$) in $MIF^{-/-}$ mice injected with $MIF^{-/-}$ BMDCs. Thus, in vivo both autocrine and paracrine MIF contributed to an optimal migration of DCs to the draining lymph nodes. To test whether CD74 was involved in these effects, we quantified the migration of $CD74^{+/+}$ and $CD74^{-/-}$ BMDCs into the draining lymph nodes of wild-type recipient mice (Figure 2B). The migration of $CD74^{-/-}$ BMDCs was reduced by 35% when compared with that of $CD74^{+/+}$

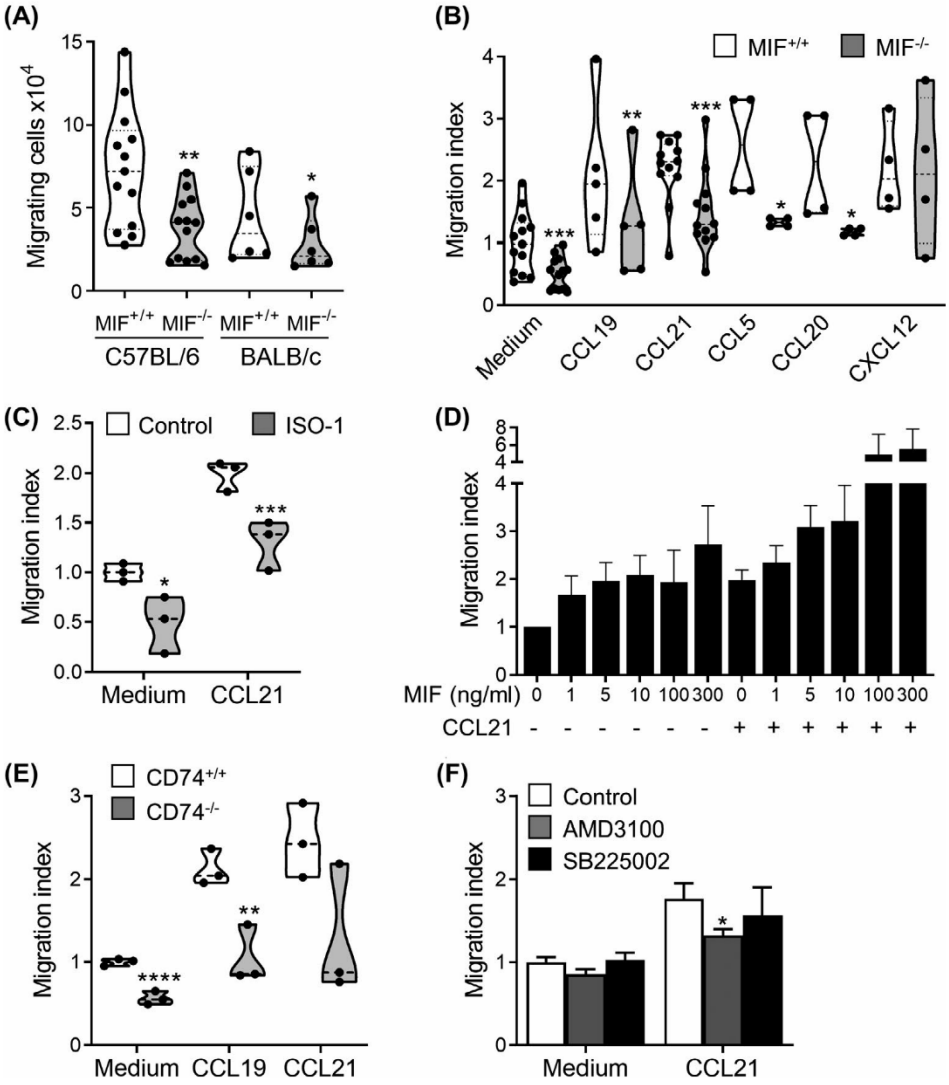

FIGURE 1 MIF promotes spontaneous and chemokine-induced migration of DCs. Spontaneous (A) and chemokine-dependent (B–F) migration of $MIF^{+/+}$ and $MIF^{-/-}$ (A,B), and $CD74^{+/+}$ and $CD74^{-/-}$ (E) BMDCs isolated from C57BL/6N (A–F) or BALB/c (A) mice (n = 3 to 13 mice per experiment) with or without pretreatment for 1 hour with ISO-1 (100 μg/mL) (C), recombinant mouse MIF (1-300 mg/mL) (D), or inhibitors of CXCR4 (AMD3100, 100 μg/mL) or CXCR2 (SB225002, 100 μM) (F). Chemoattractants CCL19, CCL21, and CXCL12 were used at 250 ng/mL, CCL5 at 500 ng/mL, and CCL20 at 100 ng/mL. Migrating cells were enumerated after 6 hours. Results are expressed as the number of migrating cells (A) or as a migration index expressed as a fold change of the experimental conditions (CCL19, CCL21, CCL5, CCL20, CXCL12) over the mean of the control (ie, spontaneous migration of $MIF^{+/+}$ BMDCs), which was set at 1 (B-F). $^{*}P < .05$, $^{**}P < .01$, $^{***}P < .005$

BMDCs ($P = .02$). These results indicate that the paracrine effects of MIF on DC migration are CD74-dependent.

3.3 | MIF regulates integrin expression and adhesion of DCs to extracellular matrix

Leukocyte integrins (Itg) and adhesion molecules interact with the extracellular matrix including collagen, laminin, and fibronectin. We therefore examined whether MIF deficiency affected the expression of various integrins and adhesion molecules such as Itgα4 (CD49d), Itgβ1 (CD29), Itgβ2 (CD18), intercellular adhesion molecule 1 (Icam1, CD54), DC-specific intercellular adhesion molecule-3-grabbing non-integrin (Dcsign, CD209a), and vascular cell adhesion molecule 1 (Vcam1, CD106). $MIF^{-/-}$ BMDCs expressed lower Itga4 and Itgb1 mRNA levels than $MIF^{+/+}$ BMDCs (1.6-fold and 1.4-fold reduction, $P = .04$ and $P = .006$). The mRNA levels of Itgb2, Icam1, Dcsign, and Vcam1 decreased, but the differences were not statistically significant (Figure 3A). Flow cytometry analyses confirmed a reduced expression of Itgβ1 (CD29), but not of Itgβ2 (CD18), in $MIF^{-/-}$ BMDCs (Figure 3B).

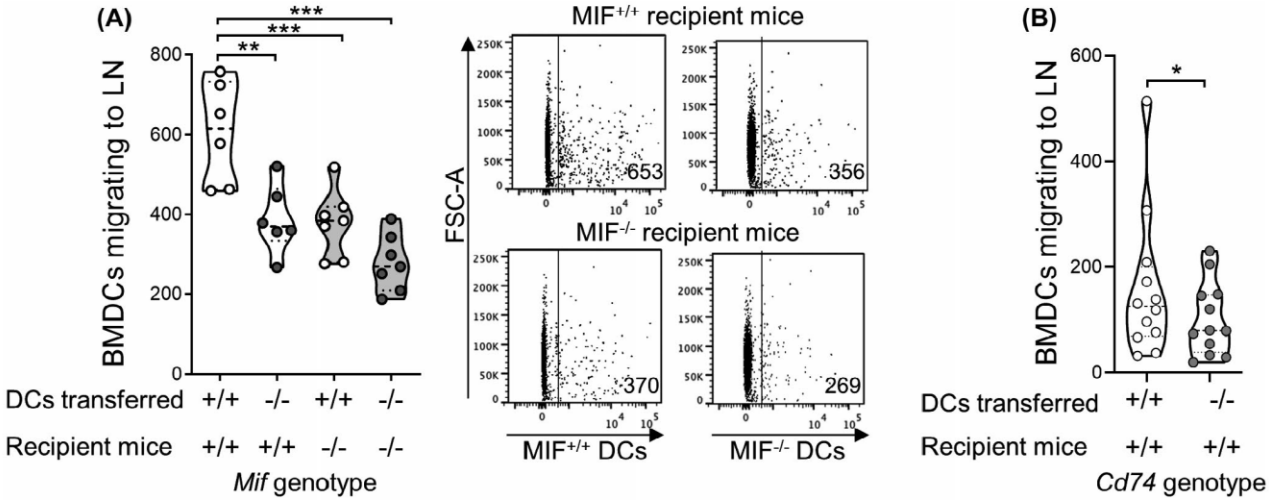

FIGURE 2 MIF deficiency impairs the migration of DCs into satellite lymph nodes. A, B, BMDCs were cultured for 72 hours with LPS (5 μg/mL). One million $MIF^{+/+}$ or $MIF^{-/-}$ (A) and $CD74^{+/+}$ or $CD74^{-/-}$ (B) BMDCs labeled with CFSE or CellVue Far red dyes were mixed in a 1:1 ratio and injected into the hind footpads of $MIF^{+/+}$ and $MIF^{-/-}$ mice (A) and $CD74^{+/+}$ mice (B). After 24 hours, popliteal lymph nodes were collected and the number of BMDCs that had migrated into the draining lymph nodes was quantified by flow cytometry. Representative dot plots of the detection of $MIF^{+/+}$ and $MIF^{-/-}$ DCs transferred into $MIF^{+/+}$ or $MIF^{-/-}$ mice are shown in panel A. Data are a pool of two (A) and one (B) experiments. Each point represents one individual mouse. Bar graphs represent mean ± SEM. $^{*}P < .05$, $^{**}P < .01$, $^{***}P < .005$

Very late antigen-4 (VLA-4) composed of heterodimers of Itgα4 and Itgβ1 interacts with VCAM1 and fibronectin. To determine whether the decreased expression of CD29 in $MIF^{-/-}$ BMDCs was functionally meaningful, we quantified the adhesion of BMDCs to fibronectin-coated glass slides. Compared to untreated $MIF^{+/+}$ BMDCs, ISO-1-treated $MIF^{+/+}$ BMDCs and $MIF^{-/-}$ BMDCs exhibited significant reductions in adherence to fibronectin by 2.3-fold and 2.8-fold ($P = .03$ and $P = .004$, respectively) (Figure 3C). Similar results were obtained when comparing $MIF^{+/+}$ and $MIF^{-/-}$ BMDCs obtained from BALB/c mice ($MIF^{+/+}$ *vs.* $MIF^{-/-}$ adherent BMDCs: 3393 ± 374 *vs.* 2324 ± 344, n = 3, $P = .01$). In agreement with these observations, spontaneous migration and CCL19 and CCL21-stimulated chemotaxis of $MIF^{-/-}$ BMDCs were 2.1- to 3.6-fold lower than those of $MIF^{+/+}$ BMDCs in migration assays performed with collagen-coated transwells (Figure S1B). These results indicate that the endogenous MIF is required for maximal expression of integrins on BMDCs for an optimal interaction with the extracellular matrix.

3.4 | MIF activates the Src/PI3K pathway

Several signaling pathways including the Src, PI3K/Akt, and MAPK regulate the migration of DCs.[66] Among these signaling modules, the RAF/MEK/ERK pathway suppresses DC migration.[67] As MIF can induce activation of PI3K/Akt, MEK/ERK1/2, and Src pathways,[45,52,55] we examined the role of PI3K/Akt, Src, and MAPK pathways in migration of DCs in transwell migration assays using specific pharmacological inhibitors. Inhibitors of PI3K (wortmannin and Ly294002) and Src (Src inhibitor 1) decreased spontaneous migration (PI3K inhibitors) and CCL21-induced chemotaxis (PI3K and Src inhibitors) of $MIF^{+/+}$ BMDCs, in line with previous observations.[66] In contrast, the inhibitor of MEK1/2 (U0126), the MAPK kinase upstream of ERK1/2, had no impact on the migration of DCs (Figure 4A and Figure S2A). Western blot analyses of the levels of phosphorylated PI3K, phosphorylated Akt, and phosphorylated Src in $MIF^{+/+}$ and $MIF^{-/-}$ BMDCs stimulated with CCL21 are shown in Figure 4B and Figure S3. CCL21 induced a rapid, robust, and transient increase in phosphorylated Akt and phosphorylated ERK1/2 and a modest increase in phosphorylated PI3K p85 and phosphorylated Src, while phosphorylated PI3K p55 was markedly reduced. Levels of phosphorylated PI3K and phosphorylated Src were reduced in $MIF^{-/-}$ BMDCs. This was not the case for phosphorylated Akt and ERK1/2. These results indicate that MIF supports the activation of kinase cascades (PI3K and Src) implicated in spontaneous and chemokine-induced migration of DCs. Of note, PI3K inhibition with wortmannin also reduced spontaneous and CCL21-induced migration of $MIF^{-/-}$ BMDCs (1.7-fold and 1.6-fold, $P = .03$ and .02, respectively), suggesting that PI3K-mediated migration of DCs is partly MIF-independent.

3.5 | MIF is involved in myosin II-dependent motility of DCs

Myosin II (MII) is an actin motor protein and essential regulator of cell morphology and cell migration.[7] MII is a hexamer composed of two heavy chains of 230 kDa, two essential light chains of 17 kDa, and two regulatory light chains

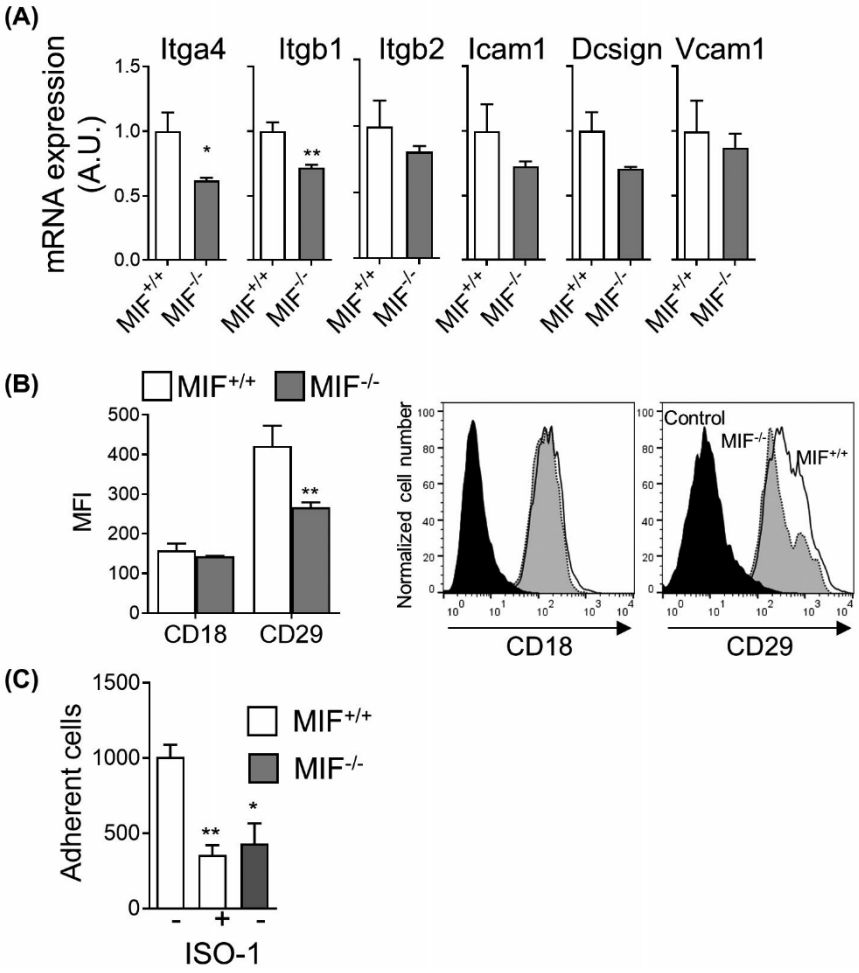

FIGURE 3 MIF-deficiency in DCs reduces integrin expression and adherence to fibronectin. A, Itga4, Itgb1, Itgb2, Icam1, Dcsign, and Vcam1 mRNA levels in $MIF^{+/+}$ and $MIF^{-/-}$ BMDCs (n = 4 mice) were determined by RT-PCR, normalized to Hprt mRNA levels and reported to the respective mRNA levels of $MIF^{+/+}$ BMDCs set at 1. B, CD18 (encoded by *Itgb2*) and CD29 (encoded by *Itgb1*) expression in $MIF^{+/+}$ and $MIF^{-/-}$ BMDCs assessed by flow cytometry (n = 3 mice) with representative histogram plots (the black area represents staining with an isotype-matched control antibody). Data are expressed as the mean fluorescence intensity (MFI). C, Number of $MIF^{+/+}$ and $MIF^{-/-}$ BMDCs adherent to fibronectin-coated glass slides. Cells were preincubated for 1 hour with or without ISO-1 (100 μg/mL) and left in contact for 30 minutes with the glass slides and adherent cells counted. Data are mean ± SD from one experiment performed with BMDCs derived from three individual mice per group and are representative of two independent experiments. $^*P < .05$, $^{**}P < .01$

of 20 kDa (MLC II). The activity of MII is dependent on the phosphorylation of MLC II at serine 19 (Ser19) and at threonine 18 (Thr18). The upstream regulators of MII include Rho GTPases and ROCK1/2. Upon activation by RhoA, ROCK1 inhibits the MLC phosphatase, thereby increasing the phosphorylation of MLC II that supports actomyosin assembly. Phosphorylation at Ser19/Thr18 induces conformational changes of MII and stimulates MII filament formation and ATPase activity that is required for cell motility.

Given the key role played by MII in the cell movement, we investigated the effects of pharmacological inhibitors of MII (blebbistatin) and ROCK (Y27632) on the migration of BMDCs. Blebbistatin and Y27632 inhibited the spontaneous migration and CCL21-dependent chemotaxis of $MIF^{+/+}$ BMDCs (blebbistatin: 2.7- and 3.8-fold decrease, $P = .05$ and $P = .012$; Y27632: 1.4- and 1.5-fold decrease, $P = .03$ and $P = .004$) (Figure 5A,B). Blebbistatin was also found to decrease the chemotaxis of $MIF^{+/+}$ BMDCs upon stimulation with CCL19, CCL5, and CCL20 (Figure S2B). Next, we examined by western blotting the effect of MIF on the phosphorylation of MLC II at Ser19 and Thr18/Ser19 II in $MIF^{+/+}$ and $MIF^{-/-}$ BMDCs after stimulation with CCL21. CCL21 induced a rapid (peaking after one minute) and persistent (up until 60 minutes) elevation of phosphorylated MLC II in $MIF^{+/+}$ BMDCs, which was delayed, of lower magnitude and of shorter duration in $MIF^{-/-}$ BMDCs (Figure 5C, Figure S4). These data indicate that MIF promotes MII-dependent motility of DCs.

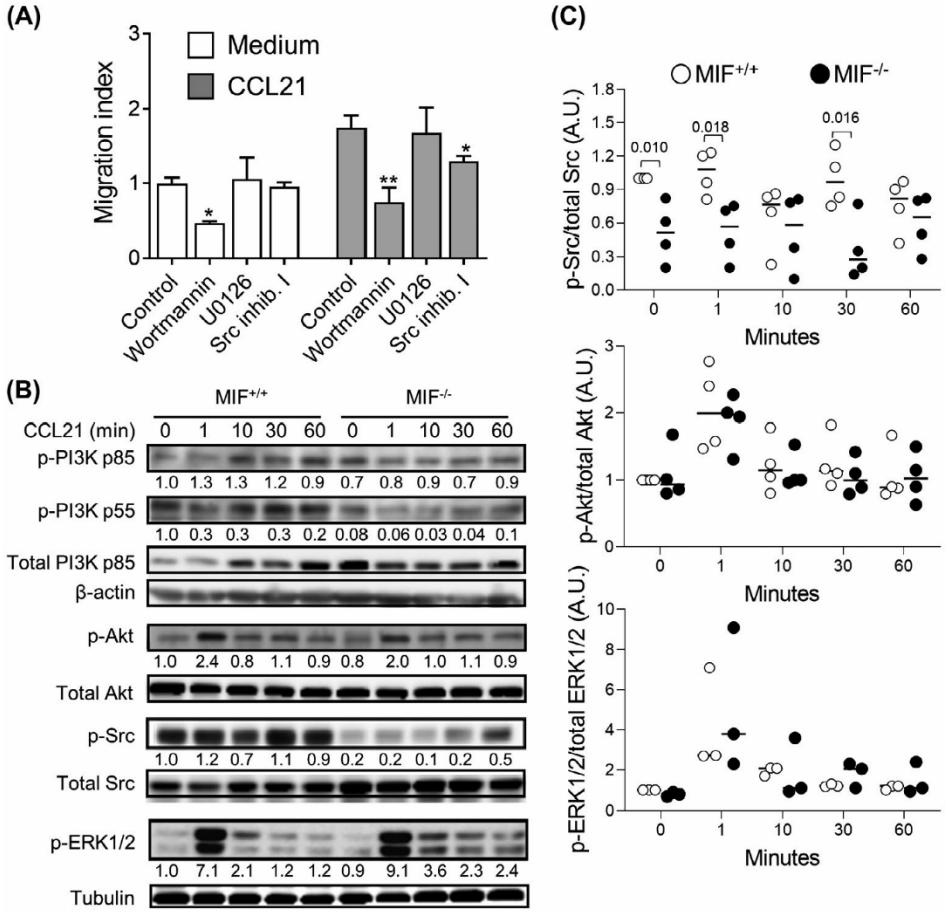

FIGURE 4 Reduced baseline and chemokine-induced phosphorylation of PI3K and Src in MIF deficient DCs. A, Spontaneous migration and CCL21-induced (250 ng/mL) chemotaxis of $MIF^{+/+}$ and $MIF^{-/-}$ BMDCs with or without pre-treatment for 1 hour with wortmannin (1 μM), U0126 (10 μM), or Src Inhibitor I (10 nM). The migration index was calculated as described in the legend of Figure 1. Data are mean ± SEM from BMDCs derived from four individual mice per group. $*P < .05$, $**P < .01$, $***P < .005$. B, Western blots of phosphorylated (p) and total PI3K, Akt, Src, ERK1/2, β-actin, and tubulin in $MIF^{+/+}$ and $MIF^{-/-}$ BMDCs cultured with CCL21 (250 ng/mL) for 0 to 60 minutes. Full-size blots are shown in Figure S3. Signal intensities were quantified by imaging. Ratios of phosphorylated over total protein or tubulin (phosphorylated ERK1/2) were normalized to those of $MIF^{+/+}$ BMDCs set at 1. Data are representative of one (PI3K), three (ERK1/2), and four (Src and Akt) independent experiments. C, Quantitative assessment of phosphorylated Src, Akt, and ERK1/2. Each dot represents one independent experiment. Statistically significant *P* values are shown in the graph

4 | DISCUSSION

Using genetic and pharmacological approaches, we showed that MIF promotes steady-state migration and chemotaxis of BMDCs in vitro and in vivo in a classical model of adoptive transfer and homing of DCs to the lymph nodes. The impairment of DC migration was especially striking when transferring MIF-deficient DCs into MIF-deficient recipient mice, indicating that MIF is playing an active role in DC recruitment and lymph node trafficking by haptotaxis. Mechanistically, MIF migration stimulating activity was mediated by the promotion of cellular adhesion via the expression of β1 integrin (CD29) and the activation of the Src/PI3K signaling pathway, which induced cellular locomotion through MII-dependent contraction (Figure 6).

Many of the biological effects of MIF require the activation of a receptor complex consisting of CD74, the ligand-binding unit, and CD44, the signal-transducing element. Via a pseudo(E)LR motif and a chemokine-mimicking N-like loop, MIF also functions as a non-canonical ligand for the chemokine receptors CXCR2 and CXCR4.[44,68] Working in concert with CD74, CXCR2 or CXCR4 mediates MIF chemokine-like activity for monocytes, eosinophils, neutrophils, NKT cells, T cells, or B cells.[44,57,58,68,69] MIF also facilitates CXCL1-induced neutrophil chemotaxis.[56] The present data provide genetic evidence that CD74 was required for maximal spontaneous migration and chemotaxis of DCs. In sharp contrast, a previous study reported an increased migration of CD74-deficient DCs.[70] The reasons underlying these diametrically opposed results remain unclear. Our data are consistent with

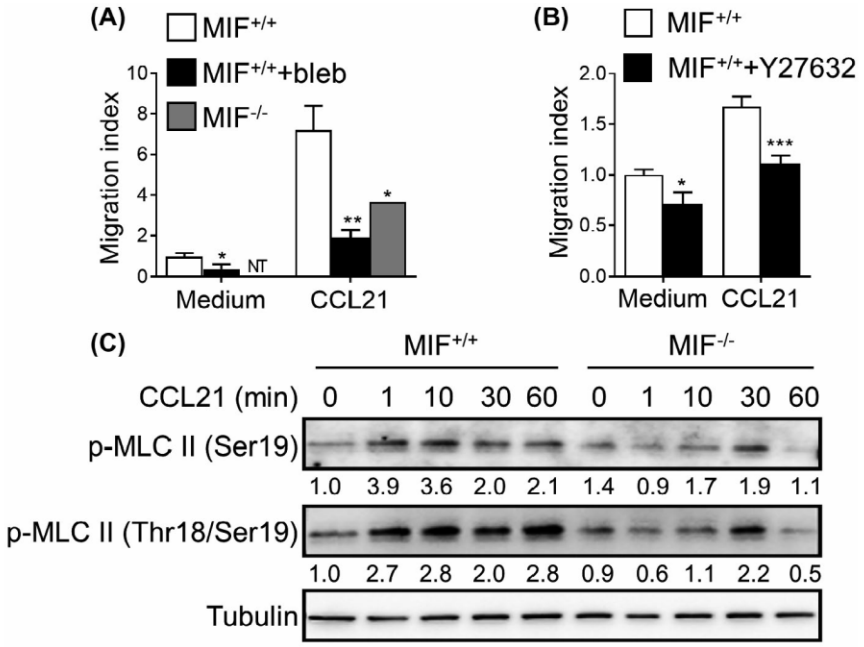

FIGURE 5 Reduced chemokine-induced myosin II phosphorylation in MIF deficient DCs. A, B, Spontaneous and CCL21-induced (250 ng/mL) migration of $MIF^{+/+}$ and $MIF^{-/-}$ BMDCs with or without pre-treatment for 1 hour with blebbistatin (bleb, 100 μM) (A) or Y27632 (5 μM) (B). The migration index was calculated as described in the legend of Figure 1. Data are mean ± SD from 3 (A) or 4-9 (B) mice. $*P < .05$, $**P < .01$, $***P < .005$. C, Expression levels of phosphorylated (p) MLC II (at Ser19 and Thr18/Ser19) and tubulin by $MIF^{+/+}$ and $MIF^{-/-}$ BMDCs cultured for 0-60 minutes with CCL21 (250 ng/mL). Samples were analyzed by Western blotting and signals quantified by imaging. Phosphorylated MLC II over tubulin ratios was normalized to those obtained from control $MIF^{+/+}$ BMDCs set at 1. Data are representative of two experiments. Full-size blots are shown in Figure S4

studies that showed a role for CD74 in the migration of monocytes, NKT cells, B cells, and CLL cells.[44,57,58,68,69] CD74-dependent promotion of DC migration by MIF relied on the activation of the Src and PI3K kinases, which is in agreement with previous studies, demonstrating the activation of these pathways by MIF.[43,45,52,55] Given that CXCR4 inhibition only modestly affected MIF migratory effects and that genetic deficiency or pharmacological inhibition of CXCR4 causes major defect of myelopoiesis and DC maturation and survival,[71-75] we did not perform in vivo experiments using CXCR4 targeting approaches. p53 and CSN5/JAB1 have been reported to affect the cell motility in a MIF-independent manner.[76-78] We did not investigate whether MIF promoted DC migration via p53 or CSN5/JAB1, but are not aware of previous findings suggesting that it might be the case.

MIF has been involved in the recruitment of antigen-presenting cells in the epidermis or in the dermis.[79] Transwell cell migration experiments carried out with a competitive inhibitor of CXCR2 (SB22502 at 100 nM) resulted in a 34% reduction of the migration of immature human DCs. With the same experimental setting, we found that CXCR2 inhibition with SB22502 tested at wide dose range (30 nM to 300 μM; shown using 100 μM in Figure 1F) had no impact on BMDCs migration. In contrast, inhibition of CXCR4 resulted in a modest but statistically significant reduction of BMDC chemotaxis, in line with studies showing an involvement of the MIF/CXCR4 axis in monocyte and T-cell chemotaxis.[44,75] Integrins play an essential role in haptotactic migration of leukocytes driven by ligands in the extracellular matrix.[1,80] The exploration of the mechanisms involved in MIF-dependent DC migration indicated that MIF modulates the expression of β1 integrin. These findings are consistent with earlier studies in which MIF upregulated the expression of αvβ3 integrin in endometrial adenocarcinoma and chondrosarcoma cells and of β1 integrin in podocytes.[81-84]

Functionally, integrin expression was associated with increased motility of chondrosarcoma cells and increased adhesion of podocytes.[82,84] β2 integrins have been implicated in the arrest of monocytes induced by MIF[44] and in the CCL2-dependent emigration of monocytes out of blood vessels.[85] Of note, the activation of CD74 by MIF in CLL cells resulted in the expression of Tap63 and of VLA-4, a heterocomplex of α4 and β1 integrins that enabled the migration of CLL to the bone marrow.[86] VLA-4 mediated MIF-induced cellular recruitment of macrophages and the adhesion and arrest of leukocytes on the endothelium through VCAM-1 or fibronectin. In line with these findings, we observed that MIF-modulated Itga4 mRNA expression with the reduced adherence of $MIF^{-/-}$ or ISO-1 treated BMDCs to fibronectin-coated glass slides. Overall,

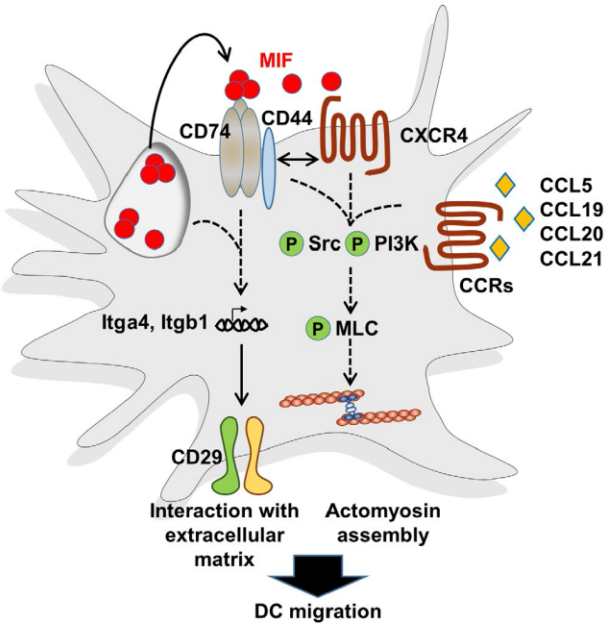

FIGURE 6 Scheme of MIF-mediated effects on migration of DCs. Functional MIF receptor complex is composed of CD74, CD44, and CXCR4. Autocrine or paracrine source of MIF binding to CD74, either alone or in combination with CCL5, CCL19, CCL20, and CCL 21-induced activation of CCRs, triggers the Src and PI3K signaling pathway resulting in the phosphorylation of MLC II that induces actomyosin assembly and ATPase activity and DC motility. MIF signaling through CD74 sustains the expression of Itga4 and Itgb1 encoding for CD29, which allows interaction with the extracellular matrix. Taken together the present findings suggest that MIF promotes integrin-dependent and integrin-independent DC trafficking through a CD74/Src/PI3K/MLC II pathway

these data are consistent with the notion that integrins mediate adhesion-dependent migration of DCs in a two-dimensional environment, whereas an actin-protrusive and integrin-independent mode of locomotion is critical for migration in three-dimensional environments.[5]

Upon binding of extracellular matrix proteins, integrin ligands, chemokines, cytokines, and growth factors to their cognate receptors, the family of Rho GTPases activates a signaling cascade that drives MII-dependent actinomyosin formation, cell protrusion, and motility of leukocytes including DCs.[1,7] The Rho-associated protein kinases (ROCK1 and ROCK2) inhibit the activity of MLC phosphatase, thus augmenting the state of MLC II phosphorylation by MLC kinase, which supports DCs migration. We found that inhibition of ROCK or of MII reduced the steady-state migration and chemotaxis of BMDCs. Mechanistically, MIF exerted its effects through the phosphorylation of the MLC II chains at Thr18 and Ser19. In a similar fashion, MIF promoted the activity of the Rho GTPase Rac1 and the migration of human lung adenocarcinoma cells and the induction of MLC kinase activity in fibroblasts.[87,88]

Taken together with previous work conducted in tumor and immune cells, our data indicate that MIF affects leukocyte trafficking in an integrin-dependent (transendothelial migration) or integrin-independent (migration into lymphoid organs) manner mainly via an interaction with the CD74 receptor and the activation of a Src/PI3K signaling pathway (Figure 6). This is the first report unraveling the signaling pathway, whereby MIF drives the activation of cell motility in immune cells. These observations reinforce the view that MIF plays a central role in promoting inflammatory and immune responses and that targeting MIF or its receptors are attractive immunotherapeutic approaches for the management of pathological conditions.

ACKNOWLEDGMENTS

The authors were supported by funding from the Swiss National Science Foundation (SNSF) grant number 310030_138488 and CRSII3_147662S (TC) and 316030_145014 and 310030_173123 (TR), the Société Académique Vaudoise (Lausanne, Switzerland) (TR), the Wilhelm-Sander Foundation grant number 2017.009.1 (JB), and the Deutsche Forschungs-gemeinschaft (DFG) grant SFB1123/A3 (JB). CT was supported by the European Sepsis Academy Horizon 2020 Marie Skłodowska-Curie Action: Innovative Training Network (MSCA-ESA-ITN, grant number 676129) and received a scholarship from the Société Académique Vaudoise (Lausanne, Switzerland). We thank Ms Amiel Olivoz-Ortiz for her involvement in the present study and Simona Gerra for help with the rMIF preparations. We thank Prof. Richard Bucala (Yale University School of Medicine, New Haven, CT) for the generous gift of $CD74^{-/-}$ knockout mice.

CONFLICT OF INTEREST

All authors declare no conflict of interest.

AUTHOR CONTRIBUTIONS

Study conception and design: T. Roger and T. Calandra. Acquisition of data: A. Ives, D. Le Roy, C. Théroude, and T. Roger. Analysis and interpretation of data: A. Ives, D. Le Roy, C. Théroude, J. Bernhagen, T. Roger, and T. Calandra. Drafting of manuscript: A. Ives, T. Roger, and T. Calandra. Final approval of the submitted manuscript: all authors.

ORCID

Jürgen Bernhagen https://orcid.org/0000-0003-2996-2652
Thierry Roger https://orcid.org/0000-0002-9358-0109
Thierry Calandra https://orcid.org/0000-0003-3051-1285

REFERENCES

1. Weninger W, Biro M, Jain R. Leukocyte migration in the interstitial space of non-lymphoid organs. *Nat Rev Immunol*. 2014;14:232-246.

2. Schulz O, Hammerschmidt SI, Moschovakis GL, Forster R. Chemokines and chemokine receptors in lymphoid tissue dynamics. *Annu Rev Immunol*. 2016;34:203-242.
3. Worbs T, Hammerschmidt SI, Forster R. Dendritic cell migration in health and disease. *Nat Rev Immunol*. 2017;17:30-48.
4. Vestweber D. How leukocytes cross the vascular endothelium. *Nat Rev Immunol*. 2015;15:692-704.
5. Lammermann T, Bader BL, Monkley SJ, et al. Rapid leukocyte migration by integrin-independent flowing and squeezing. *Nature*. 2008;453:51-55.
6. Huse M. Mechanical forces in the immune system. *Nat Rev Immunol*. 2017;17:679-690.
7. Bros M, Haas K, Moll L, Grabbe S. RhoA as a key regulator of innate and adaptive immunity. *Cells*. 2019;8(7):733.
8. See P, Dutertre CA, Chen J, et al. Mapping the human DC lineage through the integration of high-dimensional techniques. *Science*. 2017;356:eaag3009.
9. Nutt SL, Chopin M. Transcriptional networks driving dendritic cell differentiation and function. *Immunity*. 2020;52:942-956.
10. Randolph GJ, Ivanov S, Zinselmeyer BH, Scallan JP. The lymphatic system: integral roles in immunity. *Annu Rev Immunol*. 2017;35:31-52.
11. Permanyer M, Bosnjak B, Forster R. Dendritic cells, T cells and lymphatics: dialogues in migration and beyond. *Curr Opin Immunol*. 2018;53:173-179.
12. Altan-Bonnet G, Mukherjee R. Cytokine-mediated communication: a quantitative appraisal of immune complexity. *Nat Rev Immunol*. 2019;19:205-217.
13. Calandra T, Roger T. Macrophage migration inhibitory factor: a regulator of innate immunity. *Nat Rev Immunol*. 2003;3:791-800.
14. Kang I, Bucala R. The immunobiology of MIF: function, genetics and prospects for precision medicine. *Nat Rev Rheumatol*. 2019;15:427-437.
15. Merk M, Mitchell RA, Endres S, Bucala R. D-dopachrome tautomerase (D-DT or MIF-2): doubling the MIF cytokine family. *Cytokine*. 2012;59:10-17.
16. Roger T, Schlapbach LJ, Schneider A, et al. Plasma levels of macrophage migration inhibitory factor and d-dopachrome tautomerase show a highly specific profile in early life. *Front Immunol*. 2017;8:26.
17. Calandra T, Bernhagen J, Metz CN, et al. MIF as a glucocorticoid-induced modulator of cytokine production. *Nature*. 1995;377:68-71.
18. Lugrin J, Ding XC, Le Roy D, et al. Histone deacetylase inhibitors repress macrophage migration inhibitory factor (MIF) expression by targeting MIF gene transcription through a local chromatin deacetylation. *Biochim Biophys Acta*. 2009;1793:1749-1758.
19. Calandra T, Bernhagen J, Mitchell RA, Bucala R. The macrophage is an important and previously unrecognized source of macrophage migration inhibitory factor. *J Exp Med*. 1994;179:1895-1902.
20. Morelli AE, Zahorchak AF, Larregina AT, et al. Cytokine production by mouse myeloid dendritic cells in relation to differentiation and terminal maturation induced by lipopolysaccharide or CD40 ligation. *Blood*. 2001;98:1512-1523.
21. Roger T, Ding X, Chanson AL, Renner P, Calandra T. Regulation of constitutive and microbial pathogen-induced human macrophage migration inhibitory factor (MIF) gene expression. *Eur J Immunol*. 2007;37:3509-3521.
22. Roger T, David J, Glauser MP, Calandra T. MIF regulates innate immune responses through modulation of Toll-like receptor 4. *Nature*. 2001;414:920-924.
23. Mitchell RA, Liao H, Chesney J, et al. Macrophage migration inhibitory factor (MIF) sustains macrophage proinflammatory function by inhibiting p53: regulatory role in the innate immune response. *Proc Natl Acad Sci U S A*. 2002;99:345-350.
24. Roger T, Froidevaux C, Martin C, Calandra T. Macrophage migration inhibitory factor (MIF) regulates host responses to endotoxin through modulation of Toll-like receptor 4 (TLR4). *J Endotoxin Res*. 2003;9:119-123.
25. Piette C, Deprez M, Roger T, Noel A, Foidart JM, Munaut C. The dexamethasone-induced inhibition of proliferation, migration, and invasion in glioma cell lines is antagonized by macrophage migration inhibitory factor (MIF) and can be enhanced by specific MIF inhibitors. *J Biol Chem*. 2009;284:32483-32492.
26. Baugh JA, Chitnis S, Donnelly SC, et al. A functional promoter polymorphism in the macrophage migration inhibitory factor (MIF) gene associated with disease severity in rheumatoid arthritis. *Genes Immun*. 2002;3:170-176.
27. Donn R, Alourfi Z, De Benedetti F, et al. Mutation screening of the macrophage migration inhibitory factor gene: positive association of a functional polymorphism of macrophage migration inhibitory factor with juvenile idiopathic arthritis. *Arthritis Rheum*. 2002;46:2402-2409.
28. Renner P, Roger T, Calandra T. Macrophage migration inhibitory factor: gene polymorphisms and susceptibility to inflammatory diseases. *Clin Infect Dis*. 2005;41(Suppl 7):S513-S519.
29. Emonts M, Sweep FC, Grebenchtchikov N, et al. Association between high levels of blood macrophage migration inhibitory factor, inappropriate adrenal response, and early death in patients with severe sepsis. *Clin Infect Dis*. 2007;44:1321-1328.
30. Awandare GA, Martinson JJ, Were T, et al. MIF (macrophage migration inhibitory factor) promoter polymorphisms and susceptibility to severe malarial anemia. *J Infect Dis*. 2009;200:629-637.
31. Renner P, Roger T, Bochud PY, et al. A functional microsatellite of the macrophage migration inhibitory factor gene associated with meningococcal disease. *FASEB J*. 2012;26:907-916.
32. Roger T, Delaloye J, Chanson AL, Giddey M, Le Roy D, Calandra T. Macrophage migration inhibitory factor deficiency is associated with impaired killing of gram-negative bacteria by macrophages and increased susceptibility to *Klebsiella pneumoniae* sepsis. *J Infect Dis*. 2013;207:331-339.
33. Roger T, Schneider A, Weier M, et al. High expression levels of macrophage migration inhibitory factor sustain the innate immune responses of neonates. *Proc Natl Acad Sci U S A*. 2016;113:E997-E1005.
34. Savva A, Brouwer MC, Roger T, et al. Functional polymorphisms of macrophage migration inhibitory factor as predictors of morbidity and mortality of pneumococcal meningitis. *Proc Natl Acad Sci U S A*. 2016;113:3597-3602.
35. Froidevaux C, Roger T, Martin C, Glauser MP, Calandra T. Macrophage migration inhibitory factor and innate immune responses to bacterial infections. *Crit Care Med*. 2001;29:S13-S15.
36. Al-Abed Y, Dabideen D, Aljabari B, et al. ISO-1 binding to the tautomerase active site of MIF inhibits its pro-inflammatory activity and increases survival in severe sepsis. *J Biol Chem*. 2005;280:36541-36544.
37. Bilsborrow JB, Doherty E, Tilstam PV, Bucala R. Macrophage migration inhibitory factor (MIF) as a therapeutic target for rheumatoid arthritis and systemic lupus erythematosus. *Expert Opin Ther Targets*. 2019;23:733-744.

38. Kerschbaumer RJ, Rieger M, Volkel D, et al. Neutralization of macrophage migration inhibitory factor (MIF) by fully human antibodies correlates with their specificity for the beta-sheet structure of MIF. *J Biol Chem*. 2012;287:7446-7455.
39. Ouertatani-Sakouhi H, El-Turk F, Fauvet B, et al. Identification and characterization of novel classes of macrophage migration inhibitory factor (MIF) inhibitors with distinct mechanisms of action. *J Biol Chem*. 2010;285:26581-26598.
40. Ouertatani-Sakouhi H, El-Turk F, Fauvet B, et al. A new class of isothiocyanate-based irreversible inhibitors of macrophage migration inhibitory factor. *Biochemistry*. 2009;48:9858-9870.
41. Gunther S, Fagone P, Jalce G, Atanasov AG, Guignabert C, Nicoletti F. Role of MIF and D-DT in immune-inflammatory, autoimmune, and chronic respiratory diseases: from pathogenic factors to therapeutic targets. *Drug Discov Today*. 2019;24:428-439.
42. Leng L, Metz CN, Fang Y, et al. MIF signal transduction initiated by binding to CD74. *J Exp Med*. 2003;197:1467-1476.
43. Shi X, Leng L, Wang T, et al. CD44 is the signaling component of the macrophage migration inhibitory factor-CD74 receptor complex. *Immunity*. 2006;25:595-606.
44. Bernhagen J, Krohn R, Lue H, et al. MIF is a noncognate ligand of CXC chemokine receptors in inflammatory and atherogenic cell recruitment. *Nat Med*. 2007;13:587-596.
45. Schwartz V, Kruttgen A, Weis J, et al. Role for CD74 and CXCR4 in clathrin-dependent endocytosis of the cytokine MIF. *Eur J Cell Biol*. 2012;91:435-449.
46. Alampour-Rajabi S, El Bounkari O, Rot A, et al. MIF interacts with CXCR7 to promote receptor internalization, ERK1/2 and ZAP-70 signaling, and lymphocyte chemotaxis. *FASEB J*. 2015;29:4497-4511.
47. Hudson JD, Shoaibi MA, Maestro R, Carnero A, Hannon GJ, Beach DH. A proinflammatory cytokine inhibits p53 tumor suppressor activity. *J Exp Med*. 1999;190:1375-1382.
48. Filip AM, Klug J, Cayli S, et al. Ribosomal protein S19 interacts with macrophage migration inhibitory factor and attenuates its pro-inflammatory function. *J Biol Chem*. 2009;284:7977-7985.
49. Kim MJ, Kim WS, Kim DO, et al. Macrophage migration inhibitory factor interacts with thioredoxin-interacting protein and induces NF-kappaB activity. *Cell Signal*. 2017;34:110-120.
50. Kleemann R, Hausser A, Geiger G, et al. Intracellular action of the cytokine MIF to modulate AP-1 activity and the cell cycle through Jab1. *Nature*. 2000;408:211-216.
51. Mitchell RA, Metz CN, Peng T, Bucala R. Sustained mitogen-activated protein kinase (MAPK) and cytoplasmic phospholipase A2 activation by macrophage migration inhibitory factor (MIF). Regulatory role in cell proliferation and glucocorticoid action. *J Biol Chem*. 1999;274:18100-18106.
52. Lue H, Thiele M, Franz J, et al. Macrophage migration inhibitory factor (MIF) promotes cell survival by activation of the Akt pathway and role for CSN5/JAB1 in the control of autocrine MIF activity. *Oncogene*. 2007;26:5046-5059.
53. Santos LL, Lacey D, Yang Y, Leech M, Morand EF. Activation of synovial cell p38 MAP kinase by macrophage migration inhibitory factor. *J Rheumatol*. 2004;31:1038-1043.
54. Roger T, Chanson AL, Knaup-Reymond M, Calandra T. Macrophage migration inhibitory factor promotes innate immune responses by suppressing glucocorticoid-induced expression of mitogen-activated protein kinase phosphatase-1. *Eur J Immunol*. 2005;35:3405-3413.
55. Lue H, Kapurniotu A, Fingerle-Rowson G, et al. Rapid and transient activation of the ERK MAPK signalling pathway by macrophage migration inhibitory factor (MIF) and dependence on JAB1/CSN5 and Src kinase activity. *Cell Signal*. 2006;18:688-703.
56. Santos LL, Fan H, Hall P, et al. Macrophage migration inhibitory factor regulates neutrophil chemotactic responses in inflammatory arthritis in mice. *Arthritis Rheum*. 2011;63:960-970.
57. Klasen C, Ohl K, Sternkopf M, et al. MIF promotes B cell chemotaxis through the receptors CXCR4 and CD74 and ZAP-70 signaling. *J Immunol*. 2014;192:5273-5284.
58. de Souza HS, Tortori CA, Lintomen L, et al. Macrophage migration inhibitory factor promotes eosinophil accumulation and tissue remodeling in eosinophilic esophagitis. *Mucosal Immunol*. 2015;8:1154-1165.
59. Zhang H, Ye YL, Li MX, et al. CXCL2/MIF-CXCR2 signaling promotes the recruitment of myeloid-derived suppressor cells and is correlated with prognosis in bladder cancer. *Oncogene*. 2017;36:2095-2104.
60. Bozza M, Satoskar AR, Lin G, et al. Targeted disruption of migration inhibitory factor gene reveals its critical role in sepsis. *J Exp Med*. 1999;189:341-346.
61. Fingerle-Rowson G, Petrenko O, Metz CN, et al. The p53-dependent effects of macrophage migration inhibitory factor revealed by gene targeting. *Proc Natl Acad Sci U S A*. 2003;100:9354-9359.
62. Ciarlo E, Roger T. Screening the impact of sirtuin inhibitors on inflammatory and innate immune responses of macrophages and in a mouse model of endotoxic shock. *Methods Mol Biol*. 2016;1436:313-334.
63. Ciarlo E, Heinonen T, Herderschee J, et al. Impact of the microbial derived short chain fatty acid propionate on host susceptibility to bacterial and fungal infections in vivo. *Sci Rep*. 2016;6:37944.
64. Ciarlo E, Heinonen T, Theroude C, et al. Trained immunity confers broad-spectrum protection against bacterial infections. *J Infect Dis*. 2020;222:1869-1881.
65. Lubetsky JB, Dios A, Han J, et al. The tautomerase active site of macrophage migration inhibitory factor is a potential target for discovery of novel anti-inflammatory agents. *J Biol Chem*. 2002;277:24976-24982.
66. Randolph GJ, Ochando J, Partida-Sanchez S. Migration of dendritic cell subsets and their precursors. *Annu Rev Immunol*. 2008;26:293-316.
67. Hogstad B, Berres ML, Chakraborty R, et al. RAF/MEK/extracellular signal-related kinase pathway suppresses dendritic cell migration and traps dendritic cells in Langerhans cell histiocytosis lesions. *J Exp Med*. 2018;215:319-336.
68. Weber C, Kraemer S, Drechsler M, et al. Structural determinants of MIF functions in CXCR2-mediated inflammatory and atherogenic leukocyte recruitment. *Proc Natl Acad Sci U S A*. 2008;105:16278-16283.
69. Hsieh CY, Chen CL, Lin YS, et al. Macrophage migration inhibitory factor triggers chemotaxis of CD74+CXCR2+ NKT cells in chemically induced IFN-gamma-mediated skin inflammation. *J Immunol*. 2014;193:3693-3703.
70. Faure-Andre G, Vargas P, Yuseff MI, et al. Regulation of dendritic cell migration by CD74, the MHC class II-associated invariant chain. *Science*. 2008;322:1705-1710.
71. Lopez MJ, Seyed-Razavi Y, Jamali A, Harris DL, Hamrah P. The chemokine receptor CXCR4 mediates recruitment of CD11c+ conventional dendritic cells into the inflamed murine cornea. *Invest Ophthalmol Vis Sci*. 2018;59:5671-5681.

72. Umemoto E, Otani K, Ikeno T, et al. Constitutive plasmacytoid dendritic cell migration to the splenic white pulp is cooperatively regulated by CCR7- and CXCR4-mediated signaling. *J Immunol*. 2012;189:191-199.
73. Kabashima K, Sugita K, Shiraishi N, Tamamura H, Fujii N, Tokura Y. CXCR4 engagement promotes dendritic cell survival and maturation. *Biochem Biophys Res Commun*. 2007;361:1012-1016.
74. Kohara H, Omatsu Y, Sugiyama T, Noda M, Fujii N, Nagasawa T. Development of plasmacytoid dendritic cells in bone marrow stromal cell niches requires CXCL12-CXCR4 chemokine signaling. *Blood*. 2007;110:4153-4160.
75. Kontos C, El Bounkari O, Krammer C, et al. Designed CXCR4 mimic acts as a soluble chemokine receptor that blocks atherogenic inflammation by agonist-specific targeting. *Nat Commun*. 2020;11:5981.
76. Mao L, Le S, Jin X, Liu G, Chen J, Hu J. CSN5 promotes the invasion and metastasis of pancreatic cancer by stabilization of FOXM1. *Exp Cell Res*. 2019;374:274-281.
77. Hwang CI, Matoso A, Corney DC, et al. Wild-type p53 controls cell motility and invasion by dual regulation of MET expression. *Proc Natl Acad Sci U S A*. 2011;108:14240-14245.
78. Vogl AM, Phu L, Becerra R, et al. Global site-specific neddylation profiling reveals that NEDDylated cofilin regulates actin dynamics. *Nat Struct Mol Biol*. 2020;27:210-220.
79. Brocks T, Fedorchenko O, Schliermann N, et al. Macrophage migration inhibitory factor protects from nonmelanoma epidermal tumors by regulating the number of antigen-presenting cells in skin. *FASEB J*. 2017;31:526-543.
80. Kechagia JZ, Ivaska J, Roca-Cusachs P. Integrins as biomechanical sensors of the microenvironment. *Nat Rev Mol Cell Biol*. 2019;20:457-473.
81. Bondza PK, Metz CN, Akoum A. Macrophage migration inhibitory factor up-regulates alpha(v)beta(3) integrin and vascular endothelial growth factor expression in endometrial adenocarcinoma cell line Ishikawa. *J Reprod Immunol*. 2008;77:142-151.
82. Lee CY, Su MJ, Huang CY, et al. Macrophage migration inhibitory factor increases cell motility and up-regulates alphavbeta3 integrin in human chondrosarcoma cells. *J Cell Biochem*. 2012;113:1590-1598.
83. Khoufache K, Bazin S, Girard K, et al. Macrophage migration inhibitory factor antagonist blocks the development of endometriosis in vivo. *PLoS ONE*. 2012;7:e37264.
84. Chen CA, Chang JM, Yang YL, Chang EE, Chen HC. Macrophage migration inhibitory factor regulates integrin-beta1 and cyclin D1 expression via ERK pathway in podocytes. *Biomed Pharmacother*. 2020;124:109892.
85. Gregory JL, Morand EF, McKeown SJ, et al. Macrophage migration inhibitory factor induces macrophage recruitment via CC chemokine ligand 2. *J Immunol*. 2006;177:8072-8079.
86. Binsky I, Lantner F, Grabovsky V, et al. TAp63 regulates VLA-4 expression and chronic lymphocytic leukemia cell migration to the bone marrow in a CD74-dependent manner. *J Immunol*. 2010;184:4761-4769.
87. Rendon BE, Roger T, Teneng I, et al. Regulation of human lung adenocarcinoma cell migration and invasion by macrophage migration inhibitory factor. *J Biol Chem*. 2007;282:29910-29918.
88. Swant JD, Rendon BE, Symons M, Mitchell RA. Rho GTPase-dependent signaling is required for macrophage migration inhibitory factor-mediated expression of cyclin D1. *J Biol Chem*. 2005;280:23066-23072.

SUPPORTING INFORMATION

Additional Supporting Information may be found online in the Supporting Information section.

How to cite this article: Ives A, Le Roy D, Théroude C, Bernhagen J, Roger T, Calandra T. Macrophage migration inhibitory factor promotes the migration of dendritic cells through CD74 and the activation of the Src/PI3K/myosin II pathway. *The FASEB Journal*. 2021;35:e21418. https://doi.org/10.1096/fj.202001605R

6.6. The big sepsis game